

Reference

NBS
Publi-
cations

NAT'L INST. OF STAND & TECH



A11105 977757



NBS TECHNICAL NOTE 1042

U.S. DEPARTMENT OF COMMERCE /National Bureau of Standards

Shielded Balanced and Coaxial Transmission Lines — Parametric Measurements and Instrumentation Relevant to Signal Waveform Transmission in Digital Service

-QC
100
.U5753
No. 1042
1981

NATIONAL BUREAU OF STANDARDS

The National Bureau of Standards¹ was established by an act of Congress on March 3, 1901. The Bureau's overall goal is to strengthen and advance the Nation's science and technology and facilitate their effective application for public benefit. To this end, the Bureau conducts research and provides: (1) a basis for the Nation's physical measurement system, (2) scientific and technological services for industry and government, (3) a technical basis for equity in trade, and (4) technical services to promote public safety. The Bureau's technical work is performed by the National Measurement Laboratory, the National Engineering Laboratory, and the Institute for Computer Sciences and Technology.

THE NATIONAL MEASUREMENT LABORATORY provides the national system of physical and chemical and materials measurement; coordinates the system with measurement systems of other nations and furnishes essential services leading to accurate and uniform physical and chemical measurement throughout the Nation's scientific community, industry, and commerce; conducts materials research leading to improved methods of measurement, standards, and data on the properties of materials needed by industry, commerce, educational institutions, and Government; provides advisory and research services to other Government agencies; develops, produces, and distributes Standard Reference Materials; and provides calibration services. The Laboratory consists of the following centers:

Absolute Physical Quantities² — Radiation Research — Thermodynamics and Molecular Science — Analytical Chemistry — Materials Science.

THE NATIONAL ENGINEERING LABORATORY provides technology and technical services to the public and private sectors to address national needs and to solve national problems; conducts research in engineering and applied science in support of these efforts; builds and maintains competence in the necessary disciplines required to carry out this research and technical service; develops engineering data and measurement capabilities; provides engineering measurement traceability services; develops test methods and proposes engineering standards and code changes; develops and proposes new engineering practices; and develops and improves mechanisms to transfer results of its research to the ultimate user. The Laboratory consists of the following centers:

Applied Mathematics — Electronics and Electrical Engineering² — Mechanical Engineering and Process Technology² — Building Technology — Fire Research — Consumer Product Technology — Field Methods.

THE INSTITUTE FOR COMPUTER SCIENCES AND TECHNOLOGY conducts research and provides scientific and technical services to aid Federal agencies in the selection, acquisition, application, and use of computer technology to improve effectiveness and economy in Government operations in accordance with Public Law 89-306 (40 U.S.C. 759), relevant Executive Orders, and other directives; carries out this mission by managing the Federal Information Processing Standards Program, developing Federal ADP standards guidelines, and managing Federal participation in ADP voluntary standardization activities; provides scientific and technological advisory services and assistance to Federal agencies; and provides the technical foundation for computer-related policies of the Federal Government. The Institute consists of the following centers:

Programming Science and Technology — Computer Systems Engineering.

¹Headquarters and Laboratories at Gaithersburg, MD, unless otherwise noted; mailing address Washington, DC 20234.

²Some divisions within the center are located at Boulder, CO 80303.

Shielded Balanced and Coaxial Transmission Lines — Parametric Measurements and Instrumentation Relevant to Signal Waveform Transmission in Digital Service

NATIONAL BUREAU
OF STANDARDS
LIBRARY

SEP 16 1981

Not at -- Key

32100

.U5753

NO 1048

1981

W. L. Gans
N. S. Nahman

Electromagnetic Technology Division
National Engineering Laboratory
National Bureau of Standards
Boulder, Colorado 80303

Final report prepared for:
Department of the Army
U.S. Army Communications Command
Communications - Electronic Engineering and Installations Agency
Fort Huachuca, Arizona 85613



NBS technical note

U.S. DEPARTMENT OF COMMERCE, Malcolm Baldrige, Secretary

NATIONAL BUREAU OF STANDARDS, Ernest Ambler, Director

Issued June 1981

NATIONAL BUREAU OF STANDARDS TECHNICAL NOTE 1042

Nat. Bur. Stand. (U.S.), Tech. Note 1042, 260 pages (June 1981)

CODEN: NBTNAE

TABLE OF CONTENTS

	Page
1. INTRODUCTION	1
1.1 Background	1
1.2 Project Objective	2
1.3 Report Organization	2
2. DESCRIPTION OF THE TRANSMISSION LINE MODEL AND THE DEFINITION OF THE MODEL PARAMETERS.	4
2.1 The General Transmission Line Equations	4
2.2 The s^m Model and Its Parameters	6
2.3 s-Domain Circuit Properties of the Model	8
2.4 High Frequency Attenuation and Phase Shift	10
3. MEASUREMENT METHODS FOR THE DETERMINATION OF THE TRANSMISSION LINE PARAMETERS	19
3.1 The Need for Measurements	19
3.2 Measurement of the per Unit Length Resistance and Capacitance, R and C	20
3.3 Measurement of the Nominal Characteristic Impedance, R_o	20
3.4 Insertion Measurements for the Determination of the High Frequency Loss Parameter and the Exponent m	22
4. AN OVERVIEW OF THE COMPUTER CALCULATION FOR THE TRANSMISSION LINE IMPULSE AND STEP RESPONSES	34
4.1 Data Acquisition Method.	34
4.2 Fourier Transformation of $\hat{e}_{d1}(nT)$ and $\hat{e}_{d2}(nT)$	34
4.3 The Calculation of $\hat{S}_{21}(k/2NT)$ and $\hat{\alpha}_1(k/2NT)$	35
4.4 The Extraction of the Model Parameters K and m	36
4.5 Simulation of the Impulse Response	38
4.6 Determination of the dc Level for the Impulse Response, $\hat{h}(nT)$	38
4.7 Simulation of the Step Response	39
5. TYPICAL RESULTS FOR TRANSMISSION CHARACTERIZATION AND RESPONSE	44
5.1 Description of the Cable	44
5.2 The Results	44
6. USE OF TIME DOMAIN MEASUREMENTS TO ESTIMATE MAXIMUM CABLE BIT RATE AND BIT-ERROR-RATE DEGRADATION	58
6.1 Digital Communications System Model	58
6.2 Maximum Bit Rate Estimation	58
6.3 Code Dependence	60
6.4 Bit-Error-Rate Degradation	61
7. CABLE TESTING USING TIME DOMAIN REFLECTOMETRY	81
7.1 The General Theory of Time Domain Reflection and Transmission	81
7.2 The Step Response of the Sending-End Voltage	87
7.3 A Practical Method for Measuring the Step Response of the Sending-End Voltage	92
REFERENCES	104

	page
APPENDIX A -- MEASURED AND MODELED CABLE DATA	105
A.1 Cable Parameter Tables	105
A.2 Cable Graphical Data	108
APPENDIX B -- CABLE MEASUREMENT AND ANALYSIS COMPUTER PROGRAMS	185
B.1 APMS System Calibration Programs and Subroutines	185
B.1.1 Y-Axis Calibration Subroutine	185
B.1.2 X-Axis Calibration Subroutine	187
B.1.3 Calibration Data Acquisition Subroutine	190
B.1.4 Linear Least Squares Curve Fit Subroutine	195
B.1.5 General Matrix Multiplication Subroutine	196
B.2 Cable Measurement Programs and Subroutines	197
B.2.1 Main Cable Time Domain Transfer Function Measurement Program	197
B.2.2 Sweep-Sequential Waveform Acquisition Subroutine	203
B.2.3 Point-Sequential Waveform Acquisition Subroutine	208
B.2.4 Assembly Language Fast Fourier Transform Subroutine	213
B.2.5 General Time Domain/Frequency Domain Plot Program	221
B.3 Cable Modeling and Analysis Programs	231
B.3.1 Main Cable Model Program for Calculations of "m", "K", and Cable Impulse Response	231
B.3.2 Main Cable Model Program for Calculation of Cable Step Response, Bit Error Waveform and Cable Square Wave Response	239
B.3.3 Main Cable Model Program for Calculation of Unit Step TDR Waveform	245
B.3.4 Main Program for Calculation of Cable Matching Network Resistors	247
B.3.5 Main Program for Calculation of the Error Function	249
B.3.6 Function Subroutine for Calculation of the Gamma Function	250
B.3.7 Subroutine for Accurate Calculations of Cable Time Domain Impulse Response dc Level	251
APPENDIX C -- TIME DOMAIN DATA ACQUISITION SYSTEM DESCRIPTION	254

SHIELDED BALANCED AND COAXIAL TRANSMISSION LINES -
PARAMETRIC MEASUREMENTS AND INSTRUMENTATION RELEVANT TO
SIGNAL WAVEFORM TRANSMISSION IN DIGITAL SERVICE

W. L. Gans and N. S. Nahman

A method is presented for determining the impulse and step responses of a shielded cable using time domain terminal measurements and a physically based mathematical model for the transmission line properties of the cable. The method requires a computer controlled time domain measurement system and was implemented using the NBS Automatic Pulse Measurement System (APMS). Data are also developed for the frequency domain complex propagation function (attenuation and its related minimum-phase shift). The method is applied to 12 shielded paired-conductor (balanced) cables and 5 coaxial cables. Time domain responses are presented for three nominal cable lengths, 60 m (200 ft), 150m (500 ft), and 300m (1000 ft). The time domain responses are applied to the estimation of bit error rate increases due to the insertion of the cables into a digital signaling system employing a balanced polar NRZ waveform. Also discussed is the application of the time domain responses to time domain reflectometry techniques for cable acceptance tests and field-site testing of installed cables.

Key words: bit error rate; coaxial transmission lines; digital communication impulse response; instrumentation; measurements; shielded balanced transmission lines; time domain; transmission line model; waveform.

1. INTRODUCTION

1.1 Background

Nominal frequency response data supplied by cable manufacturers are not sufficient for the complete evaluation or simulation of cables (transmission lines) in digital systems. Data which must be acquired prior to engineering analysis for digital transmission are the driving-point and transfer impulse responses. These are most easily obtained through pulse or time domain testing.

Furthermore, time domain measurement methods and performance data for the characterization of balanced digital-service, shielded transmission lines [60m (200 ft) to 300 m (1000 ft) lengths] are required for the design, signal analysis, and circuit monitoring relevant to the digital-service transmission line interconnections between the Technical Control Facility (TCF) and the Radio/Microwave Exchange (MUX) as encountered in U.S. Army telecommunication installations. Also, time domain measurement methods are required for the identification and location of installation and/or operating faults which can impair the digital waveform fidelity, which in turn can cause a degradation of the digital signaling capacity. Such measurement methods and their interpretation fundamentally depend upon a knowledge of typical impulse responses.

Because response data suitable for digital cable simulation was not available, the U.S. Army Communications - Electronics Engineering Installation Agency (USACEEIA) sought assistance from the National Bureau of Standards (NBS) to develop the required data for a specified group of commercially available cables. The NBS Time Domain Metrology Group was uniquely qualified to render such assistance

by virtue of their experience in (1) the development and use of the NBS Automatic Pulse Measurement System and (2) the characterization of transient responses for shielded cables. The subject report summarizes the work performed by the NBS Time Domain Metrology Group for USACEEIA and is for the most part a catalog of cable impulse responses and associated transfer functions.

1.2 Project Objective

The overall project objective contained three components; listed in order of their relative technical priority, they were:

1. Determine and compile from measurements the parametric data necessary for engineering design and computer simulation of typical shielded cables for digital service. Demonstrate the use of the data to provide time domain and frequency domain simulation.
2. Simulate time domain reflectometry reference signatures suitable for cable field testing and fault location.
3. Demonstrate a time domain data acquisition system capable of (a) acquiring the signal waveforms of a transmission line under test conditions and (b) provide measured cable parameters suitable for subsequent batch processing in a central computer system for engineering design and simulation studies.

Originally, it was proposed to accomplish each one of the above components individually in a specific phase of the work during the contract duration. However, to allow for cable and component delivery delays, and the natural interaction between the objective components, the work was not rigidly accomplished in specific phases. The subject report presents the results of the work in accomplishing objective-components (1), (2), and (3) above.

1.3 Report Organization

This report is divided into eight chapters and two appendices, the first chapter being the present introduction. Chapter 2 presents the transmission line model, the definition of parameters, and a discussion of the model frequency dependence.

Chapter 3 describes the measurement methods used to obtain the frequency and time domain data required for the calculation of the transmission line parameters.

Chapter 4 provides a qualitative overview of the computer calculations for (1) the extraction or determination of the transmission line parameters, (2) the impulse response, and (3) the step response.

Chapter 5 presents an example of the typical results for the determination of the transmission line parameters and the corresponding frequency and time domain responses for a given cable.

Chapter 6 describes a method of estimating the bit-error-rate degradation of a balanced polar NRZ waveform produced by a given length of cable.

Chapter 7 discusses the time domain reflectometry method for testing cables which is suitable for acceptance and field-site tests. Typical results are given for the worst case situations of open and short-circuit discontinuities.

Appendix A is a catalog of complex phasor transfer functions, their associated time domain responses (both reflection and transmission) for selected commercially available shielded cables of different lengths, usually 60 m (200 ft), 150 m (500 ft), and 300 m (1000 ft). The cables included are:

- A. Shielded Paired-Conductor Transmission Lines: RG 22, U.S. Army WD-37, and ten commercially available cables designated as cables A through J.
- B. Coaxial-conductor Transmission Lines: RG58C, RG59B, RG214, RG223, and a commercially available triaxial cable designated as cable K.

Appendix B contains the computer programs which were used in the NBS APMS to accomplish the cable measurements, characterization and simulation. Appendix C is a description of one design for a time domain data acquisition system (NBS APMS).

2. DESCRIPTION OF THE TRANSMISSION LINE MODEL AND THE DEFINITION OF THE MODEL PARAMETERS

In this chapter a brief discussion of the general transmission line equations is presented so as to provide a basis for the formulation of the transmission line simulation model. Following the introductory discussion, the simulation model parameters are defined and the transmission line equations are expressed in terms of the model parameters. Finally, various limiting cases of the model versus frequency are discussed to provide insight as to the correlation of the model with experiment.

2.1 The General Transmission Line Equations

A uniform transmission line can be characterized in terms of a series impedance per unit length, $Z(s)$, and a shunt admittance per unit length, $Y(s)$, fig. 2.1. This follows from the uniformity property which simply means that the transmission line geometric form and material composition does not change with length, i.e., any segment of the transmission line possesses the same values of $Z(s)$ and $Y(s)$. The specific functional forms of $Z(s)$ and $Y(s)$ depend upon geometric form and material parameters. In practice $Z(s)$ and $Y(s)$ are combined to form two other functions which naturally appear in the transmission line equations and are called the characteristic impedance $Z_o(s)$ and the propagation function $\gamma(s)$.

$$Z_o(s) = \sqrt{\frac{Z(s)}{Y(s)}} \quad , \text{ ohms} \quad (2-1)$$

$$\gamma(s) = \sqrt{Z(s)Y(s)} \quad , \text{ per unit length} \quad (2-2)$$

For a transmission line of length l connected between a generator $E_g(s)$ of impedance $Z_g(s)$ and a load impedance $Z_l(s)$, fig. 2.2, the transfer and driving point equations are given by [1], respectively,

$$\frac{E_r(s)}{E_g(s)} = 2 \left[\frac{Z_o(s)}{Z_g(s) + Z_o(s)} \right] \left[\frac{Z_l(s)}{Z_l(s) + Z_o(s)} \right] \left[\frac{e^{-l\gamma(s)}}{1 - \rho_s(s) \rho_r(s) e^{-2l\gamma(s)}} \right] \quad (2-3)$$

$$\frac{E_s(s)}{I_s(s)} = Z_o(s) \frac{1 + \rho_r(s) e^{-2l\gamma(s)}}{1 - \rho_r(s) e^{-2l\gamma(s)}} \quad (2-4)$$

where the reflection coefficients $\rho_s(s)$ $\rho_r(s)$ are obtained from

$$\rho_i(s) = \frac{Z_i(s) - Z_o(s)}{Z_i(s) + Z_o(s)} \quad (2-5)$$

These equations describe a transmission line network which is not terminated at either end in the transmission line characteristic impedance.

When a termination $Z_1(s)$ is equal to $Z_0(s)$, then the corresponding $\rho_1(s)$ is zero, and the transmission line is said to be matched at that end. There are three possible situations for matched terminations:

1. Doubly matched $Z_g(s) = Z_l(s) = Z_0(s)$

$$\left. \begin{aligned} \frac{E_r(s)}{E_g(s)} &= \frac{e^{-2\gamma(s)}}{2} \\ \rho_g = \rho_r &= 0 \end{aligned} \right\} \quad (2-6)$$

$$\left. \begin{aligned} \frac{E_s(s)}{I_s(s)} &= Z_0(s) \\ \rho_g = \rho_r &= 0 \end{aligned} \right\} \quad (2-7)$$

2. Matched Load $Z_l(s) = Z_0(s)$

$$\left. \begin{aligned} \frac{E_r(s)}{E_g(s)} &= \left[\frac{Z_0(s)}{Z_g(s) + Z_0(s)} \right] e^{-2\gamma(s)} \\ \rho_l &= 0 \end{aligned} \right\} \quad (2-8)$$

$$\left. \begin{aligned} \frac{E_s(s)}{I_s(s)} &= Z_0(s) \\ \rho_l &= 0 \end{aligned} \right\} \quad (2-9)$$

3. Matched Generator $Z_g(s) = Z_0(s)$

$$\left. \begin{aligned} \frac{E_r(s)}{E_g(s)} &= \left[\frac{Z_l(s)}{Z_l(s) + Z_0(s)} \right] e^{-2\gamma(s)} \\ \rho_g &= 0 \end{aligned} \right\} \quad (2-10)$$

$$\left. \begin{aligned} \frac{E_g(s)}{I_s(s)} &= Z_0(s) \frac{1 + \rho_r(s) e^{-2\gamma(s)}}{1 - \rho_r(s) e^{-2\gamma(s)}} \\ \rho_g &= 0 \end{aligned} \right\} \quad (2-11)$$

Equations (2-3) through (2-11) reduce to the lossless or ideal cases when

$$Z(s) = sL \quad (2-12)$$

and

$$Y(s) = sC \quad (2-13)$$

which in turn yield a delay propagation function and a resistive characteristic impedance, respectively,

$$\gamma(s) = s\sqrt{LC} \quad (2-14)$$

and

$$Z_o(s) = R_o = \sqrt{\frac{L}{C}} \quad (2-15)$$

Under such conditions, there is no distortion with propagation, and also the transmission line can be terminated with a resistor, R_o , for reflection-free transmission.

For practical shielded cables, there are losses present, which in turn, means that both $\gamma(s)$ and $Z_o(s)$ will be complicated functions of s . The resultant propagation along the line will distort pulses due to the nature of $\gamma(s)$. Also, because $Z_o(s)$ is s dependent, resistive terminations R_g , R_ℓ will not match (equal) the characteristic impedance; under such conditions in equations (2-3) through (2-11), the voltage divider terms and their combinations which form the reflection coefficients,

$$\frac{Z_o(s)}{R_g + Z_o(s)} ; \quad \frac{Z_\ell(s)}{R_\ell + Z_o(s)} ; \quad \frac{R_1 - Z_o(s)}{R_1 + Z_o(s)} ,$$

contribute to the overall distortion of the transmitted pulse as they are not independent of s .

2.2 The s^m Model and Its Parameters

The physically-based mathematical model used in this work was originally developed by Nahman in 1962 for the sub-nanosecond to nanosecond domain transient analysis of coaxial-conductor cables [2]. Subsequent investigation by Nahman and Riad using the NBS APMS showed that the model could also be used to simulate shielded paired-conductor cables of parallel or twisted conductor construction [3].

The model specifies $Z(s)$ and $Y(s)$ as

$$Z(s) = R + sL + Ks^m , \quad 0 < m < 1 \quad (2-16)$$

and

$$Y(s) = sC \quad (2-17)$$

where

$$R \equiv \text{dc resistance/unit length} \quad (2-18)$$

$$L \equiv \text{Inductance/unit length} \quad (2-19)$$

$$K \equiv \text{High frequency loss coefficient/unit length} \quad (2-20)$$

$$m \equiv \text{High frequency loss exponent} \quad (2-21)$$

$$C \equiv \text{Capacitance/unit length} \quad (2-22)$$

Consequently, the model equivalent circuit per unit length is as shown in fig. 2.3. The propagation function and the characteristic impedance are then given by

$$\gamma(s) = \left[(R + sL + Ks^m) sC \right]^{1/2}, \quad 0 < m < 1 \quad (2-23)$$

and

$$Z_o(s) = \left[(R + sL + Ks^m) / sC \right]^{1/2}, \quad 0 < m < 1 \quad (2-24)$$

In the high frequency region, i.e., when s is such that

$$sL \gg Ks^m \gg R \quad (2-25)$$

the model series impedance is closely approximated by

$$Z(s)_{\text{HF}} = sL + Ks^m \quad (2-26)$$

which in turn gives for $\gamma(s)$ and $Z_o(s)$

$$\gamma(s)_{\text{HF}} = s \sqrt{LC} \left(1 + \frac{Ks^m}{sL} \right)^{1/2} \quad (2-27)$$

and

$$Z_o(s)_{\text{HF}} = \sqrt{\frac{L}{C}} \left(1 + \frac{Ks^m}{sL} \right)^{1/2}. \quad (2-28)$$

Because

$$\frac{Ks^m}{sL} \ll 1 \quad (2-29)$$

then

$$\left(1 + \frac{Ks^m}{sL} \right)^{1/2} \doteq 1 + \frac{Ks^m}{2sL} \quad (2-30)$$

Defining

$$\delta(s) = \frac{Ks^m}{2sL} \quad (2-31)$$

then the high frequency $\gamma(s)$ and $Z_o(s)$ may be expressed as

$$\gamma(s)_{\text{HF}} = s \sqrt{LC} \left[1 + \delta(s) \right], \quad |\delta(s)| \ll 1 \quad (2-32)$$

and

$$Z_o(s)_{\text{HF}} = \sqrt{\frac{L}{C}} \left[1 + \delta(s) \right], \quad |\delta(s)| \ll 1. \quad (2-33)$$

In the limit as $|s|$ approaches infinity, (2-32) and (2-33) yield the time delay per unit length and the high frequency or geometric or nominal characteristic impedance, respectively,

$$\lim_{|s| \rightarrow \infty} \left[\gamma(s)_{\text{HF}} \right] = s \sqrt{LC} \quad (2-34)$$

$$\lim_{|s| \rightarrow \infty} \left[Z_o(s)_{\text{HF}} \right] = \sqrt{\frac{L}{C}} \quad (2-35)$$

which defines the time delay per unit length

$$T = \sqrt{LC} \quad (2-36)$$

and the high frequency characteristic impedance,

$$R_o = \sqrt{\frac{L}{C}} \quad (2-37)$$

2.3 s-Domain Circuit Properties of the Model

Consider the circuit of fig. 2.4 which is the circuit of fig. 2.2 with

$$Z_g(s) = Z_l(s) = R_o \quad (2-38)$$

$$\gamma(s) = [(R + sL + Ks^m)sc]^{1/2} \quad (2-23)$$

$$Z_o(s) = [(R + sL + Ks^m) / sc]^{1/2} \quad (2-24)$$

Here, the transmission line is terminated at each end in the nominal or high frequency characteristic impedance, R_o . This is a doubly mismatched situation for low frequencies, but this is the usual case encountered in practice. In all that follows in this report, the generator and load impedances will be equal to R_o . Consequently, equations (2-3) through (2-5) become

$$\frac{E_r(s)}{E_g(s)} = 2 \left[\frac{Z_o(s)}{R_o + Z_o(s)} \right] \left[\frac{R_o}{R_o + Z_o(s)} \right] \left[\frac{e^{-l\gamma(s)}}{1 - [\rho(s)]^2 e^{-2l\gamma(s)}} \right] \quad (2-39)$$

$$\frac{E_s(s)}{I_s(s)} = Z_o(s) \frac{1 + \rho(s)e^{-2l\gamma(s)}}{1 - \rho(s)e^{-2l\gamma(s)}} \quad (2-40)$$

$$\rho_s(s) = \rho_r(s) = \rho(s) = \frac{R_o - Z_o(s)}{R_o + Z_o(s)} \quad (2-41)$$

For the purposes of the following discussion, it is convenient to express equations (2-38) and (2-39) in terms of the hyperbolic functions

$$\cosh l\gamma(s) = \frac{e^{l\gamma(s)} + e^{-l\gamma(s)}}{2} \quad (2-42)$$

$$\sinh l\gamma(s) = \frac{e^{l\gamma(s)} - e^{-l\gamma(s)}}{2} \quad (2-43)$$

Doing so, there results

$$\frac{E_r(s)}{E_g(s)} = \frac{2 Z_o(s) R_o}{2[R_o^2 + Z_o^2(s)] \sinh l\gamma(s) + 4 R_o Z_o(s) \cosh l\gamma(s)} \quad (2-44)$$

$$\frac{E_s(s)}{I_s(s)} = Z_o(s) \frac{R_o \cosh l\gamma(s) + Z_o(s) \sinh l\gamma(s)}{Z_o(s) \cosh l\gamma(s) + R_o \sinh l\gamma(s)} \quad (2-45)$$

Consideration of fig. 2.4 for $s = 0$ (dc) leads to the network shown in fig. 2.5 and the following conclusions:

1. The transfer function $E_r(o)/E_g(o)$, is equal to $R_o/(2 R_o + lR)$.
2. The impedance looking into the line, $E_s(o)/I_s(o)$, is equal to $lR + R_o$.

To demonstrate that these two conclusions are consistent with the mathematical model, consider (2-44) and (2-45) when $|s| \rightarrow 0$. First of all,

$$Z_o(s) \xrightarrow{|s| \rightarrow 0} \sqrt{\frac{R}{sC}} \quad (2-46)$$

$$\gamma(s) \xrightarrow{|s| \rightarrow 0} \sqrt{sCR} \quad (2-47)$$

and in the limit,

$$\lim_{|s| \rightarrow 0} Z_o(s) \rightarrow \infty \quad (2-48)$$

$$\lim_{|s| \rightarrow 0} \gamma(s) \rightarrow 0 \quad (2-49)$$

Putting (2-46) and (2-49) into (2-44) and (2-45) gives for $|s| \rightarrow 0$

$$\left[\frac{E_r(s)}{E_g(s)} \right]_{|s| \rightarrow 0} \rightarrow \frac{2 R_o \sqrt{sCR}}{2(R_o^2 sC + R) \sinh l \sqrt{sCR} + 4 R_o \sqrt{sCR} \cosh l \sqrt{sCR}} \quad (2-50)$$

$$\left[\frac{E_s(s)}{I_s(s)} \right]_{|s| \rightarrow 0} \rightarrow \frac{\sqrt{sCR} R_o \cosh l \sqrt{sCR} + R \sinh l \sqrt{sCR}}{\sqrt{sCR} \cosh l \sqrt{sCR} + R_o sC \sinh l \sqrt{sCR}} \quad (2-51)$$

When $|s| = 0$, (2-50) and (2-51) both yield 0/0 and are indeterminate. After differentiating the numerators and the denominators, and again applying the limit, the results are

$$\lim_{|s| \rightarrow 0} \left[\frac{E_r(s)}{E_g(s)} \right] = \frac{R_o}{2 R_o + l R} \quad (2-52)$$

$$\lim_{|s| \rightarrow 0} \left[\frac{E_s(s)}{I_s(s)} \right] = R_o + l R \quad (2-53)$$

which agrees with the earlier conclusions.

Next, consider the high frequency behavior of the circuit. Putting (2-32) and (2-33) into (2-44) and (2-45) yields

$$\begin{aligned} \left. \frac{E_r(s)}{E_g(s)} \right|_{\text{HF}} &= \frac{1}{e^{sTl[1 + \delta(s)]} + \frac{[\delta(s)]^2}{2[1 + \delta(s)]} \sinh \{sTl[1 + \delta(s)]\}} \\ &\doteq e^{-sTl[1 + \delta(s)]} \end{aligned} \quad (2-54)$$

and

$$\begin{aligned} Z_s(s) \Big|_{\text{HF}} &= R_o [1 + \delta(s)] \frac{e^{sTl[1 + \delta(s)]} + \delta(s) \sinh \{sTl[1 + \delta(s)]\}}{e^{sTl[1 + \delta(s)]} + \delta(s) \cosh \{sTl[1 + \delta(s)]\}} \\ &= R_o [1 + \delta(s)] \end{aligned} \quad (2-55)$$

as $|\delta(s)| \ll 1$. Note that $Z_s(s)$ is equal to $Z_o(s) \Big|_{\text{HF}}$.

2.4 High Frequency Attenuation and Phase Shift

Equation (2-54) can be written as

$$\left. \frac{E_r(s)}{E_g(s)} \right|_{\text{HF}} = e^{-sTl} e^{-sTl\delta(s)} \quad (2-56)$$

where the first factor represents the time delay of the cable (linear phase shift in the frequency domain), while the second contains the distortion due to high frequency losses. The inverse Laplace transform of (2-56) would yield the initial or early time response of the circuit impulse response. Consequently, (2-56) exhibits the time delay and then the initial impulse response.

In the frequency domain the transfer function is

$$\left. \frac{E_r(j\omega)}{E_g(j\omega)} \right|_{\text{HF}} = e^{-j\omega l T} e^{-\frac{lTK}{2L} (j\omega)^m}$$

or from (2-36) and (2-37),

$$\frac{E_r(j\omega)}{E_g(j\omega)} = e^{-j\omega\ell T} e^{-\frac{\ell K}{2R_o}(j\omega)^m}, \quad 0 < m < 1 \quad (2-57)$$

The attenuation $\alpha_1(\omega)$ and the phase $\beta(\omega)$ of the transfer function are defined by

$$\frac{E_r(j\omega)}{E_g(j\omega)} = e^{-\alpha_1(\omega) - j\beta(\omega)} \quad (2-58)$$

and are

$$\alpha_1(\omega) = \text{Real Part of } \frac{\ell K}{2R_o}(j\omega)^m \quad (2-60)$$

$$\beta(\omega) = \omega\ell T + \text{Imaginary Part of } \frac{\ell K}{2R_o}(j\omega)^m. \quad (2-61)$$

In the phase $\beta(\omega)$, the first term is the linear phase shift associated with the transmission line time delay. In network terminology $\exp(-j\omega\ell T)$ is an all-pass function possessing a linear phase shift. The second term in the phase is uniquely related to the attenuation because the two terms are the real and imaginary parts of an analytic function along the frequency axis, $j\omega$, of the complex frequency plane $s = \sigma + j\omega$; thus the factor in (2-57)

$$F_1(j\omega) = e^{-\frac{\ell K}{2R_o}(j\omega)^m} \quad 0 < m < 1 \quad (2-61)$$

is a minimum phase function. Hence, it is seen that the frequency dependent attenuation has associated with it a frequency dependent (non-linear) phase function.

Defining

$$\beta(\omega) = \beta_o(\omega) + \beta_1(\omega) \quad (2-62)$$

where

$$\beta_o(\omega) = \omega\ell T \quad (2-63)$$

$$\beta_1(\omega) = \text{Imaginary Part of } \frac{-\ell K}{2R_o}(j\omega)^m \quad (2-64)$$

the minimum phase complex exponent is then

$$A(j\omega) = \alpha_1(\omega) + j\beta_1(\omega) \quad (2-65)$$

It is equal to the exponent of (2-57) with the linear phase shift removed, i.e.,

$$\ln \left\{ e^{j\omega\ell T} \frac{E_r(j\omega)}{E_g(j\omega)} \right\} = \alpha_1(\omega) + j\beta_1(\omega)$$

$$\alpha_1(\omega) + j\beta_1(\omega) = \frac{\ell K}{2R_o}(j\omega)^m \quad (2-66)$$

$$\alpha_1(\omega) + j \beta_1(\omega) = \frac{\ell K}{2R_0} \omega^m \left(\cos \frac{m\pi}{2} + j \sin \frac{m\pi}{2} \right) \quad (2-67)$$

Hence,

$$\alpha_1(\omega) = \frac{\ell K}{2R_0} \omega^m \cos m\pi/2, \text{ nepers/unit length} \quad (2-68)$$

and

$$\beta_1(\omega) = \frac{\ell K}{2R_0} \omega^m \sin m\pi/2, \text{ radians/unit length} \quad (2-69)$$

which shows that both the attenuation and phase vary as ω^m . Their ratio is

$$\frac{\alpha_1(\omega)}{\beta_1(\omega)} = \cot m\pi/2. \quad (2-70)$$

Figure 2.6 shows a log-log graph illustrating equations (2-68) through (2-70). Note that the linear slope (i.e., the measured slope using a linear scale) is equal to the fractional power, m . Similarly, a graph of the attenuation $\alpha_1(\omega)$ in dB (8.68 nepers equals one dB) or the minimum phase $\beta_1(\omega)$ in degrees (0.0175 radians equals one degree) would have a linear slope of m .

For frequencies ranging from DC to very high frequencies, the log-log attenuation graph for the model has two asymptotes, fig. 2.7. For very low frequencies the attenuation asymptotically approaches the value set by the transfer ratio (2-52), i.e.,

$$\alpha(\omega) = 20 \log \frac{2 R_0 + \ell R}{R_0}. \quad (2-71)$$

On the other hand, for very high frequencies $\alpha(\omega)$ asymptotically approaches the fractional power response (2-68); in dB, the asymptotic response is

$$\alpha_1(\omega) \Big|_{\text{dB}} = 8.68 \frac{\ell K}{2R_0} |\omega|^m \cos m\pi/2, \text{ dB}. \quad (2-72)$$

Consequently, the model high frequency loss parameter K and the exponent m can be determined from experimental data in the asymptotic high frequency region, provided, of course, that the model is consistent with the physical situation.

In practice, some care must be taken in fitting the model to the experimental data. Specifically, the slope of log-log plot in the high frequency region may not be constant, fig. 2.8; this in turn requires a judgement as to how to select a suitable constant slope curve which is tangent to the log-log attenuation curve in the high frequency region, fig. 2.8. Because the NBS measurement system has a dynamic range of better than 40 dB, the experimental data in the 0 to 30 dB range will possess a good signal to noise ratio. Consequently, the determination of m and K is accomplished by fitting in the 30 dB range. The effectiveness of the fit can only be evaluated by comparing the simulated output waveform based upon the modeled impulse response with that of the observed waveform as will be demonstrated in Chapters 4 and 5.

Finally, one other comment should be made regarding the s^m model. The shunt admittance/unit length $Y(s)$ is specified as being a pure susceptance sC , (2-17); thus $Y(s)$ contains no conductance G which would represent one particular form of dielectric loss. However, in the computer program written for this work $Y(s)$ has the provision for the form

$$Y(s) = G + sC \quad (2-73)$$

so that such a loss form can be easily included if needed. In the cables considered here, G was negligible (as it was infinitesimal, or for all practical purposes, zero). This is not to say that the s^m model excludes all dielectric loss effects when $G = 0$. To the contrary, the slope m and the coefficient K can be effected by high frequency losses due to small dielectric losses in combination with conductor losses.

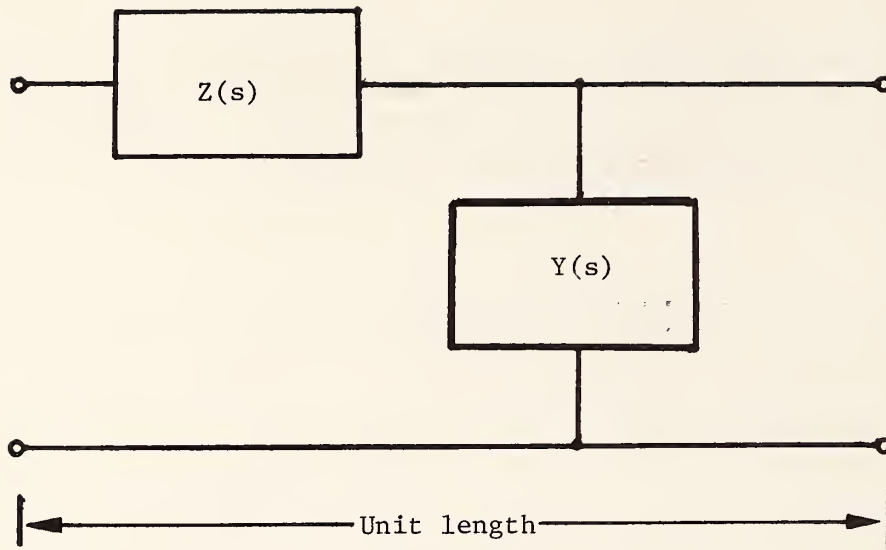


Figure 2.1 The transmission line equivalent circuit per unit length.

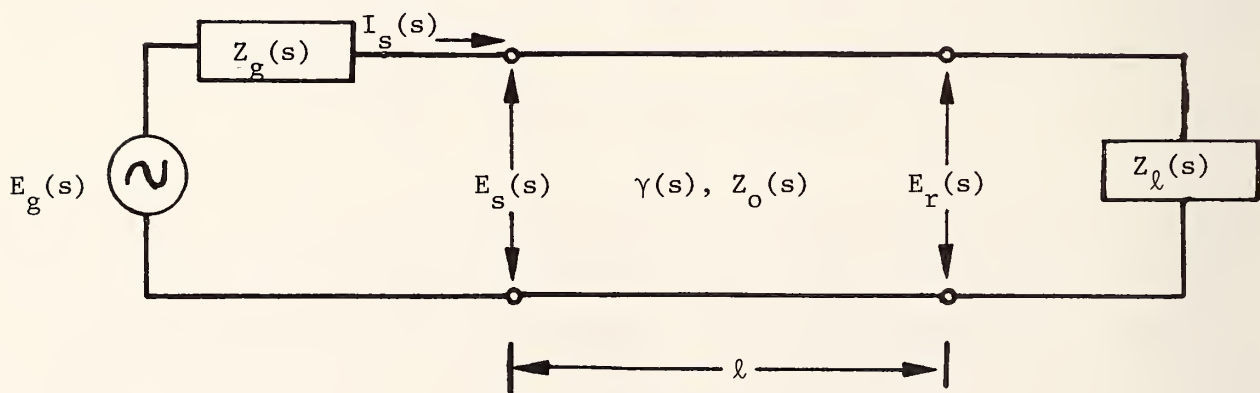


Figure 2.2 The basic transmission circuit consisting of a generator, a transmission line, and a load.

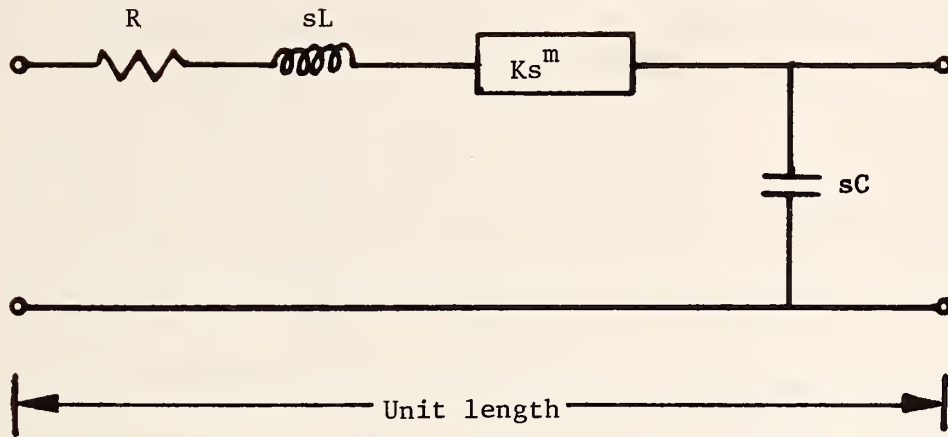


Figure 2.3 The equivalent circuit per unit length for the physically-based mathematical model.

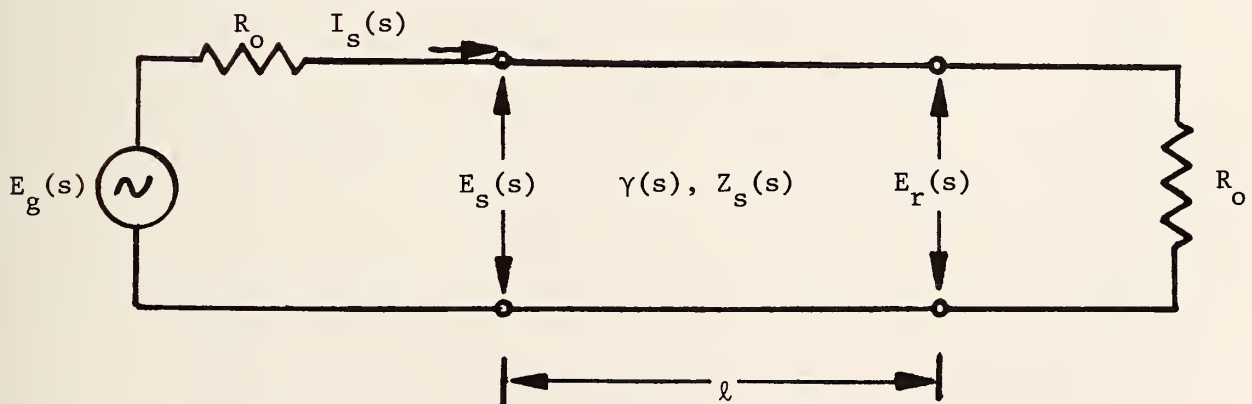


Figure 2.4 The transmission line circuit terminated at each end in R_o , the nominal characteristic impedance. This is a doubly mismatched transmission line because $Z_o(s)$ is not equal to R_o for all s .

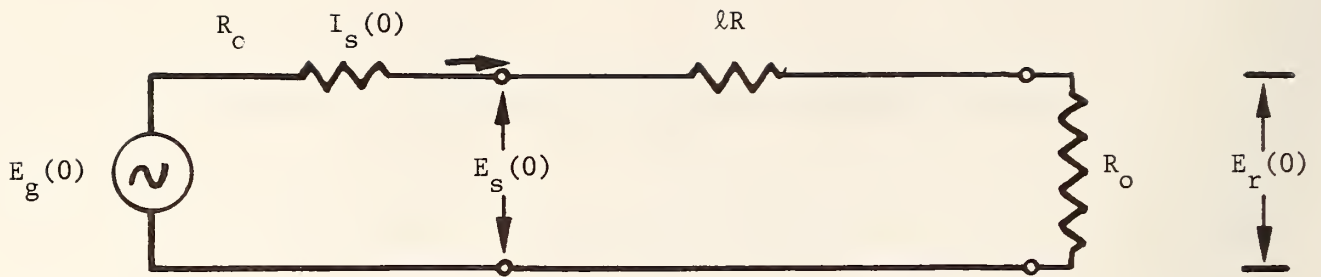


Figure 2.5 The transmission line circuit when $s = 0$ (dc)

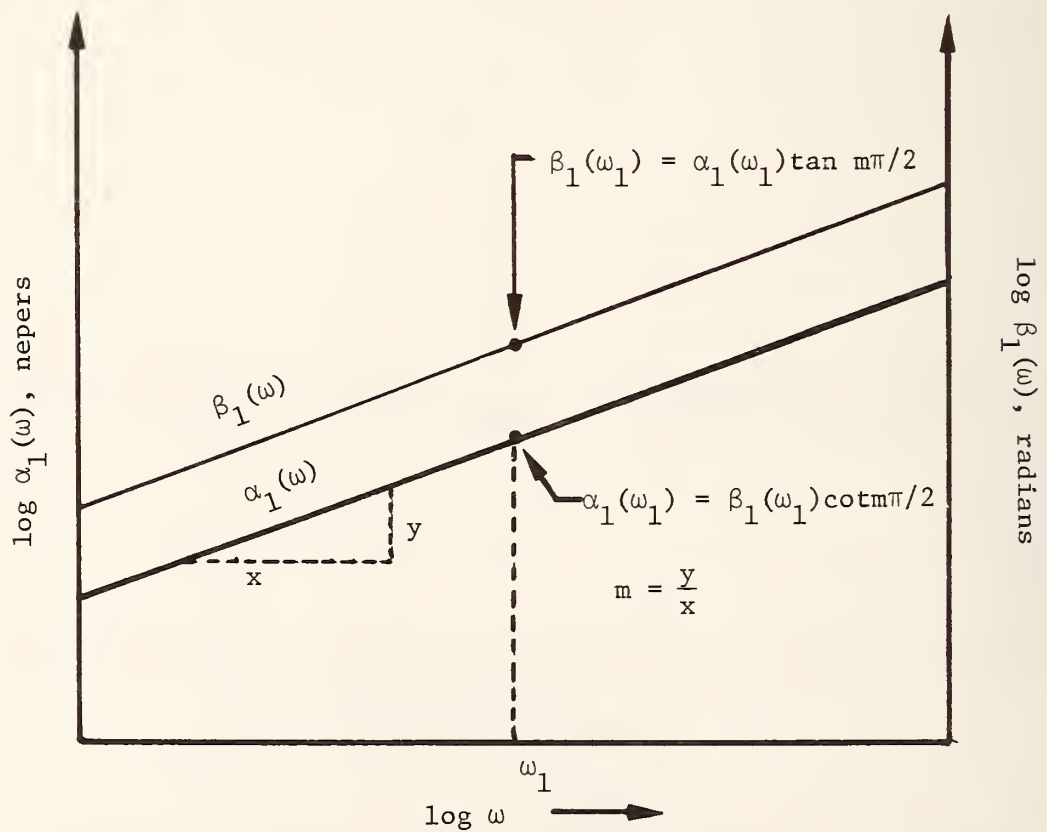


Figure 2.6 Log-log graph of the minimum phase attenuation $\alpha_1(\omega)$ and phase $\beta_1(\omega)$. The slope y/x as measured with a linear scale is equal to m .

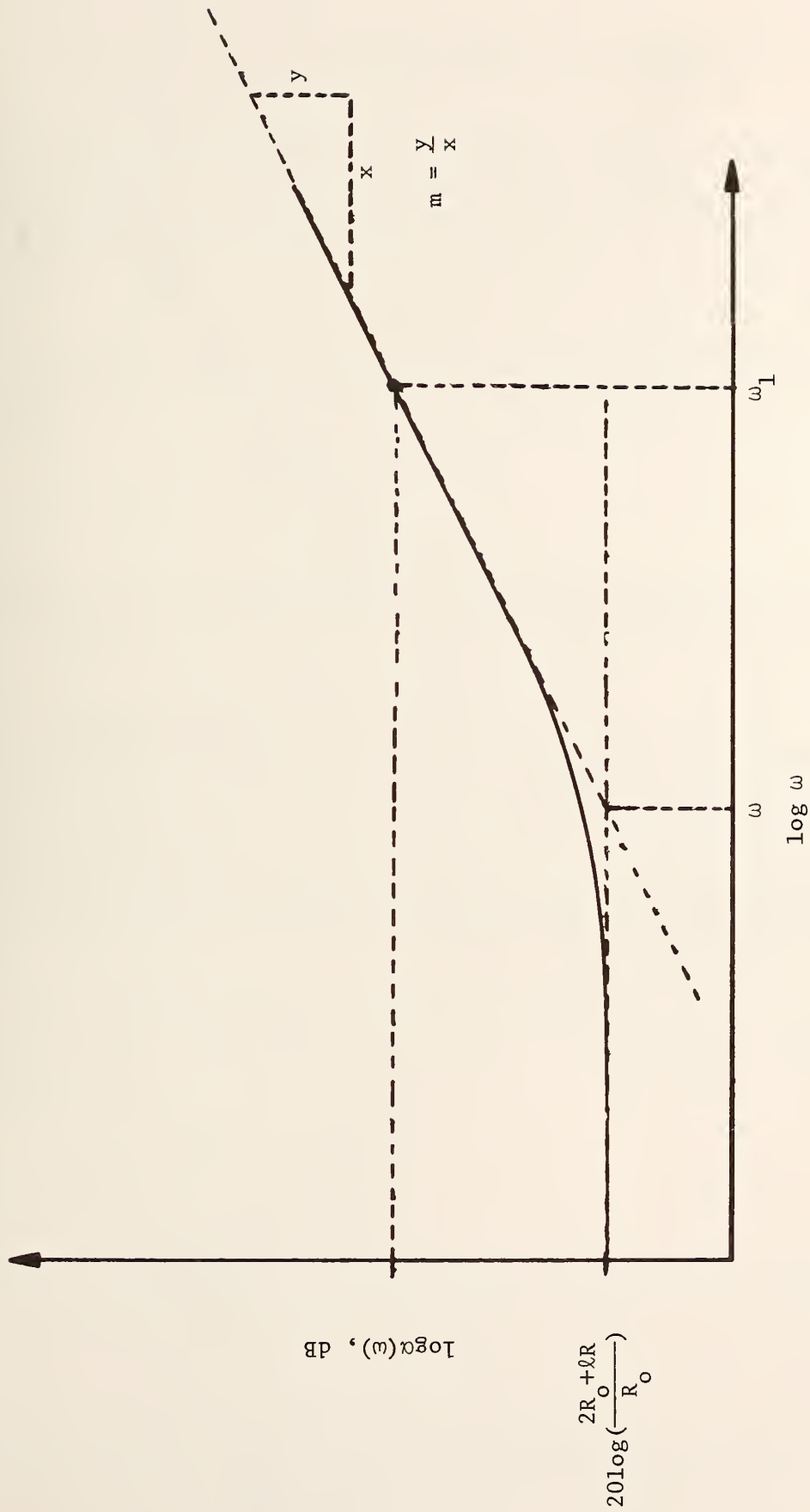


Figure 2.7 The asymptotes for the log-log attenuation vs. (angular) frequency. Vertical and horizontal scales have identical decade spacing.

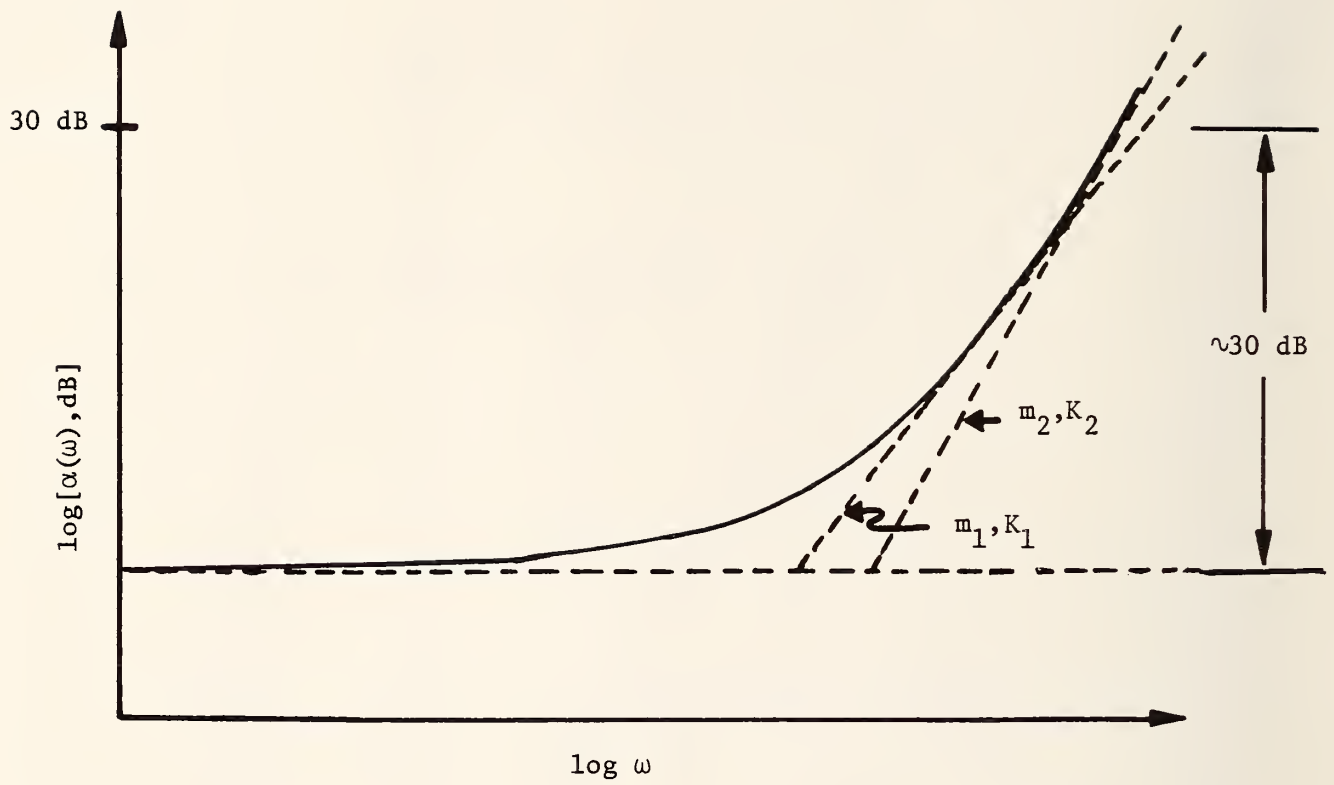


Figure 2.8 Two constant slope curves tangent to a log-log attenuation vs. (angular) frequency curve.

3. MEASUREMENT METHODS FOR THE DETERMINATION OF THE TRANSMISSION LINE PARAMETERS

In this chapter the measurement methods required to determine the transmission line model parameters are presented. A brief discussion is presented on the need for measurements and some relations between the basic parameters. Then specific measurement methods are described for the determination of R, C, R_o , m and K. L is determined from C and R_o .

3.1 The Need for Measurements

A commercially available or military cable may be characterized in terms of a set of nominal frequency domain transmission line parameters. Typically, they are

R - resistance/unit length

C - capacitance/unit length

R_o - high frequency or nominal characteristic impedance (also called the geometric characteristic impedance).

$\alpha_1(f)$ - attenuation frequency, f.

These parameters are representative of the particular cable type and have been derived from measurements on many different runs of cable. The values can be significantly different from those of a single cable sample and also can vary from manufacturer to manufacturer. Consequently, for precise estimates of the frequency domain performance of a given length of cable, the parameter values should be experimentally determined, i.e., measured. For system design applications the nominal parameter values are used with the hope that they are representative design center values. The main point being stressed here is that the manufacturer's technical specifications are always representative values; individual samples may vary.

For time domain applications, knowledge of the parameters R, C, R_o and $\alpha_1(f)$ are also required along with the phase shift, $\beta_1(f)$, which is uniquely related to $\alpha_1(f)$. $\beta_1(f)$ is the minimum phase shift component of the total cable phase shift, $\beta(f)$, (2-62) written explicitly in terms of frequency, f, i.e., $f = \omega/2\pi$.

$$\beta(f) = \beta_o(f) + \beta_1(f) \tag{3-1}$$

$$= 2\pi f T l + \beta_1(f) \tag{3-2}$$

where $\beta_o(f)$ is the phase shift due to the inherent transmission delay/unit length, T.

The delay/unit length is related to the velocity of propagation, v, and therefor, related to the inductance/unit length, L, and the capacitance/unit length, C.

$$v = \frac{1}{T} = \frac{1}{\sqrt{LC}}, \text{ unit length/sec.} \tag{3-3}$$

Also, the nominal or high frequency characteristic impedance, R_o , is dependent upon L and C,

$$R_o = \sqrt{\frac{L}{C}}, \text{ ohms.} \tag{3-4}$$

Consequently, if C is specified, then a knowledge of v or R_0 determines L . Alternately, v and R_0 may be specified which in turn determine L and C ,

$$L = \frac{R_0}{v} \quad (3-5)$$

and

$$C = \frac{1}{vR_0} . \quad (3-6)$$

The relations (3-3) through (3-6) are useful in both the time domain and frequency domain modeling; furthermore, some manufacturers specify v and R_0 rather than C and R_0 .

3.2 Measurement of the per Unit Length Resistance and Capacitance, R and C

Normally, R and C are specified by the manufacturer. If for some reason they must be determined experimentally, bridge measurements may be used. R is determined by measuring the loop resistance, ℓR using a D.C. resistance bridge, figs. 3.1 and 3.2. Similarly, C is determined using a 1 kHz capacitance bridge. With a bridge having one terminal grounded, the measurement is straight-forward for a coaxial conductor unbalanced cable, fig. 3.3. However, for a shielded paired-conductor cable, in general, three capacitance measurements have to be made to determine the total cable capacitance, ℓC_{AB} ,

$$\ell C_{AB} = \ell \left[C_1 + \frac{C_2 C_3}{C_2 + C_3} \right] . \quad (3-7)$$

The terminal designations are defined in fig. 3.4 while the equivalent circuit capacitances are defined in fig. 3.5. The measurement technique follows the procedure in [4] and consists of the following capacitance measurements: (1) C' , A to ground with B grounded, (2) C'' , A to ground with A and B shorted together, (3) C''' , B to ground with A grounded. The values of ℓC_1 , ℓC_2 , ℓC_3 are then given by

$$\ell C_1 = \frac{C' - C'' + C'''}{2} \quad (3-8)$$

$$\ell C_2 = \frac{C' + C'' - C'''}{2} \quad (3-9)$$

$$\ell C_3 = \frac{-C' + C'' + C'''}{2} . \quad (3-10)$$

3.3 Measurement of the Nominal Characteristic Impedance, R_0

The nominal characteristic impedance R_0 is actually the limit of the high frequency impedance (2-33, 2-37) and is conceptually viewed as the characteristic impedance which depends solely upon the inductance and capacitance per unit length. Furthermore, R_0 is resistive, i.e., independent of s .

For large values $|s|$, the characteristic impedance is

$$Z_o(s) = \sqrt{\frac{L}{C}} [1 + \delta(s)] \quad , \quad |\delta(s)| \ll 1 \quad (2-33)$$

HF

or

$$= R_o [1 + \delta(s)] \quad (3-11)$$

Now consider for the moment, that a step of current I_g/s is applied to the impedance (3-11). The voltage across $Z_o(s)$ at $t = 0^+$ would jump up to $I_g R_o$ volts and then commence to vary with time as dictated by the inverse Laplace transform of $I_g R_o \delta(s)/s$, fig. 3.6. By applying a step of voltage from a resistive source R_g to the input of a long length of cable, it is possible to calculate the value of R_o from the initial response of the sending end voltage $e_s(t)$, fig. 3.7.

First of all, when a signal is abruptly applied to a transmission line, the transmission line appears as an impedance equal to the characteristic impedance $Z_o(s)$. This is why the term surge impedance is also used in place of characteristic impedance. The impedance continues to appear as $Z_o(s)$ until reflections from the receiving end arrive back at the sending end. If the line is terminated in $Z_o(s)$ then there will be no reflections, and the line will continue to appear as an impedance equal to $Z_o(s)$. More will be said about such phenomena in the chapter on time domain reflectometry (Chapter 7).

Furthermore, for the initial response, only the high frequency components of $Z_o(s)$ contribute to the response. Consequently, for some time interval, say t_1 , the high frequency approximation to $Z_o(s)$ (3-11) would be valid for predicting the initial response of the transmission line, as shown by the solid-line portion of $e_s(t)$ between 0 and t_1 in fig. 3.7. Also, in fig. 3.7 t_2 denotes qualitatively the time required for reflections to return to the sending end from the open circuited receiving end. The value of t_2 is set by l and must be large enough so that reflections do not interfere with the observation of the abrupt rise in the neighborhood of $t=0^+$.

Consequently, the initial response of the cable to a voltage step of magnitude E_g is given by

$$E_s(s) = \frac{E_g}{s} \frac{Z_o(s)}{R_g + Z_o(s)} \quad \text{HF} \quad (3-12)$$

$$= \frac{E_g}{s} \frac{R_o + R_o \delta(s)}{R_g + R_o + R_o \delta(s)} \quad (3-13)$$

or approximated by

$$E_s(s) \approx \frac{E_g}{s} \frac{R_o}{R_g + R_o} [1 + \delta(s)] \quad (3-14)$$

because $R_o \gg R_o |\delta(s)|$ and $R_o + R_g$ is larger than R_o . In the time domain, the initial response of $e_s(t)$ consists of an abrupt jump E ,

$$E = \frac{E_g R_o}{R_g + R_o} \quad (3-15)$$

and then a slower upward trailing, fig. 3.7. From (3-15) R_o is obtained as

$$R_o = \frac{E}{E_g - E} R_g \quad (3-16)$$

If R_g happens to equal R_o , then E would equal $E_g/2$. An example of an initial response expressible mathematically in closed form is given for $m = 0.5$ in [5].

The measurement of R_o can be implemented by the methods shown in figs. 3.8 and 3.9 for the coaxial-conductor cable and the shielded paired-conductor cable, respectively. For the coaxial-conductor cable measurement, the effective generator impedance is 50Ω .

For the paired-conductor case the generator impedance is 100Ω and the sampling oscilloscope display is set for channel A minus channel B which yields a display voltage

$$e_d(t) = e_A(t) - e_B(t) = e_s(t) \quad (3-17)$$

Also, remember that the ground connection must be connected to the signal-ground, i.e., the zero potential for the balanced-transmission line (refer to fig. 3.5). For both cases, the cable length l should be long enough so that reflections do not occur in the region of the initial response, fig. 3.7.

Closely related to the measurement of R_o is the use of time domain reflectometry (TDR) to evaluate or test cables. The reader is referred to Chapter 7 of this report and in particular, Section 7.3 on a practical measurement method for observing the sending-end voltage.

3.4 Insertion Measurements for the Determination of the High Frequency Loss Parameter and the Exponent m

The loss parameter K and the exponent m are determined by model-fitting to data obtained from a time domain (pulse) insertion measurement, the basic method being shown in fig. 3.10. $e_{d1}(t)$ and $e_{d2}(t)$ are the observable quantities displayed on an oscilloscope before and after the insertion of the cable of length l between a generator and matched load. The generator and load impedances are both equal to the nominal transmission line characteristic impedance. Denoting the inverse Laplace transform as $\mathcal{L}^{-1}\{\}$, $e_{d1}(t)$ and $e_{d2}(t)$ are given by

$$e_{d1}(t) = \mathcal{L}^{-1} \left\{ T(s) \frac{E_g(s)}{2} \right\} \quad (3-18)$$

$$e_{d2}(t) = \mathcal{L}^{-1} \left\{ T(s) 2E_g(s) \left[\frac{Z_o(s)}{R_o + Z_o(s)} \right] \left[\frac{R_o}{R_o + Z_o(s)} \right] \left[\frac{e^{-l\gamma(s)}}{1 - [\rho(s)]^2 e^{-2l\gamma(s)}} \right] \right\} \quad (3-19)$$

where $T(s)$ is the oscilloscope transfer function (input to display), and $\tau(t)$ its inverse transform or impulse response. Also,

$$\rho(s) = \frac{R_o - Z_o(s)}{R_o + Z_o(s)} \quad (3-20)$$

Aside from the factor $T(s)$ (3-19) is taken from (2-39), while (3-20) is from (2-41). The ratio, $E_{d2}(s)/E_{d1}(s)$, is equal to $E_2(s)/E_1(s)$,

$$\frac{E_2(s)}{E_1(s)} = 4 \left[\frac{Z_o(s)}{R_o + Z_o(s)} \right] \left[\frac{R_o}{R_o + Z_o(s)} \right] \left[\frac{e^{-\ell\gamma(s)}}{1 - [\rho(s)]^2 e^{-2\ell\gamma(s)}} \right] \quad (3-21)$$

because $T(s)$ cancels out along with the pulse dependence, $E_g(s)$. The ratio $E_2(s)/E_1(s)$ is equal to the scattering network parameter $S_{21}(s)$.

Briefly, the transmission line can be represented by the scattering parameters $S_{11}(s)$, $S_{22}(s)$, and $S_{12}(s) = S_{21}(s)$. Figure 3.11 shows a transmission line inserted into another uniform transmission system of characteristic impedance $Z_o(s)$. In general, the incident and reflected voltages on the $Z_o(s)$ transmission line system are

$$V_{r1}(s) = V_{i1}(s) S_{11}(s) + V_{i2}(s) S_{12}(s) \quad (3-22)$$

and

$$V_{r2}(s) = V_{i1}(s) S_{21}(s) + V_{i2}(s) S_{22}(s) \quad (3-23)$$

The terminal voltages of the inserted transmission line are

$$V_1(s) = V_{i1}(s) + V_{r1}(s) \quad (3-24)$$

and

$$V_2(s) = V_{i2}(s) + V_{r2}(s) \quad (3-25)$$

When the uniform transmission line is terminated in $Z_o(s)$, fig. 3.12, $V_{i2}(s)$ is zero, and the voltages become

$$V_{r1}(s) = V_{i1}(s) S_{11}(s) \quad (3-26)$$

$$V_{r2}(s) = V_{i1}(s) S_{21}(s) \quad (3-27)$$

$$V_1(s) = V_{i1}(s) + V_{r1}(s) \quad (3-28)$$

$$V_2(s) = V_{r2}(s) \quad (3-29)$$

The voltage $V_2(s)$ corresponds to $E_2(s)$ in (3-21). If the inserted transmission line in fig. 3.12 is removed from the circuit and terminals 1 and 2 connected together, then $V_{r1}(s)$ is zero, and

$$V_1(s) = V_{i1}(s) \quad (3-30)$$

which corresponds to $E_1(s)$ in (3-21). Then from (3-27), (3-29), and (3-30), there results

$$\frac{E_2(s)}{E_1(s)} = S_{21}(s) \quad (3-31)$$

Returning now to consideration of (3-21), in terms of the model for high frequencies $\gamma(s)$ and $Z_o(s)$ become

$$\left. \gamma(s) \right]_{\text{HF}} = s T [1 + \delta(s)] \quad |\delta(s)| \ll 1 \quad (2-32)$$

and

$$\left. Z_o(s) \right]_{\text{HF}} = R_o [1 + \delta(s)] \quad |\delta(s)| \ll 1 \quad (2-33)$$

which reduces (3-21) to

$$\left. \frac{E_2(s)}{E_1(s)} \right]_{\text{HF}} = e^{-sT\ell} - T\ell\delta(s) \quad (3-32)$$

or in terms of the Fourier transform

$$\left. \frac{E_2(j\omega)}{E_1(j\omega)} \right]_{\text{HF}} = e^{-j\omega T\ell} - T\ell\delta(j\omega). \quad (3-33)$$

Thus, the model attenuation at high frequencies

$$\left. \alpha_1(\omega) \right]_{\text{dB}} = 20 \log \left[\left. \frac{E_1(j\omega)}{E_2(j\omega)} \right]_{\text{HF}} \right] = 8.68 \frac{\rho K}{2R_o} |\omega|^m \cos m\pi/2, \quad (3-34)$$

can be compared with the Fourier transform attenuation data computed from the experimentally observed waveforms, $e_1(t)$ and $e_2(t)$, in order to determine K and m . As discussed in section 2.3 and illustrated in figs. 2.6 - 2.8, this is accomplished in a tractable way using a log-log graph, $\log \alpha_1(\omega)$ vs. $\log \omega$.

In practice, the insertion measurements are carried out using a 50 ohm sampling oscilloscope system which has two channels. Because R_o may not be equal to 50 ohms or 100 ohms (for coaxial-conductor or paired-conductor cable, respectively) resistive impedance matching networks may be required, figs. 3.13 and 3.14. The matching networks are in an "L" configuration, each different value of R_o requiring its own matching network. The networks used in this study are summarized in fig. 3.15.

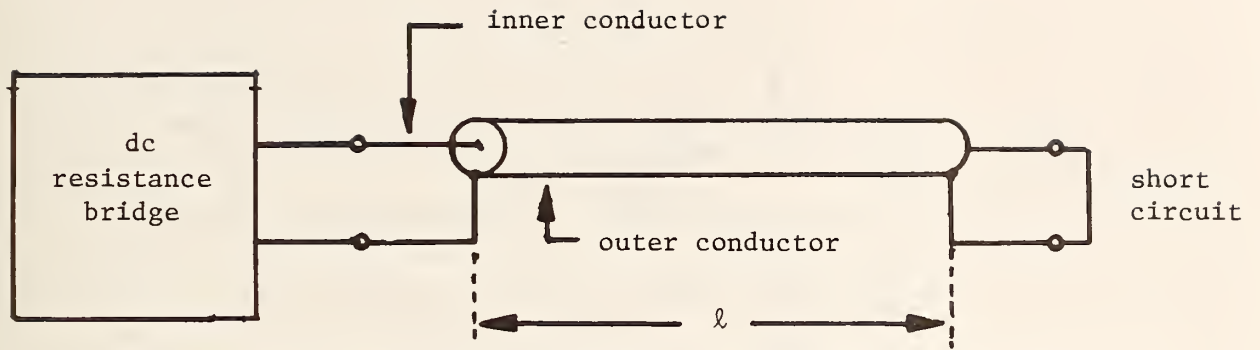


Figure 3.1 Measurement of the total coaxial-conductor cable resistance, ℓR .

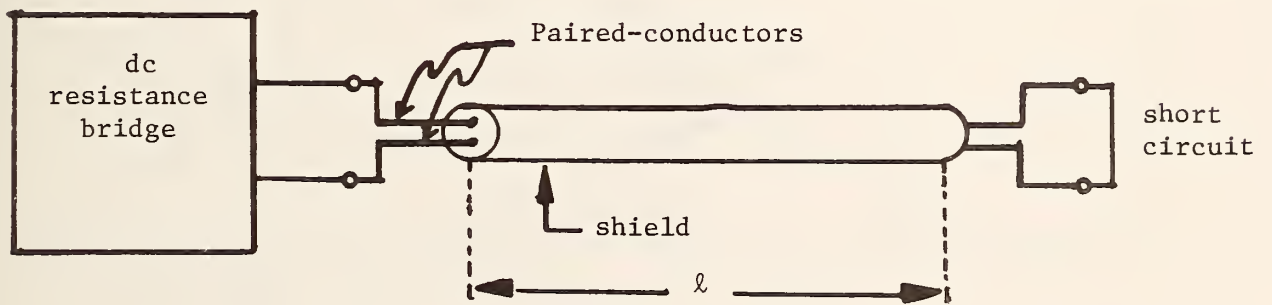


Figure 3.2 Measurement of the total shielded paired-conductor cable resistance, ℓR .

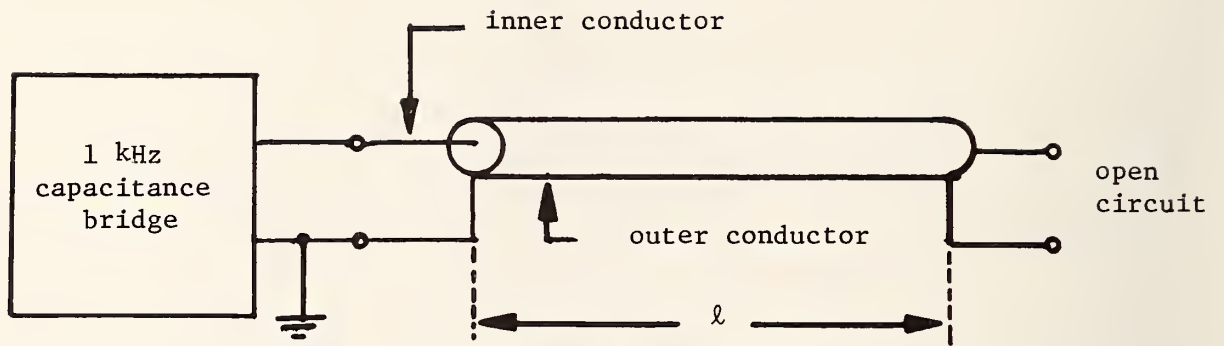


Figure 3.3 Measurement of the total coaxial-conductor cable capacitance, lC .

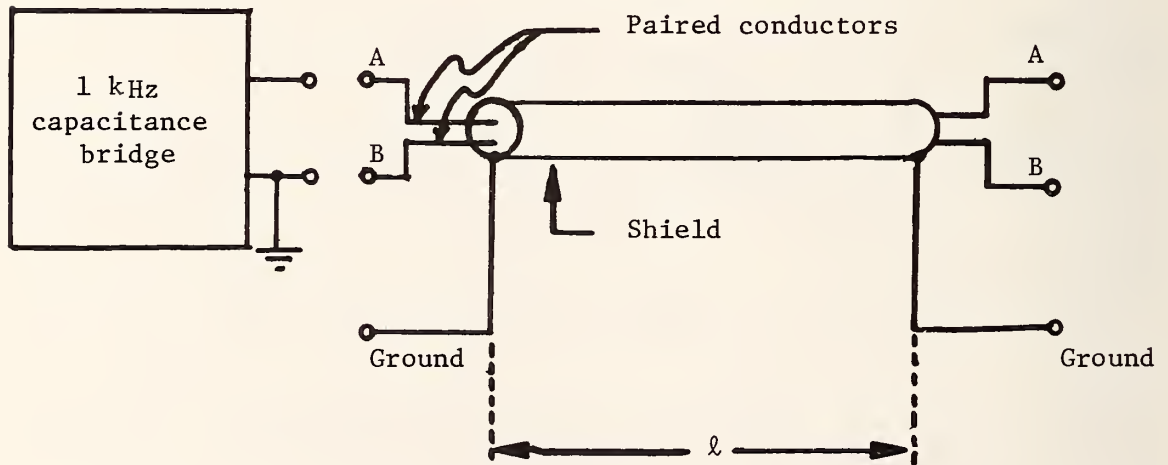
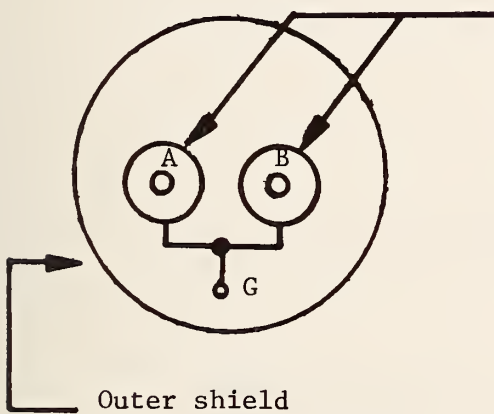
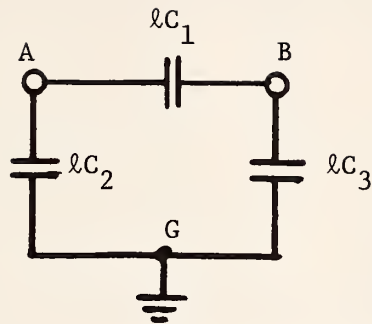
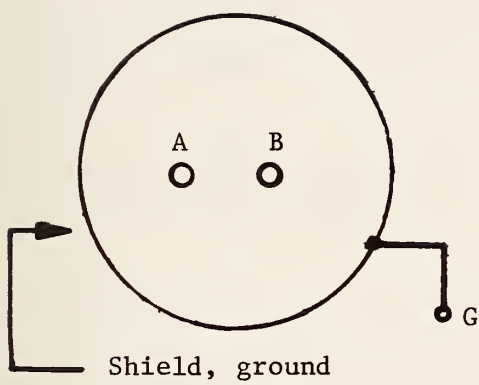


Figure 3.4 Terminal designations for measuring the total shielded paired-conductor cable capacitance, lC .



Individual coaxial shields on each paired-conductor; ground terminal is the zero potential for the balanced transmission line

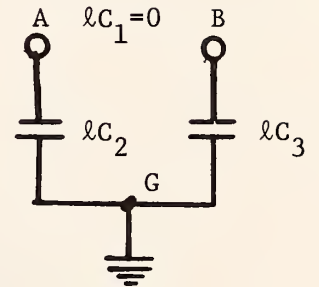


Figure 3.5 Shielded paired-conductor configurations and their equivalent capacitance circuits.

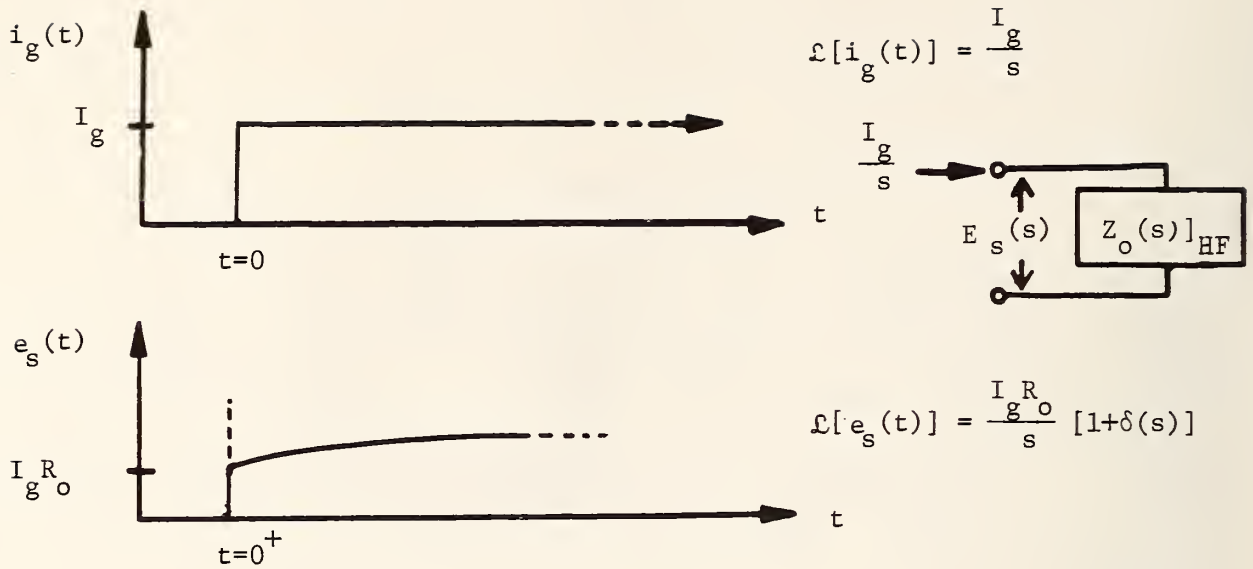


Figure 3.6 The response of $Z_o(s)_{HF}$ to a current step of magnitude I_g .

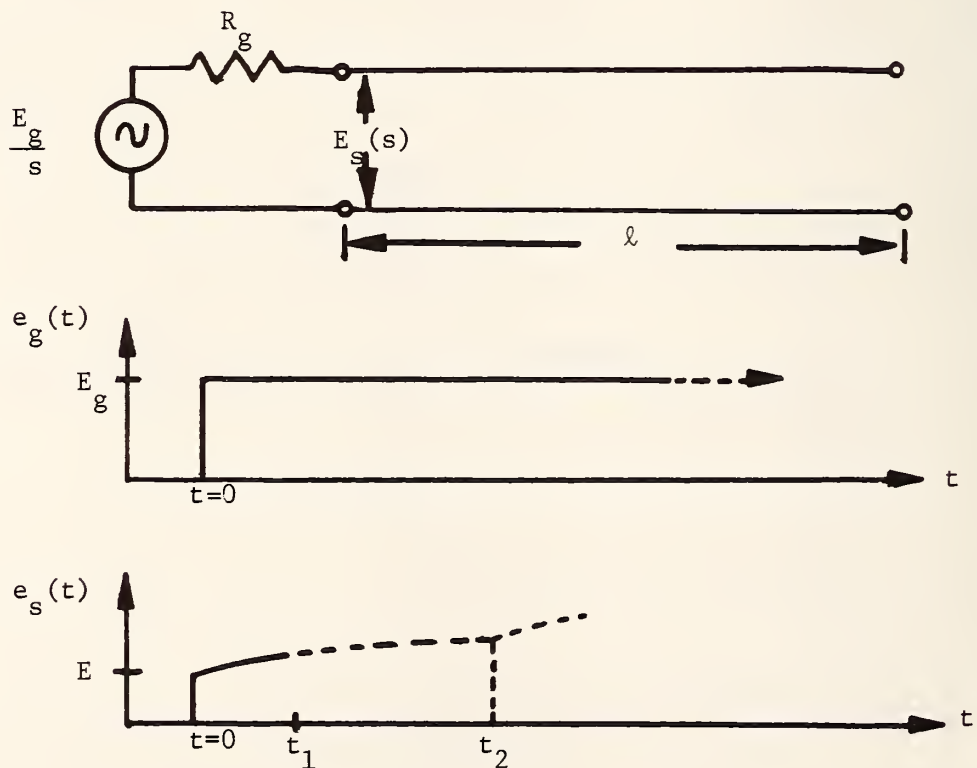


Figure 3.7 The initial response (solid line) of the sending end voltage $e_s(t)$ due to a voltage step from a generator having a resistive source impedance.

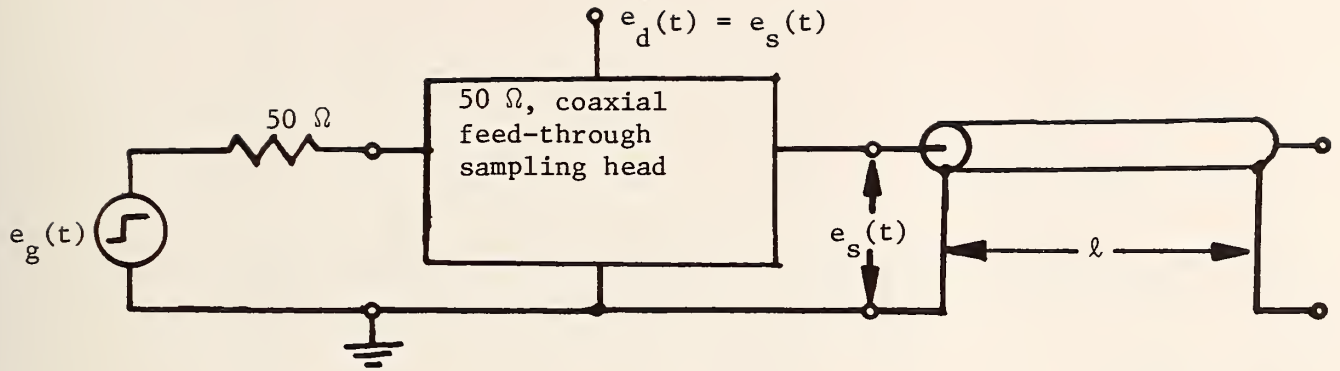


Figure 3.8 R_o measurement set-up for a coaxial-conductor cable (unbalanced lines, generally).

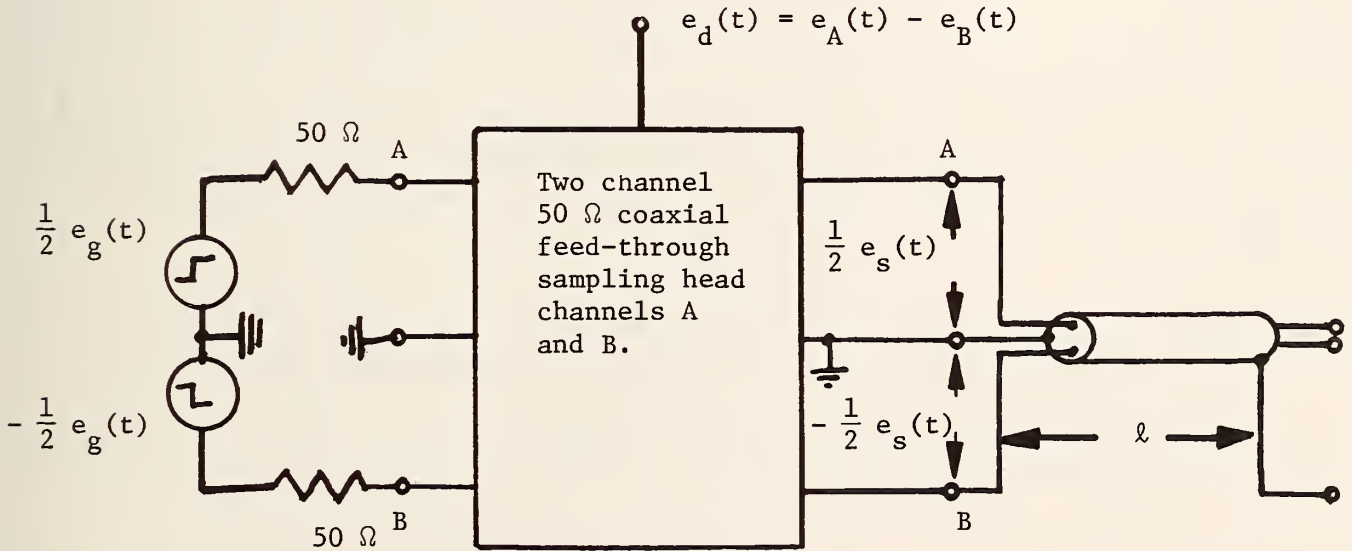


Figure 3.9 R_o measurement set-up for a shielded paired-conductor cable (balanced lines, generally).

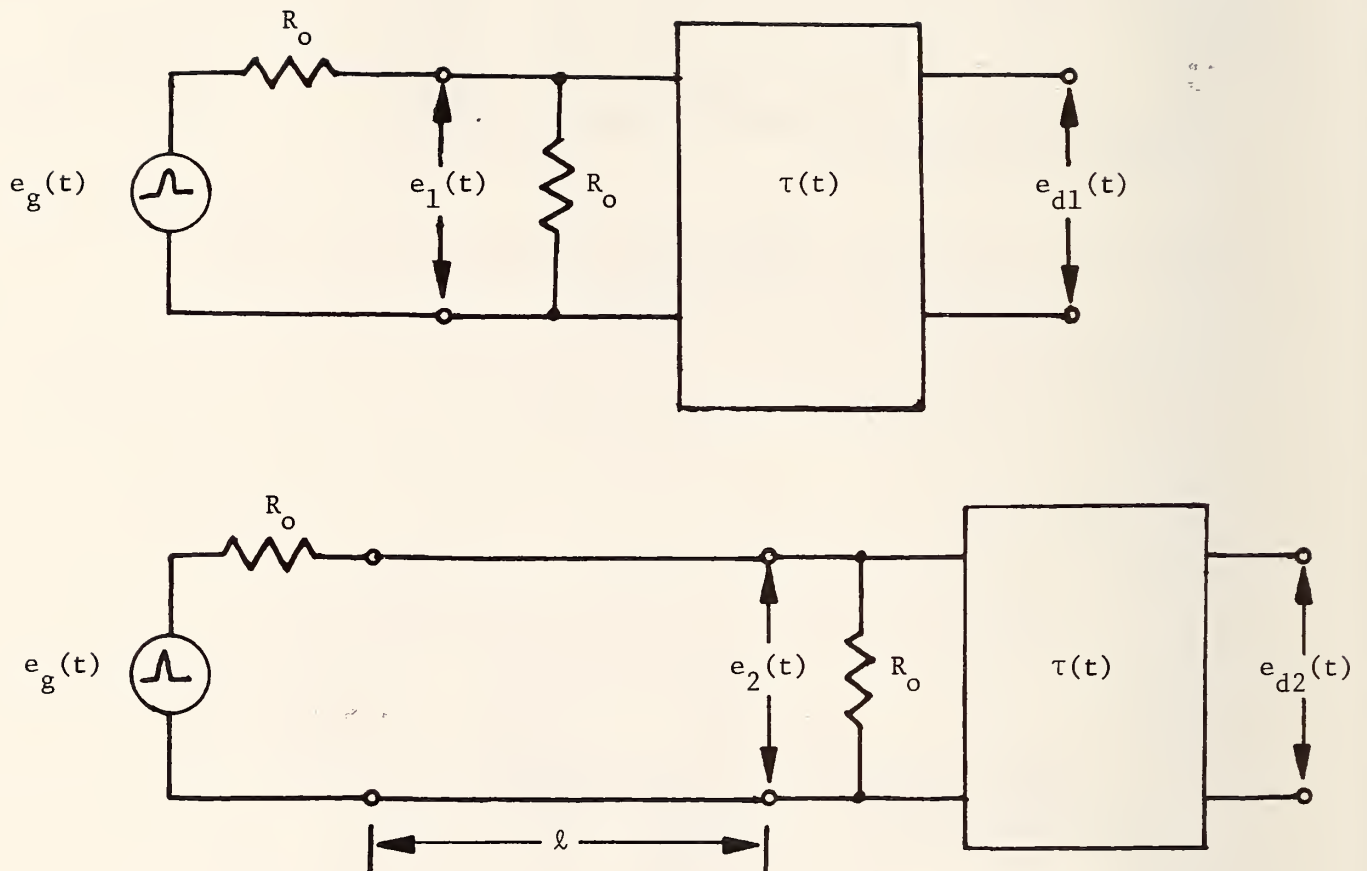


Figure 3.10 The time domain insertion method; $e_{d1}(t)$ and $e_{d2}(t)$ are the observables corresponding to $e_1(t)$ and $e_2(t)$, respectively, before and after the insertion of the cable of length ℓ . $\tau(t)$ is the impulse response of the oscilloscope.

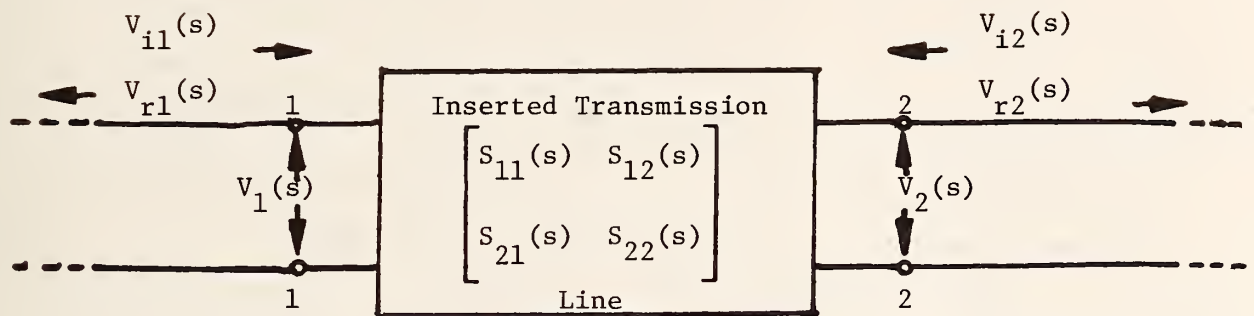


Figure 3.11 The scattering parameter representation of a transmission line inserted into a uniform transmission line system of characteristic impedance $Z_0(s)$.

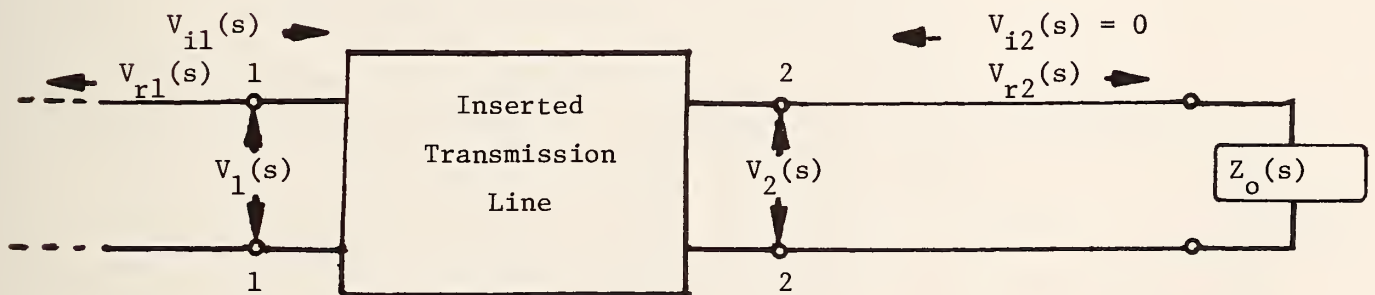


Figure 3.12 Uniform transmission line system terminated in its characteristic impedance $Z_0(s)$.

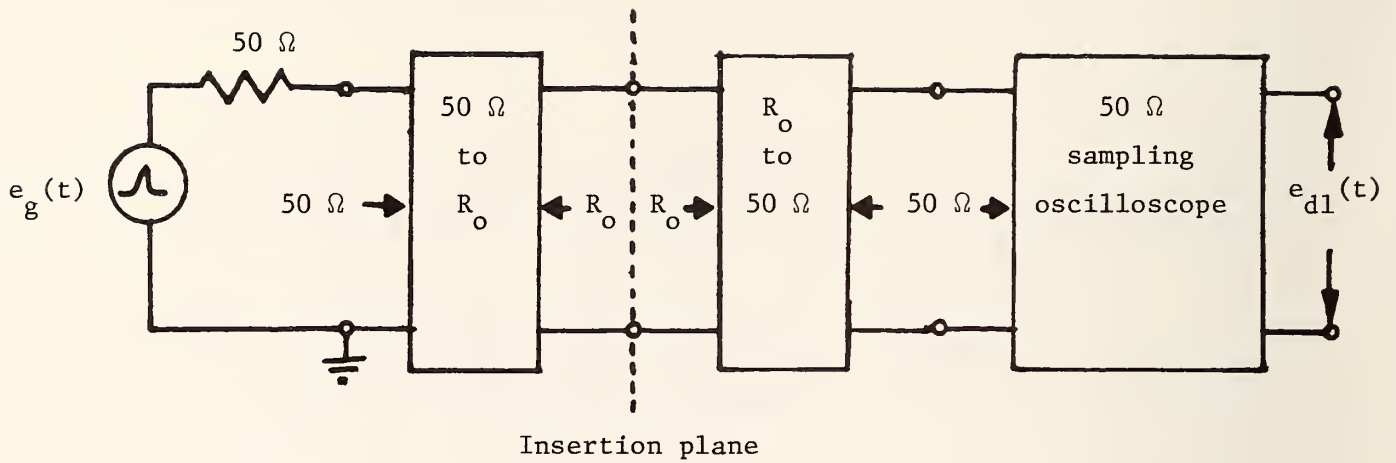


Figure 3.13 Practical implementation of the time domain insertion method for a coaxial-conductor cable.

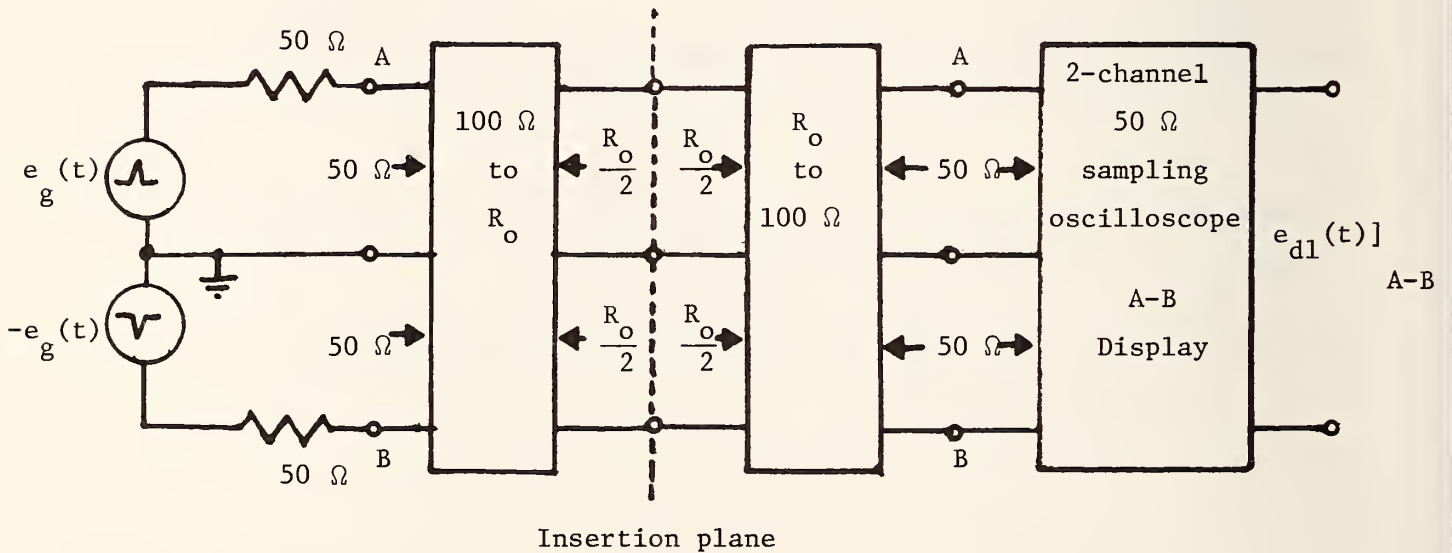
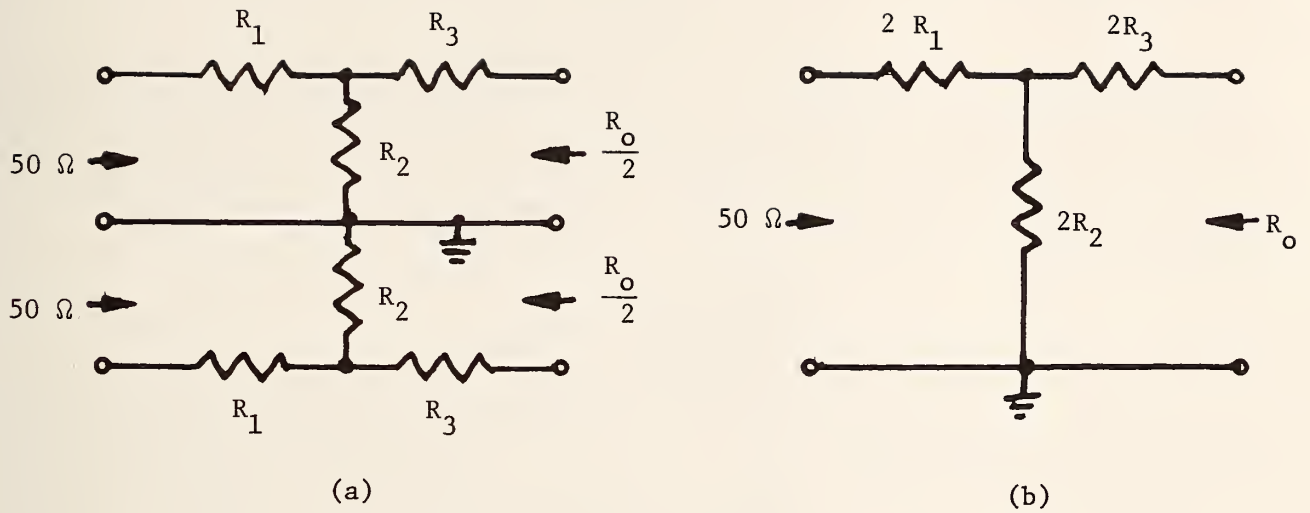


Figure 3.14 Practical implementation of the time domain insertion method for a shielded-paired-conductor cable.



R_o	R_1	R_2	R_3
75	25	75	0
78	23.45	83.1	0
95	11.18	212.25	0
98	7.07	692.00	0
124	0	113.6	27.27

Figure 3.15 The resistive impedance matching networks, 50 ohms to R_o .
 (a) Shielded paired-conductor cables,
 (b) Coaxial-conductor cables.

4. AN OVERVIEW OF THE COMPUTER CALCULATION FOR THE TRANSMISSION
LINE IMPULSE AND STEP RESPONSES

In this chapter a qualitative overview is presented which describes the computer calculations for the extraction of model parameters from measured data and the simulation of the impulse and step responses. The calculations are accomplished by the NBS Automatic Pulse Measurement System (APMS) [6,7].

4.1 Data Acquisition Method

The data is generated by repetitive pulse excitation and is displayed by a sampling oscilloscope interfaced to and controlled by a minicomputer system, i.e., the NBS Automatic Pulse Measurement System (APMS). For a given display waveform, say $e_{d2}(t)$, the data is acquired by making 500 observations at a fixed time position t_1 of 500 repetitions of the signal; the mean value [8,9] of the observations $\overline{e_{d2}(t_1)}$ is calculated by the computer,

$$\overline{e_{d2}(t_1)} = \frac{\sum_r^{500} [e_{d2}(t_1)]_r}{500} \quad (4-1)$$

The time window, T_w , is represented by 1024 uniformly spaced points; consequently, a set of 1024 mean values represent the waveform, fig. 4.1,

$$\hat{e}_{d2}(nT) = \sum_{n=0}^{1023} \left\{ \delta(t-nT) \overline{e_{d2}(nT)} \right\} \quad (4-2)$$

where $\delta(t)$ is the unit delta or impulse function multiplied by the strength $\overline{e_{d2}(nT)}$ and where

$$T = T_w/1024. \quad (4-3)$$

Refer to figs. 4.5 and 4.6 for a graphical explanation of the delta function train (4.2). The waveforms $e_{d1}(t)$ and $e_{d2}(t)$ of the time domain insertion method, fig. 3.10, are both acquired by the procedure just described and will be denoted by $\hat{e}_{d1}(nT)$ and $\hat{e}_{d2}(nT)$, corresponding to the form of (4.2).

4.2 Fourier Transformation of $\hat{e}_{d1}(nT)$ and $\hat{e}_{d2}(nT)$

The discrete acquired waveforms $\hat{e}_{d1}(nT)$ and $\hat{e}_{d2}(nT)$ are each transformed to the frequency domain using the Fast Fourier Transform (FFT) algorithm for the discrete Fourier transformation [10]. To do so, for each waveform a 2048 point time window is used which includes 1024 points of zero value, fig. 4.2. The extension of the waveform to 2048 points increases the frequency resolution by decreasing the spacing between the discrete frequencies to one half of that available from the unaugmented waveform, fig. 4.3 and 4.4. The frequency domain spacing Δf is equal to $1/T_w$ and the frequency window, F_w remains unchanged when both N and T_w are doubled, but the number of points in F_w are doubled.

The result of the FFT operation yields the discrete functions $\hat{E}_{d1}(\frac{k}{2NT})$ and $\hat{E}_{d2}(\frac{k}{2NT})$ which represent complex values at the discrete frequencies $k/2NT$, e.g., the discrete waveform, $\hat{e}_{d2}(nT)$, of fig. 4.2 transforms to

$$\hat{E}_{d2}(\frac{k}{2NT}) = \sum_{n=0}^{2N-1} \hat{e}_{d2}(nT) e^{-j2\pi nk/2N} \quad ; \quad k = 0, 1, \dots, 2N-1 \quad (4-4)$$

where N equals 1024; consequently, $\hat{E}_{d2}(k/2NT)$ consists of 2048 complex values, one value for each of the 2048 discrete frequencies, $k/2NT$. Furthermore, $\hat{E}_{d2}(k/2NT)$ is a symmetrical periodic function and as such contains only 1024 distinct values.

4.3 The Calculation of $\hat{S}_{21}(k/2NT)$ and $\hat{\alpha}_1(k/2NT)$

The discrete insertion ratio $\hat{S}_{21}(k/2NT)$ is computed in the same manner as its continuous counterpart,

$$S_{21}(j\omega) = \frac{E_{d2}(j\omega)}{E_{d1}(j\omega)}, \quad (3-31)$$

hence

$$\hat{S}_{21}(k/2NT) = \frac{\hat{E}_{d2}(k/2NT)}{\hat{E}_{d1}(k/2NT)} \quad (4-5)$$

$$= |\hat{S}_{21}(k/2NT)| \angle \hat{\beta}_1(k/2NT) \quad (4-6)$$

where $k=0,1,\dots,2N-1$, and $|\hat{S}_{21}|$ and $\hat{\beta}_1$ are the magnitude and phase of the discrete function \hat{S}_{21} at the discrete frequencies $k/2NT$, respectively.

However, an averaging process is used in arriving at $\hat{S}_{21}(k/2NT)$. The process is repeated using six different acquisitions for $\hat{E}_{d2}(k/2NT)$ and a single acquisition for $\hat{E}_{d1}(k/2NT)$. Then, the resultant $\hat{S}_{21}(k/2NT)$ data sets are expressed in terms of the discrete attenuation $\hat{\alpha}_1(k/2NT)$ and phase $\hat{\beta}_1(k/2NT)$,

$$\text{Attenuation, } \hat{\alpha}_1(k/2NT) \equiv 20 \log |\hat{S}_{21}(k/2NT)|^{-1}, \text{ dB}$$

$$\text{Phase, } \hat{\beta}_1(k/2NT) = -\tan^{-1} \left\{ \frac{\text{Imag. Pt. } \hat{S}_{21}(k/2NT)}{\text{Real Pt. } \hat{S}_{21}(k/2NT)} \right\}, \text{ degrees.}$$

and the mean values are determined by

$$\overline{\hat{\alpha}_1(k/2NT)} = \frac{\sum_r^6 20 \log |\hat{S}_{21}(k/2NT)|_r^{-1}}{6}, \text{ dB} \quad (4-7)$$

$$\overline{\hat{\beta}_1(k/2NT)} = \frac{\sum_r^6 [\hat{\beta}_1(k/2NT)]_r}{6}, \text{ degrees} \quad (4-8)$$

where

$$[\hat{S}_{21}(k/2NT)]_r^{-1} = \frac{[\hat{E}_{d1}(k/2NT)]}{[\hat{E}_{d2}(k/2NT)]_r} \quad (4-9)$$

$$= |\hat{S}_{21}(k/2NT)|_r^{-1} \angle -[\hat{\beta}_1(k/2NT)]_r. \quad (4-10)$$

and $[\hat{E}_{d2}(k/2NT)]_r$ corresponds to the r-th acquisition from $e_{d2}(t)$, i.e., $[\hat{e}_{d2}(nT)]_r$.

The discrete values $\hat{\alpha}_1(k/2NT)$ and $\hat{\beta}_1(k/2NT)$, (4-7) and (4-8), are computed for the first three hundred harmonics, because in most cases 300 harmonics cover a magnitude range of about 0 to -30 dB. The capability for any other number of harmonics is retained in the computer program. At each value of frequency, the standard deviation [8] for (4-7) and (4-8) are computed as a measure of the consistency of the data. In particular, the standard deviation of the attenuation, σ_s , is given by

$$\sigma_s(k/2NT) = \left[\frac{\sum_r^6 \left[\hat{\alpha}_1(k/2NT) - \hat{\alpha}_1(k/2NT)_r \right]^2}{5} \right]^{1/2}. \quad (4-11)$$

Past experience has shown that consistent data yields σ_s values in a typical range of 0.02 to 0.2 dB for an attenuation range of one to 30 dB.

4.4 The Extraction of the Model Parameters K and m

The parameters K and m are obtained by fitting the model at high frequencies to the (mean) attenuation data $[\hat{\alpha}_1(k/2NT)]$ as was pointed out in the discussion of (3-34) and figs. 2.6 - 2.8. The values of K and m of the equation

$$\alpha_1(\omega) = \left(\frac{8.68 \ell \cos m\pi/2}{2 R_o} \right) K |\omega|^m \quad (3-34)$$

can be determined from the straight-line parameters of the equation resulting from the log of (3-34),

$$\log \alpha_1(\omega) = \log \left(\frac{8.68 \ell \cos m\pi/2}{2 R_o} \right) + \log K + m \log |\omega|; \quad (4-12)$$

that is,

$$\log \hat{\alpha}_1(k/2NT) = \log \left(\frac{8.68 \ell \cos m\pi/2}{2 R_o} \right) + \log K + m \log |k/2NT|. \quad (4-13)$$

The parameters log K and m can be determined from the straight-line parameters of the logarithm of the mean attenuation (4-7), $\log [\hat{\alpha}_1(k/2NT)]$.

The slope m is determined by calculating the log-log graph slope from two values of the graph separated by 50 abscissa points, e.g., k=50, and k=100. The slope so determined is designated m_1 . Next K is calculated using m, in (4-13) from

$$\log \hat{\alpha}_1(k/2NT) = \log \left(\frac{8.68 \ell \cos m_1\pi/2}{2 R_o} \right) + \log K + m_1 \log |k/2NT| \quad (4-14)$$

by an iterative solution method; the result is designated K_1 .

The process for calculating m_1 and K_1 is repeated using the next two points k=51 and k=101; the results are designated m_2 and K_2 . The process is repeated 150 times ending with k=200 and k=250. The mean values of m_r and K_r are then determined as

$$\bar{m} = \sum_{r=1}^{150} m_r / 150 \quad (4-15)$$

and

$$\bar{K} = \sum_{r=1}^{150} K_r / 150 \quad (4-16)$$

The calculation process is started at $k=50$, rather than $k=0$ to avoid the small errors which appear at the beginning of the frequency window due to system errors, noise, etc.

Finally, the entire process is repeated three times; starting from $e_{d1}(t)$ and $e_{d2}(t)$ the complete operations of sections 4.1, 4.2, and 4.3 are repeated to yield three independent functions $[\hat{\alpha}_1(k/2NT)]_1$, $[\hat{\alpha}_1(k/2NT)]_2$, and $[\hat{\alpha}_1(k/2NT)]_3$ from which three sets of mean values for m and K are determined:

$$\left[\overline{\hat{\alpha}_1(k/2NT)} \right]_1 \longrightarrow [\bar{m}]_1, \quad [\bar{K}]_1$$

$$\left[\hat{\alpha}_1(k/2NT) \right]_2 \longrightarrow [\bar{m}]_2, \quad [\bar{K}]_2$$

$$\left[\hat{\alpha}_1(k/2NT) \right]_3 \longrightarrow [\bar{m}]_3, \quad [\bar{K}]_3$$

Then, the mean values for $[\bar{m}]$ and $[\bar{K}]$ are calculated, where

$$[\bar{m}] = \frac{[\bar{m}]_1 + [\bar{m}]_2 + [\bar{m}]_3}{3} \quad (4-17)$$

$$[\bar{K}] = \frac{[\bar{K}]_1 + [\bar{K}]_2 + [\bar{K}]_3}{3} \quad (4-18)$$

and the resultant values are the ones used for the model parameters m and K . The standard deviations, σ_m and σ_K are also calculated for control purposes to insure that the data are consistent. They are

$$\sigma_m = \left[\sum_{r=1}^3 \frac{\{ [\bar{m}] - [\bar{m}]_r \}^2}{2} \right]^{1/2} \quad (4-19)$$

and

$$\sigma_K = \left[\sum_{r=1}^3 \frac{\{ [\bar{K}] - [\bar{K}]_r \}^2}{2} \right]^{1/2} \quad (4-20)$$

4.5 Simulation of the Impulse Response

The impulse response of a cable of length ℓ doubly terminated in its nominal characteristic impedance R_o is obtained from (2-39) with $E_g(s) = 1$,

$$H(s) = 2 \left[\frac{Z_o(s)}{R_o + Z_o(s)} \right] \left[\frac{R_o}{R_o + Z_o(s)} \right] \left[\frac{e^{-\ell\gamma(s)}}{1 - [\rho(s)]^2 e^{-2\ell\gamma(s)}} \right] \quad (4-21)$$

where

$$Z_o = [(R + sL + Ks^m)/sC]^{1/2}$$

$$\gamma(s) = [(R + sL + Ks^m)sc]^{1/2}$$

$$\rho(s) = \frac{R_o - Z_o(s)}{R_o + Z_o(s)} \quad (2-41)$$

The received voltage (4-21) due to a unit impulse for $e_g(t)$, $E_g(s) = 1$, is equal to one half of $E_2(s)/E_1(s)$, (3-21); consequently, from (3-31) the impulse response is

$$H(s) = \frac{1}{2} S_{21}(s) \quad (4-22)$$

Using the model parameters (R , L , K , m , and C) which are now known, a discrete 1024 point representation of the insertion function $\frac{1}{2}S_{21}(s)$ is constructed. Next, the inverse discrete Fourier transformation of $\frac{1}{2}\hat{S}_{21}(k/NT)$ will yield the discrete time-domain impulse response,

$$\hat{h}(nT) = \frac{1}{N} \sum_{k=0}^{N-1} \frac{1}{2} \hat{S}_{21}(k/NT) e^{j2\pi nk/N}; \quad n = 0, 1, \dots, N-1. \quad (4-23)$$

A typical display for $\hat{h}(nT)$ would be similar to $\hat{e}_{d2}(nT)$, fig. 4.1.

4.6 Determination of the dc Level for the Impulse Response, $\hat{h}(nT)$

The dc level of the impulse response must be established before the step response can be calculated. Theoretically, the point $n = 0$ should yield $\hat{h}(0) = 0$; if such were the case, then by setting the level of $\hat{h}(nT)$ equal to zero at $n = 0$, the dc level would be properly located. However, due to the system errors in the region of $0 \leq n < 10$, the zero level can not be determined. Similar effects are encountered at the end of the time window near $n = 1024$.

Physically, the impulse response of the cable at the end of the time window is not equal to zero; it will be a small value, 10^{-4} , (typically 10^{-3} of the peak value of the impulse response). Consequently, to set the dc level, the voltage at a specified time, say n_1 , is calculated using the model and the identified model parameters. To do so, the Fourier components of the transfer function (impulse response) are summed for a specified time, typically, at 90% of the time window, $0.9 T_w$. At the present time on the APMS this summation of the Fourier series requires considerable computation time, e.g.,

several hours, because a large number of harmonics must be summed without recourse to array processing computation. Typically, for a 1 KHz separation of harmonics 5.12×10^3 harmonics are required for a one microsecond time window containing 1024 data points (harmonics from 1 kHz to 512 MHz). The typical convergence at $0.9 T_w$ is such that the voltage converges to about $10^{-3} V_{\max}$ with a peak oscillatory variation in the range of $10^{-4} V_{\max}$ to $10^{-5} V_{\max}$.

Once the voltage for n_1 has been computed, then the dc level of the impulse response waveform, $\hat{h}(nT)$, is shifted so that the value of $\hat{h}(n_1T)$ is equal to the computed voltage at n_1 .

4.7 Simulation of the Step Response

The impulse response (4-23) may be expressed in the form

$$\hat{h}(nT) = \sum_{n=0}^{1023} h(nT)\delta(t-nT) \quad (4-24)$$

where

$$T = T_w/1024 \quad (4-25)$$

and each term for the product $h(nT)\delta(t-nT)$ is given by a corresponding sum over k in (4-23).

The discrete step response is obtained by integrating (4-24) and then sampling the result to provide discrete data values. Integrating the impulse train (4-24) gives

$$f(t) = \int \hat{h}(nT) dt = T \sum_{m=0}^n h(mT)u(t-mT) \quad (4-26)$$

where $u(t)$ is the unit step function. (4-26) is a staircase waveform whose envelope is the integral of the impulse train. By sampling $f(t)$ at the points $t = nT$, the discrete waveform for the step response is obtained as

$$\hat{f}(nT) = T \sum_{n=0}^{1023} f(nT)\delta(t-nT) \quad (4-27)$$

$$= T \sum_{n=0}^{1023} \delta(t-nT) \sum_{m=0}^n h(mT). \quad (4-28)$$

The integration of the impulse response (4-24) to yield the step response (4-28) is illustrated graphically in figs. 4-5 through 4-8.

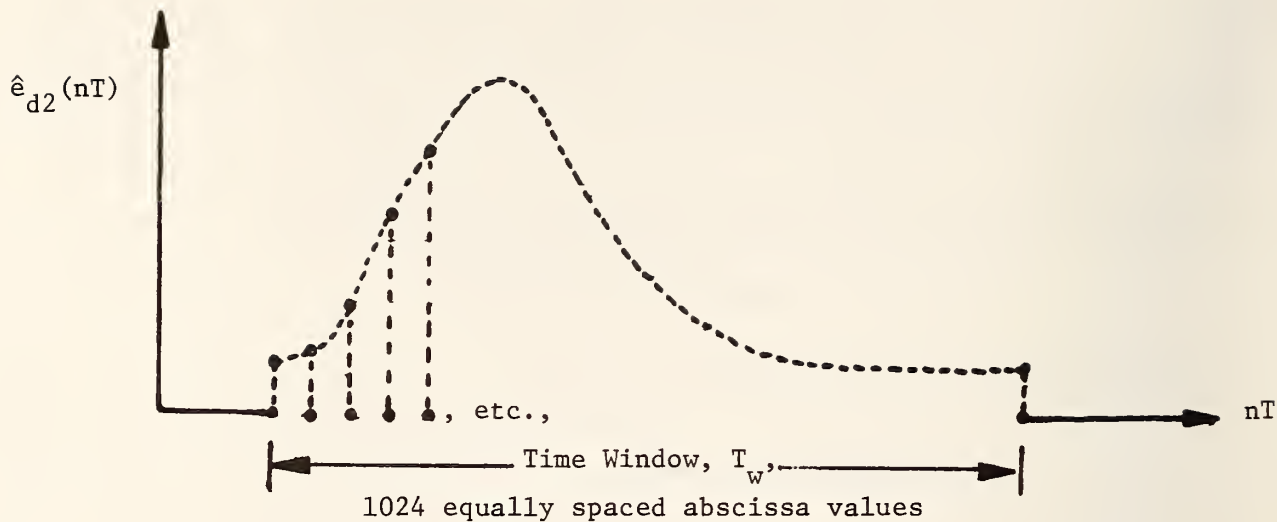


Figure 4.1 A given display waveform is represented by 1024 data points, each point being the mean value of 500 observations.

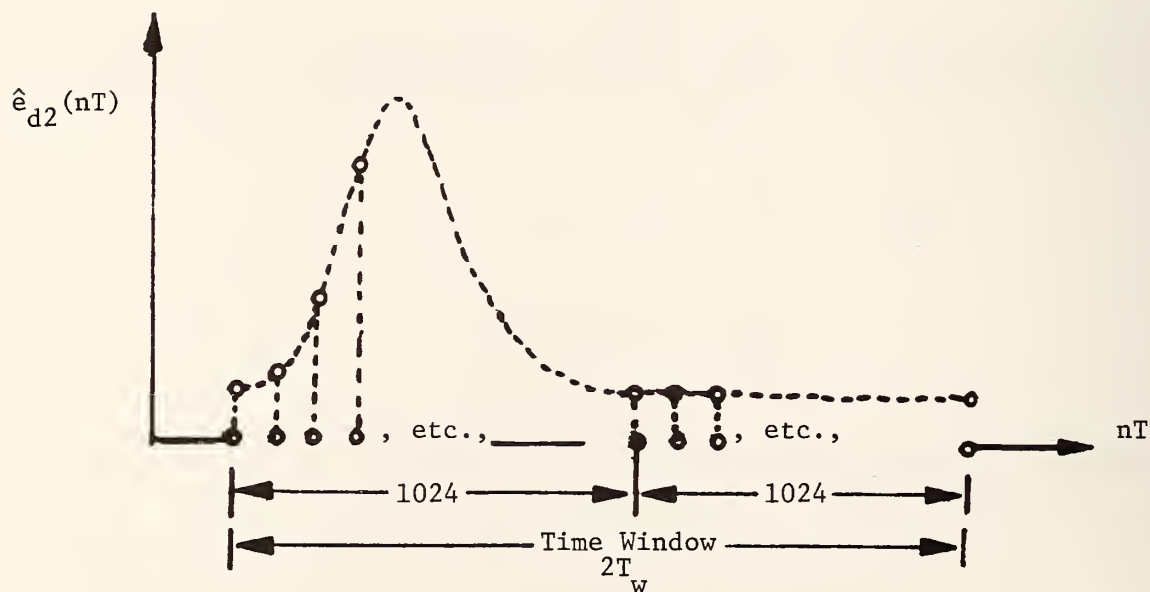


Figure 4.2 A given display waveform of 1024 points augmented by 1024 zeros to yield a total time window of 2048 points.

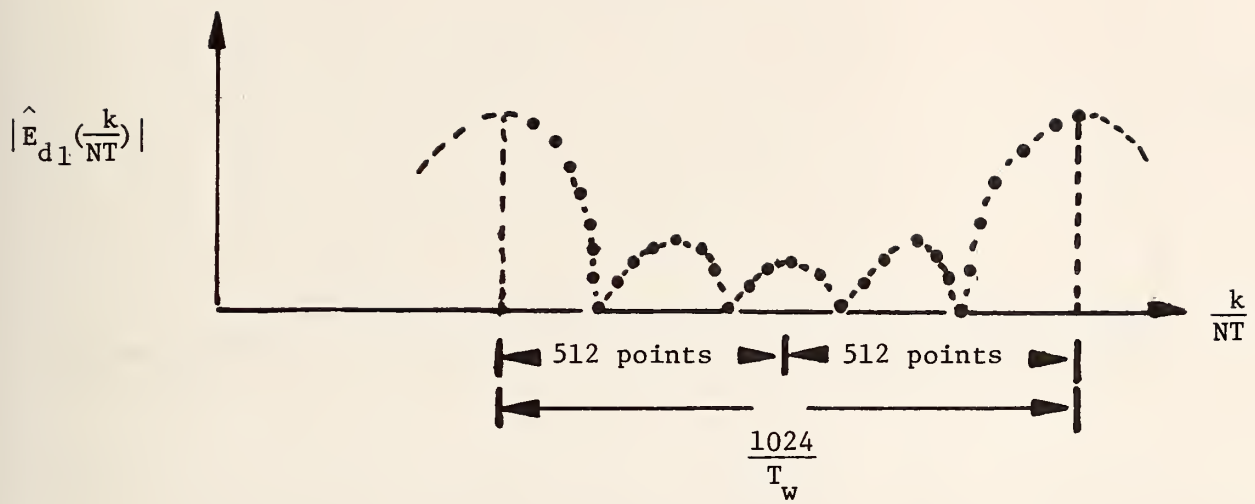


Figure 4.3 One cycle of the periodic 1024 discrete Fourier transform corresponding to $\hat{e}_{d1}(nT)$, fig. 4.1.

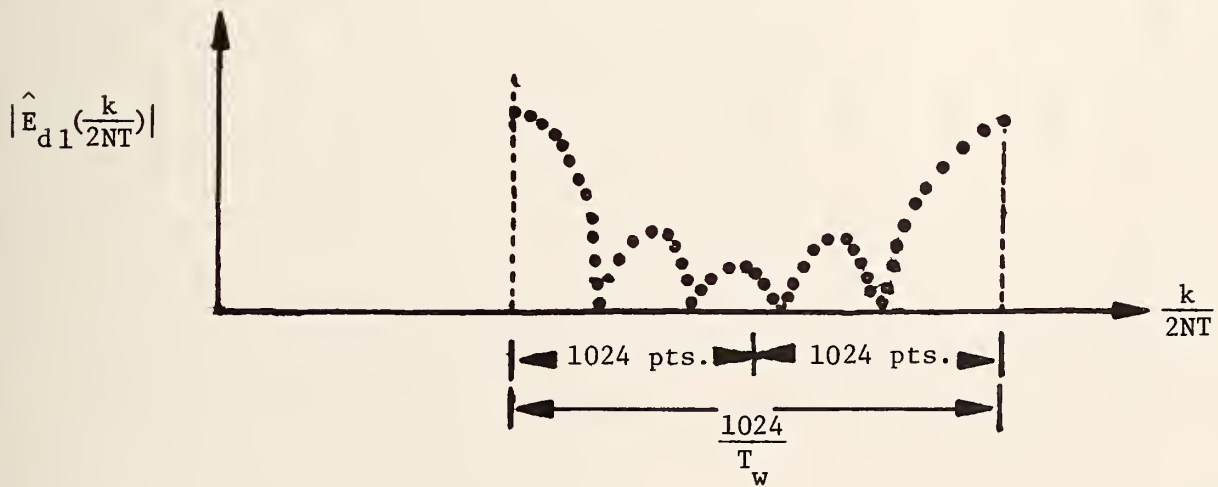


Figure 4.4 One cycle of the periodic 2048 point discrete Fourier transform corresponding to the augmented-zero waveform, fig. 4.2.

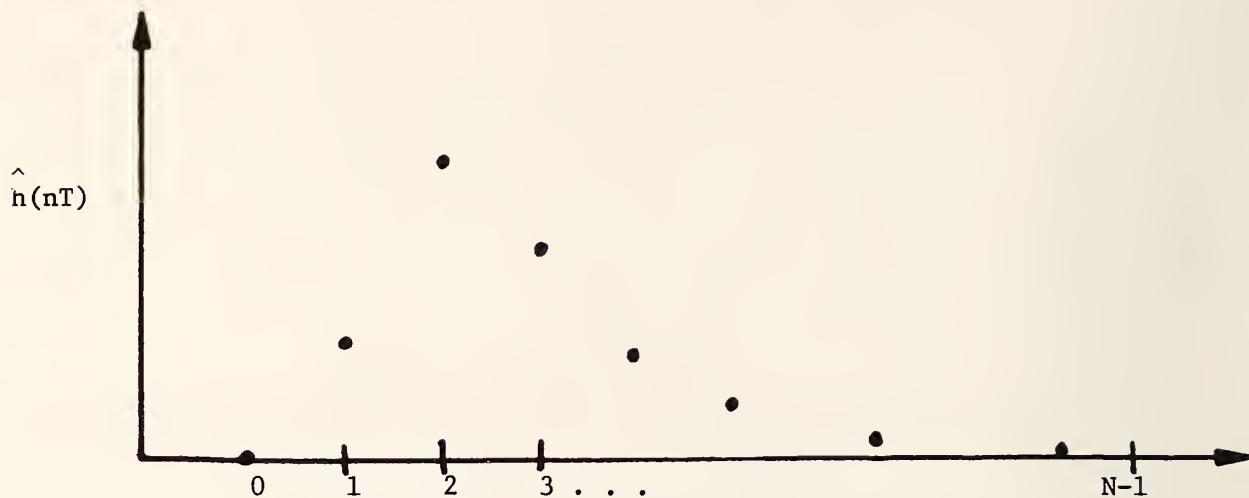


Figure 4.5 The sequence of values representing the discrete impulse response $\hat{h}(nT)$.

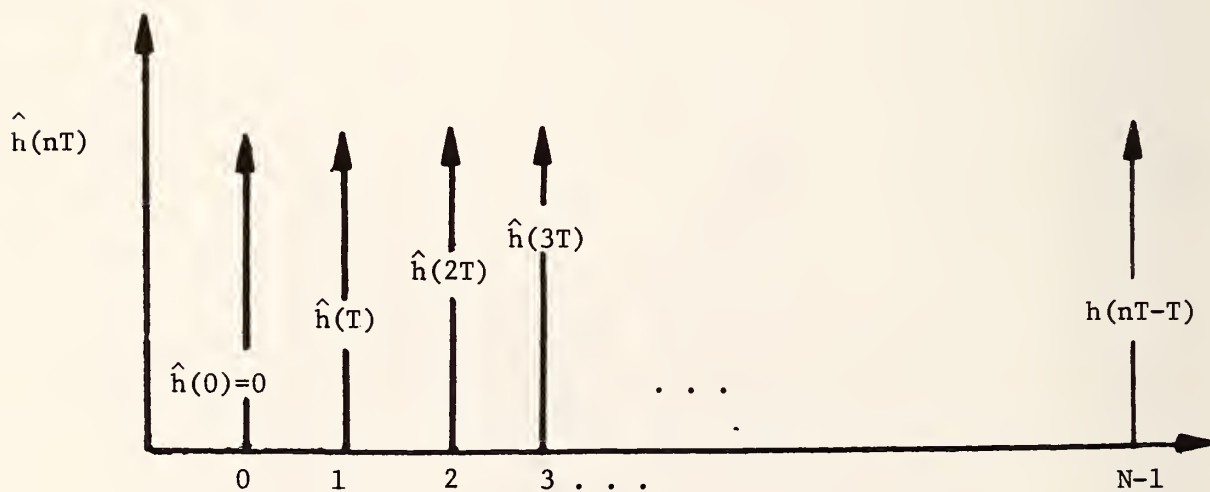


Figure 4.6 The sequence $\hat{h}(nT)$ represented as a train of delta functions of varying strengths. Keep in mind that each delta function is infinite in amplitude while its strength is given by its integral. This representation corresponds to (4.24) and is the mathematical representation for a sequence of values.

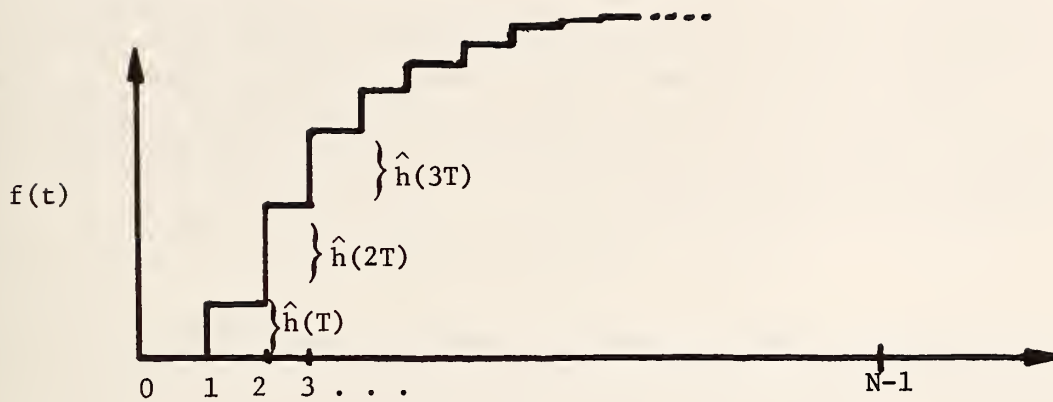


Figure 4.7 The integral of the delta-function train, fig. 4.6; yields a staircase function. Each step along the staircase corresponds to the strength of the corresponding impulse in fig. 4.6. $f(t)$ is a piece-wise continuous function, (4-26).

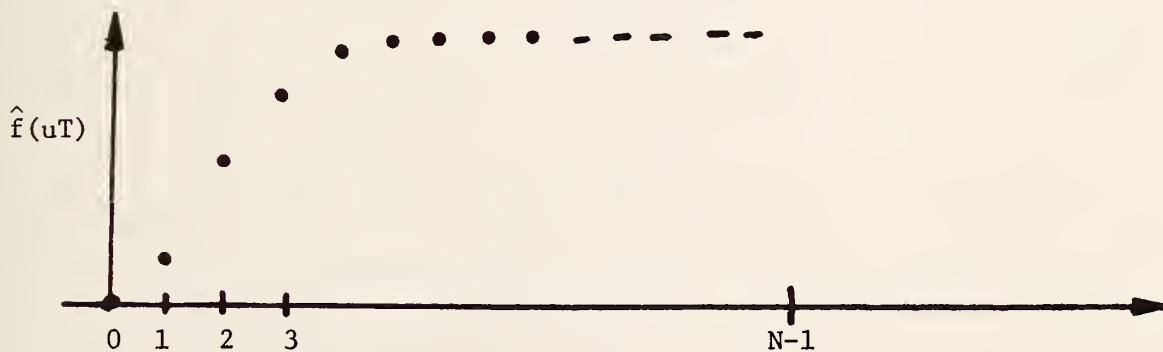


Figure 4.8 The sequence of values representing the discrete step response $\hat{f}(uT)$. This is the discrete function corresponding to the piece-wise continuous function (4-28) shown in Fig. 4.7.

5. TYPICAL RESULTS FOR TRANSMISSION CHARACTERIZATION AND RESPONSE

In this chapter typical results are presented for the determination of the transmission line parameters and the corresponding frequency and time domain responses. These results are typical of the data obtained for all of the cables considered in this report; data on specific cable types vs. length are given in Appendix A. Here, a single cable type of fixed length is used to illustrate results for parameter characterization and response simulation.

5.1 Description of the Cable

The cable results reported below were obtained using a 320 meter (1050 ft.) length of shielded paired-conductor transmission line. This cable is commercially available and for the purposes of this report is designated by the letter I. The nominal specifications for the cable are as follows:

Nominal characteristic impedance - 124 ohms
Overall diameter - 1.07 cm (0.420 in.)
Inductance/unit length - 620 nH/m (189 nH/ft)
Capacitance/unit length - 40.3 pf/m (12.3 pf/ft)
Resistance/unit length - 61.7×10^{-3} ohms/m (18 ohms/ft.)

5.2 The Results

The results are divided into three groups. The first one illustrates the acquired time domain insertion voltages and the subsequent computed (FFT) complex frequency domain data for the insertion ratio $S_{21}(j\omega)$. The second section shows the model simulated responses obtained. In the third section the simulation results for the impulse and step responses are shown.

Figures 5-1 and 5-2 show the acquired waveforms $\hat{e}_{d1}(nT)$ and $\hat{e}_{d2}(nT)$ which are the discrete insertion waveforms corresponding to equations (3-18) and (3-19); they were acquired in the manner discussed in Section 4.1. Next, the discrete Fourier transforms of $\hat{e}_{d1}(nT)$ and $\hat{e}_{d2}(nT)$ are computed and are used to calculate the complex ratio $[\hat{E}_{d2}(k/2NT)]/[\hat{E}_{d1}(k/2NT)]$ which is the insertion ratio $\hat{S}_{21}(k/2NT)$, Sections 4.2 and 4.3. Table 5-1 lists the complex data for $\hat{S}_{21}(k/2NT)$, (4.10), along with the standard deviations of each value of $|\hat{S}_{21}|$ and the phase B_1 . Figure 5-3 shows a log-log graph of the attenuation $\alpha(k/2NT)$, (4.7). The phase data in Table 5-1 is used only to ascertain that the data for $\hat{S}_{21}(k/2NT)$ possesses a small enough standard deviation in the phase data, which in conjunction with a small standard deviation for the magnitude $|\hat{S}_{21}|$, indicates that the data is consistent.

The parameters m and K are extracted from the data shown in fig. 5-3 according to the theory in Section 3.4 and by the method of Section 4.4. Using the extracted values of m and K , the simulated cable attenuation $\hat{a}_1(k/2NT)$ and its associated minimum phase shift $\hat{\beta}_1(k/2NT)$ are calculated, figs. 5-4 and 5-5.

By taking the inverse discrete Fourier transform, using the inverse FFT algorithm, of the frequency domain simulation data, the simulated impulse response of the cable, $\hat{h}(nT)$, is obtained, fig. 5-6. The D. C. level of the impulse response has been carefully established by the procedure described in section 4.6. To validate the (simulated) impulse response, the acquired reference waveform $\hat{e}_{d1}(nT)$ is convolved with the impulse response and the result is compared to the acquired insertion waveform $\hat{e}_{d2}(nT)$. Figure 5-7 shows $\hat{e}_{d2}(nT)$, fig. 5-2, with an expanded time scale while fig. 5-8 shows the result of convolving $\hat{e}_{d1}(nT)$, fig. 5-1 with the simulated impulse response $\hat{h}(nT)$, fig. 5-6. Comparison of figs. 5- and 5-8 shows no significant differences in shape, hence the model parameters accurately characterize the cable.

The step response of the cable, $\hat{f}(nT)$, is obtained by integration of the impulse response $\hat{h}(nT)$, fig. 5-6, as discussed in Section 4.7; the result is shown in fig. 5-9. Note that step response $\hat{f}(nT)$ has reached the normalized value of about 0.86 at the end of the time window, 999 nanoseconds. According to eq. (2-52) the final value referred to the sending end generator voltage E_g would be $R_o/(2R_o + lR)$ or 0.463 for this particular cable (parameter values given in Section 5.1). Without losses at dc ($R = 0$), this value would be 0.5. Normalizing the lossless value to 1.0, gives a final value dc value, i.e., the value for $t = \infty$) of 0.926. Consequently, it is seen that the cable response has not reached the true final value of 0.926 in one microsecond. Consequently, the transmission line could not accurately transmit pulses changing state every microsecond.

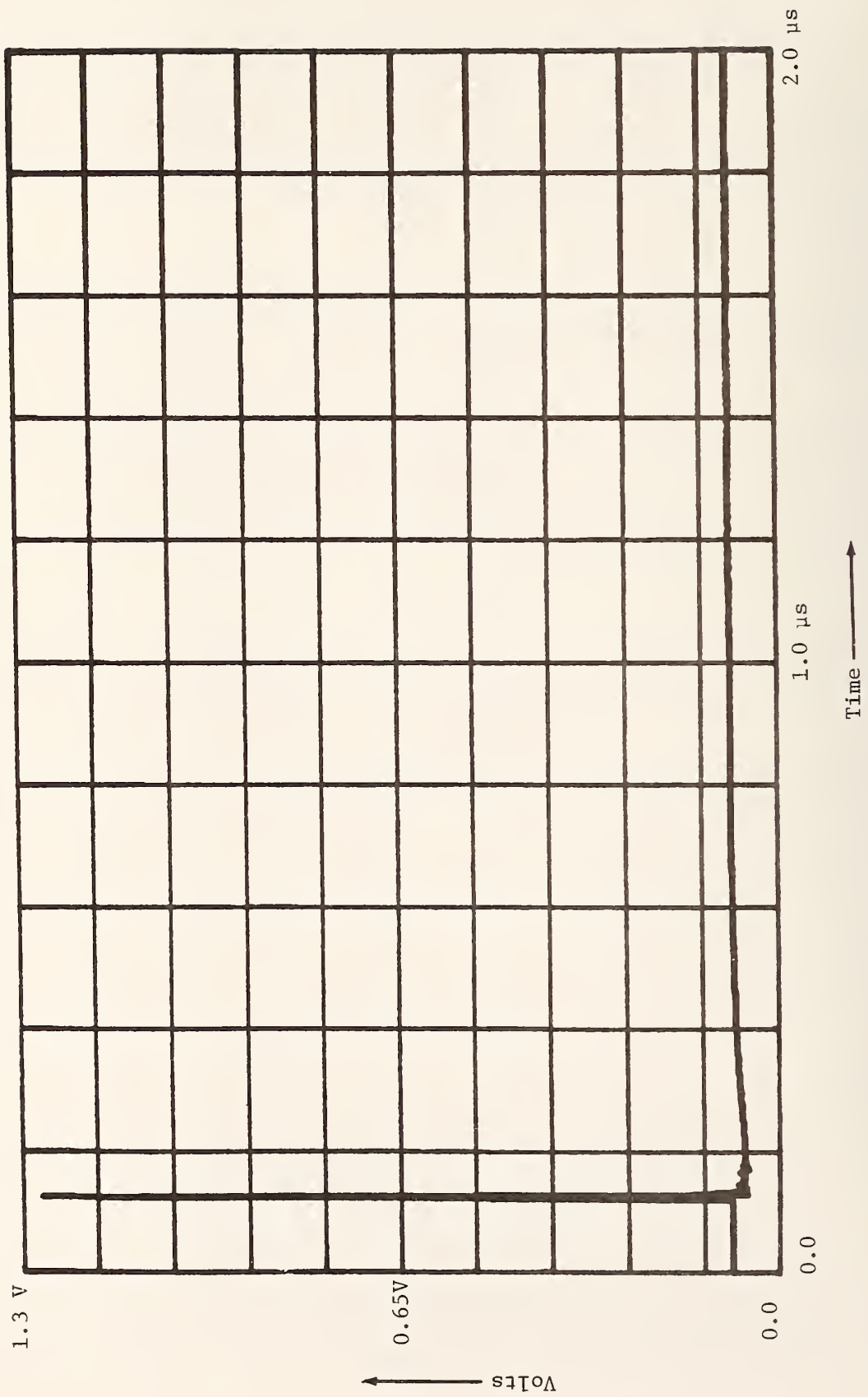


Figure 5.1 The acquired waveform \dot{e}_{d1} (nT) for 320.04 meters (1050 ft.) of cable I.

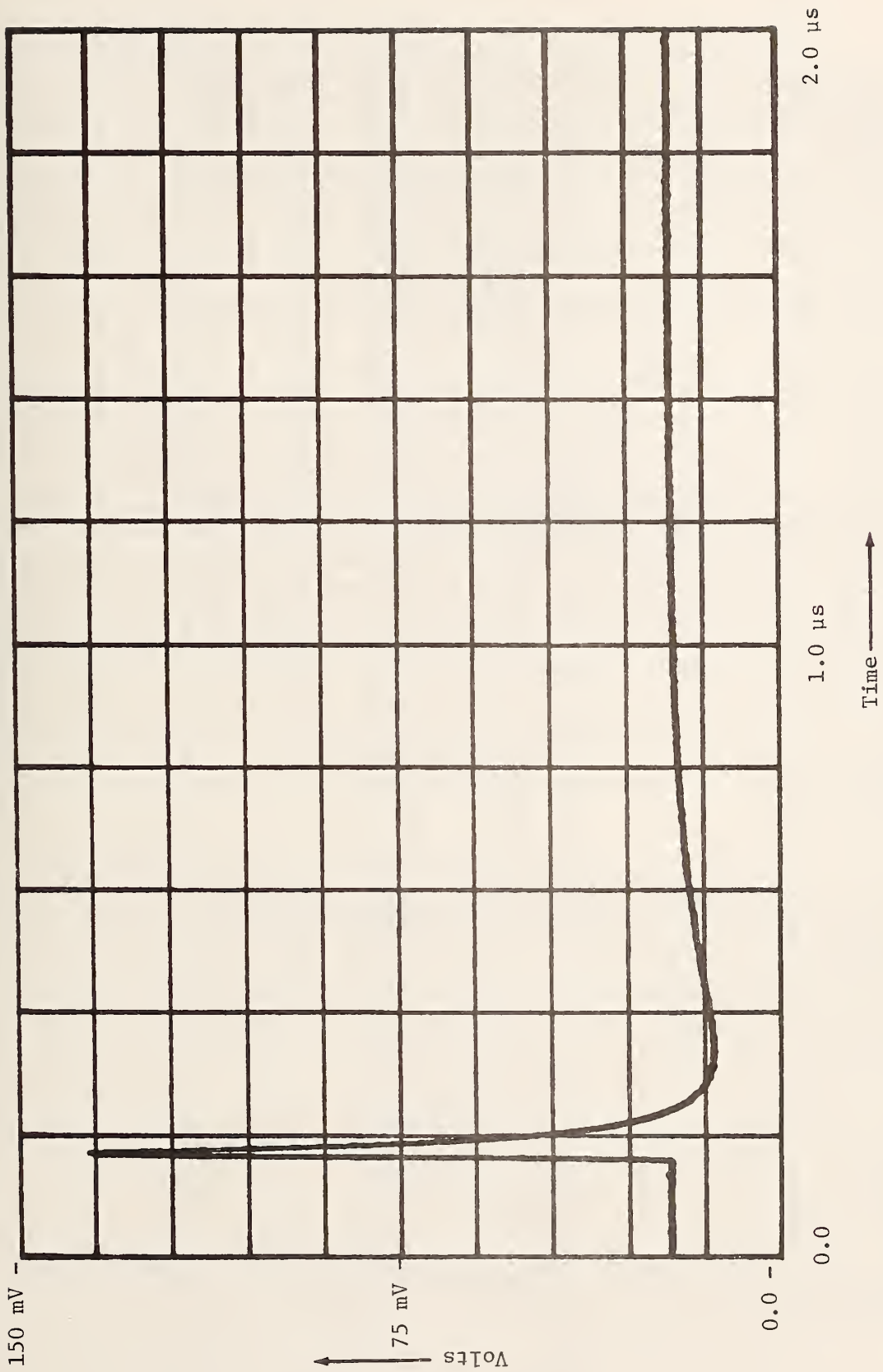


Figure 5.2 The acquired waveform \hat{e}_{d2} (nT) for 320.04 meters (1050 ft.) of cable I.

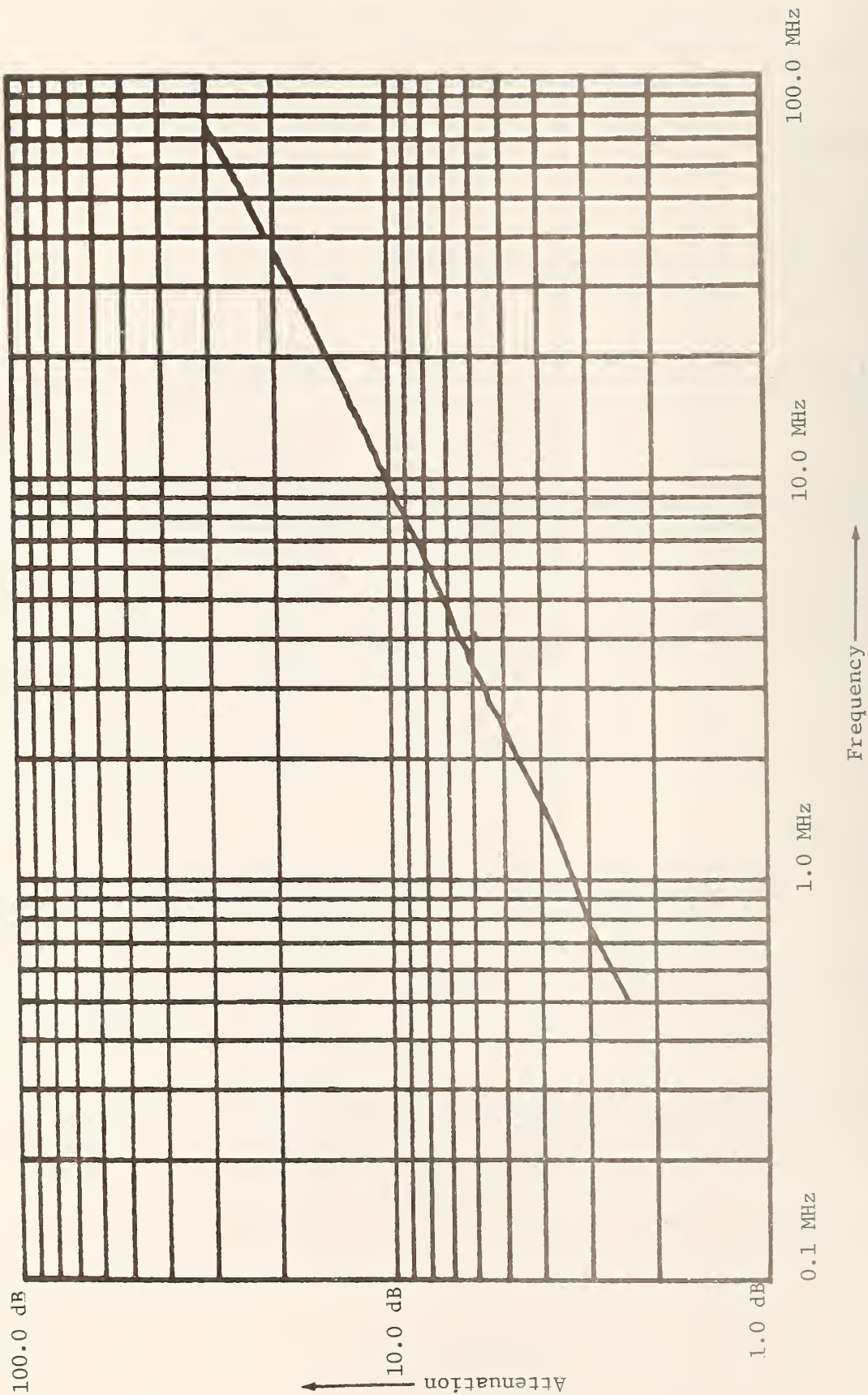


Figure 5.3 The attenuation α (k/nT) computed from the acquired waveforms \hat{e}_{d1} (nT) and \hat{e}_{d2} (nT) for 320.04 meters (1050 ft.) of cable I.

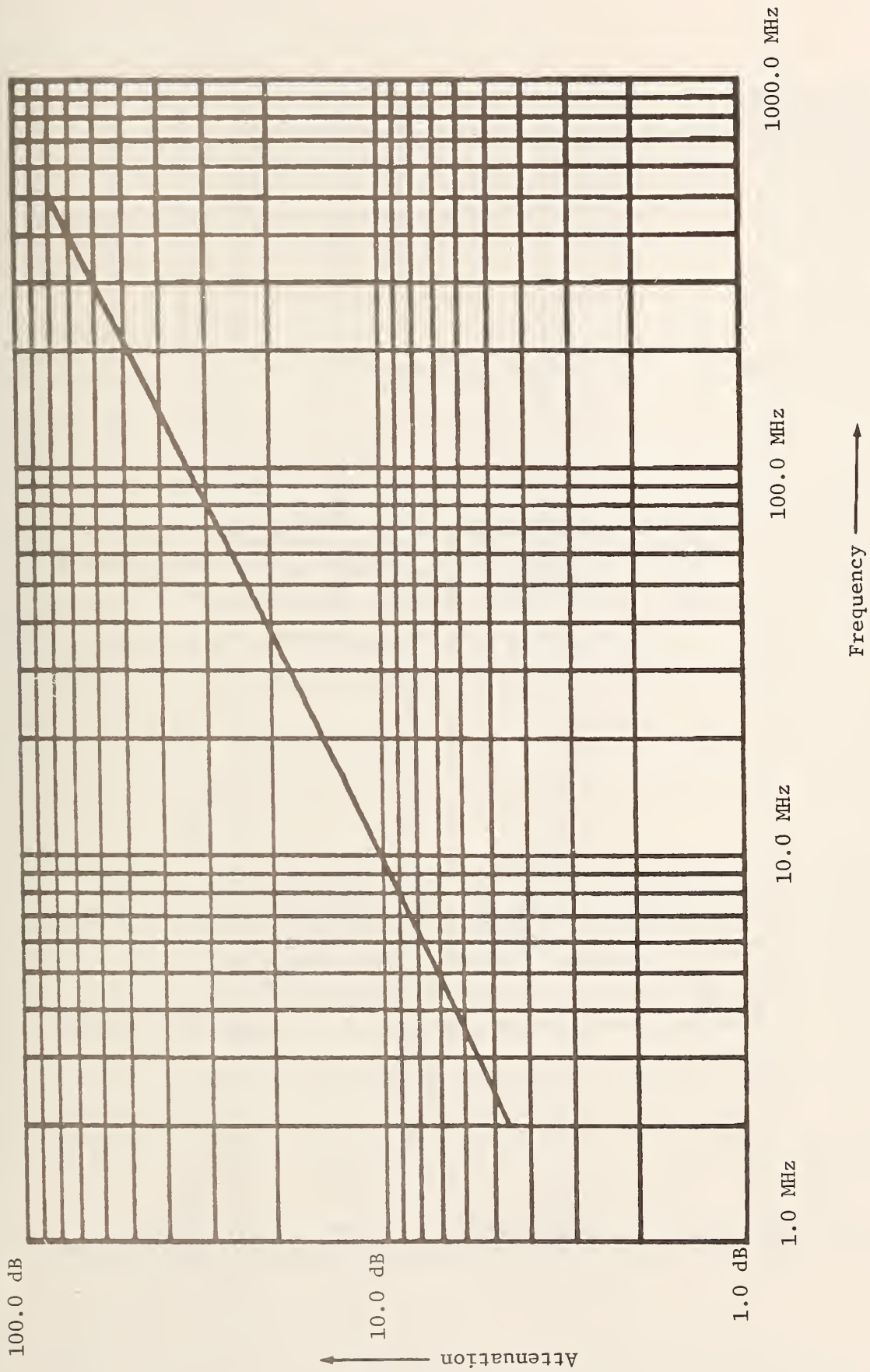


Figure 5.4 Simulated cable attenuation $\hat{\alpha}_1$ (k/2NT) for 320.04 meters (1050 ft.) of cable I.

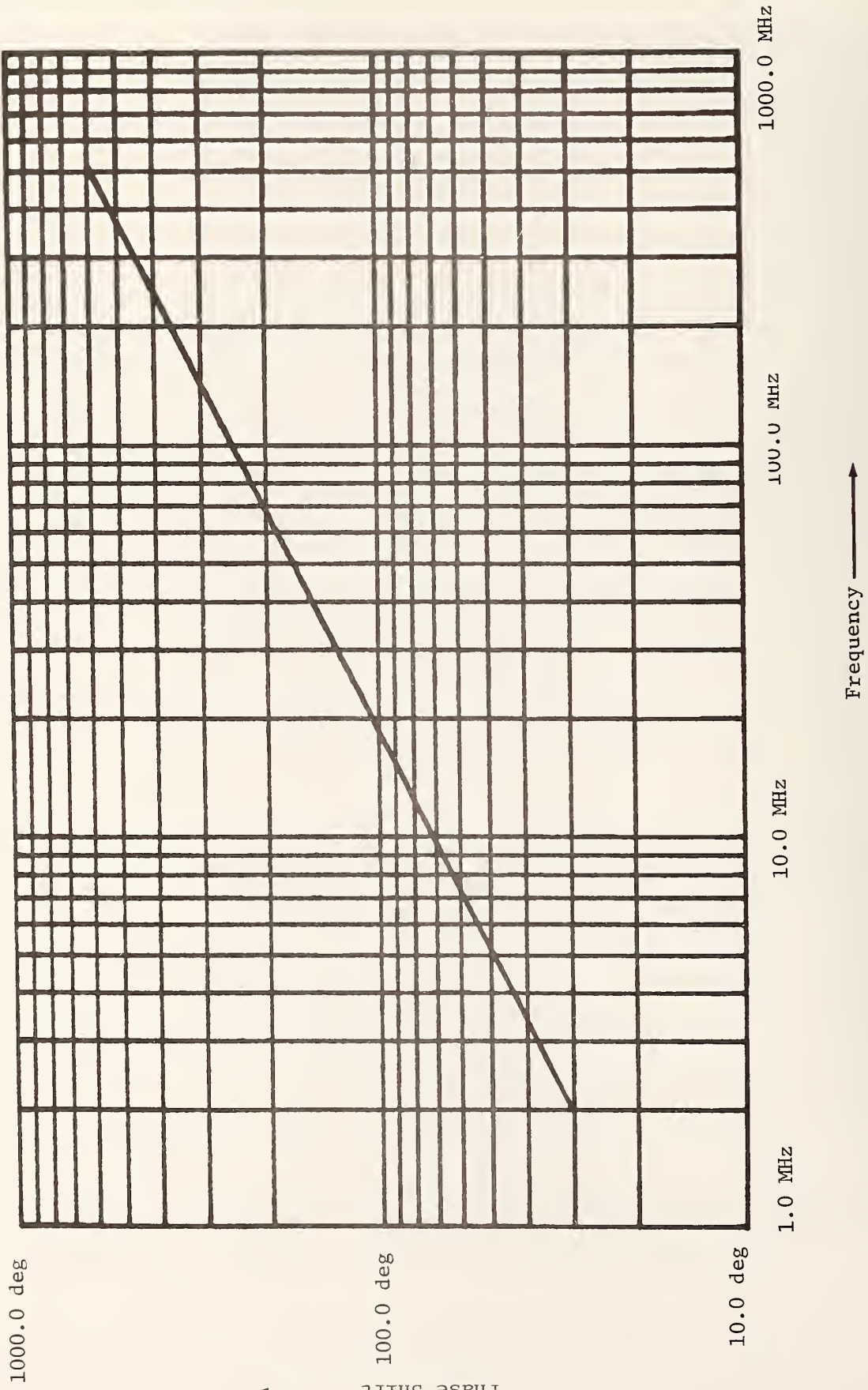


Figure 5.5 Simulated minimum phase, $\hat{\beta}_1$ (k/2NI), associated with the simulated attenuation, Fig. 5.4, for 320.04 meters (1050 ft.)

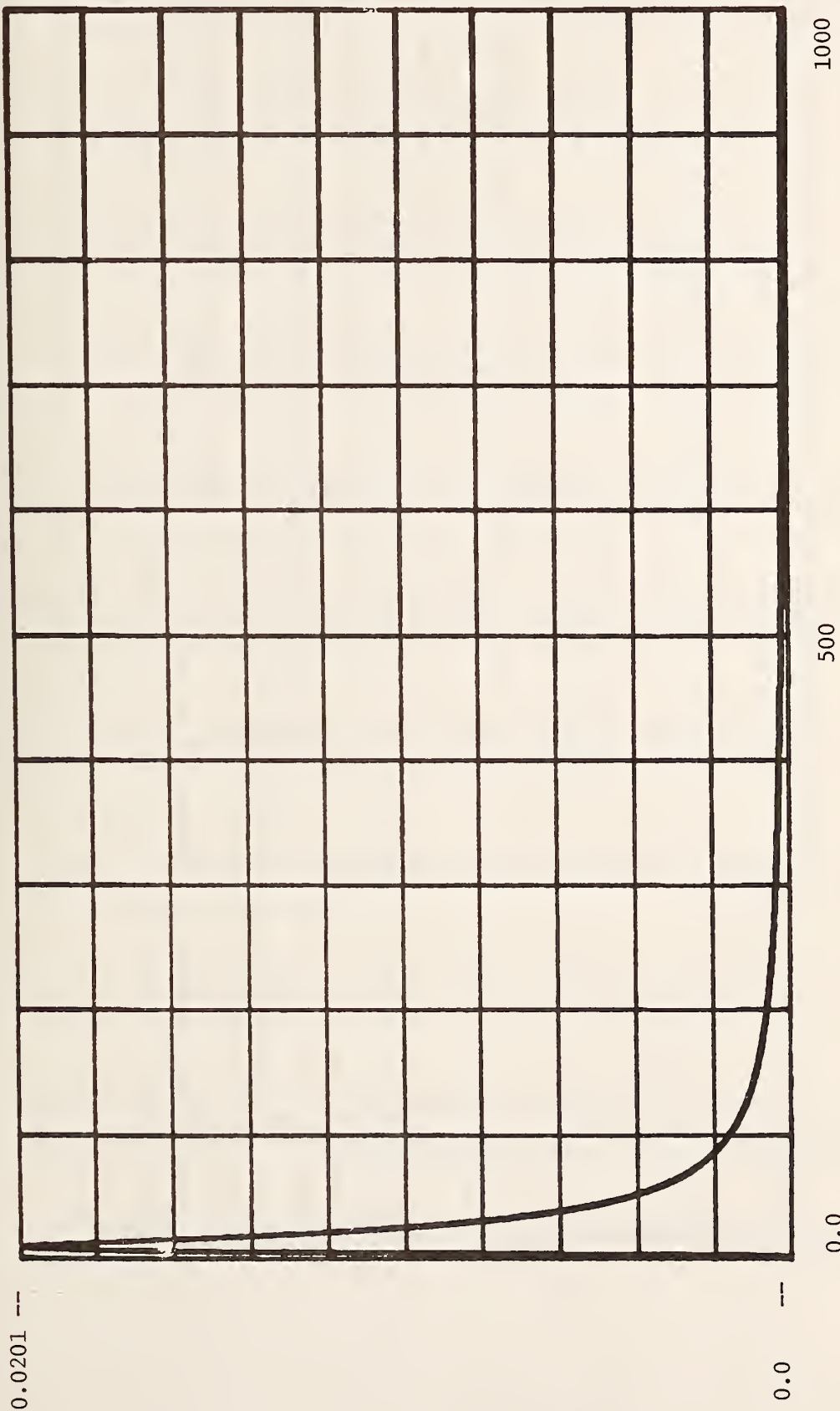


Figure 5.6 The simulated impulse response, $\hat{h}(k/2NT)$ for 320.04 meters (1050 ft.) of cable I. Abscissa units are nanoseconds and ordinate units are seconds⁻¹.

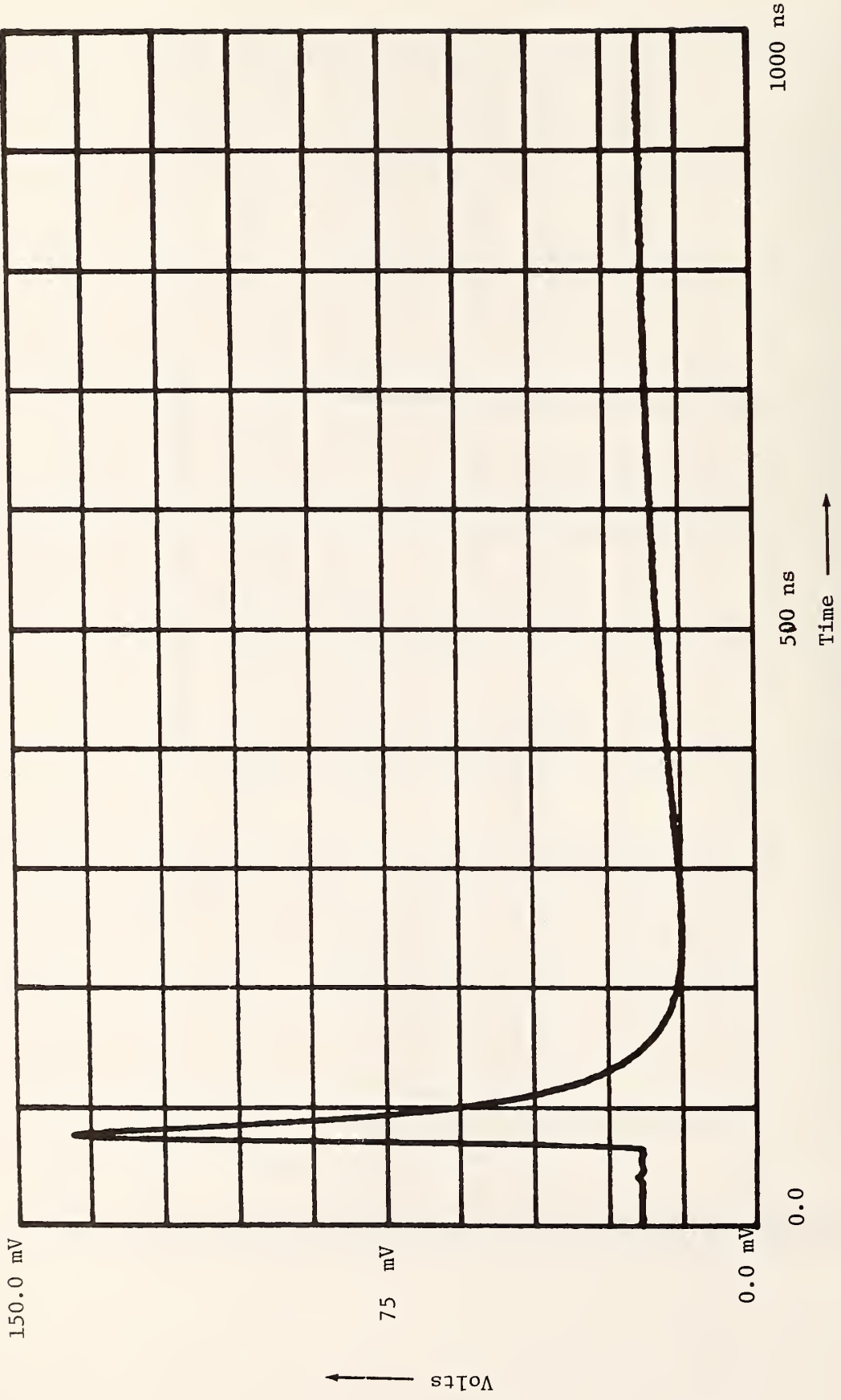


Figure 5.7 The insertion voltage \hat{e}_{d2} (nT) of Fig. 5.2 with an expanded time scale for 320.04 meters (1050 ft.) of cable I.

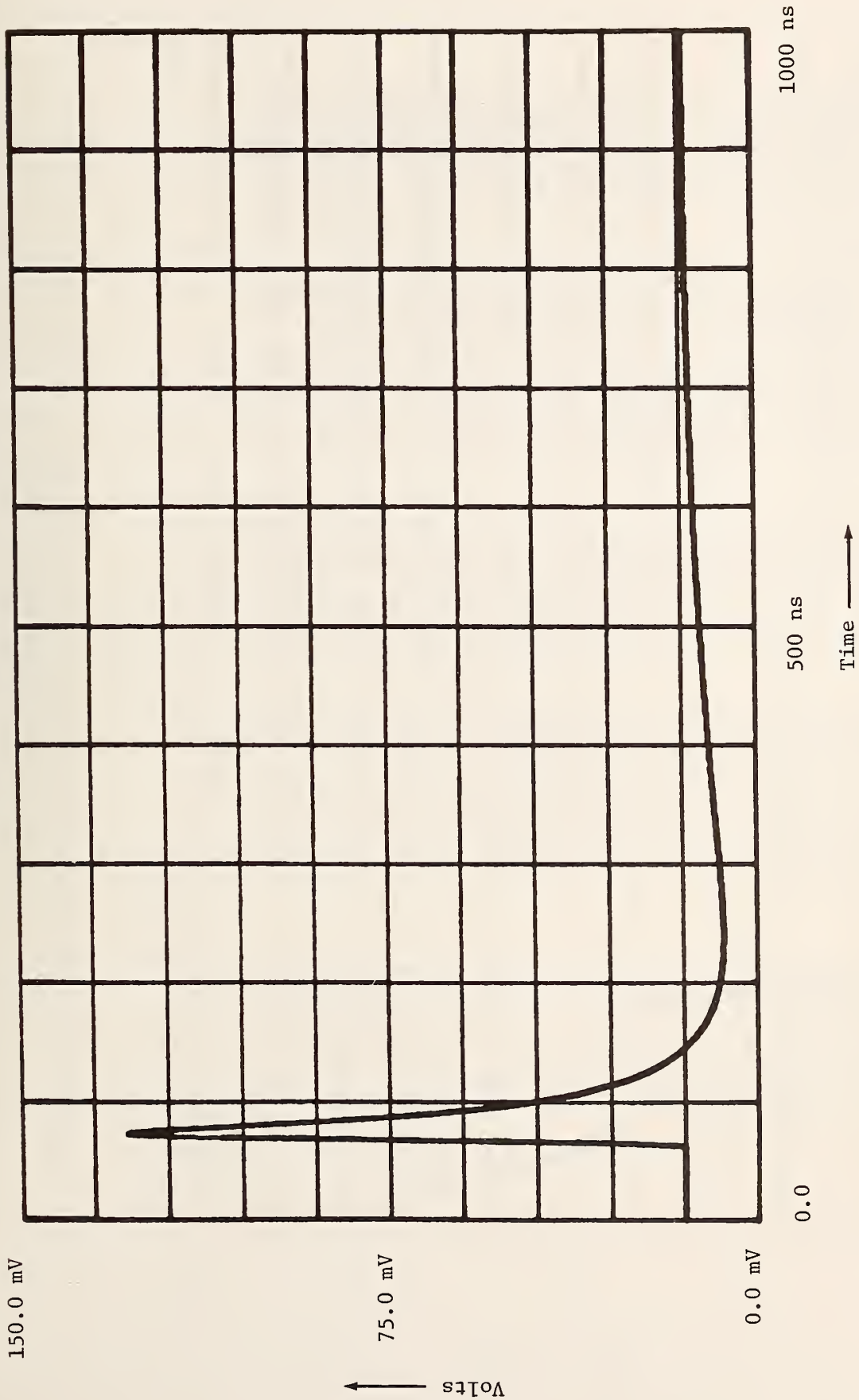


Figure 5.8 The result of convolving \hat{e}_{d1} (nT), Fig. 5.1, with the simulated impulse response, \hat{h} (nT), Fig. 5.6 for 320.04 meters (1050 ft.) of cable I.

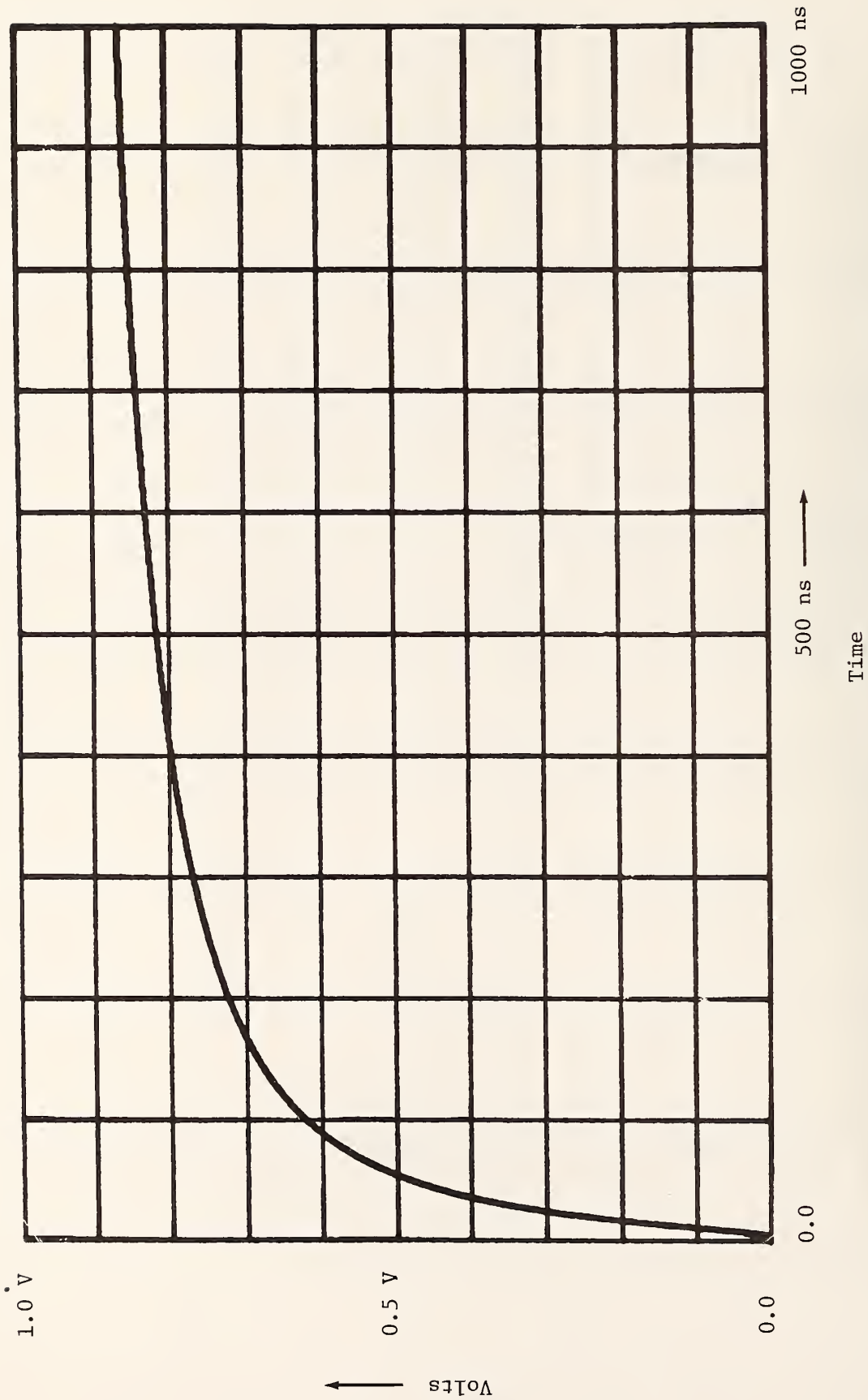


Figure 5.9 The simulated step response, $\hat{f}(nT)$, obtained by integration of the impulse response, Fig. 5.6, for 320.03 meters (1050 ft.) of cable I.

List of magnitude and phase for the insertion ratio $\hat{S}_{21}(k/2N)$ including the standard deviations of the magnitude and phase.

NUMBER OF MEASUREMENTS=		6			
FREQUENCY	SMEAN	SIGMA	PMEAN	SIGMA	
0.25 MHZ	-1.189 DB	0.245 DB	-7.652 DEG	1.684 DEG	
0.50 MHZ	-2.361 DB	0.011 DB	-19.745 DEG	0.695 DEG	
0.75 MHZ	-2.947 DB	0.016 DB	-25.454 DEG	0.362 DEG	
1.00 MHZ	-3.277 DB	0.026 DB	-31.625 DEG	0.128 DEG	
1.25 MHZ	-3.592 DB	0.035 DB	-37.583 DEG	0.161 DEG	
1.50 MHZ	-3.913 DB	0.026 DB	-43.739 DEG	0.141 DEG	
1.75 MHZ	-4.269 DB	0.019 DB	-49.228 DEG	0.133 DEG	
2.00 MHZ	-4.555 DB	0.018 DB	-54.615 DEG	0.213 DEG	
2.25 MHZ	-4.854 DB	0.027 DB	-59.708 DEG	0.206 DEG	
2.50 MHZ	-5.099 DB	0.017 DB	-65.161 DEG	0.180 DEG	
2.75 MHZ	-5.449 DB	0.015 DB	-70.022 DEG	0.281 DEG	
3.00 MHZ	-5.590 DB	0.015 DB	-74.542 DEG	0.229 DEG	
3.25 MHZ	-5.840 DB	0.019 DB	-80.301 DEG	0.262 DEG	
3.50 MHZ	-6.138 DB	0.017 DB	-84.516 DEG	0.257 DEG	
3.75 MHZ	-6.249 DB	0.013 DB	-89.369 DEG	0.348 DEG	
4.00 MHZ	-6.519 DB	0.028 DB	-94.357 DEG	0.294 DEG	
4.25 MHZ	-6.595 DB	0.012 DB	-98.546 DEG	0.313 DEG	
4.50 MHZ	-6.836 DB	0.010 DB	-103.310 DEG	0.302 DEG	
4.75 MHZ	-7.017 DB	0.018 DB	-108.012 DEG	0.281 DEG	
5.00 MHZ	-7.215 DB	0.009 DB	-112.526 DEG	0.418 DEG	
5.25 MHZ	-7.369 DB	0.017 DB	-116.716 DEG	0.382 DEG	
5.50 MHZ	-7.503 DB	0.014 DB	-121.250 DEG	0.407 DEG	
5.75 MHZ	-7.664 DB	0.016 DB	-125.550 DEG	0.296 DEG	
6.00 MHZ	-7.781 DB	0.014 DB	-130.024 DEG	0.293 DEG	
6.25 MHZ	-7.963 DB	0.025 DB	-134.540 DEG	0.384 DEG	
6.50 MHZ	-8.122 DB	0.016 DB	-139.743 DEG	0.476 DEG	
6.75 MHZ	-8.286 DB	0.011 DB	-143.066 DEG	0.515 DEG	
7.00 MHZ	-8.437 DB	0.009 DB	-147.183 DEG	0.533 DEG	
7.25 MHZ	-8.578 DB	0.011 DB	-151.560 DEG	0.581 DEG	
7.50 MHZ	-8.763 DB	0.016 DB	-155.600 DEG	0.555 DEG	

Table 5-1 - continued

7.75	MHZ	9.918	DB	0.018	DB	-159.781	DEG	0.549	DEG
8.00	MHZ	9.926	DB	0.031	DB	-163.929	DEG	0.619	DEG
8.25	MHZ	9.934	DB	0.023	DB	-168.440	DEG	0.704	DEG
8.50	MHZ	9.942	DB	0.028	DB	-172.567	DEG	0.624	DEG
8.75	MHZ	9.950	DB	0.017	DB	-176.736	DEG	0.625	DEG
9.00	MHZ	9.955	DB	0.019	DB	-181.106	DEG	0.751	DEG
9.25	MHZ	9.965	DB	0.016	DB	-185.286	DEG	0.769	DEG
9.50	MHZ	9.975	DB	0.021	DB	-189.494	DEG	0.755	DEG
9.75	MHZ	9.989	DB	0.015	DB	-193.510	DEG	0.721	DEG
10.00	MHZ	10.000	DB	0.019	DB	-197.866	DEG	0.765	DEG
10.25	MHZ	10.013	DB	0.033	DB	-201.947	DEG	0.832	DEG
10.50	MHZ	10.027	DB	0.019	DB	-206.303	DEG	0.801	DEG
10.75	MHZ	10.040	DB	0.033	DB	-210.445	DEG	0.754	DEG
11.00	MHZ	10.055	DB	0.033	DB	-214.336	DEG	0.838	DEG
11.25	MHZ	10.070	DB	0.023	DB	-218.627	DEG	0.878	DEG
11.50	MHZ	10.087	DB	0.022	DB	-222.737	DEG	0.892	DEG
11.75	MHZ	10.094	DB	0.023	DB	-227.050	DEG	0.838	DEG
12.00	MHZ	10.069	DB	0.022	DB	-230.983	DEG	0.926	DEG
12.25	MHZ	10.154	DB	0.041	DB	-234.947	DEG	0.962	DEG
12.50	MHZ	10.271	DB	0.026	DB	-239.091	DEG	0.982	DEG
12.75	MHZ	10.378	DB	0.028	DB	-243.056	DEG	1.063	DEG
13.00	MHZ	10.491	DB	0.024	DB	-247.209	DEG	0.942	DEG
13.25	MHZ	10.624	DB	0.017	DB	-251.143	DEG	0.926	DEG
13.50	MHZ	10.724	DB	0.017	DB	-255.116	DEG	0.963	DEG
13.75	MHZ	10.847	DB	0.020	DB	-259.098	DEG	0.967	DEG
14.00	MHZ	10.931	DB	0.033	DB	-263.061	DEG	1.039	DEG
14.25	MHZ	10.955	DB	0.017	DB	-267.339	DEG	1.135	DEG
14.50	MHZ	10.990	DB	0.029	DB	-271.182	DEG	1.196	DEG
14.75	MHZ	10.947	DB	0.027	DB	-275.256	DEG	1.079	DEG
15.00	MHZ	10.914	DB	0.009	DB	-279.179	DEG	1.092	DEG
15.25	MHZ	10.616	DB	0.031	DB	-283.179	DEG	1.205	DEG
15.50	MHZ	10.717	DB	0.041	DB	-287.247	DEG	1.008	DEG
15.75	MHZ	10.835	DB	0.041	DB	-291.287	DEG	1.086	DEG
16.00	MHZ	10.931	DB	0.028	DB	-295.330	DEG	1.227	DEG
16.25	MHZ	10.931	DB	0.020	DB	-299.232	DEG	0.987	DEG

Table 5-1 - continued

16.50	MHZ	13.037	DB	0.024	DB	303.281	DEG	1.169	DEG
16.75	MHZ	13.130	DB	0.023	DB	307.043	DEG	1.110	DEG
17.00	MHZ	13.186	DB	0.033	DB	311.191	DEG	1.078	DEG
17.25	MHZ	13.320	DB	0.049	DB	315.320	DEG	1.246	DEG
17.50	MHZ	13.420	DB	0.025	DB	319.073	DEG	1.107	DEG
17.75	MHZ	13.501	DB	0.039	DB	323.049	DEG	1.299	DEG
18.00	MHZ	13.603	DB	0.052	DB	327.025	DEG	1.434	DEG
18.25	MHZ	13.705	DB	0.045	DB	330.912	DEG	1.375	DEG
18.50	MHZ	13.800	DB	0.022	DB	334.835	DEG	1.393	DEG
18.75	MHZ	13.915	DB	0.041	DB	338.712	DEG	1.308	DEG
19.00	MHZ	13.999	DB	0.017	DB	342.416	DEG	1.149	DEG
19.25	MHZ	14.072	DB	0.050	DB	346.479	DEG	1.306	DEG
19.50	MHZ	14.203	DB	0.030	DB	350.432	DEG	1.436	DEG
19.75	MHZ	14.288	DB	0.033	DB	354.134	DEG	1.332	DEG
20.00	MHZ	14.373	DB	0.050	DB	358.204	DEG	1.462	DEG
20.25	MHZ	14.490	DB	0.031	DB	362.072	DEG	1.477	DEG
20.50	MHZ	14.572	DB	0.031	DB	366.004	DEG	1.619	DEG
20.75	MHZ	14.687	DB	0.051	DB	369.978	DEG	1.496	DEG
21.00	MHZ	14.779	DB	0.046	DB	373.849	DEG	1.405	DEG
21.25	MHZ	14.898	DB	0.034	DB	377.812	DEG	1.619	DEG
21.50	MHZ	14.979	DB	0.053	DB	381.474	DEG	1.410	DEG
21.75	MHZ	15.055	DB	0.042	DB	385.683	DEG	1.457	DEG
22.00	MHZ	15.209	DB	0.039	DB	389.469	DEG	1.636	DEG
22.25	MHZ	15.375	DB	0.035	DB	393.058	DEG	1.637	DEG
22.50	MHZ	15.548	DB	0.035	DB	396.967	DEG	1.557	DEG
22.75	MHZ	15.425	DB	0.036	DB	400.884	DEG	1.627	DEG
23.00	MHZ	15.534	DB	0.030	DB	404.783	DEG	1.733	DEG
23.25	MHZ	15.615	DB	0.037	DB	408.479	DEG	1.772	DEG
23.50	MHZ	15.713	DB	0.058	DB	412.354	DEG	1.843	DEG
23.75	MHZ	15.794	DB	0.042	DB	415.859	DEG	1.719	DEG
24.00	MHZ	15.834	DB	0.028	DB	419.792	DEG	1.959	DEG
24.25	MHZ	15.938	DB	0.074	DB	423.687	DEG	1.853	DEG
24.50	MHZ	16.012	DB	0.020	DB	427.494	DEG	1.611	DEG
24.75	MHZ	16.119	DB	0.036	DB	431.419	DEG	1.783	DEG
25.00	MHZ	16.227	DB	0.024	DB	435.090	DEG	1.782	DEG

6. USE OF TIME DOMAIN MEASUREMENTS TO ESTIMATE MAXIMUM CABLE BIT RATE AND BIT-ERROR-RATE DEGRADATION

This chapter is concerned with developing a method for using the time domain measurement techniques and data presented in the previous five chapters to obtain estimates of two parameters of great interest to the digital communication system designer. These are (1) the maximum bit rate that may be transmitted through a given length and type of cable, and (2) the bit-error-rate that may be expected for a given system signal-to-noise ratio. It will be shown that a rather unusual plot of the cable step response may be used to estimate these two parameters.

6.1 Digital Communications System Model

Since the purpose of this study is to characterize certain transmission lines (as opposed to complete communication systems) for digital communication applications, a simple idealized transmitter/receiver model has been chosen. By avoiding more complex "realistic" system models it becomes simpler to observe the deleterious effects of the transmission line, alone, in an otherwise perfect system.

The chosen system model is shown in fig. 6.1. The following important assumptions have been made with respect to this transmitter/receiver model:

- a. The transmitter generates a binary non-return-to-zero (NRZ) signal of perfect rectangular pulse shape. That is, a "zero" is represented by a constant zero-volts output, a "one" by a constant V -volts output and the transitions from a "zero" to a "one" or vice versa are instantaneous. The transmitter bit rate is controlled by the trigger generator.
- b. The receiver is a perfect, triggerable threshold detector such that at any time t it may be triggered to sample the input signal and decide if the input voltage is less than or greater than some voltage V_{TH} . If the receiver decision is "less than V_{TH} ", then a "zero" is assumed to have been received; and if the decision is "greater than V_{TH} ", then a "one" is assumed to have been received.
- c. The trigger generator and variable delay are assumed to allow perfect timing control between the transmitter and receiver for any bit rate. Thus, compensation for any cable delay is provided and the delay may be "fine tuned" to allow a receiver sample to be taken at any chosen time within a bit period.
- d. The transmitter output impedance, the receiver input impedance and the summing circuit's input and output impedance are matched to the high frequency limit of the cable characteristic impedance; i.e., $\sqrt{L/C}$ (see eqn. 2-35).

(The noise source will be discussed in Section 6.4; for the discussion in this section switch S_1 is assumed to be open.)

6.2 Maximum Bit Rate Estimation

From the model assumptions it is evident that the transmitter/receiver pair, connected directly together, represents a system with no bandwidth (or, equivalently, bit rate) limitation. That is, since the transmitter voltage transitions are assumed to be instantaneous, and the receiver has no speed of sampling restrictions, then the system can operate perfectly at any bit rate. In addition, it should be noted that this system is not code dependent; it will work perfectly for any particular sequence of "ones" and "zeros" generated by the transmitter.

If a section of transmission line is now connected into the system at the insertion plane indicated in fig. 6.1, two changes in the operation of the system occur; the system becomes bit rate limited and code dependent. In order to analyze and quantize these cable-induced system limitations, the example measurements on 1050 ft. of cable I presented in Chapter 5 will be extended

The step response for cable I for $0 \leq t < 1 \mu\text{s}$ is shown in fig. 6.2. This, of course, is the voltage that would be observed at the receiver if a "one" were transmitted preceded by an infinite (in theory) string of "zeros". At the end of the time window the voltage is only about 0.86 V and, as was shown in Chapter 5, will rise to only 0.926V as $t \rightarrow \infty$. The fact that the received voltage never reaches V volts is due to the DC resistive losses in the cable.

If the situation were reversed such that a "zero" were sent at $t = 0$, preceded by an infinite string of "ones", the response voltage seen at the receiver would be as shown in fig. 6.3. That is, it would be 0.926 V at $t = 0$, decay to 0.066 V at $t = 1 \mu\text{s}$ ($0.926 \text{ V} - 0.86 \text{ V}$) and finally reach 0 V as $t \rightarrow \infty$.

From this information the receiver may now be adjusted for optional operation. That is, a threshold level, V_{TH} , and a sampling time t_s may be chosen to maximize the receiver's ability to accurately detect whether a "one" or a "zero" was transmitted. In both the "zero"-to-"one" and "one"-to-"zero" transitions mentioned above the received voltage varied between the limits of 0 V and 0.926 V in the interval $0 \leq t \leq \infty$. Thus a logical choice for V_{TH} is $V_f/2$ where V_f is a function of the type and length of cable and, as was discussed in Chapter 5, is calculated as

$$V_f = V \frac{2 R_o}{2 R_o + \ell R} \quad (6-1)$$

For the cable I parameters listed in Chapter 5 ($R_o = 124 \Omega$, $\ell = 1050 \text{ ft.}$ and $R = 18.8 \text{ m } \Omega/\text{ft}$) substitution into eqn. 6-1 yields $V_f = 0.926 \text{ V}$ and thus $V_{\text{TH}} = 0.463 \text{ V}$. Any other choice of V_{TH} will bias the receiver such that it no longer would have an equal ability to detect a "one" and a "zero".

The logical choice for a receiver sampling time is at the end of a bit period (note that this choice applies only to this model, e.g., no time jitter). From fig. 6.2 it is observed that in the time window $0 \leq t \leq 1 \mu\text{s}$ the "one" voltage is maximum at $t = 1 \mu\text{s}$. Also, from fig. 6.3, the "zero" voltage is minimum at $t = 1 \mu\text{s}$. Therefore, since the received "one" or "zero" voltage is either rising or decaying monotonically, the best time to sample is always at the end of a bit period, regardless of the actual value of the bit period.

Figure 6.4 is a superposition of the positive and negative step responses shown in figs. 6.2 and 6.3. As expected, the two curves intersect at $V_{\text{TH}} = V_f/2$ which occurs at $t \approx 50 \text{ ns}$. If the system were operated at the bit rate corresponding to this intersect time; i.e., $\text{BR} = 1/50 \text{ ns} = 20 \text{ Mb/s}$, then the receiver voltage at the sample time would be V_{TH} regardless of whether a "one" or a "zero" were sent. Furthermore, if the system were operated at any faster rate, say at $\text{BR} = 1/10 \text{ ns} = 100 \text{ MB/s}$, then the receiver would always be wrong because a "one" signal (or a "zero" signal) would not have had sufficient time to reach a value above (or below) V_{TH} . Also, if the system were operated at any slower rate, say at $\text{BR} = 1/100 \text{ ns} = 10 \text{ Mb}$, the receiver would always be correct because a "one" signal (or a "zero" signal) would have had sufficient time to reach a value above (or below) V_{TH} .

Thus it is observed that the insertion of the cable into the otherwise unlimited-bit-rate system imposes a maximum bit rate limitation, and also that the value of this maximum bit rate may be obtained

as the reciprocal of the intersect time of the positive and negative cable step responses.

It is admittedly difficult to extract receiver voltage versus bit rate information from fig. 6.4. But by redrawing the positive and negative cable step response voltages on an X-axis scaling of \log_{10} (bit rate) instead of time it becomes a simple matter to relate the intersect point to a maximum bit rate. This plot is shown in fig. 6.5 and represents the desired objective of this section. From it the maximum permissible bit rate for correct system operation may be read directly by observing the point on the X-axis, or bit rate axis, at which the two curves intersect, in this case about 20 Mb/s.

Since this plot (fig. 6.5) is central to the remaining developments of this chapter, a few additional remarks about it are in order. The data from which it is derived, the positive and negative cable step responses of fig. 6.4, consist of two discrete time signals, each of 1024 points in a 1 μ s window. That is, the step responses are really a set of 1024 voltage points spaced 1 μ s/1024 points or about 1 ns apart. Therefore, when plotted versus reciprocal time, or frequency, they range from 1 MHz (1/1 μ s) to about 1 GHz (1/1 ns). As shown in fig. 6.5, then, the signals of fig. 6.4 are contained in the frequency interval from 10^6 b/s to 10^9 b/s.

Since it is economically unfeasible to calculate these step responses beyond the order of 1 μ s, (or equivalently, below 1 Mb/s), due to computer memory and speed limitations, a straight line approximation has been used for the step response voltages between 1 μ s and 1 s or 1 Mb/s and 1 b/s. Because the actual "one" voltage lies above and the actual "zero" voltage lies below their corresponding straight lines in this time or frequency interval, this straight line approximation is a conservative or "worst case" approximation.

6.3 Code Dependence

From the shapes of the cable step responses of figs. 6.2 and 6.3 it is evident that intersymbol interference will occur at the receiver when a cable is placed in the system. Just as in the case of an RC exponential response, the positive modeled cable step response reaches V_f only as $t \rightarrow \infty$. Therefore, the voltage sampled at the receiver at the end of a bit period will depend not only on whether a "one" or a "zero" was sent in that period but also on the particular sequence of "ones" and "zeros" sent for all time before the bit period in question. In other words, the presence of this intersymbol interference, caused by the infinitely long cable step response "tails", implies that the system is code dependent.

One approach to the analysis of this code dependence on system operation would be to analyze separately the effects of all possible code sequences. However, a much simpler method exists which is to find the worst case and best case code sequences as lower and upper bounds for correct system operation.

The worst case is exactly the one referred to in the last section; an infinite string of "zeros" for all $t < 0$, a transition to "one" at $t = 0$ and an infinite string of "ones" for $t > 0$. In other words it is represented by the (positive or negative) cable step response. If even a single "one" had occurred at some time $t < 0$, then the voltage at the receiver would not be exactly 0 V at $t = 0$. Rather, it would be slightly greater than 0 V due to the fact that the decay back to 0 V, even from a single "one" only occurs as $t \rightarrow \infty$. Therefore, if one or more "ones" occurred before $t = 0$ and if a "one" is transmitted at $t = 0$ as described above, then the step response commencing at $t = 0$ will begin from some voltage greater than 0 V. The received voltage will thus have a "head start" towards V_{TH} and will rise to that value sooner than in the case of all "zeros" preceding $t = 0$. Of all possible code sequences preceding $t = 0$, then, the one consisting of all "zeros" will yield the worst case because it is the only one that forces the transition to a "one" to begin at 0 V. The same argument may be used to show that the worst case for a "one"-to "zero" transition is the negative cable step response.

The best case is the sequence "one"- "zero"- "one"- "zero" occurring over all time. Fig. 6.6 (a through f) shows that this is true. Figure 6.6a is a plot of the transmitter signal for 64 bits of a "one"- "zero"- "one"- "zero" code sequence. (For all $t < 0$ the transmitter output is 0 V.) Figure 6.6b is the time domain convolution of this transmitter signal with the impulse response of 1050 feet of cable I, that is, figure 6.6b is a plot of the receiver signal that results from the transmitter signal passing through the above cable at a 4 Mb/s rate. The plots shown in fig. 6.6c through f are of the receiver signal that would be observed if the transmitter bit rate were increased to 8, 16, 32 and 64 Mb/s respectively.

All of these responses may be thought of as transient responses starting at 0 V and eventually oscillating symmetrically about V_{TH} as $t \rightarrow \infty$. The worst case mentioned above is graphically illustrated by observing the first "zero" to "one" transition occurring at $t = 0$. For the responses shown in fig. 6.6b, c and d, corresponding to 4, 8 and 16 Mb/s, respectively, the first "one" rises to a voltage greater than V_{TH} thus implying that no errors will be made. For the 32 and 64 Mb/s responses, however, the first "one" does not reach V_{TH} ; an error in detection of this "one" is certain. This tends to confirm the conclusion drawn from fig. 6.5 that the cutoff bit rate for proper system operation is about 20 Mb/s.

The fact that the "one"- "zero"- "one"- "zero" sequence over all time is the best case may be deduced from the five responses shown in fig. 6.6 by observing that, regardless of the bit rate, all of the responses end up oscillating symmetrically about V_{TH} as $t \rightarrow \infty$. Therefore, even for very high bit rates, when the receiver response signal reaches steady state the detector will properly discriminate between a "zero" and a "one".

Neither of these code sequences, the single step over all time or the square wave over all time, contain any information, of course, but they do represent the code boundaries. That is, for a given bit rate, they represent the minimum and maximum number of transitions allowable per unit of time. Therefore, any arbitrary "real" code sequence will have a receiver response somewhere between these worst and best case responses. Consequently, the worst case plot shown in fig. 6.5 may be used to prudently estimate the maximum bit rate that may be transmitted over a given type and length of cable.

6.4 Bit-Error-Rate Degradation

In the previous sections in this chapter it was shown that the overlay plot of the positive and negative cable step responses versus bit rate may be used to estimate the maximum bit rate that may be transmitted over a given type and length of cable under ideal conditions. Quite often, though, there is noise present in communications systems such that even if the system were operating at a bit rate less than the cutoff bit rate, there is a nonzero probability of error simply due to the noise. This error probability is usually quantitatively characterized by the parameter "bit error rate" (BER) which is the probability that an error will be made in the detection of any given bit. A BER of 10^{-6} , for example, means that the probability of misinterpreting any given bit is one in one million, or, stated another way, it can be expected on the average that for every one million bits sent, one will be misinterpreted.

The goal of this section is to develop a method for determining the change in BER of an idealized communication system by the addition of a given type and length of cable. The assumed communication system is the same as that defined in section 6.1 and shown in fig. 6.1 but with the noise source switch

now closed. It will be further assumed that the noise source voltage output is Gaussian white noise; that is, uncorrelated noise with a Gaussian density function given as,

$$p(v) = \frac{1}{\sqrt{2\pi\sigma^2}} e^{-(v-\mu)^2/2\sigma^2}, \quad (6-2)$$

where μ is the noise mean, assumed to be zero, and σ is the noise standard deviation or rms value.

In order to determine the BER degradation due to the insertion of a cable into the system it is first necessary to calculate the BER of the system with the transmitter connected directly to the receiver. In this case a "one" is represented by a transmitter output of V volts and a "zero" by the 0 volts. As before, the receiver threshold voltage is set to the midpoint of the received signal range, in this case $V/2$ volts. To this signal, then, is added a Gaussian noise voltage with zero mean and rms value σ .

If a "zero" is assumed to be sent then the probability of an error in detection is simply the probability that the received voltage (signal plus noise) will exceed $V/2$ volts. From the assumed Gaussian density function this is,

$$P(v > V/2) = \int_{V/2}^{\infty} \frac{1}{\sqrt{2\pi\sigma^2}} e^{-v^2/2\sigma^2} dv. \quad (6-3)$$

Likewise, if a "one" is assumed to be sent then the probability of detection error is the probability that the received voltage is less than $V/2$ and is given as

$$P(v < V/2) = \int_{-\infty}^{V/2} \frac{1}{\sqrt{2\pi\sigma^2}} e^{-(v-V)^2/2\sigma^2} dv. \quad (6-4)$$

Due to the symmetry of the Gaussian density function the probabilities of mistaking a "one" for a "zero" (eqn. 6-3) or a "zero" for a "one" (eqn. 6-4) are the same so either equation may be used to calculate the probability of error per bit regardless of whether a "one" or a "zero" was sent.

The actual calculation of the error probability from eqn (6-3) or (6-4) is quite difficult and fortunately unnecessary. Tables exist for the error function^[11], defined as,

$$\text{erf}(x) = \frac{2}{\sqrt{\pi}} \int_0^x e^{-y^2} dy \quad (6-5)$$

and it is easily shown [12] that the error probability above may be expressed in terms of the error function as

$$P(E) = \frac{1}{2} \left[1 - \text{erf} \left(\frac{V}{2\sqrt{2}\sigma} \right) \right]. \quad (6-6)$$

Furthermore, if the voltage peak signal to rms noise ratio is defined as

$$VSNR = \frac{V}{\sigma} \quad (6-7)$$

then the error probability per bit, or equivalently, the BER may be expressed as a function of VSNR as,

$$P(E) = \frac{1}{2} \left[1 - \operatorname{erf} \left(\frac{VSNR}{2\sqrt{2}} \right) \right]. \quad (6-8)$$

A computer-generated plot of BER versus VSNR is given in fig. 6.7a through e.

As an example of using this plot assume that the transmitter output for a "zero" is 0 volts, a "one" is 24 volts and the rms noise value is 2 volts. Then, from (6-7) the VSNR is 12. From the plot in fig. 6.7c it is observed that a VSNR of 12 yields a BER of 10^{-9} .

If the transmitter-receiver pair VSNR is known, it becomes possible to determine the new BER that would be observed by inserting of a given type and length of cable. This may be accomplished by use of the overlay step response versus bit rate plot of fig. 6.5 in conjunction with the BER versus VSNR plot of fig. 6.7 in the following manner. For a desired bit rate, the new peak signal voltage is obtained from fig. 6.5 as

$$v_p(BR) = v_1(BR) - v_0(BR). \quad (6-9)$$

That is, the new peak signal voltage is the difference between the "one" voltage and the "zero" voltage that are present at the receiver at the end of a bit period for the assumed bit rate. From fig. 6.5, for example, v_p for an assumed bit rate of 1 Mb/s is $0.86 \text{ V} - 0.07 \text{ V} = 0.79 \text{ V}$. Then, from eqn. (6-7), a new VSNR is obtained as

$$VSNR_{\text{System + Cable}} = \frac{v_p}{\sigma} = \frac{0.79\text{V}}{\sigma} = 0.79\text{V} \times VSNR_{\text{System}}. \quad (6-10)$$

Continuing the above example, if the transmitter receiver pair VSNR were 12, implying a system BER of 10^{-9} , and then 1050 ft. of cable I were placed in the system operating at 1 Mb/s, the new system VSNR would be 0.79×12 or about 9.5. From fig. 6.7b a VSNR of 9.5 yields a new BER of about 10^{-6} .

These two graphs, figs. 6.5 and 6.7a-e, may be used for a variety of system design purposes. As another example suppose that it is desired to know the maximum permissible bit rate for the system in the previous example such that the new BER (after insertion of the cable) will not exceed 10^{-7} . From fig. 6.7b this BER implies a minimum allowable VSNR of about 10.4. Then, from eqn. (6-10)

$$v_p = V \frac{VSNR_{\text{System + Cable}}}{VSNR_{\text{System}}} \quad (6-11)$$

or

$$v_p = V \frac{10.4}{12} = 0.87 \text{ V}$$

where in fig. 6.5 it is seen that this difference voltage v_p occurs for a bit rate of 200 b/s.

However, rather than using the difference voltage of eqn. 6-9, one can proceed using a single curve, e.g., the "one" curve, fig. 6.2. Due to the symmetry of the negative and positive step response, it is evident that, for any bit rate

$$v_0(\text{BR}) = V_f - v_1(\text{BR}), \quad (6-12)$$

and substitution of this expression for $v_0(\text{BR})$ into (6-9) yields

$$v_p(\text{BR}) = 2 v_1(\text{BR}) - V_f \quad (6-13)$$

or

$$v_1(\text{BR}) = \frac{1}{2} [v_p(\text{BR}) + V_f]. \quad (6-14)$$

For the example,

$$v_1(\text{BR}) = \frac{1}{2} [0.87\text{V} + 0.926\text{V}] = 0.898\text{V}$$

$$\approx 0.9.$$

Observation of the point where the $v_1(\text{BR})$ curve (the "zero"-to-"one" step response curve) passes through the 0.9 V line again yields a bit rate of approximately 200 b/s. The same answer has been obtained by reading the value of only one curve rather than by reading the difference between two curves.

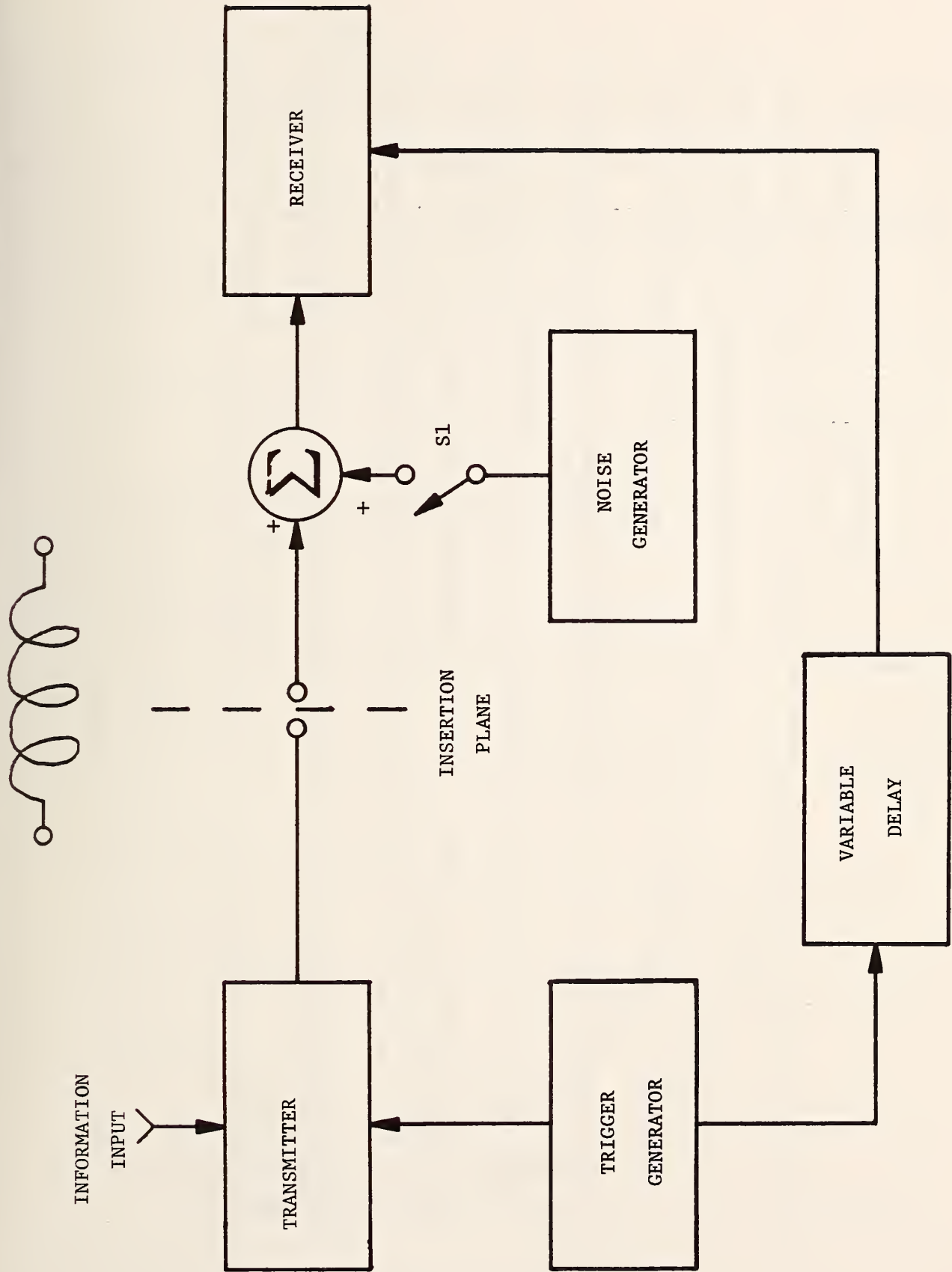


Figure 6.1 Model communications system used for analysis of maximum bit rate limitation and bit-error-rate degradation caused by transmission lines.

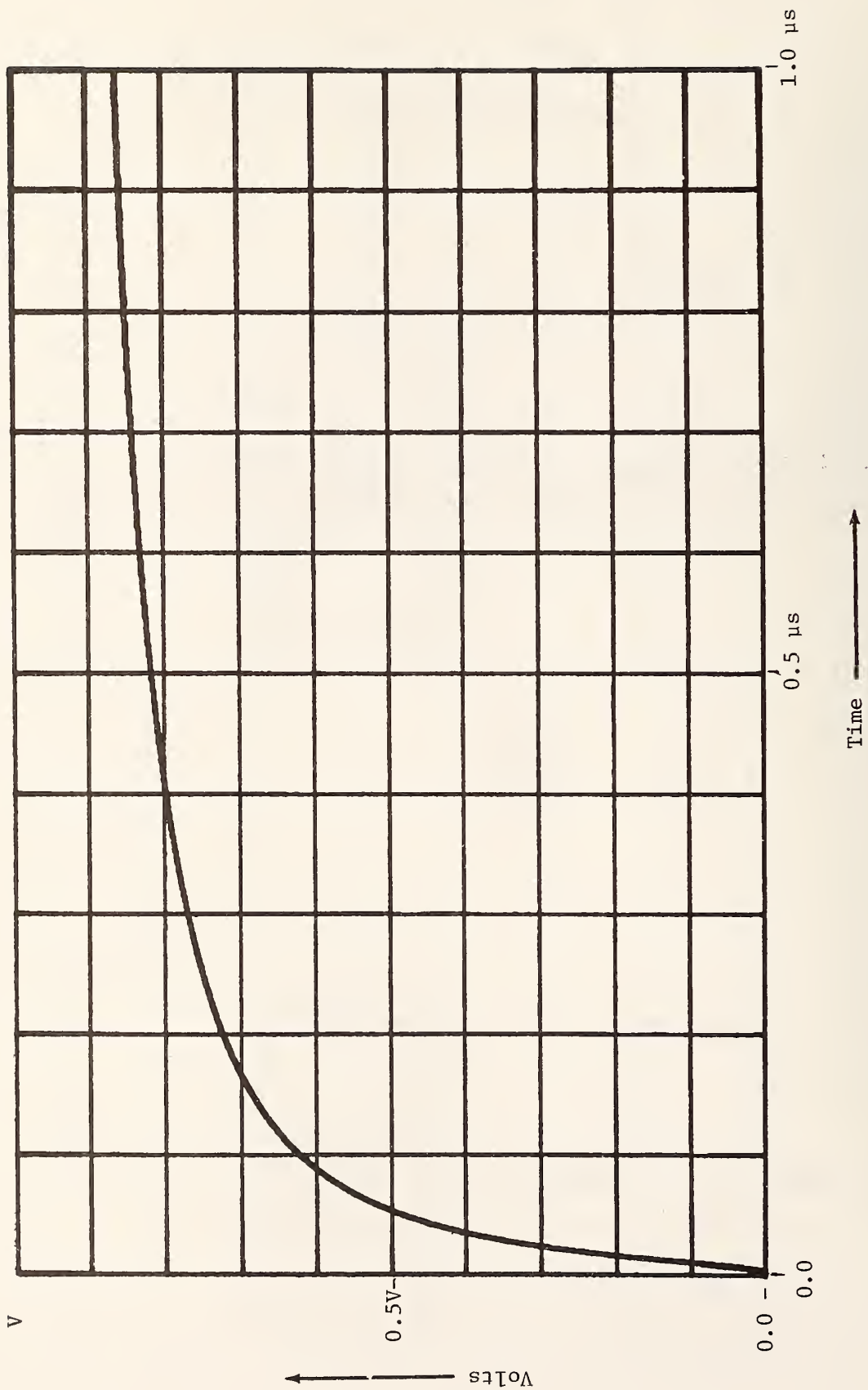


Figure 6.2. "Zero"-to "one" step response of 320.04 meters (1050 ft.) of cable I.

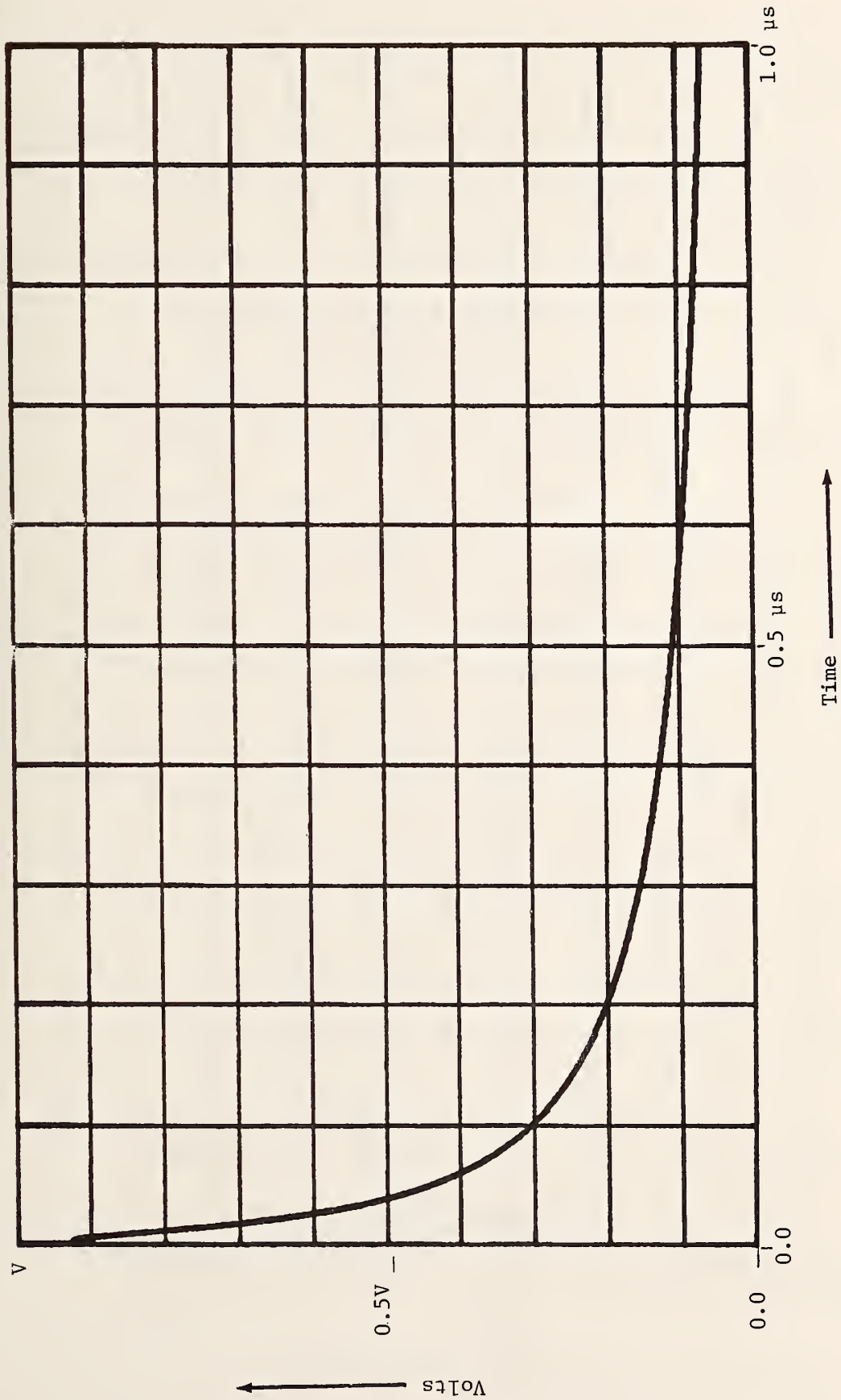


Figure 6.3. "One"-to-"zero" step response of 320.04 meters (1050 ft.) of cable I.

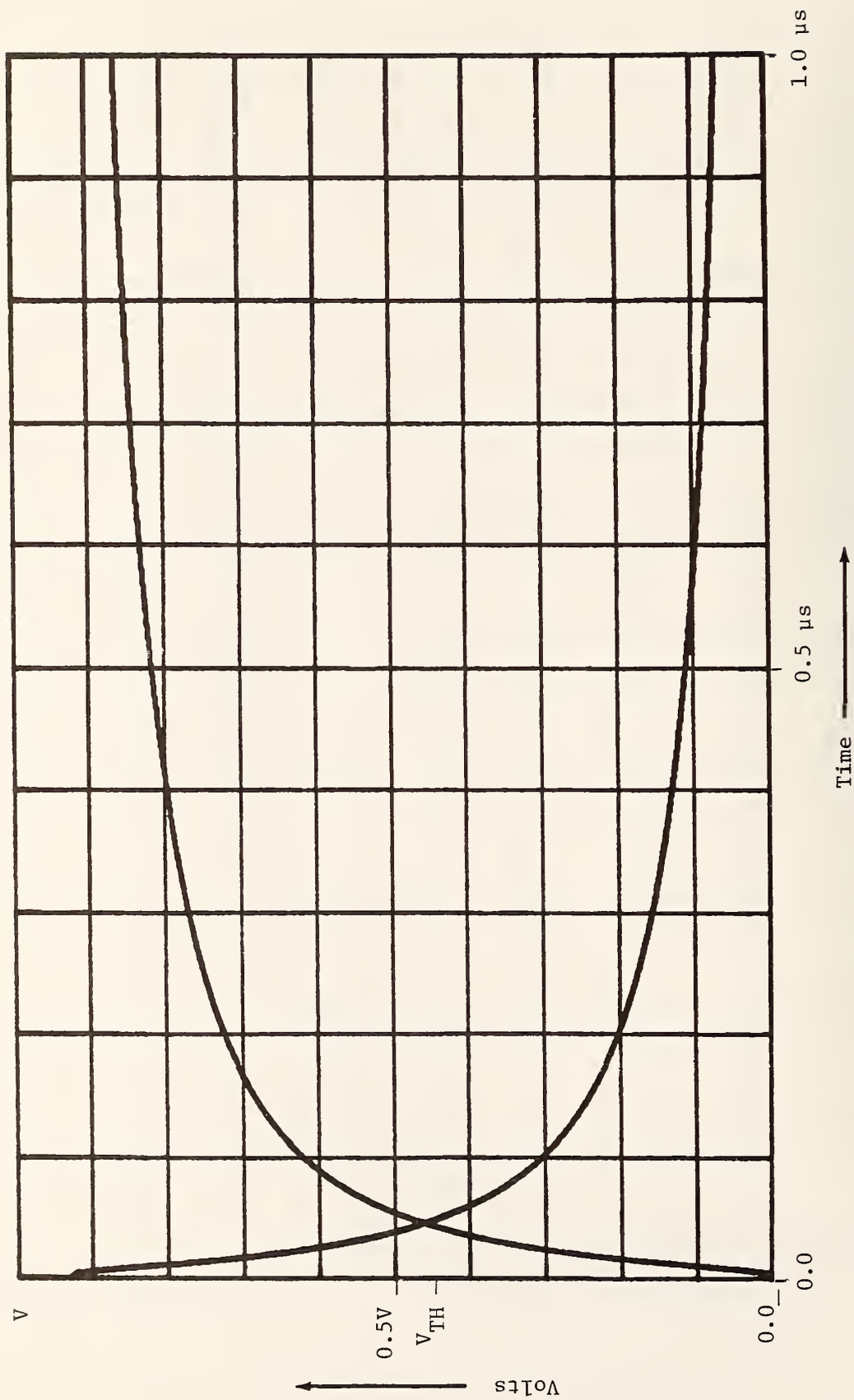


Figure 6.4. Superposition of positive and negative step responses of 320.03 meters (1050 ft.) of cable I.

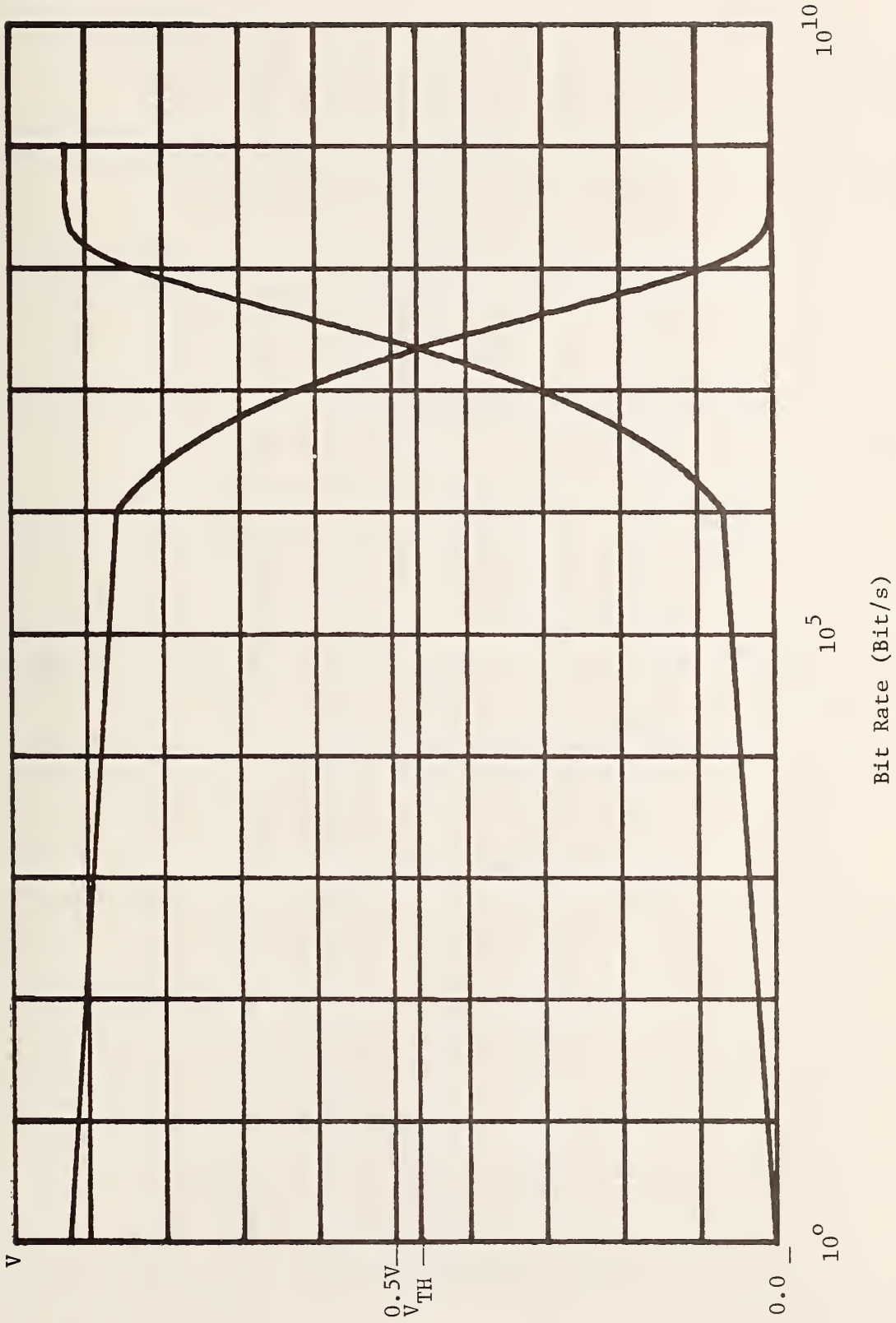


Figure 6.5. Superposition of positive and negative step responses of 320.04 meters (1050 ft.) of cable I plotted as a function of bit rate.

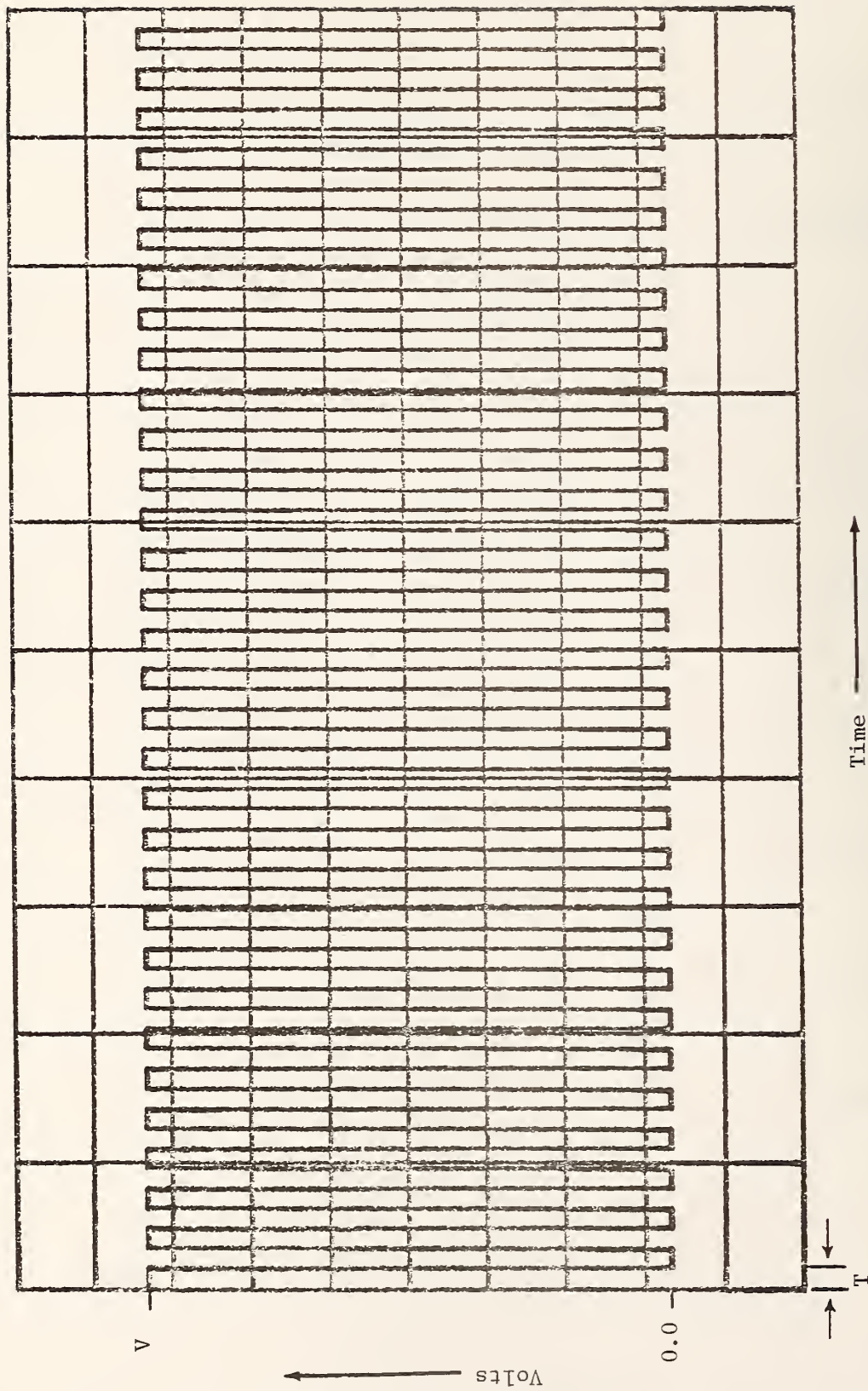


Figure 6.6a. Transmitter output signal consisting of 64 bits of alternating "ones" and "zeros" commencing at $t = 0$.

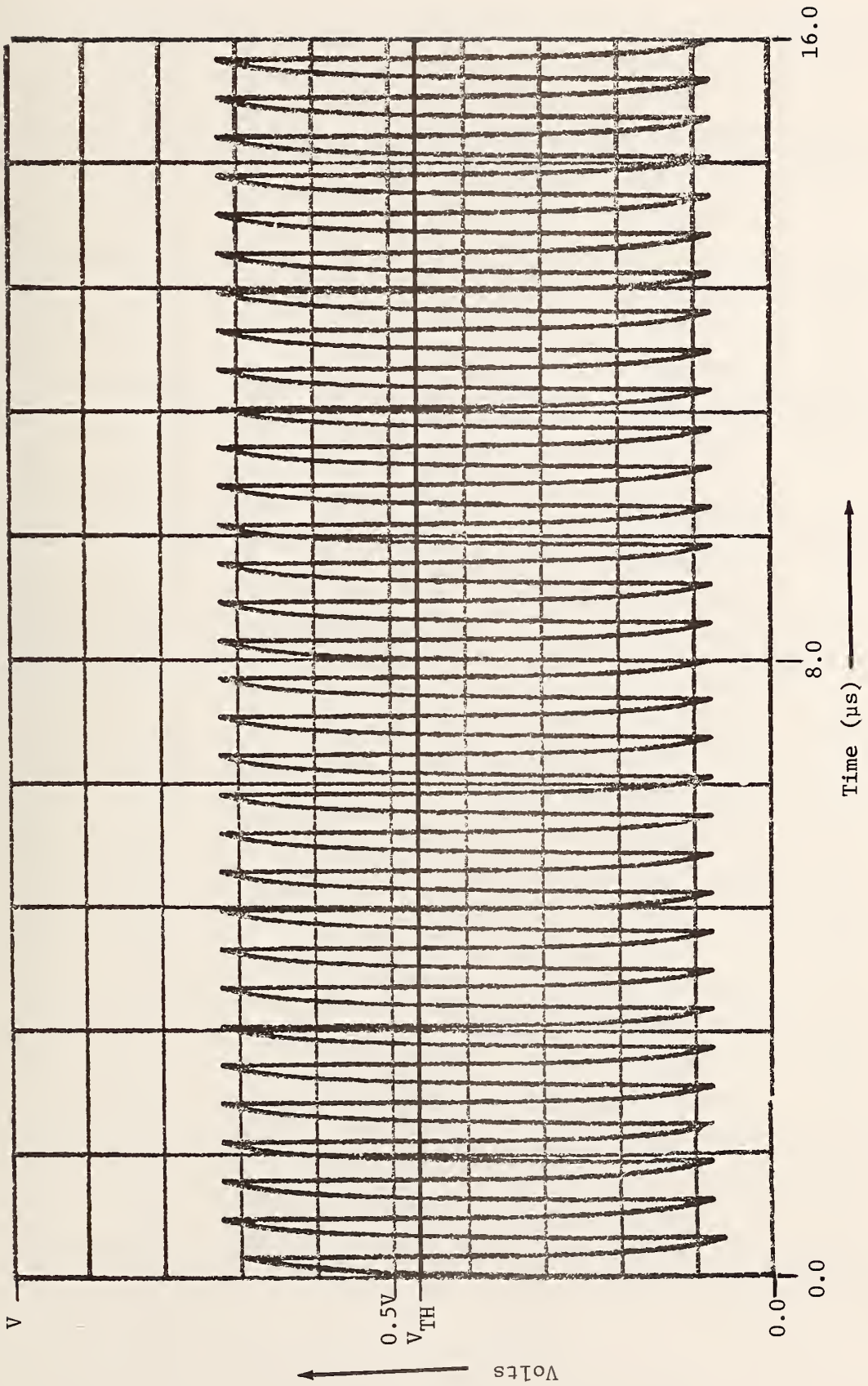


Figure 6.6b. Received signal response for transmitter bit rate of 4 Mb/s through 320.04 meters (1050 ft.) of cable I.

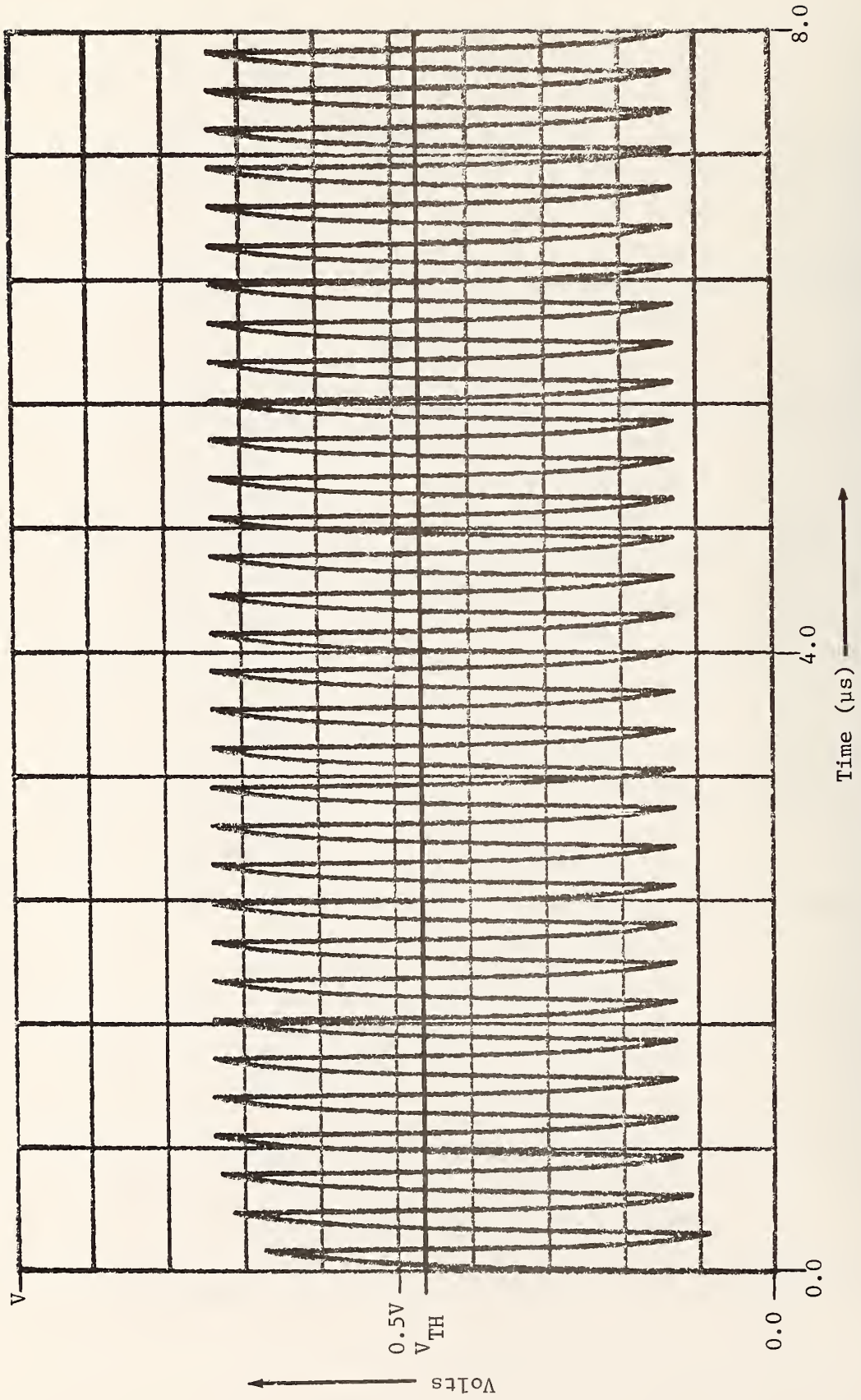


Figure 6.6c. Received signal response for transmitter bit rate of 8 Mb/s through 320.04 meters (1050 ft.) of cable I.

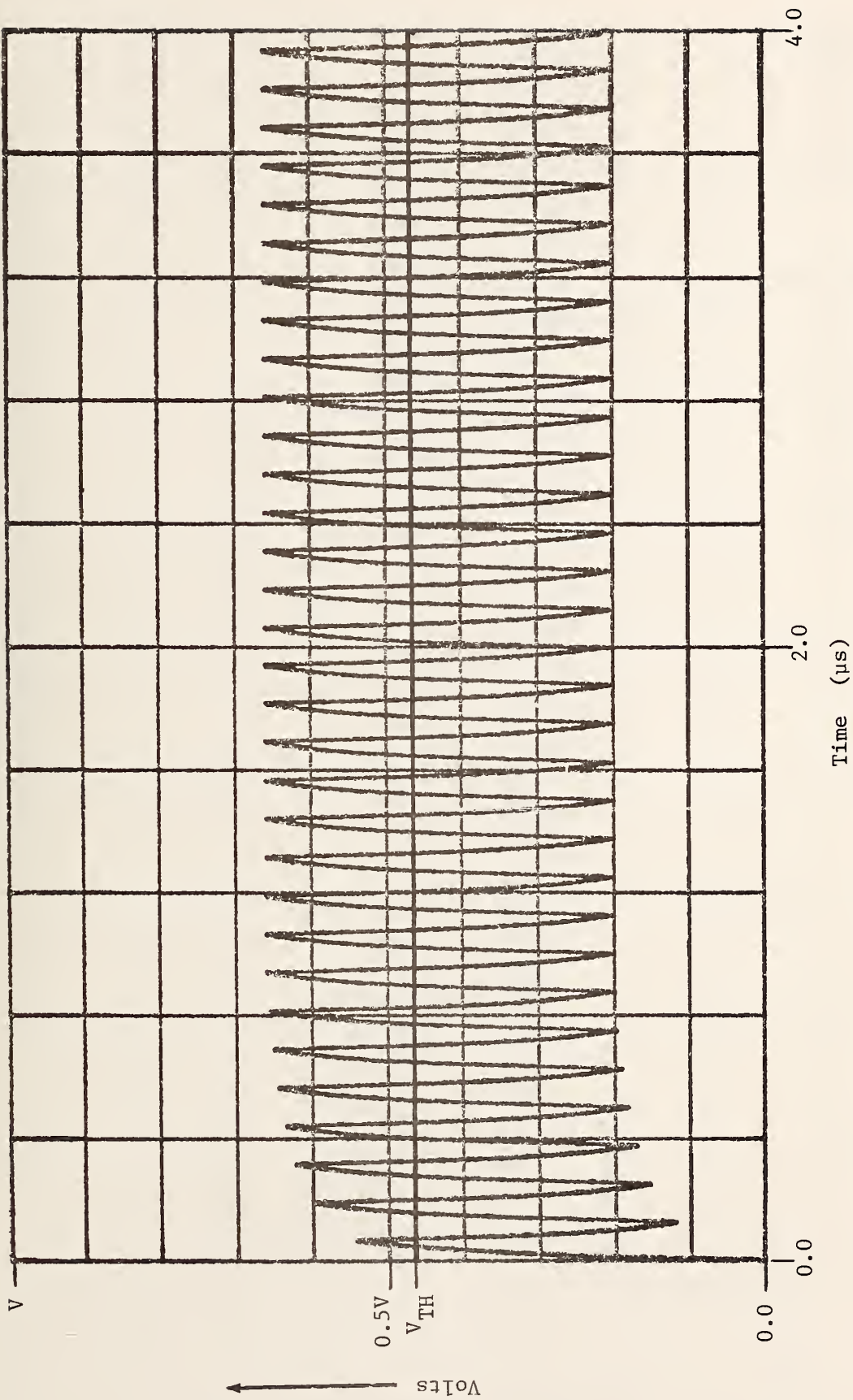


Figure 6.6d. Received signal response for transmitter bit rate of 16 Mb/s through 320.04 meters (1050 ft.) of cable I.

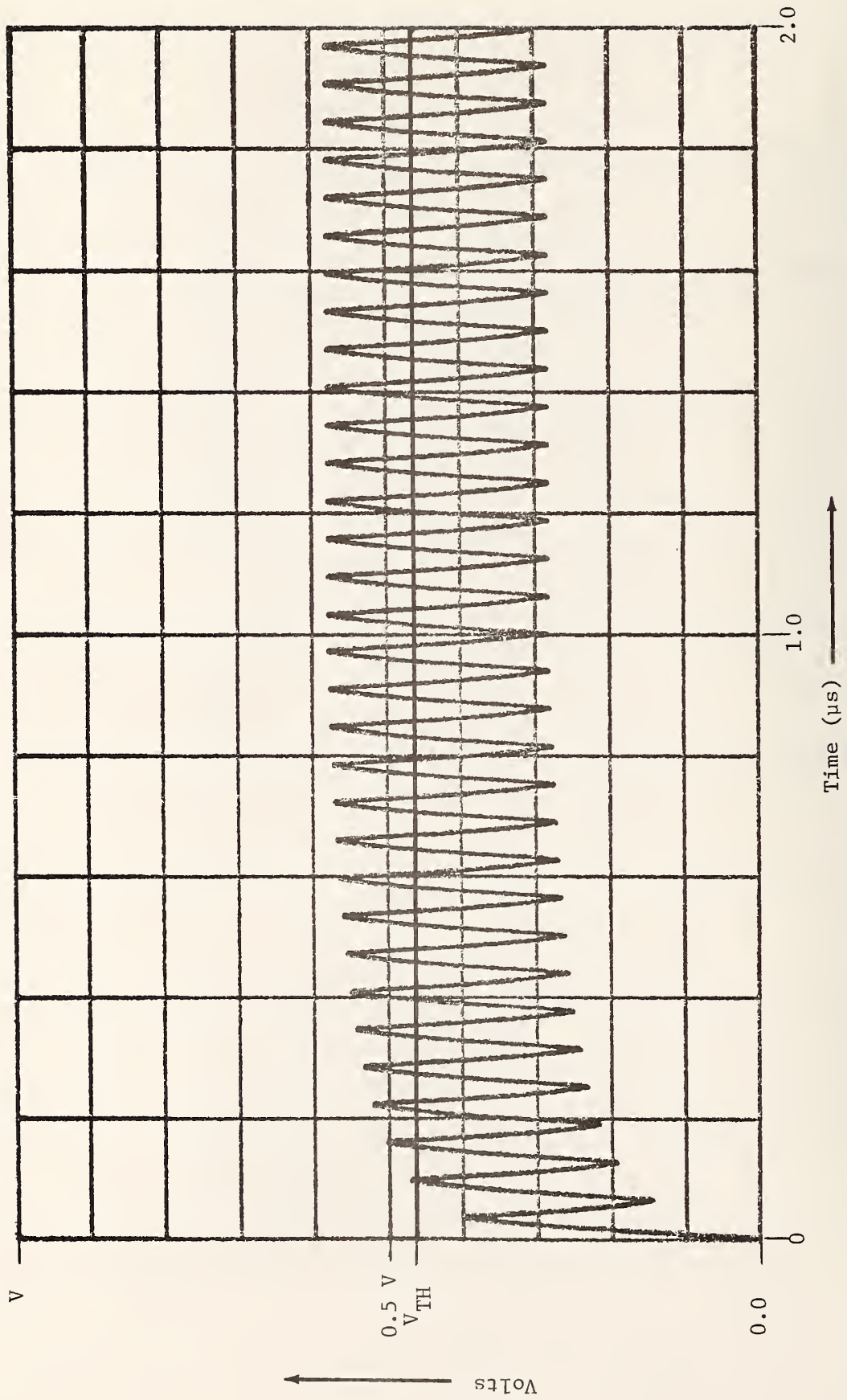


Figure 6.6e. Received signal response for transmitter bit rate of 32 Mb/s through 320.04 meters (1050 ft.) of cable I.

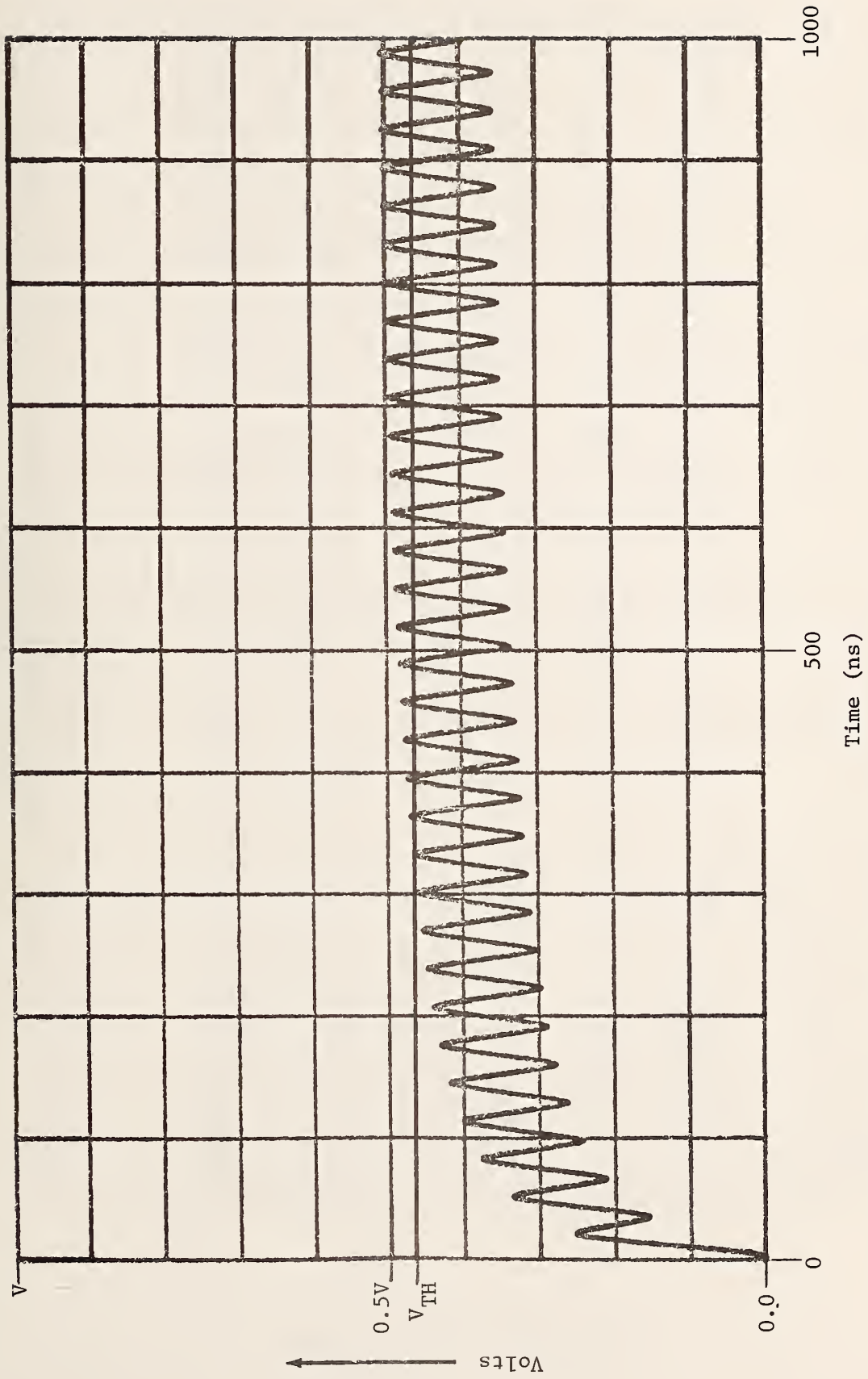


Figure 6.6f. Received signal response for transmitter bit rate of 64 Mb/s through 320.04 meters (1050 ft.) of cable I.

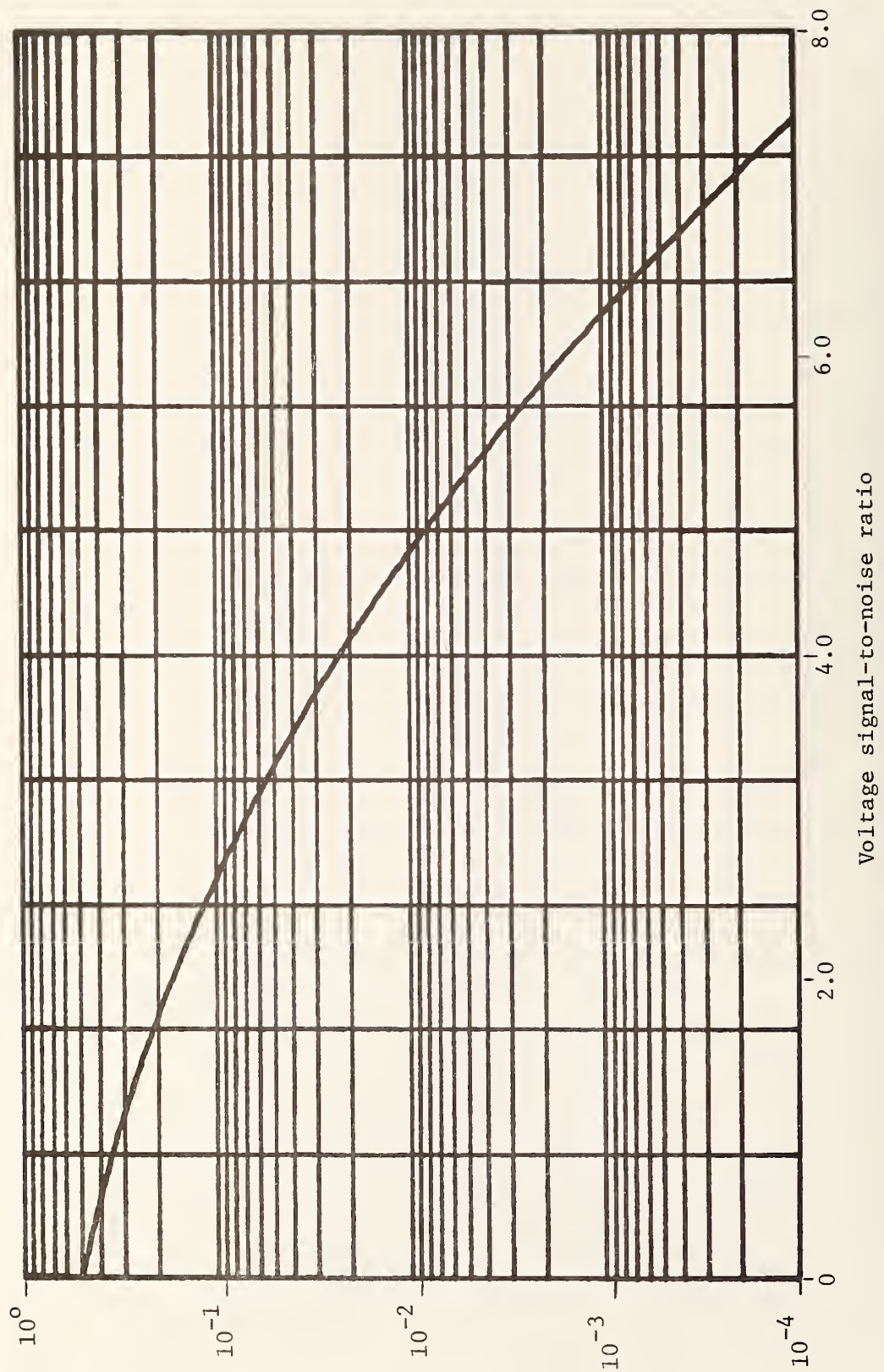


Figure 6.7a P(E) versus VSNR curve for VSNR from 0.0 to 8.0

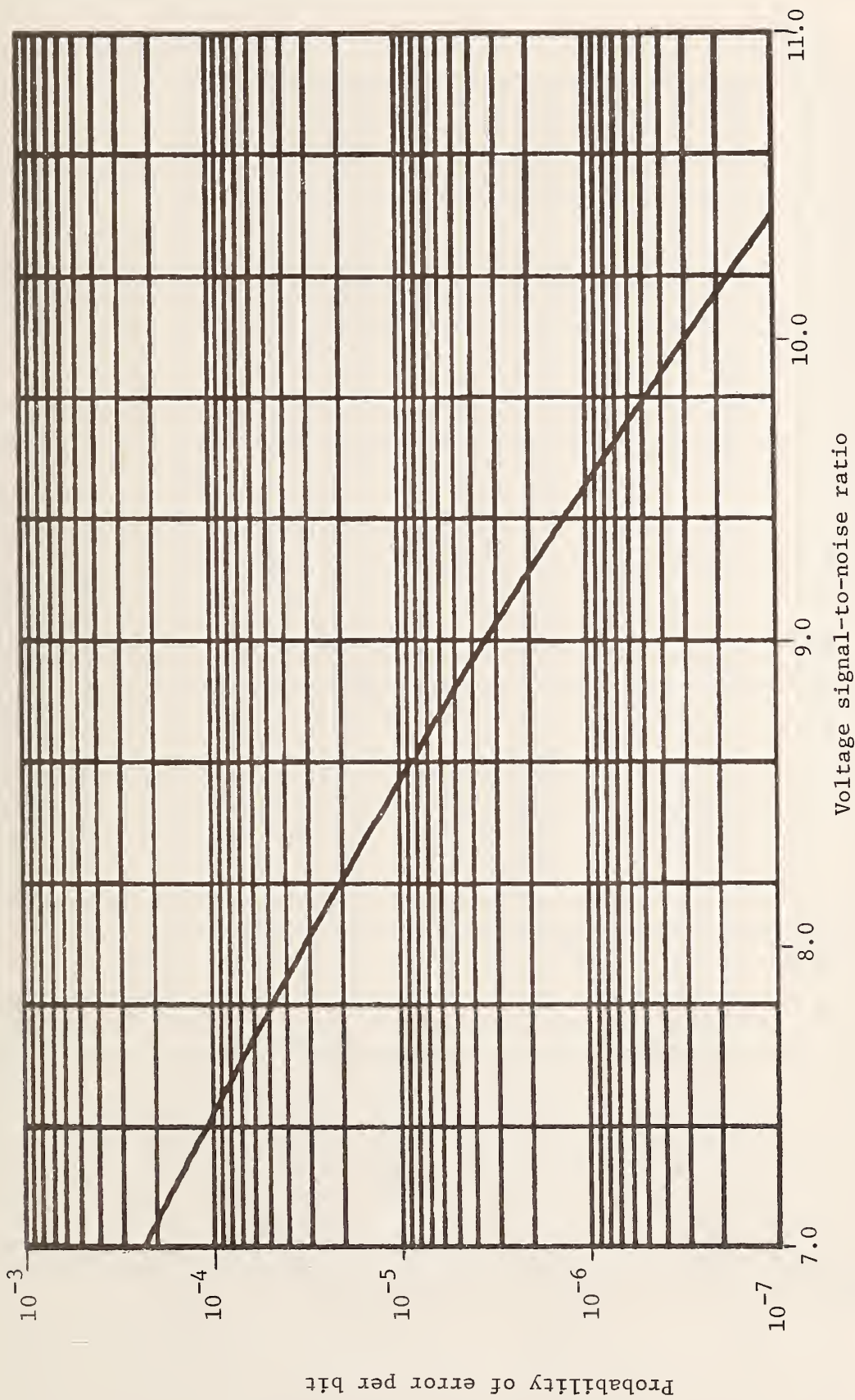


Figure 6.7b. $P(E)$ versus VSNR for VSNR from 7.0 to 11.0.

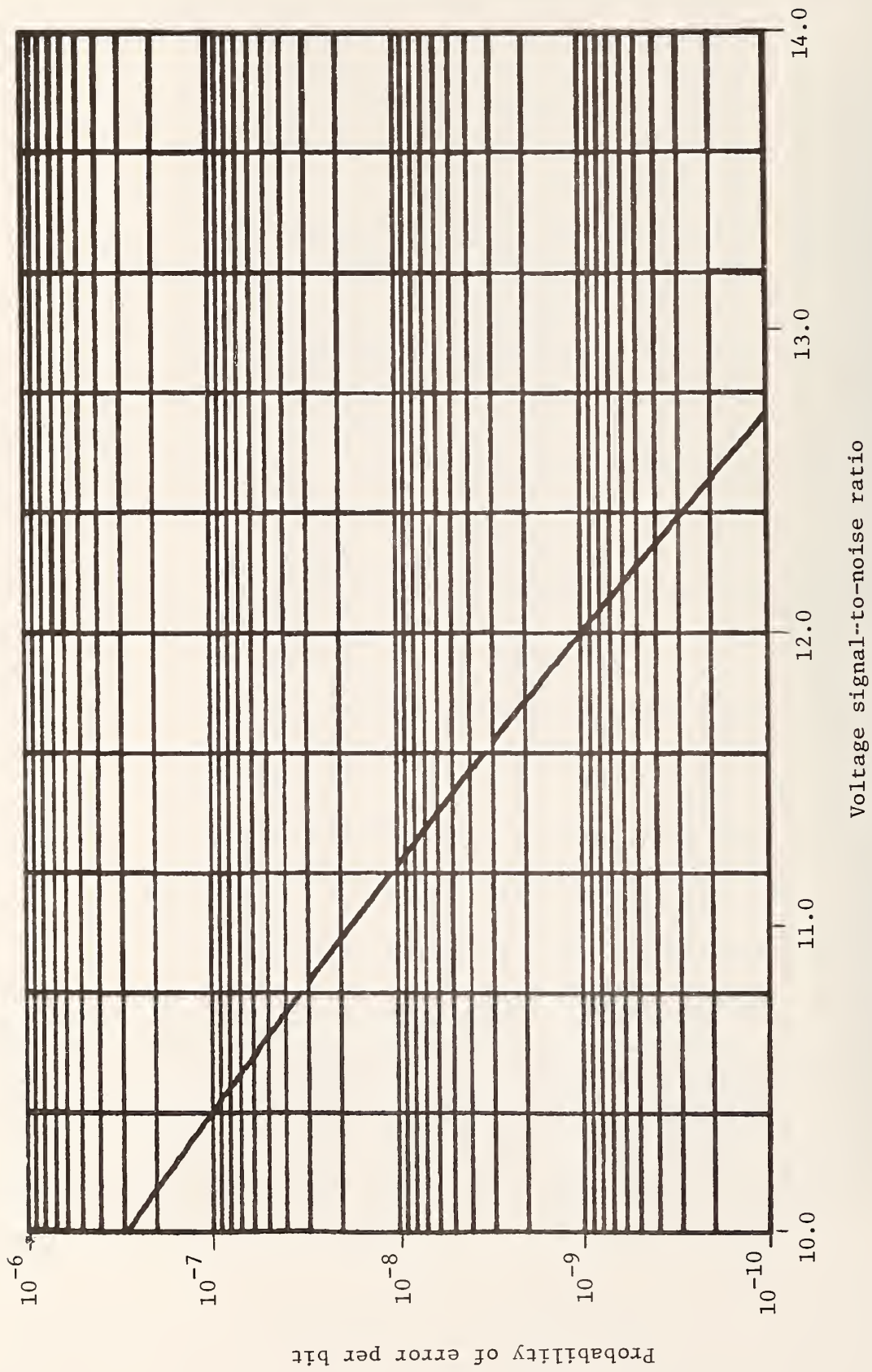


Figure 6.7c. P(E) versus VSNR for VSNR from 10.0 to 14.0.

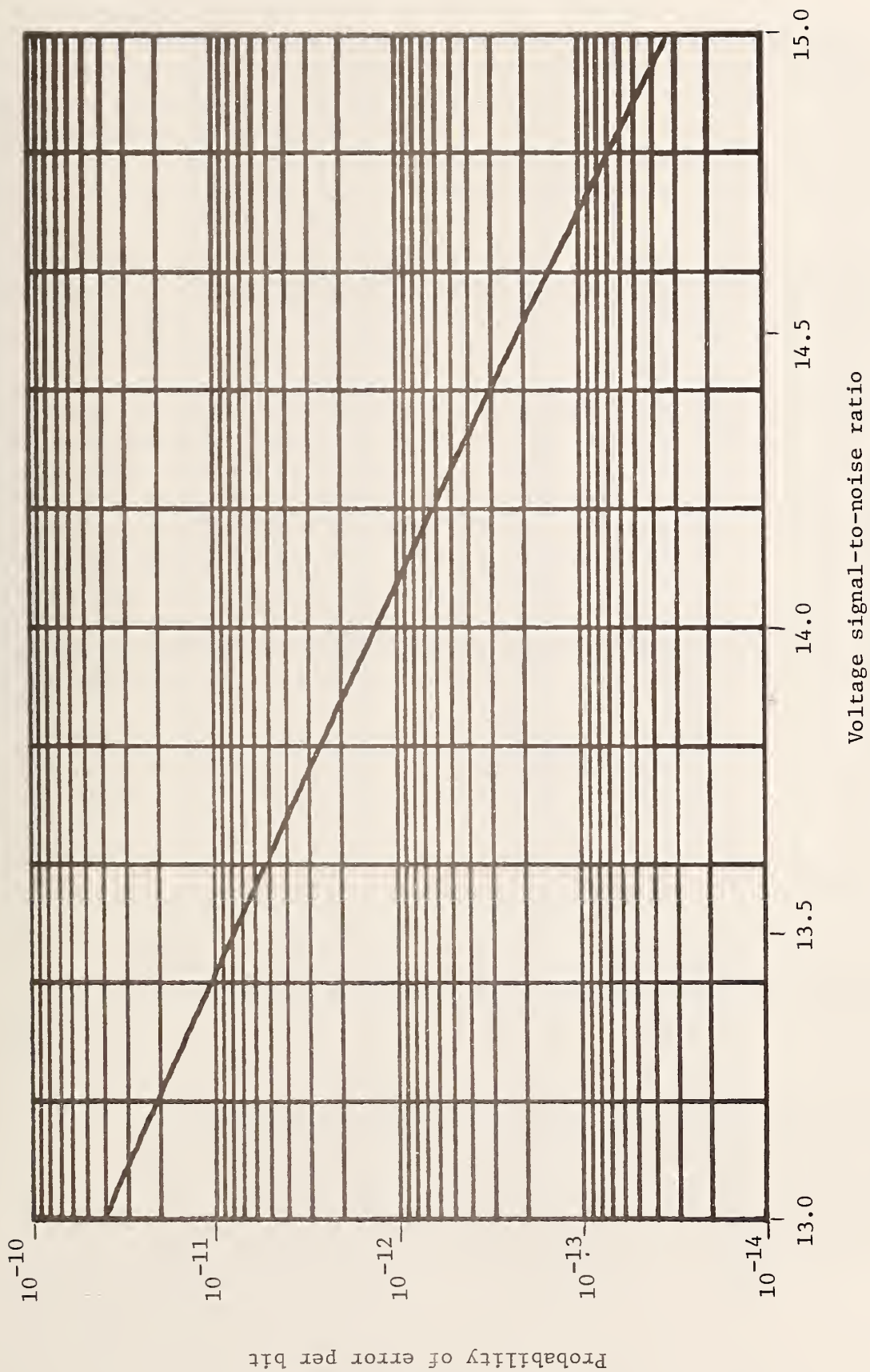


Figure 6.7d. $P(E)$ versus VSNR for VSNR from 13.0 to 15.0.

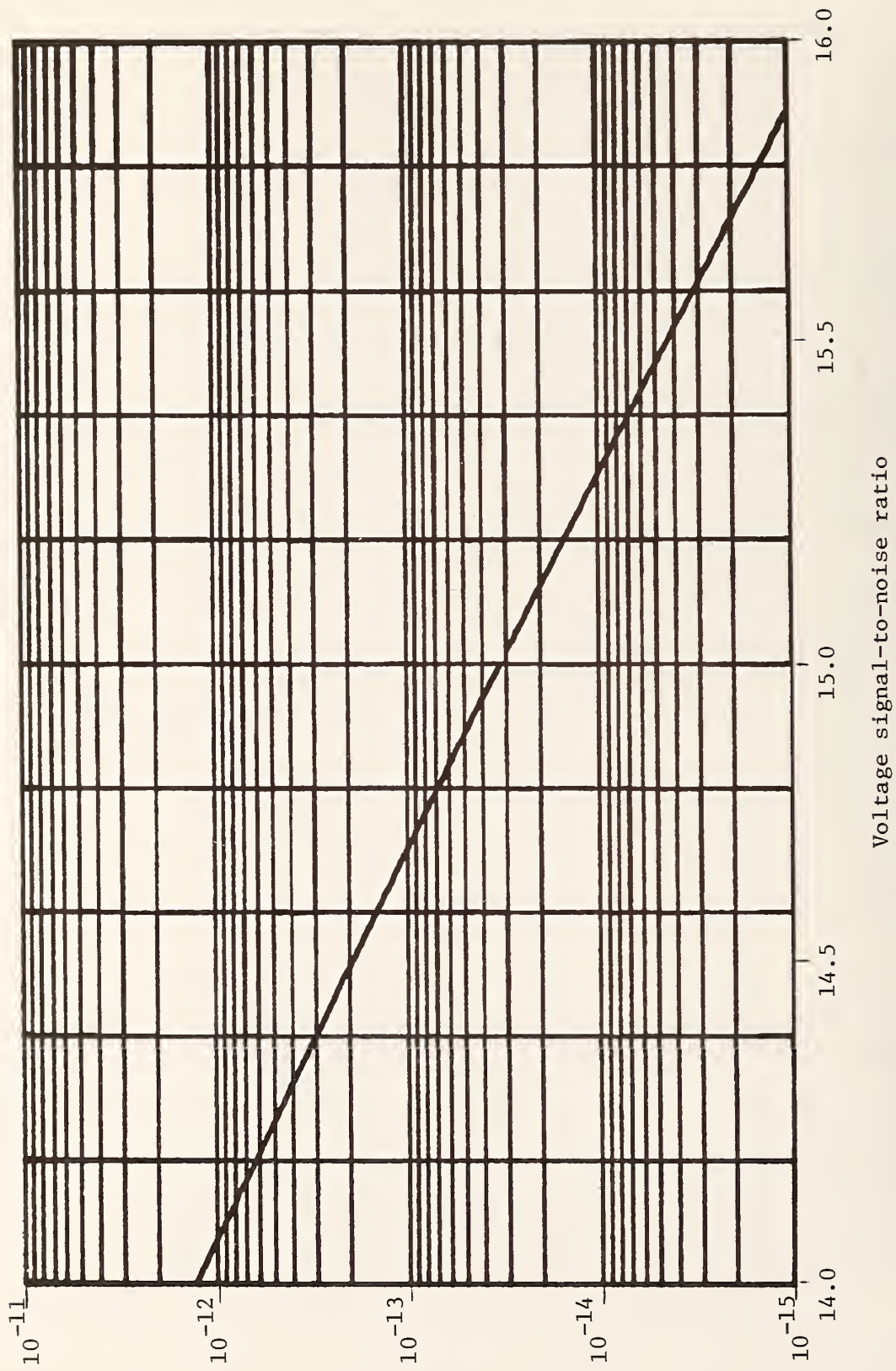


Figure 6.7e. $P(E)$ versus VSNR for VSNR from 14.0 to 16.0.

7. CABLE TESTING USING TIME DOMAIN REFLECTOMETRY

In this chapter the general principles of time domain reflection and transmission are developed and then are applied to cable testing. It is shown how the cable sending-end step responses are employed to calculate (simulate) the reference echoes (TDR responses) which characterize an undamaged cable. Departures from the reference response waveforms indicate uniform degradation of the cable and physical damage, or some combination of the two factors.

7.1 The General Theory of Time Domain Reflection and Transmission

In the classical frequency domain analysis of transmission lines containing reflections, the assumption is implicit that the sinusoidal signals are steady state signals, i.e., they have been present since the time minus infinity. In time domain measurements of transient or pulse phenomena, such is not the case. Prior to some time, say $t=0$, there was no signal present. When the pulse signal does enter the transmission line, it propagates along the line at a finite velocity arriving at observation points displaced from the input later in time. When this propagating signal encounters a discontinuity, reflected and transmitted signals are created. An observer remote from the point of reflection will not observe the reflected signal until still later in time due to the time isolation (delay) inherent in the transmission line. For people working with time domain measurements and instruments it is very important to comprehend this time isolation of reflections. As an aid to developing an understanding of this concept this section develops the analysis of a discretely loaded transmission line in terms of transmitted and reflected pulse trains. A reflection-transmission (RT) diagram is used. The resultant transmission line equations are then shown to be identical to those derived in the classical frequency domain manner.

The starting point for this discussion is based upon fig. 2.2 and the general equations (2-3) and (2-4). First, equation (2-4) is expressed in terms of $E_g(s)$ rather than $I_s(s)$ through the relation

$$I_s(s) = \frac{E_g(s) - E_s(s)}{Z_g(s)} \quad (7-1)$$

with the result

$$\frac{E_s(s)}{E_g(s)} = \left[\frac{Z_o(s)}{Z_g(s) + Z_o(s)} \right] \left[\frac{1}{1 - \rho_s(s)\rho_r(s)e^{-2\ell\gamma(s)}} \right] \left[1 + \rho_r(s)e^{-2\ell\gamma(s)} \right]. \quad (7-2)$$

For convenience, (2-3) is repeated here,

$$\frac{E_r(s)}{E_g(s)} = 2 \left[\frac{Z_o(s)}{Z_g(s) + Z_o(s)} \right] \left[\frac{Z_\ell(s)}{Z_\ell(s) + Z_o(s)} \right] \left[\frac{e^{-\ell\gamma(s)}}{1 - \rho_s(s)\rho_r(s)e^{-2\ell\gamma(s)}} \right]. \quad (7-3)$$

$\rho_s(s)$ and $\rho_r(s)$ are the reflection coefficients (2-5) produced by the sending and receiving end impedances, $Z_g(s)$ and $Z_\ell(s)$, respectively. ℓ is the transmission line length while $\gamma(s)$ and $Z_o(s)$ are the line propagation function and characteristic impedance, respectively.

The latter are given as

$$Z_o(s) = \left[\frac{Z(s)}{Y(s)} \right]^{1/2} \quad (2-1)$$

$$\gamma(s) = [Z(s) Y(s)]^{1/2} \quad (2-2)$$

where $Z(s)$ and $Y(s)$ are the transmission line equivalent circuit parameters: series impedance/unit length and shunt admittance/unit length. In general, for wave transmission on a transmission line $\gamma(s)$ is such that the limit

$$\lim_{|s| \rightarrow \infty} \left[\frac{\gamma(s)}{s} \right]$$

is equal to the time delay per unit length, T , i.e.,

$$T = \lim_{|s| \rightarrow \infty} \left[\frac{\gamma(s)}{s} \right] \quad (7-4)$$

For uniform transmission lines, the time delay/unit length is expressed in terms of the inductance and capacitance per unit length,

$$T = \sqrt{LC} \quad (7-5)$$

Also, $\gamma(s)$ can be written in the form

$$\gamma(s) = sT + \gamma'(s) \quad (7-6)$$

where sT is an all-pass function (linear phase function) and $\gamma'(s)$ is the minimum phase function (see section 2.4 for some discussion of minimum phase). For $\gamma'(s)$ to be a minimum phase function, the ratio $\gamma'(s)/s$ vanishes as $|s|$ becomes infinitely large [2].

Now consider a step generator of impedance $Z_o(s)$ applied to the system described by (7-2) and (7-3), i.e., $E_g(s) = 1/s$ and $Z_g(s) = Z_o(s)$. Then $\rho_s(s) = 0$, and (7-2) and (7-3) reduce to

$$E_s(s) = \frac{1}{2s} \left[1 + \rho_r(s) e^{-2\ell[sT + \gamma'(s)]} \right] \quad (7-7)$$

and

$$E_r(s) = \frac{1}{s} \left[\frac{Z_\ell(s)}{Z_o(s) + Z_\ell(s)} \right] e^{-\ell[sT + \gamma'(s)]} \quad (7-8)$$

Rewriting

$$E_s(s) = \frac{1}{2s} + e^{-2s\ell T} \left[\rho_r(s) e^{-2\ell\gamma'(s)} \right] \quad (7-9)$$

and

$$E_r(s) = e^{-s\ell T} \left\{ \frac{Z_\ell(s) e^{-\ell\gamma'(s)}}{s [Z_o(s) + Z_\ell(s)]} \right\} \quad (7-10)$$

Consideration of (7-9) and (7-10) leads to the following conclusions:

1. The input terminals of the line presents to the generator the characteristic impedance $Z_o(s)$ for the time interval $0 < t < 2lT$; i.e., the load impedance is not seen at the generator terminals until the incident wave travels to the load and the subsequent reflection returns to the generator terminals.
2. The output waveform is zero for $t < lT$; also, its shape is controlled by the characteristic impedance to load impedance voltage divider and the minimum phase (distorting) part of the propagation function, $\gamma'(s)$.

Generally, for arbitrary terminations, $E_s(s)$ and $E_r(s)$ each consist of an infinite sequence of terms similar to those in (7-9) and (7-10) and have their origins in the conclusions delineated above. By using the geometric series expansion

$$\left[1 - \rho_s(s)\rho_r(s)e^{-2l\gamma(s)} \right]^{-1} = \sum_{n=0}^{\infty} \left[\rho_s(s)\rho_r(s)e^{-2l\gamma(s)} \right]^n ; \quad (7-11a)$$

where

$$|\rho_s(s)\rho_r(s)e^{-2l\gamma(s)}|^2 < 1 \quad (7-11b)$$

in the second and third factors of (7-2) and (7-3), respectively, the transfer functions can be expressed as infinite sequences which represent impulse responses consisting of pulse trains. A note of caution should be entered here; for a lossless line the inequality condition in (7-11) may not be satisfied and hold for all values of s in the complex plane. Under such conditions an alternate mathematical procedure must be used [13].

Putting (7-11) into (7-2) and (7-3) yields the sending end pulse train

$$E_s(s) = E_g(s) \left[\frac{Z_o(s)}{Z_g(s) + Z_o(s)} \right] \times \sum_{n=0}^{\infty} \rho_s^n(s)\rho_r^n(s)e^{-2nl\gamma(s)} + \rho_s^n(s)\rho_r^{(n+1)}(s)e^{-(n+1)2l\gamma(s)} \quad (7-12)$$

and the receiving end pulse train,

$$E_r(s) = 2E_g(s) \left[\frac{Z_o(s)}{Z_g(s) + Z_o(s)} \right] \left[\frac{Z_l(s)}{Z_l(s) + Z_o(s)} \right] \times \sum_{n=0}^{\infty} \rho_s^n(s)\rho_r^n(s)e^{-(2n+1)l\gamma(s)} \quad (7-13)$$

where (7-12) and (7-13) are both subject to the condition specified in (7-11b). The physical situation represented by the pulse trains (7-12) and (7-13) is lucidly shown by a reflection-transmission (RT) diagram, fig. 7.1. In fact, the RT diagram itself provides an intuitive (but exact) means for writing out the terms of each pulse train.

The RT diagram is a signal flow chart embodying the reflection and transmission properties of the terminal impedances, and the wave propagation property of the connecting transmission line. To interpret the diagram the following rules are used:

1. Passage from a generator of impedance $Z_g(s)$ through a node to a line segment represents multiplication by the transfer function $Z_o(s)/[Z_g(s) + Z_o(s)]$.
2. Passage along a line segment represents multiplication by the transfer function $\exp[-l\gamma(s)]$.
3. Passage through a node to a load $Z_l(s)$ represents multiplication by the transfer function $2 Z_l(s)/[Z_l(s) + Z_o(s)]$.
4. Reflection from a node represents multiplication by the reflection coefficient $\rho_r(s) = [Z_l(s) - Z_o(s)]/[Z_l(s) + Z_o(s)]^{-1}$.

Application of the rules to the diagram in fig. 7.1 obtains the following results:

$$\begin{aligned}
 E_s(s) &= \left[E_g \frac{Z_o}{Z_g + Z_o} \right]_{\text{Gen to A}} + \left[E_g \frac{Z_o}{Z_g + Z_o} e^{-l\gamma} \rho_r e^{-l\gamma} \frac{2Z_g}{Z_g + Z_o} \right]_{\text{ABC}} \\
 &+ \left[E_g(s) \frac{Z_o}{Z_o + Z_g} e^{-l\gamma} \rho_r e^{-l\gamma} \rho_s e^{-l\gamma} \rho_r e^{-l\gamma} \frac{2 Z_g}{Z_g + Z_o} \right]_{\text{ABCDE}} + \dots \\
 &= E_g \frac{Z_o}{Z_g + Z_o} \left\{ 1 + \frac{2\rho_r Z_g}{Z_g + Z_o} e^{-2l\gamma} + \frac{2\rho_r^2 \rho_s Z_g}{Z_g + Z_o} e^{-4l\gamma} + \dots \right\} \quad (7-14)
 \end{aligned}$$

Since

$$\rho_i = \frac{Z_i - Z_o}{Z_i + Z_o}$$

the voltage divider may be written as

$$\frac{Z_i}{Z_i + Z_o} = \frac{1 + \rho_i}{2}.$$

Putting $(1 + \rho_s)/2$ into (7-14) for the factor $Z_g/(Z_g + Z_o)$ obtains the result

$$E_s(s) = E_g \frac{Z_o}{Z_g + Z_o} \left[1 + \rho_r (1 + \rho_s) e^{-2l\gamma} + \rho_r^2 \rho_s (1 + \rho_s) e^{-4l\gamma} + \dots \right] \quad (7-15)$$

which is identical to that given by expansion of (7-12). Therefore, it has been demonstrated that the RT diagram allows one to write down the equation for $E_s(s)$ directly by tracing out the signal flow while invoking the rules 1-4.

Similarly, the received voltage $E_r(s)$ is obtained from the RT diagram as

$$\begin{aligned}
E_r(s) &= \left[\begin{array}{c} E_g \frac{Z_o}{Z_g + Z_o} \\ \text{Gen to A} \end{array} \right] \left[\begin{array}{c} e^{-\ell\gamma} \frac{2Z_\ell}{Z_\ell + Z_o} \\ \text{AB} \end{array} \right] \\
&+ \left[\begin{array}{c} E_g \frac{Z_o}{Z_g + Z_o} e^{-2\ell\gamma} \rho_r e^{-\ell\gamma} \rho_s e^{-\ell\gamma} \frac{2Z_\ell}{Z_\ell + Z_o} \\ \text{ABCD} \end{array} \right] + \dots \\
&= 2 E_g \frac{Z_o}{Z_g + Z_o} \frac{Z_\ell}{Z_\ell + Z_o} \left[e^{-\ell\gamma} + \rho_r \rho_s e^{-3\ell\gamma} + \dots \right] \quad (7-16)
\end{aligned}$$

which is identical to that found by expanding (7-13).

In this report the transmission lines are lossy and are normally operated in a doubly mismatched condition due to the terminations being equal to the nominal high frequency characteristic impedance, R_o . Under such conditions, (7-15) and (7-16) become

$$E_s(s) = E_g(s) \frac{Z_o(s)}{R_o + Z_o(s)} \left[1 + \rho_r(1+\rho_s)e^{-2\ell\gamma(s)} + \rho_r\rho_s(1+\rho_s)e^{-4\ell\gamma(s)} + \dots \right] \quad (7-17)$$

and

$$E_r(s) = 2 E_g(s) \frac{Z_o(s) R_o}{[R_o + Z_o(s)]^2} \left[e^{-\ell\gamma(s)} + \rho^2 e^{-3\ell\gamma(s)} + \dots \right] \quad (7-18)$$

respectively, where

$$\rho = \rho_r = \rho_s = \frac{R_o - Z_o(s)}{R_o + Z_o(s)}. \quad (7-19)$$

Briefly, consider the received voltage $E_r(s)$. Inspection of (7-18) shows that the initial signal transfer function is due to the product of the RT input voltage transfer function, the exponential transmission factor, and the output RT voltage transfer function, i.e.,

$$E_r(s) \Big|_{0 < t < 3\ell T} = 2E_g(s) \left[\frac{Z_o(s)}{Z_o(s) + R_o} \times e^{-\ell\gamma(s)} \times \frac{R_o}{Z_o(s) + R_o} \right]. \quad (7-20)$$

This is in agreement with the RT diagram transmission/reflection rules. The condition $0 < t < 3\ell T$ describes the time interval of the initial response, which is to say that the inverse Laplace transform of (7-20) represents the time domain response only over the interval $0 < t < 3\ell T$. Refer to fig. 7-2 and the brief discussion in its caption.

$$e_r(t) = \mathcal{L}^{-1} \left[2E_g(s) \frac{Z_o(s) R_o}{Z_o(s) + R_o} e^{-\ell\gamma(s)} \right]; \quad 0 < t < 3\ell T. \quad (7-21)$$

It is important to keep in mind that (7-21) is the exact response for $e_r(t)$ over the interval $0 < t < 3\ell T$. What is unusual about this method of analysis is that even though a series expansion (7-11) has been used, a finite sequence of terms starting from the initial term is always an exact result out to some multiple of

the time ℓT . Contrast this with other series expansions where an infinite number of terms must be present for an exact result, e.g., Fourier Series, etc. The discussion now turns to the sending-end response.

The main purpose of this chapter is to develop the sending end response so that one would have a reference response or waveform for a given cable type; this response would then be used to evaluate the measured test response of samples of the given cable type. To conclude this section, consider (7-17). It is clear that for the time interval $0 < t < 2\ell T$ the response is only dependent upon the transmission line through the characteristic impedance, $Z_o(s)$, and is given by the first term from the sequence (7-17)

$$\left[E_s(s) \right]_{0 < t < 2\ell T} = E_g(s) \frac{Z_o(s)}{R_o + Z_o(s)} \quad (7-22)$$

In the next section this relation will be used to derive the reference responses. After the passage of $2\ell T$ seconds, the second term in the sequence must be added to the first to provide the temporal response out to $4\ell T$ seconds

$$\left[E_s(s) \right]_{0 < t < 4\ell T} = E_g(s) \left[\frac{Z_o(s)}{R_o + Z_o(s)} + \frac{Z_o(s)}{R_o + Z_o(s)} \rho_r (1 + \rho_s) e^{-2\ell\gamma(s)} \right] \quad (7-23)$$

Now consider the second term in detail; the term $(1 + \rho_s)$ is just $2 R_o / [R_o + Z_o(s)]$ which is the RT transfer function from the transmission line to the load R_o ; ρ_r is the reflection coefficient of the receiving end load. $Z_o(s) / [R_o + Z_o(s)]$ is the RT transfer function from the generator to the sending end, and $\exp.[-2\ell\gamma(s)]$ represents transmission over a length 2ℓ . Consequently, the second term has a physical picture which correlates with the RT diagram as follows:

$$\underbrace{\left[\frac{Z_o(s)}{R_o + Z_o(s)} \right] \times e^{-\ell\gamma(s)} \times \left[\frac{2 R_o}{R_o + Z_o(s)} \right]}_{\text{Initial voltage at receiving end (7-20)}} \times \underbrace{\left[\rho \right] \times e^{-\ell\gamma(s)}}_{\text{Reflection factor and transmission back to sending end.}}$$

In other words, the initial sending end voltage is transmitted to the load; the received voltage is then scaled by the reflection coefficient and then transmitted back to the sending end. Figure 7-3 qualitatively illustrates the time domain unit step response corresponding to (7-23). In the next section the time domain expressions for unit step excitation will be derived.

7.2 The Step Response of the Sending-End Voltage

The sending-end voltage $E_s(s)$ for $0 \leq t \leq 2\ell T$ due to a unit step is obtained from (7-22) by letting

$$E_g(s) = \frac{1}{s} \quad (7-24)$$

which obtains for the sending-end voltage

$$E_s(s) = \frac{1}{s} \frac{Z_o(s)}{R_o + Z_o(s)} ; \quad 0 \leq t \leq 2\ell T . \quad (7-25)$$

The time domain sending-end voltage is given by

$$e_s(t) = \mathcal{L}^{-1} \left\{ \frac{1}{s} \frac{Z_o(s)}{R_o + Z_o(s)} \right\} \quad 0 \leq t \leq 2\ell T . \quad (7-26)$$

This expression is also valid for all time t when the receiving-end is terminated in the characteristic impedance, $Z_o(s)$, that is; when there are no reflections from the receiving-end, the line appears to be infinitely long. For a finite length, ℓ , $e_s(t)$ is only valid for $0 \leq t \leq 2\ell T$. In terms of a circuit model, $e_s(t)$ represents a voltage division of the generator voltage, $e_g(t)$, fig. 7-4A. Qualitatively, the response is shown in fig. 7.3. If there were no reflection from the load (receiving-end), the waveform would continue to rise monotonically to unity, fig. 7.4B. From the final value theorem of the Laplace transformation, the final value of (7-26) is

$$e_s(\infty) = \lim_{|s| \rightarrow 0} s \left[\frac{1}{s} \frac{Z_o(s)}{R_o + Z_o(s)} \right] = 1 \quad (7-27)$$

Note that (7-26) is independent of ℓ ; that is to say, the step response of any length of cable will follow (7-26) until the first reflection arrives at the sending-end ($t = 2\ell T$).

Expressing (7-25) in terms of the model parameters gives

$$\begin{aligned} E_s(s) &= \frac{1}{s} \frac{\left[\frac{R + sL + Ks^m}{sC} \right]^{1/2}}{R_o + \left[\frac{R + sL + Ks^m}{sC} \right]^{1/2}} \\ &= \frac{1}{s} \frac{R_o \left[1 + \frac{R + Ks^m}{sL} \right]^{1/2}}{R_o + R_o \left[1 + \frac{R + Ks^m}{sL} \right]^{1/2}} \\ E_s(s) &= \frac{1}{s} \frac{\left[1 + \frac{R + Ks^m}{sL} \right]^{1/2}}{1 + \left[1 + \frac{R + Ks^m}{sL} \right]^{1/2}} . \end{aligned} \quad (7-28)$$

For large s (small t) (7-28) can be expanded as the ratio of two power series,

$$E_s(s) = \frac{1}{s} \frac{1 + \frac{v}{2} - \frac{v^2}{2 \cdot 4} + \frac{3 v^3}{2 \cdot 4 \cdot 6} - \frac{3.5 v^4}{2 \cdot 4 \cdot 6 \cdot 8} + \dots}{2 + \frac{v}{2} - \frac{v^2}{2 \cdot 4} + \frac{3 v^3}{2 \cdot 4 \cdot 6} - \frac{3.5 v^4}{2 \cdot 4 \cdot 6 \cdot 8} + \dots} \quad (7-29)$$

where

$$v = \frac{R + Ks^m}{sL} \quad (7-30)$$

and

$$|v| = \left| \frac{R + Ks^m}{sL} \right| < 1 \quad (7-31)$$

If the condition (7-31) is violated, the expansion (7-29) is not valid. By dividing the denominator of (7-29) into its numerator a single series in v can be obtained. This is easily done using the following method. If the product of two polynomials in v is given by

$$Y = HX$$

then the k -th coefficient of Y is given by

$$y(k) = \sum_{i=1}^{k-1} h(i) x(k+1-i). \quad (7-32)$$

For example,

$$\begin{aligned} y(1) &= h(1) x(1) \\ y(2) &= h(1) x(2) + h(2)x(1) \\ &\vdots \\ &\vdots \end{aligned}$$

and

$$Y = h(1) + h(2)v + h(3) v^2 + \dots$$

By writing out a few terms in the product, and starting with $x(1) \neq 0$, it is possible to solve for $h(k)$, i.e., the quotient of Y/X . The result is

$$h(k) = \frac{1}{x(1)} \left[y(k) - \sum_{i=1}^{k-1} h(i) x(k+1-i) \right] \quad (7-33)$$

where

$$\begin{aligned} h(1) &= \frac{y(1)}{x(1)} \\ h(2) &= \frac{1}{x(1)} \left[Y(2) - h(1) x(2) \right] \\ &\vdots \\ &\vdots \end{aligned}$$

Consequently (7-29) can be replaced by

$$E_s(s) = \frac{1}{2s} + \frac{1}{8s} v - \frac{1}{16s} v^2 + \frac{5}{128s} v^3 - \frac{14}{512s} v^4 + \dots \quad (7-34)$$

The series (7-34) is also convergent for

$$|v(s)| = \left| \frac{R + Ks^m}{sL} \right| < 1. \quad (7-35)$$

Upon substituting $v(s)$ into the series (7-34) there results a series having terms of the form As^{-q} and Bs^{-r} where q is an integer $1, 2, 3, \dots$, and r is not an integer. The time domain response is obtained by taking the inverse Laplace transform of each term using the appropriate transform pair

$$\frac{A}{s^q} \longleftrightarrow A \frac{t^{q-1}}{\Gamma(q)} u(t) \quad (7-36)$$

$$\frac{B}{s^r} \longleftrightarrow \frac{B t^{r-1}}{\Gamma(r)} u(t) \quad (7-37)$$

where $u(t)$ is the unit step and $\Gamma(r)$ the gamma function. The non integers r result from the fractional power m , $0 < m < 1$, which appears in the high frequency loss term of the model, Ks^m . The resultant time domain response is

$$e_s(t) = \frac{1}{2} u(t) + \frac{1}{8} w_1(t) - \frac{1}{16} w_2(t) + \frac{5}{128} w_3(t) - \frac{7}{256} w_4(t) + \dots \quad (7-38)$$

or in terms of the coefficient b_n ,

$$e_s(t) = \frac{1}{2} u(t) + \sum_{n=1}^{\infty} b_n w_n(t) \quad (7-39)$$

where

$$w_n(t) = \sum_{i=0}^n \frac{a_{ni} R^{n-i} K^i}{L^n \Gamma[(n+1) - im]} t^{n-im} u(t) \quad (7-40)$$

$$a_{ni} = \frac{n!}{i! (n-i)!} \quad (7-41)$$

$$b_n = \frac{\prod_{i=1}^n (2i-1)}{(2n+2) \prod_{i=1}^n (2i)} (-1)^{n+1} \quad (7-42)$$

$$n! = \Gamma(n+1) \quad (7-43)$$

$$\Gamma(n+1) = n \Gamma(n). \quad (7-44)$$

For examples of the expansion of $w_n(t)$, (7-40), $w_1(t)$ through $w_4(t)$ are given below.

$$w_1(t) = \frac{R}{L \Gamma(2)} t u(t) + \frac{K}{L \Gamma(2-m)} t^{1-m} u(t) \quad (7-45)$$

$$w_2(t) = \frac{R^2}{L^2 \Gamma(3)} t^2 u(t) + \frac{2RK}{L^2 \Gamma(3m)} t^{2-m} u(t) + \frac{K^2}{L^2 \Gamma(3-2m)} t^{2-m} u(t) \quad (7-46)$$

$$w_3(t) = \frac{R^3}{L^3 \Gamma(4)} t^3 u(t) + \frac{3R^2K}{L^3 \Gamma(4-m)} t^{3-m} u(t) + \frac{3RK^2}{L^3 \Gamma(4-2m)} t^{3-2m} u(t) \\ + \frac{K^3}{L^3 \Gamma(4-3m)} t^{3-3m} u(t) \quad (7-47)$$

$$w_4(t) = \frac{R^4}{L^4 \Gamma(5)} t^4 u(t) + \frac{4R^3K}{L^4 \Gamma(5-m)} t^{4-m} u(t) + \frac{6R^2K^2}{L^4 \Gamma(5-2m)} t^{4-2m} u(t) \\ + \frac{4RK^3}{L^4 \Gamma(5-3m)} t^{4-3m} u(t) + \frac{K^4}{L^4 \Gamma(5-4m)} t^{4-4m} u(t) \quad (7-48)$$

For a given cable, certain precautions must be taken before using the time domain series (7-38) to calculate the sending-end voltage $e_s(t)$. First of all, the condition (7-35) must be satisfied for all frequencies comprising the sending-end step response voltage $e_s(t)$. As can be seen from (7-35), there is a lower limit on $|s|$, i.e., a lower frequency limit, f_o . Letting $s = j\omega$ in (7-35) obtains

$$\left| \frac{R/L}{j\omega} + \frac{(K/L)}{(j\omega)^{1-m}} \right| < 1 \quad (7-49)$$

which can be expressed as

$$\frac{K^2}{\omega^{2(1-m)} L^2} + \frac{R^2}{\omega^2 L^2} + \frac{2RK}{\omega^{2-m} L^2} \sin \frac{(1-m)\pi}{2} < 1. \quad (7-50)$$

The frequency, $f = \omega/2\pi$, at which the left hand side of (7-50) just equals unity is defined as f_o . For frequencies equal to and less than f_o , the series (7-34) will not converge to $E_s(s)$. Consequently, the corresponding time domain series (7-38) will diverge for time greater than some value T_1 , which should be of the order of the reciprocal of f_o , i.e.,

$$T_o = 1/f_o .$$

T_1 can not be exactly specified due to the uncertainty properties of the Fourier (and Laplace)

transformation which prohibits a one to one correspondence between points in the time and frequency domain.

To demonstrate the application of the time domain step response, equation (7-38), and also its convergence properties, the sending-end step response of Cable I has been simulated using (7-38); the cable parameters are given in section 5.1. Figures 7-5 and 7-6 show the responses for the time windows of 5 and 10 microseconds, respectively. Note the initial jump to 0.5 and the subsequent slow rise thereafter increasing only by 10 to 12% of the final value (1.0). For each response the largest error occurs at the last point; they are 1.5×10^{-4} volts ($1.5 \times 10^{-2}\%$) and 3.3×10^{-3} volts (0.33%) for figs. 7.5 and 7.6, respectively. The errors occur due to the use of a finite number of terms of the series $e_s(t)$, (7-38). For figs. 7.5 and 7.6 the truncated series for (7-38) consisted of the first term $0.5 u(t)$ plus the weighted values of $w_1(t)$ through $w_6(t)$, a total of 28 terms. The error was computed by taking the magnitude of the difference between results for the truncated series and a second truncated series containing one more weighted value of $w_1(t)$. The second truncated series contained $w_8(t)$ and thus contained a total of 36 terms.

Turning now to the divergent properties of the series, it is known that (7-34) will not converge for values of $|s|$ along the real frequency axis, i.e., $|\omega|$, when ω is equal to or less than $2\pi \times 28 \times 10^3$, $f_o = 28$ KHz, (7-50). Consequently, in the neighborhood of $t=T_o=1/f_o = 35.7$ microseconds, the time domain response (7-38) should diverge even when an infinite number of its terms are used. Truncation of the series should lead to a divergent result well before 35.7 microseconds; that such is the case is shown in fig. 7-7.

Figure 7-7 presents the step responses for the time interval of 40 microseconds as a function of the number of terms of (7-38). The label 10 corresponds to 10 terms comprised of $0.5 u(t)$ plus the algebraic sum of the weighted values of $w_1(t)$ through $w_3(t)$. Similarly, 15 corresponds to 15 terms obtained from the algebraic sum of the weighted terms through $w_4(t)$. The largest number of terms, 36 yields the most accurate result. For example, at $t=10$ microseconds the responses for 28 and 36 terms are virtually identical while those for 21, 15, and 10 terms show increasing error, respectively. Also, the divergence increases as t approaches the neighborhood of T_o , 35.7 microseconds. These curves show that the divergent properties of the series (7-38) and its truncation to 28 or 36 terms have negligible effect on the computation of $e_s(t)$ out to 10 microseconds (no greater than 0.33 % error at 10 ns).

For the cables considered here, the maximum physical length is typically about 300m (1000 ft). Accordingly, for a typical relative dielectric constant of about 2.5, the maximum cable delay to be encountered would be about 1.69 microseconds ($\sqrt{2.5 \times 320/3 \times 10^8}$) and the corresponding $2\ell T$ value would be 3.38 microseconds ($2 \times 1.69 \times 10^{-6}$). In the particular case of Cable I, ℓT is equal to 1.6×10^{-6} ($320 \times \sqrt{LC}$) and $2\ell T$ is 3.2 microseconds. Accordingly, the observed response would depart from (7-38) at 3 ns in the manner shown in fig. 7-3; however, figs. 7-5 and 7-6 do accurately describe the observed response out to 3.2 ns, i.e., for the time interval before the receiving-end reflection returns to the sending-end.

7.3 A Practical Method for Measuring the Step Response of the Sending-End Voltage

When the generator impedance R_g is not equal to the high frequency characteristic impedance R_o of the cable under test, (7-28) is not valid. Specifically, in the first form of (7-28) note the R_o term; for a generator of impedance R_g , the R_o term has to be replaced by R_g . Consequently, for a generator impedance R_g all equations based on (7-28) are also invalid.

However, all is not lost because the principal result of Section 7.2, $e_s(t)$, i.e., eq. (7-38), transforms as follows:

$$\left. e_s(t) \right\}_{R_g} = \frac{2 R_o}{R_o + R_g} e_s(t). \quad (7-51)$$

The derivation of this result proceeds in the following manner. Consider fig. 7-4A in which R_o is replaced by R_g . Then, the voltage across $Z_o(s)$ is given by

$$\left. e_s(t) \right\}_{R_g} = \frac{1}{s} \frac{Z_o(s)}{R_g + Z_o(s)}. \quad (7-52)$$

Upon expressing $Z_o(s)$ in terms of the cable parameters obtains

$$\begin{aligned} \left. e_s(t) \right\}_{R_g} &= \frac{1}{s} \frac{\left[\frac{R + sL + Ks^m}{sL} \right]^{1/2}}{R_g + \left[\frac{R + sL + Ks^m}{sL} \right]^{1/2}} \\ &= \frac{1}{s} \frac{R_o \left[1 + \frac{R + Ks^m}{sL} \right]^{1/2}}{R_g + \left[1 + \frac{R + Ks^m}{sL} \right]^{1/2}} \\ &= \frac{1}{s} \frac{\left[1 + \frac{R + Ks^m}{sL} \right]^{1/2}}{\frac{R_o}{R_g} + \left[1 + \frac{R + Ks^m}{sL} \right]^{1/2}} \end{aligned} \quad (7-53)$$

where \bar{R}_g denotes R_g/R_o . Expanding the radical terms in a power series as was done in (7-28) yields

$$e_s(t) \Big|_{R_g} = \frac{1 + \frac{v}{2} - \frac{v^2}{2 \cdot 4} + \frac{3v^3}{2 \cdot 4 \cdot 6} - \frac{3 \cdot 5 \cdot v^4}{2 \cdot 4 \cdot 6 \cdot 8} + \dots}{(1 + \bar{R}_g) + \frac{v}{2} - \frac{v^2}{2 \cdot 4} + \frac{3v^3}{2 \cdot 4 \cdot 6} - \frac{3 \cdot 5 \cdot v^4}{2 \cdot 4 \cdot 6 \cdot 8} + \dots} \quad (7-54)$$

Because the quotient of polynomials, (7-54), can be expressed as

$$H = \frac{Y}{X} = \frac{1 + a_1 v + a_2 v^2 + \dots}{(1 + \bar{R}_g) + a_1 v + a_2 v^2 + \dots},$$

the k-th coefficient of H is given by

$$h(k) = \frac{1}{x(1)} \left[y(k) - \sum_{i=1}^{k-1} h(i) x(k+1-i) \right] \quad (7-33)$$

For $e_s(t) \Big|_{R_g}$, i.e., (7-54)

$$x(1) = 1 + \bar{R}_g \quad (7-56)$$

while for $e_s(t)$, (7-38)

$$x(1) = 2$$

Because $x(1)$ occurs in (7-33) only as the factor $1/x(1)$ external to the brackets, the two series expansions are related by a simple scale factor,

$$\begin{aligned} e_s(t) \Big|_{R_g} &= \frac{2}{1 + \bar{R}_g} e_s(t) \\ &= \frac{2 R_o}{R_o + R_g} e_s(t) \end{aligned}$$

which is the result given above in (7-51).

An experimental run on Cable I using a two channel 50 ohm feed-through sampling system produced the data shown in fig. 7-8. Note that the initial step is given by

$$e_s(0) \Big|_{100} = \frac{2 \times 124}{100 + 124} \left(\frac{1}{2} \right) = 0.55 \quad (7-57)$$

where R_g and R_o are 100 and 124 ohms, respectively. The measurement system is shown in fig. 7-9. When the voltage of one of the balanced generators was reduced to zero with the 50 source impedance being maintained, no significant change (none was discerned) in the energized channel's sending-end voltage, $(1/2) e_s(t)$] .
124

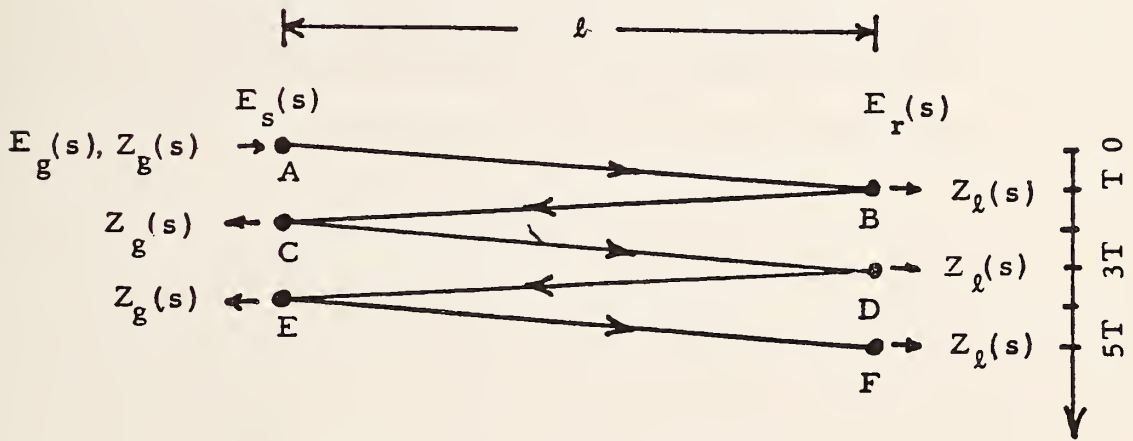
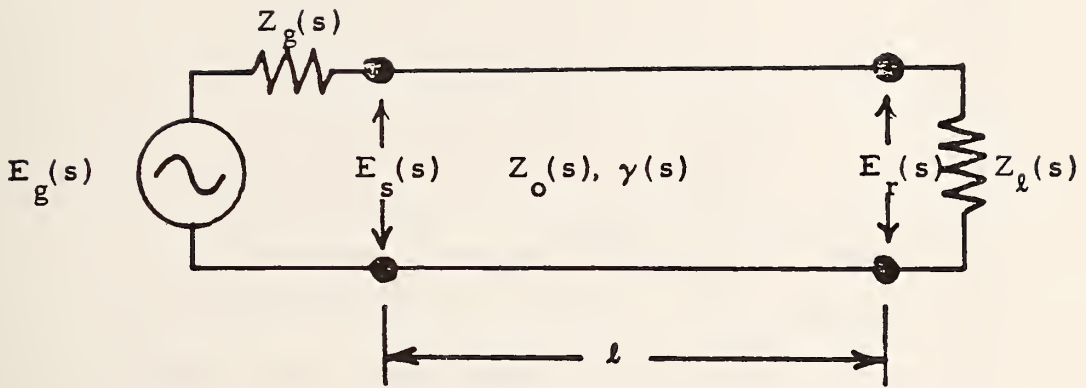


Figure 7-1. The RT diagram for a uniform transmission line connecting an arbitrary generator and load.

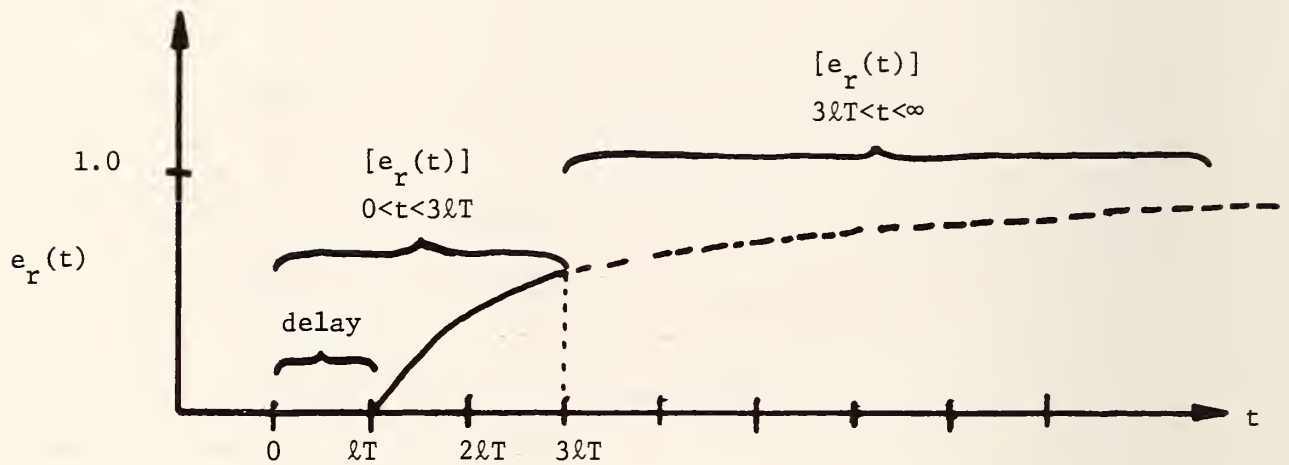


Figure 7.2 The initial received voltage $[e_r(t)]$ assuming $e_g(t)$ to be the unit-step. Equation (7-21) is the Laplace transform of this initial voltage. Note the transmission delay of lT seconds and then the emergence of the distorted step-like signal from the transmission line, lT to $3lT$ seconds.

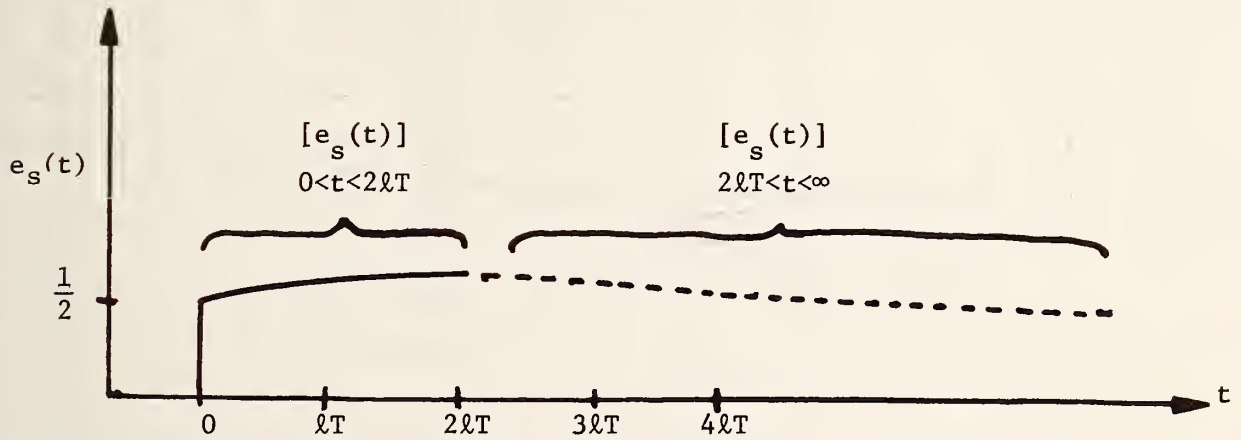


Figure 7-3. The initial sending-end voltage $[e_s(t)]$ assuming $e_g(t)$ to be $0 < t < 2lT$ the initial step. The initial voltage jumps to 0.5 volts and then rises slowly until the first reflection returns from the load.

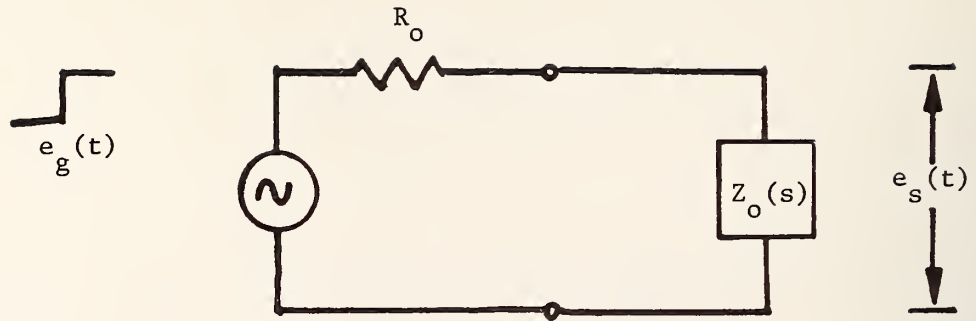


Figure 7-4A. The voltage divider circuit representing the voltage transfer from $e_g(t)$ to $e_s(t)$ for $0 < t < 2\ell T$ or for all t when $\ell = \infty$, or the line is terminated in $Z_o(s)$.

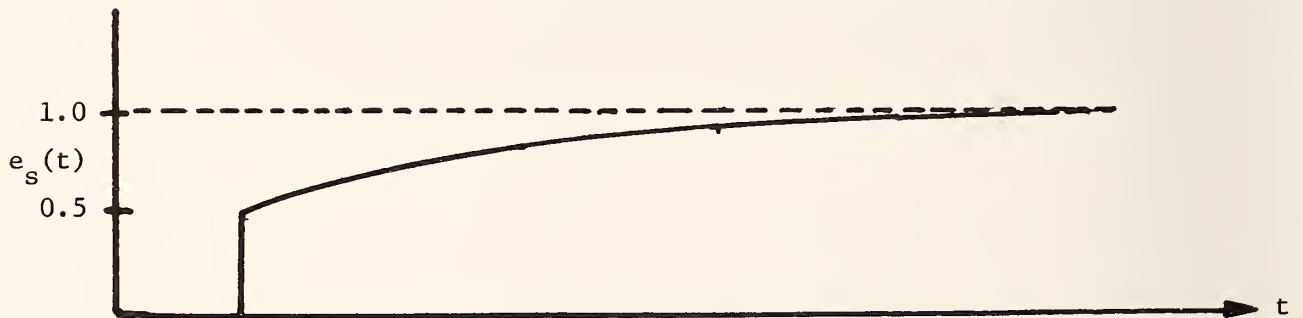


Figure 7-4B. The sending-end voltage step response when the line is infinitely long or terminated in $Z_o(s)$.

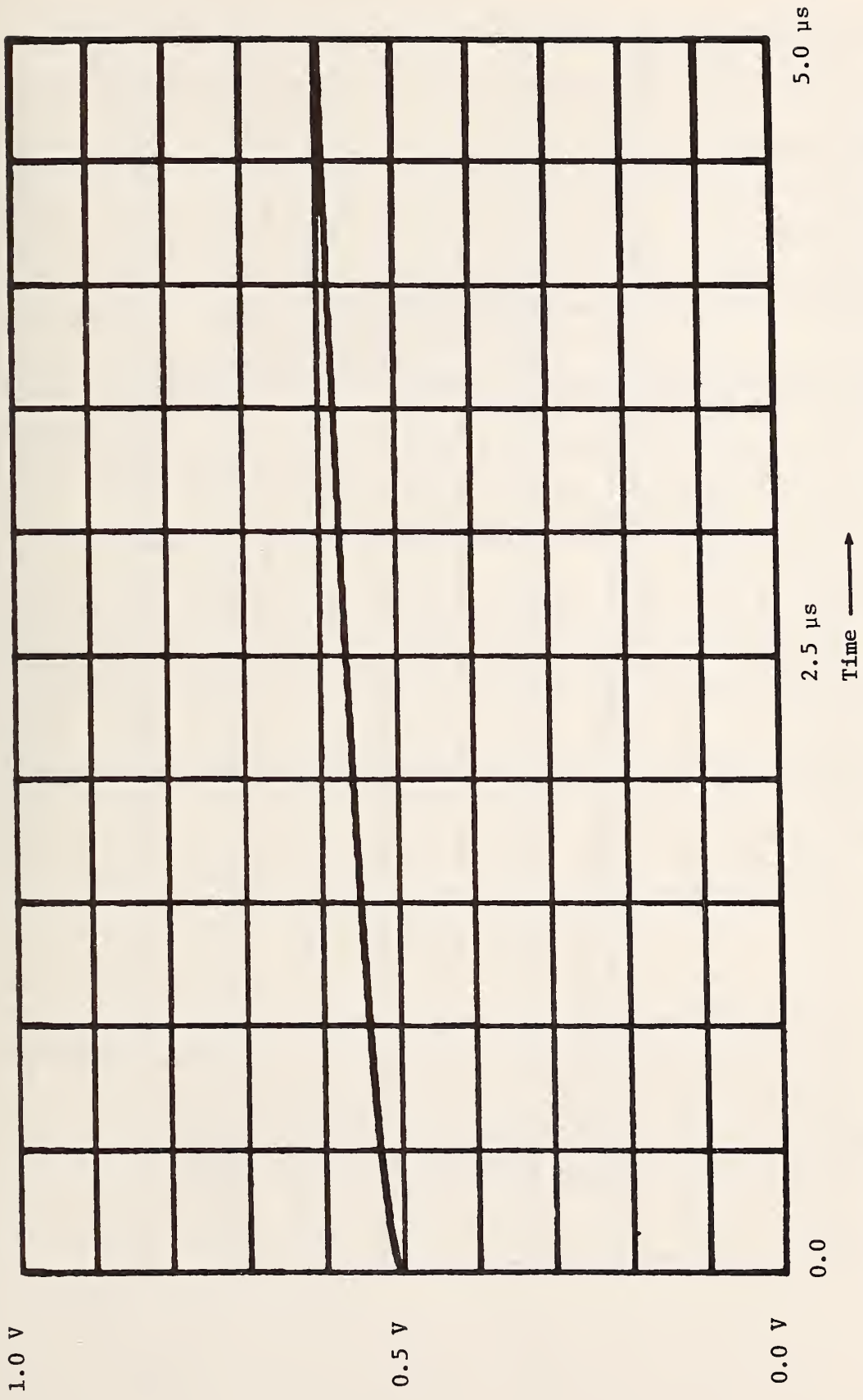


Figure 7.5 The sending-end step response for the time interval of $0 < t < 5$ microseconds.

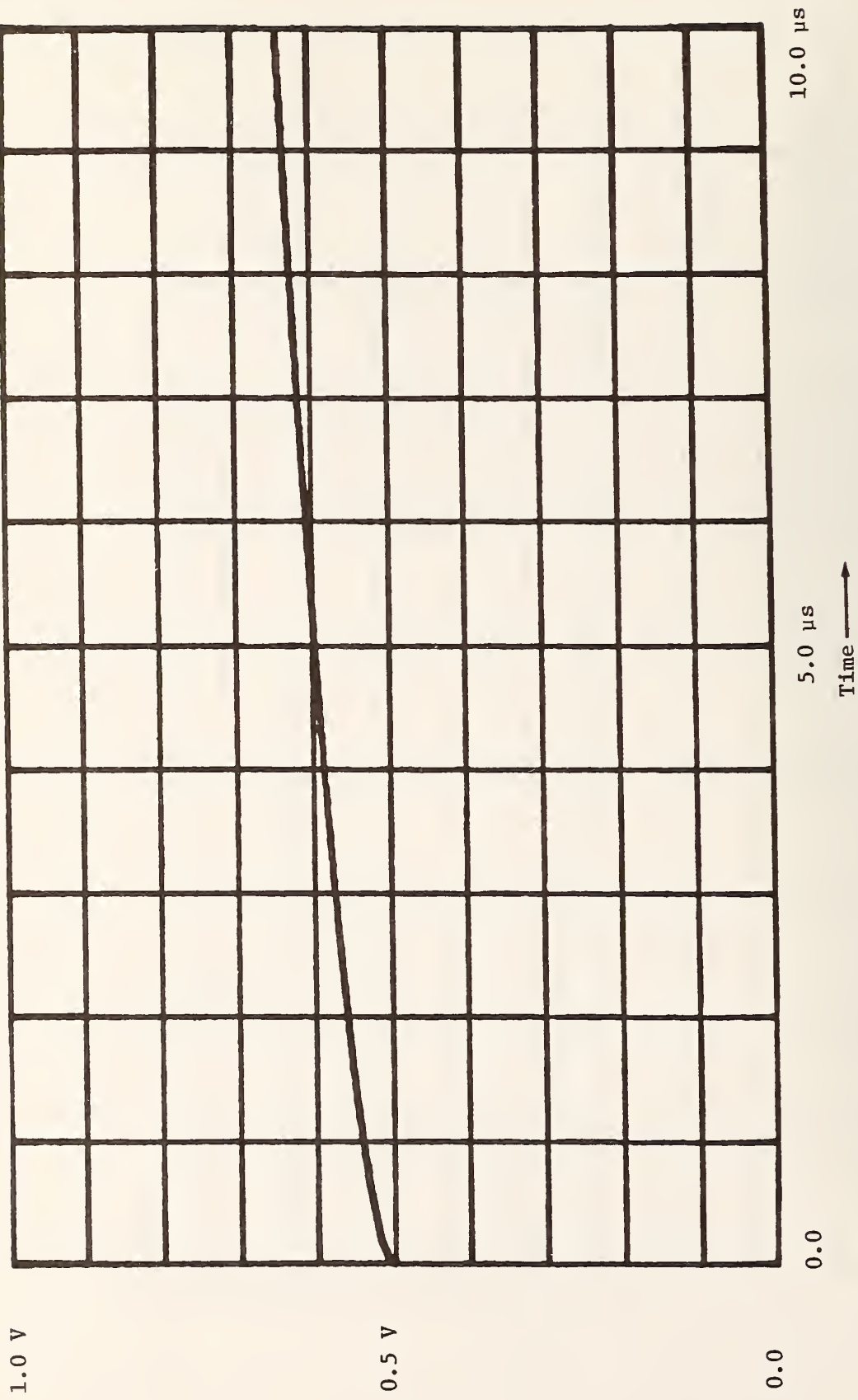


Figure 7.6 The sending-end step response for the time interval of $0 < t < 10$ microseconds.

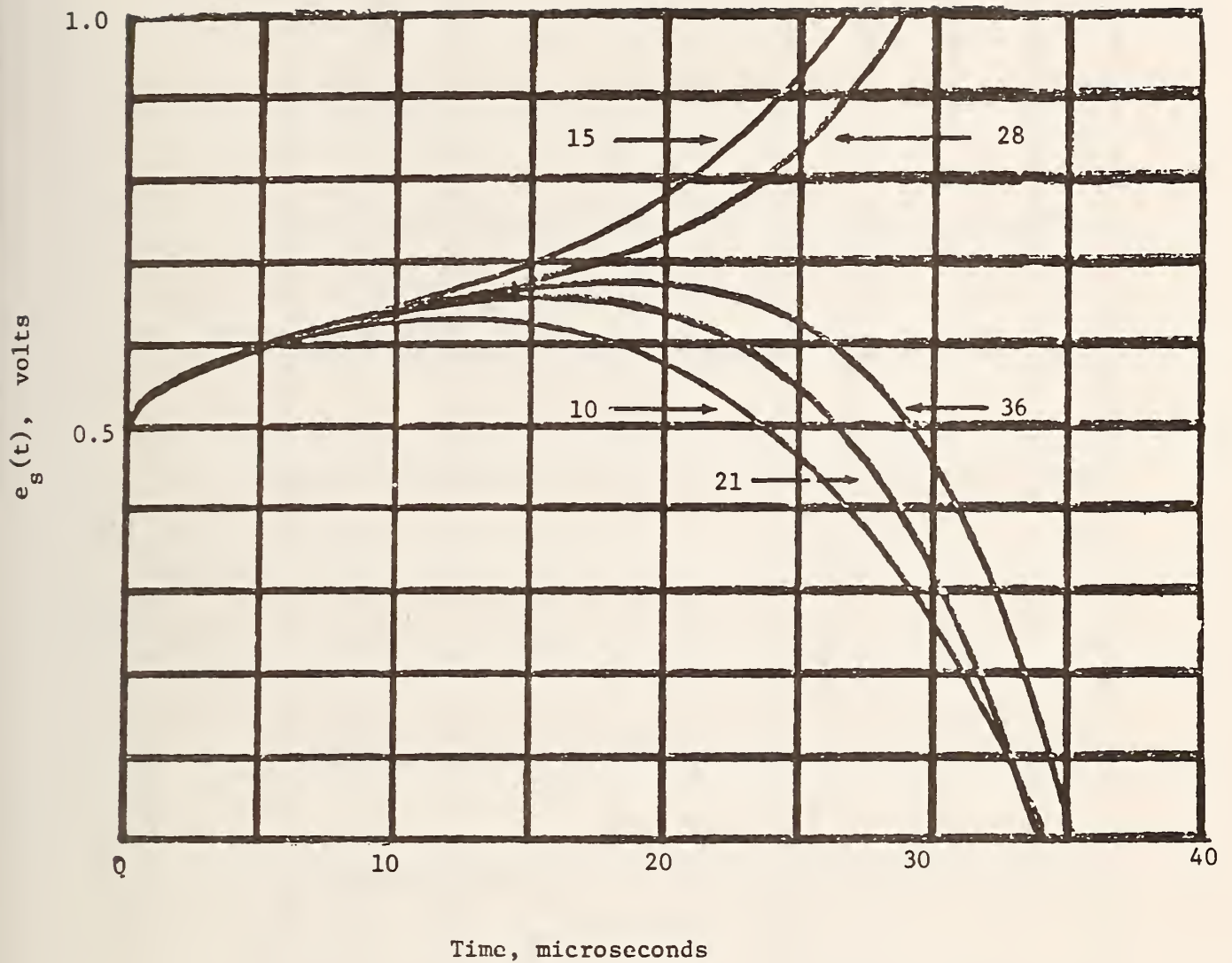


Figure 7-7. The divergent properties of the series (7-38) using the parameters for Cable I. The parametric variable 10 corresponds to 10 terms comprised of $0.5 u(t)$ plus the algebraic sum of the weighted values of $w_1(t)$ through $w_3(t)$. Similarly, 15 corresponds to 15 terms obtained from the sum through $w_4(t)$; and so on through $w_7(t)$ for 36 terms.

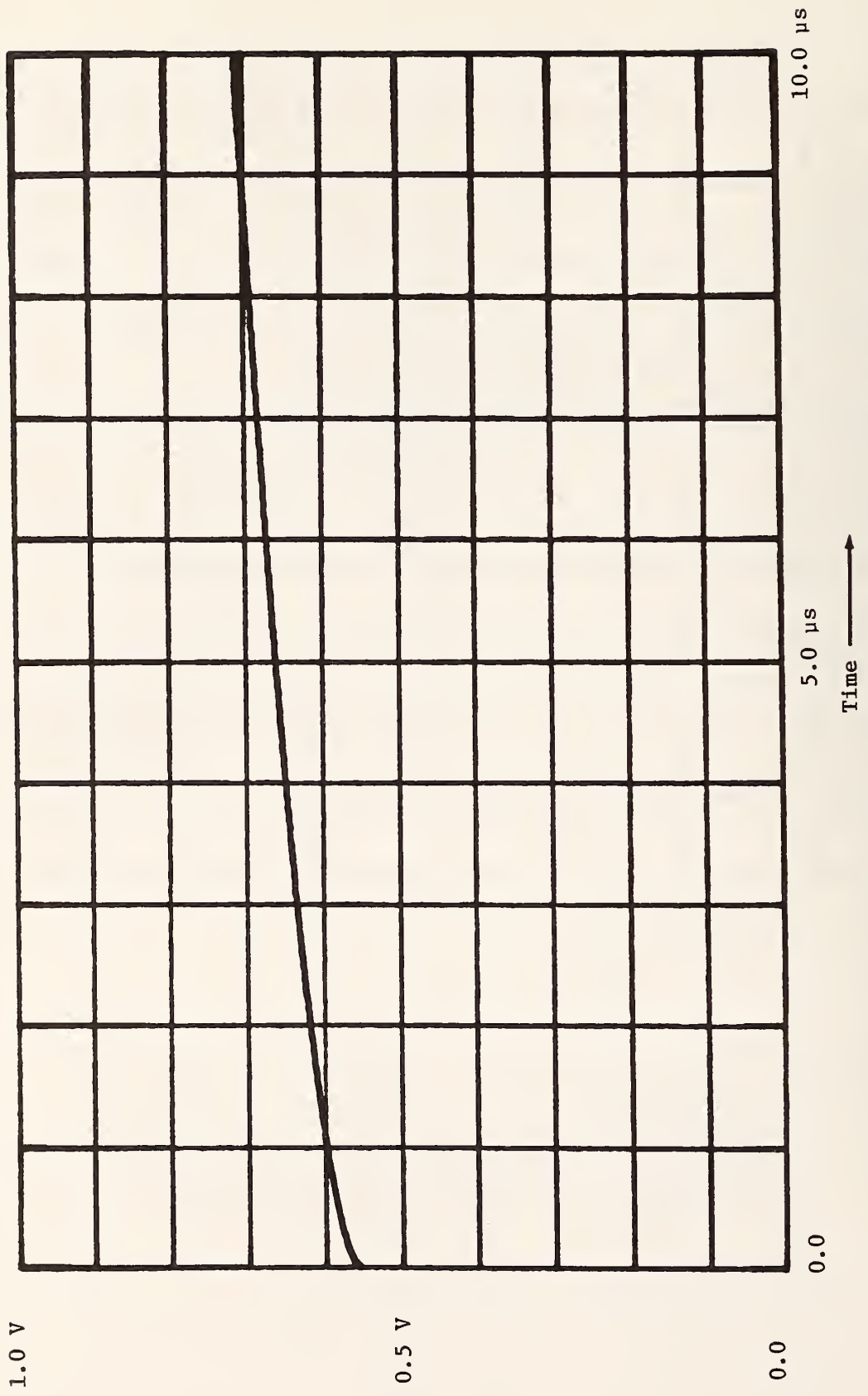


Figure 7.8 The sending-end voltage step response of cable I, $R_o = 124$ ohms, $R_g = 100$ ohms. The initial step is 0.55.

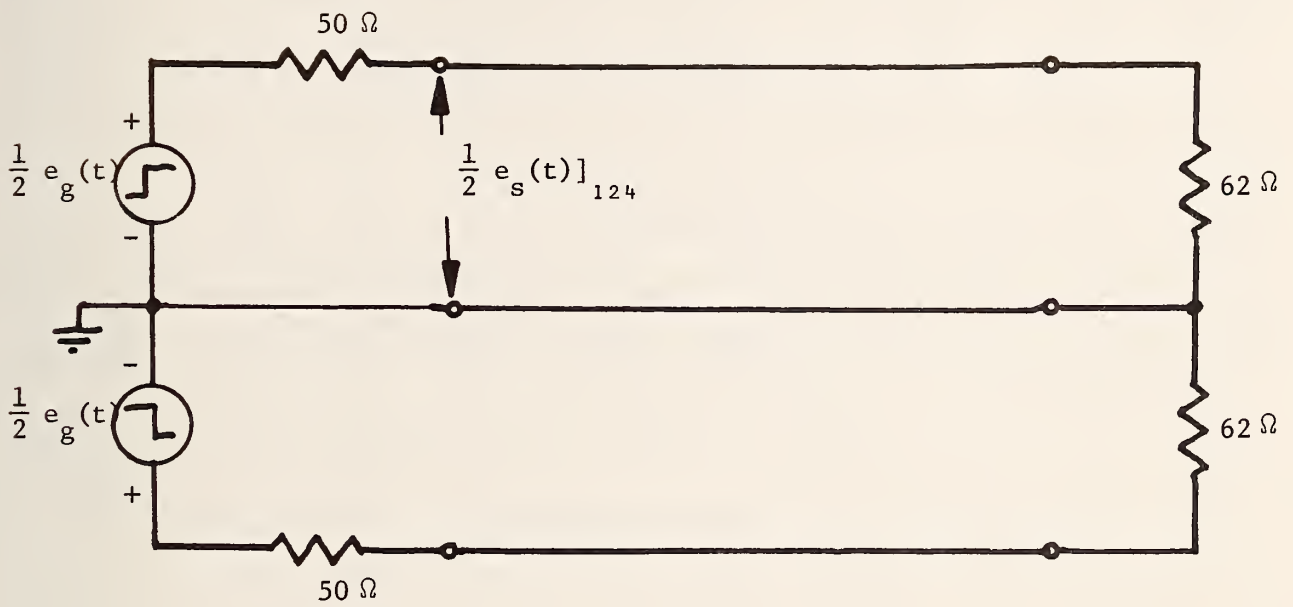


Figure 7-9 The measurement system for observing the sending-end step response. $e_g(t)$ is a unit step generator.

REFERENCES

- [1] Johnson, W. C., *Transmission Lines and Networks*, McGraw-Hill, New York 1950,
- [2] Nahman, N. S., A discussion on the transient analysis of coaxial cables considering high-frequency losses, *IRE Trans. PGCT, CT-9*, No. 2, 144-152, June, 1962.
- [3] Nahman, N. S., Signal waveform metrology at NBS, WESCON 77, Western Electronics Conference, Sept. 19-21, 1977, San Francisco, California (10 pages).
- [4] Terman, F. E. and Pettit, J. M., *Electronic Measurements*, (McGraw-Hill, New York, NY, 1952), p. 113. Also, note discussion of capacitance measurements, p. 102.
- [5] McCaa, Jr., W. D. and Nahman, N. S., Generation of reference waveforms by uniform lossy transmission lines, *IEEE Trans. Instru. and Meas.*, Vol. IM-14, Nov. 1969, pp. 382-390.
- [6] Gans, W. L., Present capabilities of the NBS automatic pulse measurement system, *IEEE Trans. I&M*, No. 4, 384-388, December 1976.
- [7] W. L. Gans and Andrews, J. R., Time domain automatic network analyzer for the measurement of RF and microwave parameters, NBS Tech. Note 672, September 1975.
- [8] Baird, D. C., *Experimentation: An Introduction to Measurement Theory and Experiment Design*, Prentice-Hall, Englewood Cliffs, N.J. 1962.
- [9] Stout, M. B., *Basic Electrical Measurements*, 2nd Ed., Prentice-Hall, Englewood Cliffs, N. J., 1960.
- [10] Brigham, E. O., *The Fast Fourier Transform*, Prentice-Hall, Englewood Cliffs, N. J., 1974.
- [11] *Tables of the Error Function and its Derivative*, National Bureau of Standards, Applied Math Series, No. 41, 1954.
- [12] Schwartz, M., *Information, Transmission, Modulation, and Noise*, McGraw-Hill, New York, N.Y., 1959, pp. 381-384.
- [13] Tai, C. T., Transients on lossless terminated transmission lines. *IEEE Trans. Ant. and Prop.*, AP-26, No. 4, 556-561, July 1978.

APPENDIX A. MEASURED AND MODELED CABLE DATA

A.1 Cable Parameter Tables

Table A-1. Cable Physical Parameters

Cable	Signal Conductor(s) Material and O.D.	Dielectric Material and O.D.	Shield(s) Material and O.D.	Jacket Material and O.D.
RG-58C/U	stranded tinned copper 0.81 mm (0.032 in)	polyethylene 2.95 mm 0.116 in)	tinned copper braid ---	black vinyl 4.95 mm (0.195 in)
RG-214/U	silver coated copper 2.26 mm (0.089 in)	polyethylene 7.24 mm (0.285 in)	silver coated copper ---	black vinyl 10.80 mm (0.425 in)
RG-223/U	silver coated copper 0.91 mm (0.036 in)	polyethylene 2.95 mm (0.116 in)	silver coated copper ---	black vinyl 5.23 mm (0.206 in)
RG-59B/U	copper covered steel 0.57 mm (0.022 in)	polyethylene 3.71 mm (0.146 in)	bare copper braid ---	black vinyl 6.15 mm (0.242 in)
A	stranded bare copper 0.33 mm (0.013 in)	polyethylene 4.11 mm (0.162 in)	tinned copper braid 4.70 mm (0.185 in)	black pvc 6.22 mm (0.245 in)
B	bare copper 1.70 mm (0.067 in)	polyethylene 7.21 mm (0.284 in)	tinned copper braid 8.07 mm (0.318 in)	black pvc 10.67 mm (0.420 in)
C	stranded tinned copper 0.97 mm (0.038 in)	polyethylene 6.10 mm (0.240 in)	tinned copper braid ---	blue vinyl 6.15 mm (0.242 in)
D	stranded tinned copper 0.56 mm (0.022 in)	polyethylene 1.12 mm (0.044 in)	bare copper braid 2.74 mm (0.108 in)	blue pvc 3.81 mm (0.150 in)
E	stranded tinned copper 0.99 mm (0.039 in)	polyethylene 1.96 mm (0.077 in)	bare copper braid 4.95 mm (0.195 in)	blue pvc 6.22 mm (0.245 in)
RG-22B/U	stranded bare copper 1.16 mm (0.046 in)	polyethylene 7.24 mm (0.285 in)	tinned copper braid ---	black vinyl 10.67 mm (0.420 in)

Table A-1., continued

Cable	Signal Conductor(s) Material and O.D.	Dielectric Material and O.D.	Shield(s) Material and O.D.	Jacket Material and O.D.
F	stranded bare copper 0.81 mm (0.032 in)	polyethylene 4.11 mm (0.162 in)	tinned copper braid 4.70 mm (0.185 in)	black pvc 6.22 mm (0.245 in)
G	stranded bare copper 1.35 mm (0.053 in)	polyethylene 7.21 mm (0.284 in)	tinned copper braid 8.08 mm (0.318 in)	black pvc 10.67 mm (0.420 in)
H	stranded bare copper 0.56 mm (0.022 in)	polyethylene 4.11 mm (0.162 in)	tinned copper 4.70 mm (0.185 in)	black pvc 6.22 mm (0.245 in)
I	stranded bare copper 0.97 mm (0.038 in)	polyethylene 7.21 mm (0.284 in)	tinned copper braid 8.08 mm (0.318 in)	black pvc 10.67 mm (0.420 in)
J	stranded tinned copper 0.56 mm (0.022 in)	polyethylene 2.06 mm (0.081 in)	bare copper braid 4.95 mm (0.195 in)	blue pvc 6.22 mm (0.245 in)
K	stranded bare copper 2.74 mm (0.108 in)	foam polyethylene 7.2 mm (0.285 in)	bare copper braid (2) ---	black polyethylene 12.19 mm (0.480 in)
WD-37	stranded bare copper 0.762 mm (0.030 in)	polypropylene 2.29 mm (0.09 in)	bare copper braid 2.97 mm (0.117 in)	black pvc ---

Table A-2. Cable Electrical Parameters

Cable	Capacitance per meter (ft) in pf	Inductance per meter (ft) in nh	Resistance per meter (ft) in mΩ	Loss slope "m"	Loss constant "K" (x10 ⁻⁴)
RG-58C/U	101.0 (30.8)	252.6 (77.0)	37.1 (11.3)	0.52975	0.16710
RG-214/U	101.0 (30.8)	252.6 (77.0)	10.3 (3.15)	0.55071	0.053034
RG-223/U	101.0 (30.8)	252.6 (77.0)	34.8 (10.6)	0.52314	0.16676
RG-59B/U	67.6 (20.6)	380.2 (115.9)	147.6 (45.0)	0.52284	0.21993
A	64.3 (19.6)	391.1 (119.2)	58.7 (17.9)	0.50981	0.62760
B	64.3 (19.6)	391.1 (119.2)	20.0 (6.1)	0.52724	0.22117
C	64.6 (19.7)	393.4 (119.9)	68.2 (20.8)	0.51395	0.71262
D	64.6 (19.7)	393.4 (119.9)	196.9 (60.0)	0.55307	0.46238
E	68.9 (21.0)	419.0 (127.7)	68.9 (21.0)	0.52174	0.51676
RG-22B/U	52.5 (16.0)	473.8 (144.4)	43.0 (13.1)	0.53103	0.23926
F	51.2 (15.6)	491.5 (149.8)	86.6 (26.4)	0.51565	0.51543
G	51.2 (15.6)	491.5 (149.8)	31.5 (9.6)	0.54819	0.17271
H	40.4 (12.3)	620.4 (189.1)	160.1 (48.8)	0.50262	0.78542
I	40.4 (12.3)	620.4 (189.1)	61.7 (18.8)	0.53952	0.25639
J	40.4 (12.3)	620.4 (189.1)	186.4 (56.8)	0.51619	0.69930
K	85.3 (26.0)	213.3 (65.0)	7.45 (2.27)	0.55829	0.039593
WD-37	43.6 (13.3)	587.2 (179.0)	137.8 (42.0)	0.57232	0.086936

A.1 Cable Graphical Data

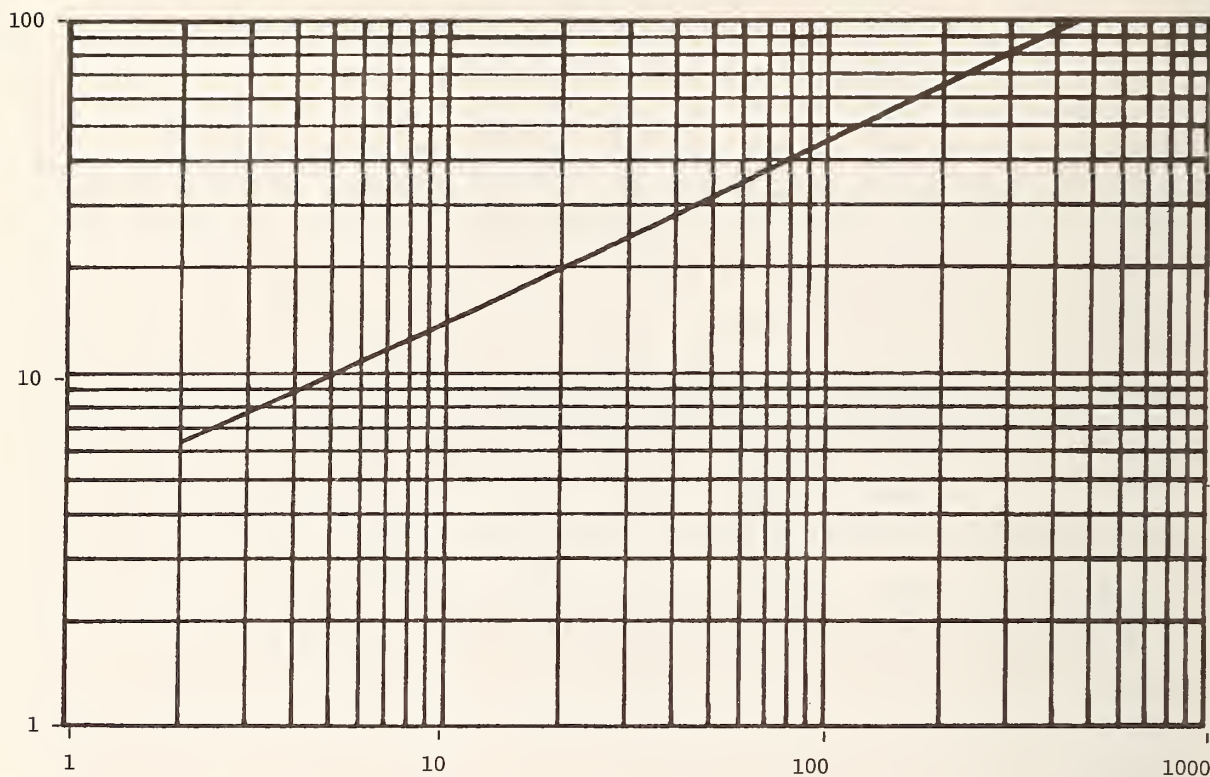


Figure A-1. Modeled attenuation plot for 304.8 meters (1000 feet) of RG-58C/U. Ordinate units are decibels and abscissa units are megahertz.

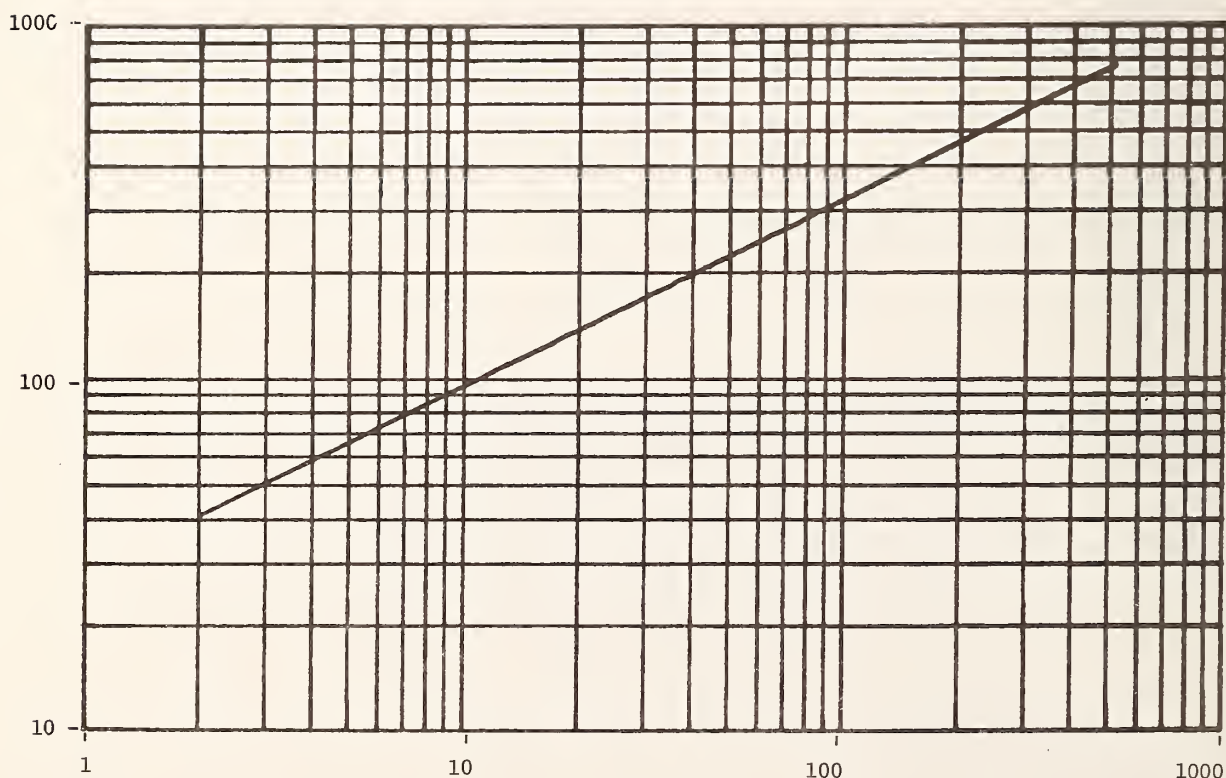


Figure A-2. Modeled minimum-phase shift plot for 304.8 meters (1000 feet) of RG-58C/U. Ordinate units are degrees and abscissa units are megahertz.

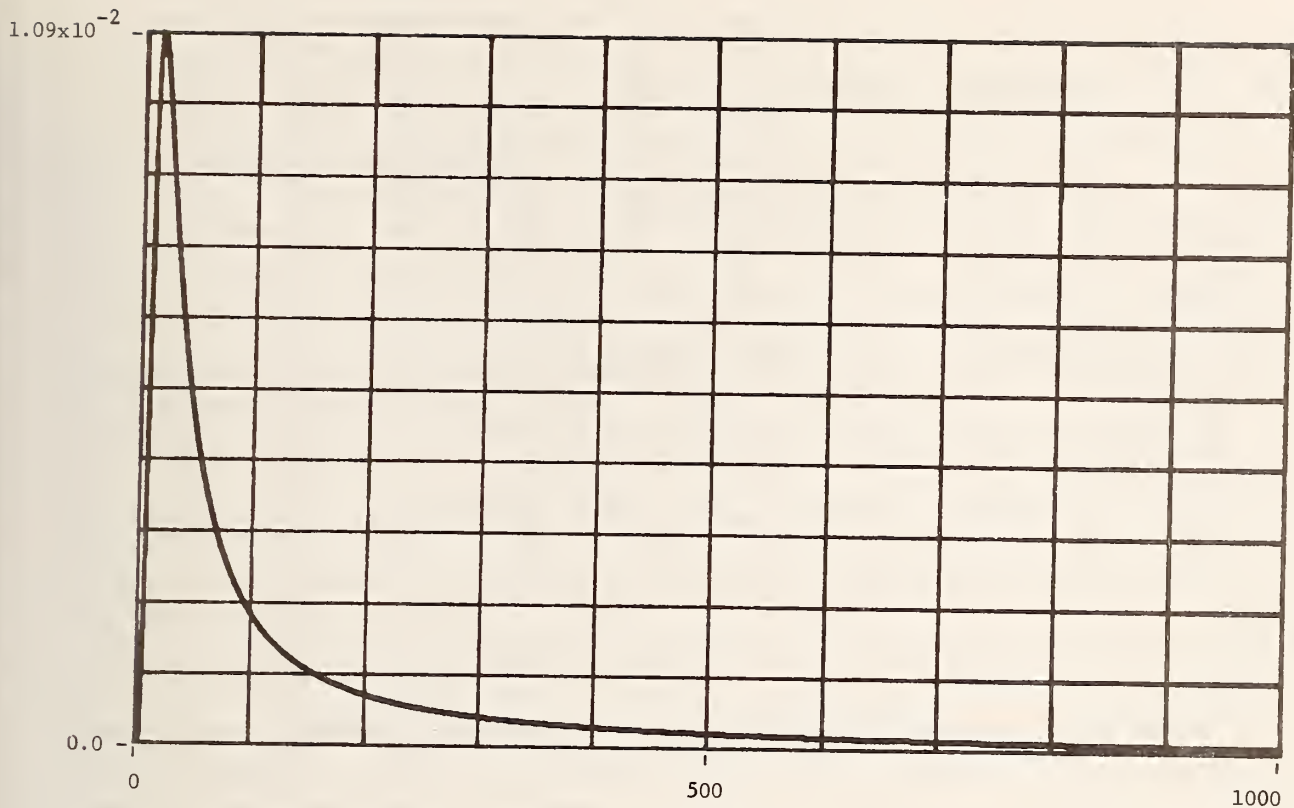


Figure A-3. Modeled and computed time domain impulse response for 304.8 meters (1000 feet) of RG-58C/U. Ordinate units are seconds⁻¹, abscissa units are nanoseconds and time spacing between points is 0.9766 ns.

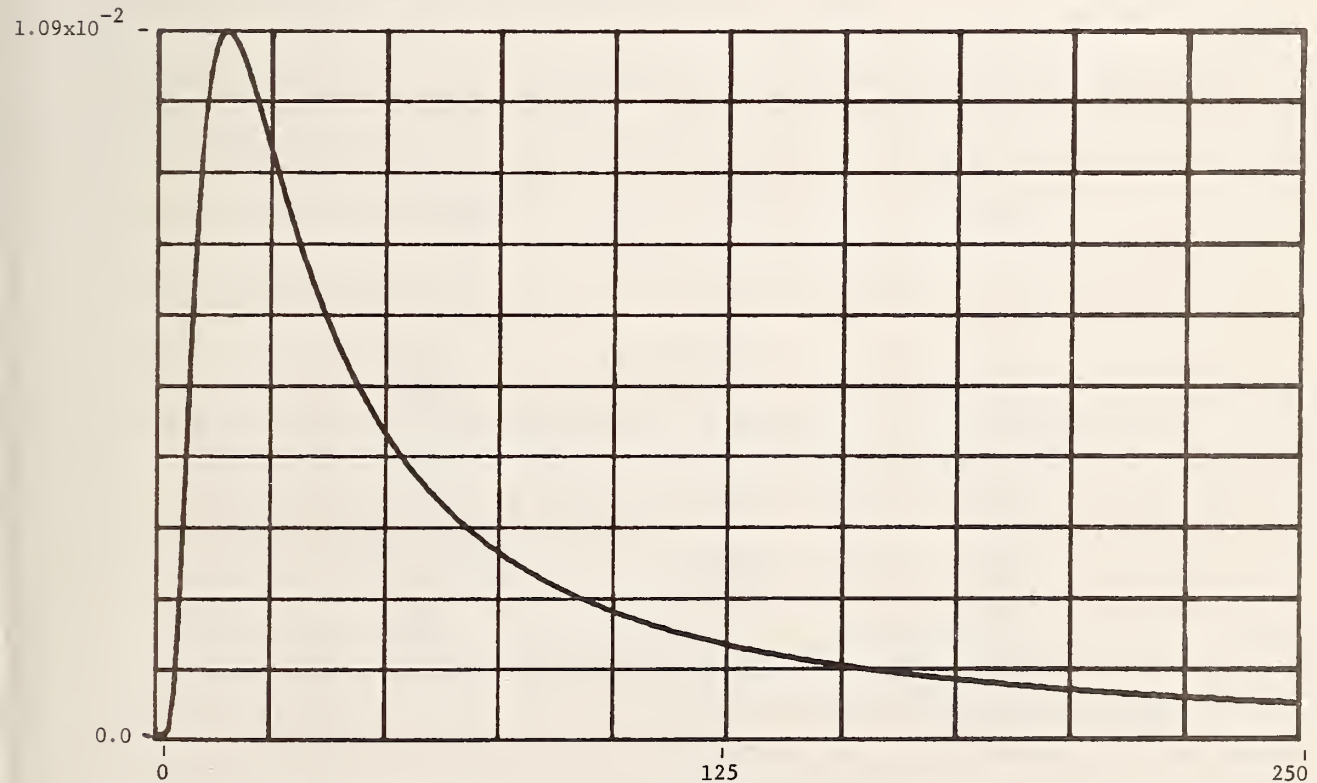


Figure A-4. Time-expanded modeled and computed time domain impulse response for 304.8 meters (1000 feet) of RG-58C/U. Ordinate units are seconds⁻¹, abscissa units are nanoseconds and time spacing between points is 0.9766 ns.

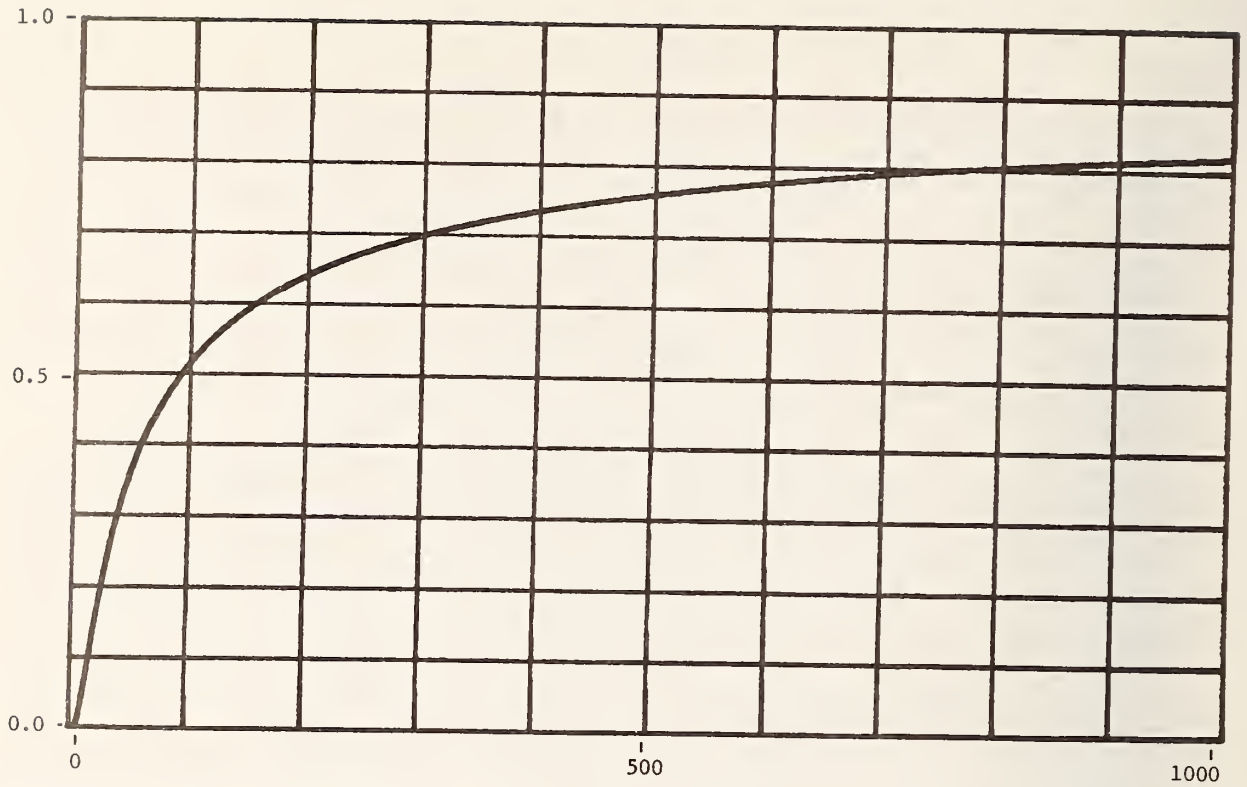


Figure A-5. Modeled and computed time domain unit step response for 304.8 meters (1000 ft) of RG-58C/U. Ordinate units are volts and abscissa units are nanoseconds.

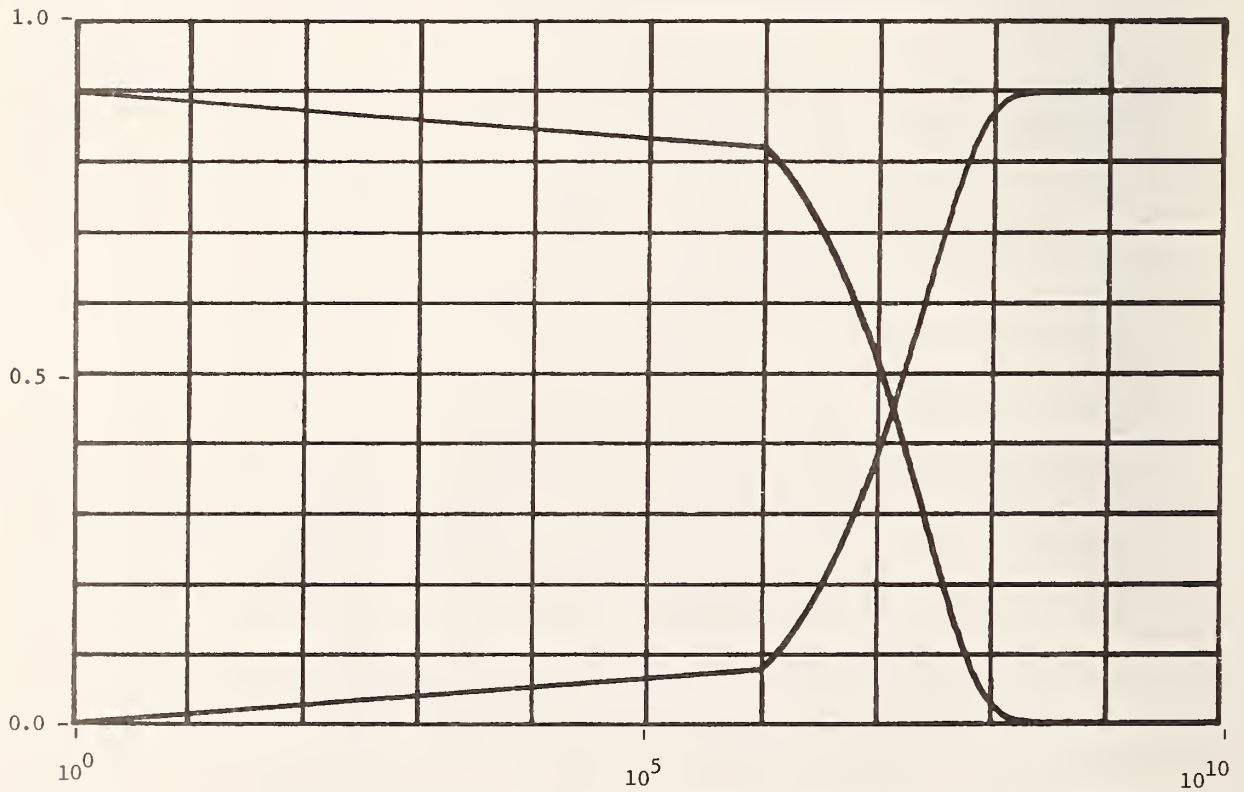


Figure A-6. Plots of "zero"/"one" cable unit step response voltages versus \log_{10} frequency for 304.8 meters (1000 ft) of cable RG-58C/U. Ordinate units are volts and abscissa units are hertz.

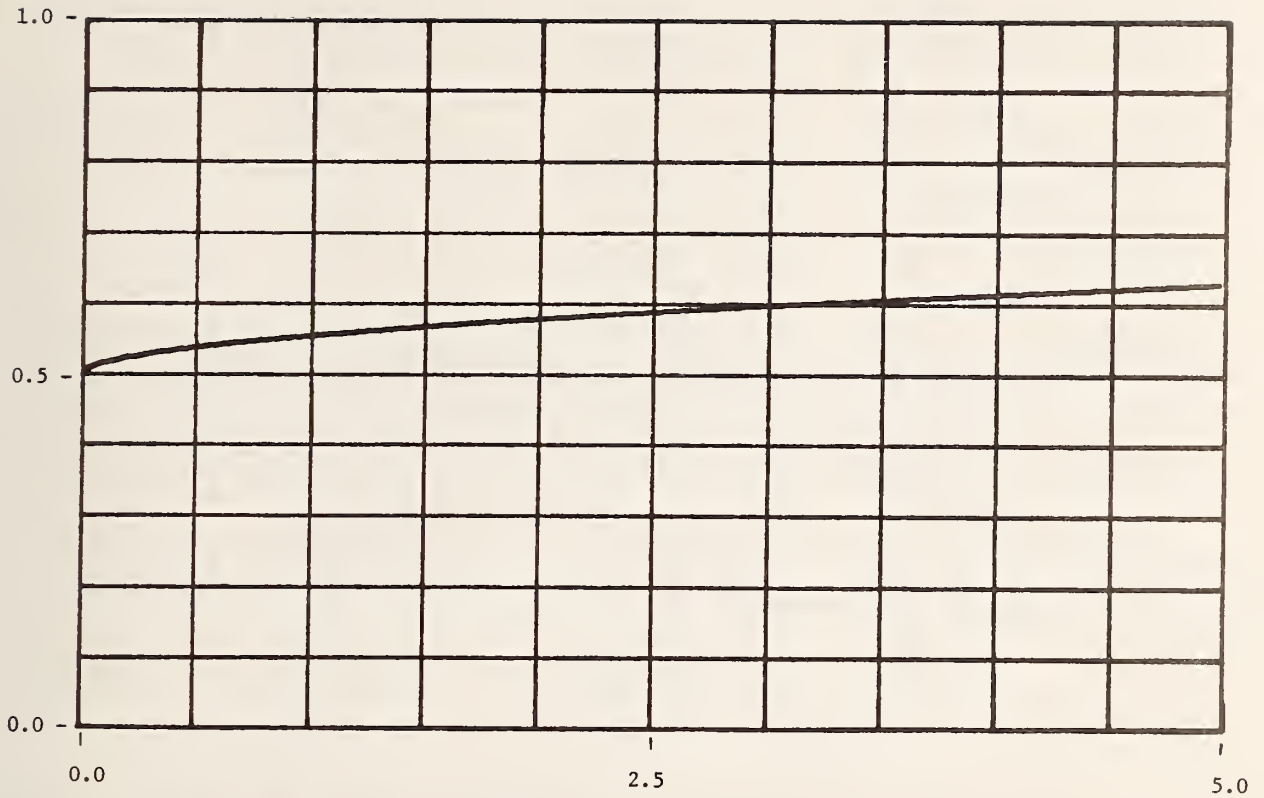


Figure A-7. TDR unit step response for cable RG-58C/U. Source step generator has assumed 50Ω resistive output impedance. Ordinate units are volts and abscissa units are microseconds.

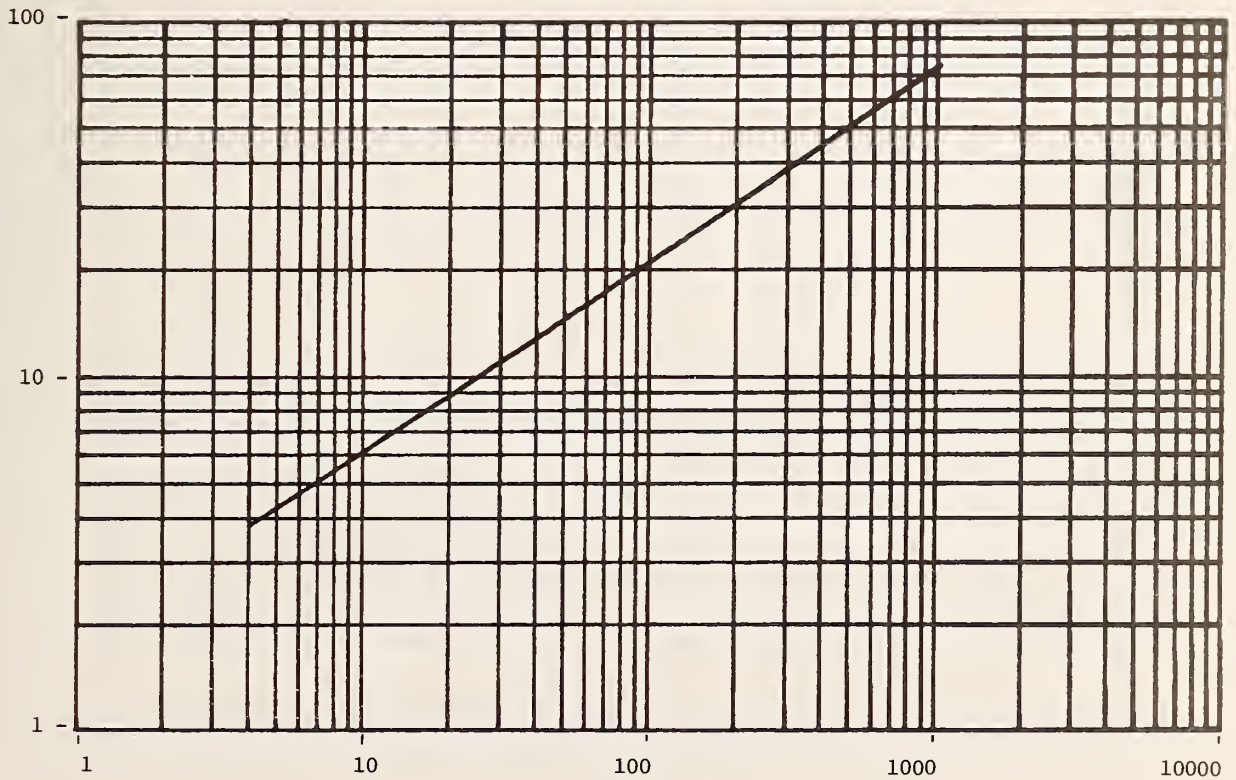


Figure A-8. Modeled attenuation plot for 304.8 meters (1000 ft) of RG-214/U. Ordinate units are decibels and abscissa units are megahertz.

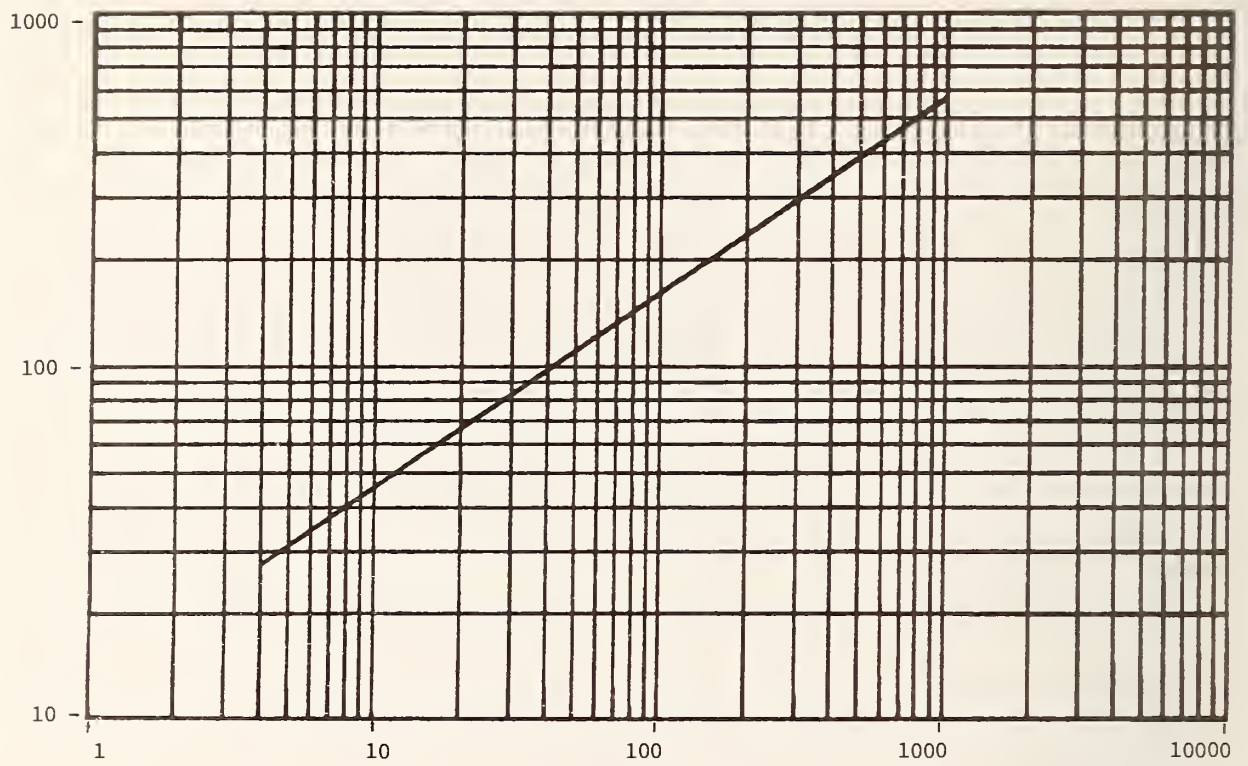


Figure A-9. Modeled minimum-phase phase shift plot for 304.8 meters (1000 ft) of RG-214/U. Ordinate units are degrees and abscissa units are megahertz.

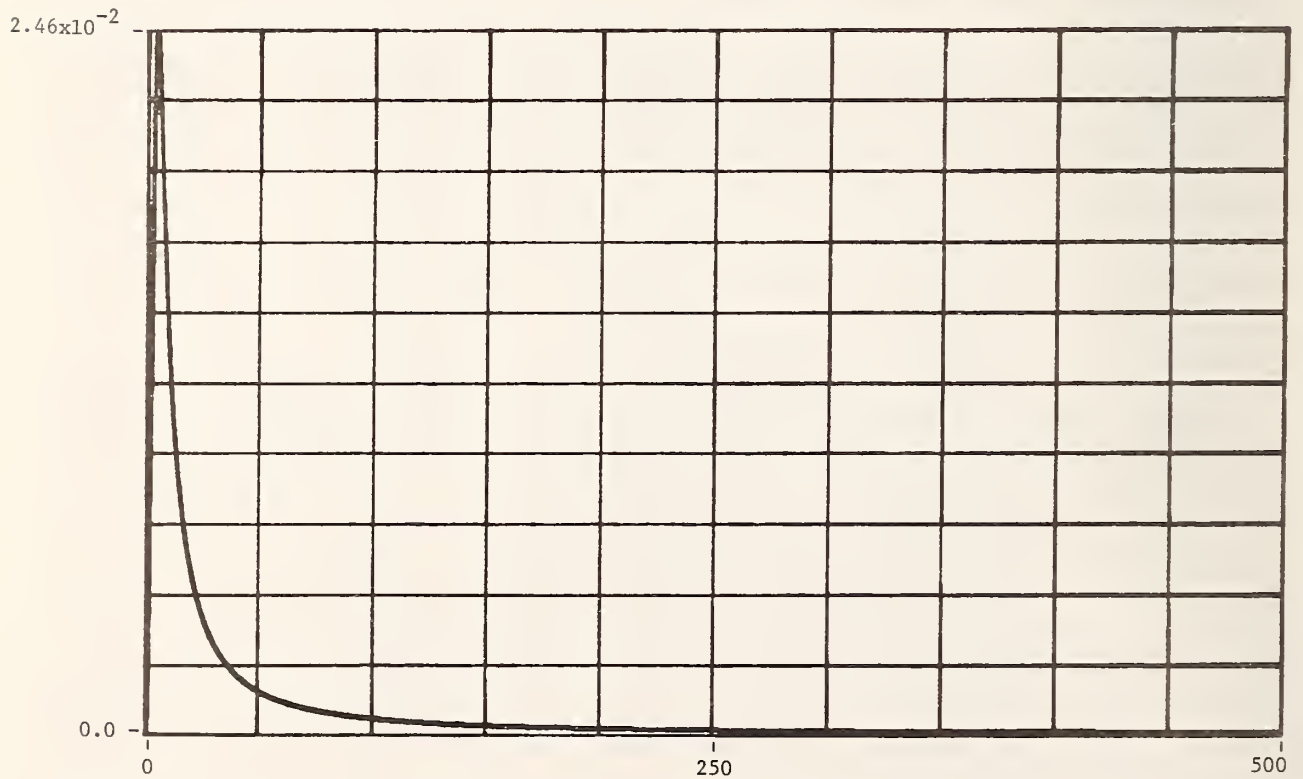


Figure A-10. Modeled and computed time domain impulse response for 304.8 meters (1000 ft) of RG-214/U. Ordinate units are seconds^{-1} , abscissa units are nanoseconds and time spacing between points is 0.9766 ns.

2.46×10^{-2}

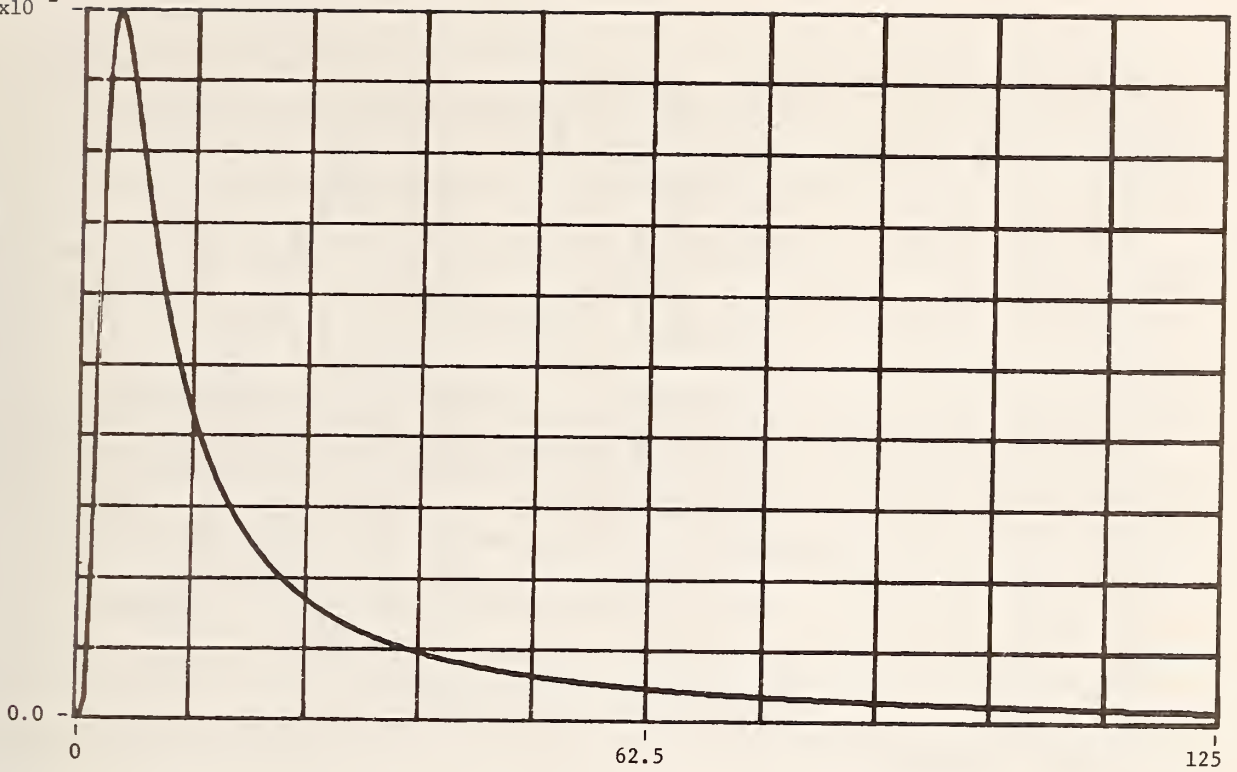


Figure A-11. Time-expanded modeled and computed time domain impulse response for 304.8 meters (1000 ft) of RG-214/U. Ordinate units are seconds⁻¹, abscissa units are nanoseconds and time spacing between points is 0.9766 ns.

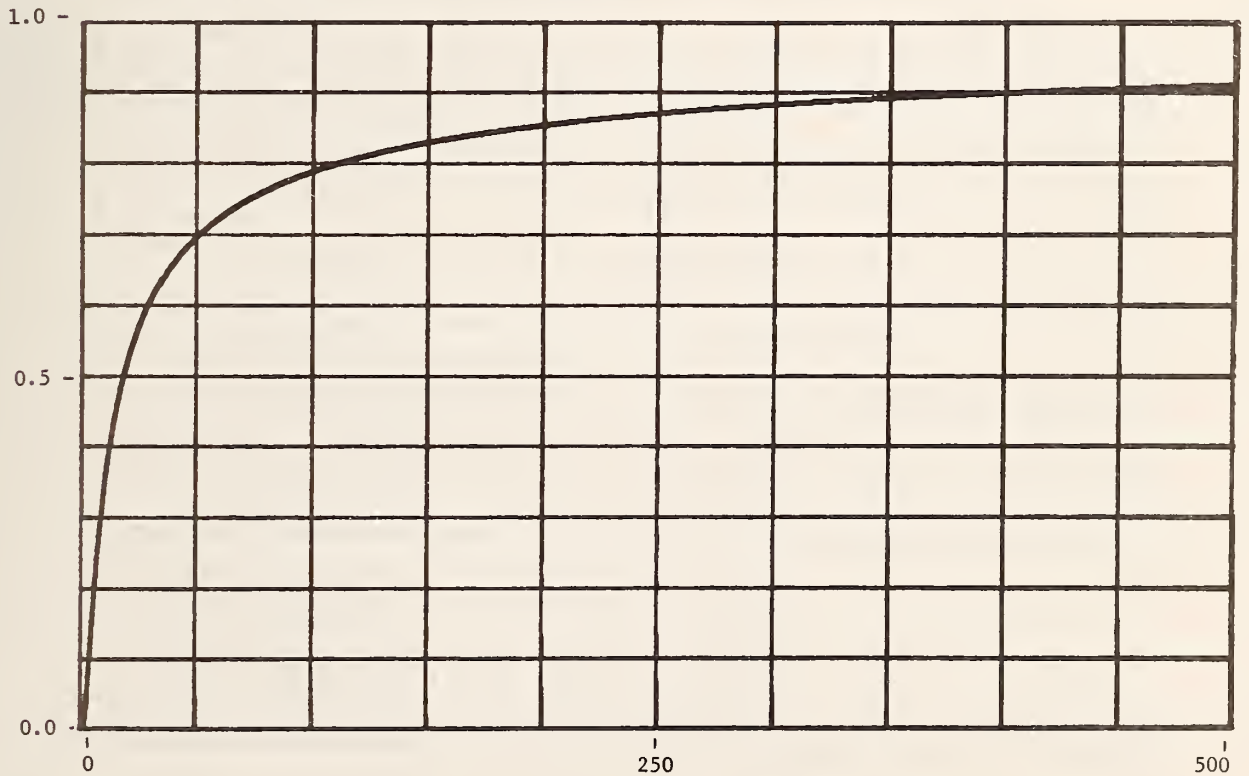


Figure A-12. Modeled and computed time domain unit step response for 304.8 meters (1000 ft) of RG-214/U. Ordinate units are volts and abscissa units are nanoseconds.

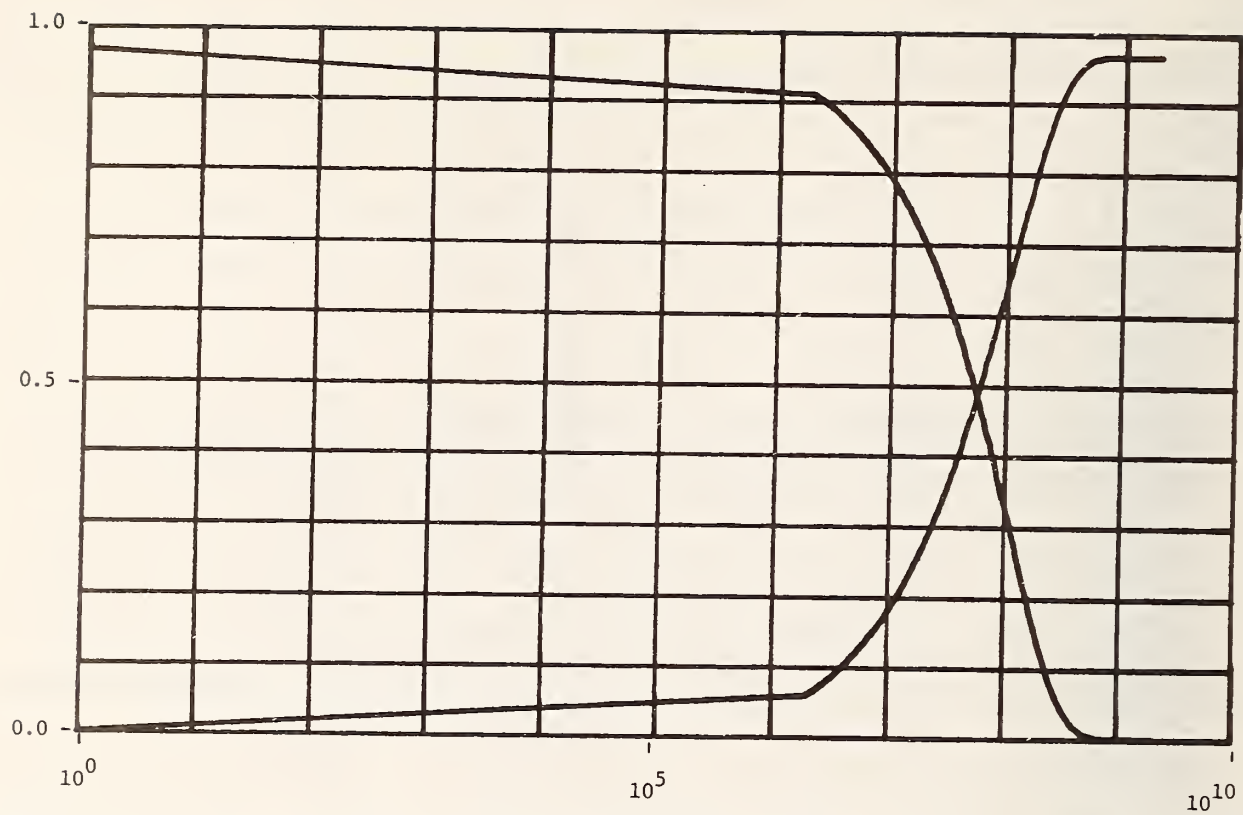


Figure A-13. Plots of "zero"/"one" cable unit step response voltages versus \log_{10} frequency for 304.8 meters (1000 ft) of cable RG-214/U. Ordinate units are volts and abscissa units are hertz.

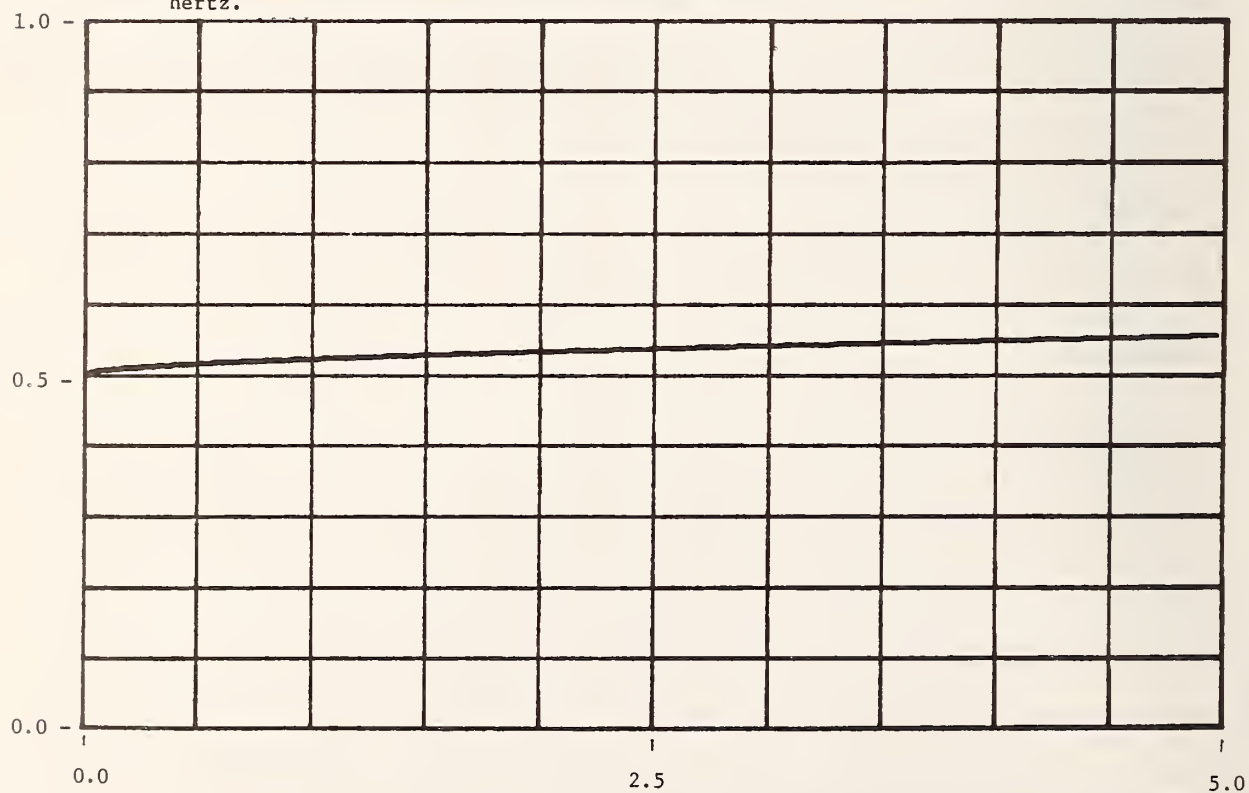


Figure A-14. TDR unit step response for cable RG-214/U. Source step generator has assumed 50Ω resistive output impedance. Ordinate units are volts and abscissa units are microseconds.

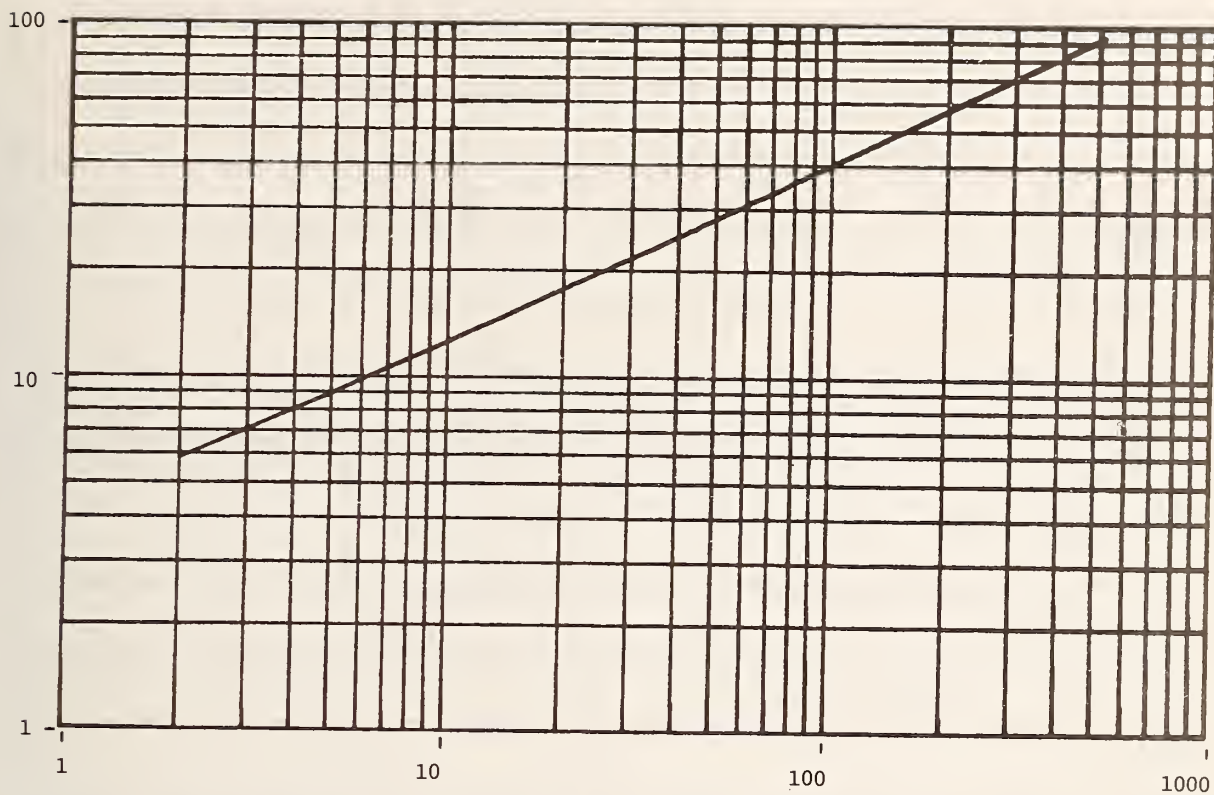


Figure A-15. Modeled attenuation plot for 304.8 meters (1000 ft) of RG-223/U. Ordinate units are decibels and abscissa units are megahertz.

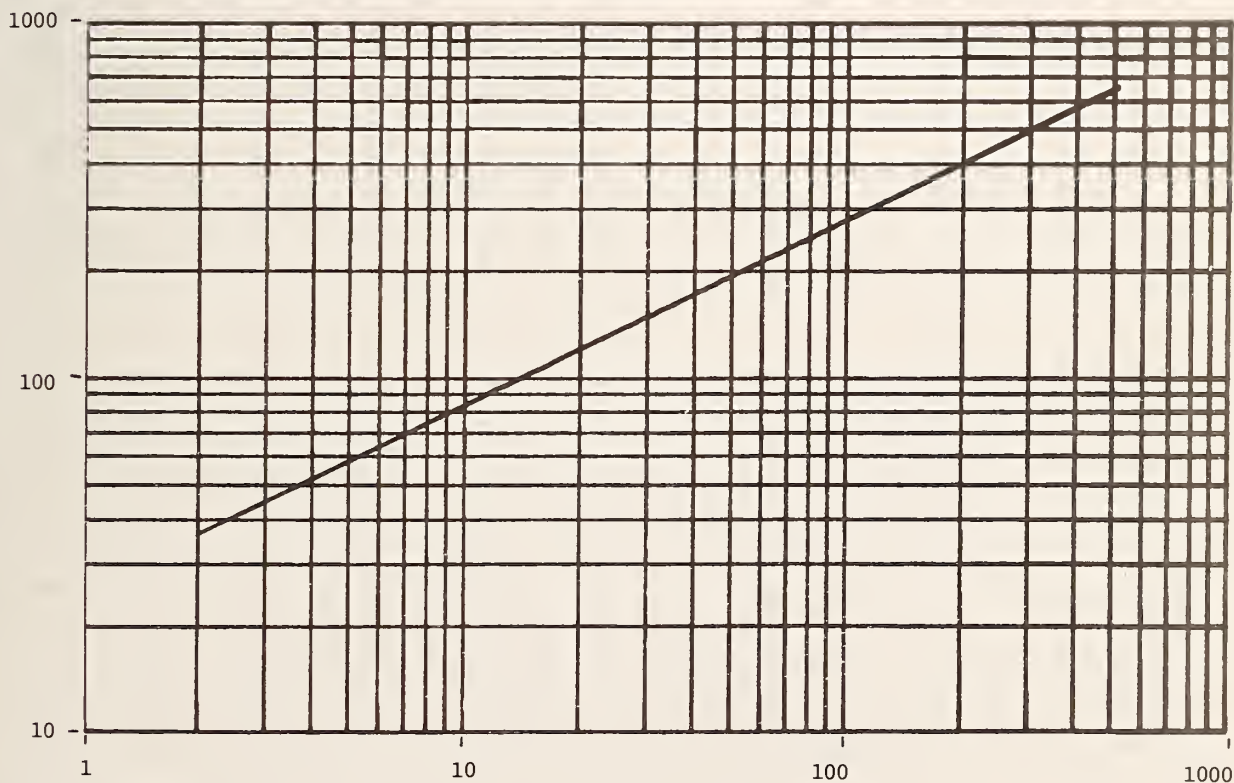


Figure A-16. Modeled minimum-phase phase shift plot for 304.8 meters (1000 ft) of RG-223/U. Ordinate units are degrees and abscissa units are megahertz.

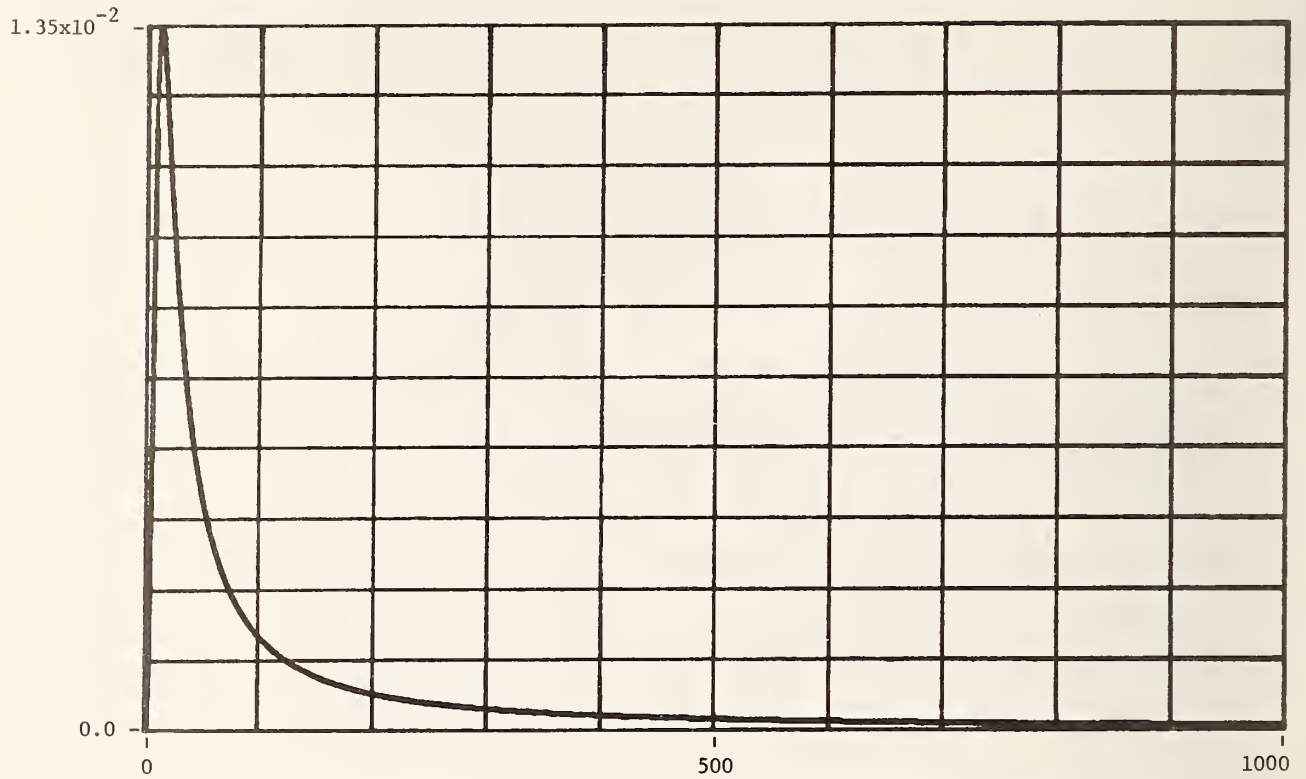


Figure A-17. Modeled and computed time domain impulse response for 304.8 meters (1000 ft) of RG-223/U. Ordinate units are seconds^{-1} , abscissa units are nanoseconds and time spacing between points is 0.9766 ns.

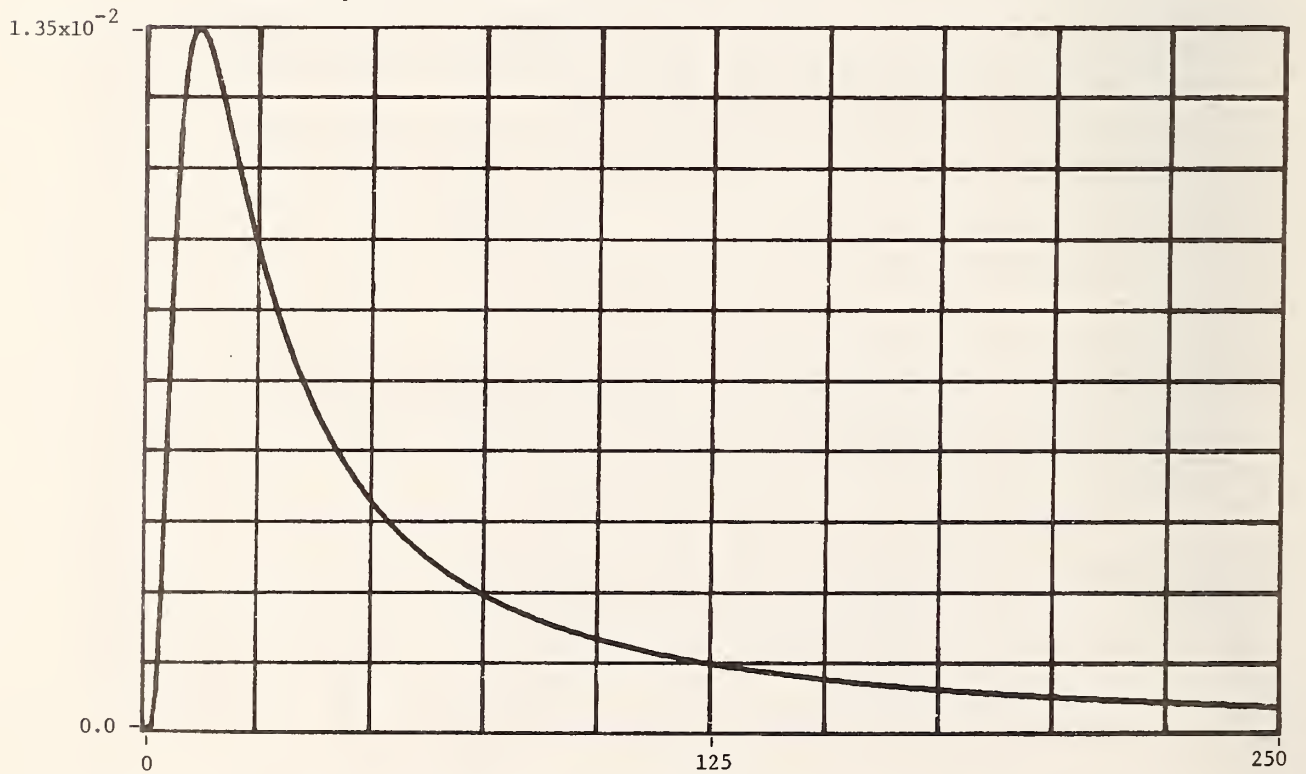


Figure A-18. Time-expanded modeled and computed time domain impulse response for 304.8 meters (1000 ft) of RG-223/U. Ordinate units are seconds^{-1} , abscissa units are nanoseconds and time spacing between points is 0.9766 ns.

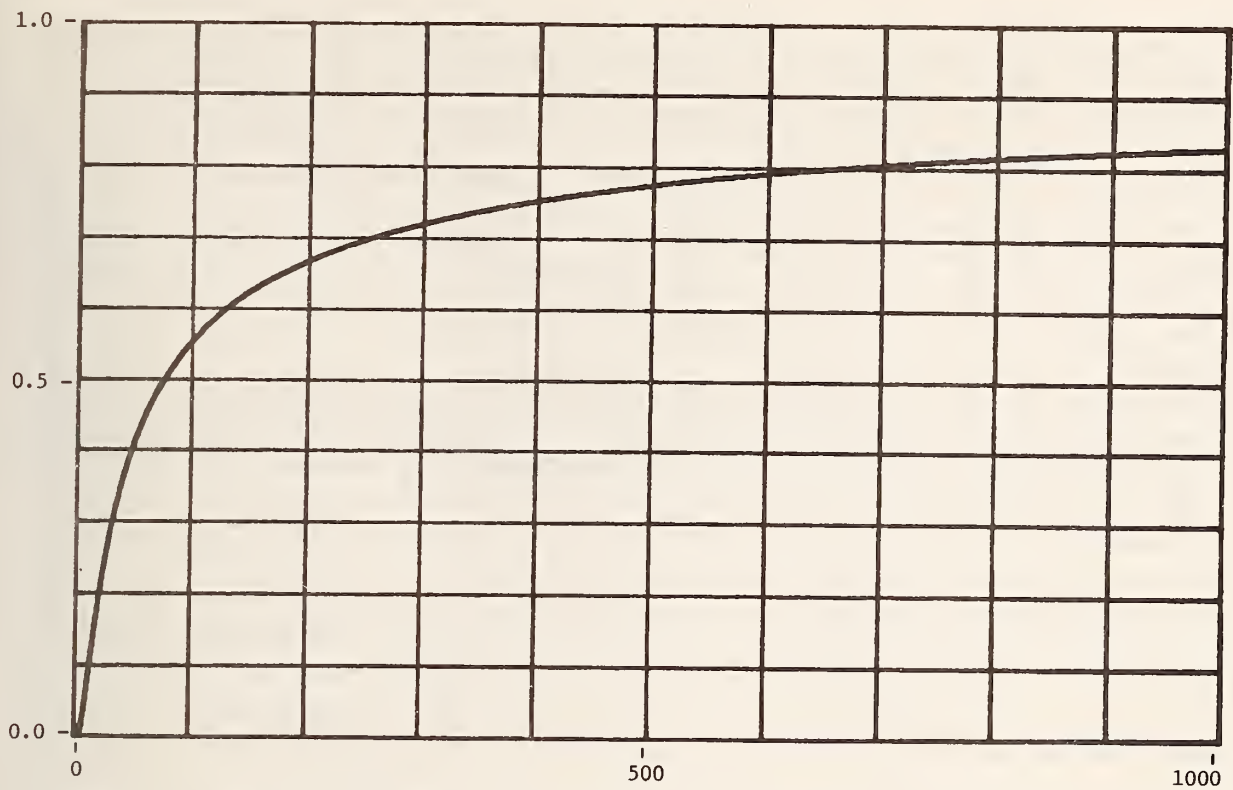


Figure A-19. Modeled and computed time domain unit step response for 304.8 meters (1000 ft) of RG-223/U. Ordinate units are volts and abscissa units are nanoseconds.

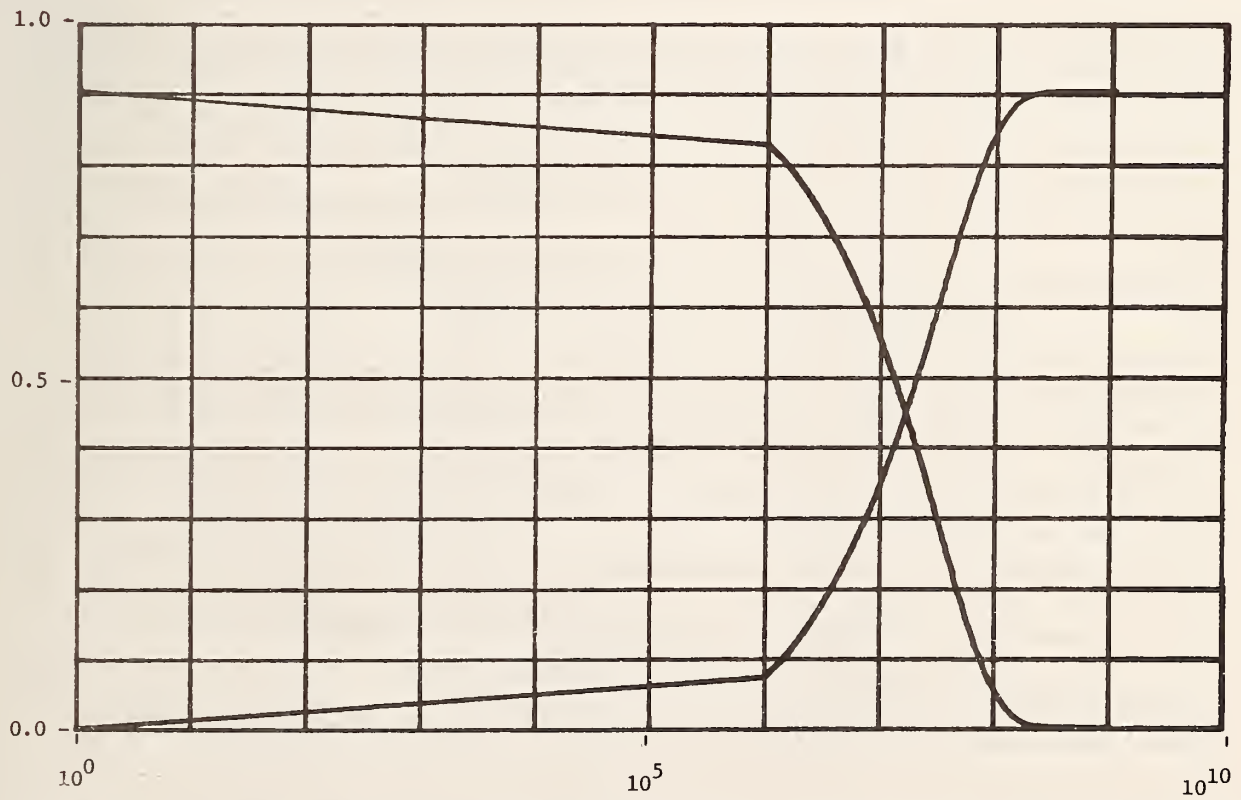


Figure A-20. Plots of "zero"/"one" cable unit step response voltages versus \log_{10} frequency for 304.8 meters (1000 ft) of cable RG-223/U. Ordinate units are volts and abscissa units are hertz.

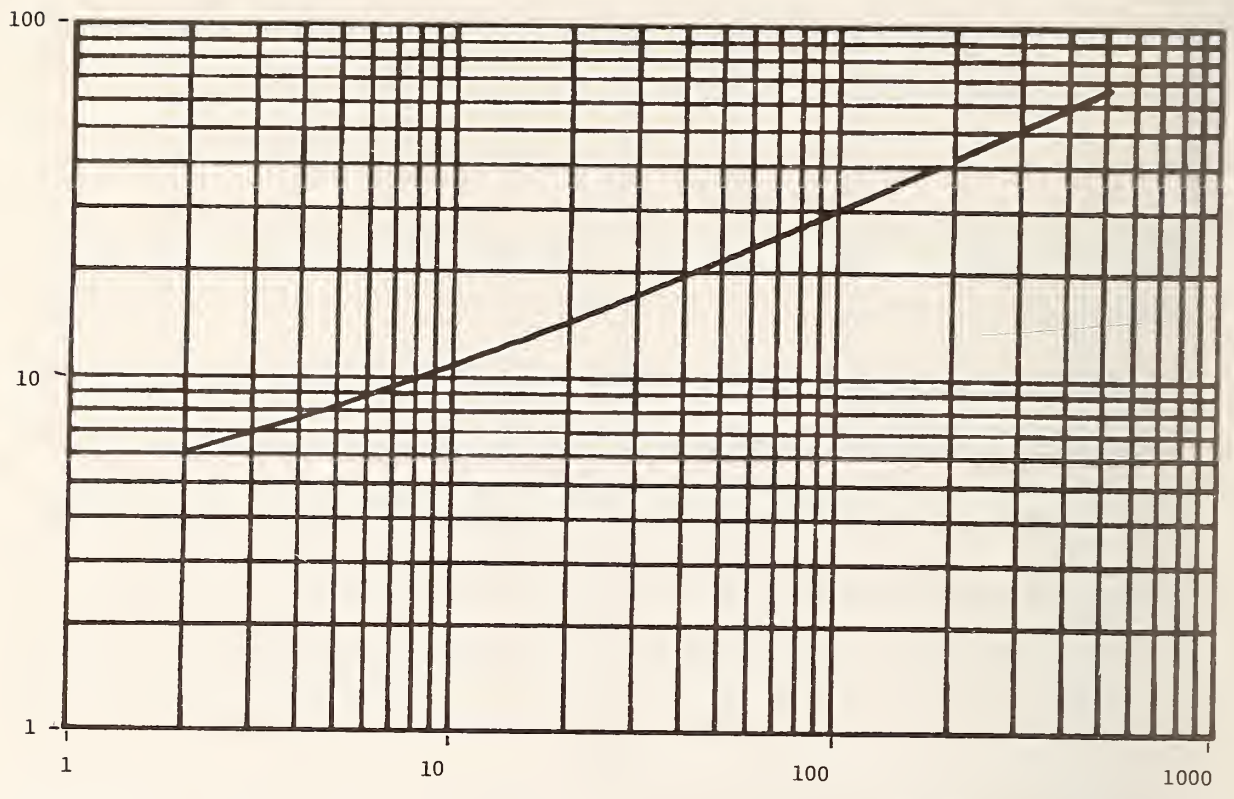


Figure A-21. Modeled attenuation plot for 304.8 meters (1000 ft) of RG-59B/U. Ordinate units are decibels and abscissa units are megahertz.

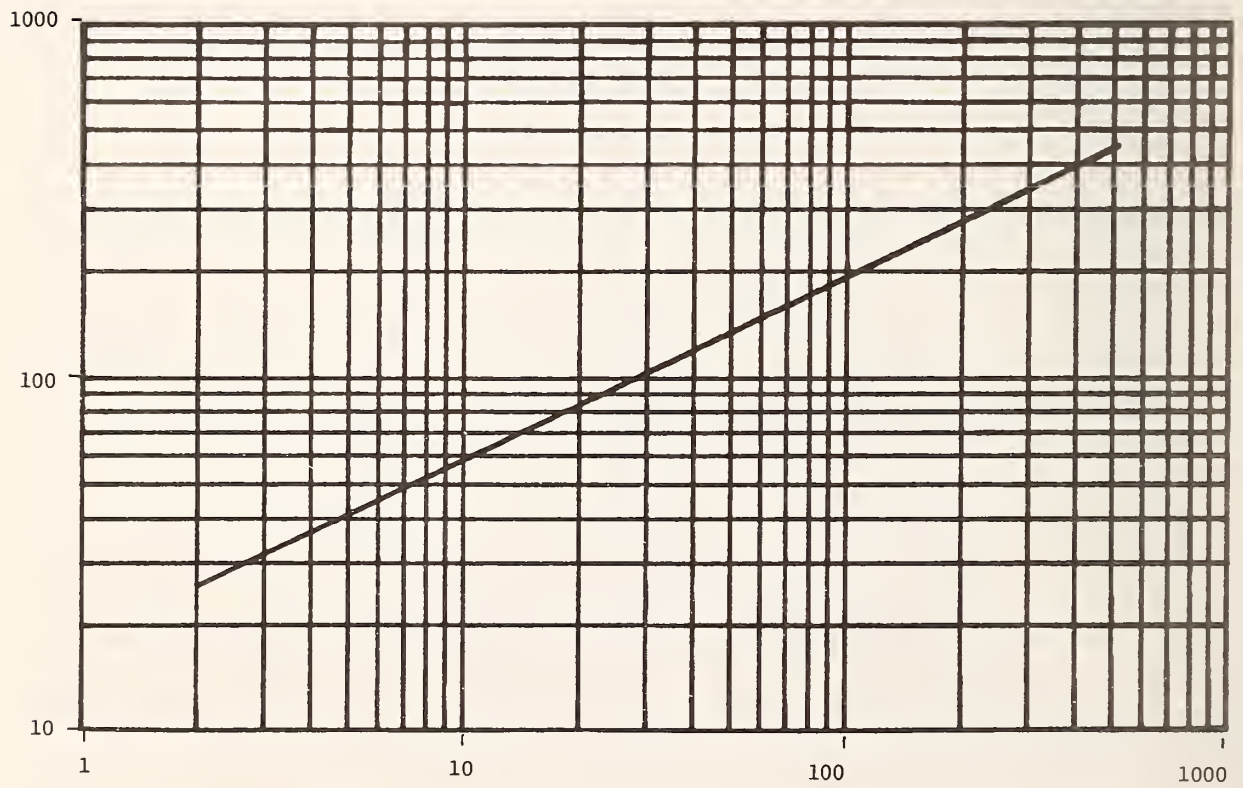


Figure A-22. Modeled minimum-phase phase shift plot for 304.8 meters (1000 ft) of RG-59B/U. Ordinate units are degrees and abscissa units are megahertz.

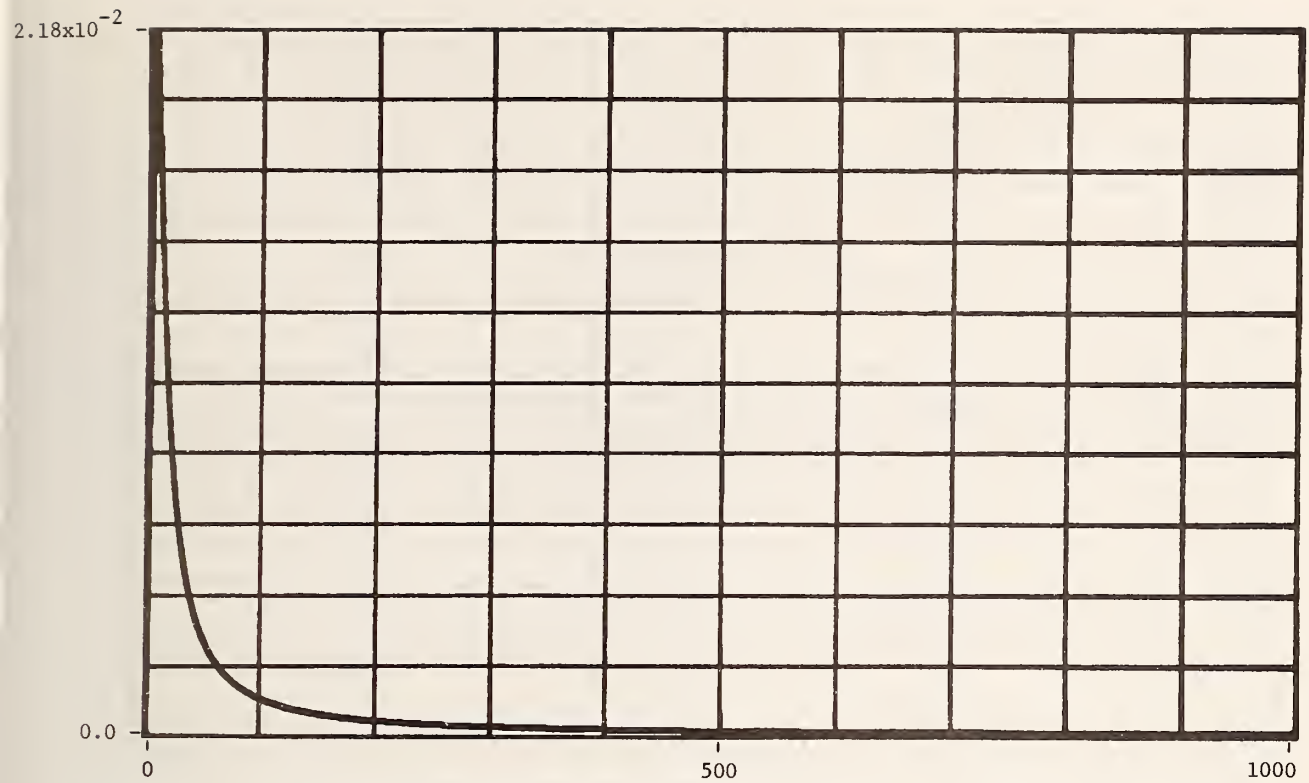


Figure A-23. Modeled and computed time domain impulse response for 304.8 meters (1000 ft) of RG-59B/U. Ordinate units are seconds⁻¹, abscissa units are nanoseconds and time spacing between points is 0.9766 ns.

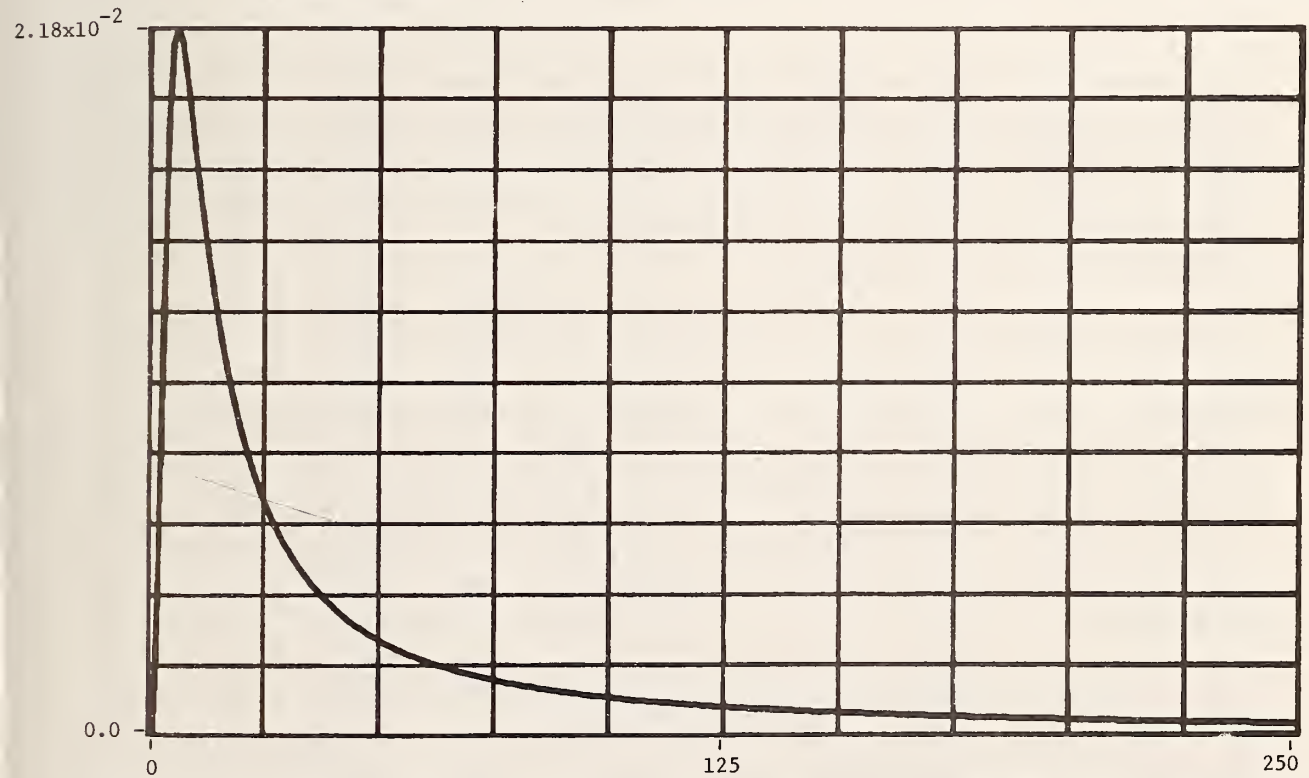


Figure A-24. Time-expanded modeled and computed time domain impulse response for 304.8 meters (1000 ft) of RG-59B/U. Ordinate units are seconds⁻¹, abscissa units are nanoseconds and time spacing between points is 0.9766 ns.

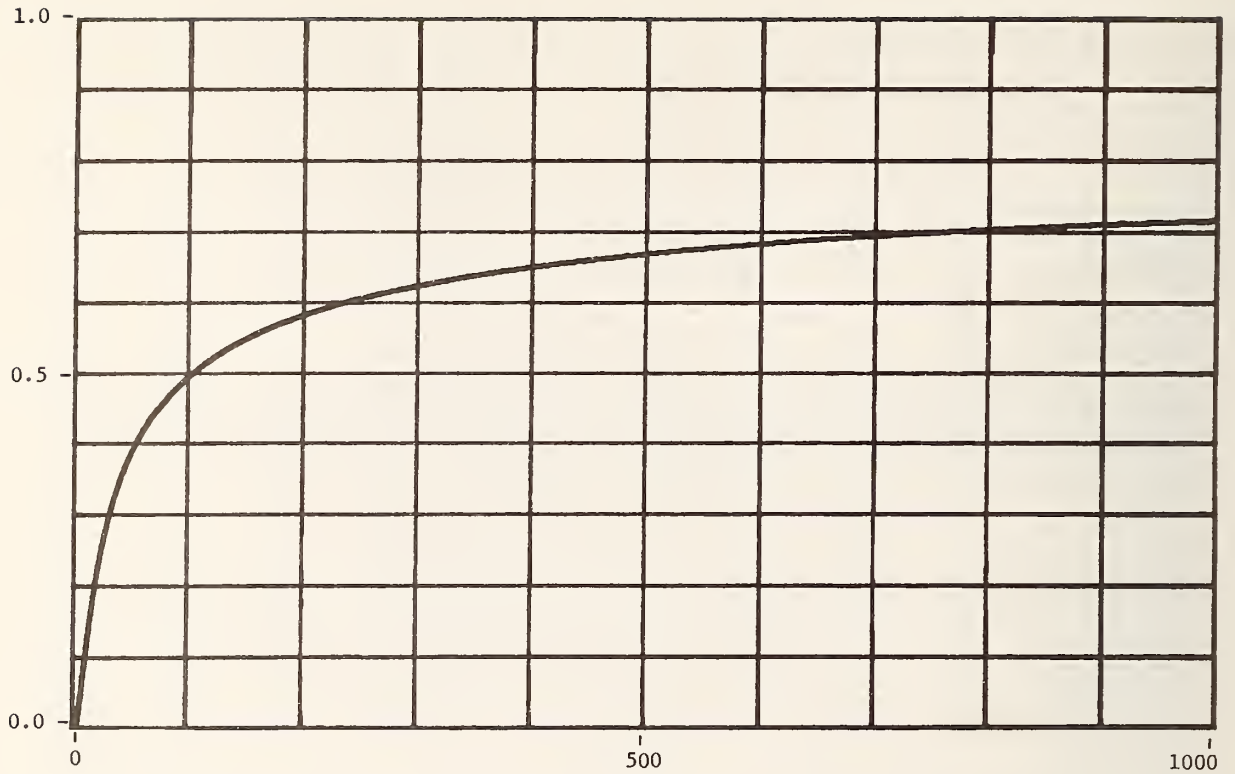


Figure A-25. Modeled and computed time domain unit step response for 304.8 meters (1000 ft) of RG-59B/U. Ordinate units are volts and abscissa units are nanoseconds.

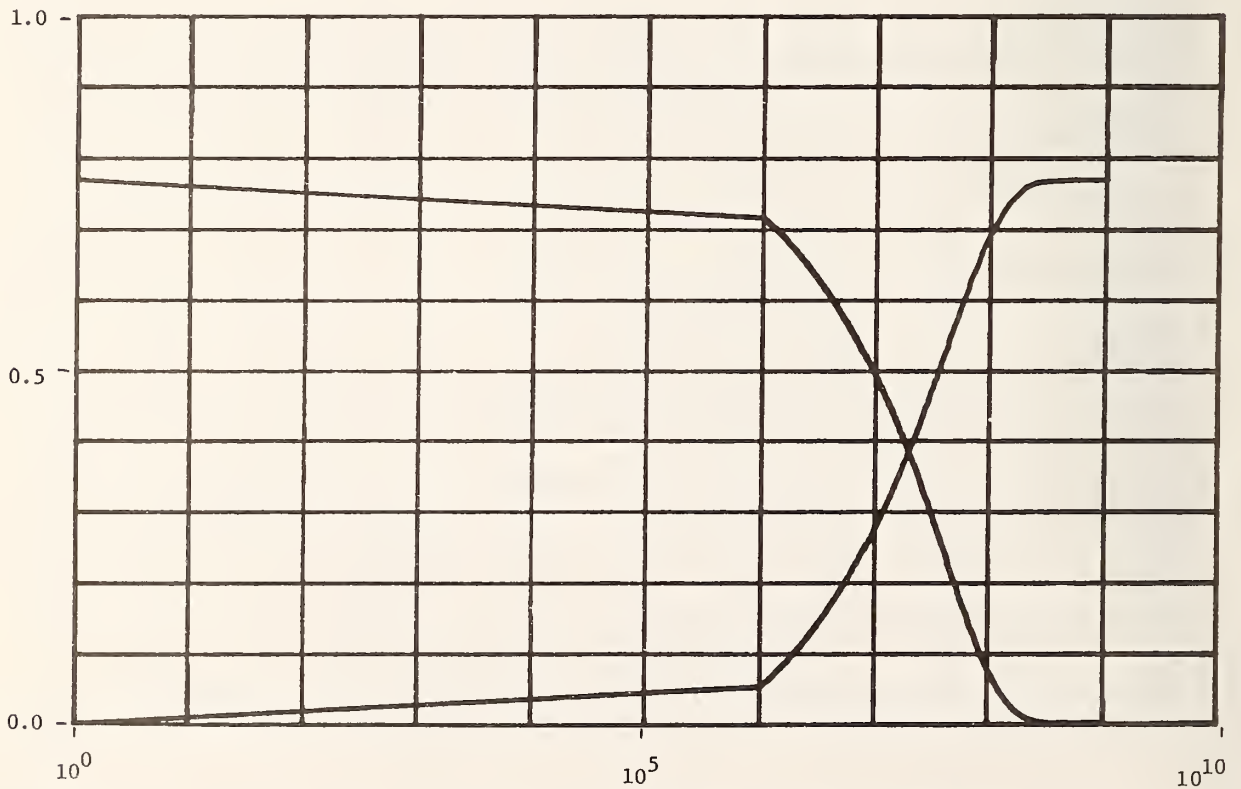


Figure A-26. Plots of "zero"/"one" cable unit step response voltages versus \log_{10} frequency for 304.8 meters (1000 ft) of cable RG-59B/U. Ordinate units are volts and abscissa units are hertz.

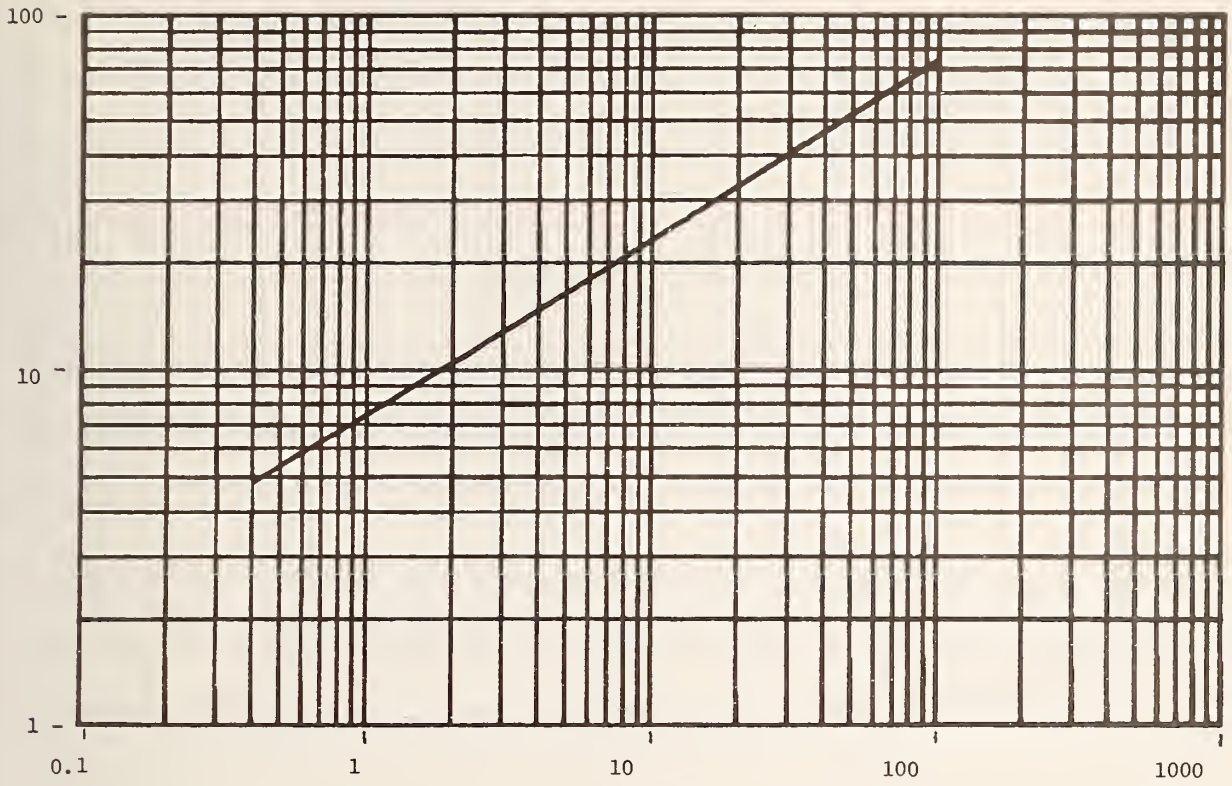


Figure A-27. Modeled attenuation plot for 304.8 meters (1000 ft) of A. Ordinate units are decibels and abscissa units are megahertz.

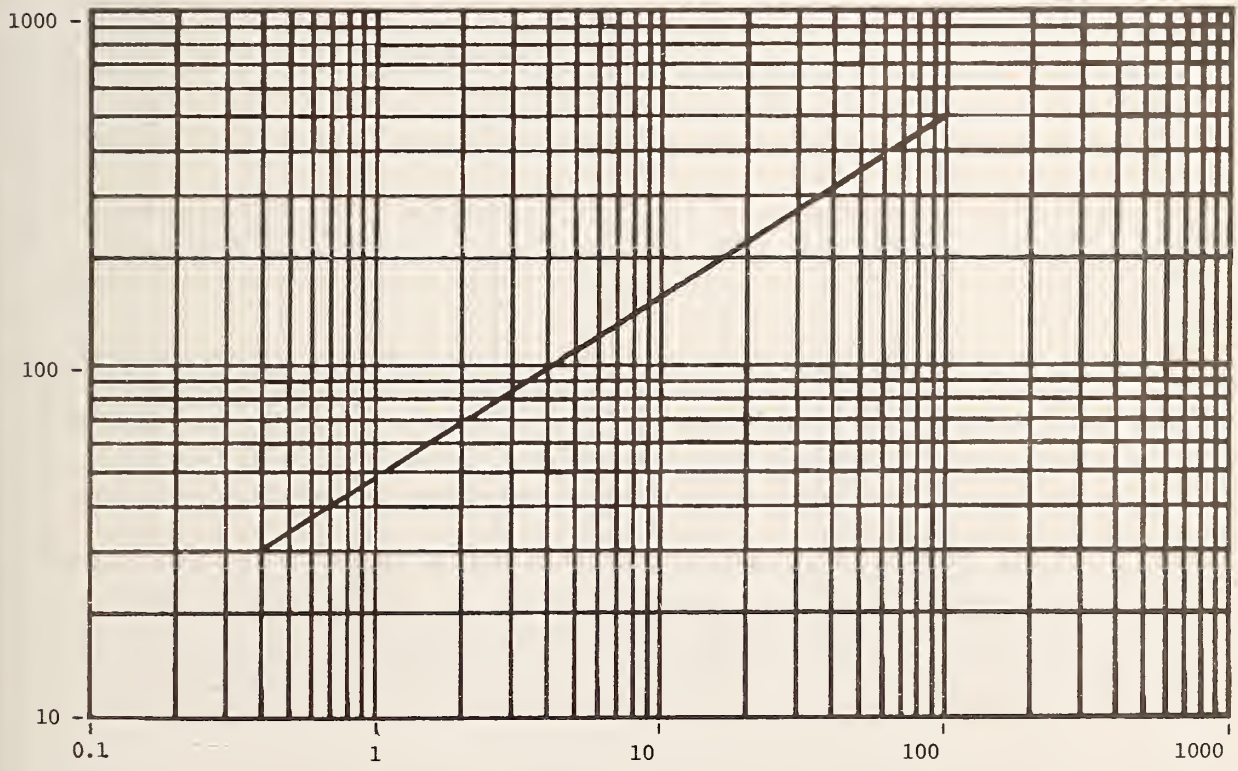


Figure A-28. Modeled minimum-phase phase shift plot for 304.8 meters (1000 ft) of A. Ordinate units are degrees and abscissa units are megahertz.

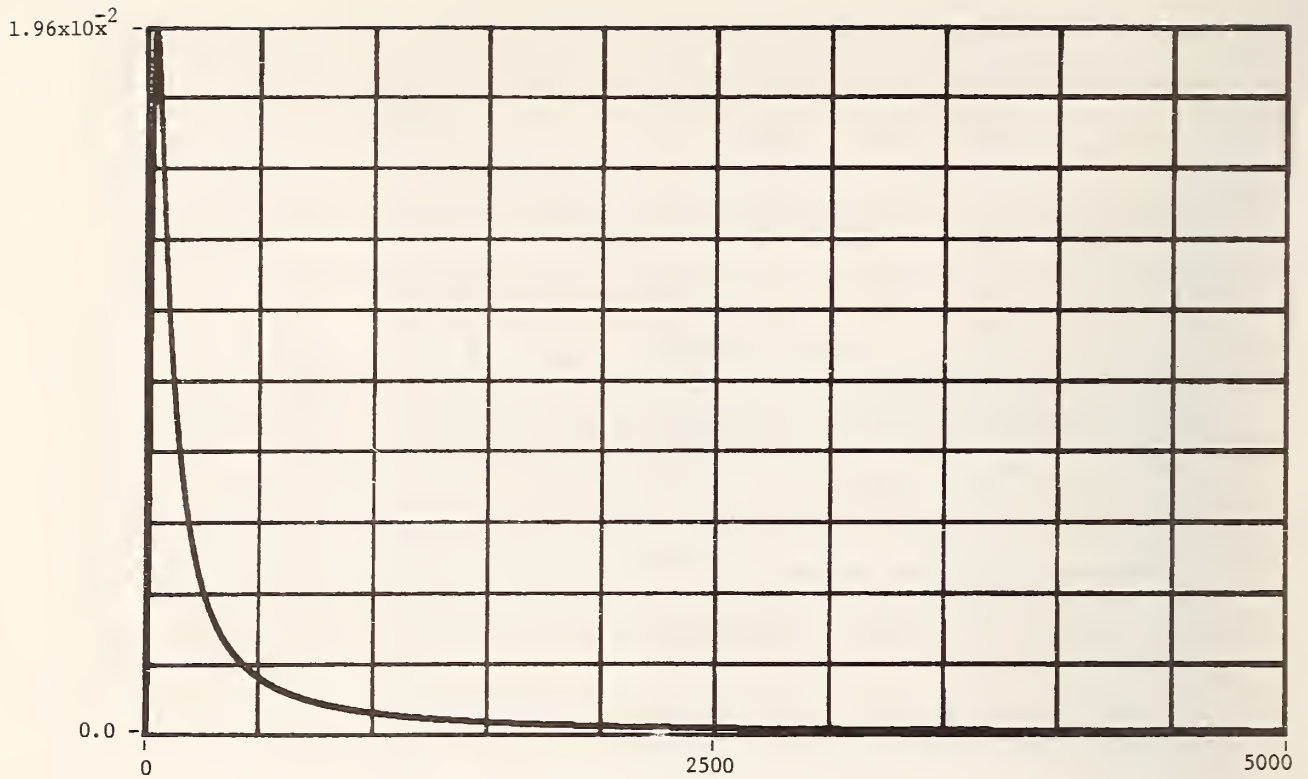


Figure A-29. Modeled and computed time domain impulse response for 304.8 meters (1000 ft) of A. Ordinate units are seconds^{-1} , abscissa units are nanoseconds and time spacing between points is 0.9766 ns.

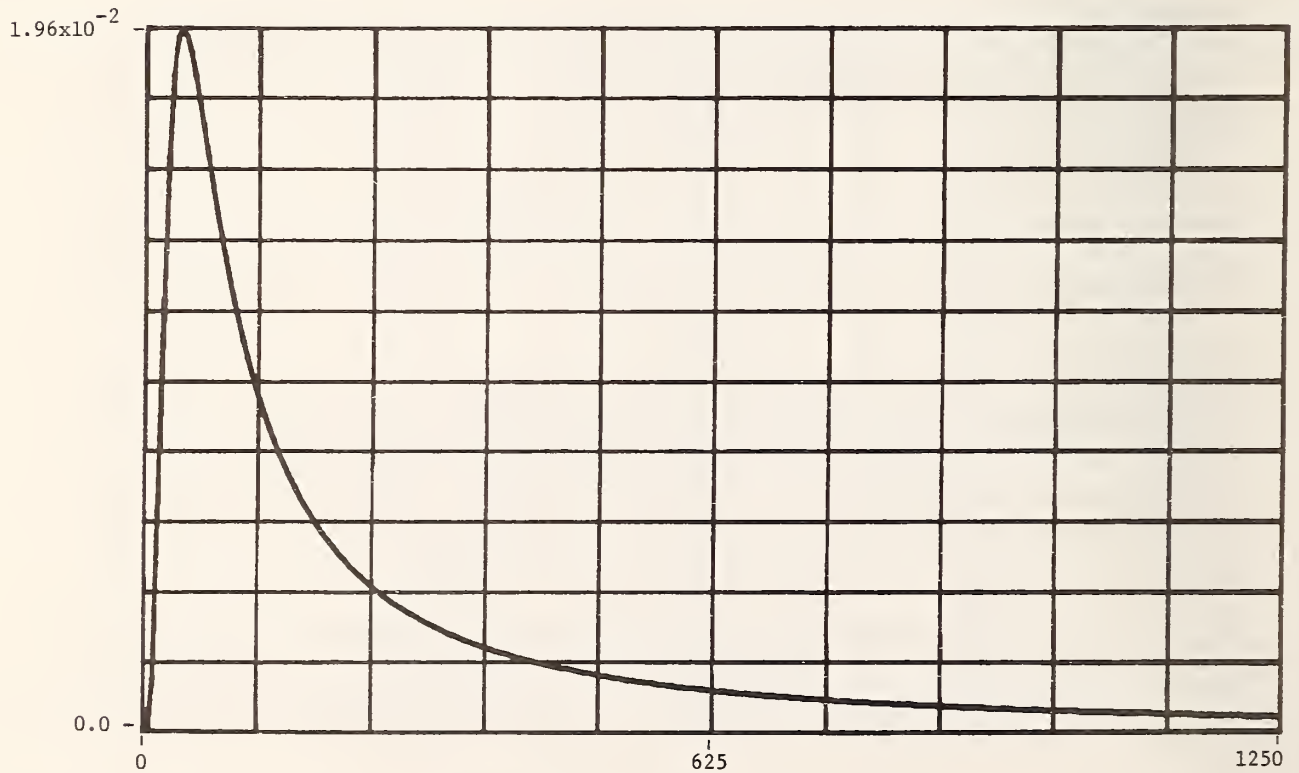


Figure A-30. Time-expanded modeled and computed time domain impulse response for 304.8 meters (1000 ft) of A. Ordinate units are seconds^{-1} , abscissa units are nanoseconds and time spacing between points is 0.9766 ns.

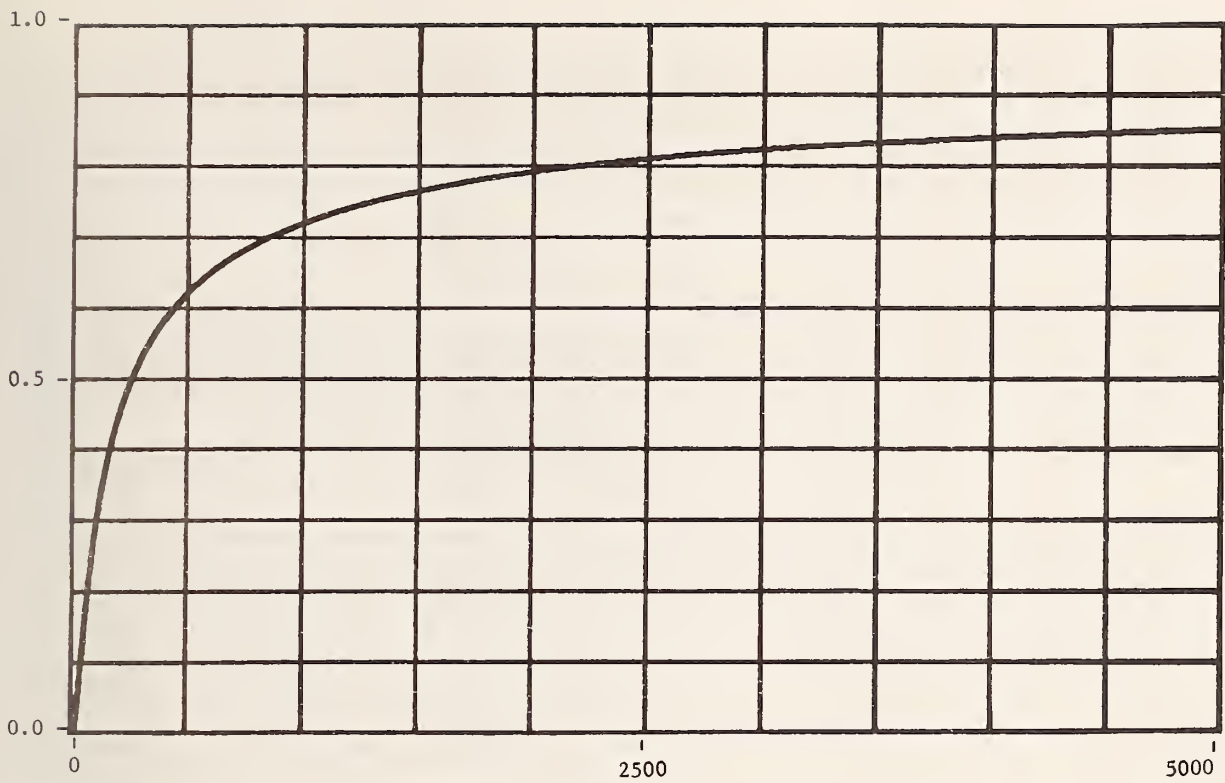


Figure A-31. Modeled and computed time domain unit step response for 304.8 meters (1000 ft) of A. Ordinate units are volts and abscissa units are nanoseconds.

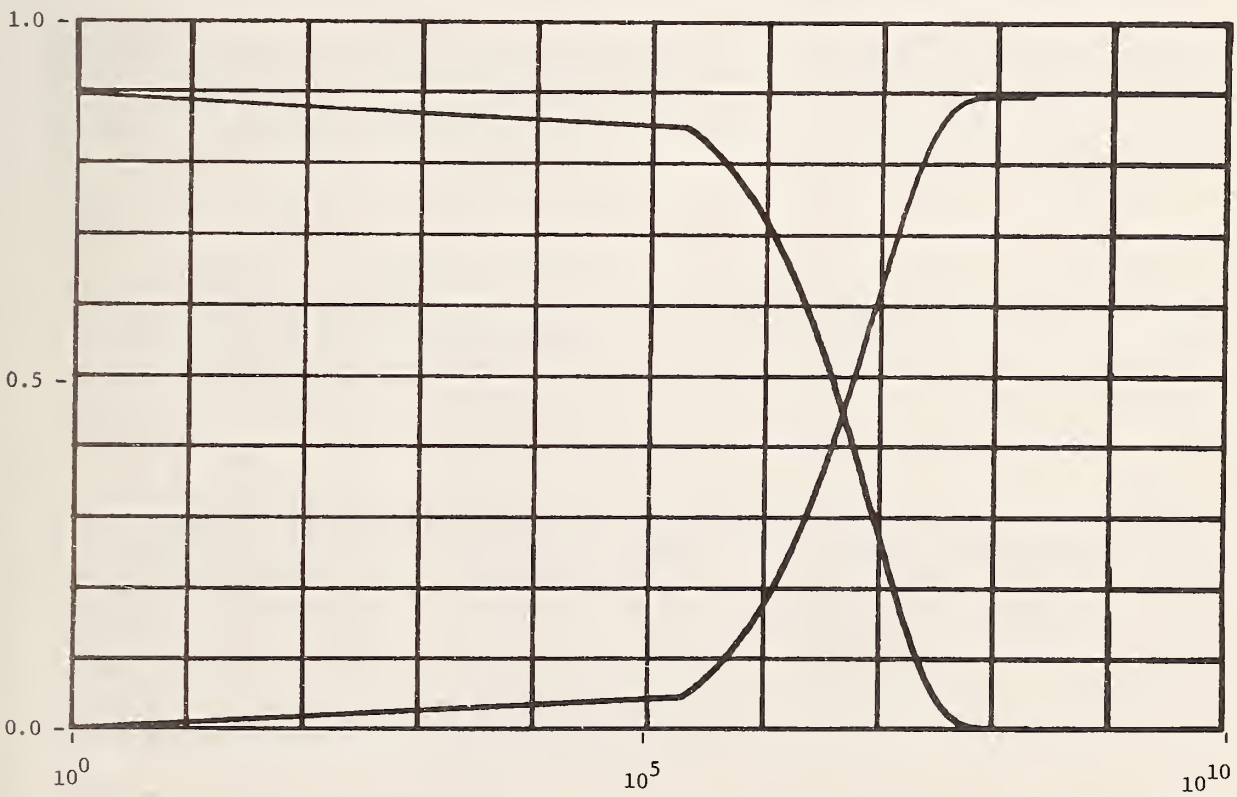


Figure A-32. Plots of "zero"/"one" cable unit step response voltages versus \log_{10} frequency for 304.8 meters (1000 ft) of cable A. Ordinate units are volts and abscissa units are hertz.

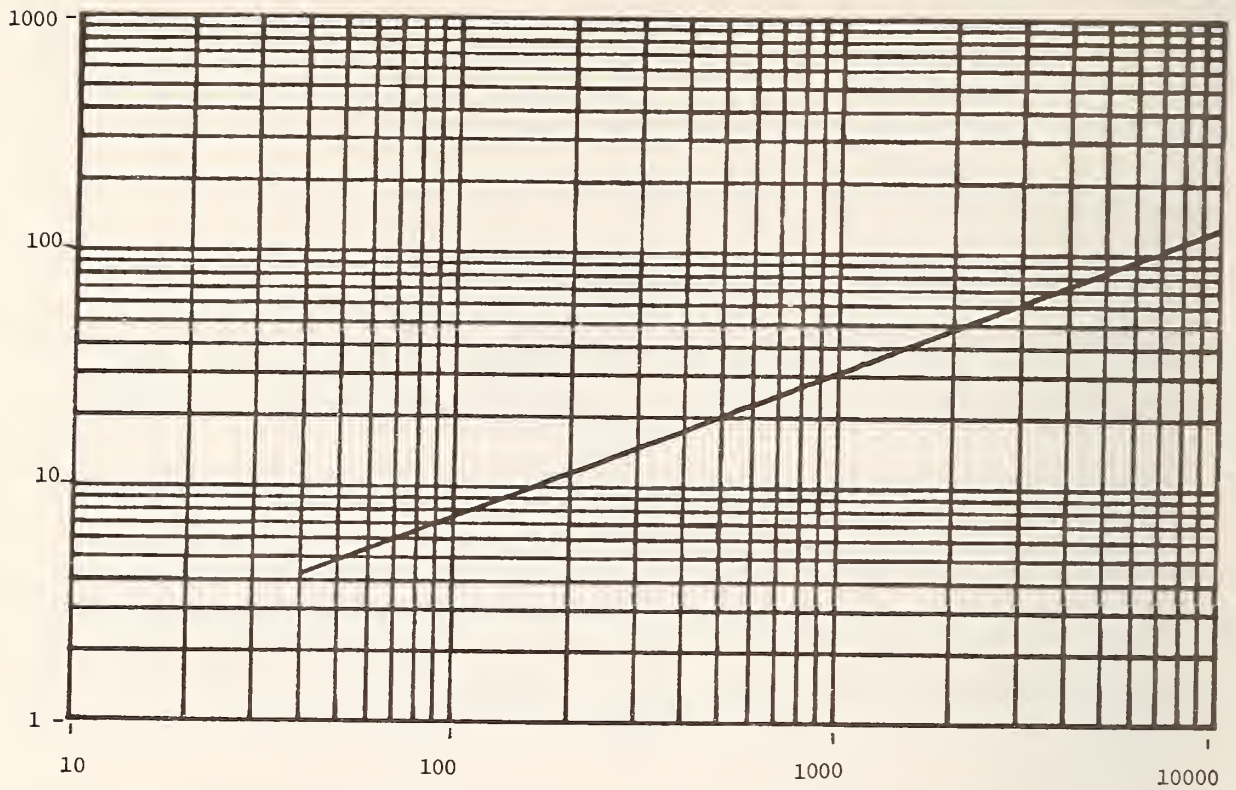


Figure A-33. Modeled attenuation plot for 60.96 meters (200 ft) of B. Ordinate units are decibels and abscissa units are megahertz.

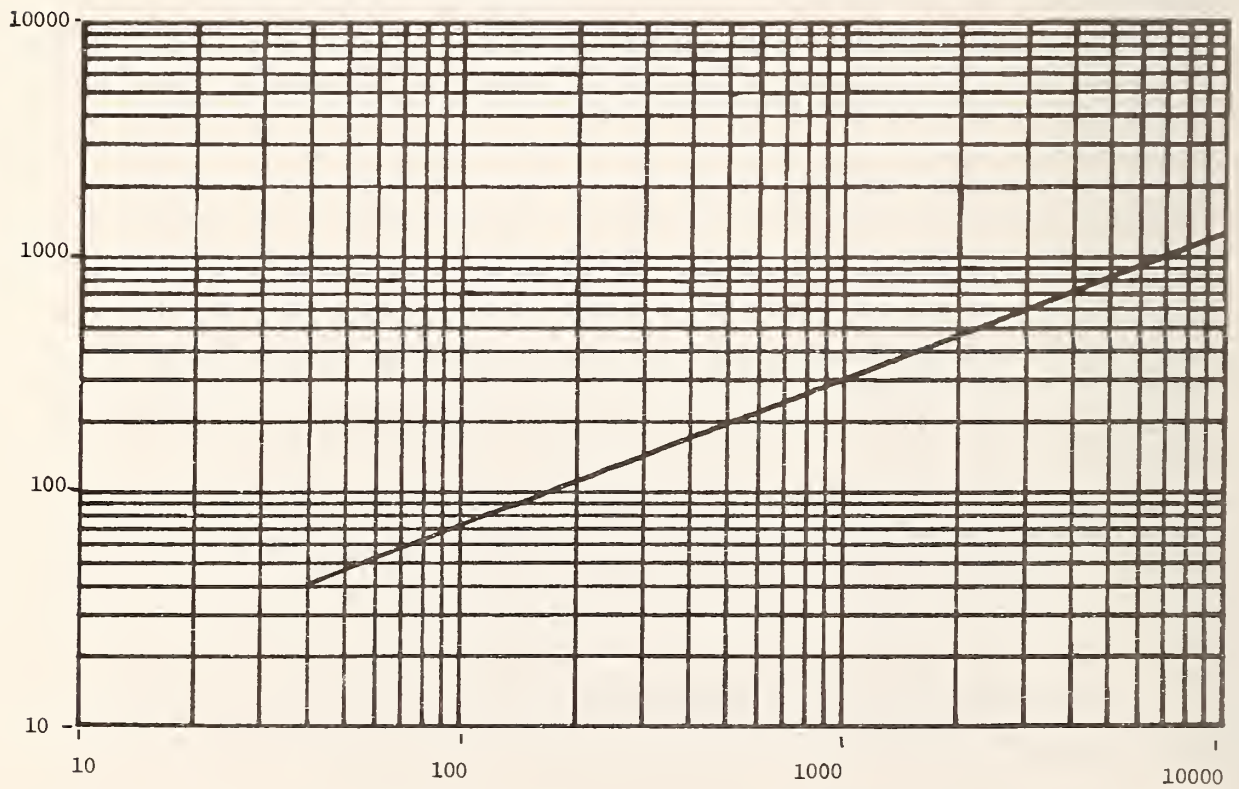


Figure A-34. Modeled minimum-phase phase shift plot for 60.96 meters (200 ft) of B. Ordinate units are degrees and abscissa units are megahertz.

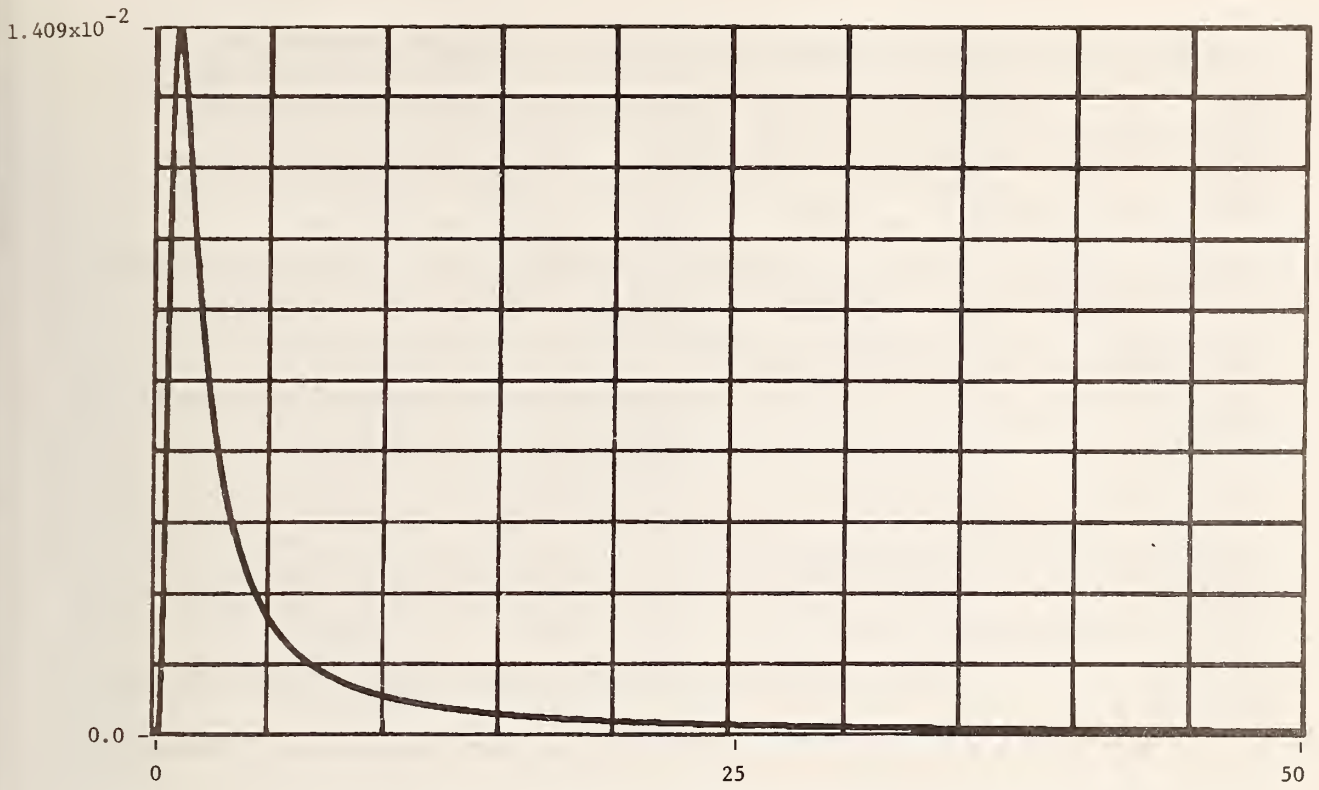


Figure A-35. Modeled and computed time domain impulse response for 60.96 meters (200 ft) of B. Ordinate units are seconds^{-1} , abscissa units are nanoseconds and time spacing between points is 0.9766 ns.

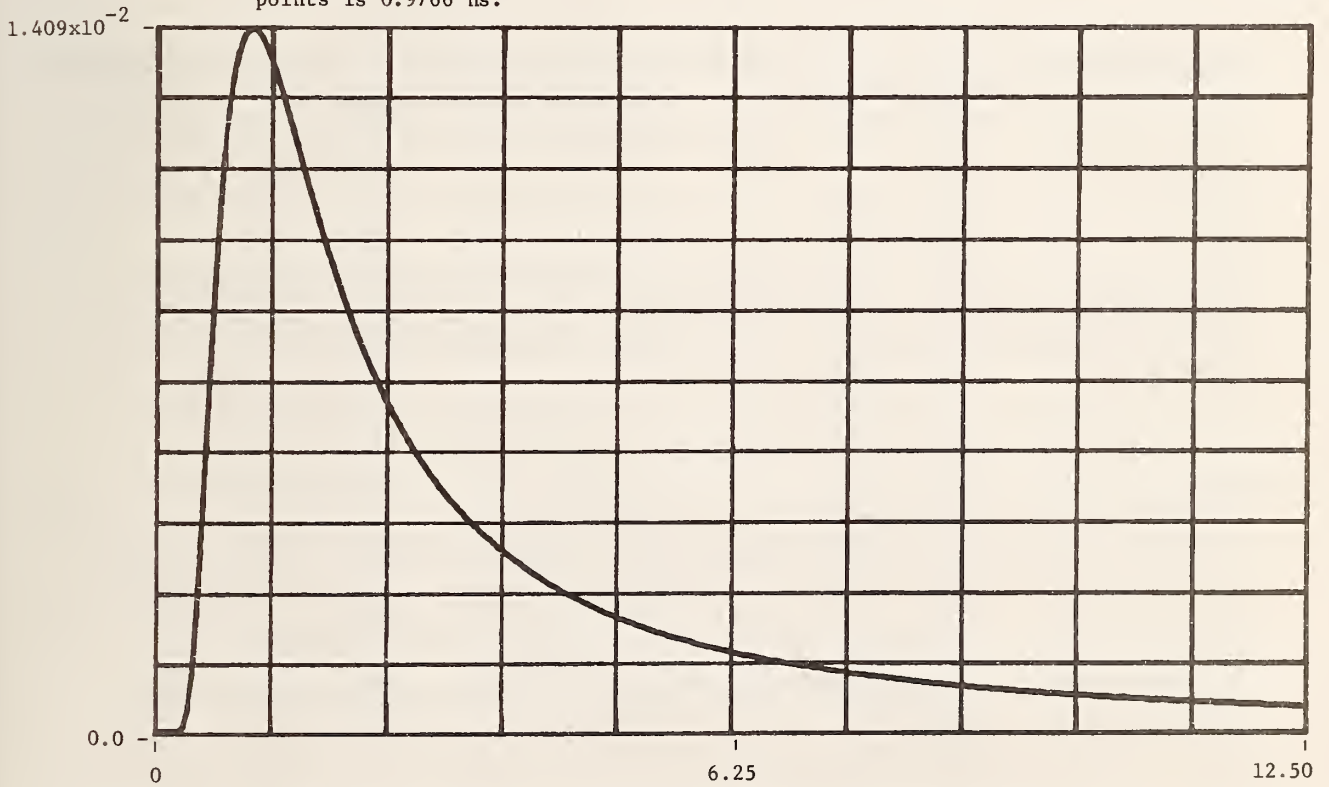


Figure A-36. Time-expanded modeled and computed time domain impulse response for 60.96 meters (200 ft) of B. Ordinate units are seconds^{-1} , abscissa units are nanoseconds and time spacing between points is 0.9766 ns.

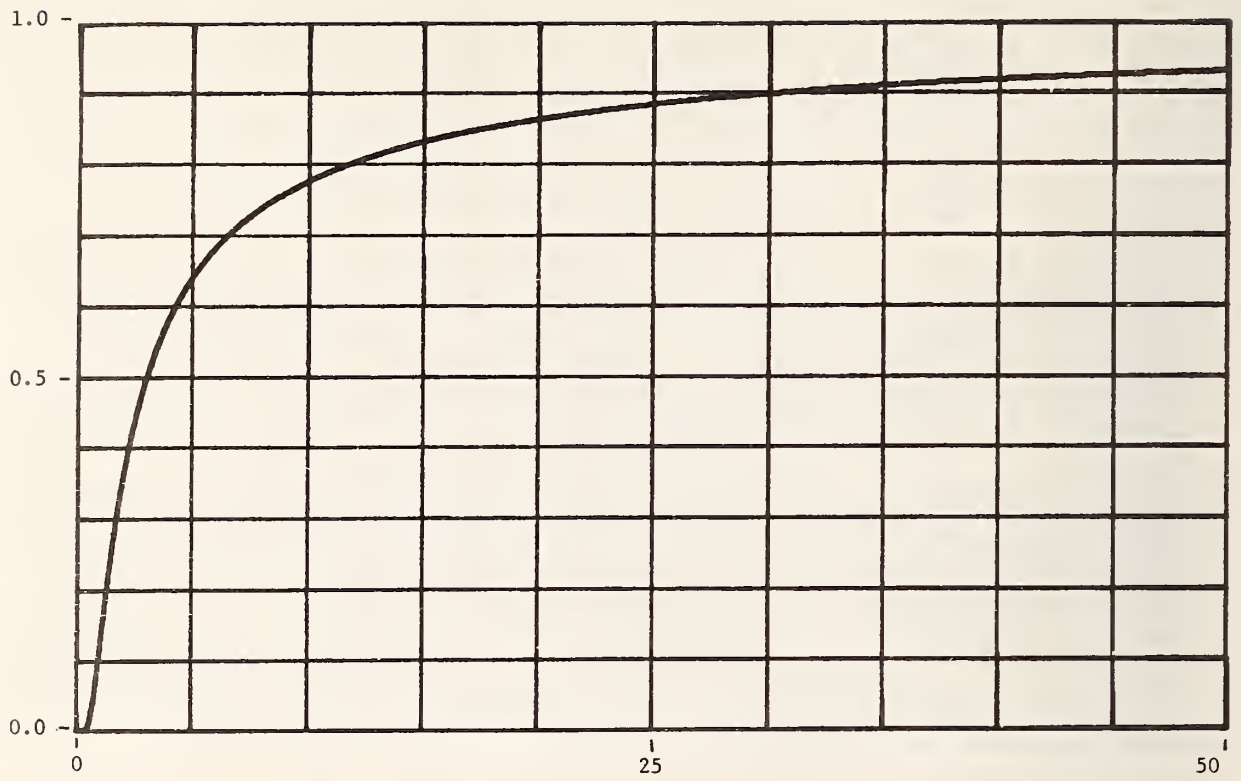


Figure A-37. Modeled and computed time domain unit step response for 60.96 meters (200 ft) of B. Ordinate units are volts and abscissa units are nanoseconds.

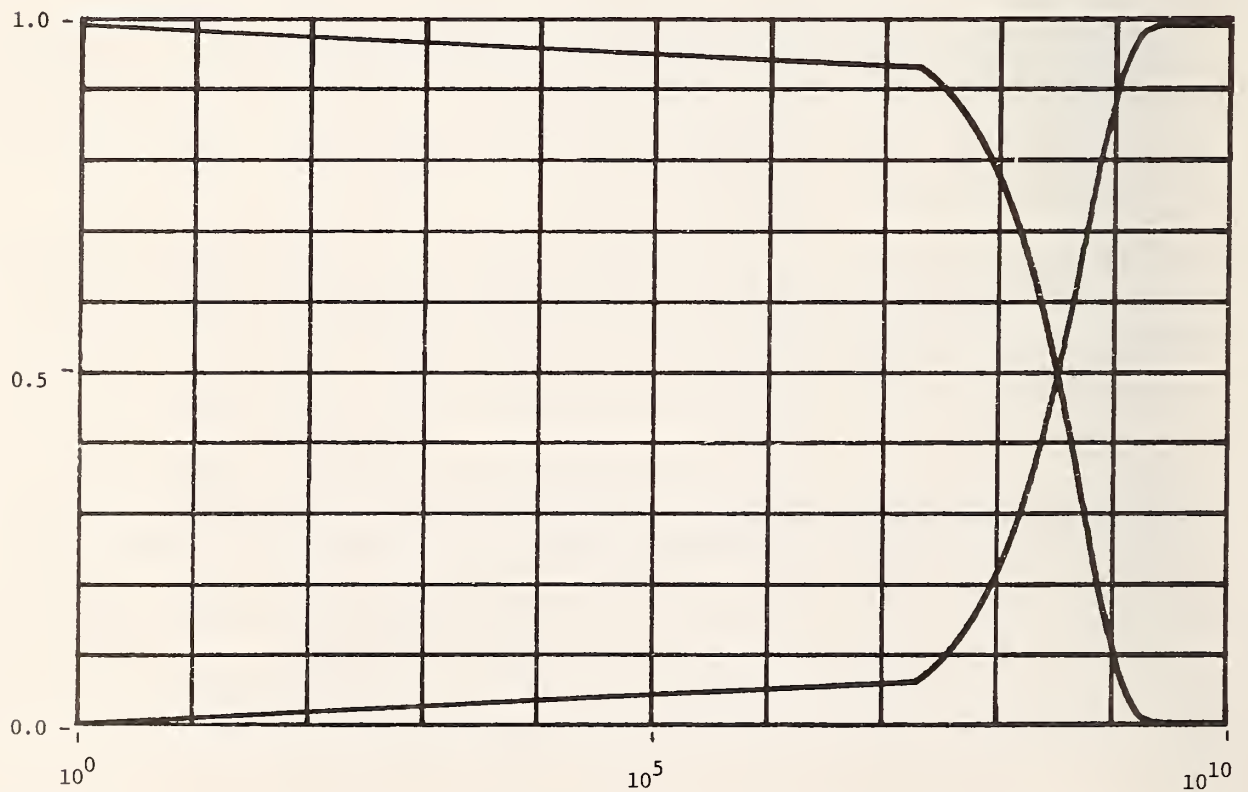


Figure A-38. Plots of "zero"/"one" cable unit step response voltages versus \log_{10} frequency for 60.96 meters (200 ft) of cable B. Ordinate units are volts and abscissa units are hertz.

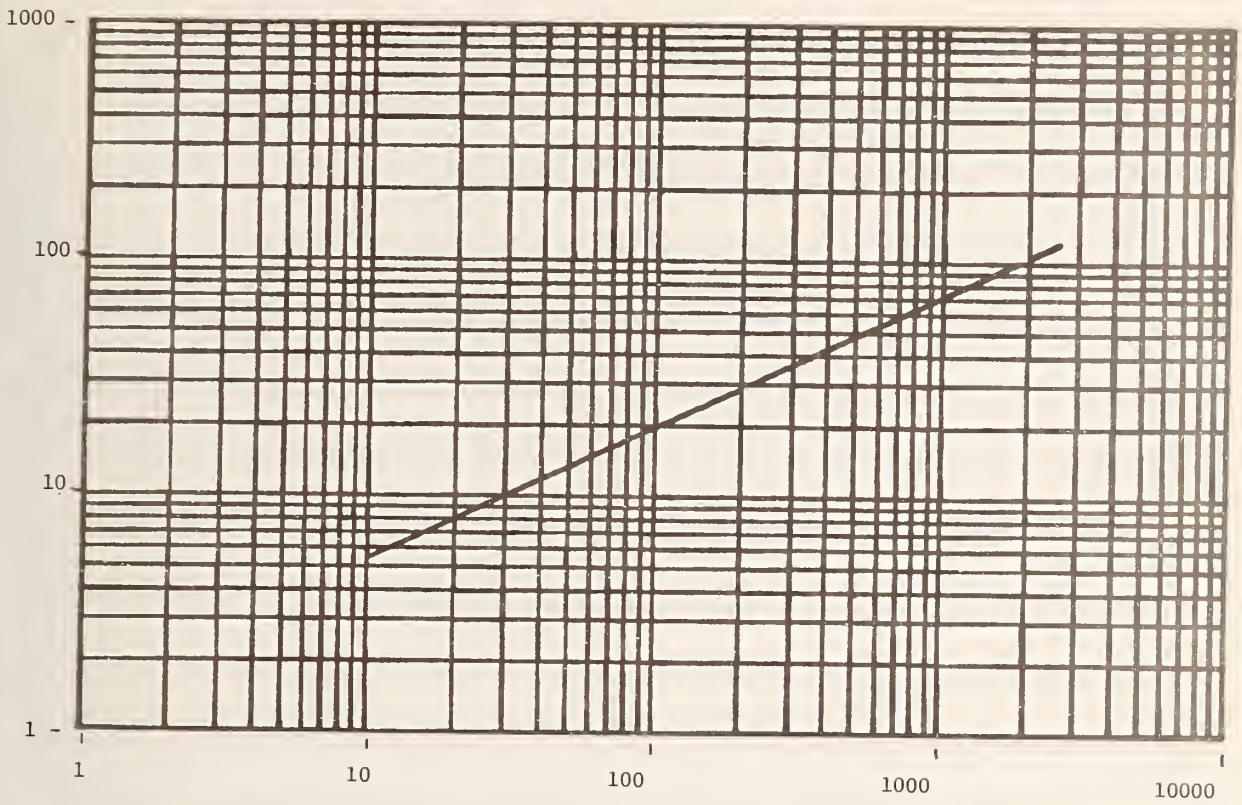


Figure A-39. Modeled attenuation plot for 152.4 meters (500 ft) of B. Ordinate units are decibels and abscissa units are megahertz.

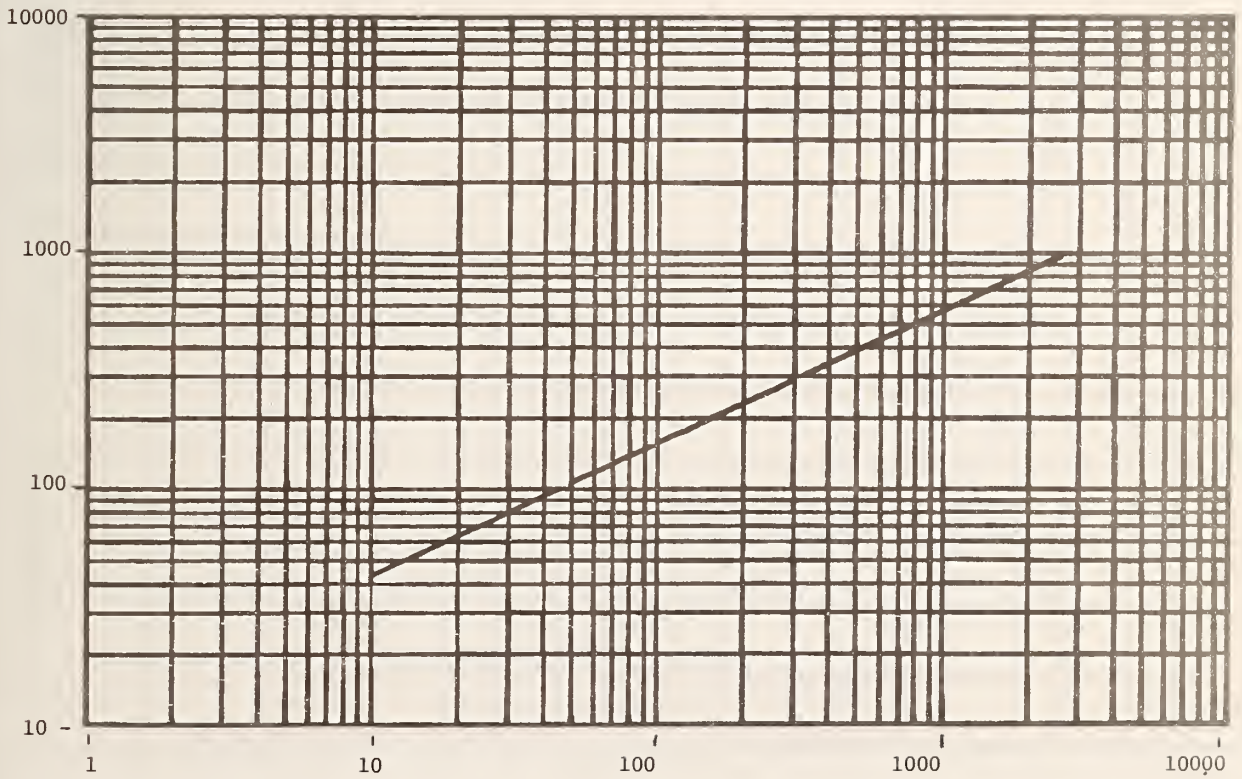


Figure A-40. Modeled minimum-phase phase shift plot for 152.4 meters (500 ft) of B. Ordinate units are degrees and abscissa units are megahertz.

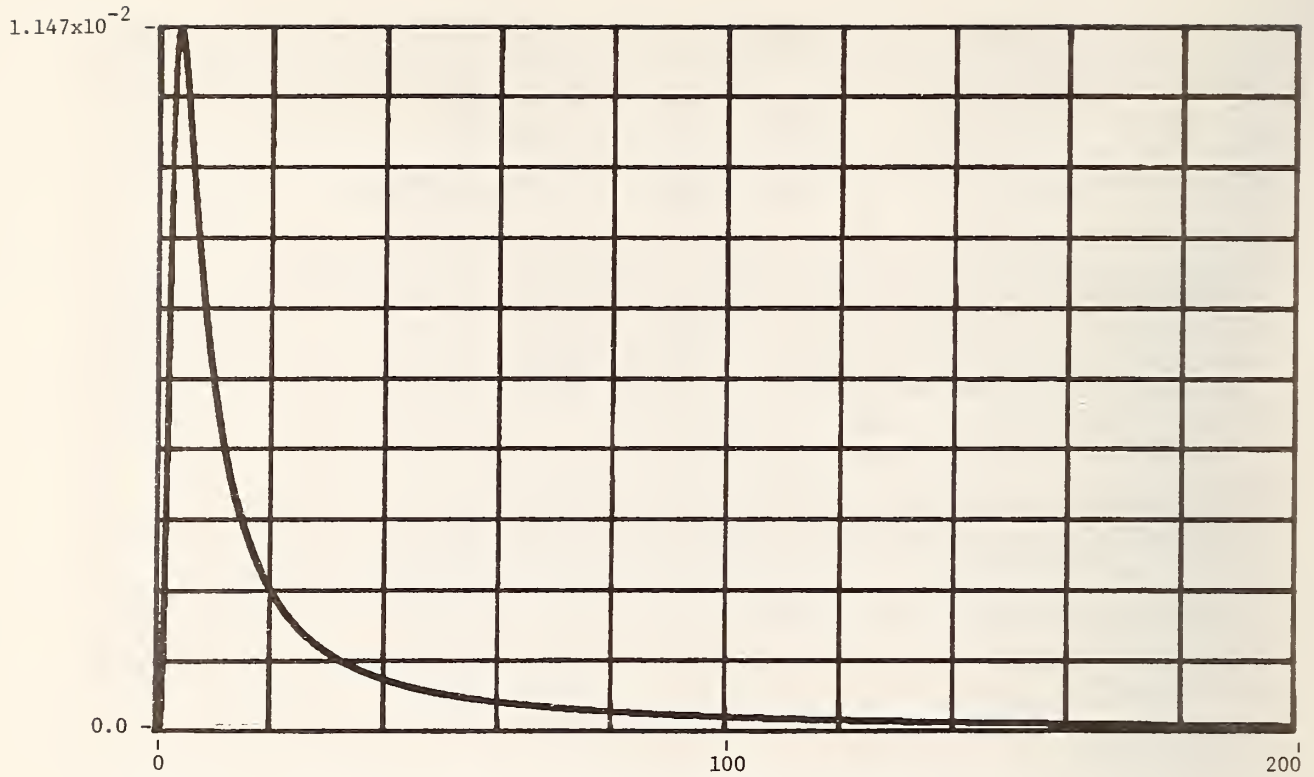


Figure A-41. Modeled and computed time domain impulse response for 152.4 meters (500 ft) of B. Ordinate units are seconds^{-1} , abscissa units are nanoseconds and time spacing between points is 0.9766 ns.

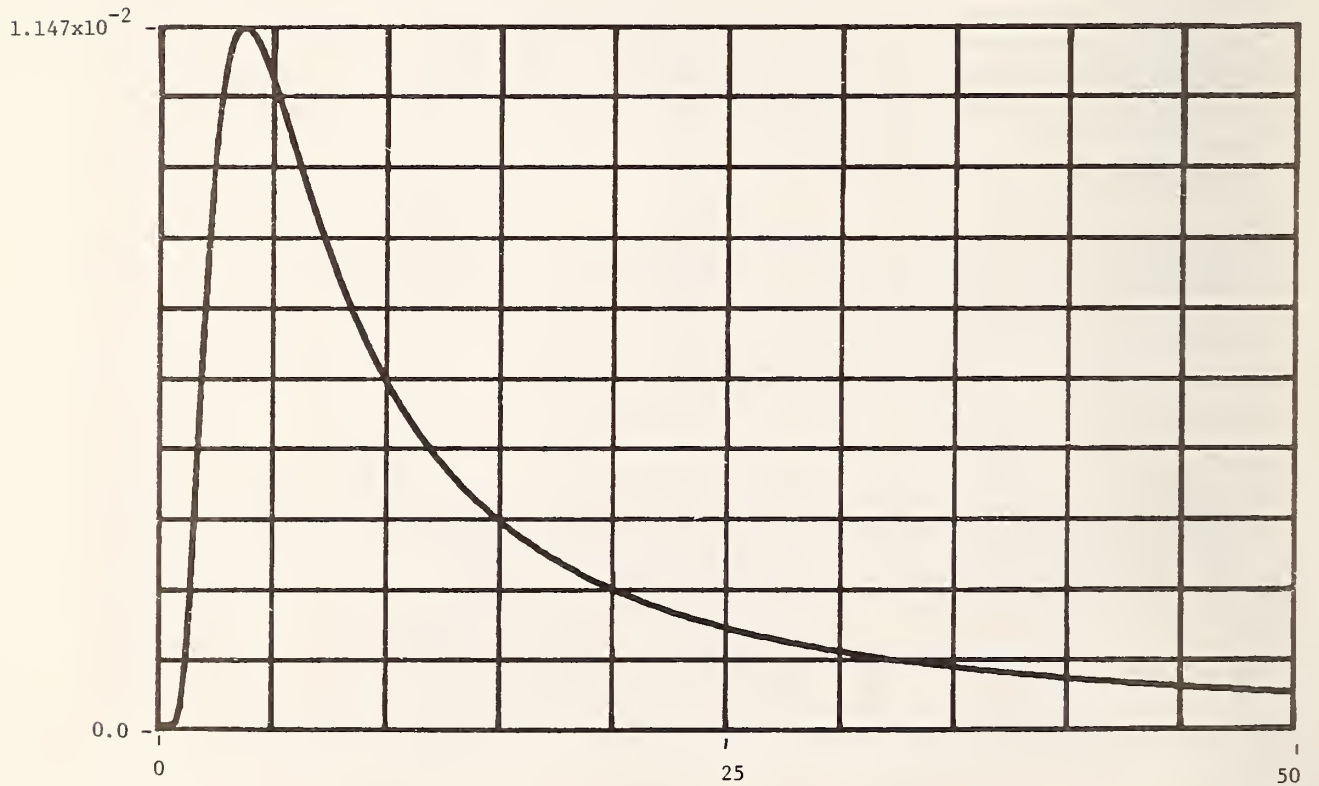


Figure A-42. Time-expanded modeled and computed time domain impulse response for 152.4 meters (500 ft) of B. Ordinate units are seconds^{-1} , abscissa units are nanoseconds and time spacing between points is 0.9766 ns.

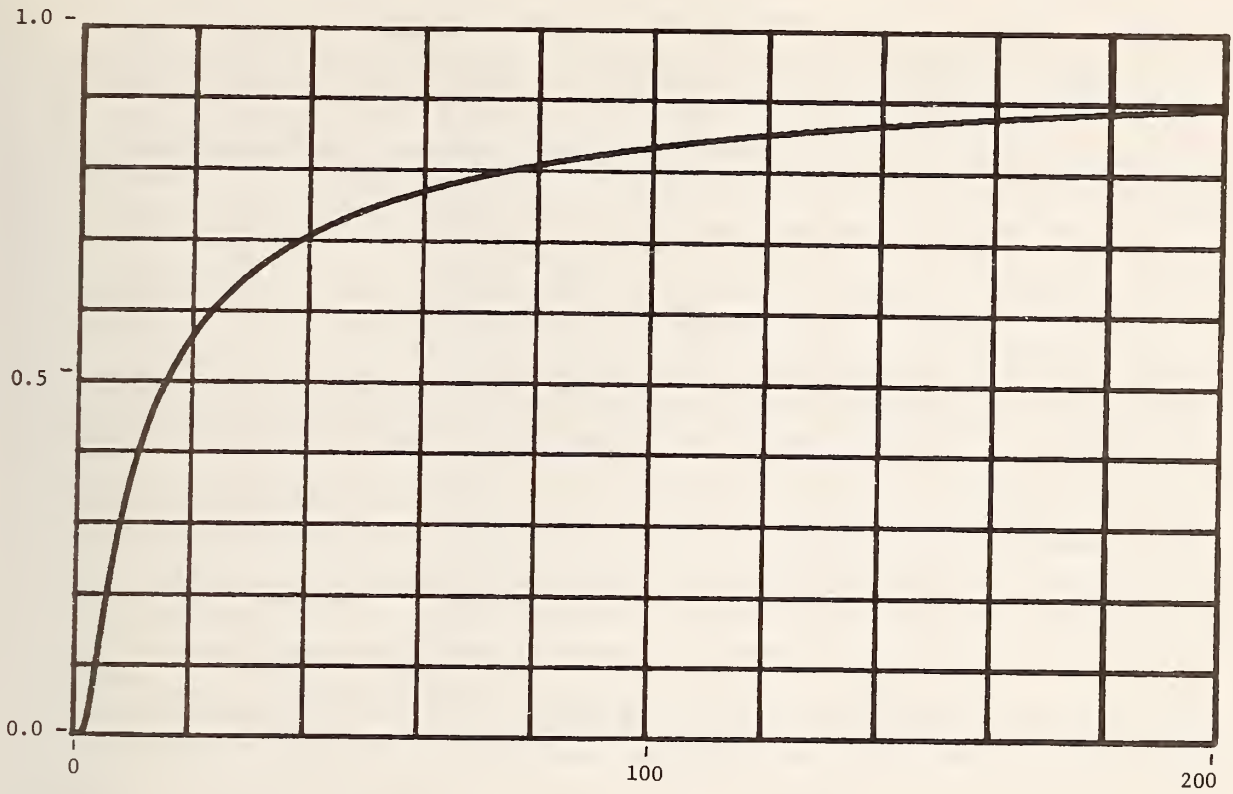


Figure A-43. Modeled and computed time domain unit step response for 152.4 meters (500 ft) of B. Ordinate units are volts and abscissa units are nanoseconds.

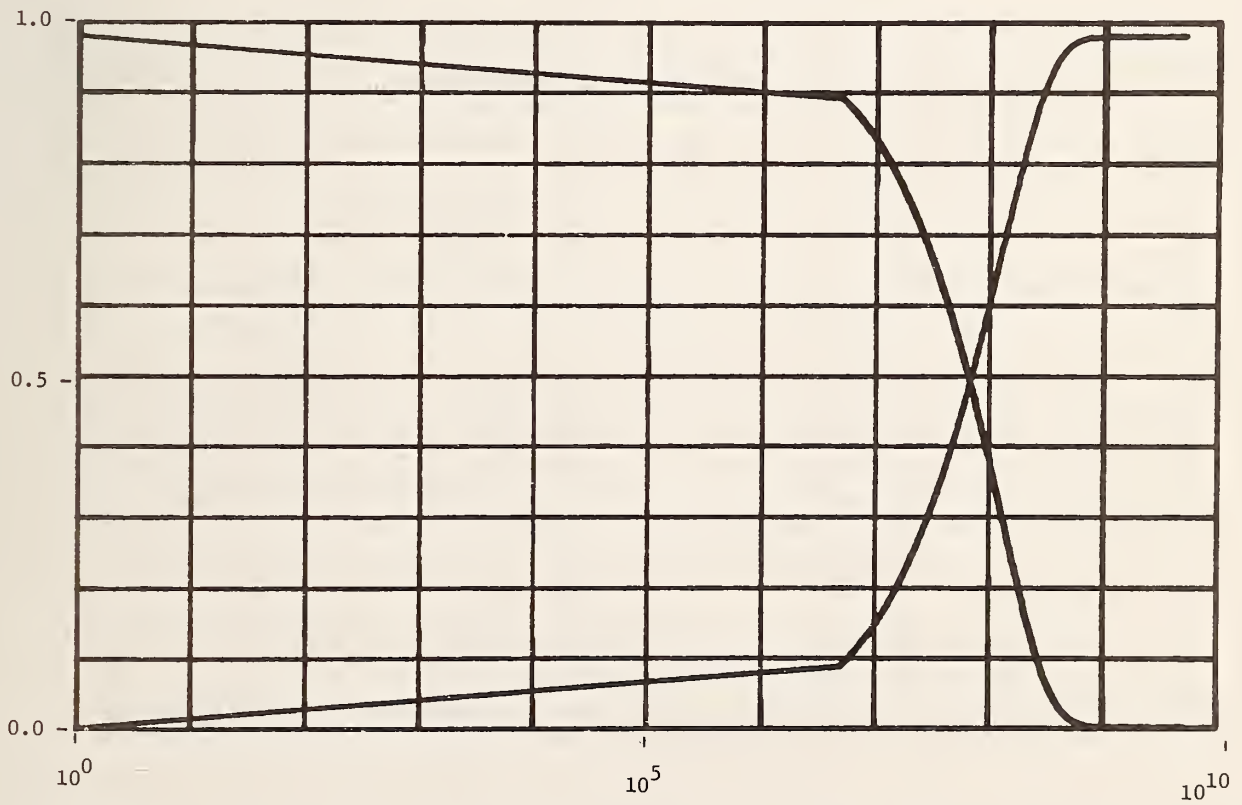


Figure A-44. Plots of "zero"/"one" cable unit step response voltages versus \log_{10} frequency for 152.4 meters (500 ft) of cable B. Ordinate units are volts and abscissa units are hertz.

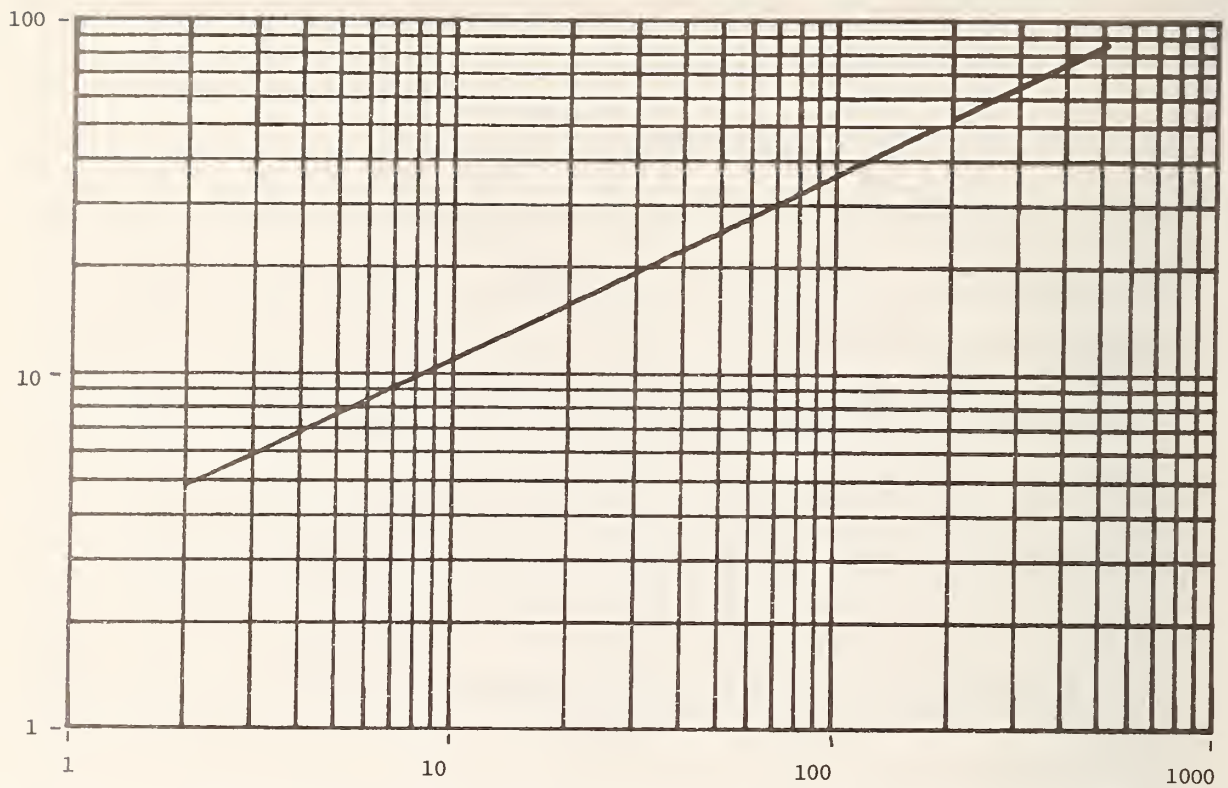


Figure A-45. Modeled attenuation plot for 333.76 meters (1095 ft) of B. Ordinate units are decibels and abscissa units are megahertz.

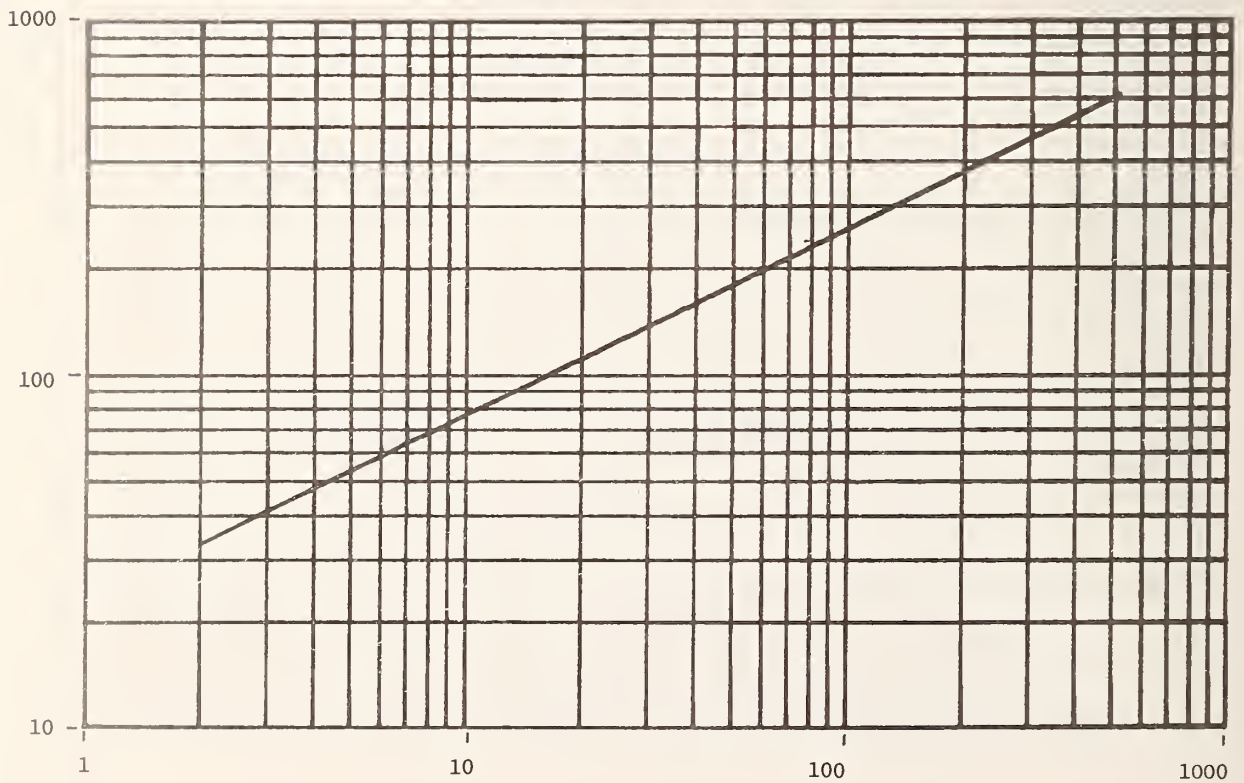


Figure A-46. Modeled minimum-phase phase shift plot for 333.76 meters (1095 ft) of B. Ordinate units are degrees and abscissa units are megahertz.

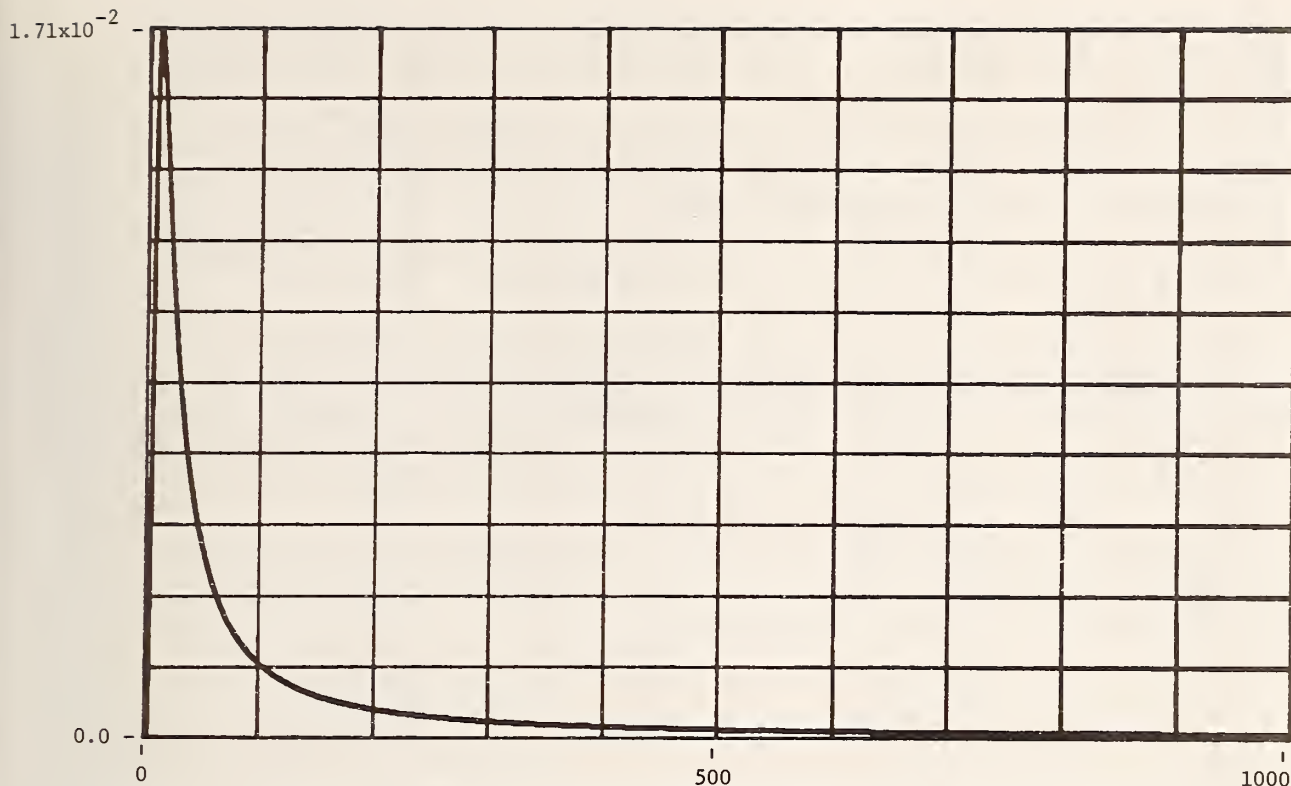


Figure A-47. Modeled and computed time domain impulse response for 333.76 meters (1095 ft) of B. Ordinate units are seconds⁻¹, abscissa units are nanoseconds and time spacing between points is 0.9766 ns.

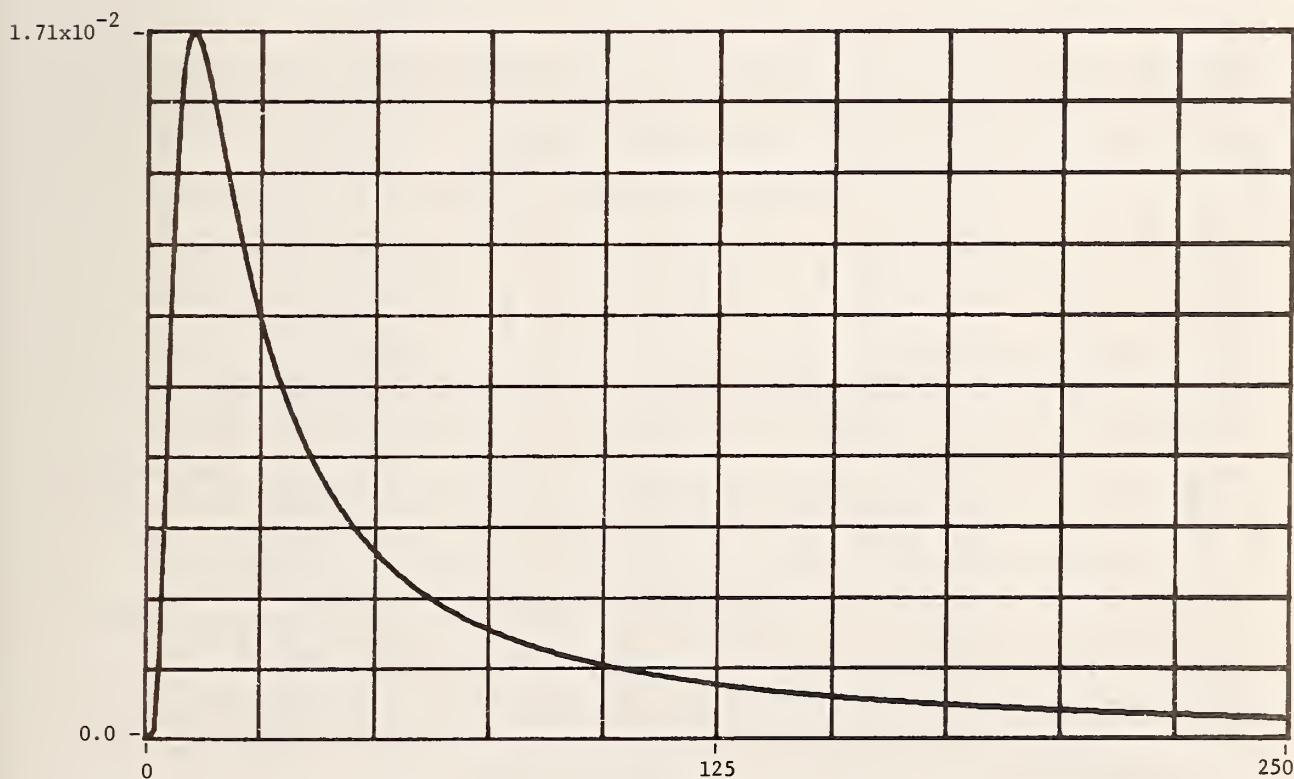


Figure A-48. Time-expanded modeled and computed time domain impulse response for 333.76 meters (1095 ft) of B. Ordinate units are seconds⁻¹, abscissa units are nanoseconds and time spacing between points is 0.9766 ns.

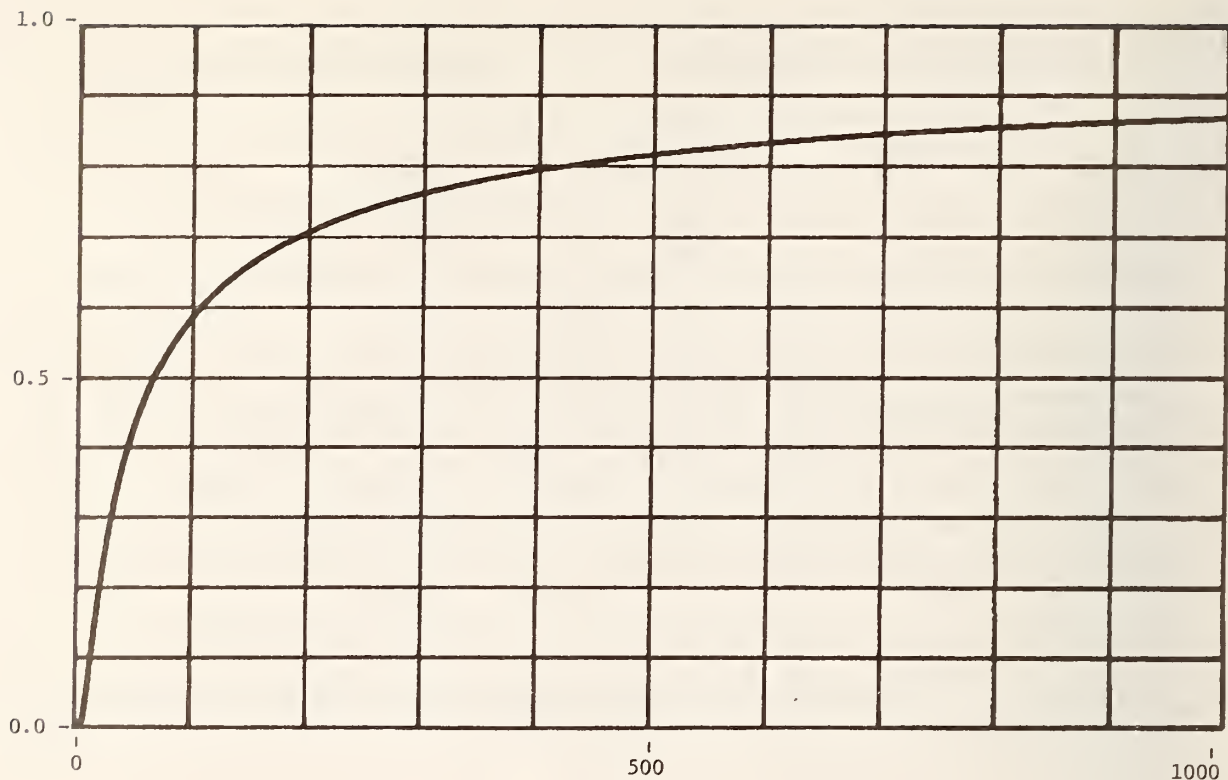


Figure A-49. Modeled and computed time domain unit step response for 333.76 meters (1095 ft) of B. Ordinate units are volts and abscissa units are nanoseconds.

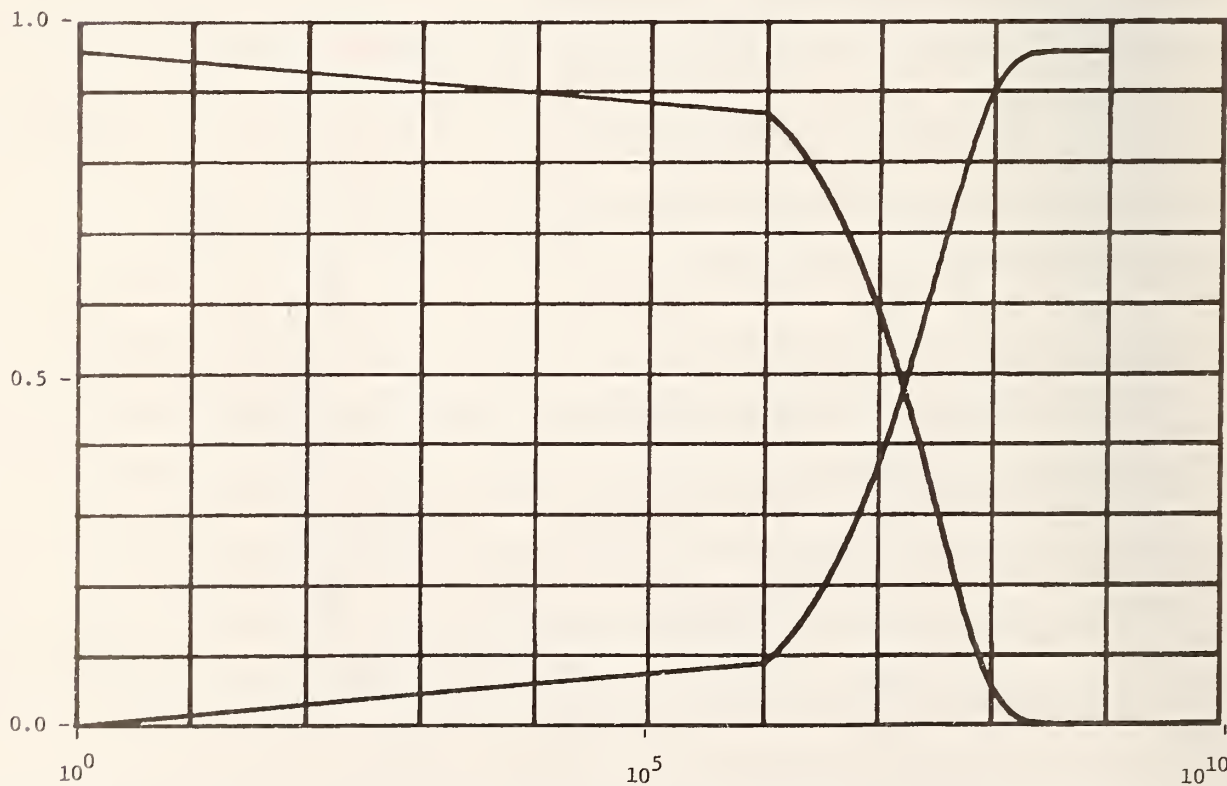


Figure A-50. Plots of "zero"/"one" cable unit step response voltages versus \log_{10} frequency for 333.76 meters (1095 ft) of cable B. Ordinate units are volts and abscissa units are hertz.

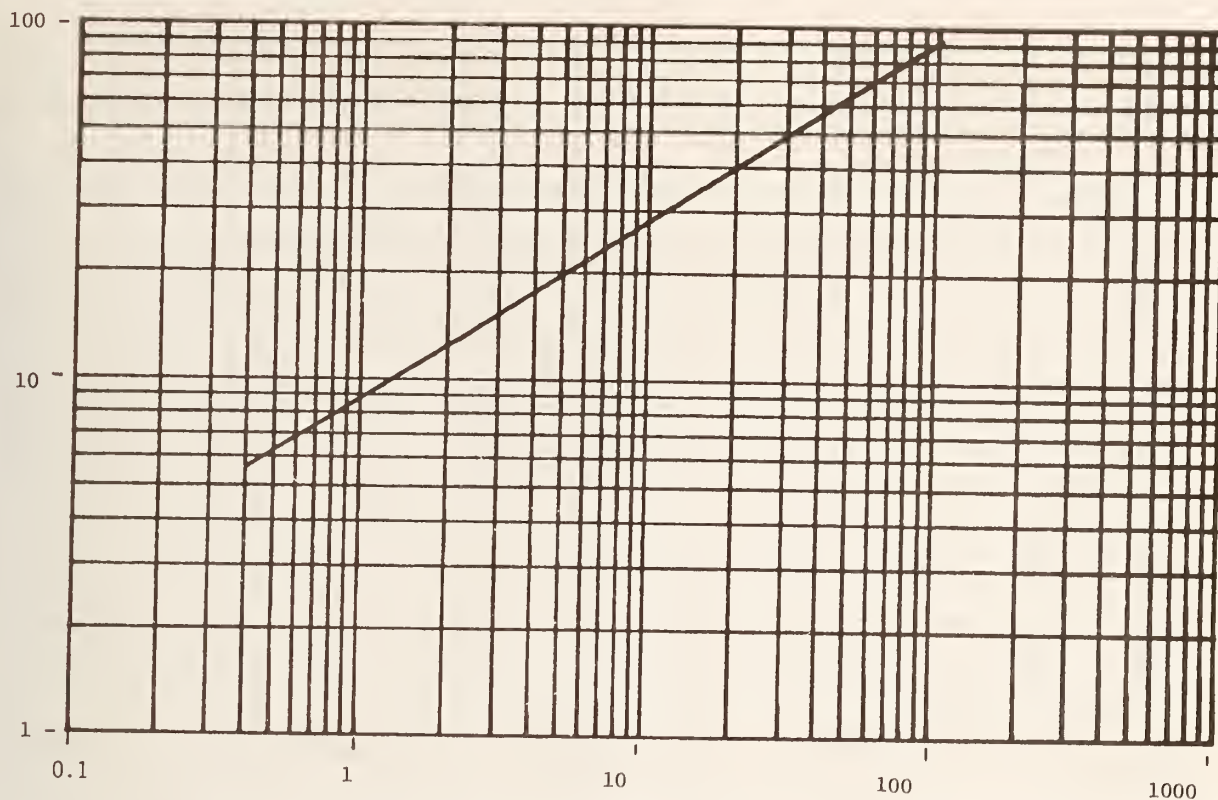


Figure A-51. Modeled attenuation plot for 304.8 meters (1000 ft) of C. Ordinate units are decibels and abscissa units are megahertz.

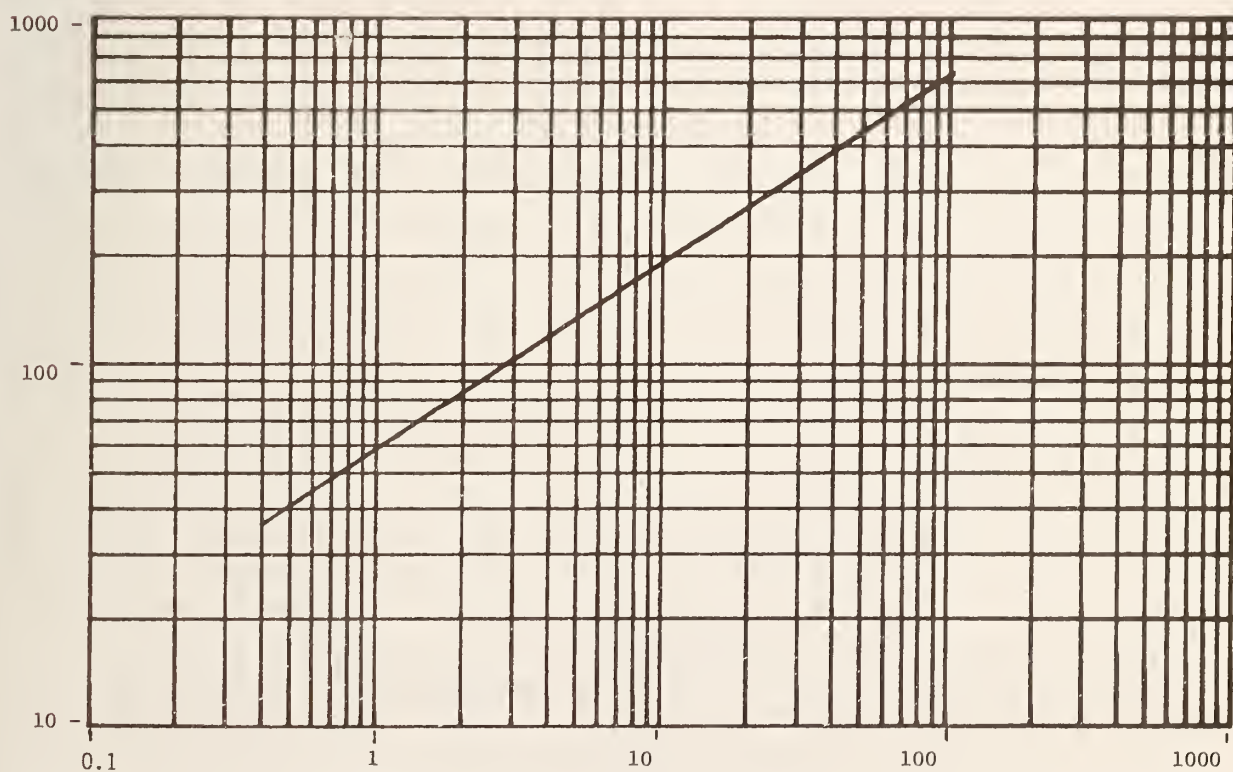


Figure A-52. Modeled minimum-phase phase shift plot for 304.8 meters (1000 ft) of C. Ordinate units are degrees and abscissa units are megahertz.

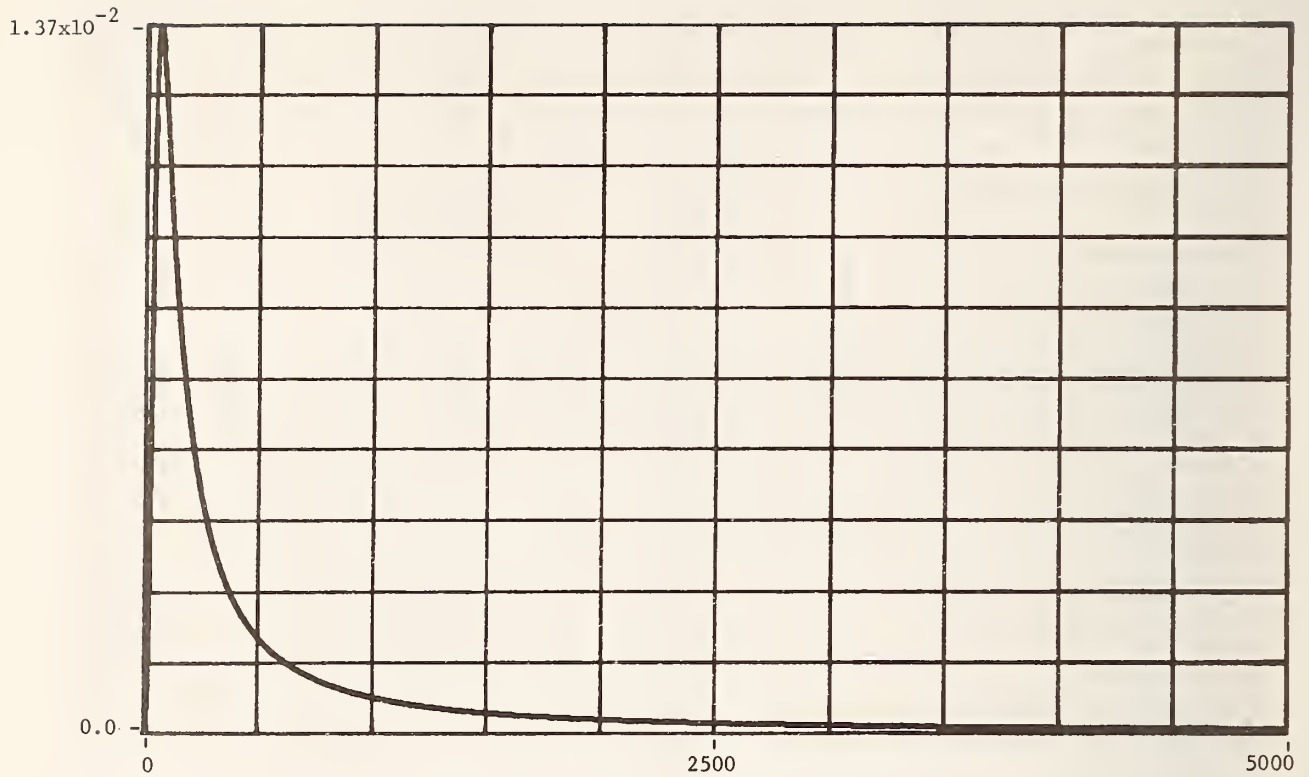


Figure A-53. Modeled and computed time domain impulse response for 304.8 meters (1000 ft) of C. Ordinate units are seconds⁻¹, abscissa units are nanoseconds and time spacing between points is 0.9766 ns.

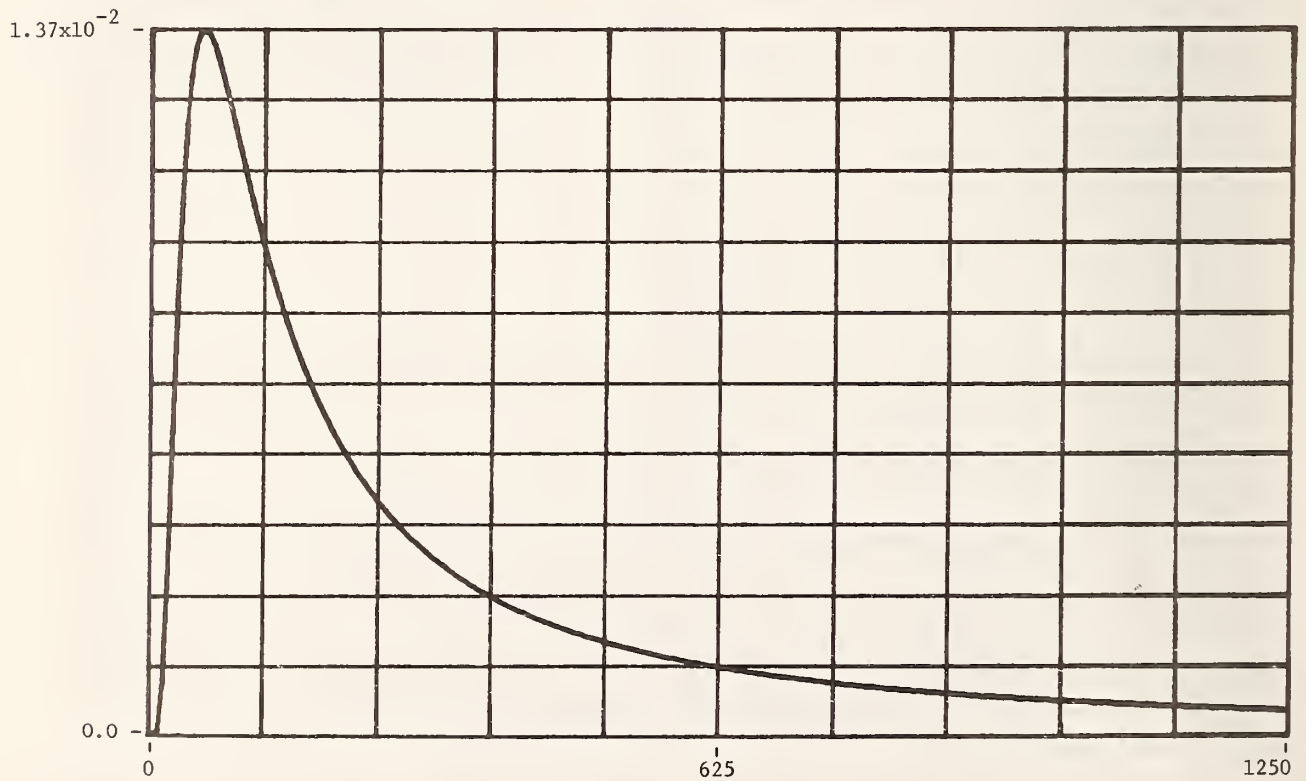


Figure A-54. Time-expanded modeled and computed time domain impulse response for 304.8 meters (1000 ft) of C. Ordinate units are seconds⁻¹, abscissa units are nanoseconds and time spacing between points is 0.9766 ns.

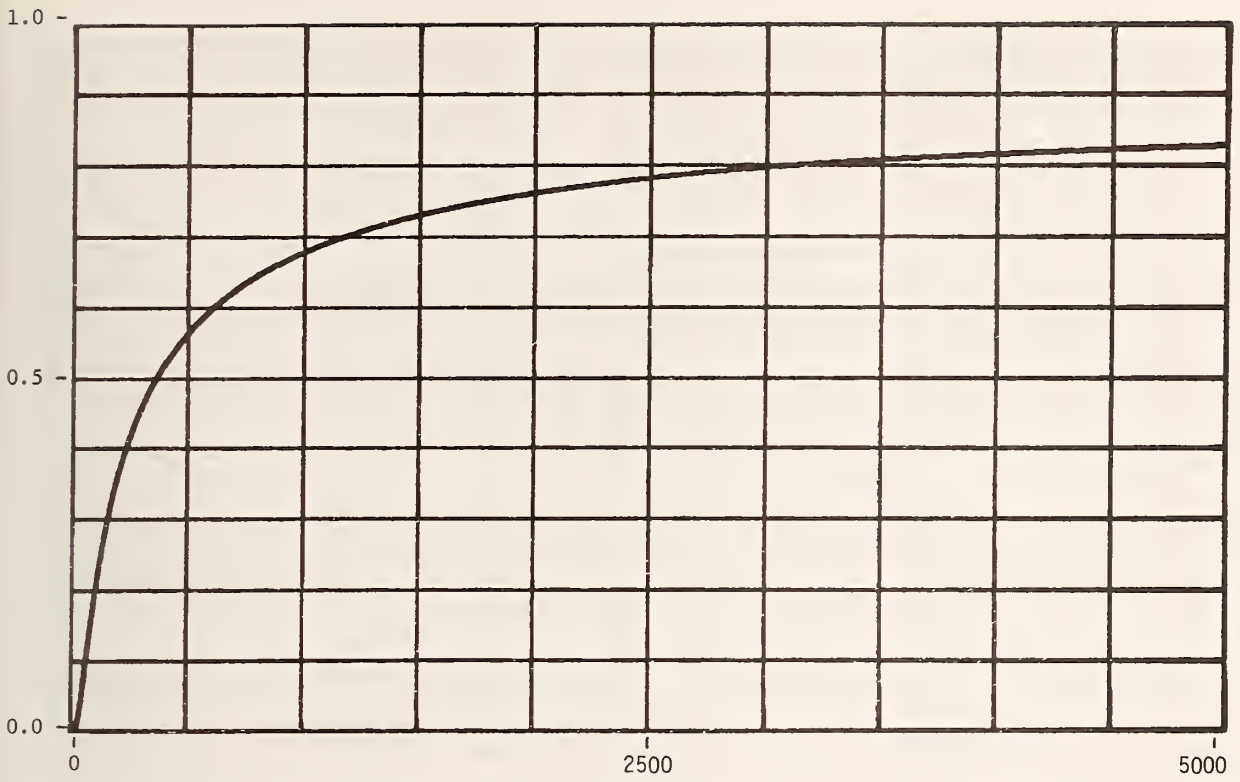


Figure A-55. Modeled and computed time domain unit step response for 304.8 meters (1000 ft) of C. Ordinate units are volts and abscissa units are nanoseconds.

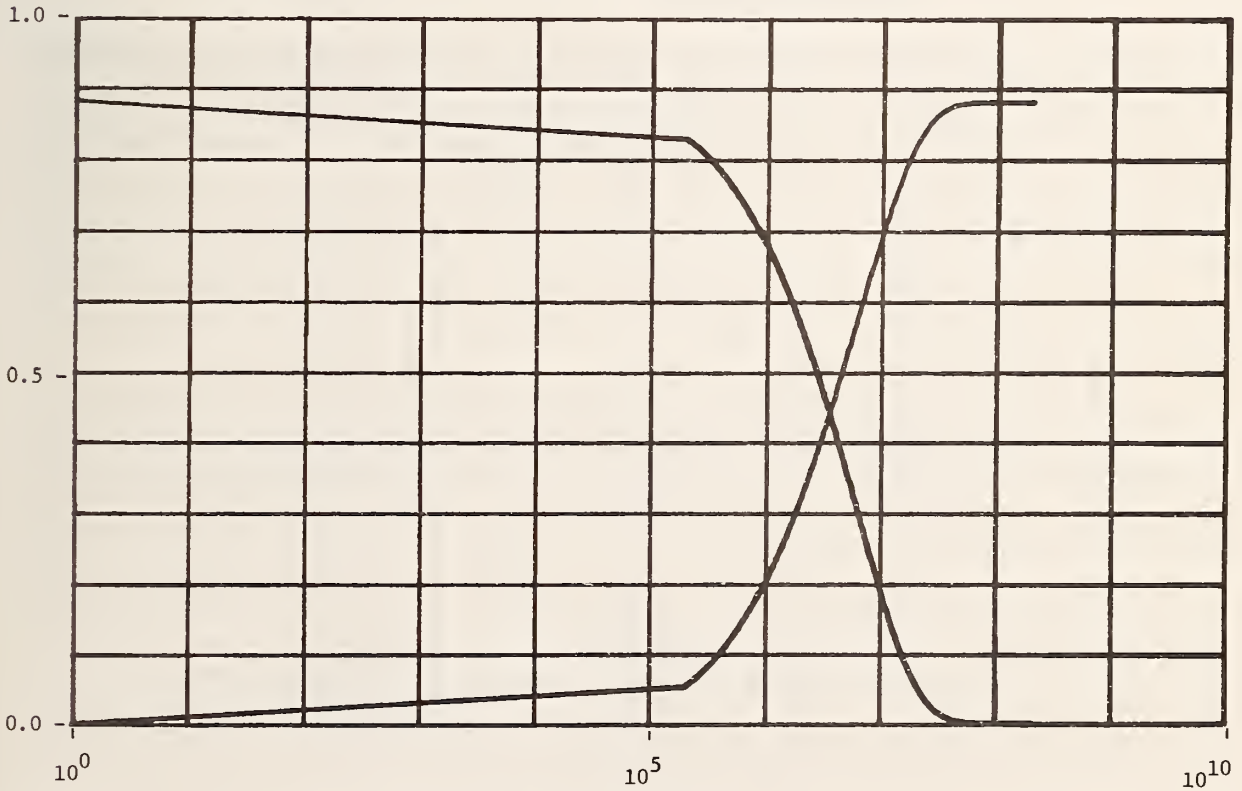


Figure A-56. Plots of "zero"/"one" cable unit step response voltages versus \log_{10} frequency for 304.8 meters (1000 ft) of cable C. Ordinate units are volts and abscissa units are hertz.

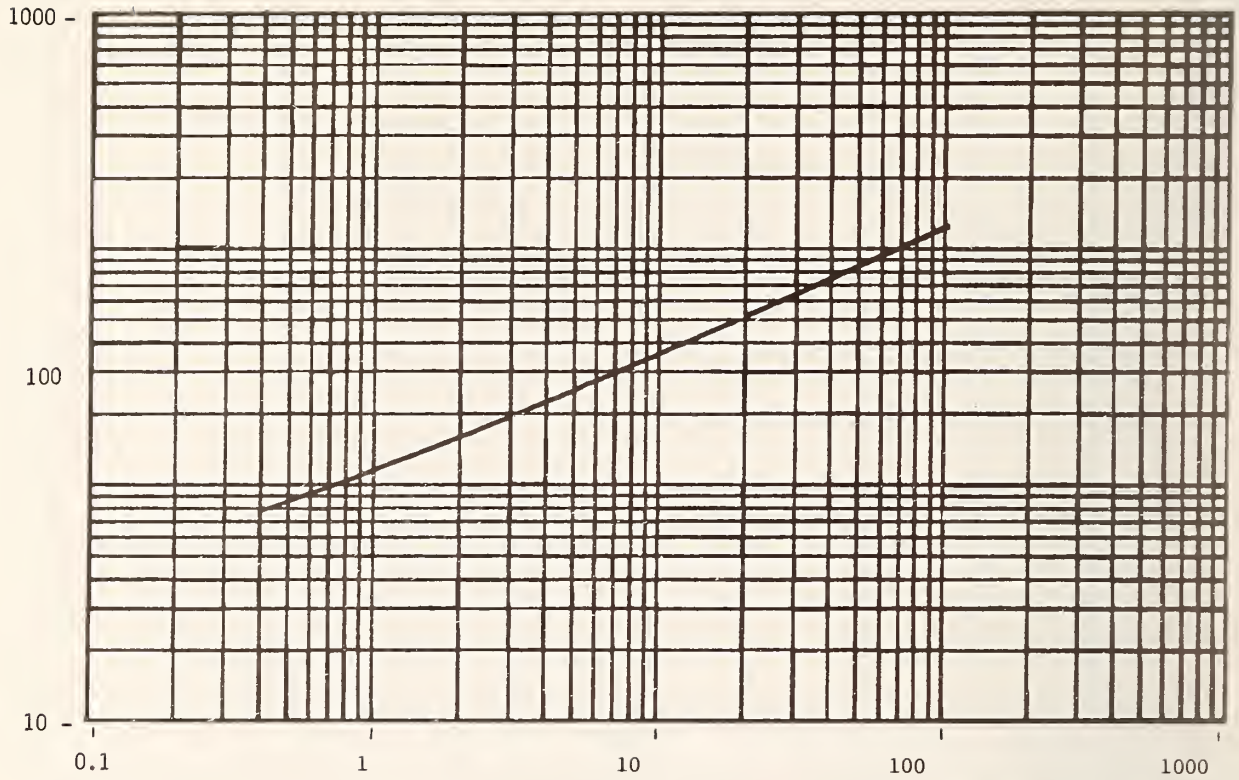


Figure A-57. Modeled attenuation plot for 304.8 meters (1000 ft) of D. Ordinate units are decibels and abscissa units are megahertz.

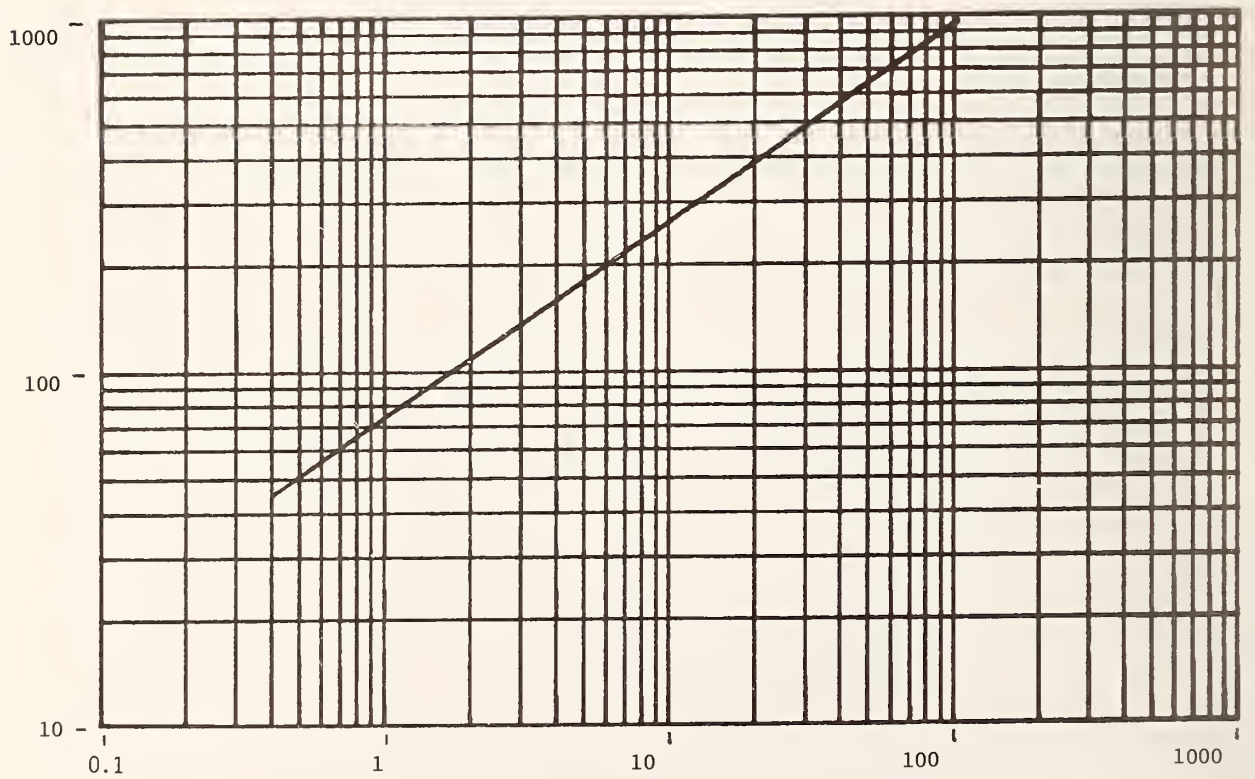


Figure A-58. Modeled minimum-phase phase shift plot for 304.8 meters (1000 ft) of D. Ordinate units are degrees and abscissa units are megahertz.

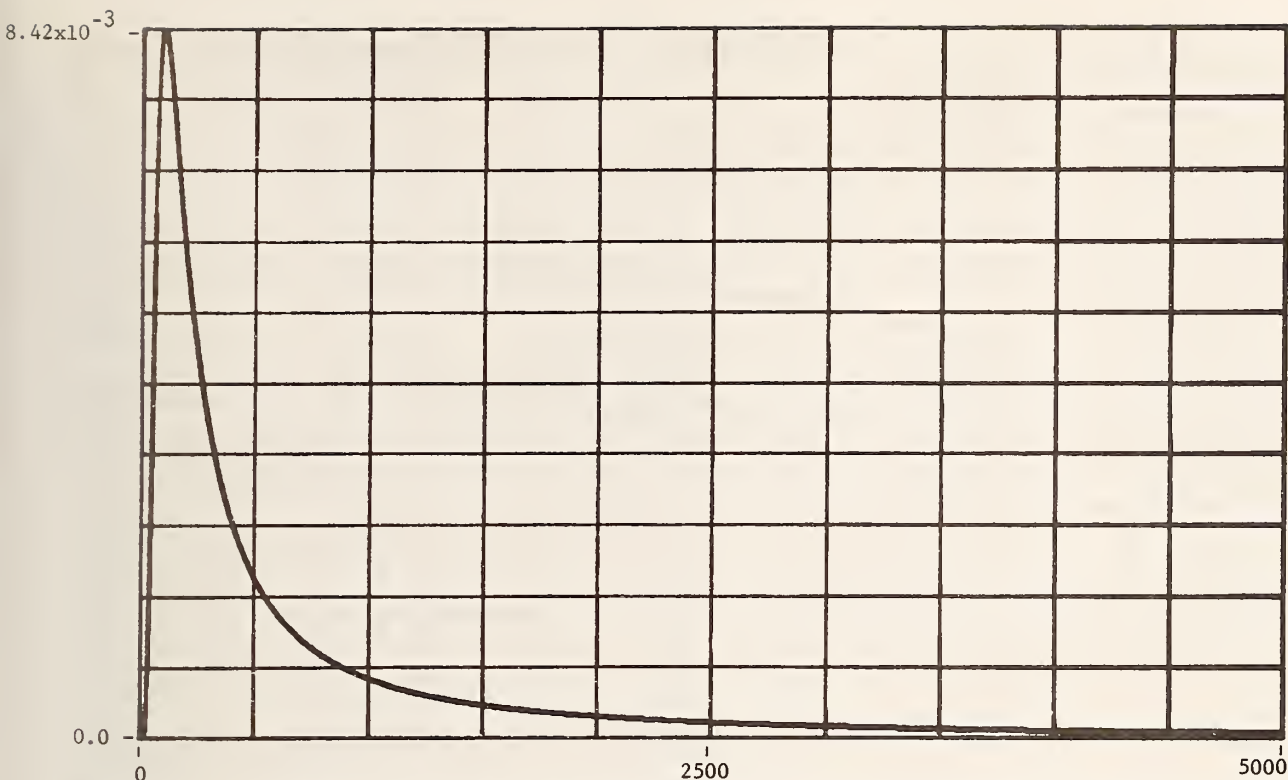


Figure A-59. Modeled and computed time domain impulse response for 304.8 meters (1000 ft) of D. Ordinate units are seconds⁻¹, abscissa units are nanoseconds and time spacing between points is 4.883 ns.

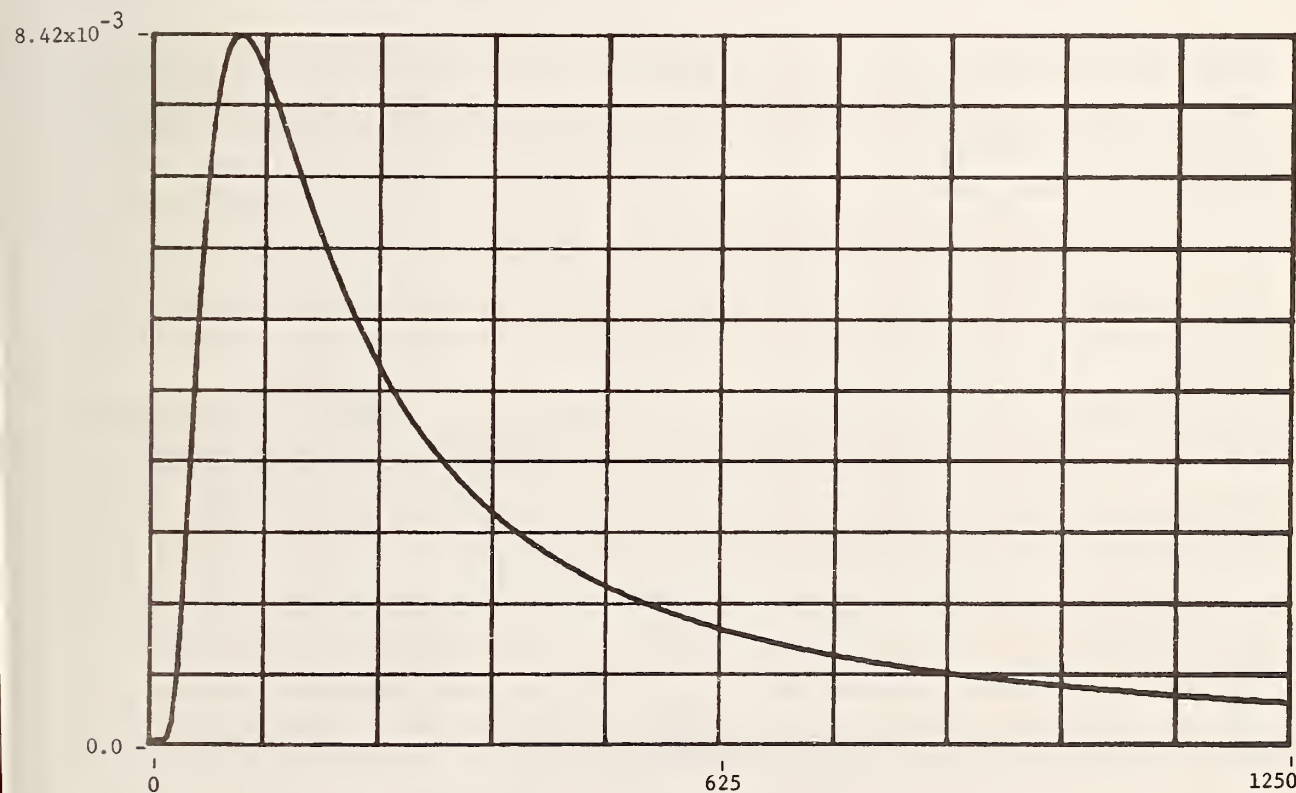


Figure A-60. Time-expanded modeled and computed time domain impulse response for 304.8 meters (1000 ft) of D. Ordinate units are seconds⁻¹, abscissa units are nanoseconds and time spacing between points is 4.883 ns.

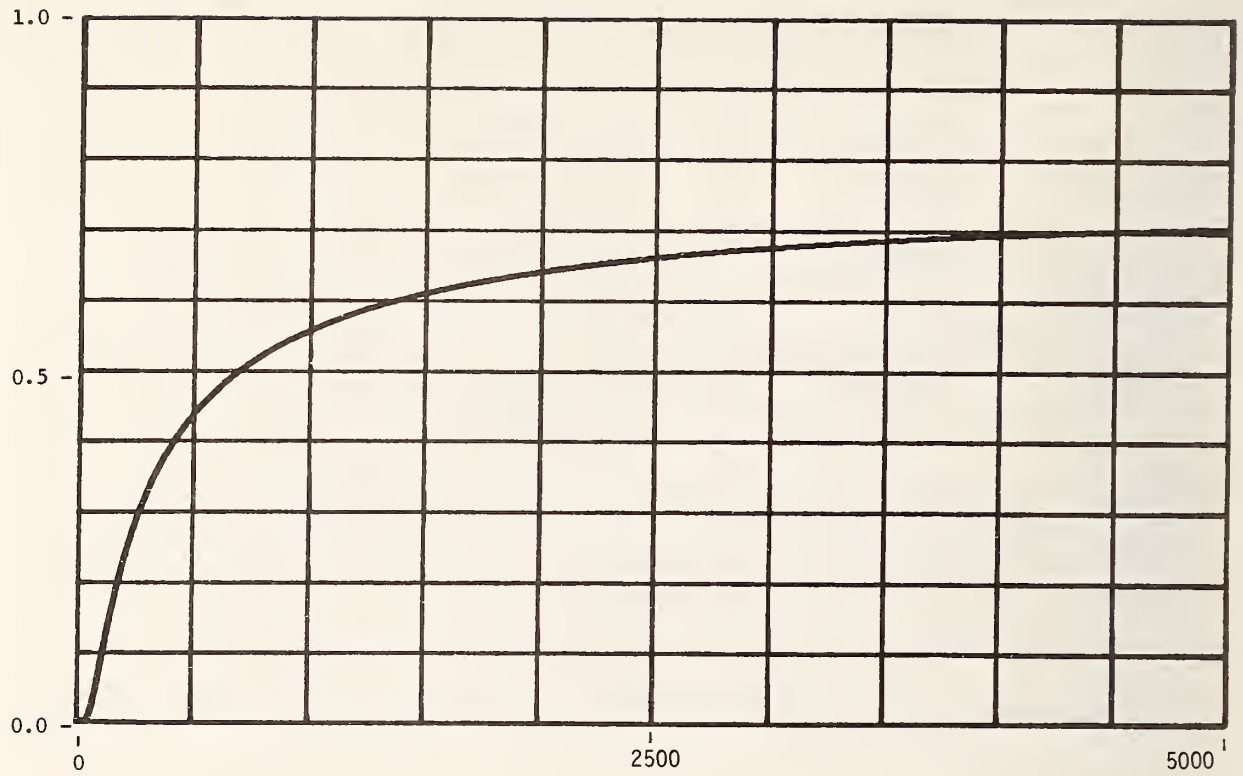


Figure A-61. Modeled and computed time domain unit step response for 304.8 meters (1000 ft) of D. Ordinate units are volts and abscissa units are nanoseconds.

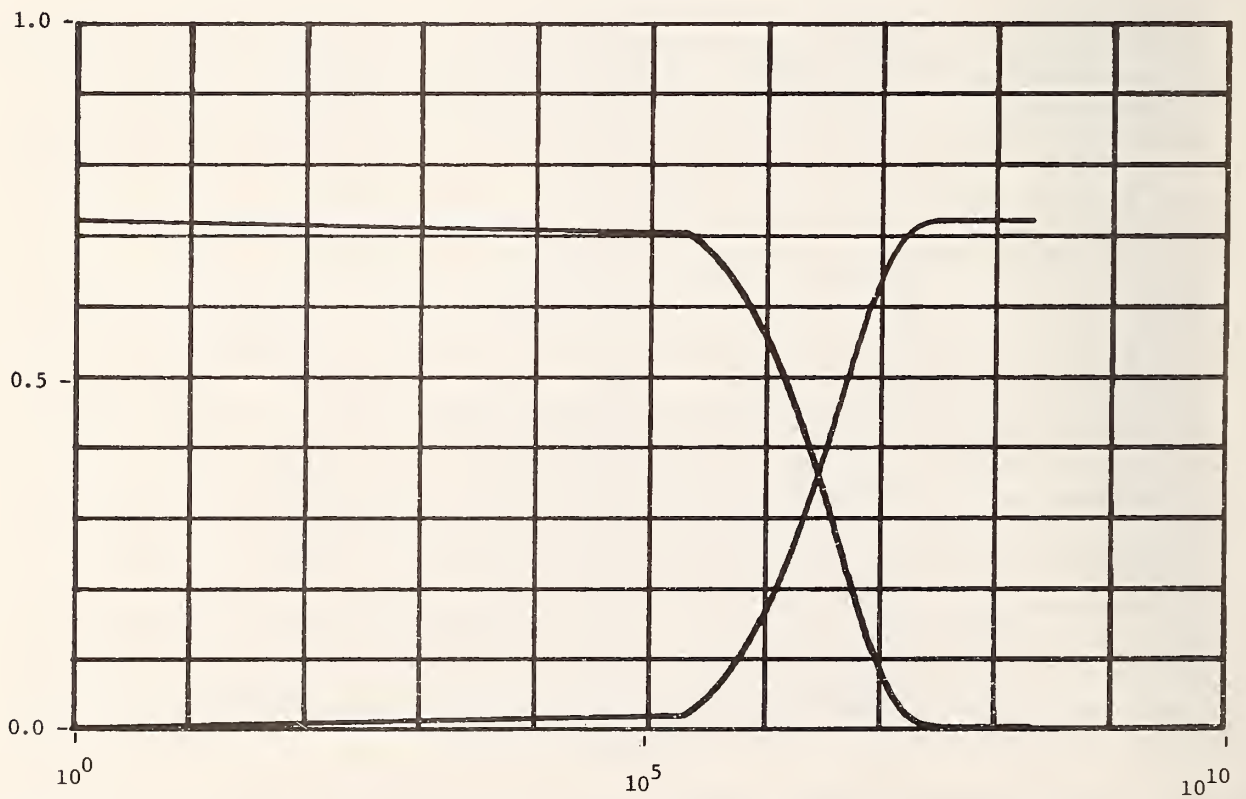


Figure A-62. Plots of "zero"/"one" cable unit step response voltages versus \log_{10} frequency for 304.8 meters (1000 ft) of cable D. Ordinate units are volts and abscissa units are hertz.

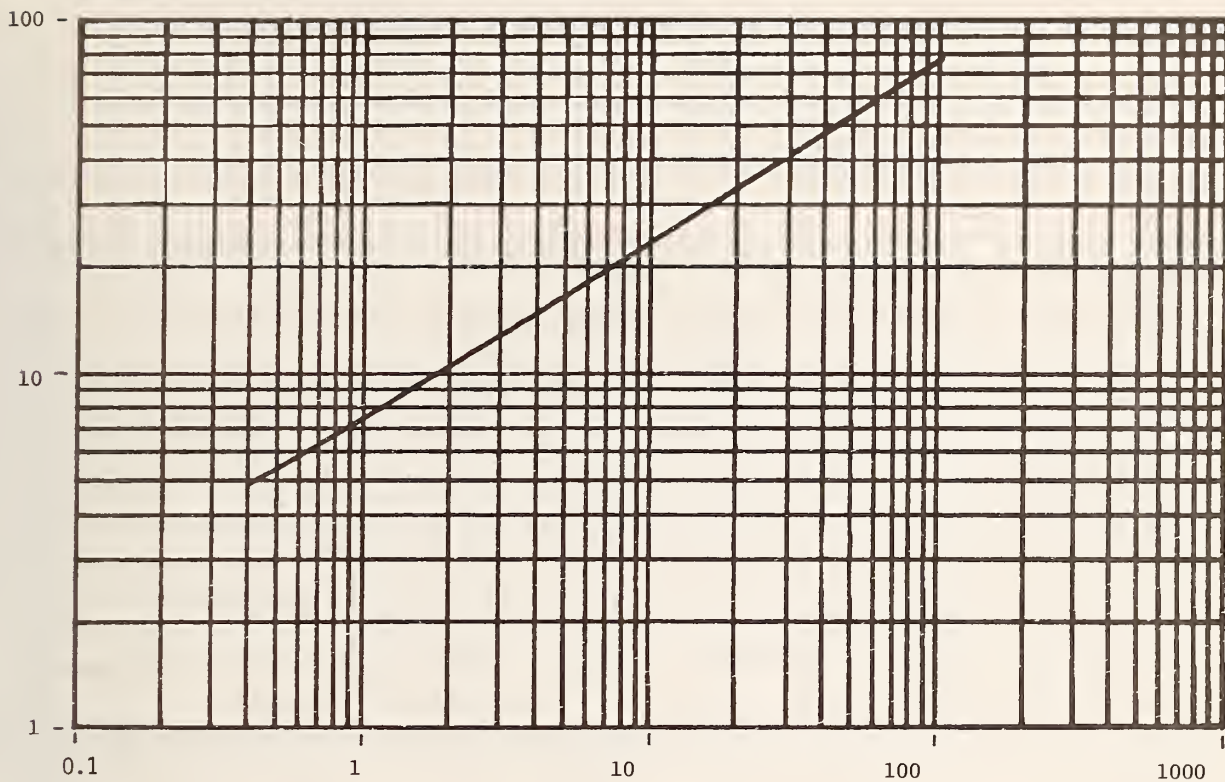


Figure A-63. Modeled attenuation plot for 304.8 meters (1000 ft) of E. Ordinate units are decibels and abscissa units are megahertz.

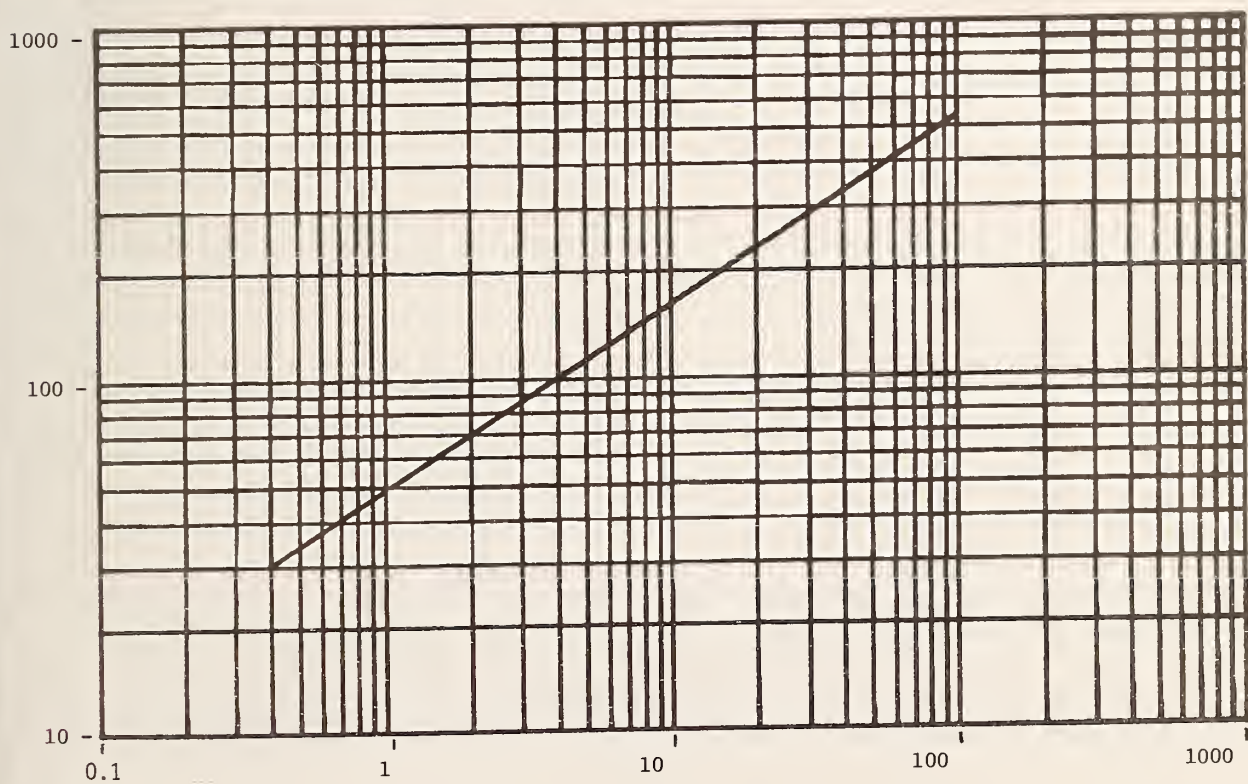


Figure A-64. Modeled minimum-phase phase shift plot for 304.8 meters (1000 ft) of E. Ordinate units are degrees and abscissa units are megahertz.

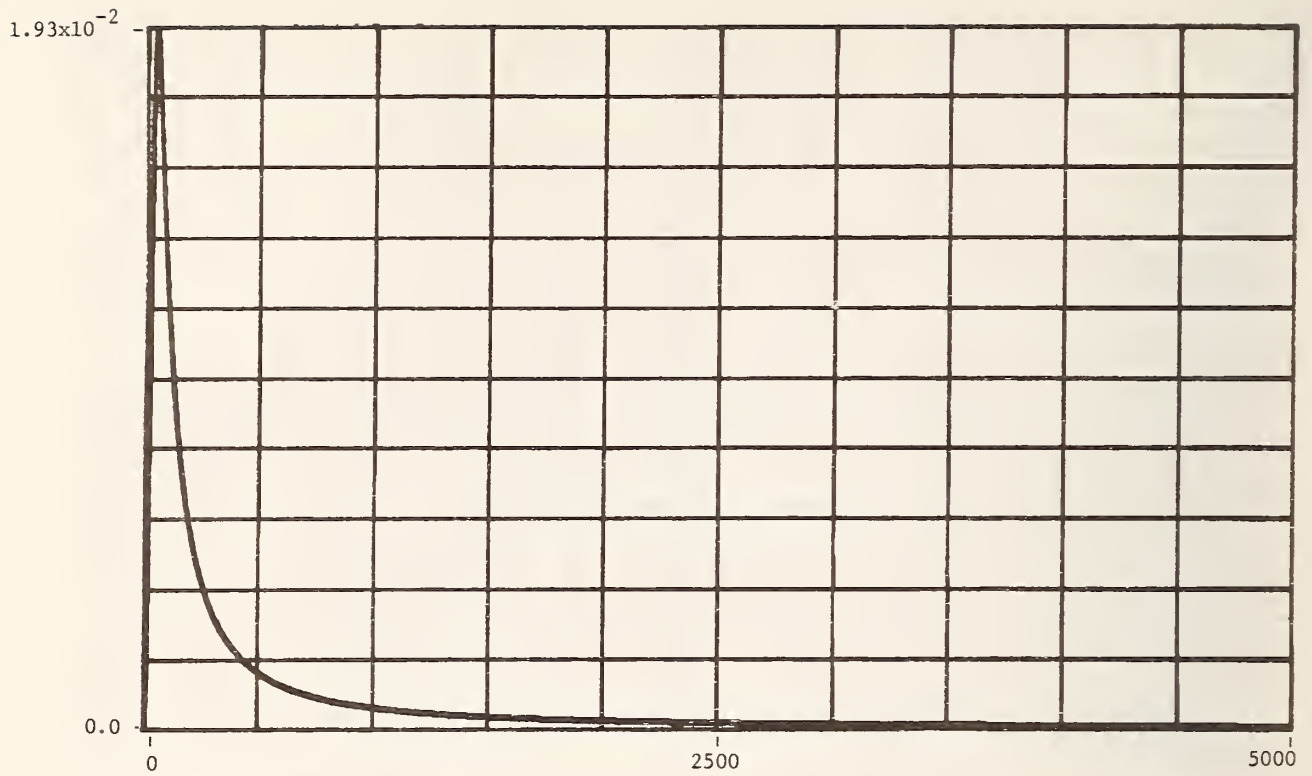


Figure A-65. Modeled and computed time domain impulse response for 304.8 meters (1000 ft) of E. Ordinate units are seconds⁻¹, abscissa units are nanoseconds and time spacing between points is 4.883 ns.

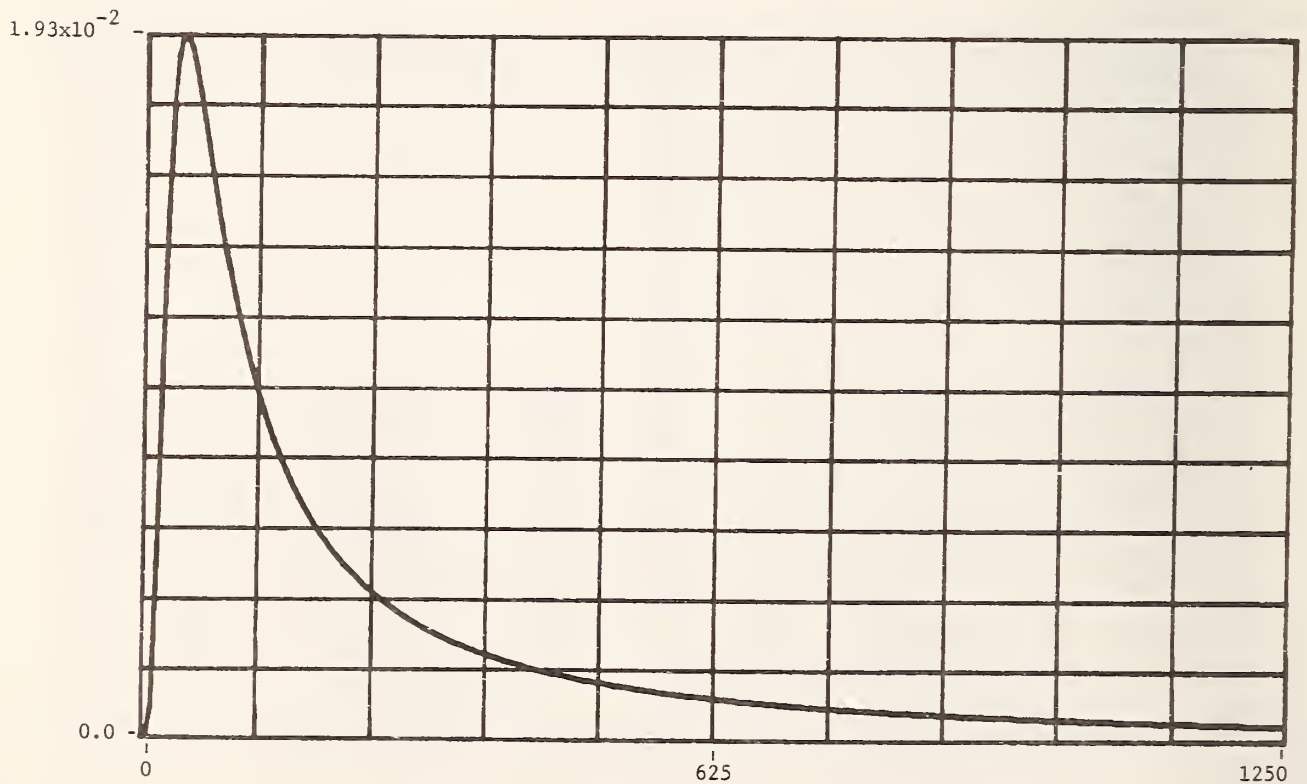


Figure A-66. Time-expanded modeled and computed time domain impulse response for 304.8 meters (1000 ft) of E. Ordinate units are seconds⁻¹, abscissa units are nanoseconds and time spacing between points is 4.883 ns.

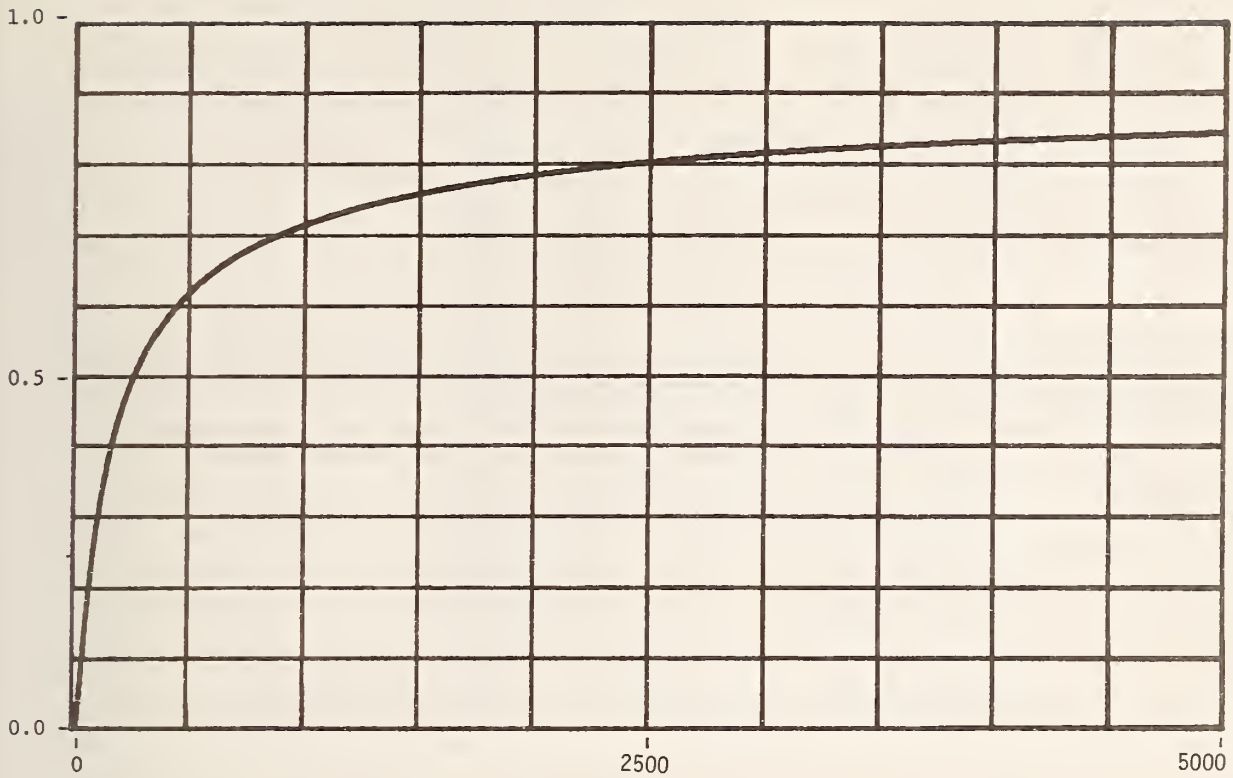


Figure A-67. Modeled and computed time domain unit step response for 304.8 meters (1000 ft) of E. Ordinate units are volts and abscissa units are nanoseconds.

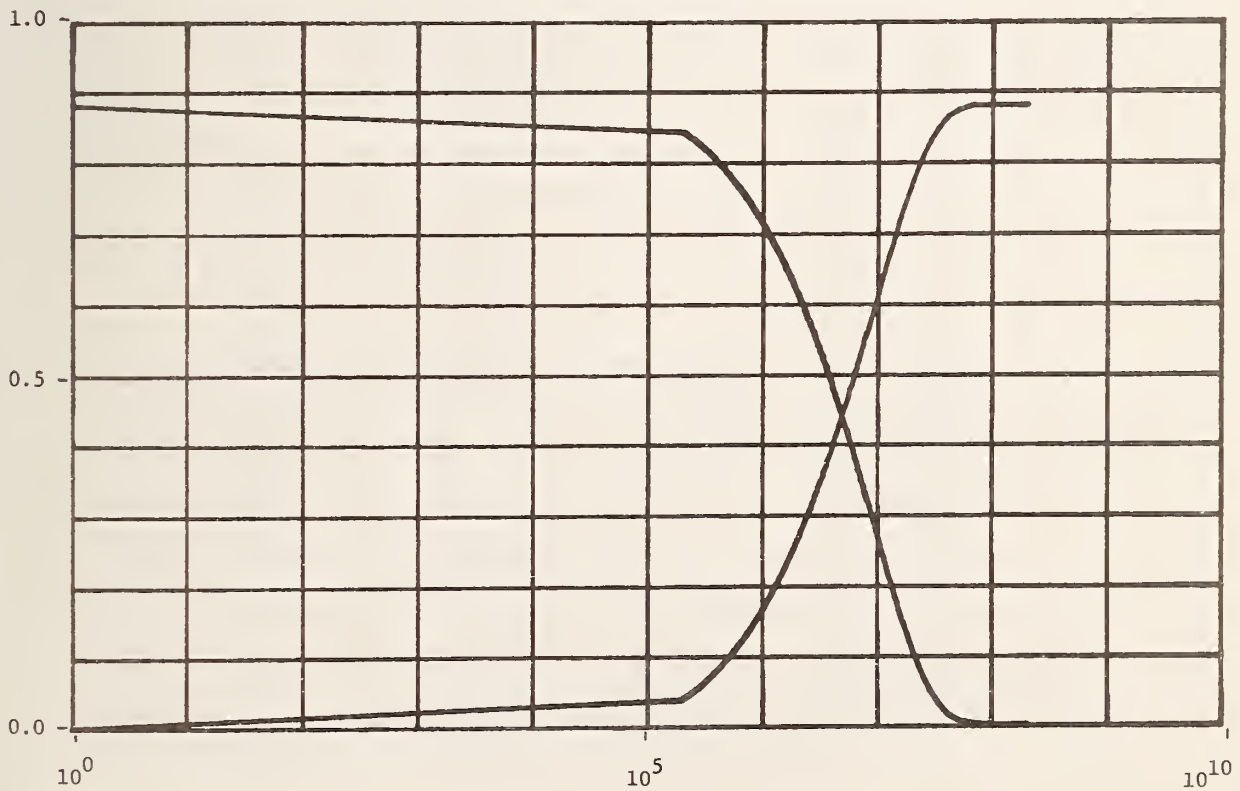


Figure A-68. Plots of "zero"/"one" cable unit step response voltages versus \log_{10} frequency for 304.8 meters (1000 ft) of cable E. Ordinate units are volts and abscissa units are hertz.

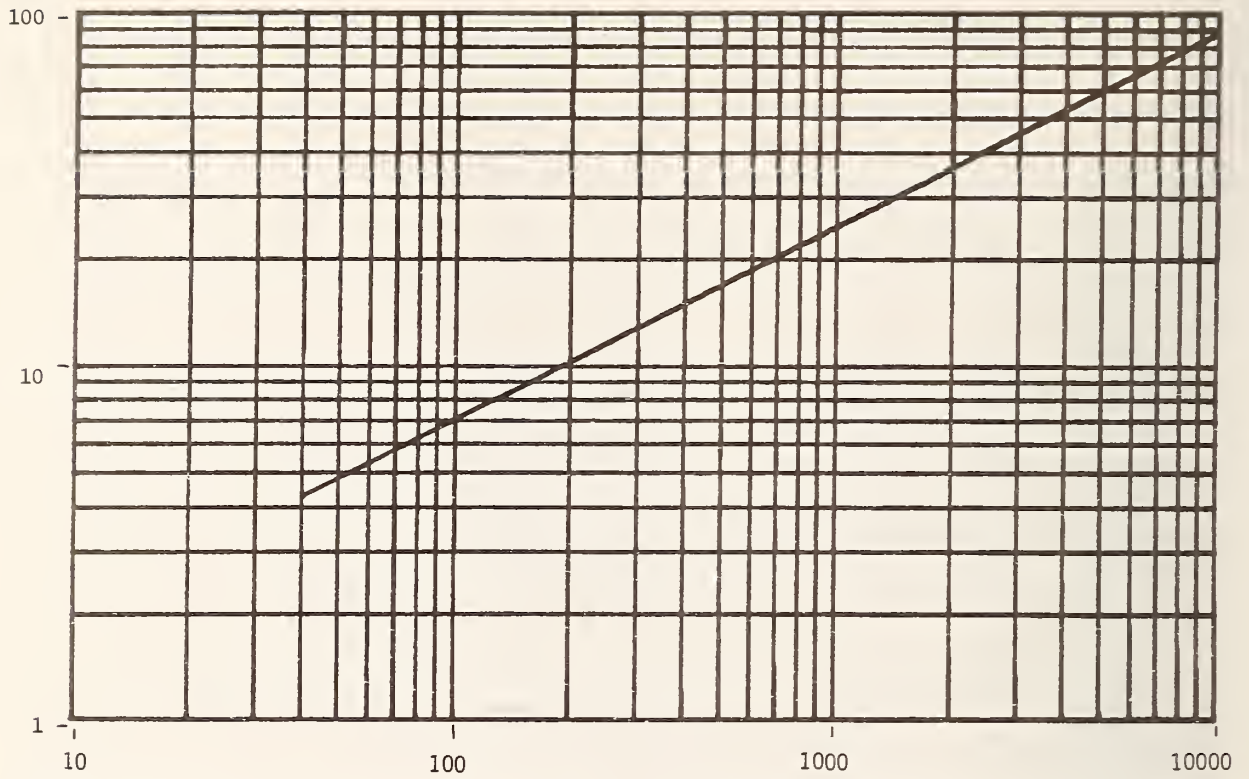


Figure A-69. Modeled attenuation plot for 60.96 meters (200 ft) of RG-22B/U. Ordinate units are decibels and abscissa units are megahertz.

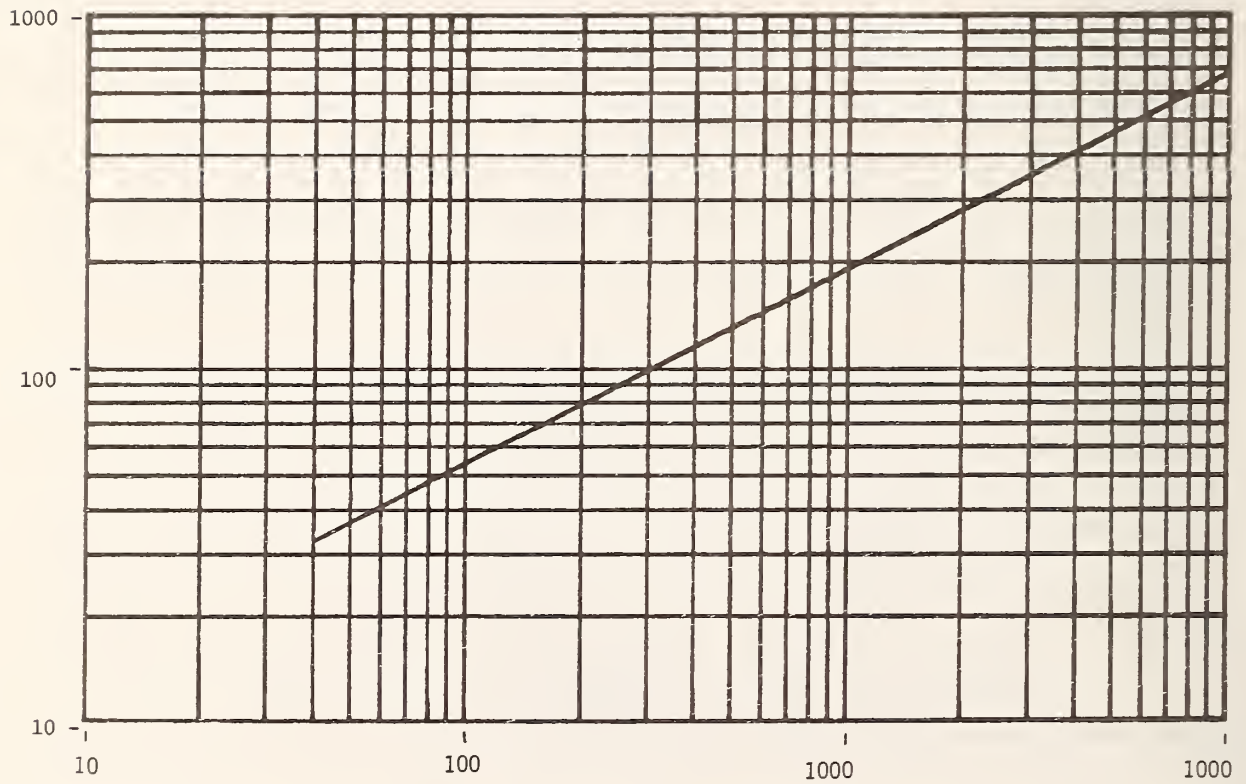


Figure A-70. Modeled minimum-phase phase shift plot for 60.96 meters (200 ft) of RG-22B/U. Ordinate units are degrees and abscissa units are megahertz.

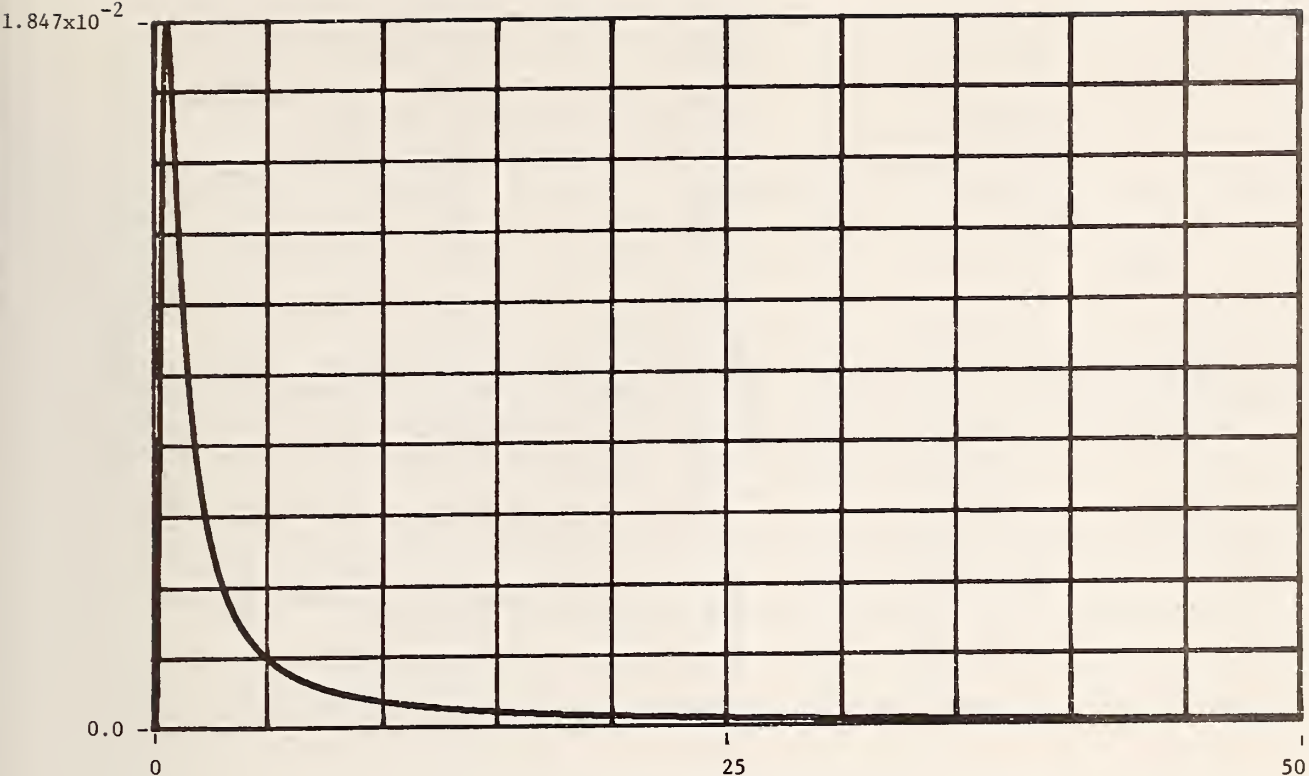


Figure A-71. Modeled and computed time domain impulse response for 60.96 meters (200 ft) of RG-22B/U. Ordinate units are seconds⁻¹, abscissa units are nanoseconds and time spacing between points is 0.9766 ns.

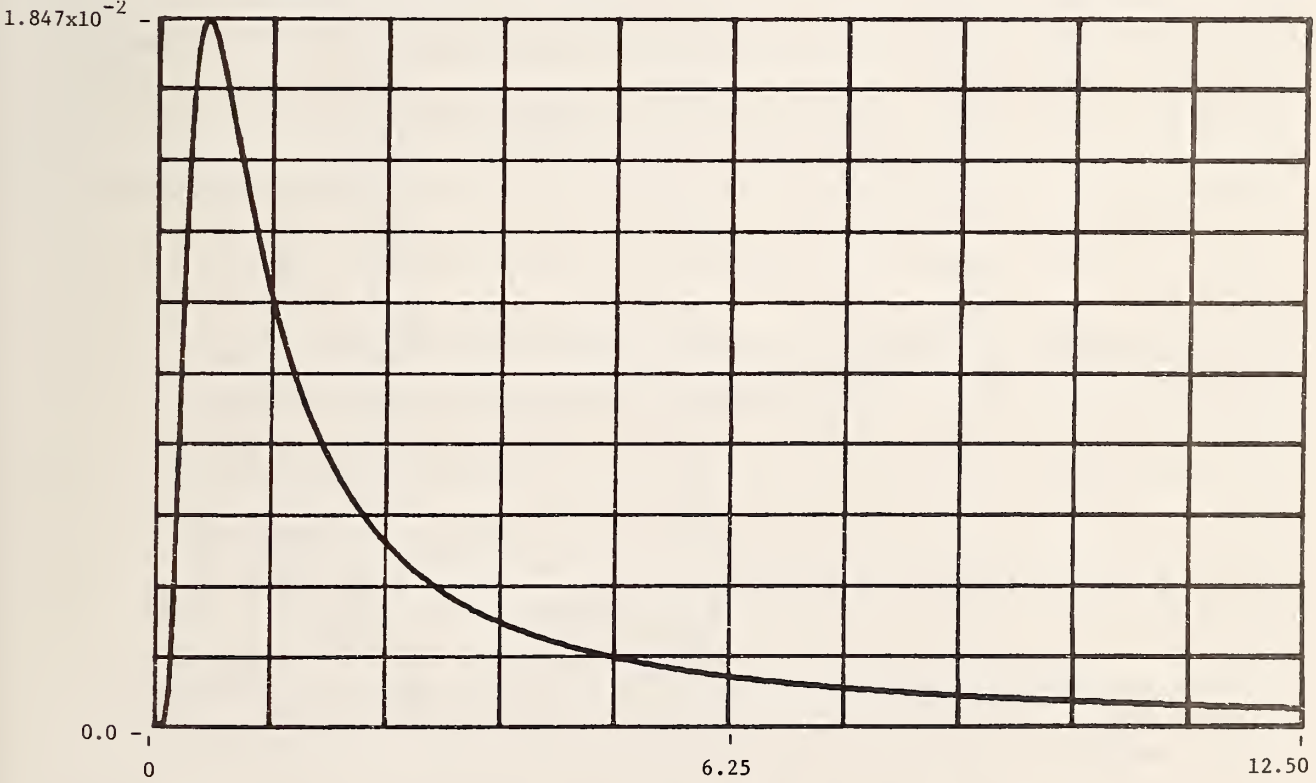


Figure A-72. Time-expanded modeled and computed time domain impulse response for 60.96 meters (200 ft) of RG-22B/U. Ordinate units are seconds⁻¹, abscissa units are nanoseconds and time spacing between points is 0.9766 ns.

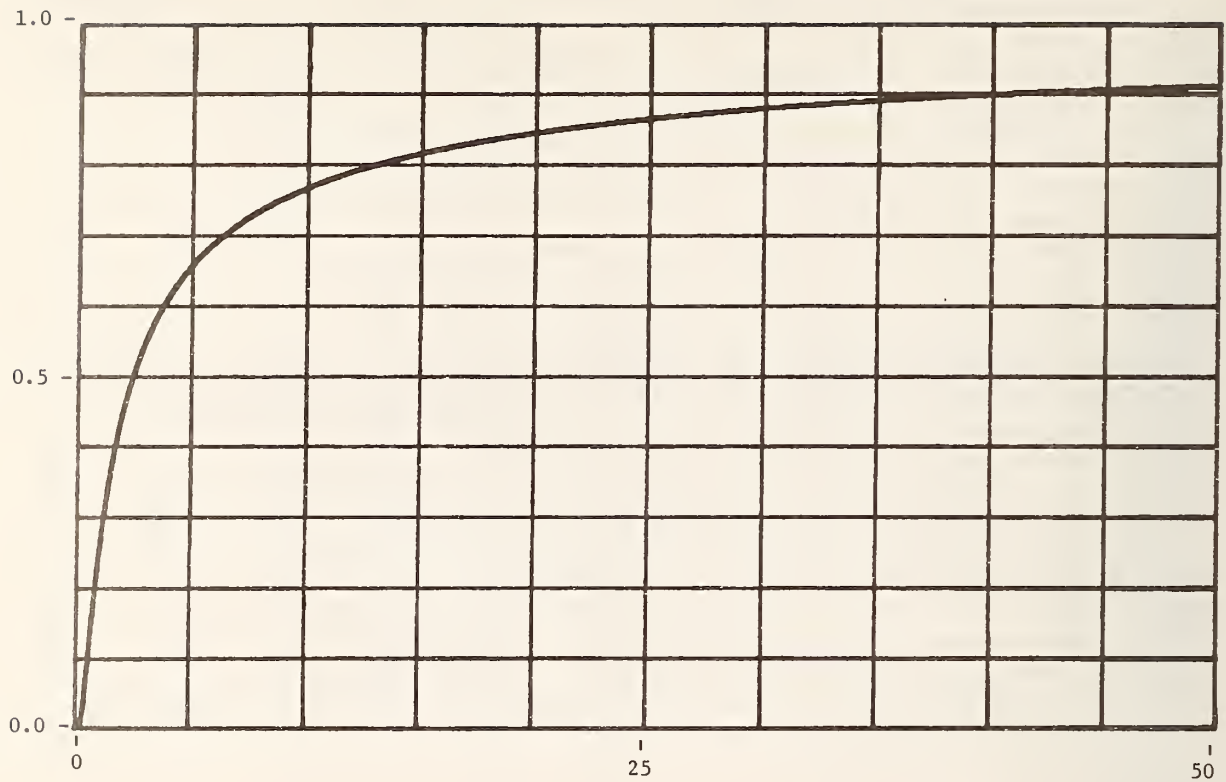


Figure A-73. Modeled and computed time domain unit step response for 60.96 meters (200 ft) of RG-22B/U. Ordinate units are volts and abscissa units are nanoseconds.

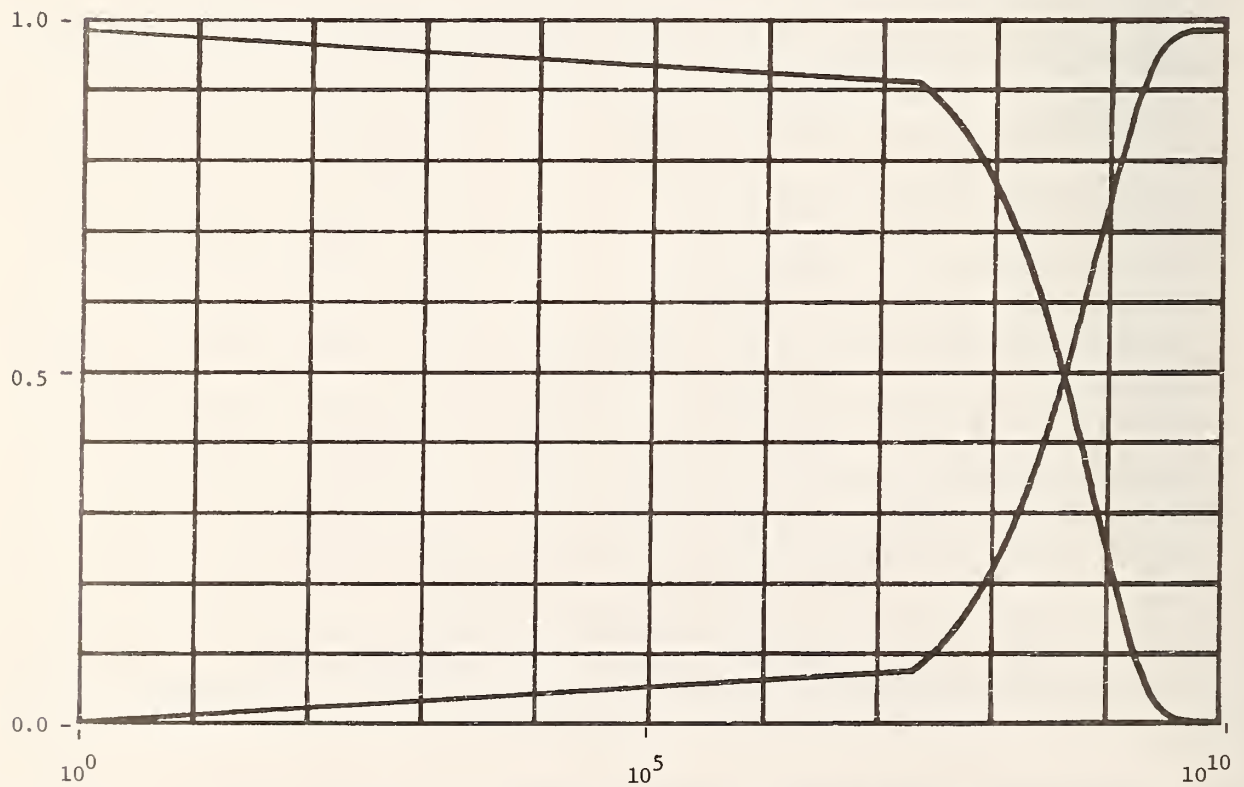


Figure A-74. Plots of "zero"/"one" cable unit step response voltages versus \log_{10} frequency for 60.96 meters (200 ft) of cable RG-22B/U. Ordinate units are volts and abscissa units are hertz.

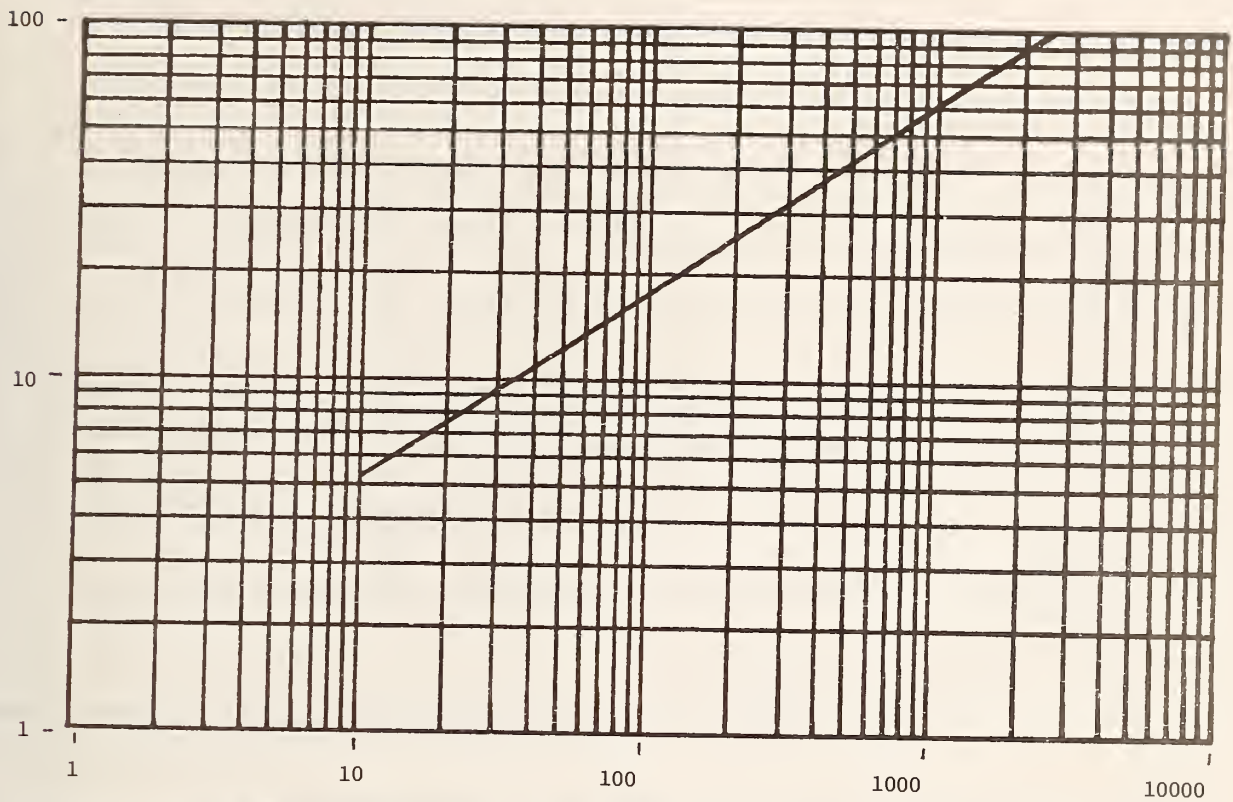


Figure A-75. Modeled attenuation plot for 152.4 meters (500 ft) of RG-22B/U. Ordinate units are decibels and abscissa units are megahertz.

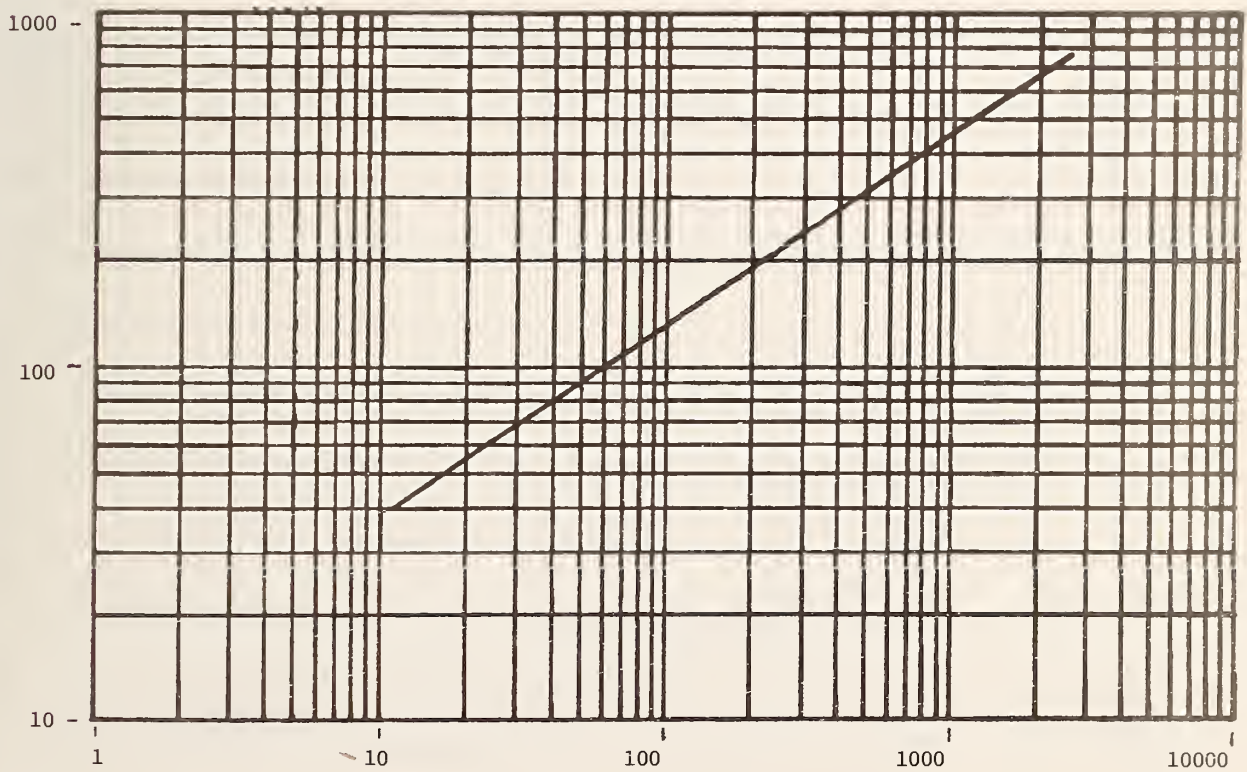


Figure A-76. Modeled minimum-phase phase shift plot for 152.4 meters (500 ft) of RG-22B/U. Ordinate units are degrees and abscissa units are megahertz.

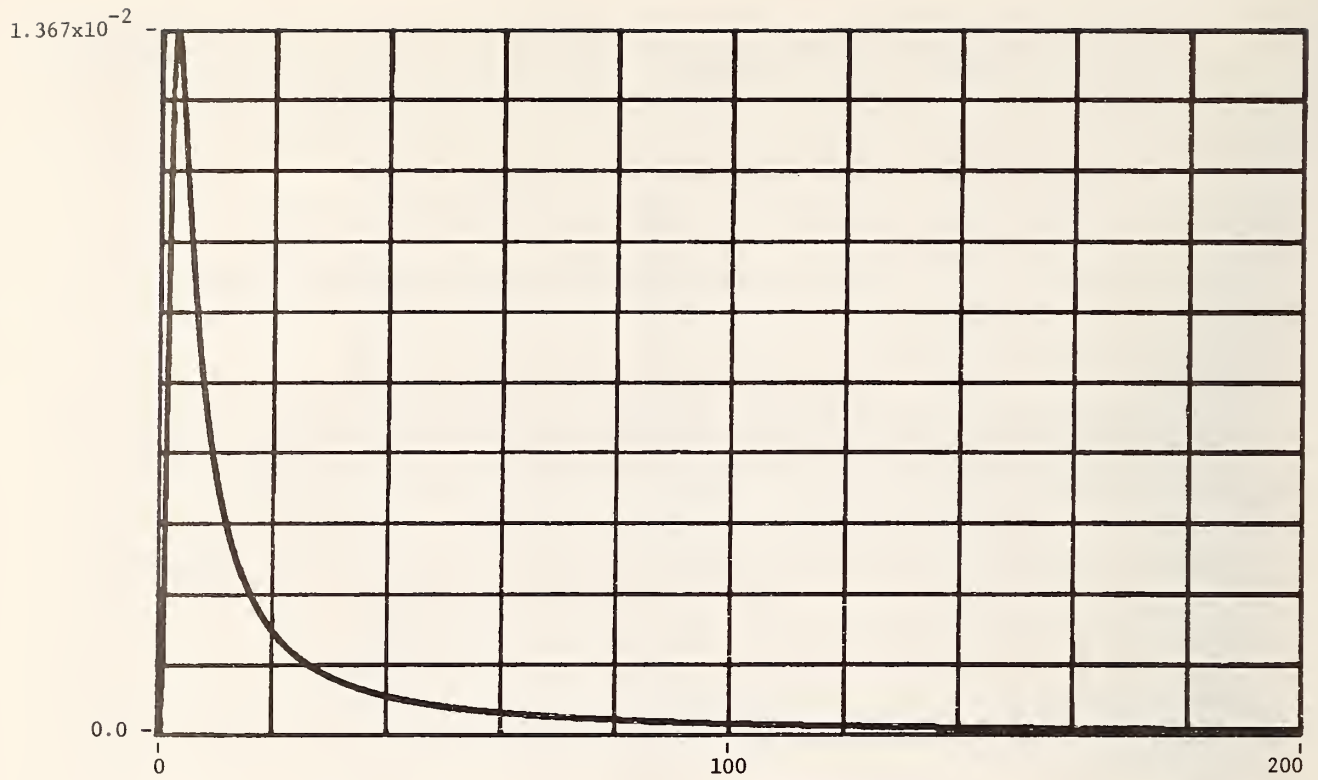


Figure A-77. Modeled and computed time domain impulse response for 152.4 meters (500 ft) of RG-22B/U. Ordinate units are seconds^{-1} , abscissa units are nanoseconds and time spacing between points is 0.1953 ns.

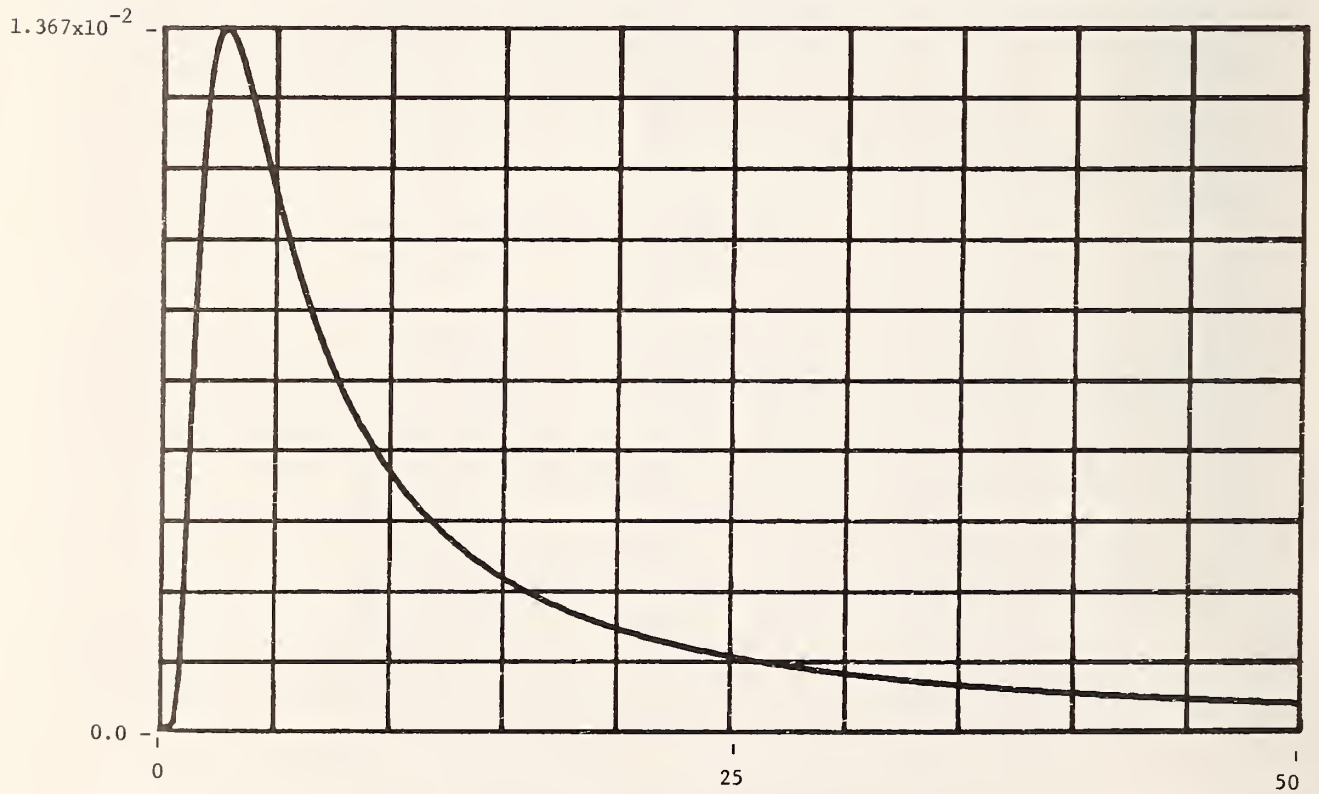


Figure A-78. Time-expanded modeled and computed time domain impulse response for 152.4 meters (500 ft) of RG-22B/U. Ordinate units are seconds^{-1} , abscissa units are nanoseconds and time spacing between points is 0.1953 ns.

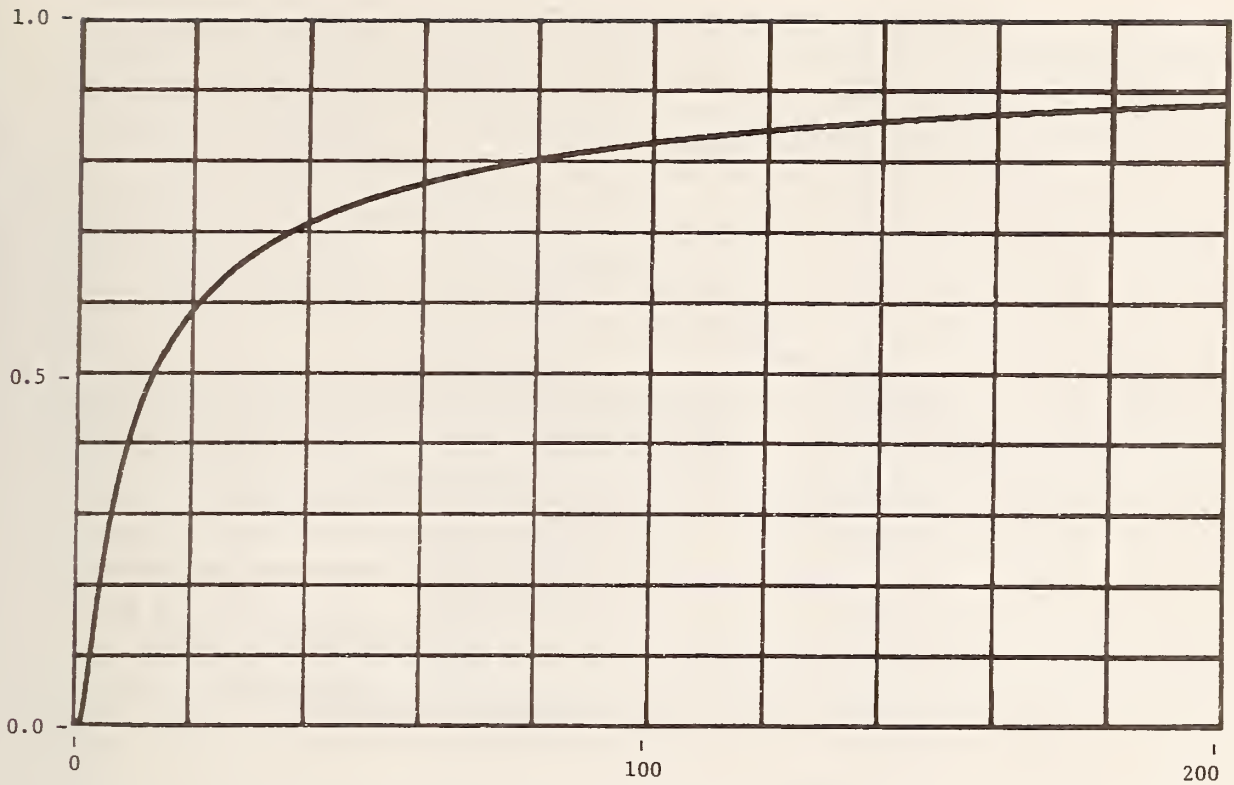


Figure A-79. Modeled and computed time domain unit step response for 152.4 meters (500 ft) of RG-22B/U. Ordinate units are volts and abscissa units are nanoseconds.

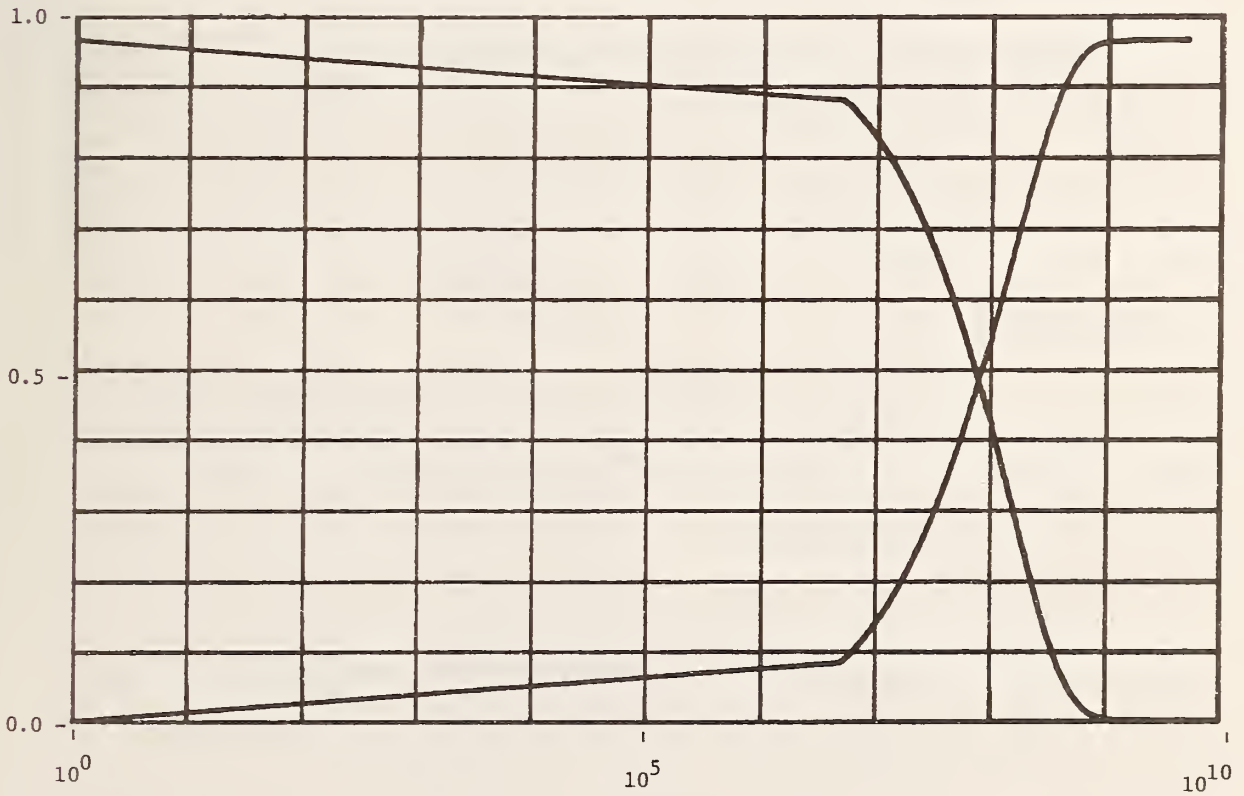


Figure A-80. Plots of "zero"/"one" cable unit step response voltages versus \log_{10} frequency for 152.4 meters (500 ft) of cable RG-22B/U. Ordinate units are volts and abscissa units are hertz.

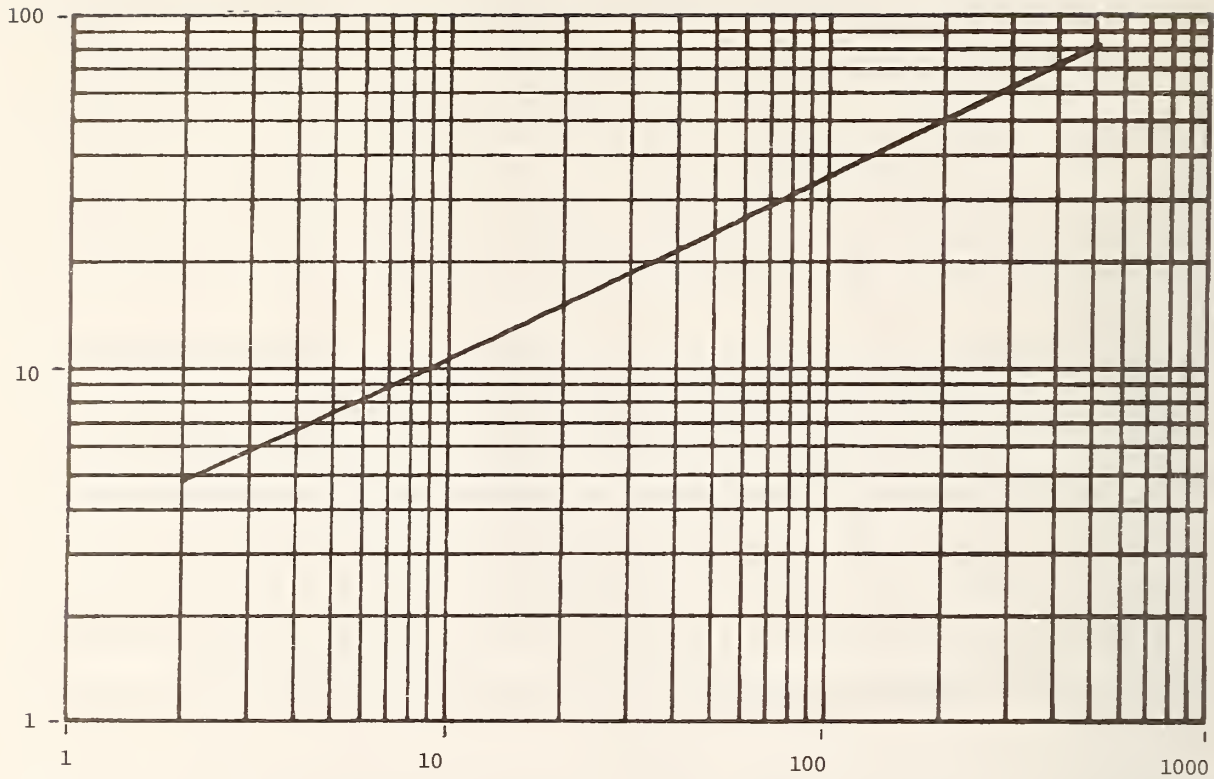


Figure A-81. Modeled attenuation plot for 304.8 meters (1000 ft) of RG-22B/U. Ordinate units are decibels and abscissa units are megahertz.

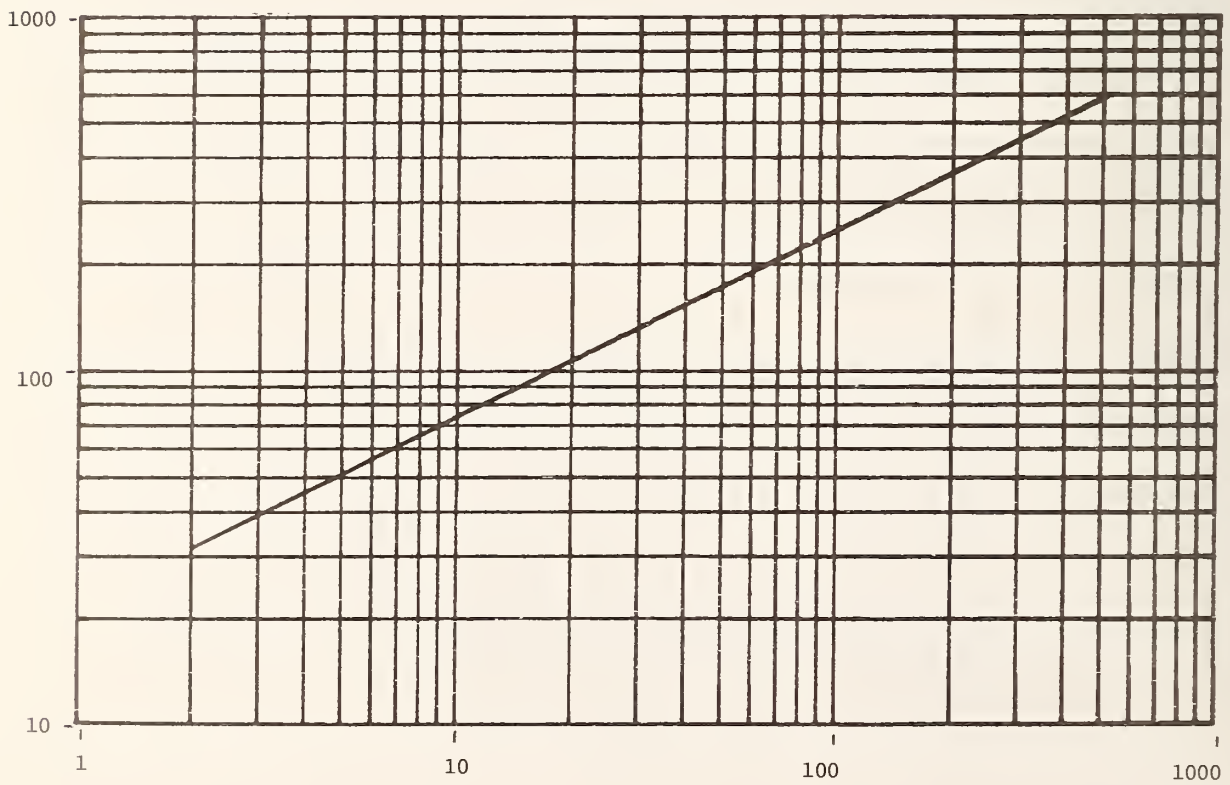


Figure A-82. Modeled minimum-phase phase shift plot for 304.8 meters (1000 ft) of RG-22B/U. Ordinate units are degrees and abscissa units are megahertz.

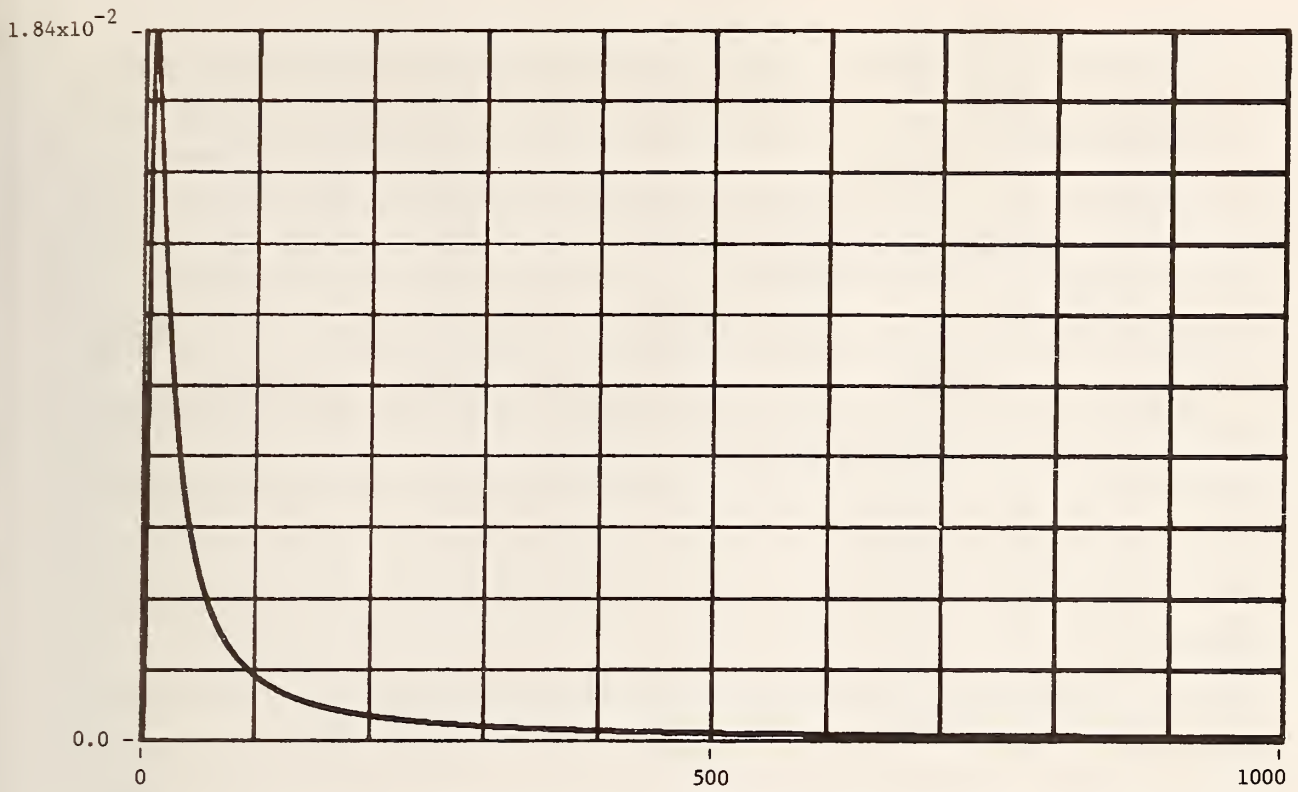


Figure A-83. Modeled and computed time domain impulse response for 304.8 meters (1000 ft) of RG-22B/U. Ordinate units are seconds⁻¹, abscissa units are nanoseconds and time spacing between points is 0.9766 ns.

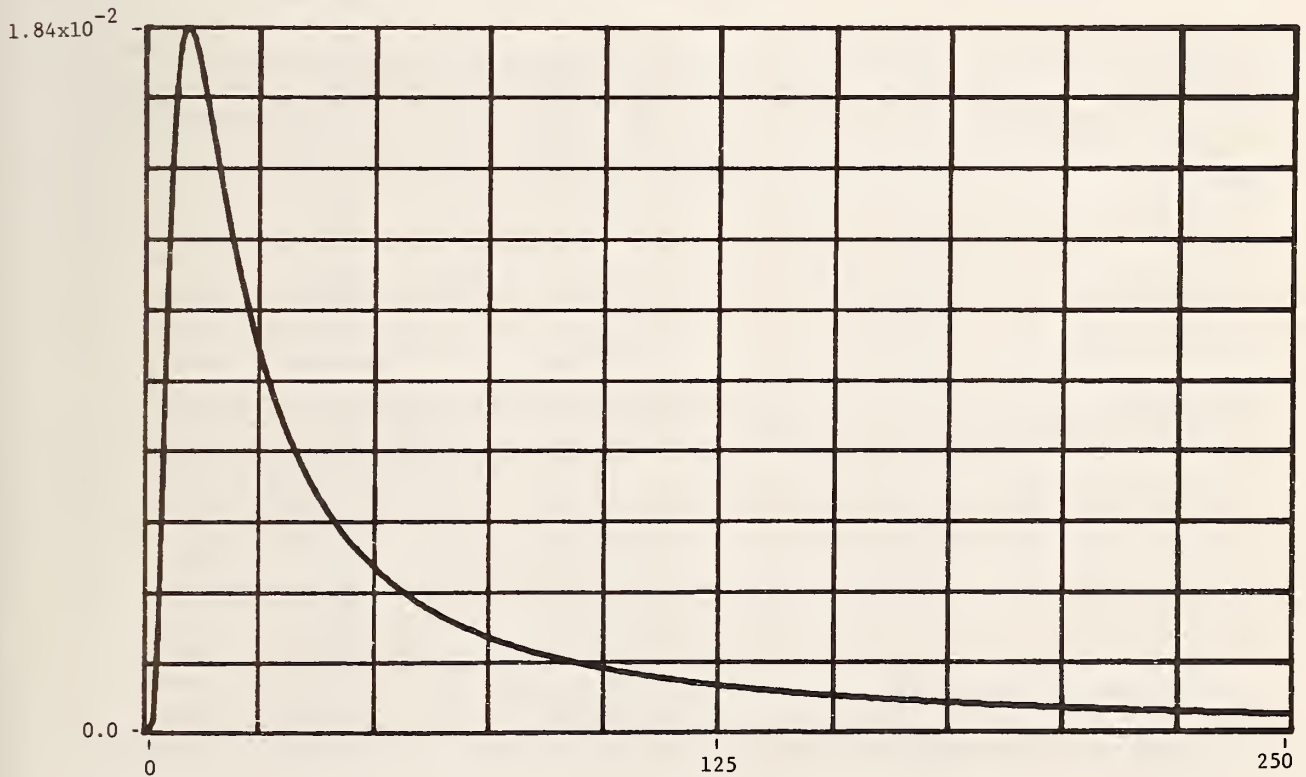


Figure A-84. Time-expanded modeled and computed time domain impulse response for 304.8 meters (1000 ft) of RG-22B/U. Ordinate units are seconds⁻¹, abscissa units are nanoseconds and time spacing between points is 0.9766 ns.

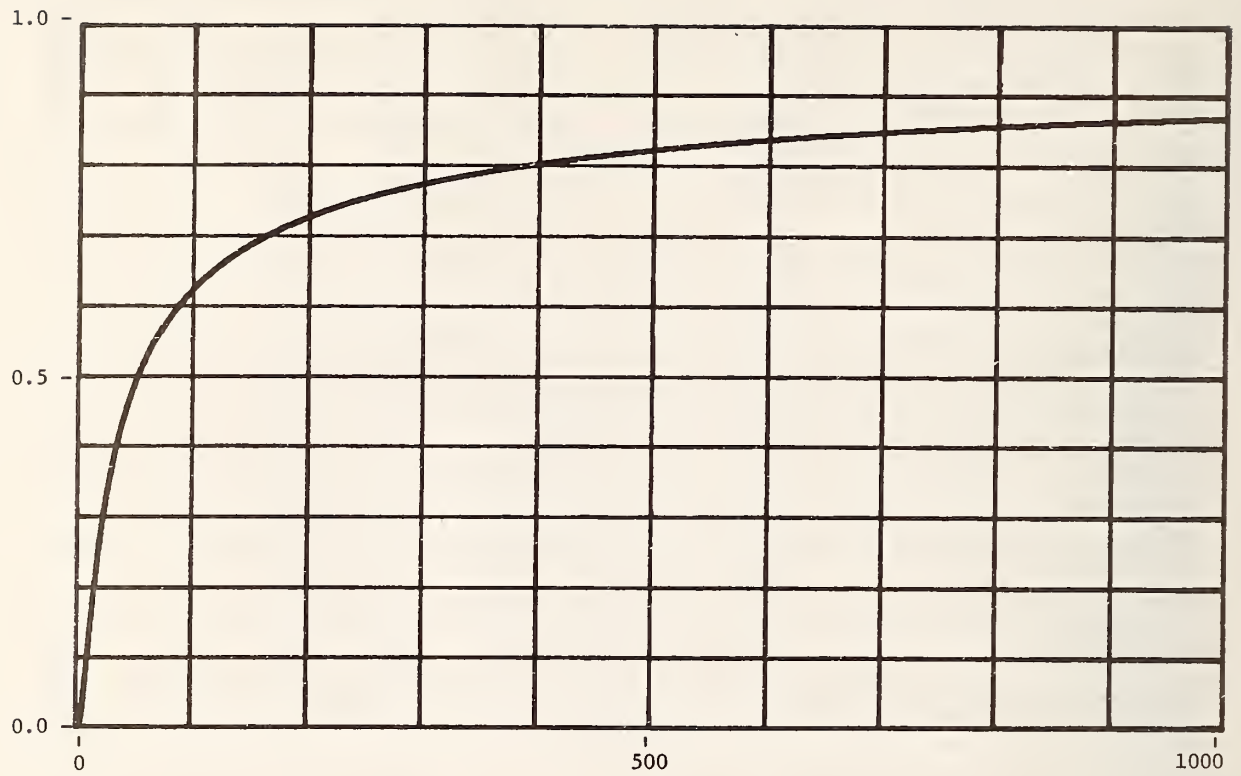


Figure A-85. Modeled and computed time domain unit step response for 304.8 meters (1000 ft) of RG-22B/U. Ordinate units are volts and abscissa units are nanoseconds.

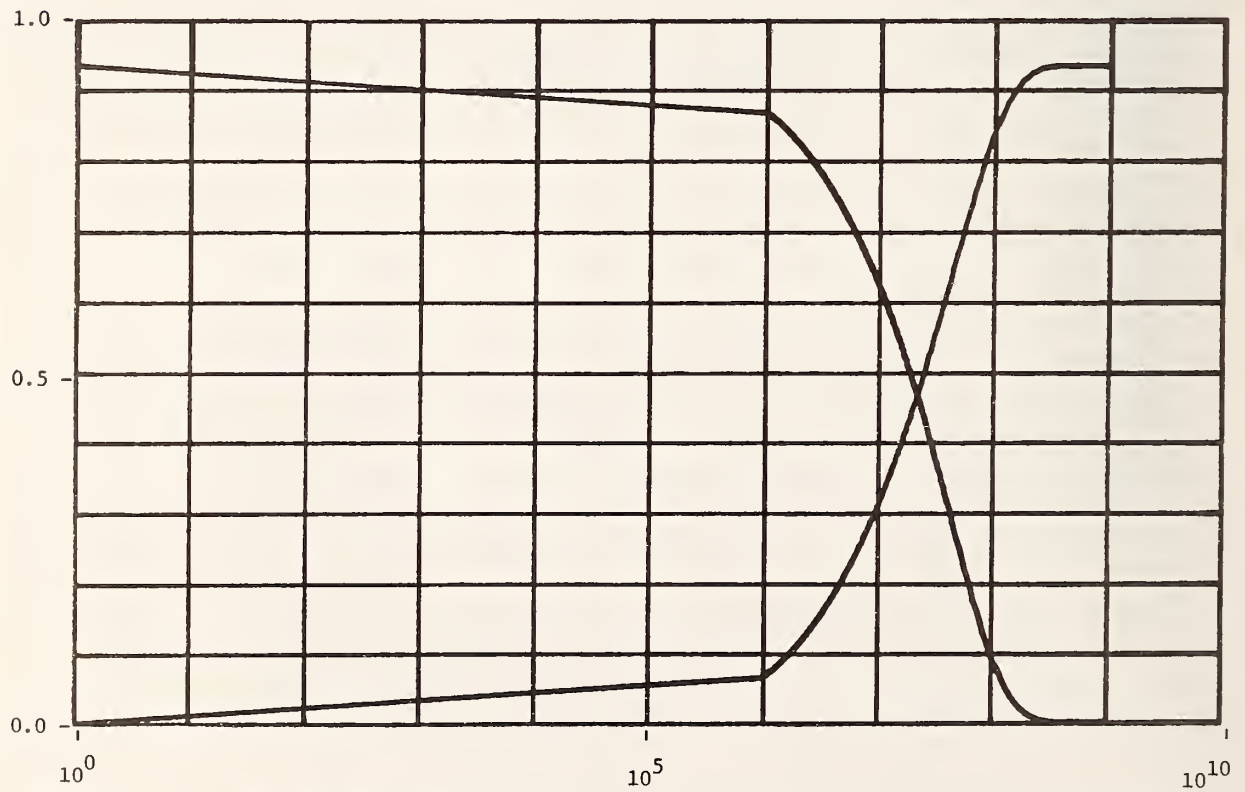


Figure A-86. Plots of "zero"/"one" cable unit step response voltages versus \log_{10} frequency for 304.8 meters (1000 ft) of cable RG-22B/U. Ordinate units are volts and abscissa units are hertz.

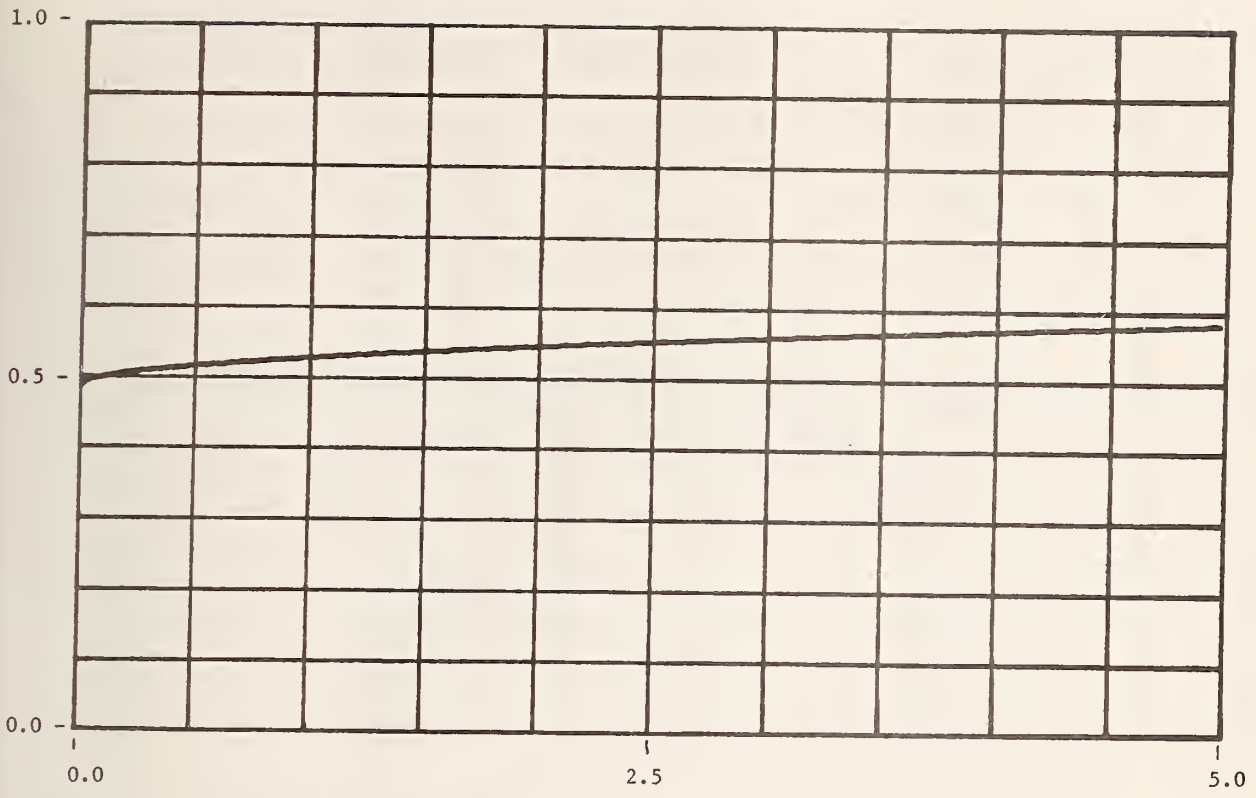


Figure A-87. TDR unit step response for cable RG-22B/U. Source step generator has assumed 50 Ω resistive output impedance. Ordinate units are volts and abscissa units are microseconds.

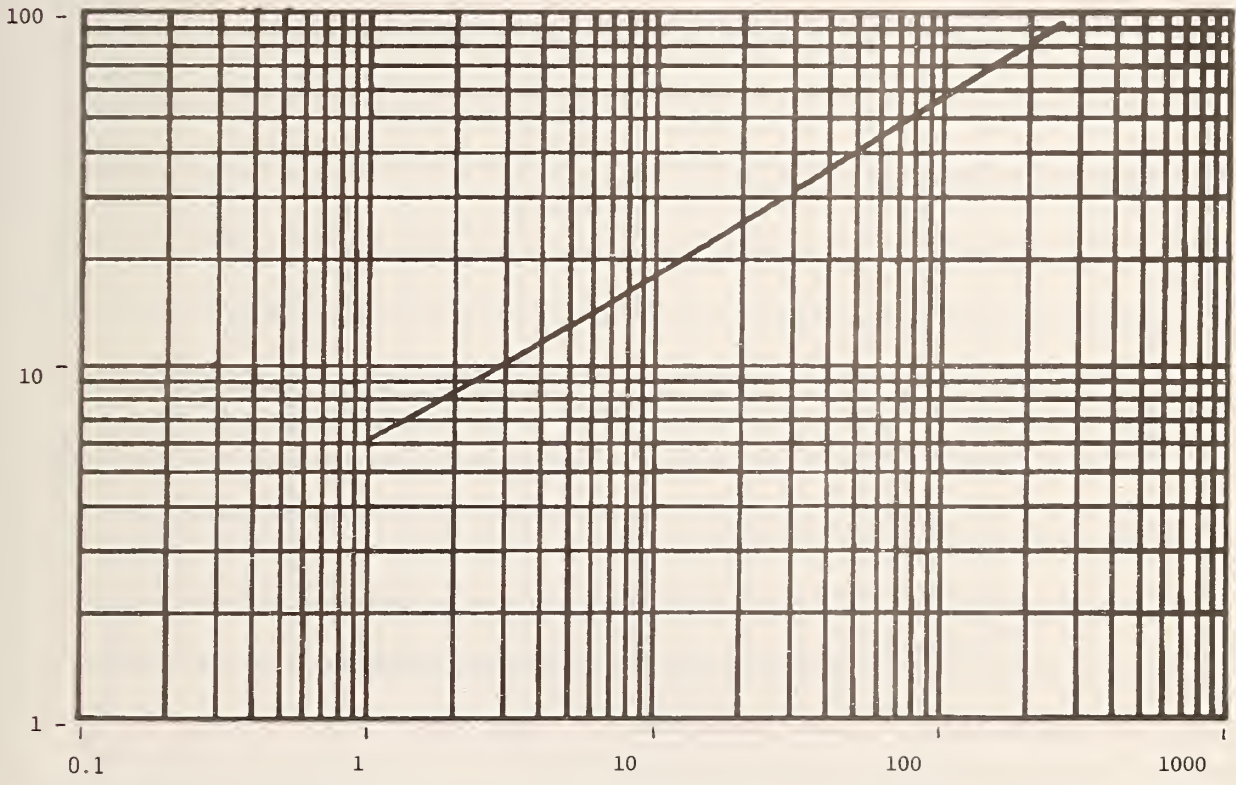


Figure A-88. Modeled attenuation plot for 320.04 meters (1050 ft) of F. Ordinate units are decibels and abscissa units are megahertz.

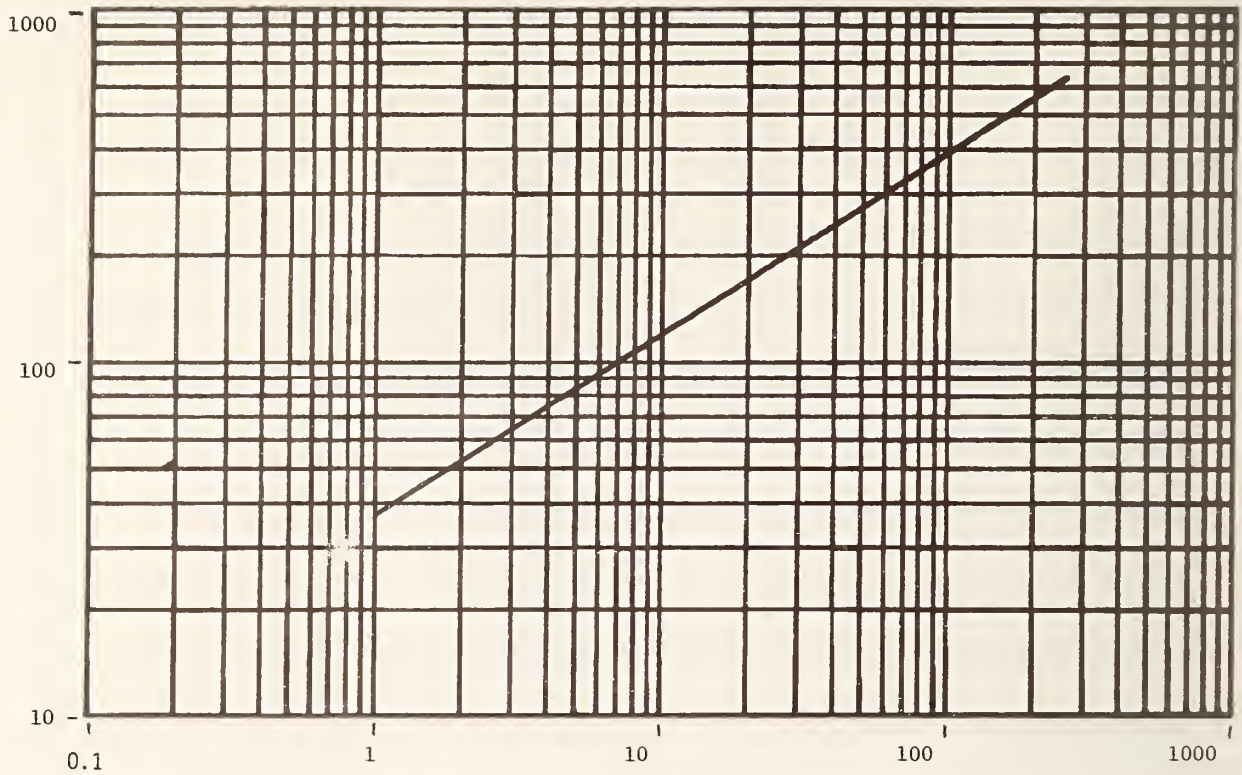


Figure A-89. Modeled minimum-phase phase shift plot for 320.04 meters (1050 ft) of F. Ordinate units are degrees and abscissa units are megahertz.

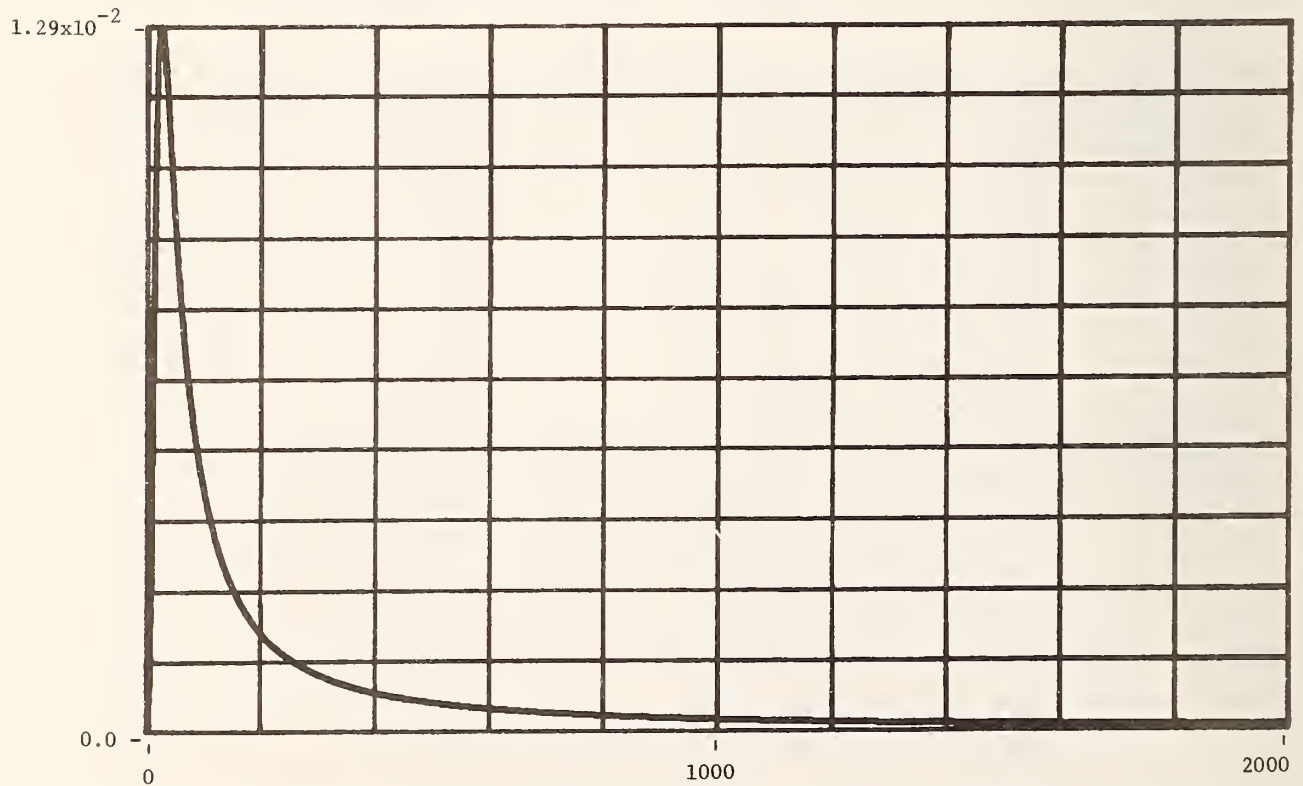


Figure A-90. Modeled and computed time domain impulse response for 320.04 meters (1050 ft) of F. Ordinate units are seconds⁻¹, abscissa units are nanoseconds and time spacing between points is 1.953 ns.

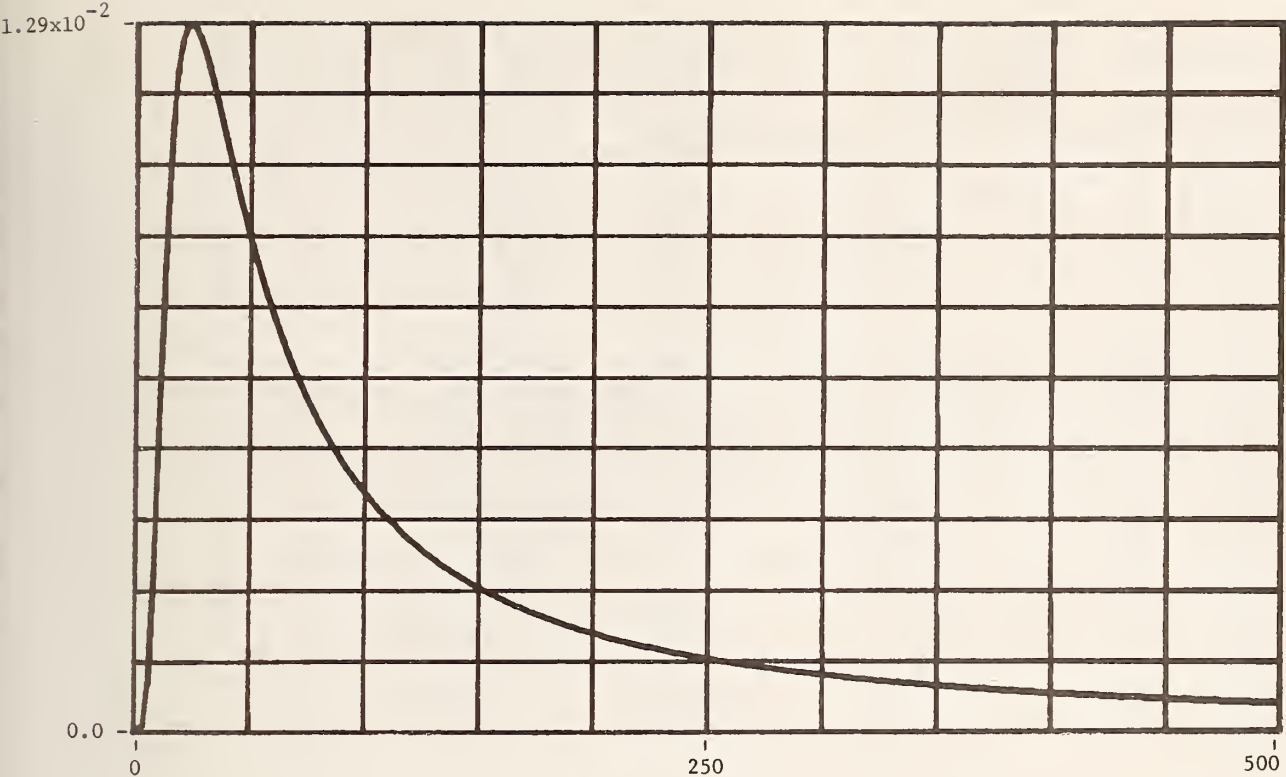


Figure A-91. Time-expanded modeled and computed time domain impulse response for 320.04 meters (1050 ft) of F. Ordinate units are seconds⁻¹, abscissa units are nanoseconds and time spacing between points is 1.953 ns.

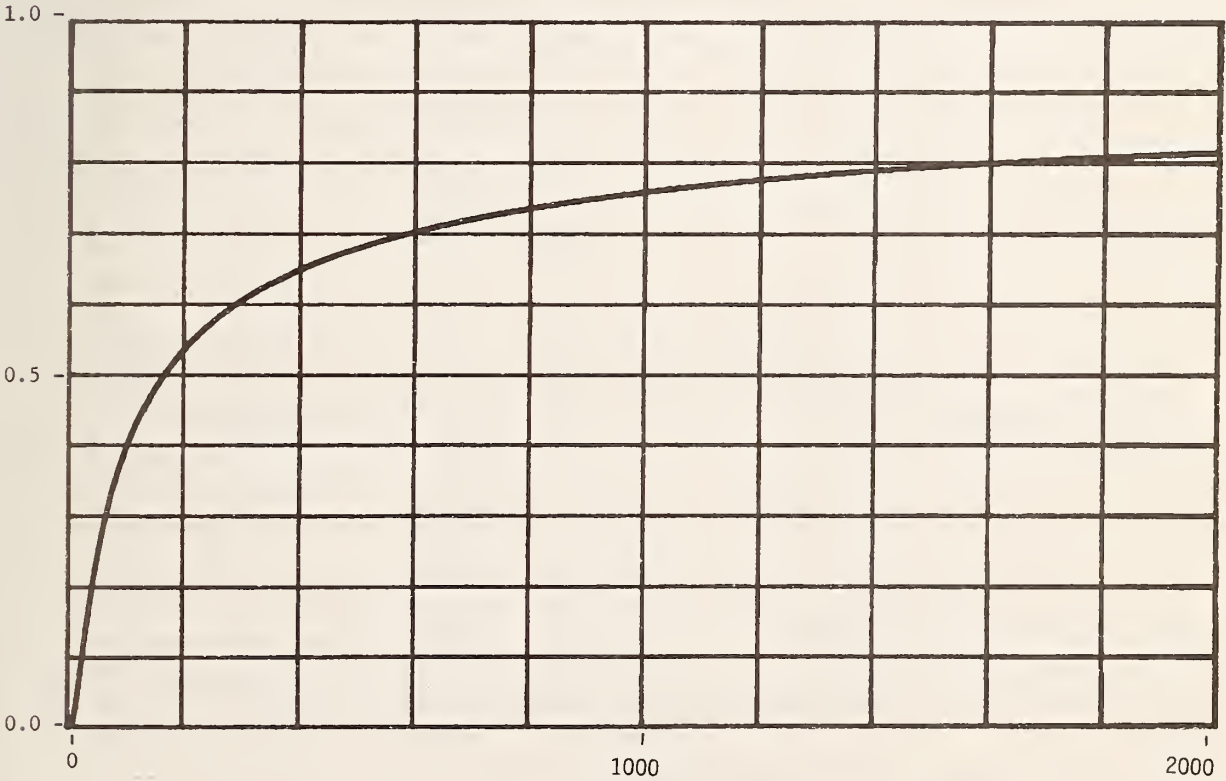


Figure A-92. Modeled and computed time domain unit step response for 320.04 meters (1050 ft) of F. Ordinate units are volts and abscissa units are nanoseconds.

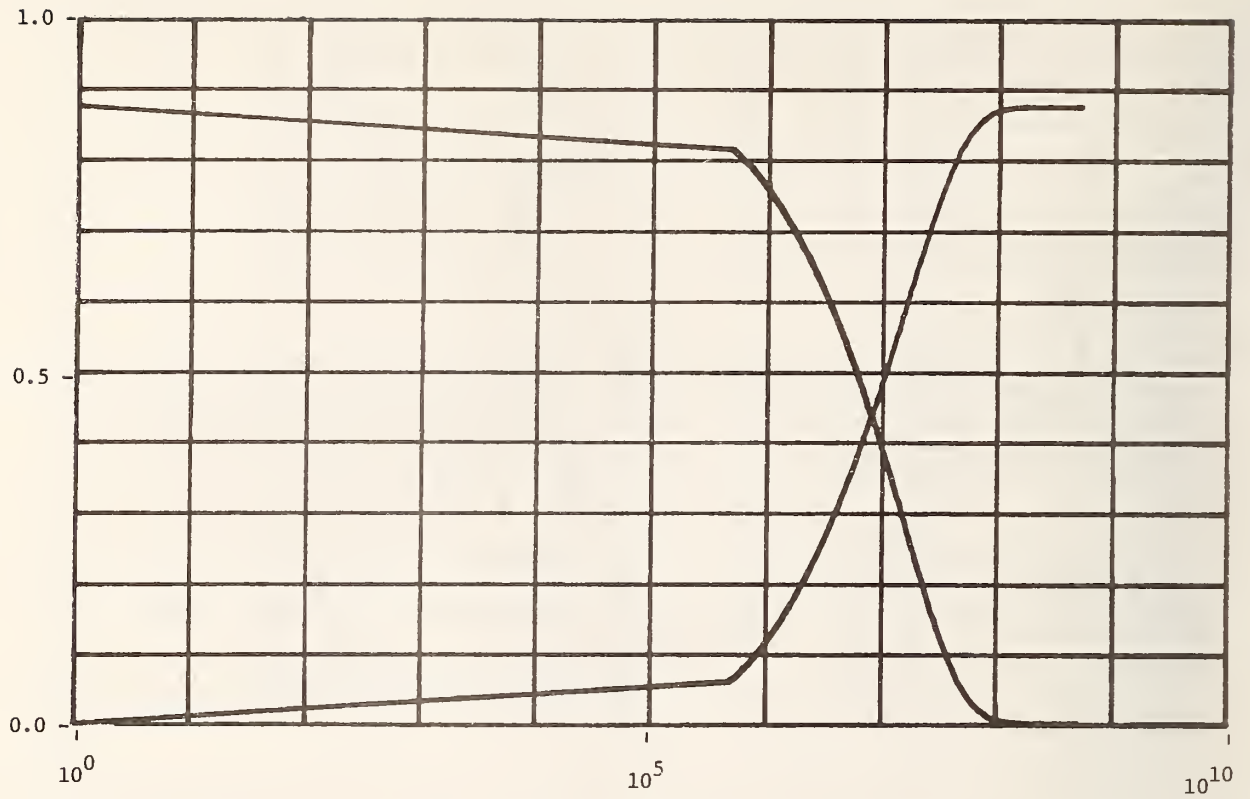


Figure A-93. Plots of "zero"/"one" cable unit step response voltages versus \log_{10} frequency for 320.04 meters (1050 ft) of cable F. Ordinate units are volts and abscissa units are hertz.

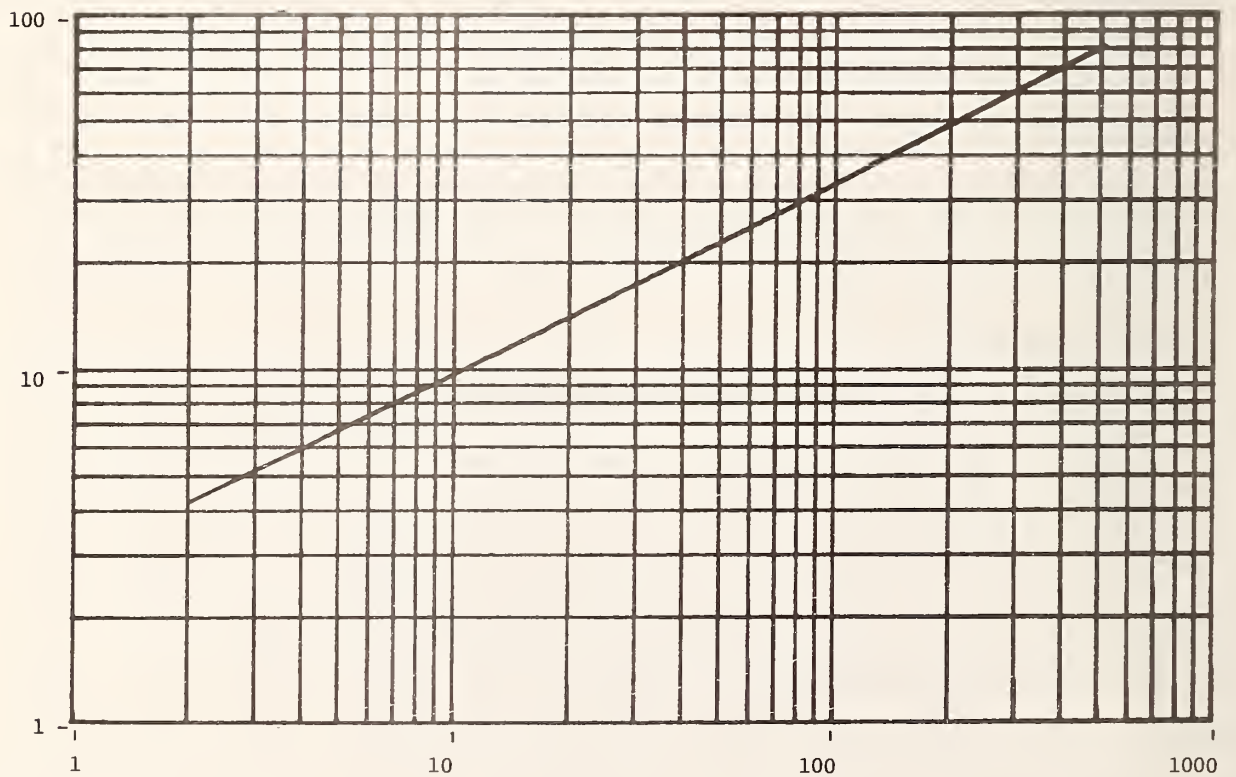


Figure A-94. Modeled attenuation plot for 323.09 meters (1060 ft) of G. Ordinate units are decibels and abscissa units are megahertz.

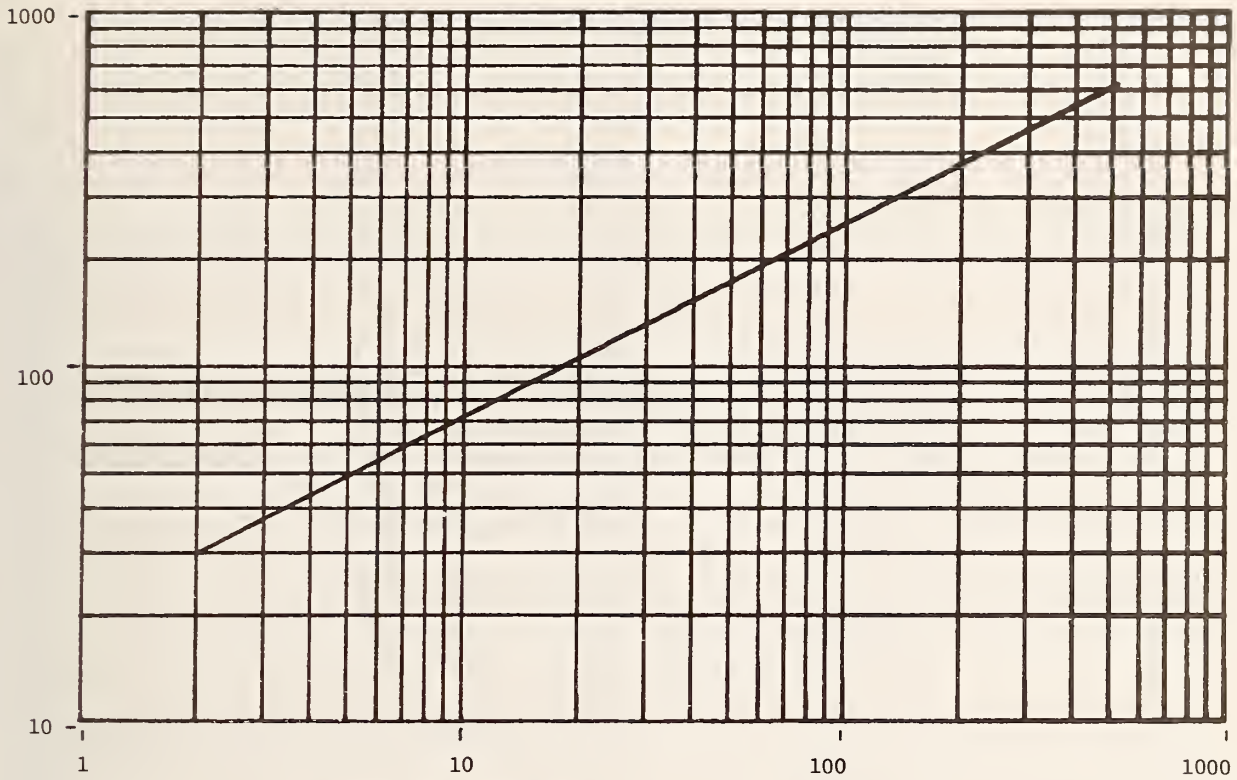


Figure A-95. Modeled minimum-phase phase shift plot for 323.09 meters (1060 ft) of G. Ordinate units are degrees and abscissa units are megahertz.

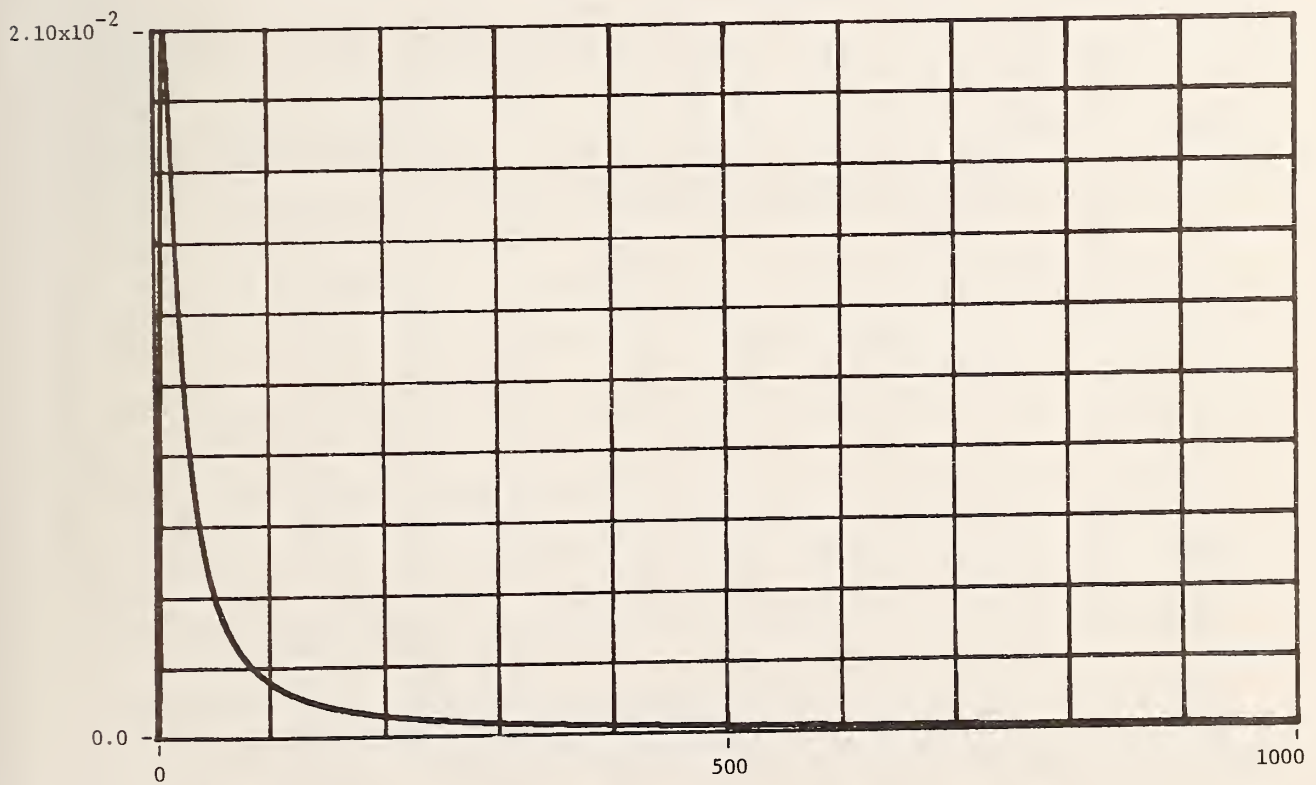


Figure A-96. Modeled and computed time domain impulse response for 323.09 meters (1060 ft) of G. Ordinate units are seconds⁻¹, abscissa units are nanoseconds and time spacing between points is 0.9766 ns.

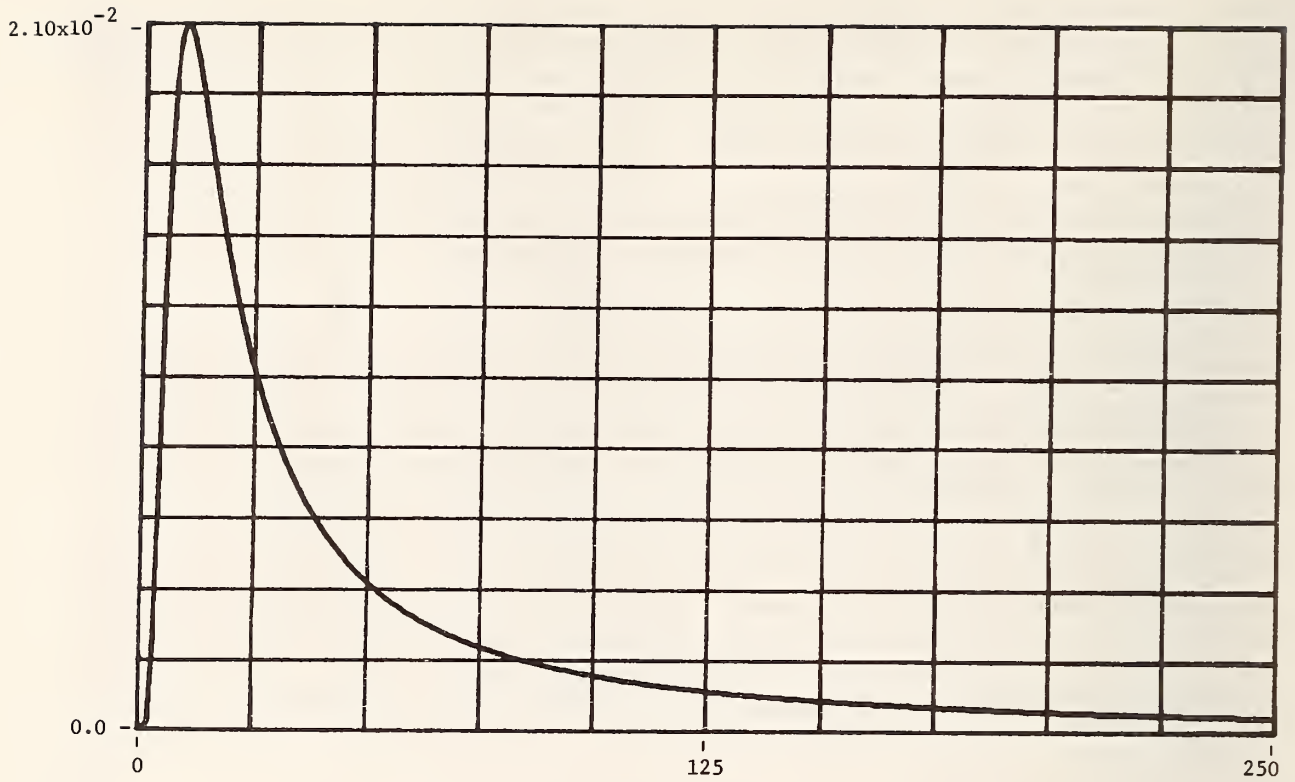


Figure A-97 . Time-expanded modeled and computed time domain impulse response for 323.09 meters (1060 ft) of G. Ordinate units are seconds⁻¹, abscissa units are nanoseconds and time spacing between points is 0.9766 ns.

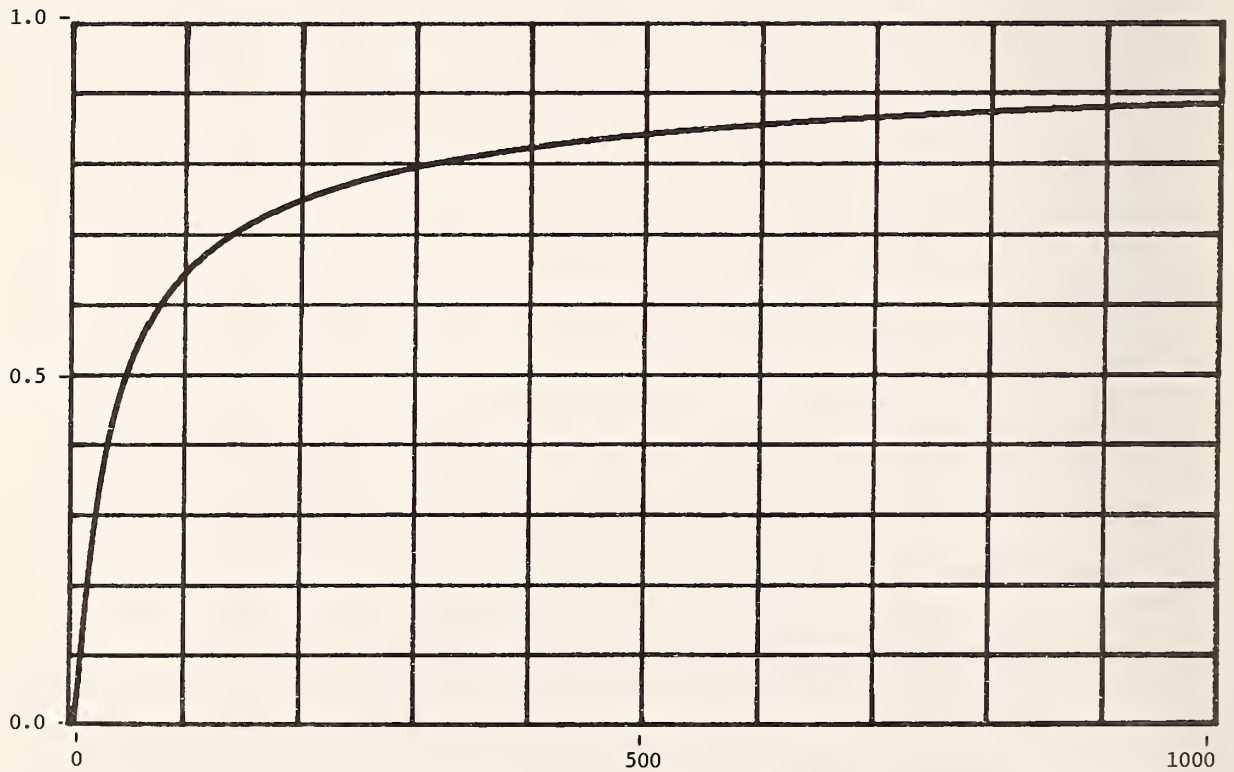


Figure A-98. Modeled and computed time domain unit step response for 323.09 meters (1060 ft) of G. Ordinate units are volts and abscissa units are nanoseconds.

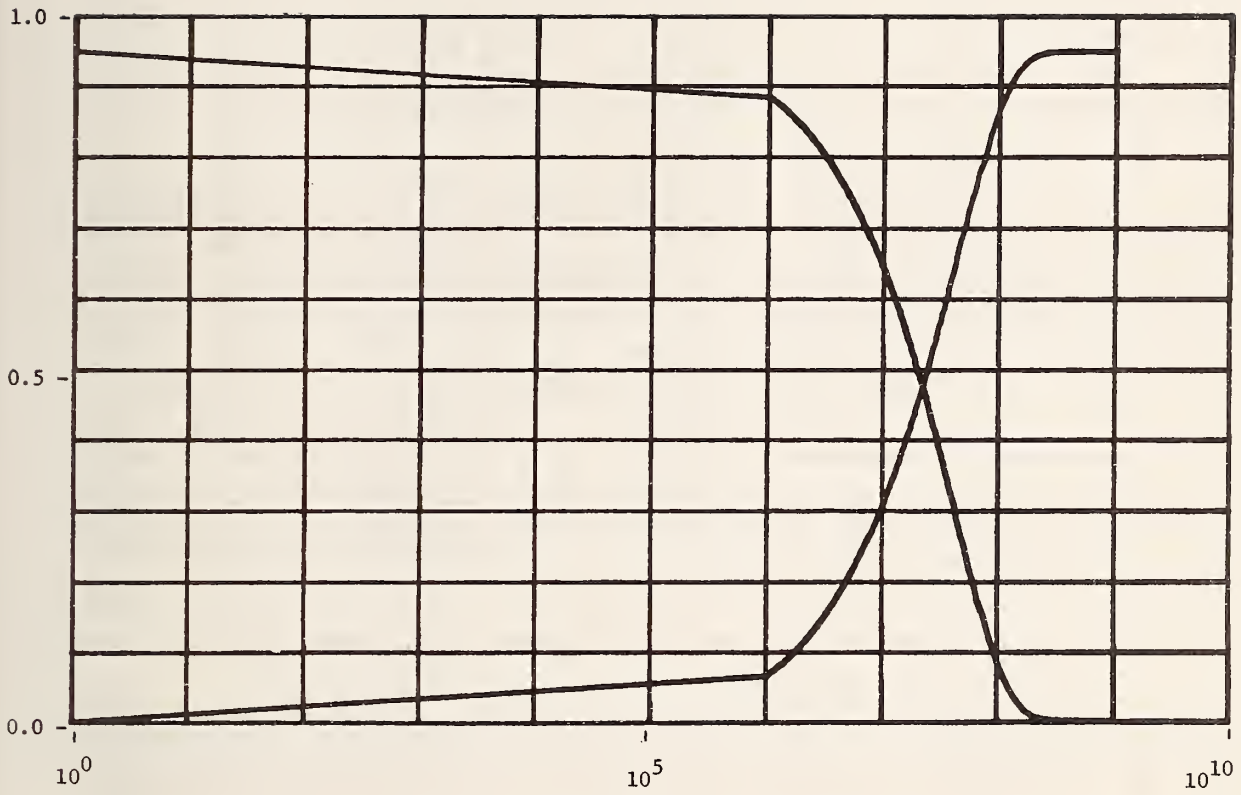


Figure A-99. Plots of "zero"/"one" cable unit step response voltages versus \log_{10} frequency for 323.09 meters (1060 ft) of cable G. Ordinate units are volts and abscissa units are hertz.

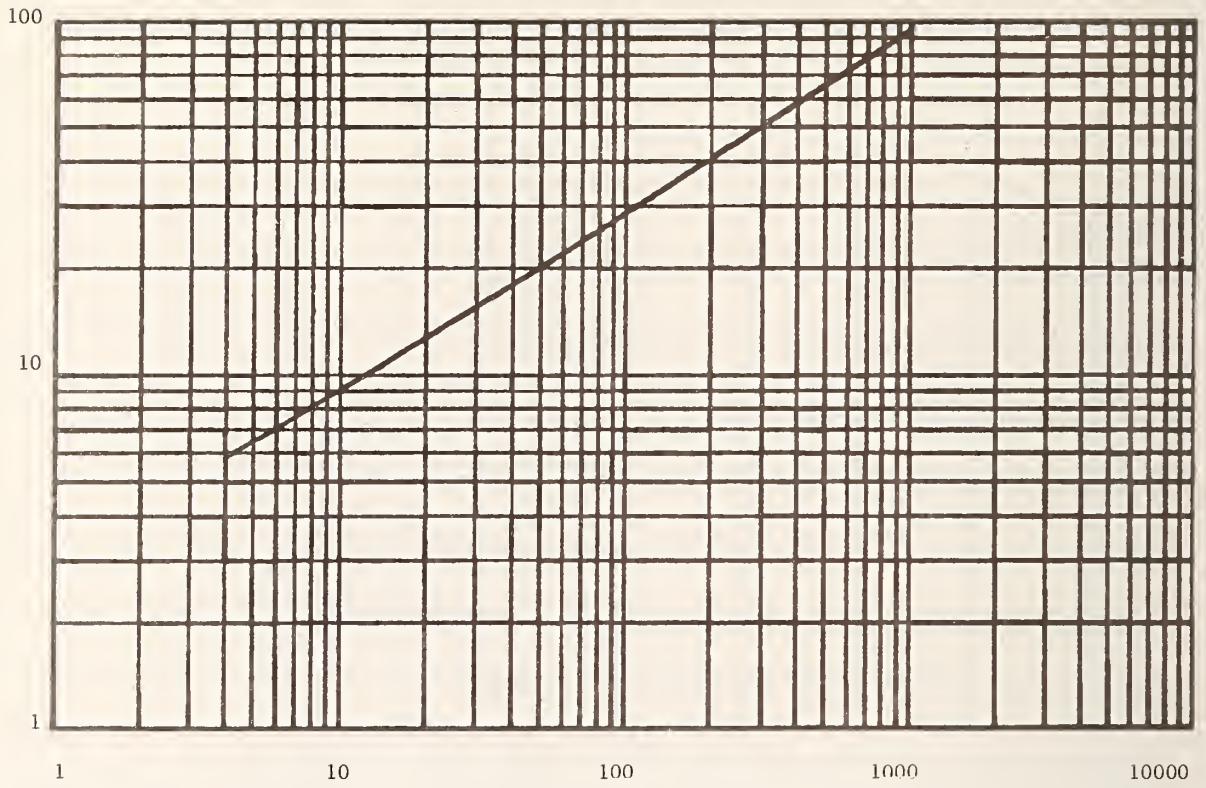


Figure A- 100. Modeled attenuation plot for 152.4 meters (500 ft) of H. Ordinate units are decibels and abscissa units are megahertz.

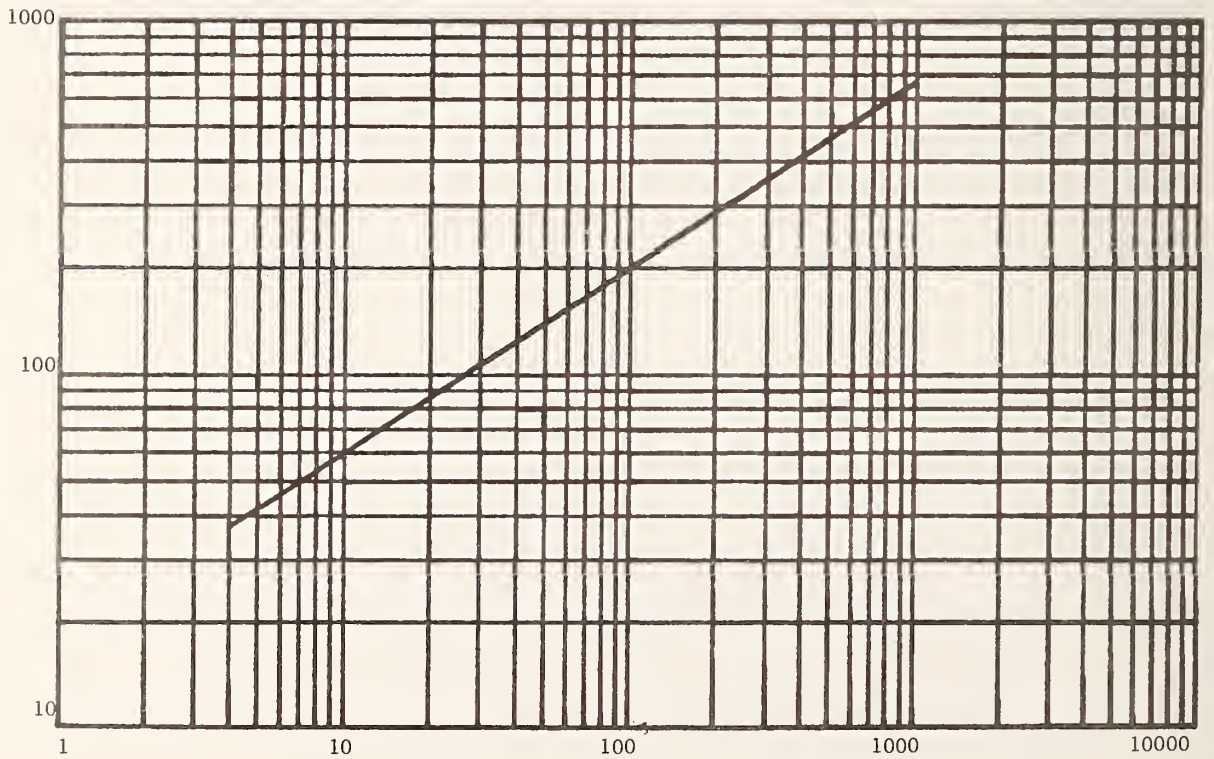


Figure A- 101. Modeled minimum-phase phase shift plot for 152.4 meters (500 ft) of H. Ordinate units are degrees and abscissa units are megahertz.

1.315×10^{-2}

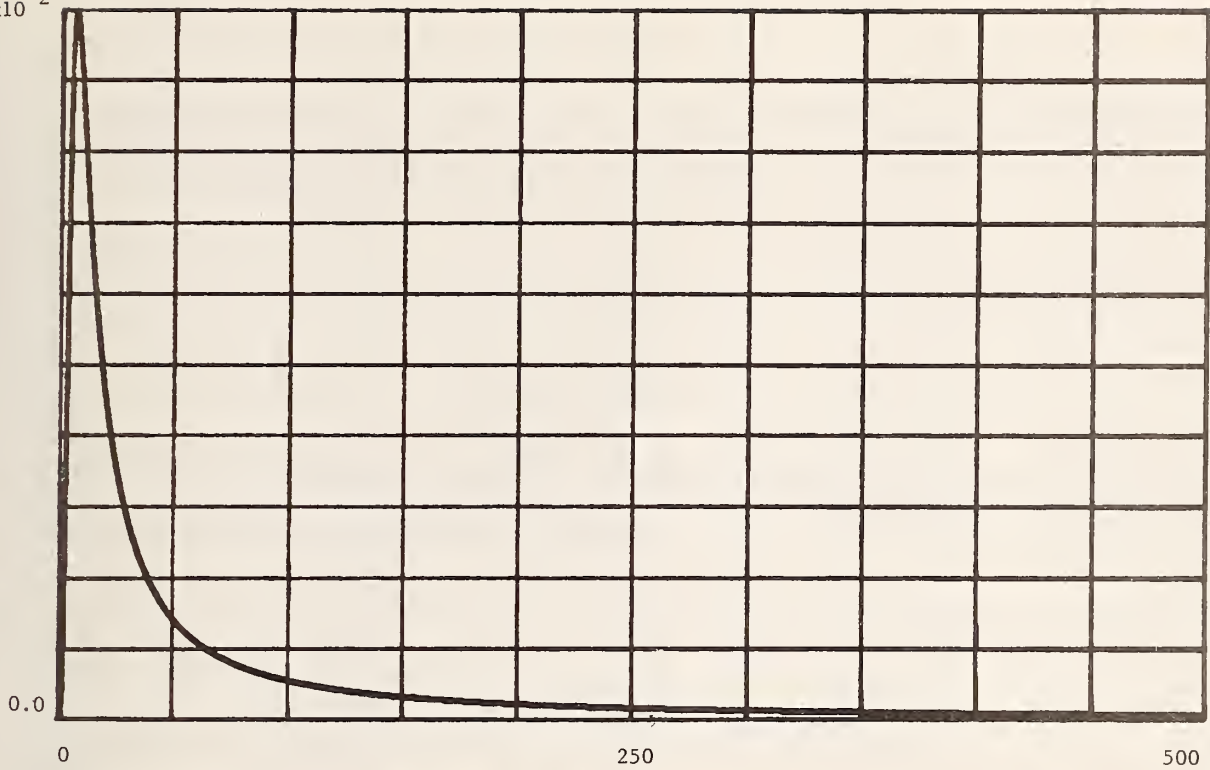


Figure A-102. Modeled and computed time domain impulse response for 152.4 meters (500 ft) of H. Ordinate units are seconds⁻¹, abscissa units are nanoseconds and time spacing between points is 4.883 ns.

1.315×10^{-2}

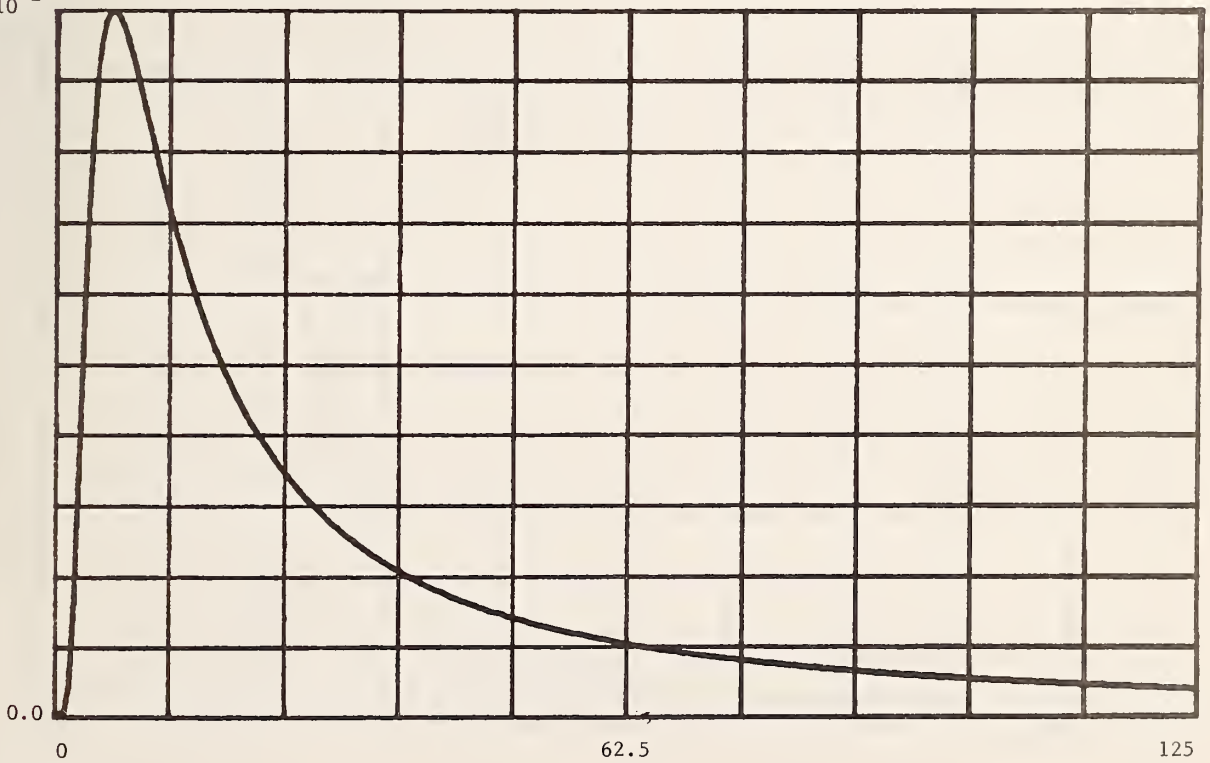


Figure A-103. Time-expanded modeled and computed time domain impulse response for 152.4 meters (500 ft) of H. Ordinate units are seconds⁻¹, abscissa units are nanoseconds and time spacing between points is 4.883 ns.

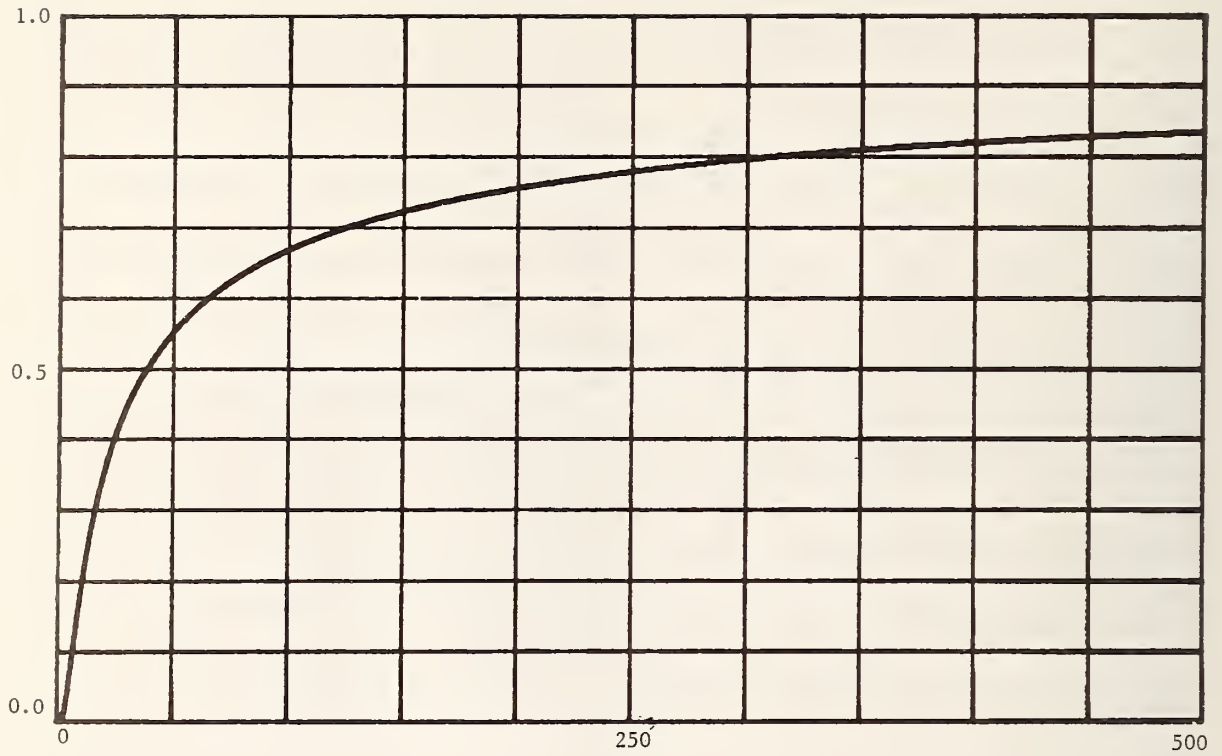


Figure A-104. Modeled and computed time domain unit step response for 152.4 meters (500 ft) of H. Ordinate units are volts and abscissa units are nanoseconds.

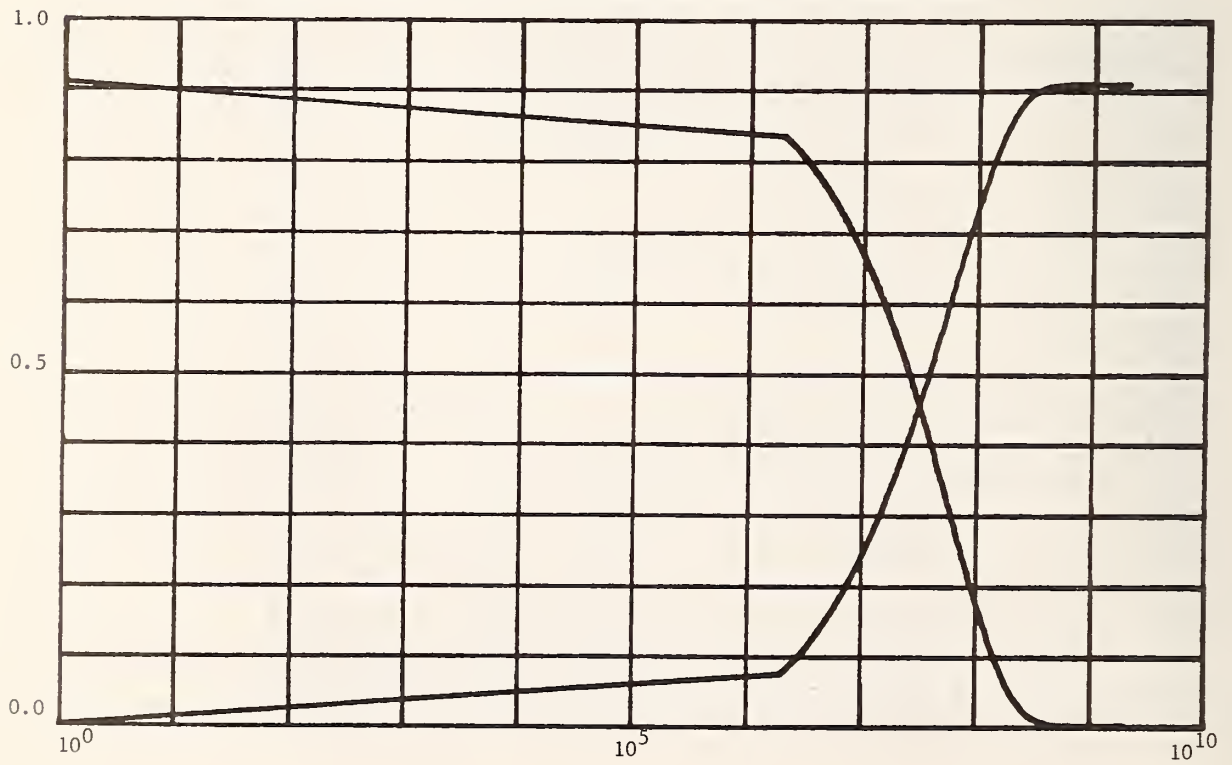


Figure A-105. Plots of "zero"/"one" cable unit step response voltages versus \log_{10} frequency for 152.4 meters (500 ft) of cable H. Ordinate units are volts and abscissa units are hertz.

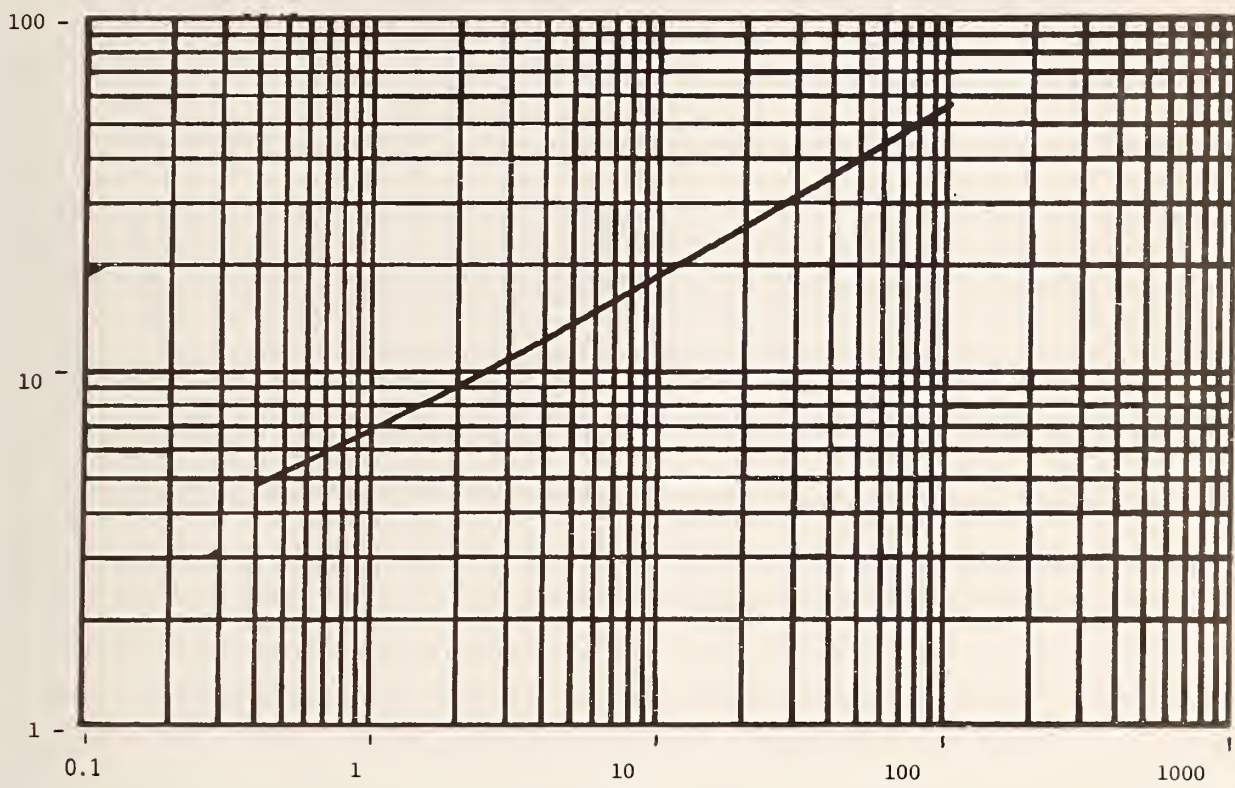


Figure A-106. Modeled attenuation plot for 326.14 meters (1070 ft) of H. Ordinate units are decibels and abscissa units are megahertz.

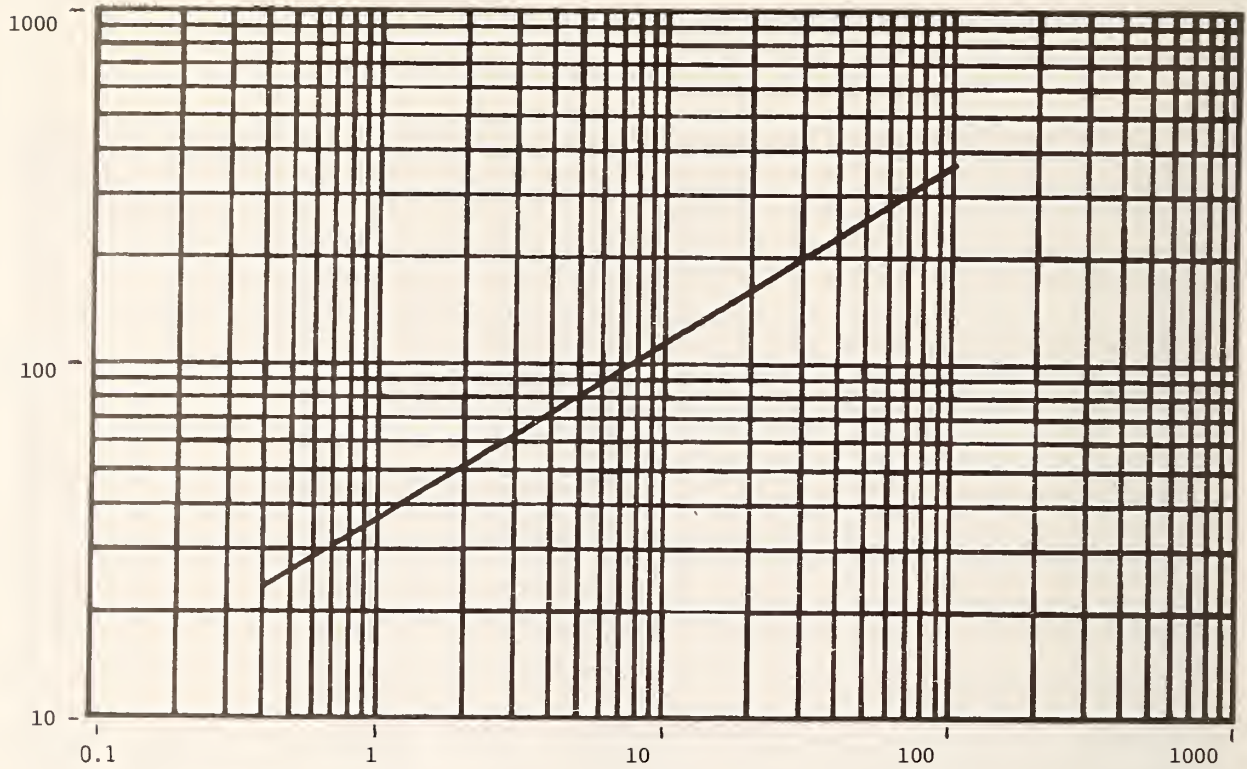


Figure A-107. Modeled minimum-phase phase shift plot for 326.14 meters (1070 ft) of H. Ordinate units are degrees and abscissa units are megahertz.

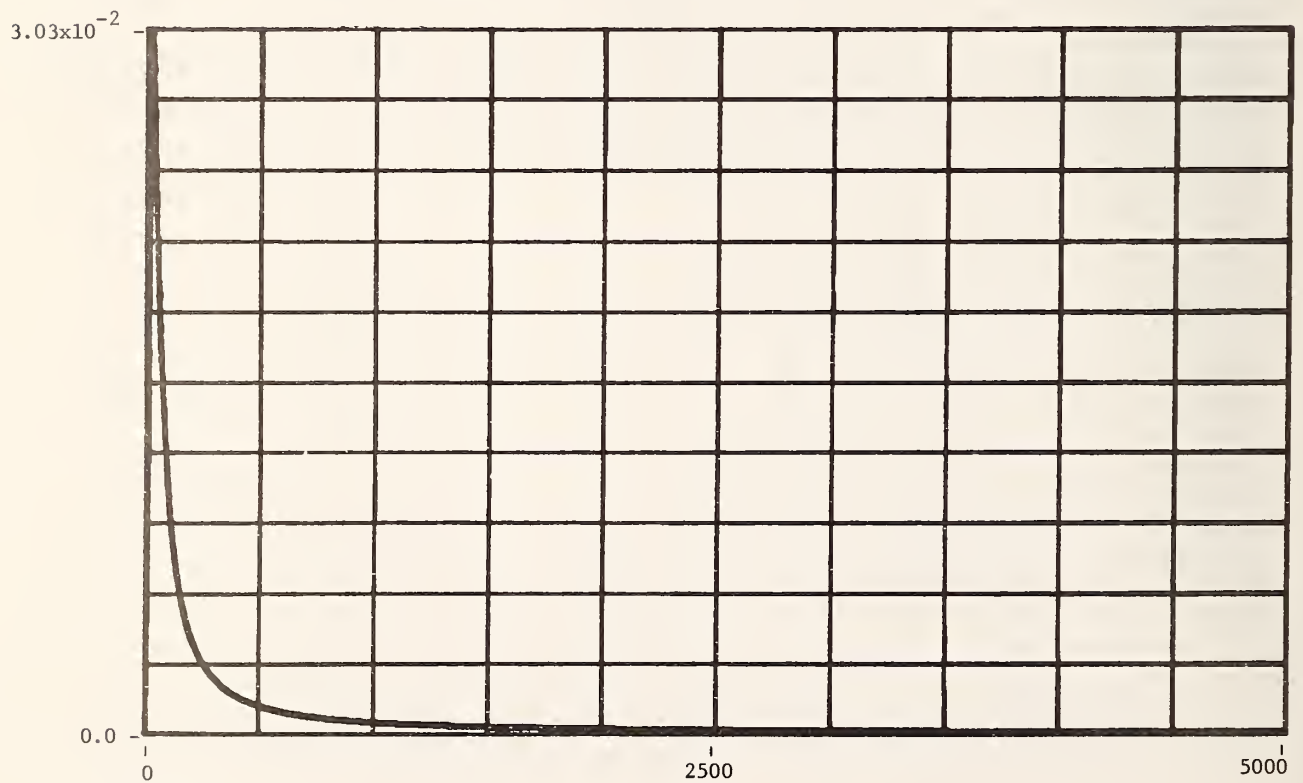


Figure A-108. Modeled and computed time domain impulse response for 326.14 meters (1070 ft) of H. Ordinate units are seconds⁻¹, abscissa units are nanoseconds and time spacing between points is 4.883 ns.

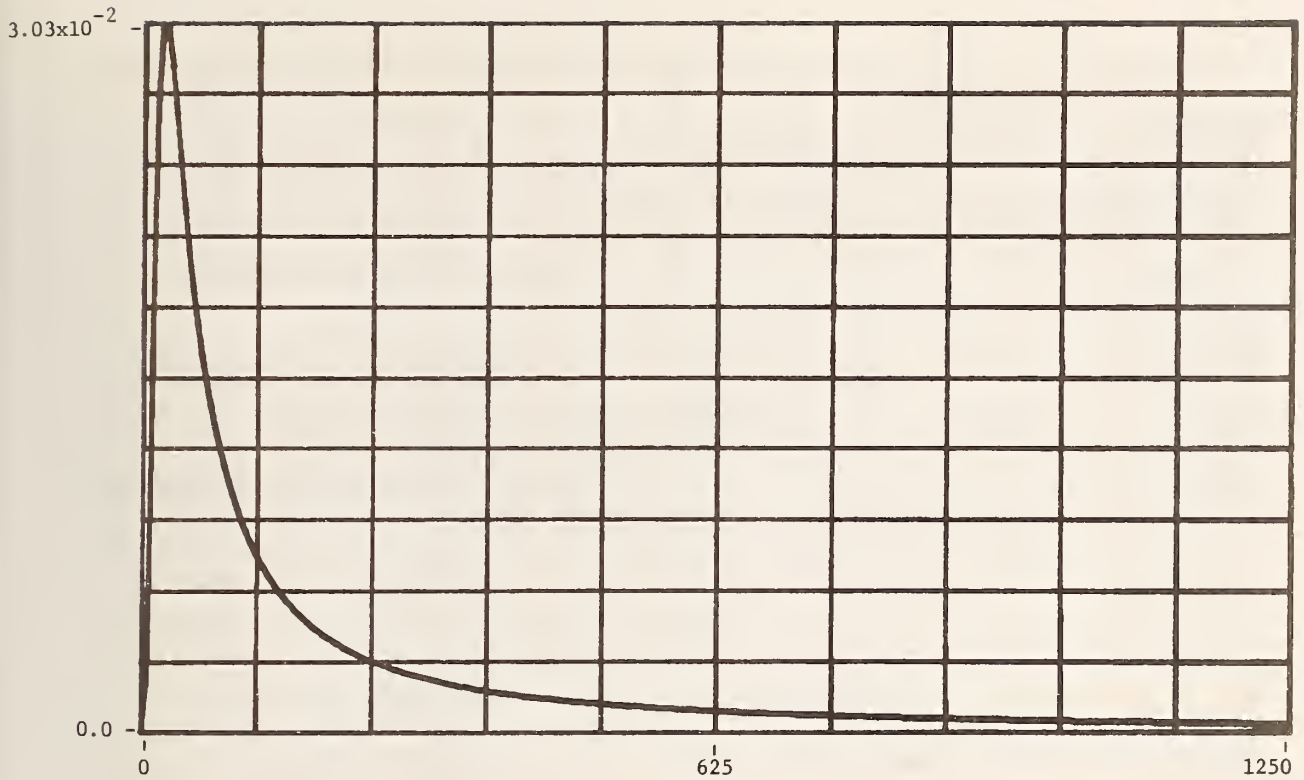


Figure A-109. Time-expanded modeled and computed time domain impulse response for 326.14 meters (1070 ft) of H. Ordinate units are seconds^{-1} , abscissa units are nanoseconds and time spacing between points is 4.883 ns.

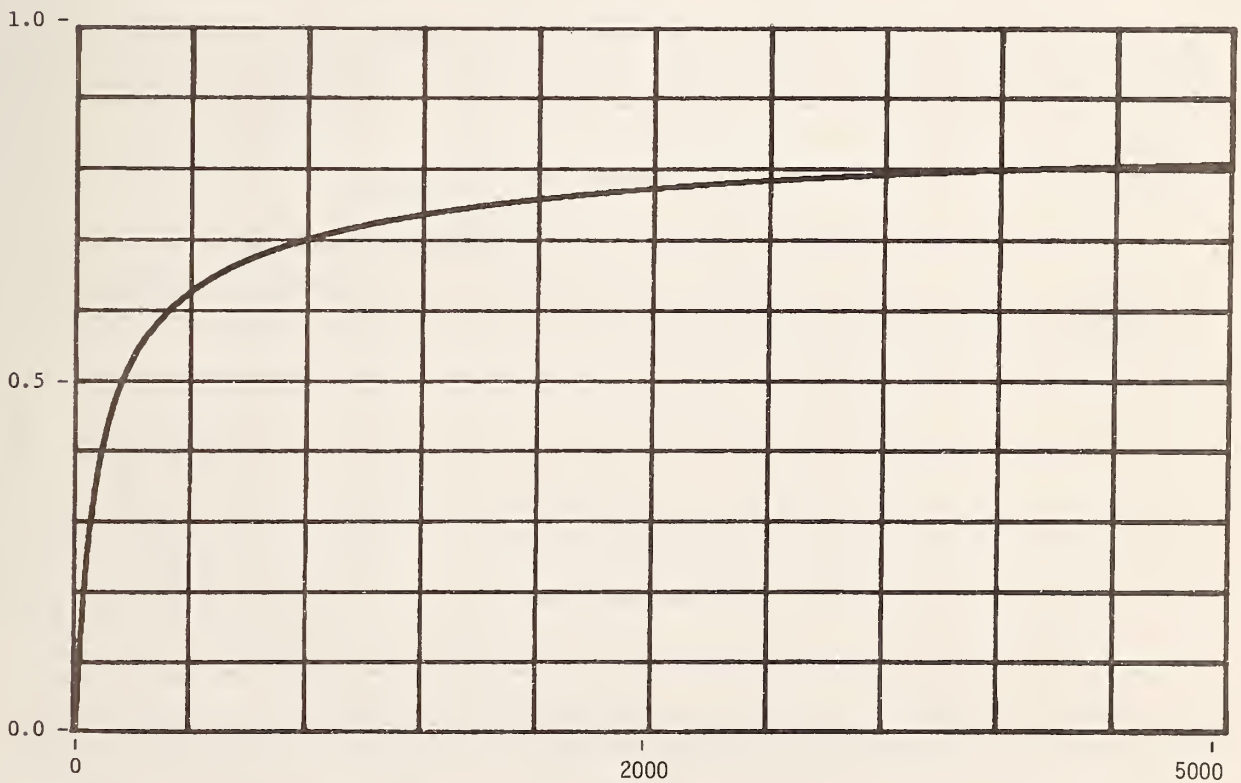


Figure A-110. Modeled and computed time domain unit step response for 326.14 meters (1070 ft) of H. Ordinate units are volts and abscissa units are nanoseconds.

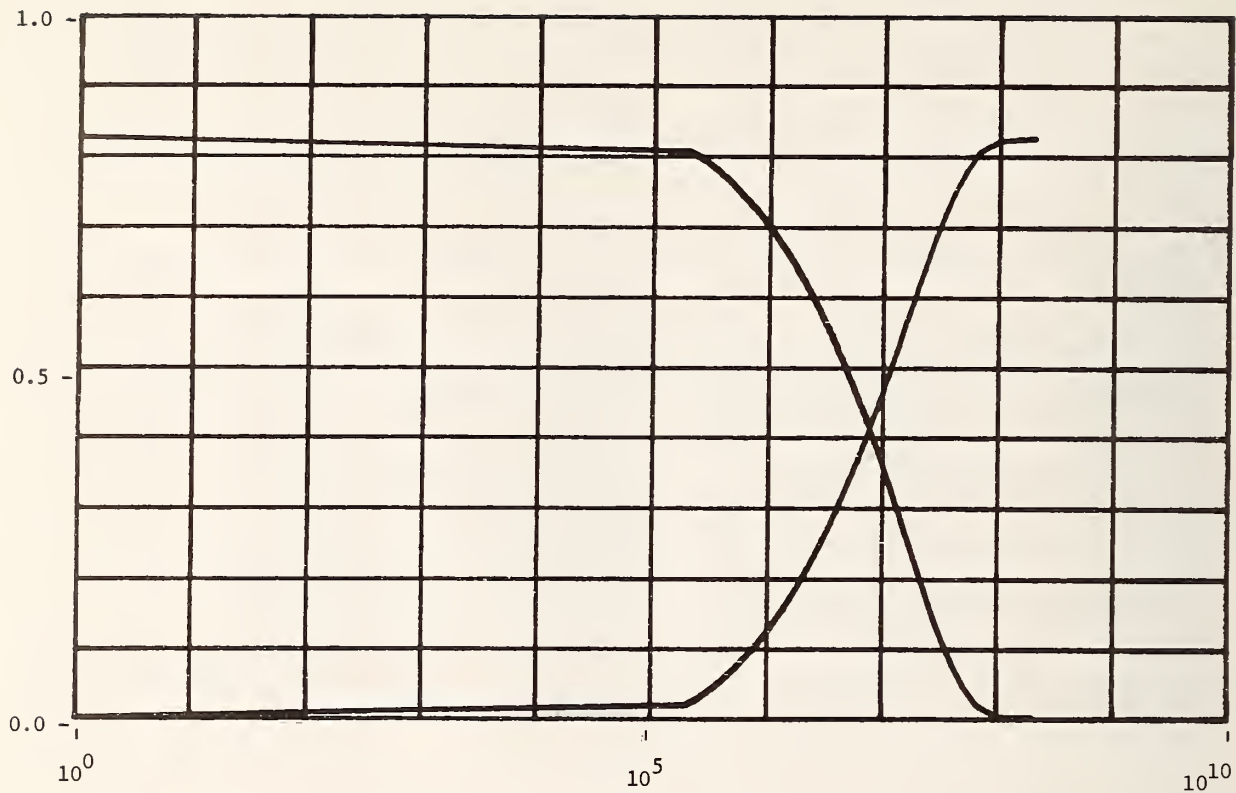


Figure A-111. Plots of "zero"/"one" cable unit step response voltages versus \log_{10} frequency for 326.14 meters (1070 ft) of cable H. Ordinate units are volts and abscissa units are hertz.

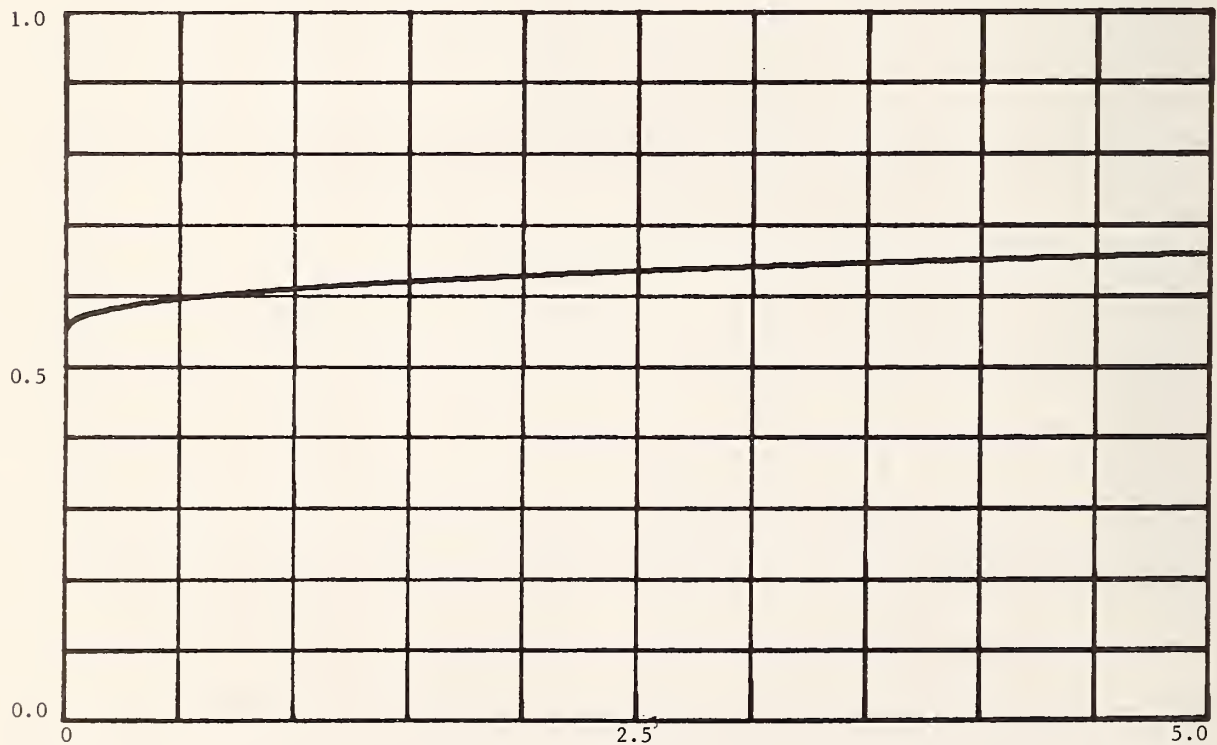


Figure A-112. TDR unit step response for cable H. Source step generator has assumed 50Ω resistive output impedance. Ordinate units are volts and abscissa are microseconds.

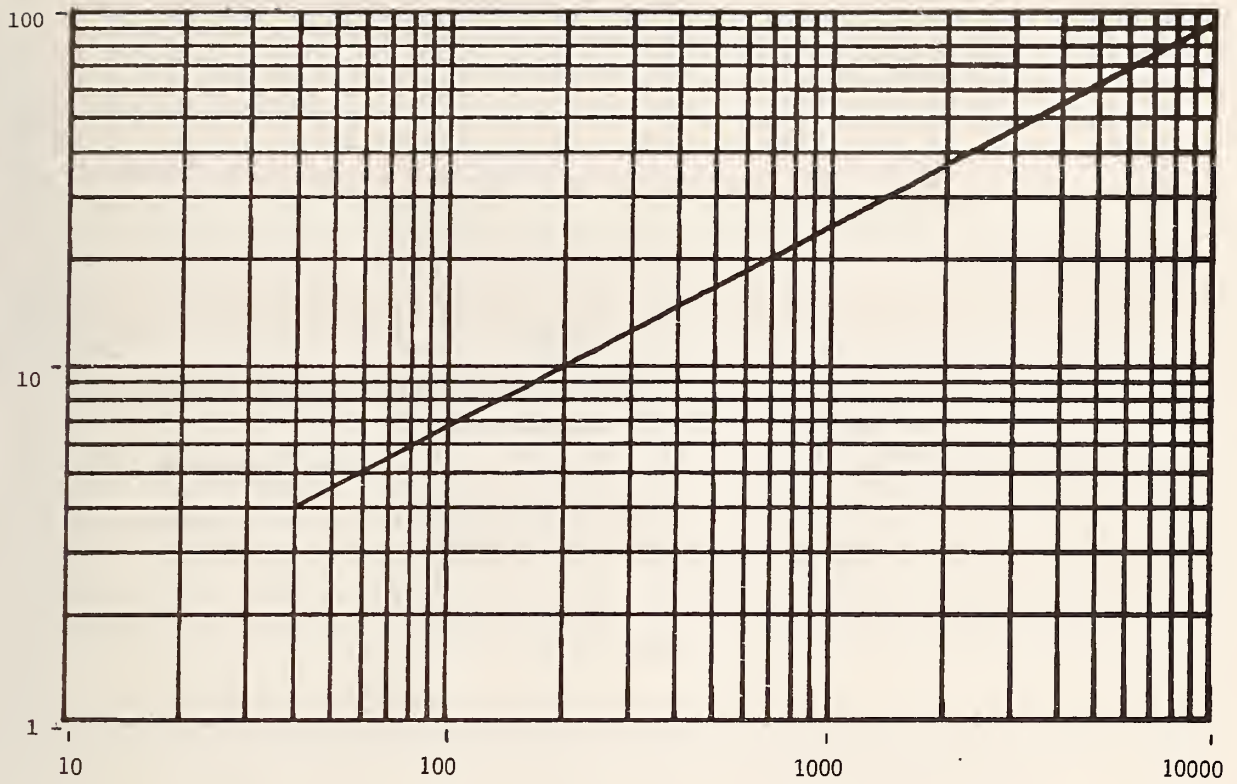


Figure A-113. Modeled attenuation plot for 60.96 meters (200 ft) of I. Ordinate units are decibels and abscissa units are megahertz.

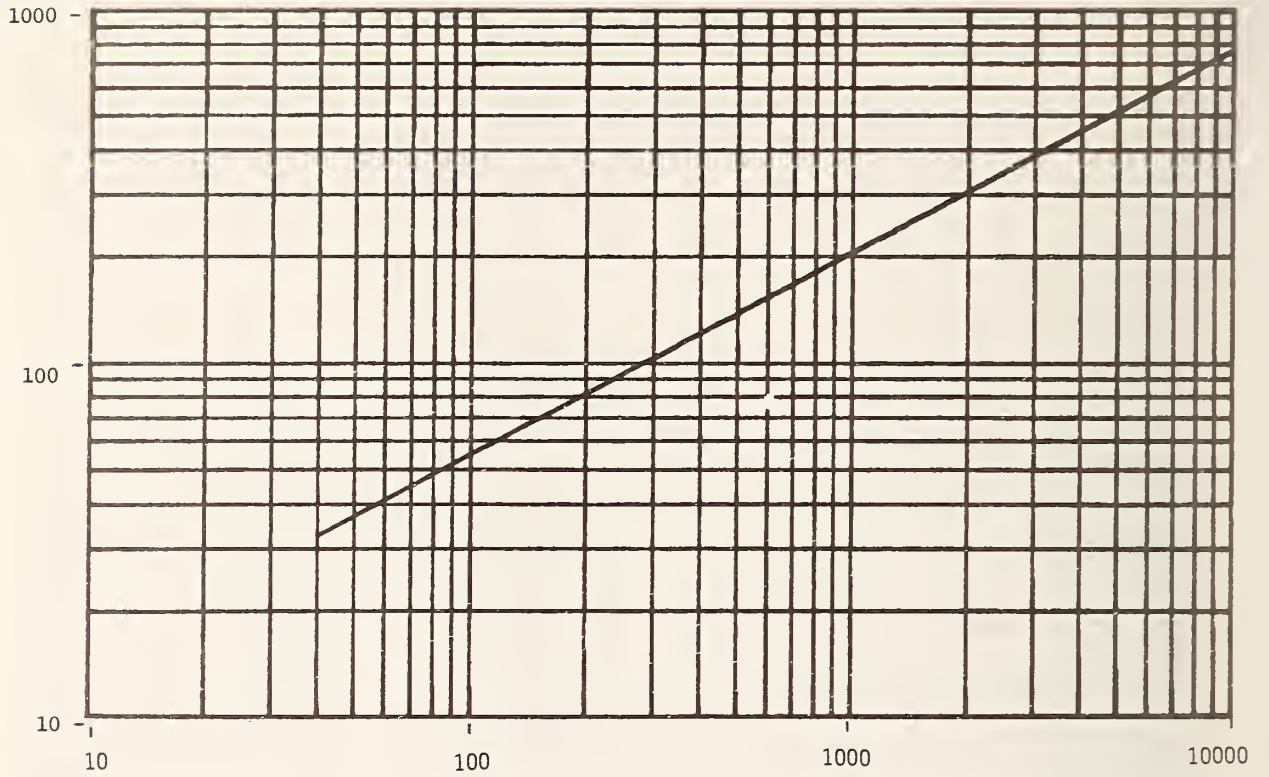


Figure A-114 Modeled minimum-phase phase shift plot for 60.96 meters (200 ft) of I. Ordinate units are degrees and abscissa units are megahertz.

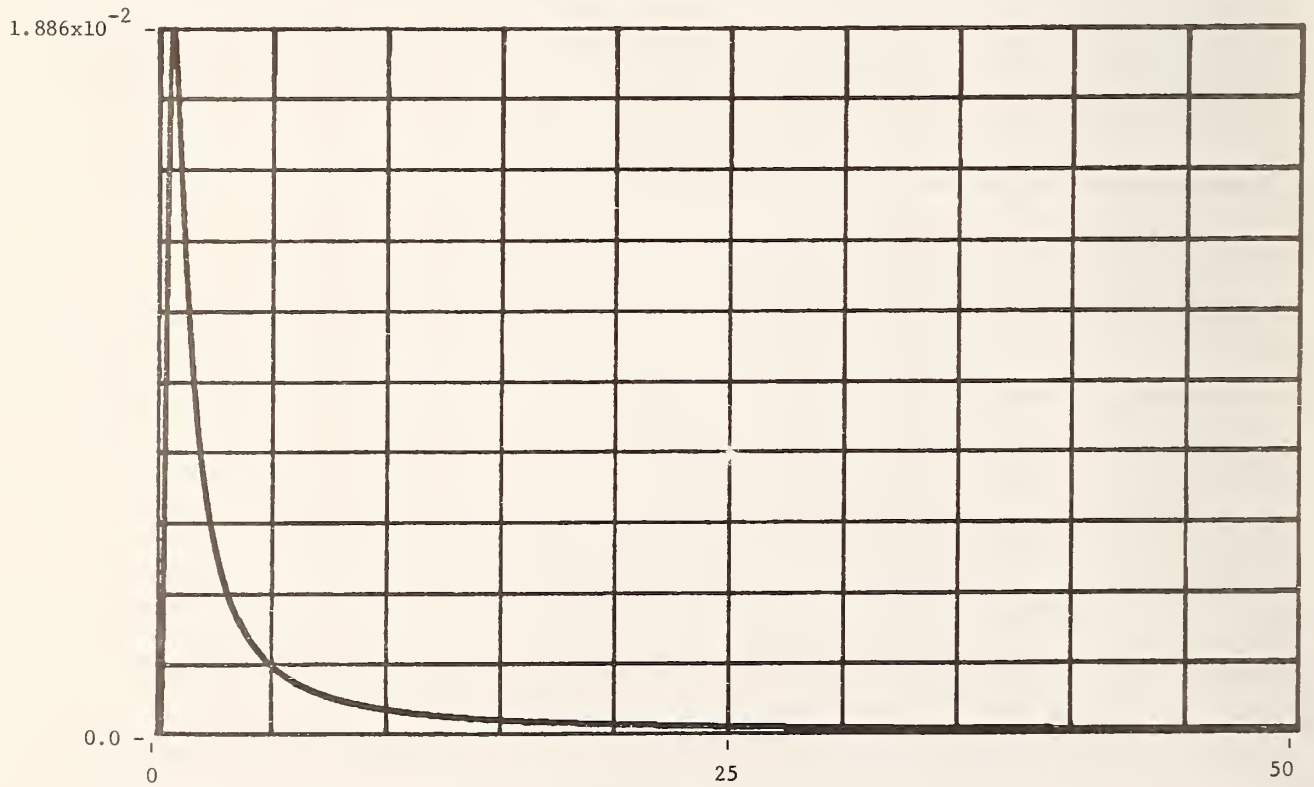


Figure A-115. Modeled and computed time domain impulse response for 60.96 meters (200 ft) of I. ordinate units are seconds⁻¹, abscissa units are nanoseconds and time spacing between points is 0.9766 ns.

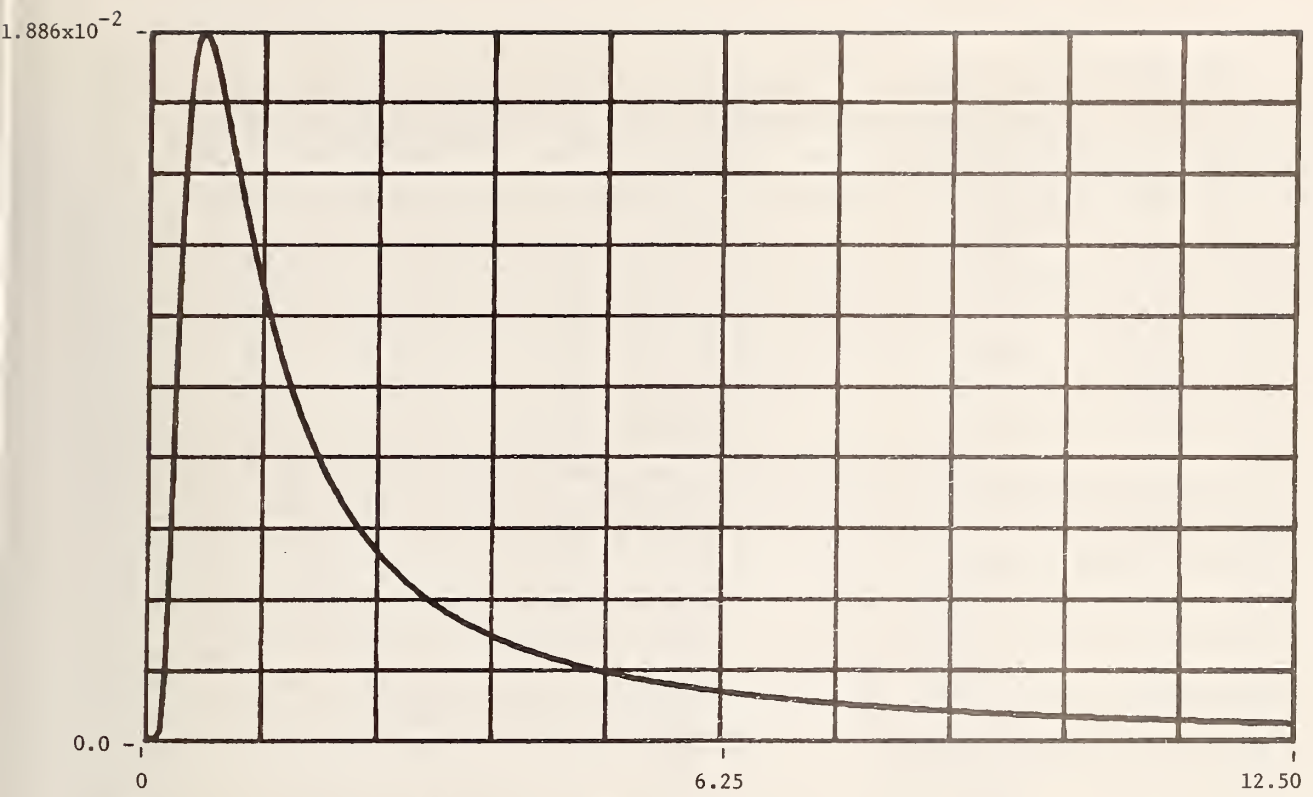


Figure A-116. Time-expanded modeled and computed time domain impulse response for 60.96 meters (200 ft) of I. Ordinate units are seconds⁻¹, abscissa units are nanoseconds and time spacing between points is 0.9766 ns.

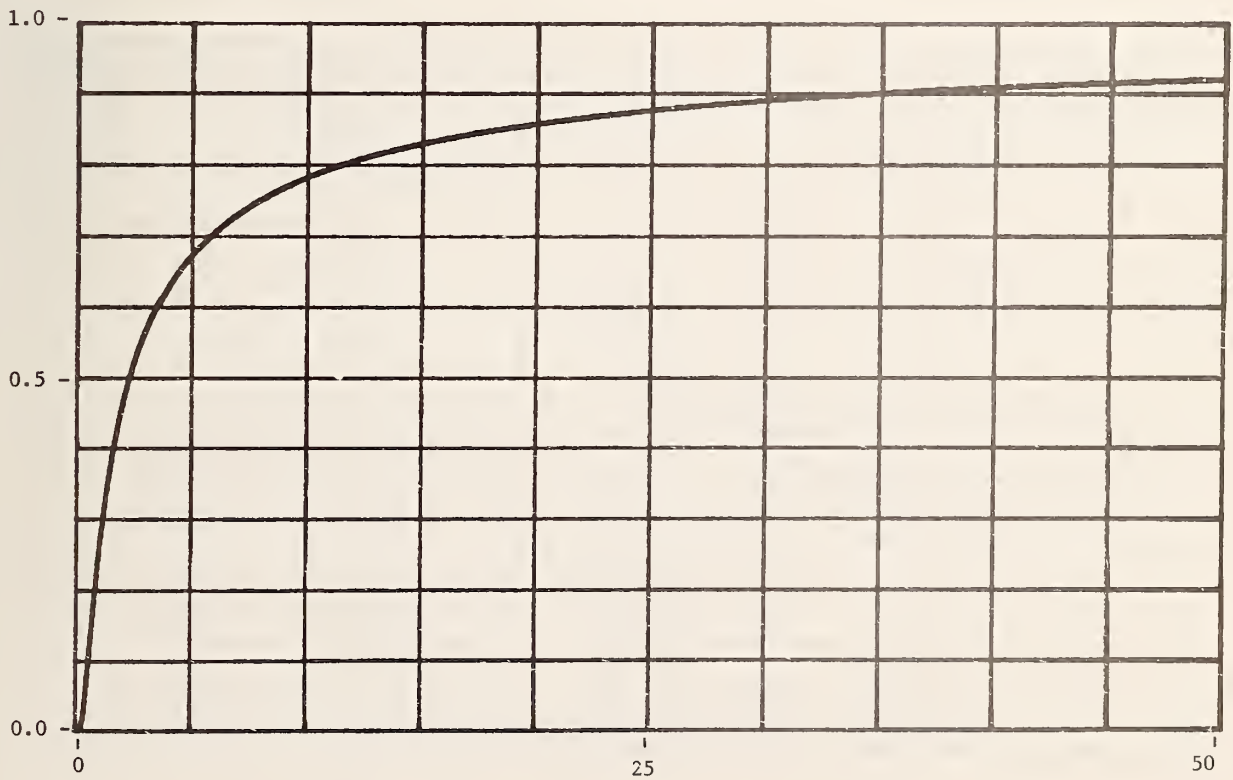


Figure A-117. Modeled and computed time domain unit step response for 60.96 meters (200 ft) of I. Ordinate units are volts and abscissa units are nanoseconds.

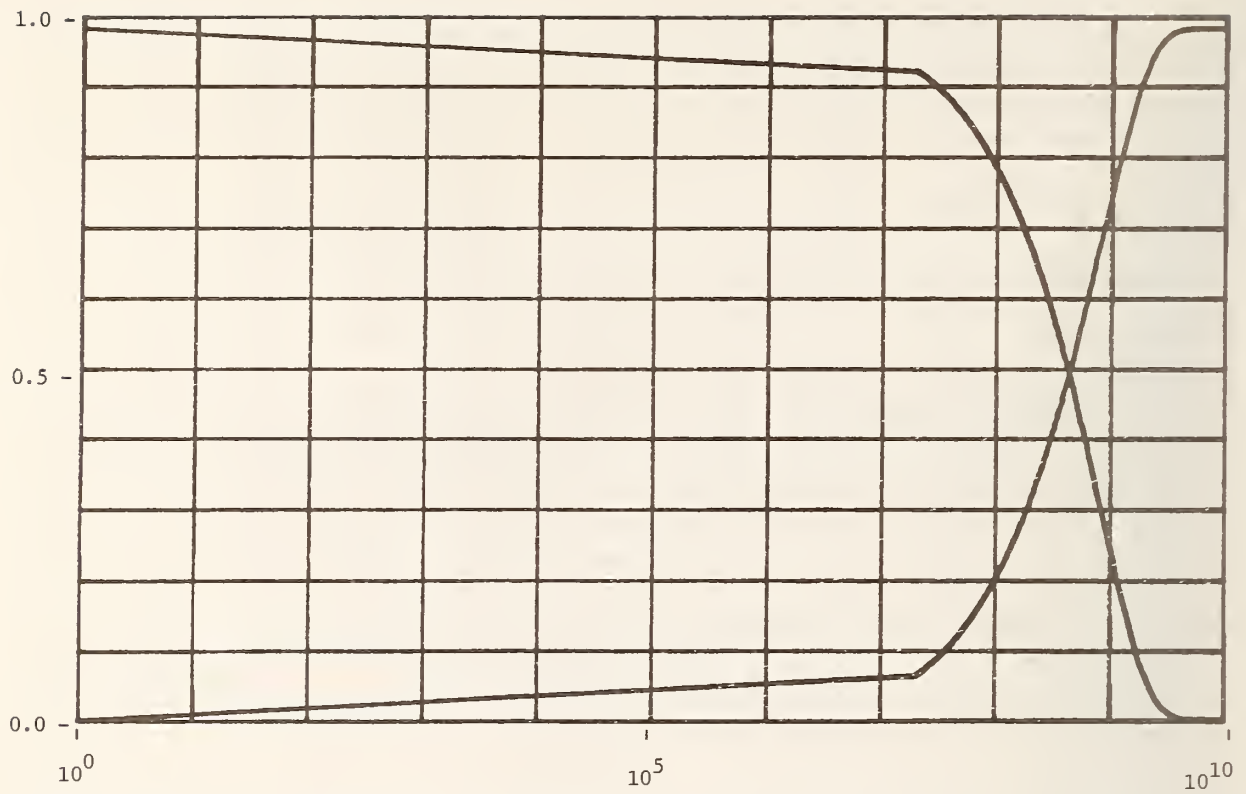


Figure A-118. Plots of "zero"/"one" cable unit step response voltages versus \log_{10} frequency for 60.96 meters (200 ft) of cable I. Ordinate units are volts and abscissa units are hertz.

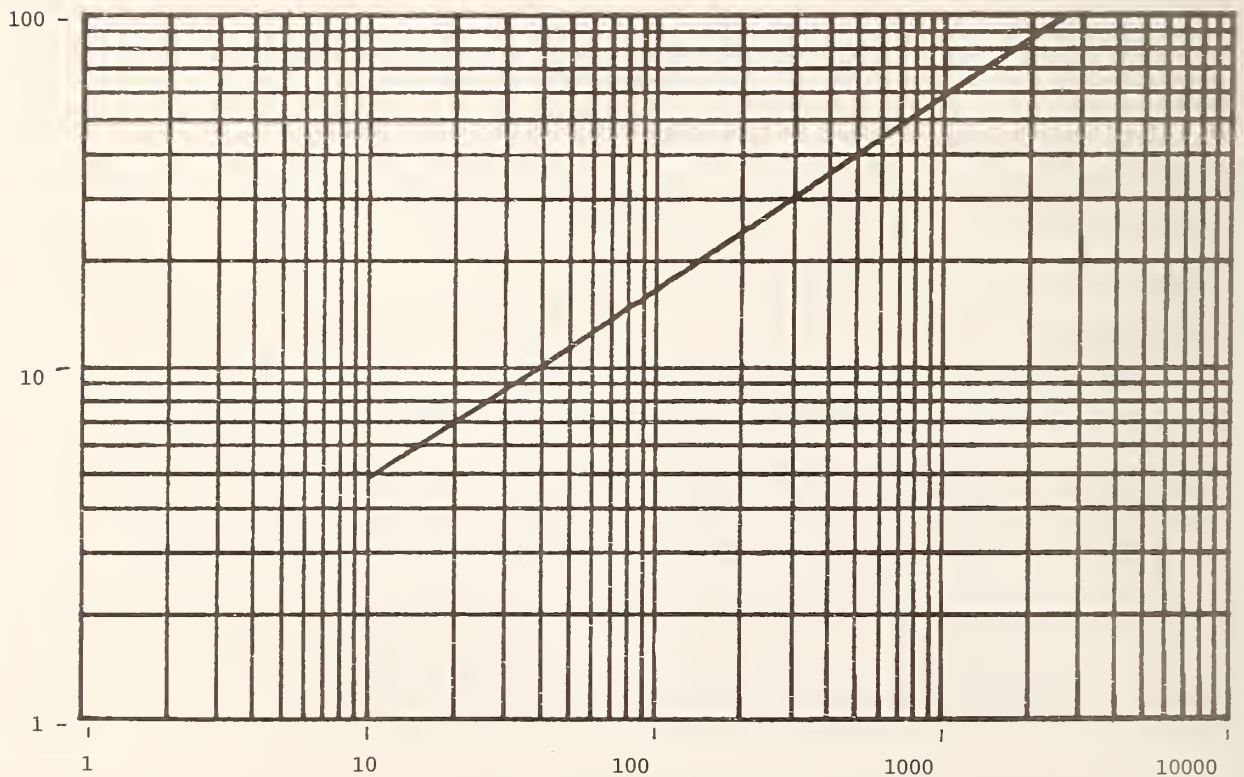


Figure A-119. Modeled attenuation plot for 152.4 meters (500 ft) of I. Ordinate units are decibels and abscissa units are megahertz.

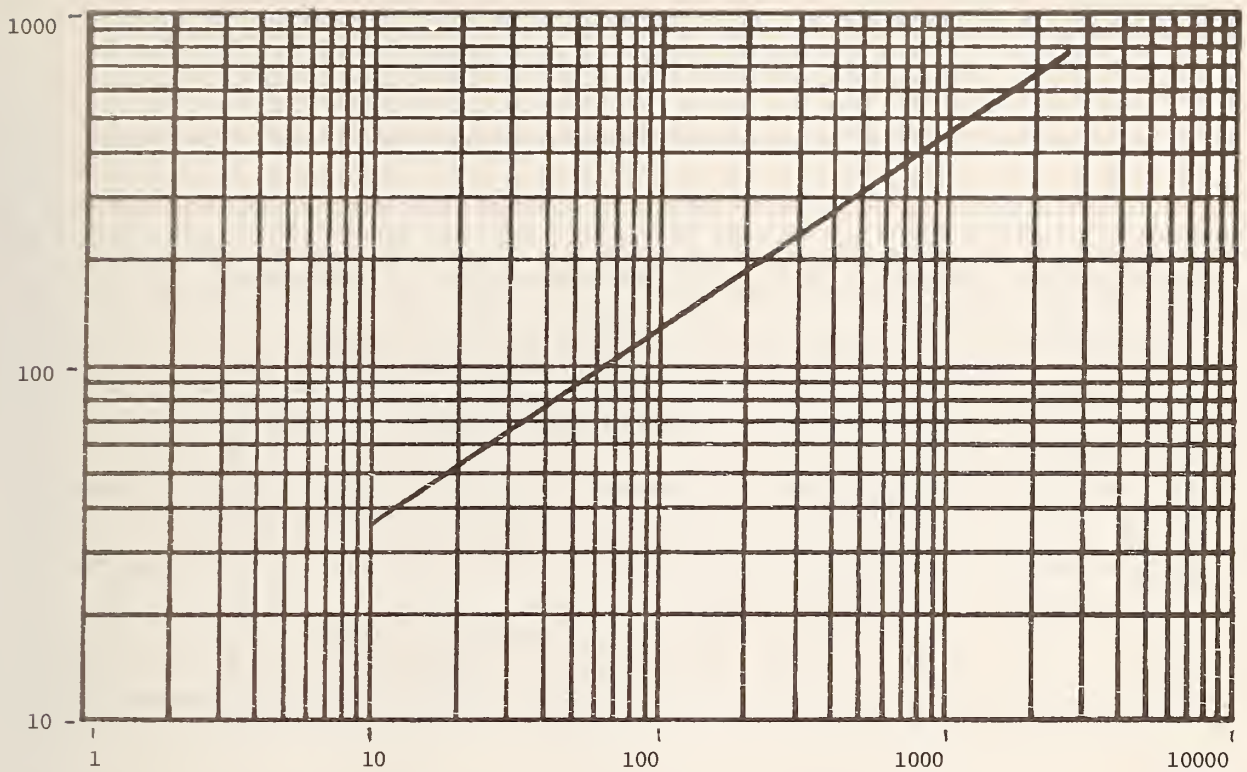


Figure A-120. Modeled minimum-phase phase shift plot for 152.4 meters (500 ft) of I. Ordinate units are degrees and abscissa units are megahertz.

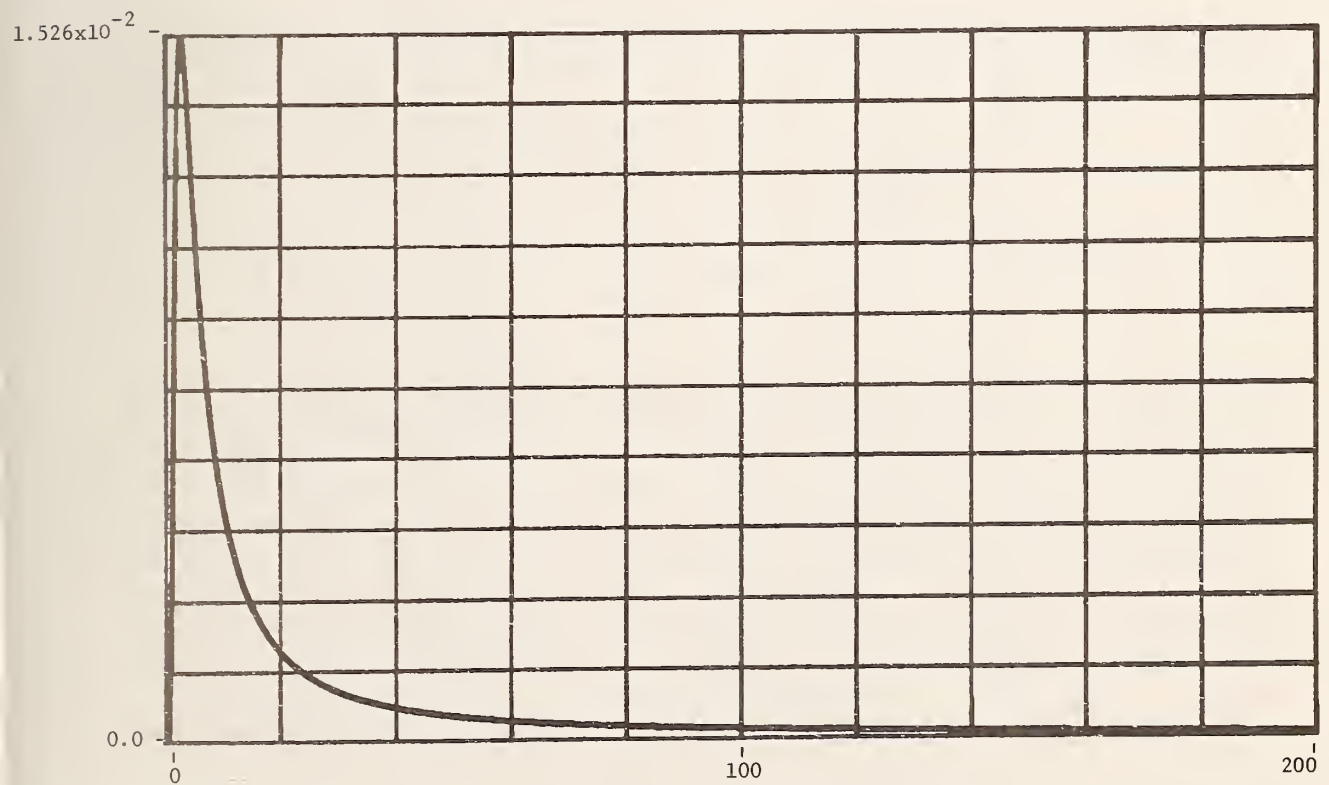


Figure A-121. Modeled and computed time domain impulse response for 152.4 meters (500 ft) of I. Ordinate units are seconds⁻¹, abscissa units are nanoseconds and time spacing between points is 0.9766 ns.

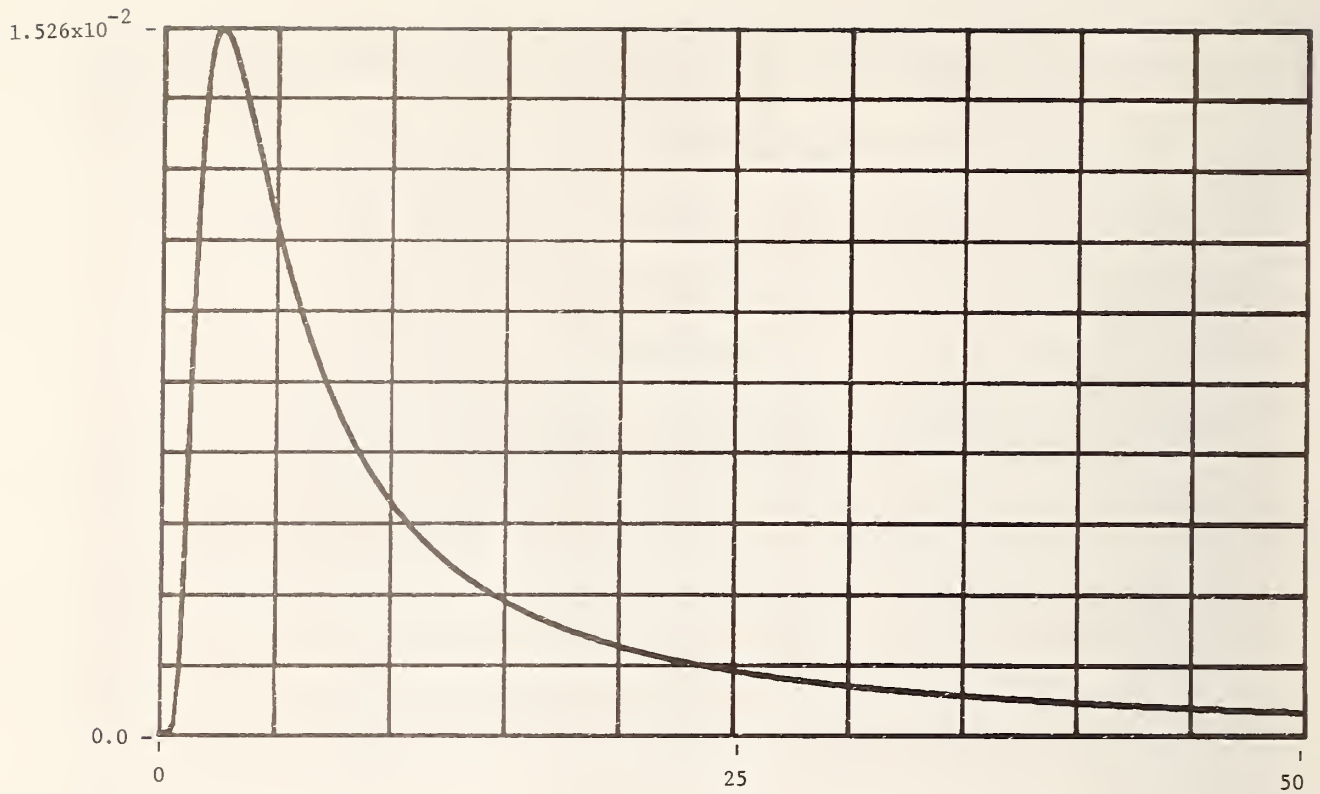


Figure A-122. Time-expanded modeled and computed time domain impulse response for 152.4 meters (500 ft) of I. Ordinate units are seconds⁻¹, abscissa units are nanoseconds and time spacing between points is 0.9766 ns.

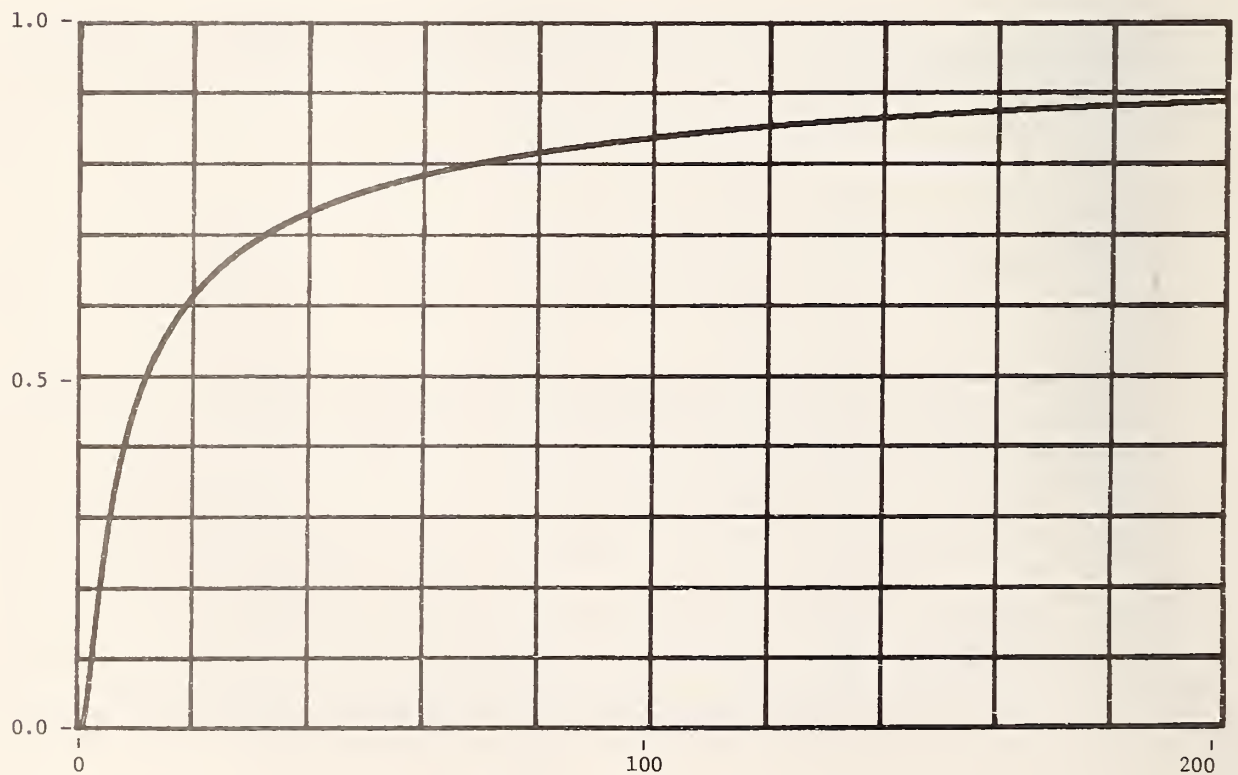


Figure A-123. Modeled and computed time domain unit step response for 152.4 meters (500 ft) of I. Ordinate units are volts and abscissa units are nanoseconds.

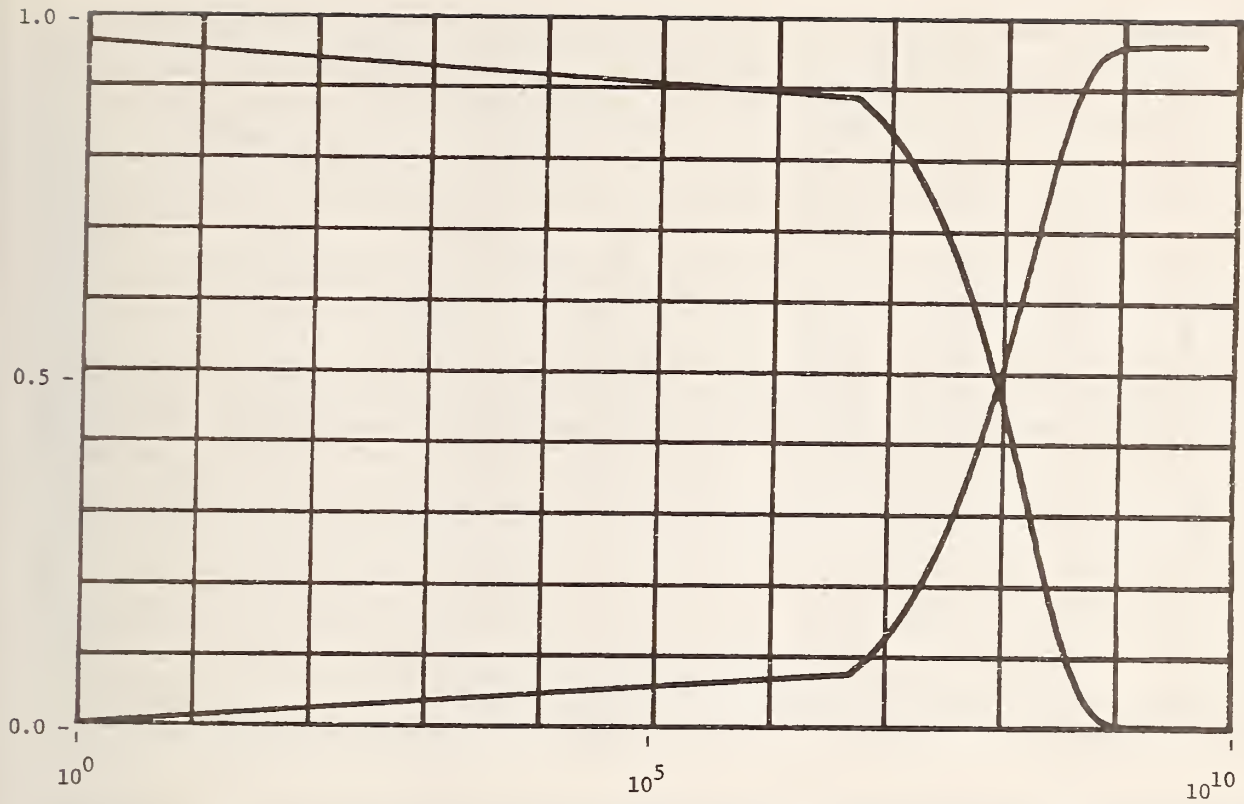


Figure A-124. Plots of "zero"/"one" cable unit step response voltages versus \log_{10} frequency for 152.4 meters (500 ft) of cable I. Ordinate units are volts and abscissa units are hertz.

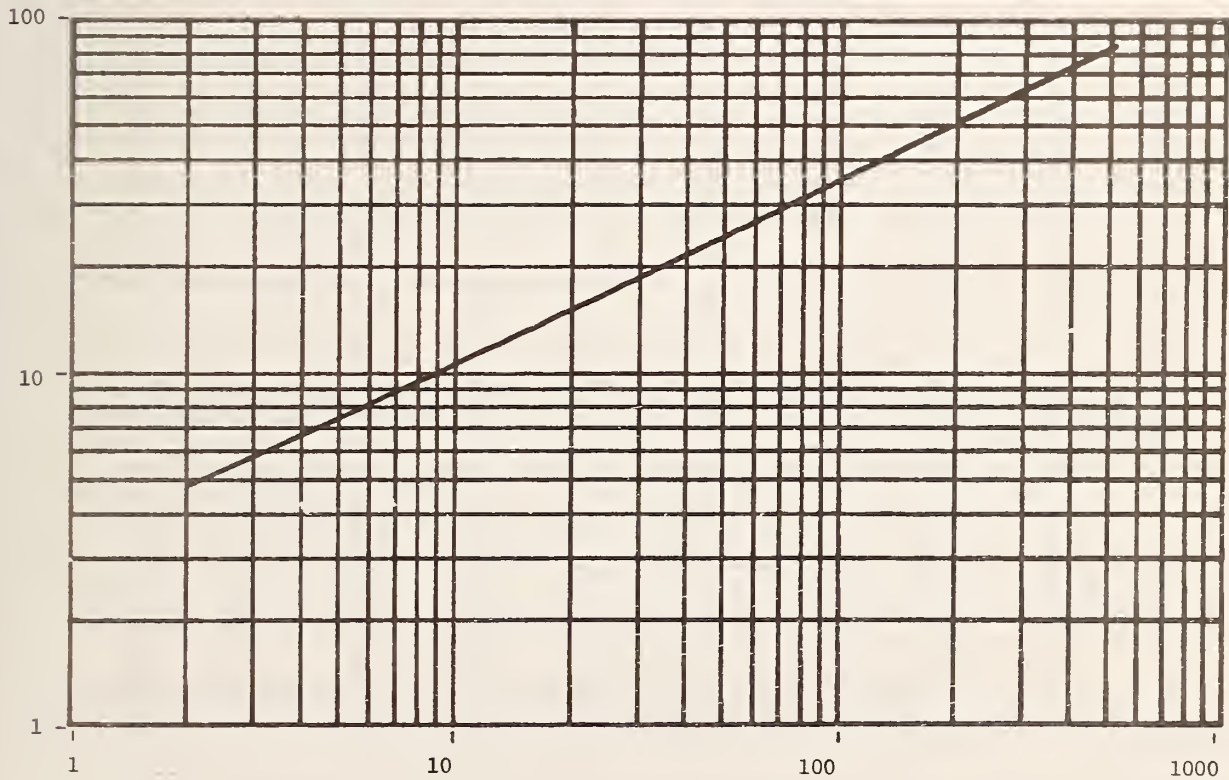


Figure A-125. Modeled attenuation plot for 320.04 meters (1050 ft) of I. Ordinate units are decibels and abscissa units are megahertz.

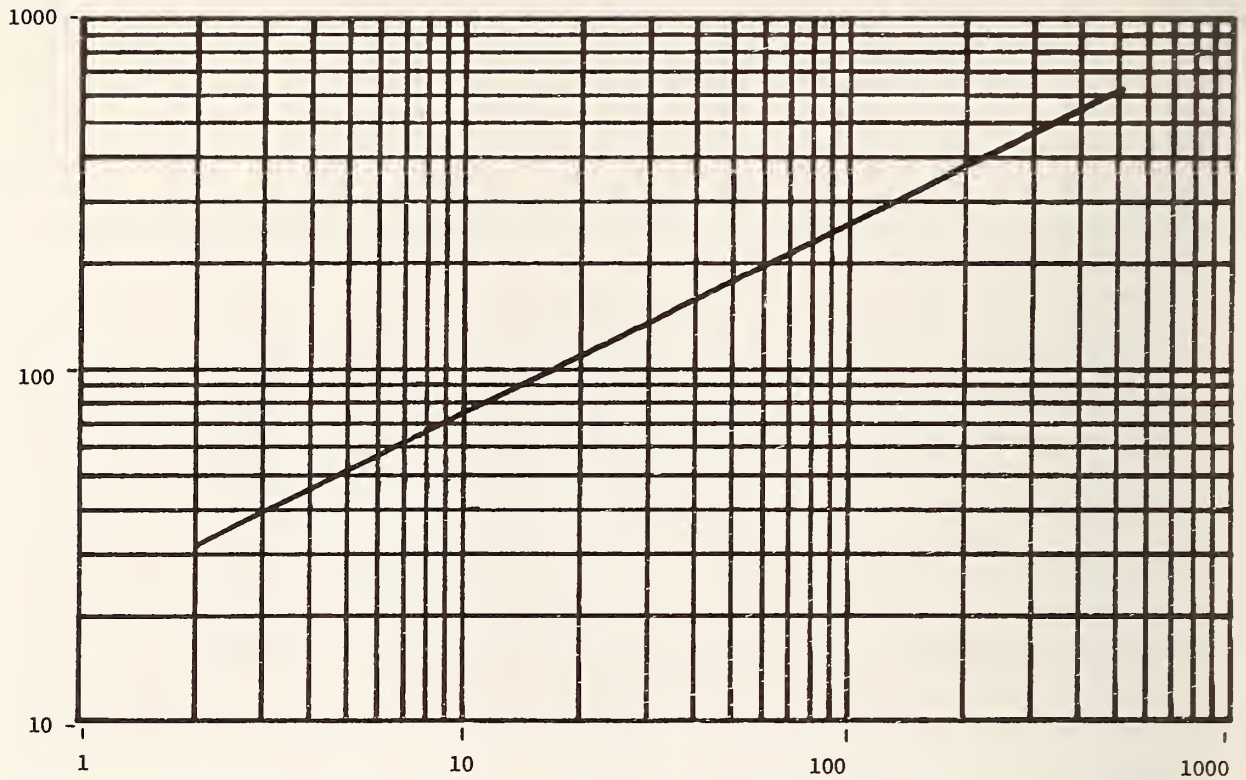


Figure A-126. Modeled minimum-phase phase shift plot for 320.04 meters (1050 ft) of I. Ordinate units are degrees and abscissa units are megahertz.

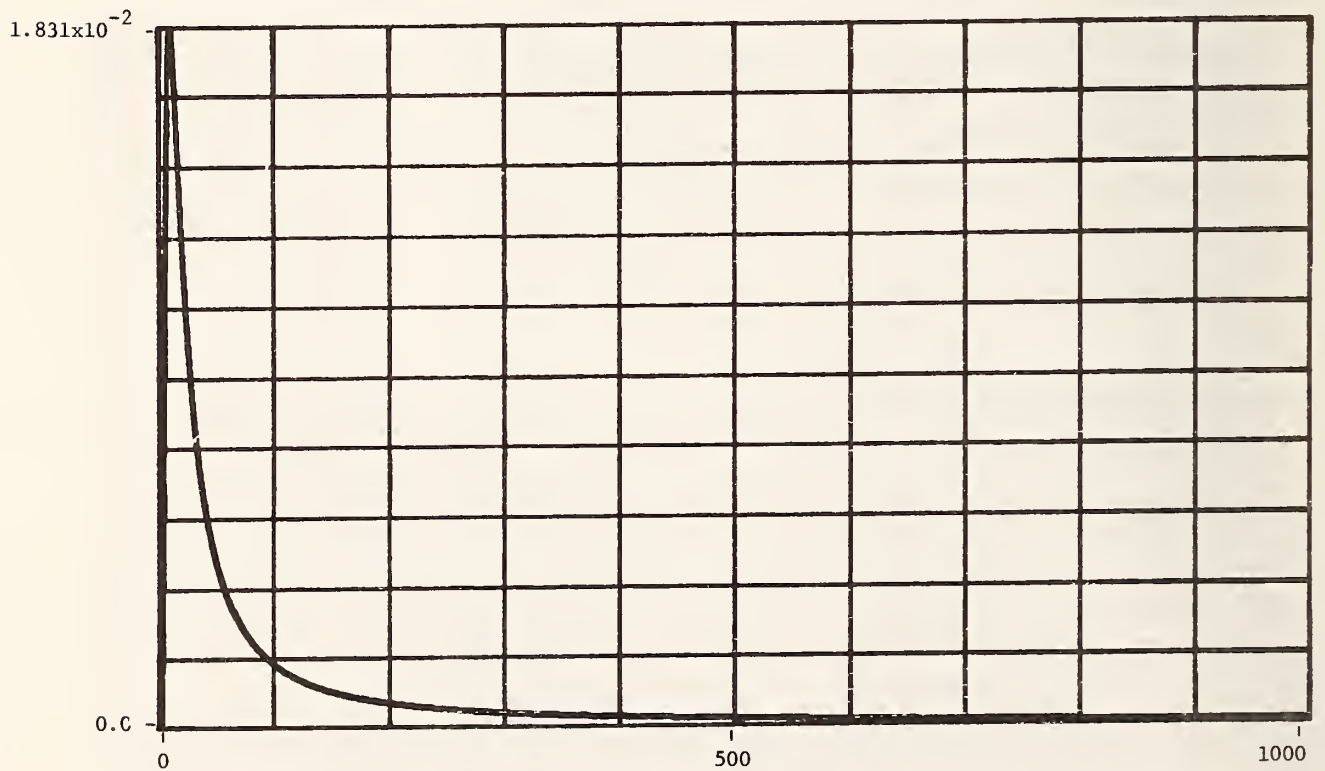


Figure A-127. Modeled and computed time domain impulse response for 320.04 meters (1050 ft) of I. Ordinate units are seconds⁻¹, abscissa units are nanoseconds and time spacing between points is 0.9766 ns.

1.831×10^{-2}

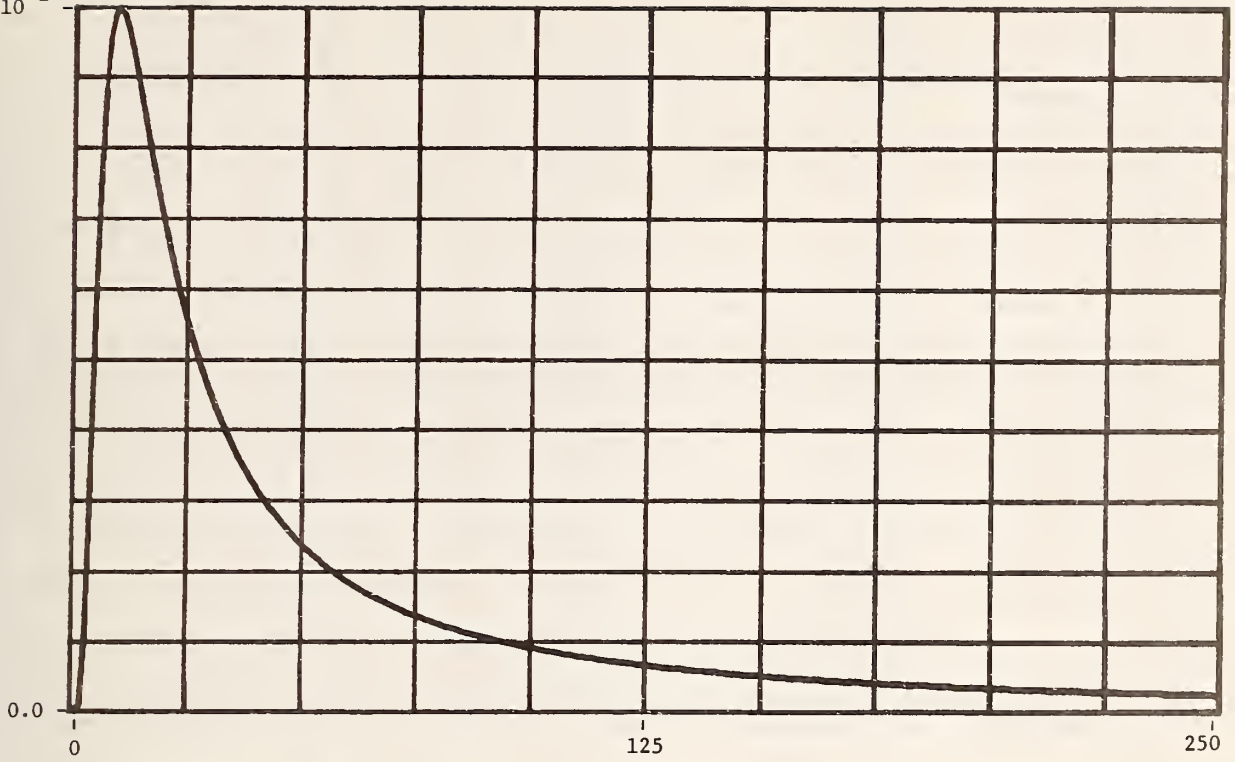


Figure A-128. Time-expanded modeled and computed time domain impulse response for 320.04 meters (1050 ft) of I. Ordinate units are seconds⁻¹, abscissa units are nanoseconds and time spacing between points is 0.9766 ns.

1.0 -

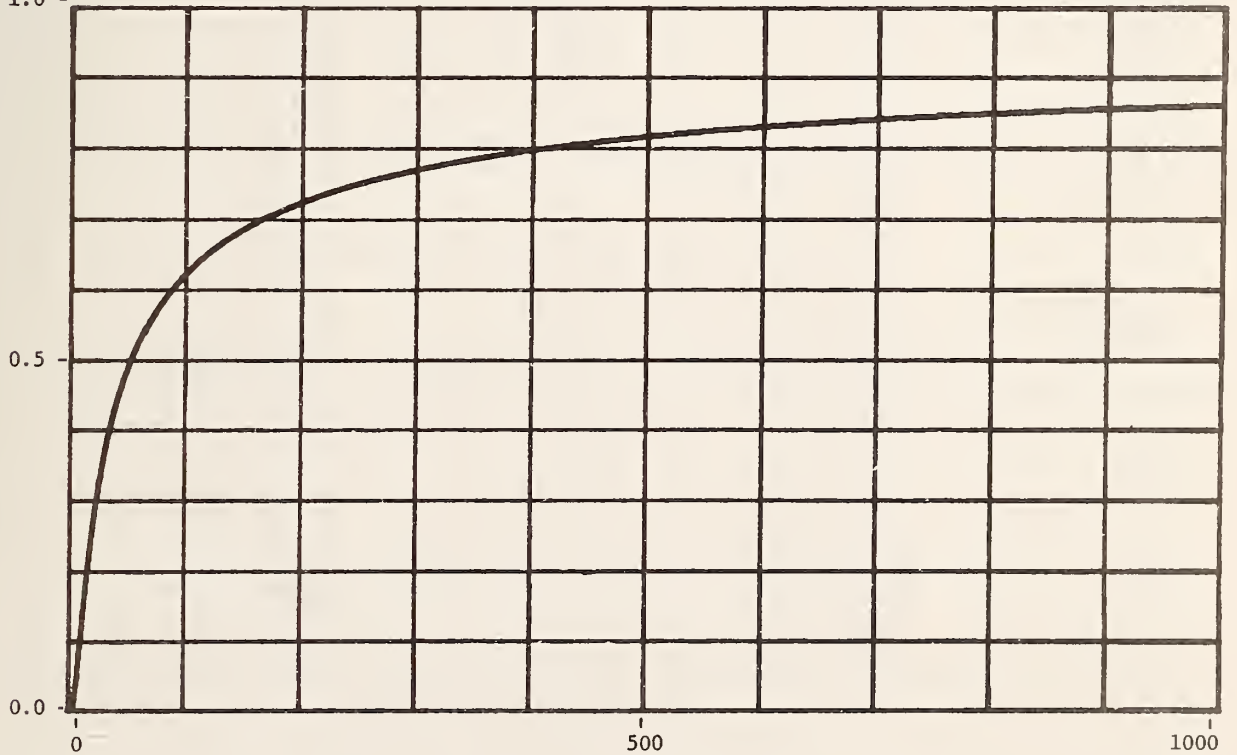


Figure A-129. Modeled and computed time domain unit step response for 320.04 meters (1050 ft) of I. Ordinate units are volts and abscissa units are nanoseconds.

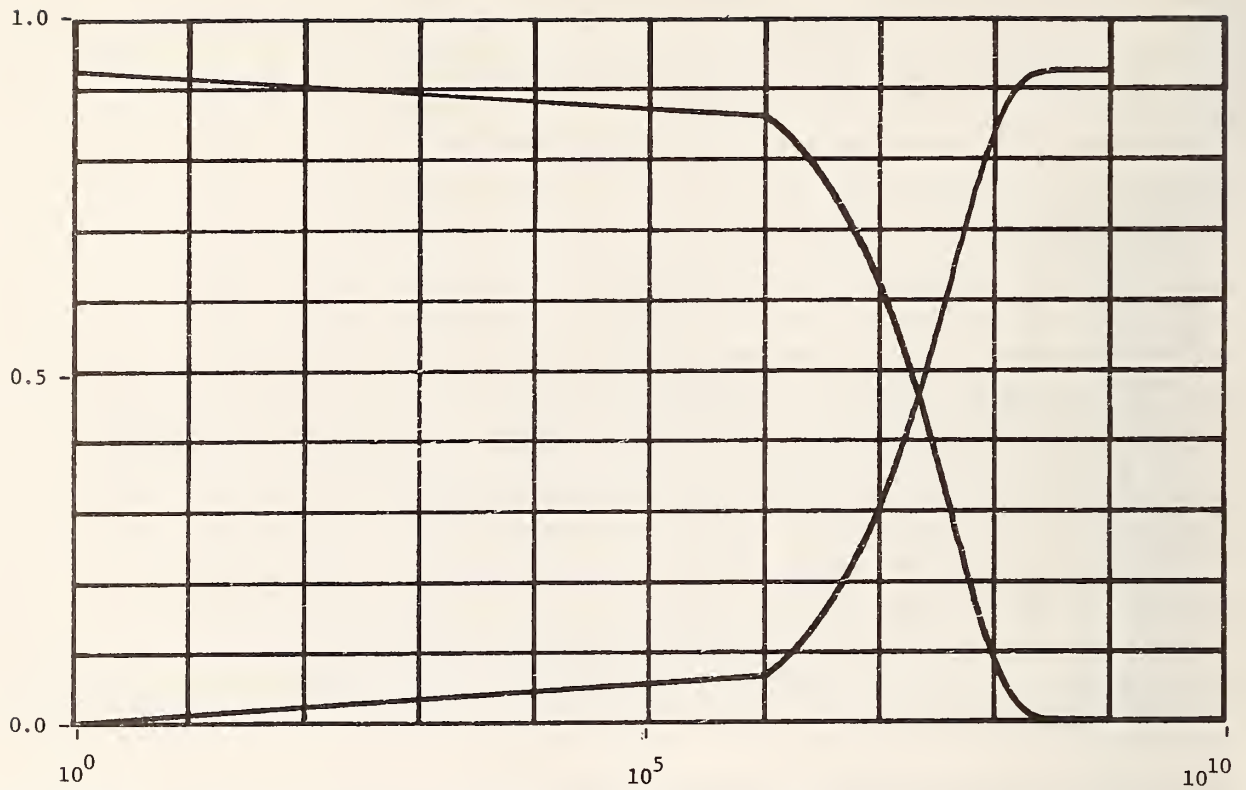


Figure A-130. Plots of "zero"/"one" cable unit step response voltages versus \log_{10} frequency for 320.04 meters (1050 ft) of cable I. Ordinate units are volts and abscissa units are hertz.

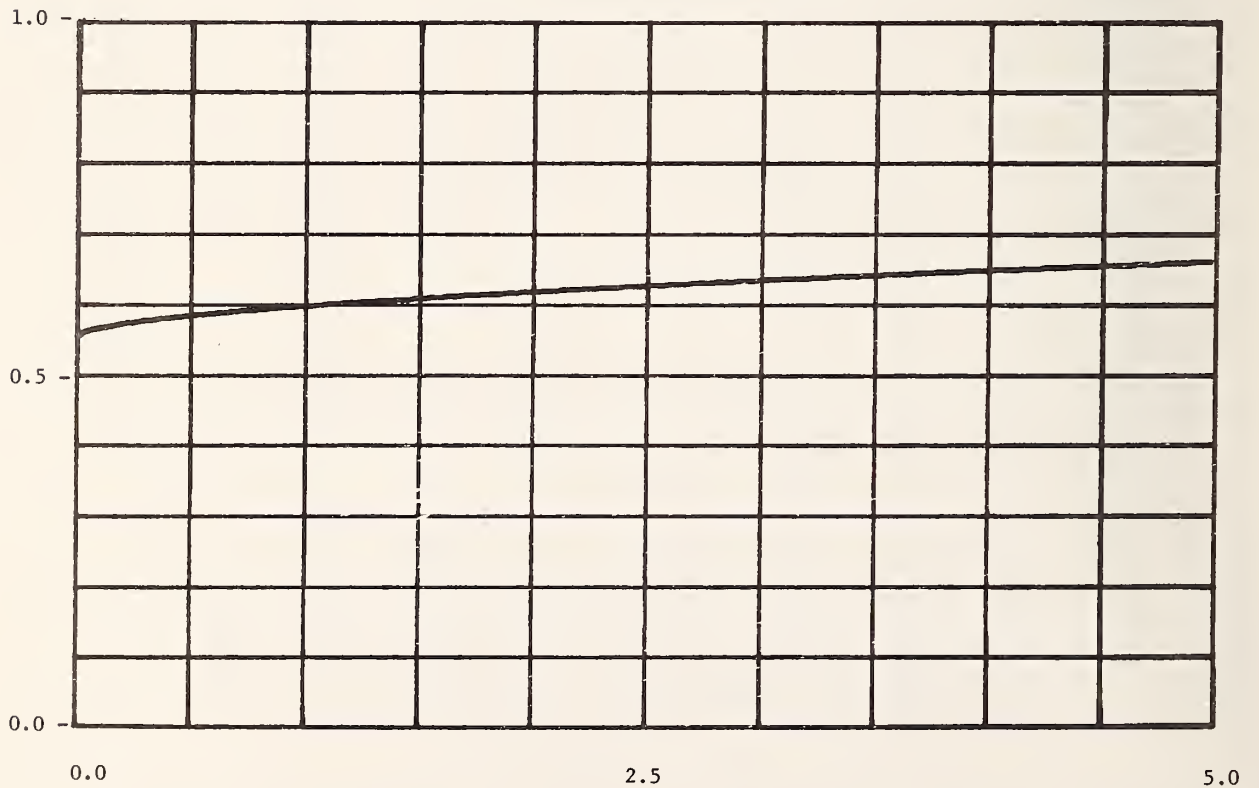


Figure A-131. TDR unit step response for cable I. Source step generator has assumed 50Ω resistive output impedance. Ordinate units are volts and abscissa units are microseconds.

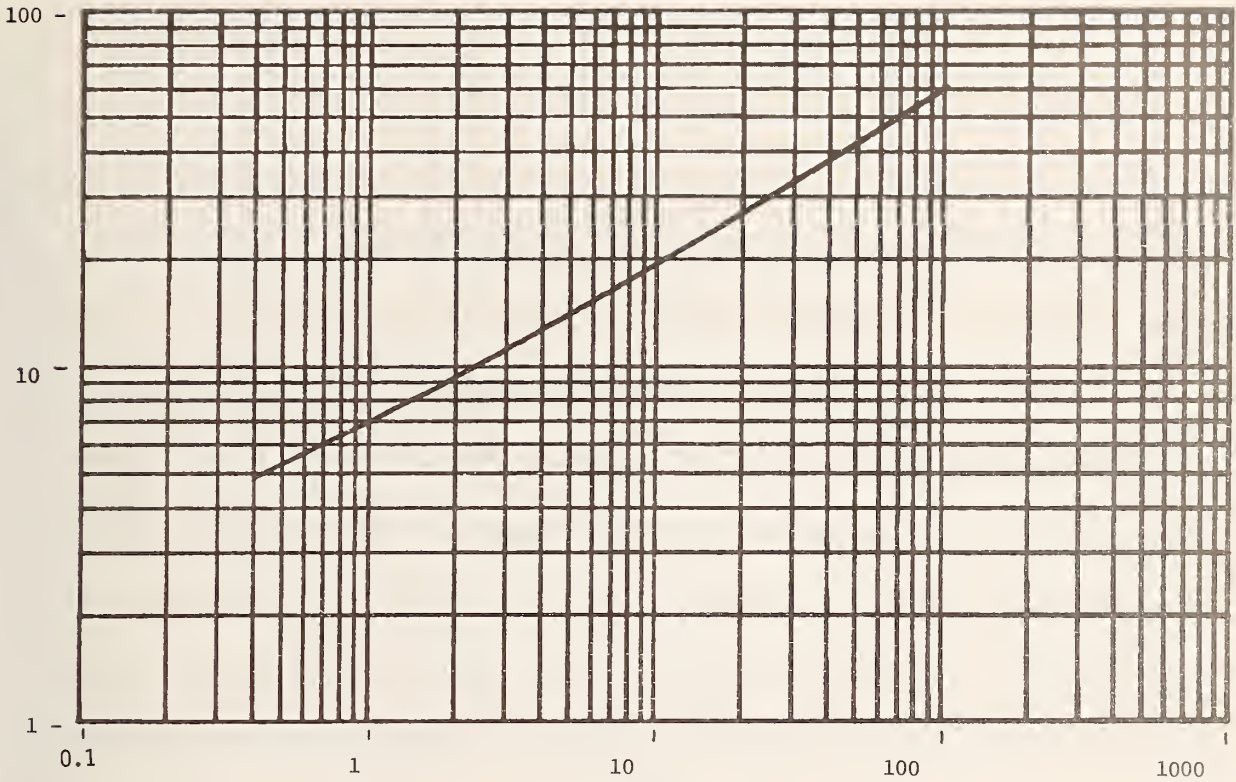


Figure A-132. Modeled attenuation plot for 304.8 meters (1000 ft) of J. Ordinate units are decibels and abscissa units are megahertz.

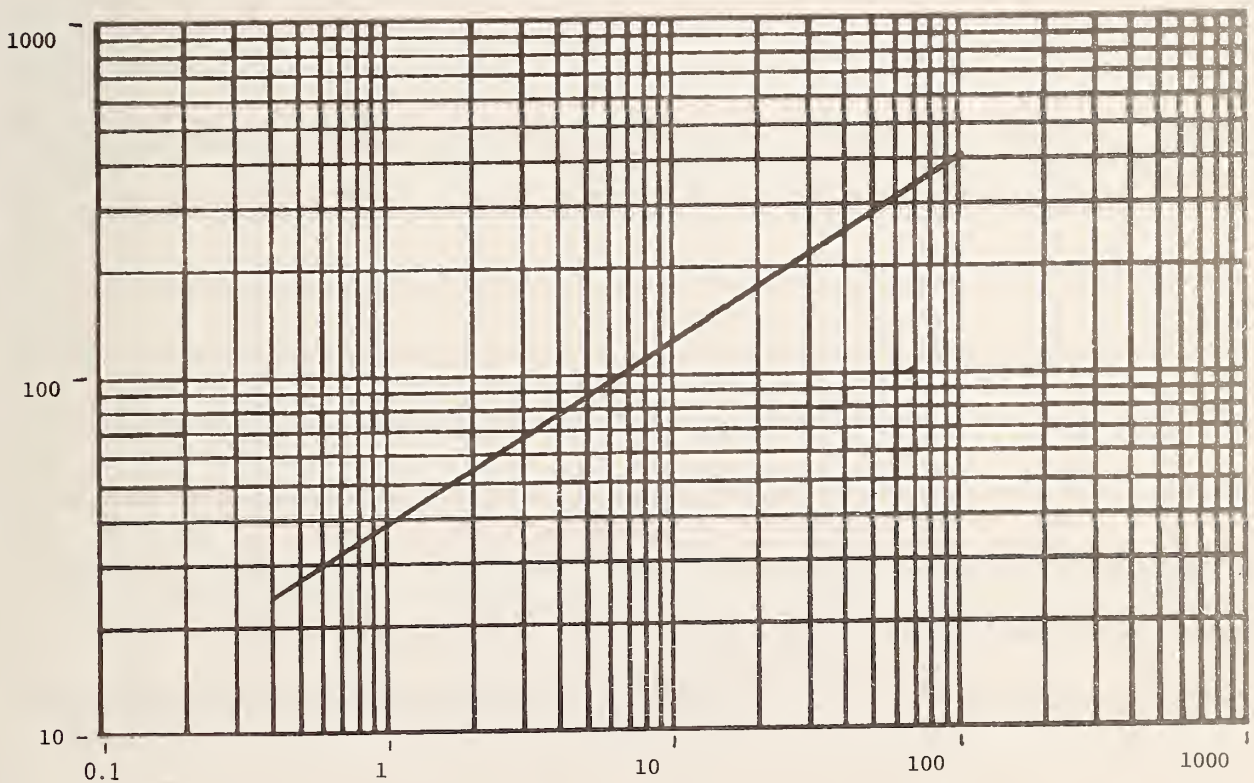


Figure A-133. Modeled minimum-phase phase shift plot for 304.8 meters (1000 ft) of J. Ordinate units are degrees and abscissa units are megahertz.

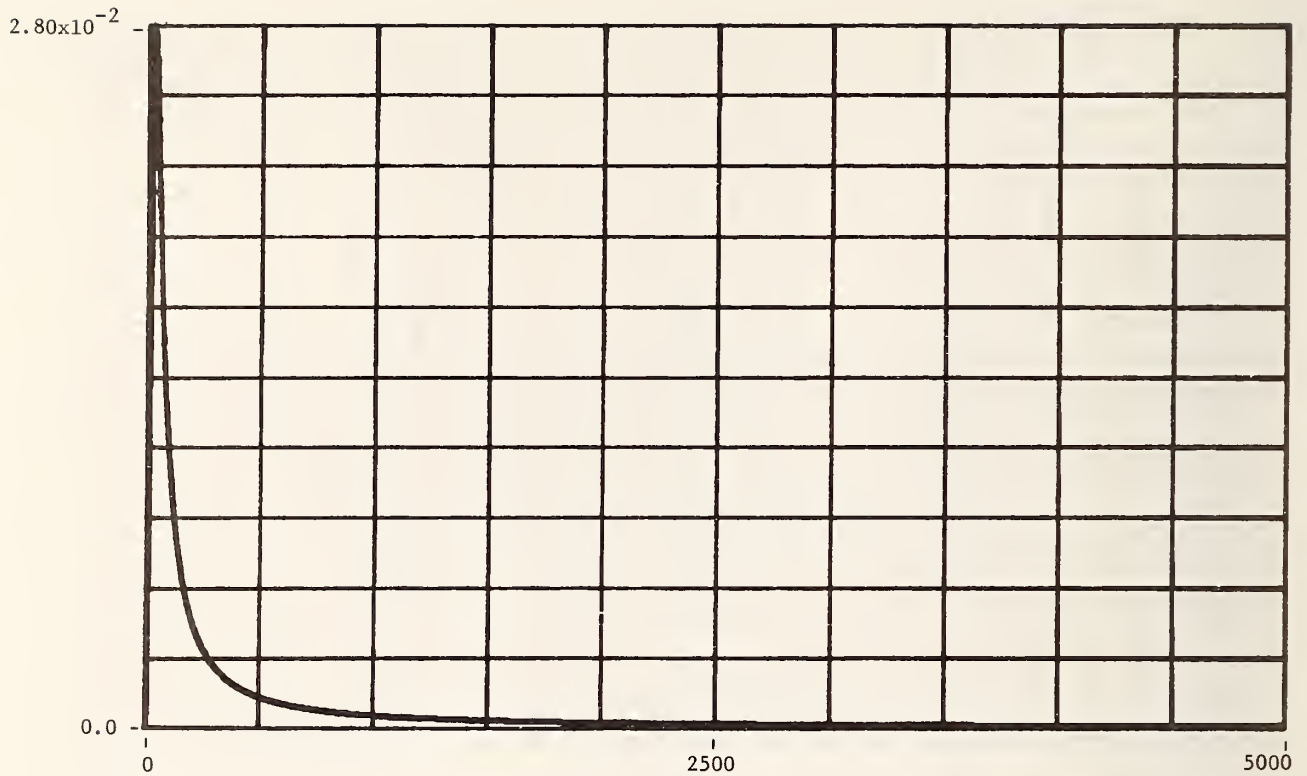


Figure A-134. Modeled and computed time domain impulse response for 304.8 meters (1000 ft) of J. Ordinate units are seconds^{-1} , abscissa units are nanoseconds and time spacing between points is 0.9766 ns.

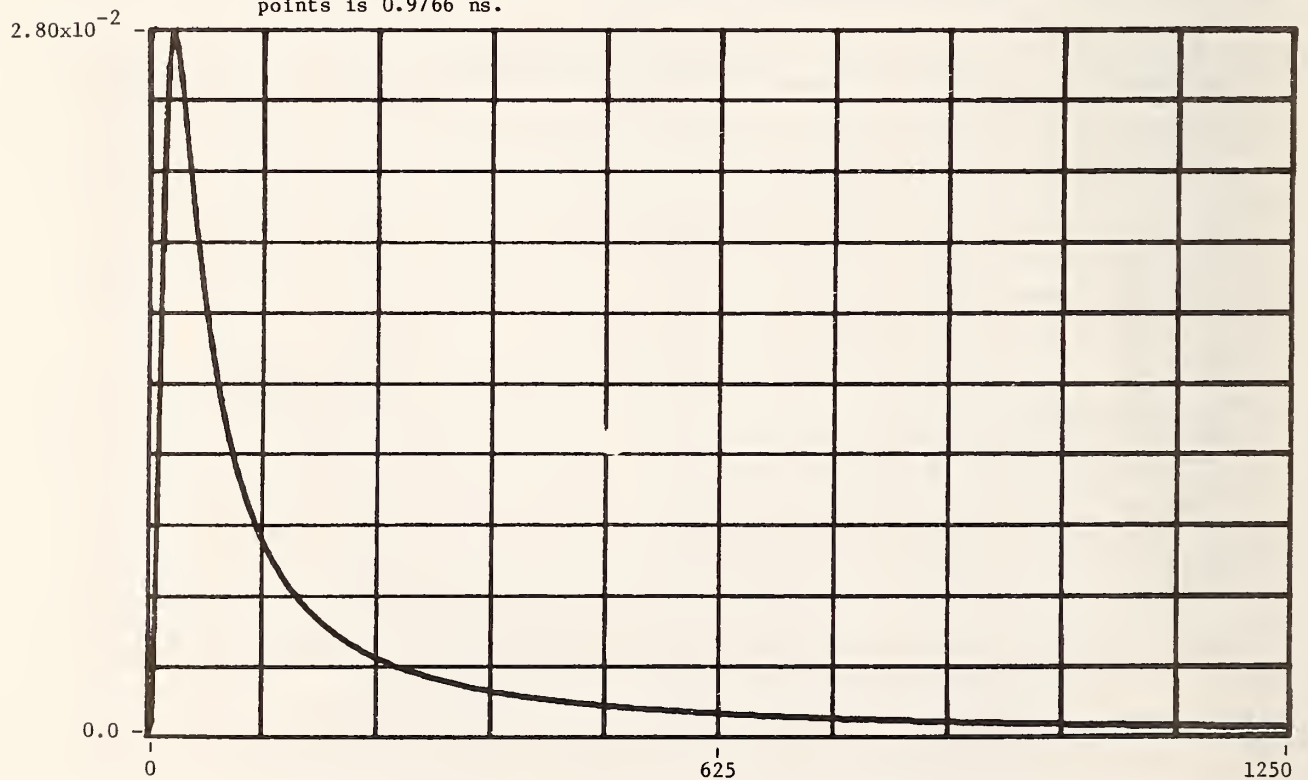


Figure A-135. Time-expanded modeled and computed time domain impulse response for 304.8 meters (1000 ft) of J. Ordinate units are seconds^{-1} , abscissa units are nanoseconds and time spacing between points is 0.9766 ns.

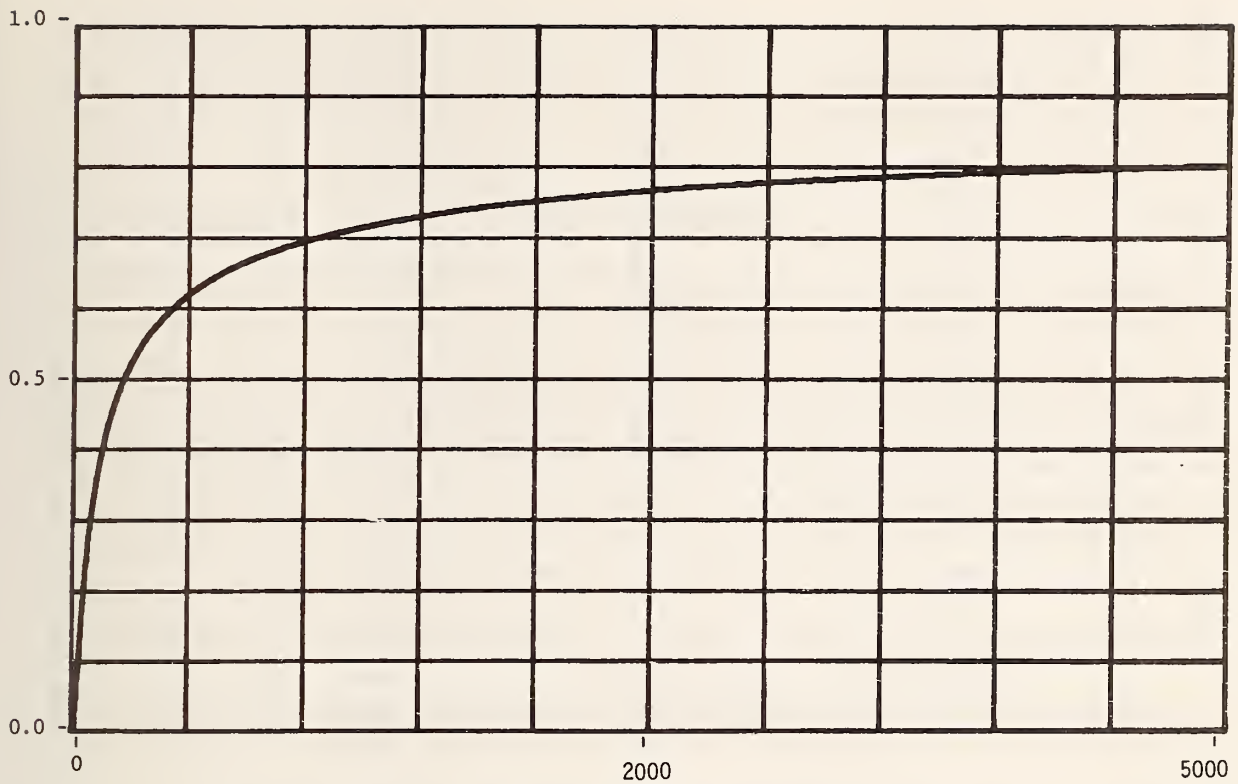


Figure A-136. Modeled and computed time domain unit step response for 304.8 meters (1000 ft) of J. Ordinate units are volts and abscissa units are nanoseconds.

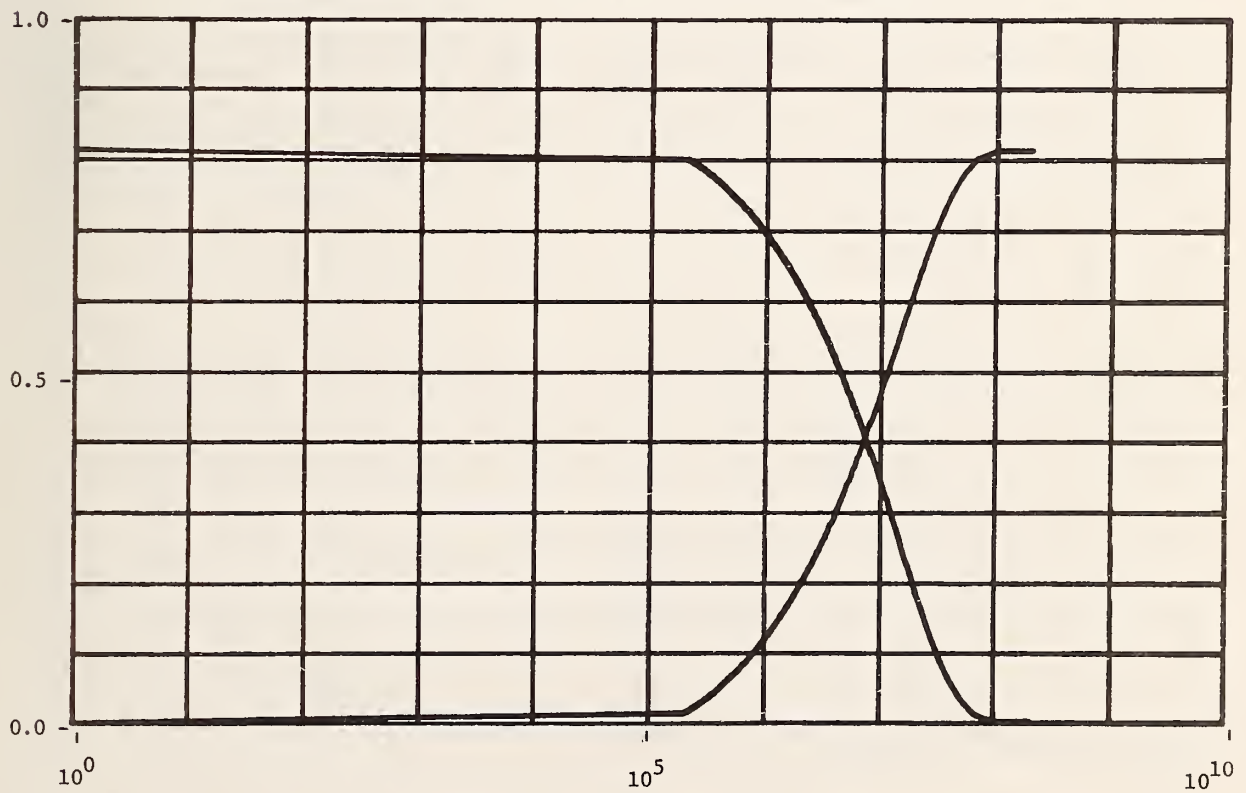


Figure A-137. Plots of "zero"/"one" cable unit step response voltages versus \log_{10} frequency for 304.8 meters (1000 ft) of cable J. Ordinate units are volts and abscissa units are hertz.

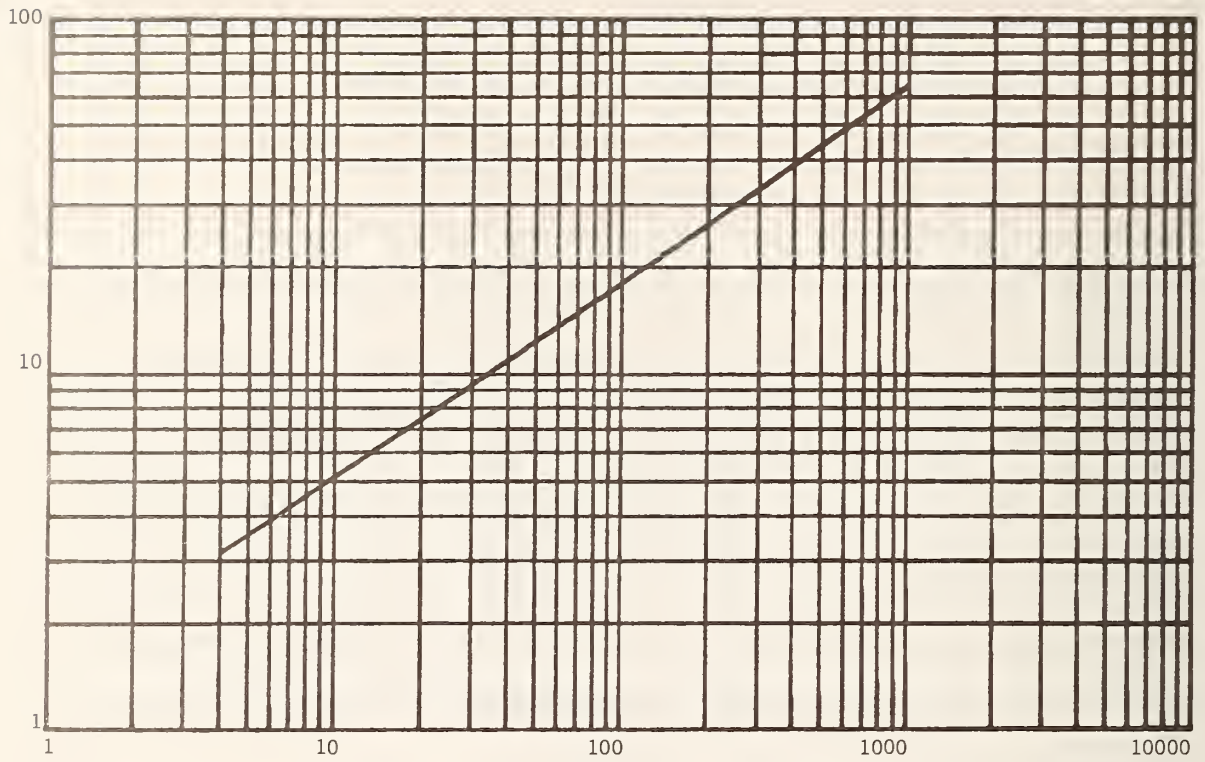


Figure A-138. Modeled attenuation plot for 304.8 meters (1000 ft) of K. Ordinate units are decibels and abscissa units are megahertz.

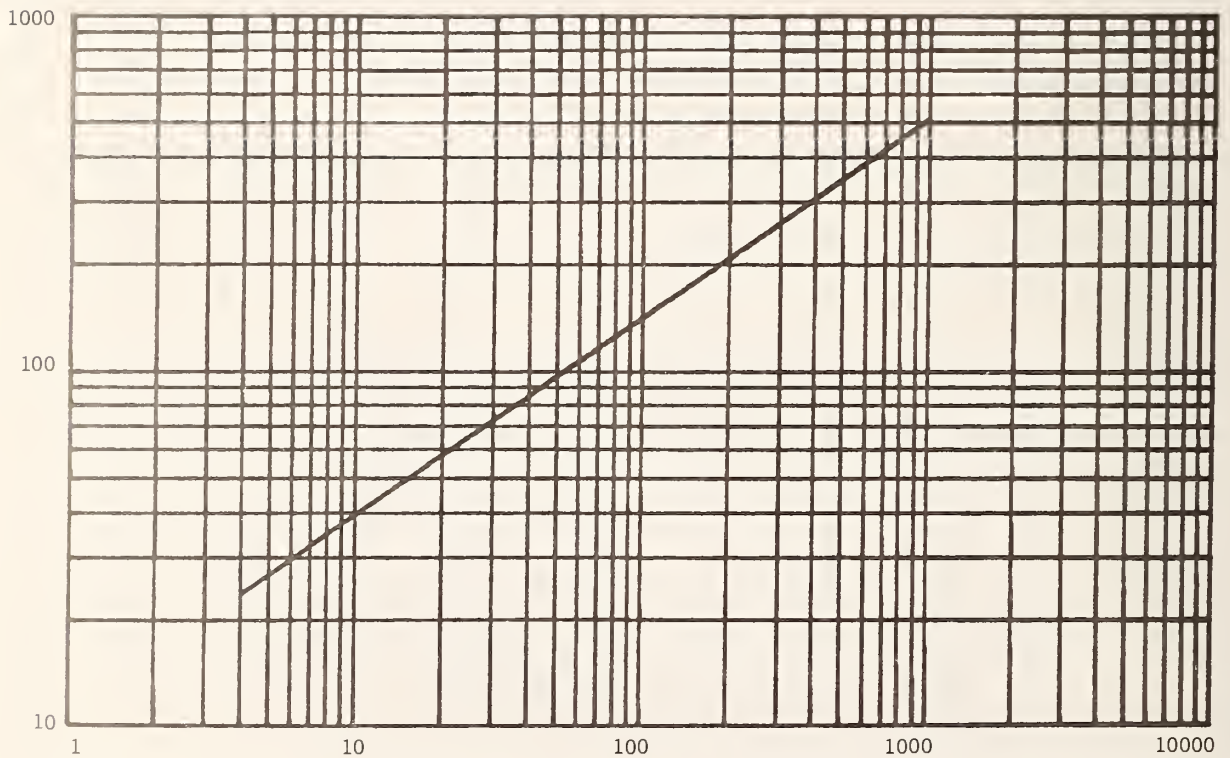


Figure A-139. Modeled minimum-phase phase shift plot for 304.8 meters (1000 ft) of K. Ordinate units are degrees and abscissa units are megahertz.

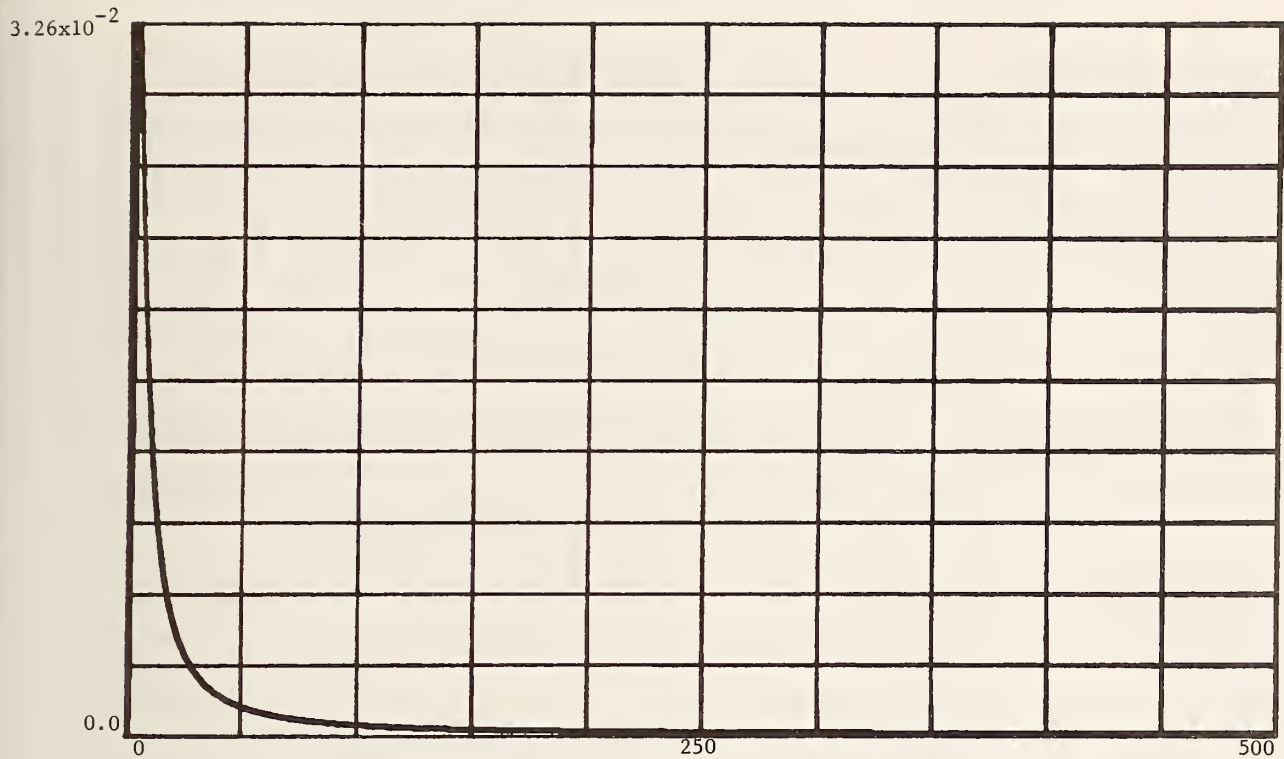


Figure A-140. Modeled and computed time domain impulse response for 304.8 meters (1000 ft) of K. Ordinate units are seconds⁻¹, abscissa units are nanoseconds and time spacing between points is 0.4883 ns.

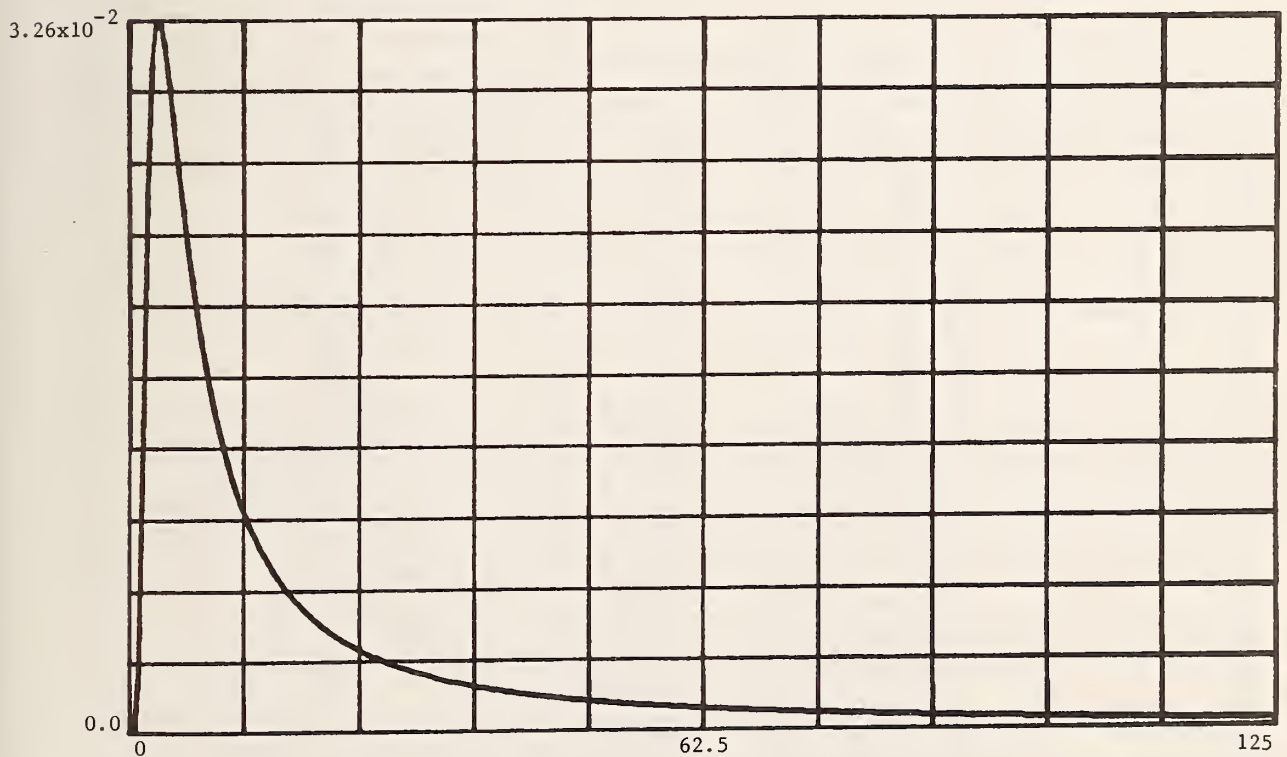


Figure A-141. Time-expanded modeled and computed time domain impulse response for 304.8 meters (1000 ft) of K. Ordinate units are seconds⁻¹, abscissa units are nanoseconds and time spacing between points is 0.9766 ns.

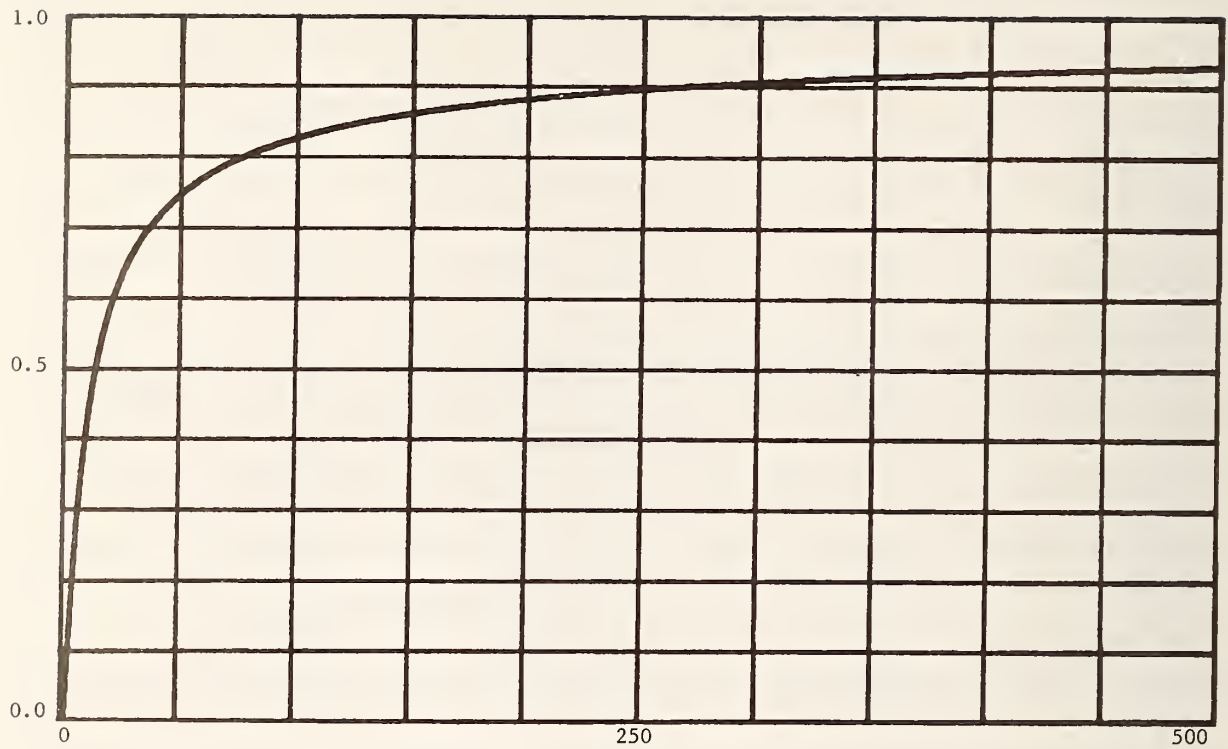


Figure A-142. Modeled and computed time domain unit step response for 304.8 meters (1000 ft) of K. Ordinate units are volts and abscissa units are nanoseconds.

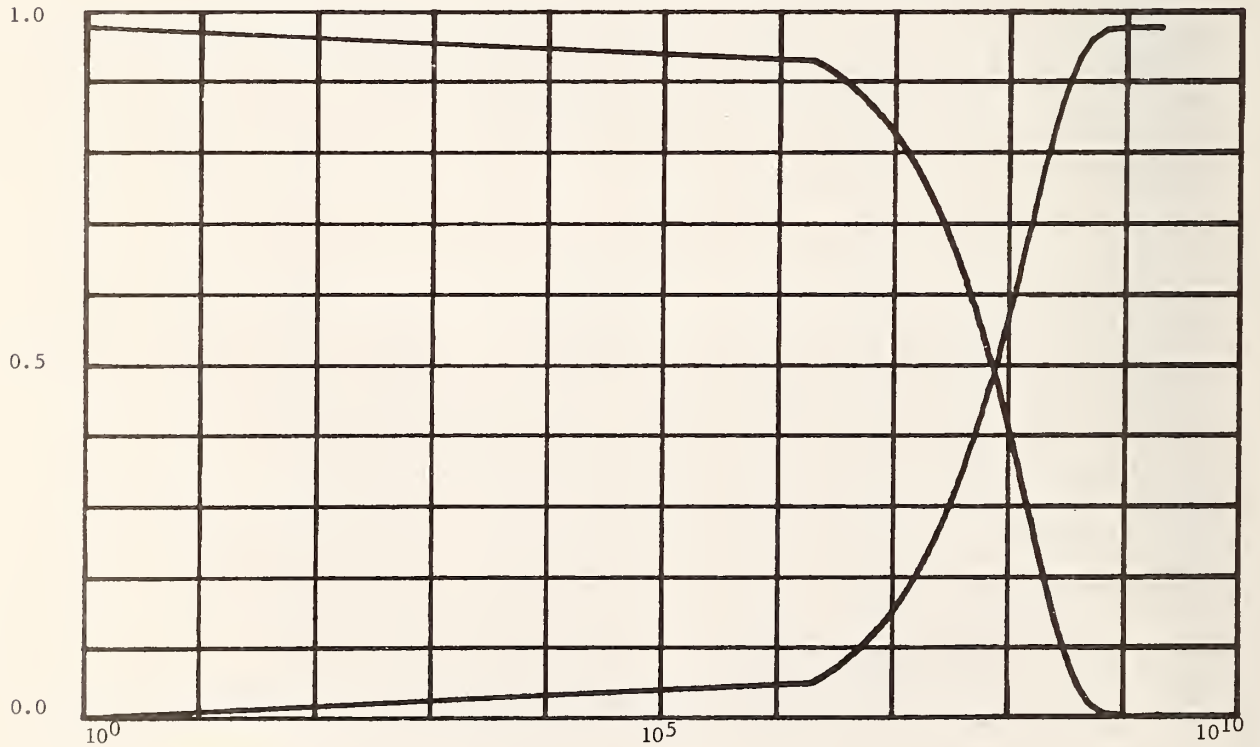


Figure A-143. Plots of "zero"/"one" cable unit step response voltages versus \log_{10} frequency for 304.8 meters (1000 ft) of cable K. Ordinate units are volts and abscissa units are hertz.

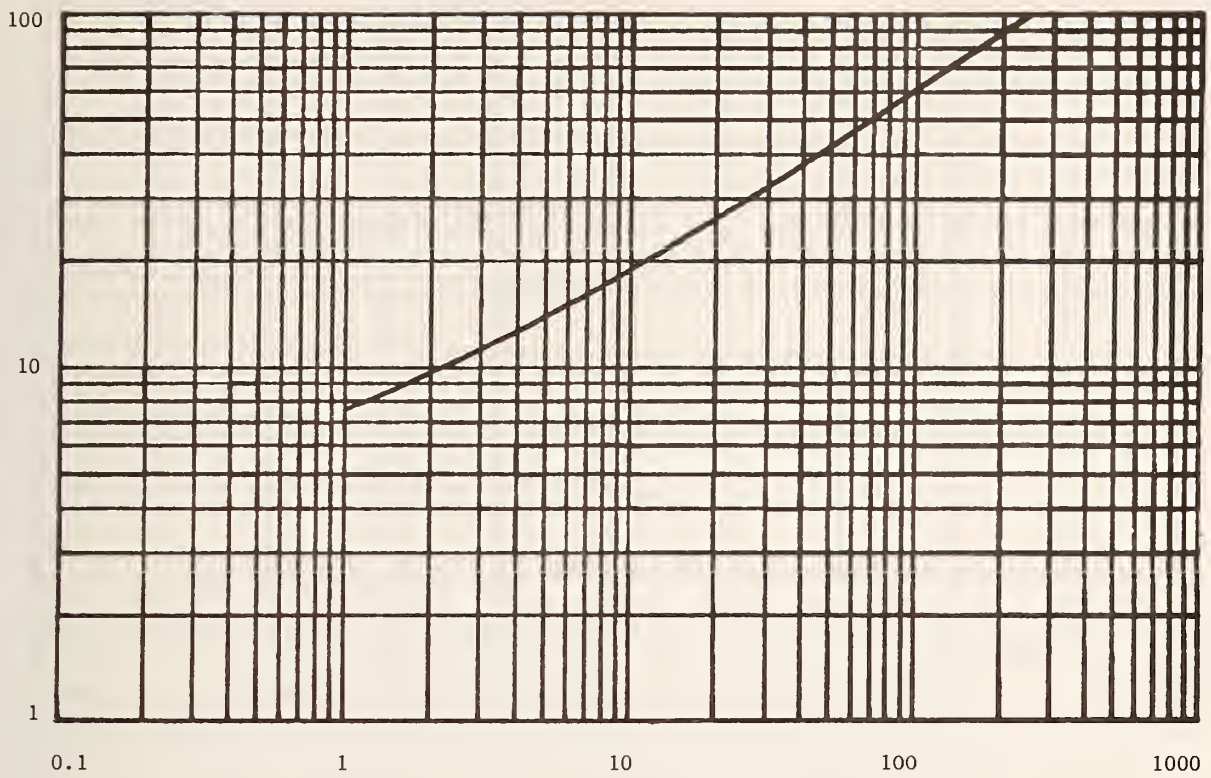


Figure A-144. Modeled attenuation plot for 402.34 meters (1320 ft) of WD-37. Ordinate units are decibels and abscissa units are megahertz.

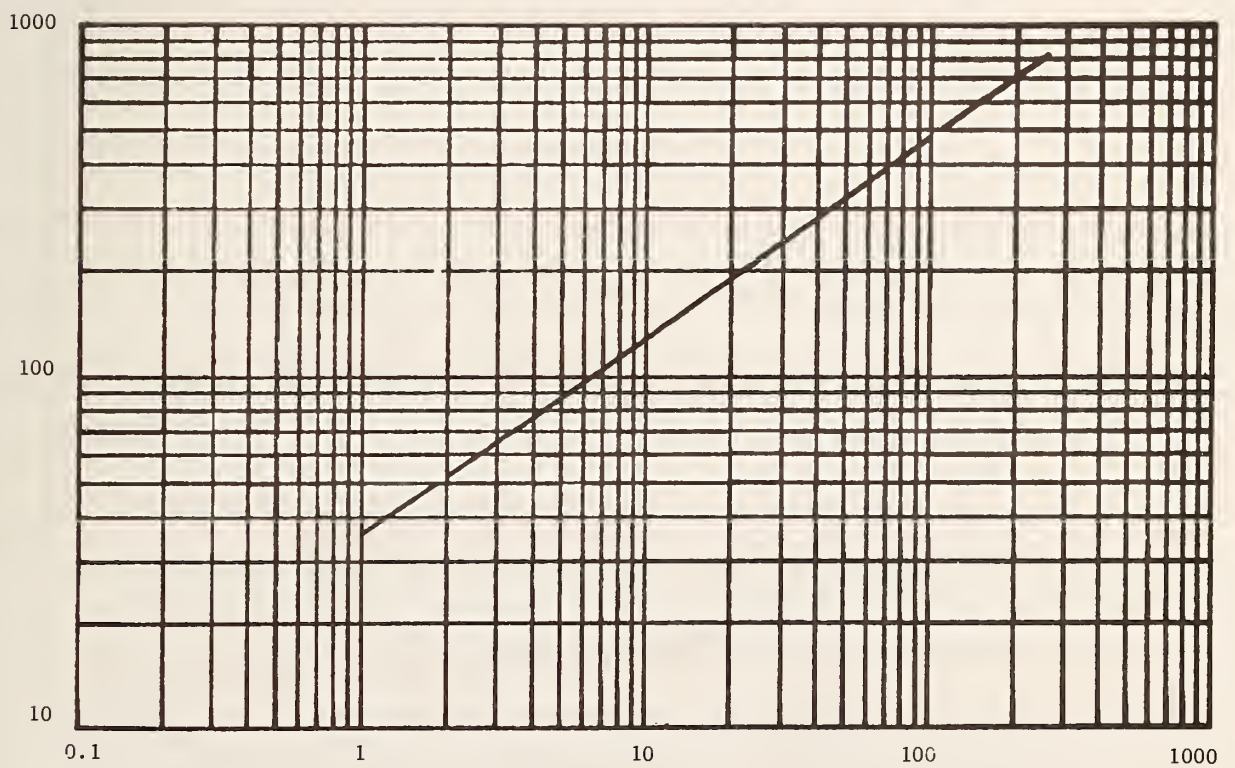


Figure A-145. Modeled minimum-phase phase shift plot for 402.34 meters (1320 ft) of WD-37. Ordinate units are degrees and abscissa units are megahertz.

1.161×10^{-2}

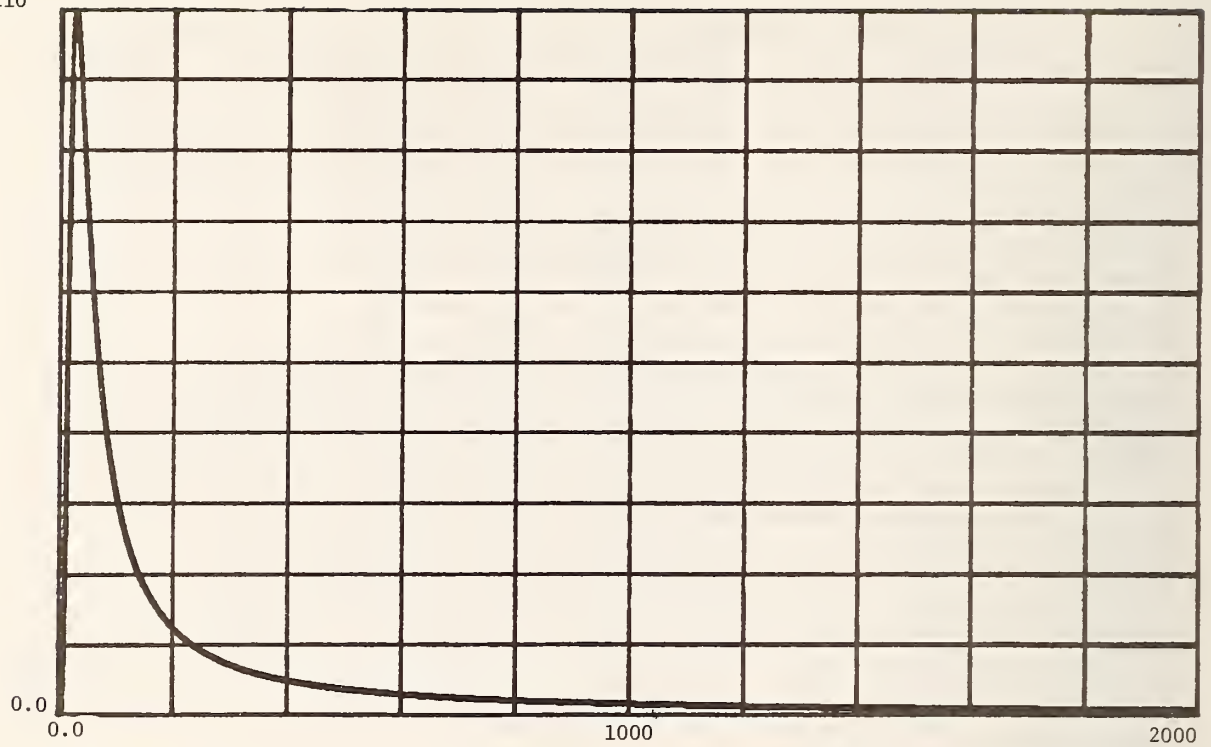


Figure A-146. Modeled and computed time domain impulse response for 402.34 meters (1320 ft) of WD-37. Ordinate units are seconds⁻¹, abscissa units are nanoseconds and time spacing between points is 1.953 ns.

1.161×10^{-2}

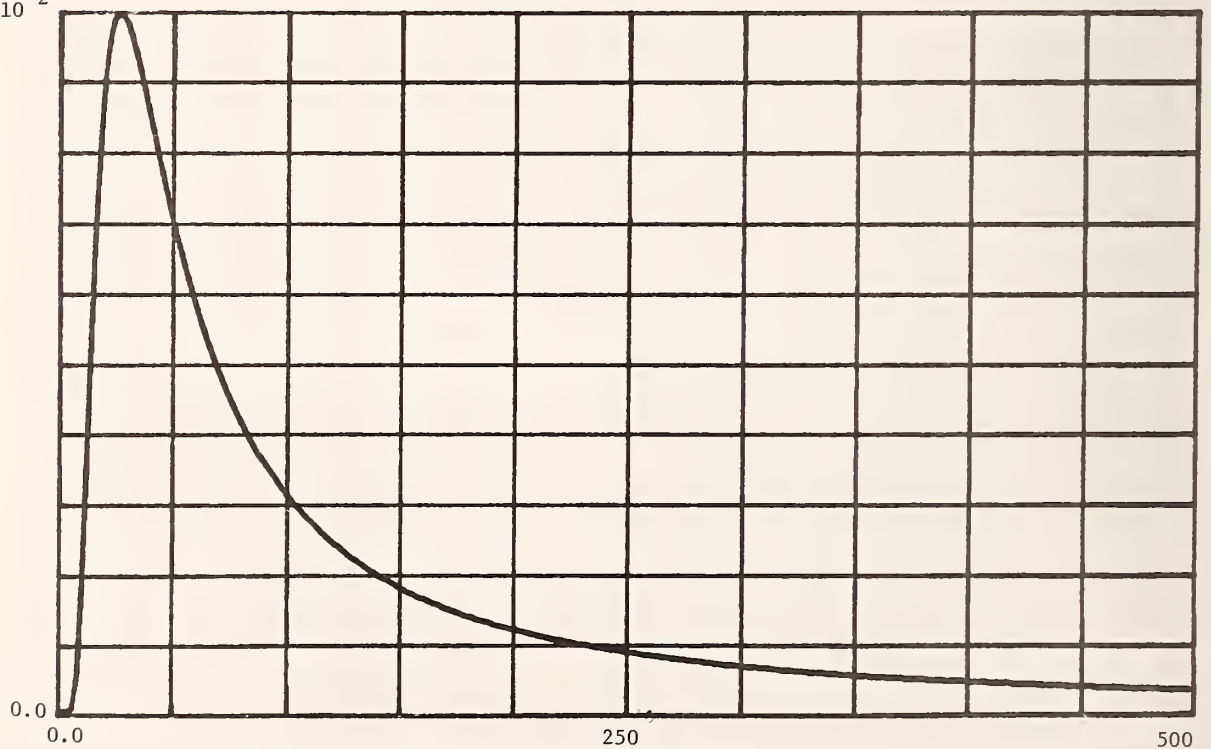


Figure A-147. Time-expanded modeled and computed time domain impulse response for 402.34 meters (1320 ft) of WD-37. Ordinate units are seconds⁻¹, abscissa units are nanoseconds and time spacing between points is 1.953 ns.

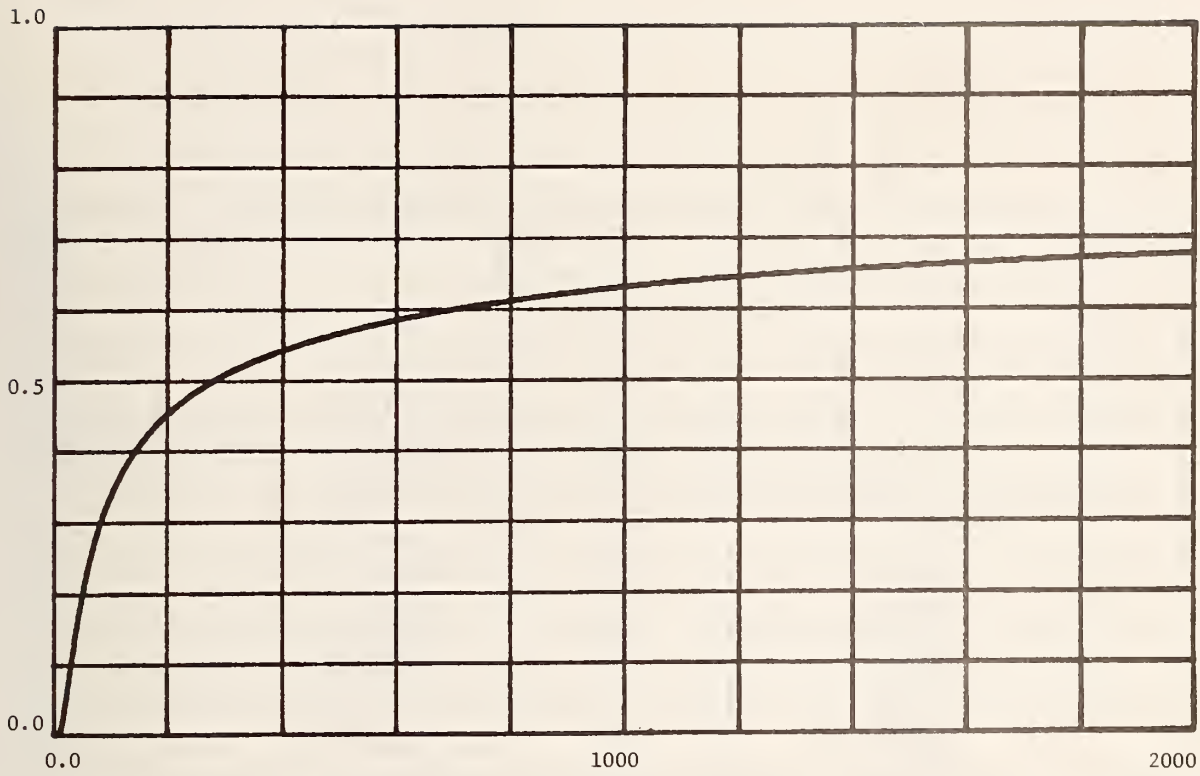


Figure A-148. Modeled and computed time domain unit step response for 402.34 meters (1320 ft) of WD-37. Ordinate units are volts and abscissa units are nanoseconds.

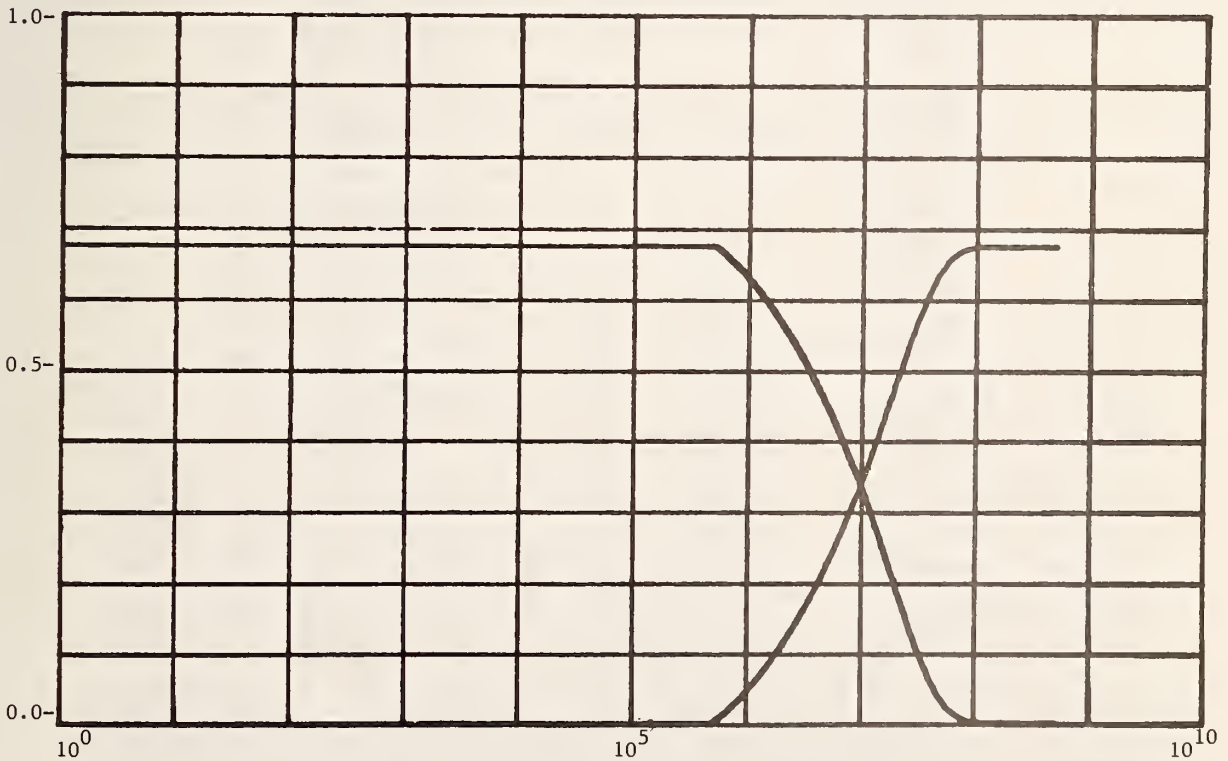


Figure A-149. Plots of "zero"/"one" cable unit step response voltages versus \log_{10} frequency for 402.34 meters (1320 ft) of WD-37. Ordinate units are volts and abscissa units are hertz.

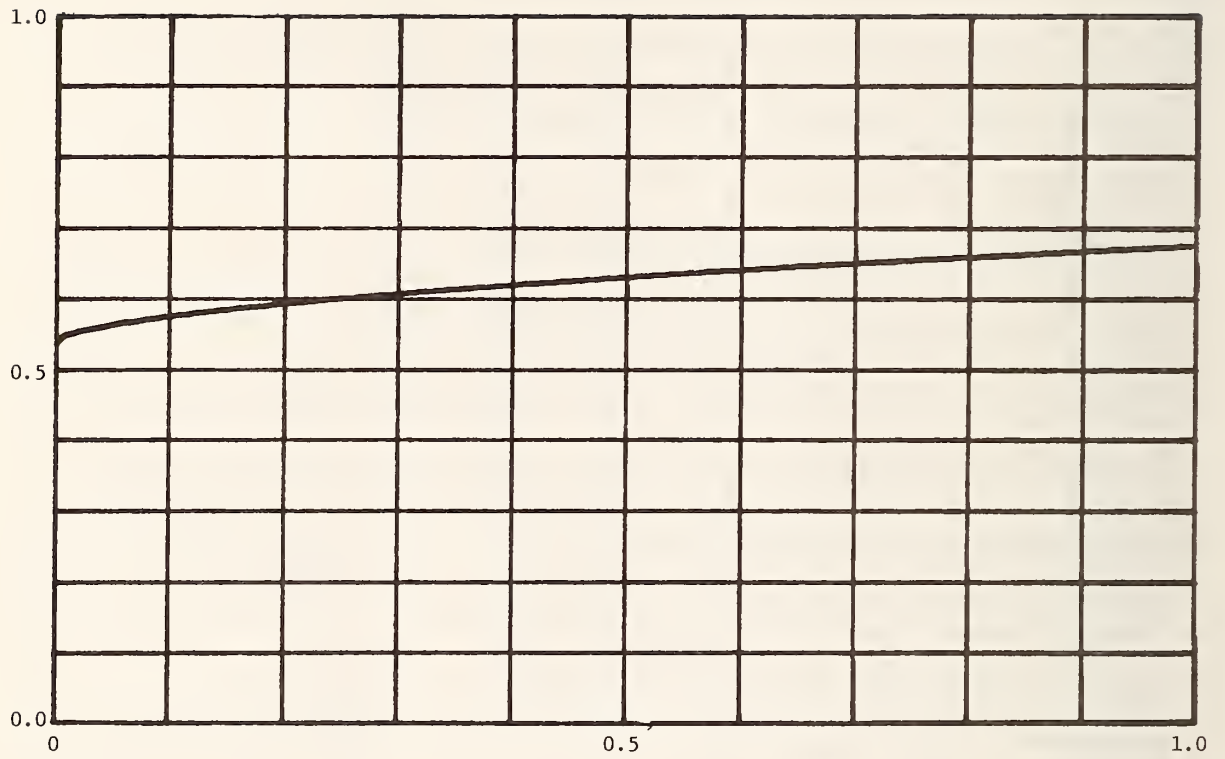


Figure A-150. TDR unit step response for cable WD-37. Source step generator has assumed 50Ω resistive output impedance. Ordinate units are volts and abscissa units are microseconds.

APPENDIX B. CABLE MEASUREMENT AND ANALYSIS COMPUTER PROGRAMS

B.1. APMS System Calibration Programs and Subroutines

B.1.1. Y-Axis Calibration Subroutine

```

T$$$
SUBROUTINE YCAL(U,ERY)
DIMENSION UKAL(9)
COMPLEX ERY(1024)
REAL IUT
ACCEPT "VERTICAL SCALE FACTOR IN MV/CM =?",IUT
TYPE " "
TYPE "APPLY MINIMUM DC VOLTAGE DESIRED TO THE SAMPLER. THEN,"
TYPE "DURING THE DUMMY DATA ACQUISITION PHASE, ADJUST THE VERTICAL"
TYPE "POSITION CONTROL ON THE S.O. TO POSITION THE SWEEP 1.0 CM"
TYPE "ABOVE THE BOTTOM LINE ON THE S.O. CRT. NOW, TYPE ANY NUMERAL"
ACCEPT "TO BEGIN THE MEASUREMENT.",IDUM
IPOINT=1024
IP=50
CALL DAT22< IP, IPOINT, ERY >
TYPE " "
CALL DAT22< IP, IPOINT, ERY >
DO 10 J=1,9
UKAL<J>=0.0
DO 20 J=1, IPOINT
UKAL<1>=UKAL<1>+REAL<ERY<J>>
UKAL<1>=UKAL<1>/IPOINT
DO 30 K=2,9
L=K-1
TYPE " "
TYPE "NOW, APPLY A DC VOLTAGE TO THE SAMPLER CORRESPONDING TO"
TYPE L, "CM UPWARD DEFLECTION OF THE SWEEP ON THE S.O. CRT."
ACCEPT "THEN, TYPE ANY NUMERAL.",IDUM
CALL DAT22<2, IPOINT, ERY >
TYPE " "
CALL DAT22< IP, IPOINT, ERY >
DO 25 J=1, IPOINT
UKAL<K>=UKAL<K>+REAL<ERY<J>>
UKAL<K>=UKAL<K>/IPOINT
CONTINUE
10
20
25
30

```

```
110 DO 110 J=1,8
      UKAL(J)=UKAL(J+1)-UKAL(J)/50.
      U=0.0
120 DO 120 J=1,8
      U=U+UKAL(J)
      U=U*1638.4*8.0)/U
      TYPE "U=",U,"MU/CM"
      RETURN
      END
```

*

B.1.2. X-Axis Calibration Subroutine

```

1$$$
SUBROUTINE XCAL(WAVE1, IHORIZ)
DIMENSION WAVE1(2048), XVAL(20), CMK(20), B1(2,1), C1(50,2), CTRK(2,50),
1CTOT(2,50), Y(50,1), CPRODX(2,2), CINX(2,2)
REAL IFREQ, IHORIZ
TYPE "SET THE S.O. TIME BASE TO THE SWEEP SPEED YOU INTEND TO USE"
TYPE "FOR THE 10%-90% RISETIME MEASUREMENT. APPLY A SIGNAL OF"
TYPE "KNOWN FREQUENCY TO THE SAMPLER SUCH THAT THE S.O. DISPLAY"
TYPE "CONTAINS BETWEEN 5 AND 15 SIGNAL PERIODS. CENTER THE SIGNAL"
TYPE "VERTICALLY ABOUT THE 5TH CM ON THE S.O."
ACCEPT "THE SIGNAL FREQUENCY IN GHZ=?", IFREQ
TYPE "DO YOU WANT CALIBRATION DONE BETWEEN SEQUENTIAL POSITIVE OR"
ACCEPT "NEGATIVE WAVEFORM SLOPES? (1=+, 0=-)", ISLOPE
I=1
CALL DAT11(50,2048,WAVE1)
TYPE ""
CALL DAT11(100,2048,WAVE1)
DO 10 J=1,2048
WAVE1(J)=WAVE1(J)/100.
L1=3
STRT=0.0
DO 20 J=L1,5
STRT=STRT+WAVE1(J)
STRT=STRT/3.0
IF (ISLOPE.EQ.1) GO TO 100
IF (STRT.GT.8192.) GO TO 40
L1=L1+1
IF (L1.GE.2040) GO TO 500
STRT=(WAVE1(L1)+WAVE1(L1+1)+WAVE1(L1+2))/3.0
GO TO 30
SNEX=(WAVE1(L1+1)+WAVE1(L1+2)+WAVE1(L1+3))/3.0
IF (SNEX.LT.STRT) GO TO 50
L1=L1+1
IF (L1.GE.2040) GO TO 500
STRT=SNEX
10
20
30
35
40

```

```

50      GO TO 40
        SNEX=WAVE1(L1+3)
        IF (SNEX.LE.8192.) GO TO 60
        L1=L1+1
        IF (L1.GE.2040) GO TO 500
        GO TO 50
60      KXVAL=L1+3
        NPOINT=11
        CALL LINE(WAVE1,B1,NPOINT,KXVAL,C1,CTR,CTOT,Y)
        XVAL(I)=(8192.-B1(1,1))/B1(2,1)
        L1=L1+3
        I=I+1
100     GO TO 35
        IF (STRT.LT.8192.) GO TO 140
        L1=L1+1
110     IF (L1.GE.2040) GO TO 500
        STRT=(WAVE1(L1)+WAVE1(L1+1)+WAVE1(L1+2))/3.0
        GO TO 100
140     SNEX=(WAVE1(L1+1)+WAVE1(L1+2)+WAVE1(L1+3))/3.0
        IF (SNEX.GT.STRT) GO TO 150
        L1=L1+1
        IF (L1.GE.2040) GO TO 500
        STRT=SNEX
        GO TO 140
150     SNEX=WAVE1(L1+3)
        IF (SNEX.GE.8192.) GO TO 160
        L1=L1+1
        IF (L1.GE.2040) GO TO 500
        GO TO 150
160     KXVAL=L1+3
        NPOINT=11
        CALL LINE(WAVE1,B1,NPOINT,KXVAL,C1,CTR,CTOT,Y)
        XVAL(I)=(8192.-B1(1,1))/B1(2,1)
        L1=L1+3
        I=I+1

```

```

500 GO TO 110
    AUG=0.0
    K=I-1
510 DO 510 J=1,K
    CMK J=XVAL(J)/204.7
    K=K-1
    DO 520 J=1,K
    XVAL(J)=XVAL(J+1)-XVAL(J)
    XVAL(J)=204.8/(IFREQXVAL(J))
    J1=J+1
600 WRITE (10,600)CMK J),CMK J1),XVAL(J)
    FORMAT(1X,"BETWEEN"F7.3" CM AND"F7.3" CM, TIME SCALE="F9.4" NS/CM")
520 CONTINUE
    DO 530 J=1,K
    AUG=AUG+XVAL(J)
    AUG=AUG/K
650 WRITE (10,650)AUG
    FORMAT (//1X,"AVERAGE TIME SCALE="F9.4" NS/CM"//)
    TYPE "WHICH TIME SCALE DO YOU WANT TO USE IN THE MAIN PROGRAM?"
    ACCEPT "(0=AVERAGE, 1=1ST INTERVAL, 2=2ND INTERVAL, ETC.)",J1
    IF (J1.NE.0) GO TO 540
    IHORIZ=AUG
    GO TO 550
540 IHORIZ=XVAL(J1)
550 RETURN
    END

```

*

B.1.3. Calibration Data Acquisition Subroutine

THIS SUBROUTINE ACQUIRES Y-AXIS DATA FROM THE SAMPLING OSCILLOSCOPE IN A SWEEP-SEQUENTIAL MANNER. IT IS CALLED FROM THE MAIN PROGRAM BY THE FORTRAN STATEMENT,

```
CALL S00X ISWP, IPNT, ARAY >
```

WHERE ISWP CONTAINS THE NUMBER OF WAVEFORM SWEEPS DESIRED AND WHERE IPNT CONTAINS THE NUMBER OF POINTS DESIRED IN EACH SWEEP. IPNT MUST BE OF THE FORM 2**N WHERE N IS A POSITIVE INTEGER. ARAY IS THE FLOATING POINT ARRAY INTO WHICH THE TOTAL WAVEFORM DATA IS PLACED AND MUST BE DIMENSIONED IN THE MAIN PROGRAM TO THE LARGEST EXPECTED NUMBER OF WAVEFORM POINTS.

THE OUTPUT ARRAY, ARAY(IPNT) CONSISTS OF SINGLE-PRECISION FLOATING POINT NUMBERS SUITABLE FOR FORTRAN ARITHMETIC OPERATIONS. TO ELIMINATE SAMPLER TRANSIENT EFFECTS FOUR SAMPLES ARE ACTUALLY TAKEN AT EACH POINT, THE FIRST THREE OF WHICH ARE DISCARDED.

SUBROUTINE S00X ISWP, IPNT, ARAY >

```

CONTINUE
.DUSR
.DUSR
LDA DACU=23 ;D/A DEVICE CODE
STA ADCU=21 ;A/D DEVICE CODE
LDA 0,T,3 ;ISWP ADDRESS
STA 0,SWP ;ADDRESS TO SWP
LDA 0,T,+1,3;IPNT ADDRESS
STA 0,PNT ;ADDRESS TO PNT
LDA 0,T,+2,3;ARAY STARTING ADDRESS
STA 0,ARY ;ADDRESS TO ARY
LDA 0,PEAC ;OCTAL 40000 TO ACK0)
LDA 1,OPNT ;# OF POINTS TO ACK1)
JMP .+2 ;THESE FIVE INSTRUCTIONS
MOVZR 0,0 ;CALCULATE THE POINT
MOVZR 1,1,SNC ;SPACING, IBITE, WHERE

```

\$\$\$
 C
 A

A	JMP	ASMPCT:	-2	; IBYTE=16,394/# OF POINTS
A	LDA		0,IBYTE	;DONE!
A	STA		2,@PNT	;# OF POINTS TO AC(2)
A	MOVZL		2,2	;DOUBLE AC(2) FOR FP ARRAY
A	NEG		2,2	;NEGATE AC(2)
A	LDA		3,ARY	;ARY ADDRESS TO AC(3)
A	SUBO		0,0	;ZERO AC(0)
A	STA		0,0,3	;ZERO ALL ARRAY LOCATIONS
A	INC		3,3	;INCREMENT POINT COUNTER
A	INC		2,2,SZR	;INCREMENT POINT COUNTER
A	JMP		-3	;NOT DONE--GET NEXT POINT
A	LDA		0,@SWP	;# OF SWEEPS TO AC(0)
A	STA		0,CNT1	;# OF SWEEPS TO CNT1
A	LDA		0,@PNT	;# OF POINTS/SWEEP TO AC(0)
A	STA		0,IPT	;# OF POINTS/SWEEP TO IPT
A	LDA		0,IBYTE	;POINT SPACING TO AC(0)
A	STA		0,CNT2	;POINT SPACING TO CNT2
A	LDA		0,DUM	;DUMMY SAMPLE # TO AC(0)
A	STA		0,DCNT	;DUMMY SAMPLE # TO DCNT
A	LDA		0,ARY	;ARY SA TO AC(0)
A	STA		0,DATA0	;ARRAY SA TO DATA0
A	STA		0,CT1	;ARRAY SA TO CT1
A	STA		0,CT2	;ARRAY SA TO CT2
A	SUBO		0,0	;ZERO AC(0)
A	DOA		0,DACU	;ADDRESS D/A #0
A	DOB		0,DACU	;OUTPUT ZERO TO D/A #0
A	DOAS		0,ACCU	;START CONVERT, A/D #0
A	LDA		0,ADM1	;INTERRUPT MASK TO AC(0)
A	MSKO		0	;MASK OUT A/D INTERRUPT
A	SKPON		ACCU	;CONVERSION DONE?
A	JMP		-1	;NO, KEEP WAITING
A	DSZ		DCNT	;DUMMY SAMPLES DONE?
A	JMP		DUMY	;NO, TAKE ANOTHER
A	SUBO		2,2	;ZERO AC(2)
A	DIC		3,ACCU	;A/D OUTPUT TO AC(3)


```

A ADUMAD:
A SUBZ
A DOA
A DOB
A DOAS
A SKPON
A JMP
A JMP
A 4
A DCNT:
A ADM1:
A ACNT1:
A ACNT2:
A ADATAD:
A ACT1:
A ACT2:
A AXMASK:
A APEAC:
A ACT3:
A ACT4:
A AEXPON:
A APNT:
A IBITE:
A ARY:
A ASWP:
A AIPT:
A ASHIFT:
A
A
A
A
A
A
A
A
A
A

; JUMP AROUND SHIFT
; CLEAR AC(0)
; ADDRESS D/A #0
; X LOCATION TO D/A #0
; TAKE DUMMY SAMPLE
; A/D FINISHED?
; NO, NOT YET
; YES, RETURN
; NUMBER OF DUMMY SAMPLES +1
; DUMMY SAMPLE COUNTER
; INTERRUPT MASK WORD
; SWEEP COUNTER
; BITE SIZE (POINT SPACING)
; ARAY STARTING ADDRESS
; DATA LOAD COUNTER
; DATA STORE COUNTER
; UPPER BYTE MASK
; 2^14 IN OCTAL
; DATA LOAD COUNTER
; DATA STORE COUNTER
; FLOATING POINT NORMALIZING EXPONENT
; # OF POINTS DESIRED IN SWEEP
; BITE SIZE
; ARRAY STARTING ADDRESS
; ADDRESS OF # OF SWEEPS
; # OF POINTS/SWEEP
; MOVE THE FOUR LO-ORDER
; BITS OF THE HI-ORDER
; DATA WORD INTO THE TOP
; FOUR BITS OF THE LO-ORDER
; DATA WORD AND THROW OUT
; THE FOUR LO-ORDER BITS OF
; THE LO-ORDER DATA WORD.
; INCREMENT THE EXPONENT

TEST1
0,0
0,DACV
2,DACV
0,ADCV
ADCV
-1
RET
;NUMBER OF DUMMY SAMPLES +1
;DUMMY SAMPLE COUNTER
;INTERRUPT MASK WORD
;SWEEP COUNTER
;BITE SIZE (POINT SPACING)
;ARAY STARTING ADDRESS
;DATA LOAD COUNTER
;DATA STORE COUNTER
;UPPER BYTE MASK
;2^14 IN OCTAL
;DATA LOAD COUNTER
;DATA STORE COUNTER
;FLOATING POINT NORMALIZING EXPONENT
;# OF POINTS DESIRED IN SWEEP
;BITE SIZE
;ARRAY STARTING ADDRESS
;ADDRESS OF # OF SWEEPS
;# OF POINTS/SWEEP
0,0
1,1
0,0
1,1
0,0
1,1
0,0
1,1
1,1
1,1
2,2

JMP
SUBZ
DOA
DOB
DOAS
SKPON
JMP
JMP
4
DCNT:
ADM1:
ACNT1:
ACNT2:
ADATAD:
ACT1:
ACT2:
AXMASK:
APEAC:
ACT3:
ACT4:
AEXPON:
APNT:
IBITE:
ARY:
ASWP:
AIPT:
ASHIFT:
A
A
A
A
A
A
A
A
A
A
MOVZR
MOVZR
MOVZR
MOVZR
MOVZR
MOVZR
MOVZR
MOVZR
INC

```

```

A ATEST1:
A LDA
A LDA
A ISZ
A LDA
A ISZ
A AND#
A JMP
A MINS
A ADD
A STA
A ISZ
A STA
A ISZ
A DSZ
A JMP
A SUBZ
A MSKO
A RETURN
A END
*

RTN2
2,EXPON
0,0CT3
CT3
1,0CT3
CT3
0,3,SZR
SHIFT
2,2
2,0
0,0CT4
CT4
1,0CT4
CT4
IPT
TEST1
0,0
0

;RETURN TO SUBROUTINE
;FP EXPONENT TO AC<2>
;HI-ORDER # TO AC<0>
;INCREMENT DATA ADDRESS
;LO-ORDER # TO AC<1>
;INCREMENT DATA ADDRESS
;OVFL INTO EXPONENT?
;YES, JUMP TO SHIFT
;SWAP BYTES IN EXPONENT #
;ADD EXPON TO HI-ORDER #
;HI-ORDER FP # TO ARRAY
;INCREMENT DATA ADDRESS
;LO-ORDER FP # TO ARRAY
;INCREMENT DATA ADDRESS
;FINISHED NORMALIZING
;NO, GET NEXT POINT
;ZERO TO AC<0>
;CLEAR INTERRUPTS

```


B.1.4. Linear Least Squares Curve Fit Subroutine

```

$$$
SUBROUTINE LINE(WAVE1,B1,NPOINT,KXVAL,C1,CTR,CTOT,Y)
DIMENSION WAVE1(2048),B1(2,1),C1(NPOINT,2),CTR(2,NPOINT),
1CTOT(2,NPOINT),Y(NPOINT,1),CPROK(2,2),CINX(2,2)
KPOINT=NPOINT/2
DO 40 J=1,NPOINT
C1(J,1)=1.0
C1(J,2)=KXVAL-KPOINT+J-1
IF (C1(J,2).GT.0) GO TO 35
TYPE "ERROR---CHECK FOR FAULTY WAVEFORM ACQUISITION"
STOP
35 Y(J,1)=WAVE1(KXVAL-KPOINT+J-1)
40 CONTINUE
DO 50 J=1,NPOINT
DO 50 K=1,2
CTR(K,J)=C1(J,K)
50 CONTINUE
CALL MATMUL(CTR,C1,CPROD,2,NPOINT,2)
D=CPROK(1,1)*CPROK(2,2)-CPROK(1,2)*CPROK(2,1)
CINX(1,1)=CPROK(2,2)/D
CINX(2,1)=-CPROK(1,2)/D
CINX(1,2)=-CPROK(2,1)/D
CINX(2,2)=CPROK(1,1)/D
CALL MATMUL(CINU,CTR,CTOT,2,2,NPOINT)
CALL MATMUL(CTOT,Y,B1,2,NPOINT,1)
CONTINUE
RETURN
END
*

```

B.1.5. General Matrix Multiplication Subroutine

```
1$$$  
SUBROUTINE MATMUL(A,B,C,NROWA,NCOLA,NCOLB)  
DIMENSION A(NROWA,NCOLA),B(NCOLA,NCOLB),C(NROWA,NCOLB)  
DO 20 K=1,NCOLB  
DO 20 L=1,NROWA  
TEMP=0.0  
DO 10 J=1,NCOLA  
TEMP1=A(L,J)*B(J,K)  
TEMP=TEMP+TEMP1  
CONTINUE  
C(L,K)=TEMP  
CONTINUE  
RETURN  
END  
10  
20  
*
```

B.2. Cable Measurement Programs and Subroutines

B.2.1. Main Cable Time Domain Transfer Function Measurement Program

```

10  S21U-----MAIN PROGRAM FOR CALCULATION OF PARAMETER S21<F>
11  MAGNITUDE AND PHASE USING AN IMPULSIVE WAVEFORM. THE NUMBER OF
12  ACQUIRED DATA POINTS AND THE NUMBER OF ARRAY POINTS FOR FFT
13  PROCESSING ARE EACH SELECTABLE BUT BOTH MUST BE AN INTEGER POWER
14  OF 2. WAVEFORMS MAY BE ACQUIRED IN EITHER A SWEEP SEQUENTIAL OR
15  A POINT SEQUENTIAL MODE.
16  IN ADDITION, FREQUENCY DOMAIN AVERAGING IS POSSIBLE WITH AN
17  OUTPUT LISTING OF MEAN VALUE AND SIGMA FOR BOTH MAGNITUDE (IN DB
18  OR IN NEPERS) AND PHASE (IN DEGREES OR IN RADIAN). DUE TO MEMORY
19  LIMITATIONS ONLY THE FIRST 300 HARMONICS (OR LESS) OF S21<F>
20  ARE CALCULATED.
21  COMPLEX WAVE1<2048>,WAVE2<1025>,AV1
22  DIMENSION S<1800>,PK<1800>
23  PI=3.14159265
24  NMEAS=0
25  TYPE "REFERENCE WAVEFORM ACQUISITION READY?"
26  TYPE "WAVEFORM ACQUISITION MODE? 1=SWEEP SEQUENTIAL,"
27  ACCEPT "0=POINT SEQUENTIAL
28  ACCEPT "# OF WAVEFORM POINTS FOR DATA ACQ=?
29  ACCEPT "# OF WAVEFORM POINTS IN TOTAL=?
30  ACCEPT "NUMBER OF DUMMY DATA ACQUISITION SWEEPS =?
31  IF (<IMODE.EQ.1>) GO TO 10
32  ACCEPT "NUMBER OF POINTS PER X LOCATION=?
33  GO TO 20
34  ACCEPT "NUMBER OF TIME-AVERAGED WAVEFORMS=?
35  ACCEPT "TIME SCALE FACTOR IN NSEC/CM=?
36  ACCEPT "INDIVIDUAL S21 LISTINGS? (1=YES, 0=NO)
37  ACCEPT "VERTICAL SCALE FACTOR IN MV/CM=?
38  ACCEPT "VERT. SCALE CHANGE FOR 2ND WAVEFORM? (1=YES, 0=NO)
39  TYPE "NUMBER OF FREQUENCY DOMAIN AVERAGES =? THIS"
40  ACCEPT "NUMBER MUST BE LESS THAN OR EQUAL TO SIX.
41  TYPE "NUMBER OF HARMONICS TO BE CALCULATED =?"
42  TYPE "THIS NUMBER MUST BE LESS THAN (<# OF TOTAL POINTS>/2"
43  ACCEPT "OR 300, WHICHEVER IS THE SMALLER OF THE TWO.

```

```

",IMODE
",IDAT
",IPNT
",IP
",ISAP
",ISAP
",TIME
",NA
",VERT
",NB
",MEAS
",IHARM

```

10
20

10
11
12
13
14
15
16
17
18
19
20
21
22
23
24
25
26
27
28
29
30
31
32
33
34
35
36
37
38
39
40
41
42
43

```

30  IRUN=0
    NMEAS=NMEAS+1
    IF <NMEAS.NE.1> GO TO 50
    IF <IRUN.EQ.0> GO TO 50
    IF <N8.EQ.0> GO TO 50
    ACCEPT "VERTICAL SCALE FACTOR IN MU/CM=?
    CALL S02 <IP, IDAT, WAVE1>
    TYPE ""
    IF <IMODE.EQ.1> GO TO 60
    CALL S03 <ISWP, IDAT, WAVE1>
    GO TO 70
    CALL S02 <ISWP, IDAT, WAVE1>
    AV1=(0.0,0.0)
    DO 80 J=6,15
    AV1=AV1+WAVE1<J>
    AV1=AV1<10.0,0.0>
    DO 90 J=1,5
    WAVE1<J>=AV1
    AV1=(WAVE1<IDAT>+WAVE1<IDAT-1>+WAVE1<IDAT-2>)/3.0,0.0)
    ID=IDAT+1
    DO 100 J=ID, IPNT
    WAVE1<J>=AV1
    IF <NMEAS.NE.1> GO TO 140
    IF <IRUN.NE.0> GO TO 110
    CALL MSOPEN <5, "TIME1", "W">
    GO TO 120
    CALL MSOPEN <5, "TIME2", "W">
    WRITE <5> IDAT
    WRITE <5> TIME
    WRITE <5> VERT
    ISTEP=1
    IF <IDAT.GT.1024> ISTEP=2
    DO 130 J=1, IDAT, ISTEP
    X1=(REAL<WAVE1<J>>)/ISWP
    X1=X1/1638.4
    ", VERT

```

```

130 WRITE (5) X1
    CALL FCLOS (5)
140 CALL FFT(WAVE1, IPNT, 1)
    IF (IRUN.NE.0) GO TO 145
    IF (NMEAS.NE.1) GO TO 145
    ACCEPT "WRITE REFERENCE WAVEFORM SPECTRUM? (1=YES, 0=NO) ", ISPEC
    IF (ISPEC.EQ.0) GO TO 145
    CALL MSOPEN (5, "SPEK", "W")
    IPOINT=IPNT/2-1
    FDIU=5.*IPNT/TIME
    OYY=1.0
    WRITE (5) IPOINT
    WRITE (5) FDIU
    WRITE (5) OYY
    IPOINT=IPOINT+1
    DO 147 J=2, IPOINT
    X=20.0XALOG10(CABS(WAVE1(J)))
147 WRITE (5) X
    CALL FCLOS (5)
145 IF (IRUN.EQ.1) GO TO 160
    IHA=IHART+1
    IPN=IPNT/2+1
    DO 150 J=1, IPN
150 WAVE2(J)=WAVE1(J)
    VER=VERT
    ACCEPT "RESPONSE WAVEFORMS READY? (TYPE ANY CHARACTER)", IOUM
    IRUN=1
    GO TO 40
160 IF (N4.EQ.0) GO TO 180
    ACCEPT "READY FOR LISTING? (TYPE ANY NUMERAL)", N9
170 FORMAT (1X, F12.2" MHZ" F15.3" DB" F15.3" DEGREES")
180 SHIFT=0.0
    DO 210 J=2, IHA
    K=J-1
    AV1=(WAVE1(J)+WAVE2(J))*K/VERT/VER)

```

```

U1=20.0*ALOG10(CABS(AU1))
U2=ATAN2(AIMAG(AU1),REAL(AU1))
U2=U2/360.0/(2*PI))*U2
DA=FLOAT(IDAT)
U3=(KXDA)/(IPNT*TIME*0.01)+0.001
S(300*NMEAS-300+K)=U1
IF (J.EQ.2) GO TO 200
U5=U2
PROD=U4*U2
IF (PROD.GE.0) GO TO 200
IF (ABS(U2).LE.90.0) GO TO 200
IF (U4.GT.0) GO TO 190
SHIFT=SHIFT-360.0
GO TO 200
SHIFT=SHIFT+360.0
U2=U2+SHIFT
P(300*NMEAS-300+K)=U2
U4=U5
IF (N4.EQ.0) GO TO 210
WRITE (10,170)U3,U1,U2
CONTINUE
IF (NMEAS.EQ.MEAS) GO TO 220
GO TO 30
IF (NMEAS.EQ.1) GO TO 999
ACCEPT "READY FOR LISTING OF S21(MEAN) AND S21(SIGMA)?" ,N6
ACCEPT "LISTING IN NEPERS & RADIANES (1) OR DB AND DEGREES (2)",L1
TYPE "NUMBER OF MEASUREMENTS=",NMEAS
TYPE " "
WRITE (10,230)
FORMAT(1X,"
FREQUENCY
SIGMA" )
TYPE " "
CALL MSOPEN (5,"MNDG","W")
HARM=FLOAT(IHARM)
DUX=FLOAT(IHARM)/(IPNT*TIME*0.1)

```

190
200

210

220

230

PMEAN

SIGMA

SMEAN

```

US=1.0
WRITE (5) IHARM
WRITE (5) DIVX
WRITE (5) VS
NAU=300
IF (IHARM.LE.300) NAU=IHARM
DO 300 J=1,NAU
SMEAN=0.0
DO 240 K=1,NMEAS
SMEAN=SMEAN+SX(300*K-300+J)
SMEAN=SMEAN/NMEAS
SMNEP=-SMEAN/8.685889638
WAVE1(J)=CMPLX(SMEAN,SMNEP)
PMEAN=0.0
DO 250 K=1,NMEAS
PMEAN=PMEAN+PX(300*K-300+J)
PMEAN=PMEAN/NMEAS
PMRAD=-((PMEAN*PI)/180.0)
WAVE2(J)=CMPLX(PMRAD,0.0)
SOEU2=0.0
DO 260 K=1,NMEAS
SOEU2=SOEU2+(SMEAN-SX(300*K-300+J))*SMEAN-SX(300*K-300+J)
SOEU2=SOEU2/(NMEAS-1)
SIGMA=SQRT(SOEU2)
IF (L1.EQ.1) SIGMA=SIGMA/8.685889638
POEU2=0.0
DO 270 K=1,NMEAS
POEU2=POEU2+(PMEAN-PX(300*K-300+J))*PMEAN-PX(300*K-300+J)
POEU2=POEU2/(NMEAS-1)
PIGMA=SQRT(POEU2)
IF (L1.EQ.1) PIGMA=(PIGMA*PI)/180.0
FREQ=(J*DA)/((IPNT*TIME)*0.01)+0.001
IF (L1.EQ.1) GO TO 280
WRITE (10,340) FREQ,SMEAN,SIGMA,PMEAN,PIGMA
GO TO 290

```

```

280 WRITE (10,350) FREK, SMNEP, SIGMA, PMRAD, PIGMA
290 WRITE (5) PMEAN
300 CONTINUE
    CALL FCLOS (5)
    CALL MSOPEN (5, "MND8", "W")
    WRITE (5) IHARM
    WRITE (5) DIUX
    WRITE (5) US
    DO 310 J=1,NAU
    X1=REAL(WAVE1(J))
    WRITE (5) X1
    CALL FCLOS (5)
    CALL MSOPEN (5, "MNEP", "W")
    WRITE (5) IHARM
    WRITE (5) DIUX
    WRITE (5) US
    DO 320 J=1,NAU
    X1=AIMAG(WAVE1(J))
    WRITE (5) X1
    CALL FCLOS (5)
    CALL MSOPEN (5, "MNRAD", "W")
    WRITE (5) IHARM
    WRITE (5) DIUX
    WRITE (5) US
    DO 330 J=1,NAU
    X1=REAL(WAVE2(J))
    WRITE (5) X1
    CALL FCLOS (5)
    FORMAT(1X,F12.2" MHZ"F12.3" DB"F8.3" DB"F12.3" DEG"F8.3" DEG")
    FORMAT (1X,F12.2" MHZ"F12.3" NEP"F8.3" RAD"F12.3" RAD"F8.3" RAD")
999 END
*
```


B.2.2. Sweep-Sequential Waveform Acquisition Subroutine

THIS SUBROUTINE ACQUIRES Y-AXIS DATA FROM THE SAMPLING OSCILLOSCOPE IN A SWEEP-SEQUENTIAL MANNER. IT IS CALLED FROM THE MAIN PROGRAM BY THE FORTRAN STATEMENT,
 CALL S02(I SWP, IPNT, ARAY)
 WHERE I SWP CONTAINS THE NUMBER OF WAVEFORM SWEEPS DESIRED AND WHERE IPNT CONTAINS THE NUMBER OF POINTS DESIRED IN EACH SWEEP. IPNT MUST BE OF THE FORM $2 \cdot N$ WHERE N IS A POSITIVE INTEGER. ARAY IS THE FLOATING POINT ARRAY INTO WHICH THE TOTAL WAVEFORM DATA IS PLACED AND MUST BE DIMENSIONED IN THE MAIN PROGRAM TO THE LARGEST EXPECTED NUMBER OF WAVEFORM POINTS.
 THE OUTPUT ARRAY, ARAY(IPNT) CONSISTS OF SINGLE-PRECISION FLOATING POINT NUMBERS SUITABLE FOR FORTRAN ARITHMETIC OPERATIONS. THIS SUBROUTINE DIFFERS FROM S00 IN THAT THE ARRAY IN S02 IS COMPLEX WITH ALL IMAGINARY ELEMENTS EQUAL TO ZERO. THUS, FOR A GIVEN VALUE OF IPNT, THE ARRAY RESULTING FROM S02 WILL OCCUPY TWICE THE MEMORY OF THAT RESULTING FROM S00. TO ELIMINATE SAMPLER TRANSIENT EFFECTS, FOUR SAMPLES ARE ACTUALLY TAKEN AT EACH POINT, THE FIRST THREE OF WHICH ARE DISCARDED.
 SUBROUTINE S02(I SWP, IPNT, ARAY)
 COMPLEX ARAY(IPNT)
 CONTINUE

```

.DUSR      DACU=23 ,D/A DEVICE CODE
.DUSR      ADCU=21 ,A/D DEVICE CODE
LDA        0,T.,3 ,I SWP ADDRESS
STA        0, SWP ,ADDRESS TO SWP
LDA        0,T.+1,3,IPNT ADDRESS
STA        0,PNT ,ADDRESS TO PNT
LDA        0,T.+2,3,ARAY STARTING ADDRESS
STA        0,ARY ,ADDRESS TO ARY
LDA        0,PEAC ,OCTAL 40000 TO ACK0)
LDA        1,OPNT ,# OF POINTS TO ACK1)
.JMP      .+2 ,THESE FIVE INSTRUCTIONS

```

T\$\$
 CCC
 AA

A	.JMP	CT1	NO, TAKE ANOTHER
A	SUB0	2,2	ZERO AC<2>
A	DIC	3,ADCU	A/D OUTPUT TO AC<3>
A	LDA	0,DUM	DUMMY SAMPLE # TO AC<0>
A	STA	0,DCNT	DUMMY SAMPLE # TO DCNT
A	LDA	0,IBITE	IBITE SIZE TO AC<0>
A	SUB0	1,1	ZERO AC<1>
A	ADD	0,2	INCREMENT X LOCATION
A	DDA	1,DACU	ADDRESS D/A #0
A	DOB	2,DACU	NEXT X LOCATION TO D/A #0
A	DDAS	1,ADCU	BEGIN CONVERT, A/D #0
A	ADDZL	3,3	REMOVE LEADING ONES
A	MOVZR	3,3	FROM OUTPUT DATA FROM A/D
A	MOVZR	3,3	<EXTRANEOUS ONES ONLY>
A	LDA	0,@CT1	HIGH ORDER # TO AC<0>
A	ISZ	CT1	INCREMENT DATA ADDRESS
A	LDA	1,@CT1	LOW ORDER # TO AC<1>
A	ISZ	CT1	INCREMENT DATA ADDRESS
A	ISZ	CT1	INCREMENT DATA ADDRESS
A	ISZ	CT1	INCREMENT DATA ADDRESS
A	ADDZ	3,1,SZC	ADD TWO LOW ORDER #'S
A	INC	0,0	INCR. HI-ORDER # IF OVFL
A	STA	0,@CT2	NEW SUM TO ARAY
A	ISZ	CT2	INCREMENT DATA ADDRESS
A	STA	1,@CT2	NEW SUM TO ARAY <LO-ORDER>
A	ISZ	CT2	INCREMENT DATA ADDRESS
A	ISZ	CT2	INCREMENT DATA ADDRESS
A	ISZ	CT2	INCREMENT DATA ADDRESS
A	LDA	1,PEAC	2^14 TO AC<1>
A	SKPON	ADCU	A/D CONVERSION DONE?
A	.JMP	-1	NO, WAIT
A	DSZ	DCNT	DUMMY SAMPLES DONE?
A	.JMP	DUMAD	NO, TAKE ANOTHER
A	NI0C	ADCU	
A	SUB#	2,1,SZC	SWEEP COMPLETED

A	JMP	PTCNT	; NO, GET NEXT POINT
A	DSZ	CNT1	; ALL SWEEPS COMPLETED?
A	JMP	SWPCT	; NO, START NEXT SWEEP
A	LDA	0, DATAD	; ARRAY SA TO DATAD
A	STA	0, CT3	; ARRAY SA TO CT3
A	STA	0, CT4	; ARRAY SA TO CT4
A	LDA	3, XMASK	; BYTE MASK TO AC<3>
A	JMP	TEST1	; JUMP AROUND SHIFT
A	SUBZ	0, 0	; CLEAR AC<0>
ADUMAD:	DOA	0, DACU	; ADDRESS D/A #0
A	DOB	2, DACU	; X LOCATION TO D/A #0
A	DOAS	0, ADCU	; TAKE DUMMY SAMPLE
A	SKPON	ADCU	; A/D FINISHED?
A	JMP	-1	; NO, NOT YET
A	JMP	RET	; YES, RETURN
A	4		; NUMBER OF DUMMY SAMPLES +1
ADUM:	ADCNT:		; DUMMY SAMPLE COUNTER
ADUM1:	ADMT1:	377	; INTERRUPT MASK WORD
ADUM2:	ADNT1:	0	; SWEEP COUNTER
ADATAD:	ADNT2:	0	; BITE SIZE <POINT SPACING>
ACT1:	ADAT1:	0	; ARRAY STARTING ADDRESS
ACT2:	ADAT2:	0	; DATA LOAD COUNTER
AXMASK:	ACT1:	0	; DATA STORE COUNTER
APEAC:	ACT2:	177400	; UPPER BYTE MASK
ACT3:	APEAC:	40000	; 2~14 IN OCTAL
ACT4:	ACT3:	0	; DATA LOAD COUNTER
AEXPON:	ACT4:	0	; DATA STORE COUNTER
APNT:	AEXPON:	106	; FLOATING POINT NORMALIZING EXPONENT
AIBITE:	APNT:	0	; # OF POINTS DESIRED IN SWEEP
AARY:	AIBITE:	0	; BITE SIZE
ASWP:	AARY:	0	; ARRAY STARTING ADDRESS
AIPNT:	ASWP:	0	; ADDRESS OF # OF SWEEPS
ASHIFT:	AIPNT:	0	; # OF POINTS/SWEEP
A	MOVZR	0, 0	; MOVE THE FOUR LO-ORDER
A	MOUR	1, 1	; BITS OF THE HI-ORDER

B.2.3. Point-Sequential Waveform Acquisition Subroutine

```
T$$$
CCCCCCCCCCCCCCCCCCCC
      THIS SUBROUTINE ACQUIRES Y-AXIS DATA FROM THE SAMPLING
      OSCILLOSCOPE IN A POINT-SEQUENTIAL MANNER. IT IS CALLED
      FROM THE MAIN PROGRAM BY THE FORTRAN STATEMENT,
      CALL S03(NPNT, IPNT, ARAY)
      WHERE NPNT CONTAINS THE NUMBER OF POINTS/X LOCATION DESIRED
      AND WHERE IPNT CONTAINS THE NUMBER OF POINTS DESIRED IN
      THE TOTAL SWEEP. IPNT MUST BE OF THE FORM 2*NXN WHERE N IS A
      POSITIVE INTEGER. ARAY IS THE FLOATING POINT ARRAY INTO
      WHICH THE TOTAL WAVEFORM DATA IS PLACED AND MUST BE
      DIMENSIONED IN THE MAIN PROGRAM TO THE LARGEST EXPECTED
      NUMBER OF WAVEFORM POINTS.
      THE OUTPUT ARRAY, ARAY(IPNT), CONSISTS OF COMPLEX SINGLE-
      PRECISION FLOATING POINT NUMBERS SUITABLE FOR FORTRAN
      ARITHMETIC OPERATIONS. THE IMAGINARY PART OF EACH ARRAY
      ELEMENT IS SET TO ZERO THUS ASSUMING ONLY REAL DATA WILL
      BE ACQUIRED USING THIS SUBROUTINE. TO ELIMINATE SAMPLER
      TRANSIENT EFFECTS, THE FIRST THREE SAMPLES TAKEN AT EACH
      POINT ARE DISCARDED.
      SUBROUTINE S03(NPNT, IPNT, ARAY)
      COMPLEX ARAY(IPNT)
      CONTINUE
      .DUSR ;D/A DEVICE CODE
      .DUSR ;A/D DEVICE CODE
      LDA 0,T,3 ;NPNT ADDRESS
      STA 0,SMP ;ADDRESS TO SWP
      LDA 0,T,+1,3 ;IPNT ADDRESS
      STA 0,PNT ;ADDRESS TO PNT
      LDA 0,T,+2,3 ;ARAY STARTING ADDRESS
      STA 0,ARY ;ADDRESS TO ARY
      LDA 0,PEAC ;OCTAL 40000 TO AC(0)
      LDA 1,CPNT ;# OF POINTS TO AC(1)
      .JMP ;+2 ;THESE FIVE INSTRUCTIONS
      MOVZR 0,0 ;CALCULATE THE POINT
      MOVZR 1,1,8NC ;SPACING, IBITE, WHERE
```

AAAAAAAAAAAAAAAAAAAAAAAAADUMY:AAAAAAAAAAAAAAAA

```

JMP
STA
LDA
MOVZL
MOVZL
NEG
LDA
SUBO
STA
INC
INC
JMP
LDA
STA
LDA
STA
LDA
STA
LDA
STA
LDA
STA
LDA
STA
INC
STA
SUBO
DOA
DOB
DOAS
LDA
MSKO
SKPON
JMP
DSZ
JMP
SUBO

-2
0,IBITE
2,CBPT
2,2
2,2
2,2
3,ARY
0,0
0,0,3
3,3
2,2,SZR
-3
0,CBAP
0,CNT1
0,CBPT
0,IPT
0,IBITE
0,CNT2
0,FOUR
0,DCNT
0,ARY
0,CT1
0,0
0,CT2
0,0
0,DACU
0,DACU
0,ADCU
0,ADM1
0
ADCU
-1
DCNT
DUMY
2,2

;IBITE=16,384/# OF POINTS
;DONE!
;# OF POINTS TO AC<2>
;DOUBLE AC<2> FOR FP ARRAY
;DOUBLE AC<2> FOR CMLX ARRAY
;NEGATE AC<2>
;ARY ADDRESS TO AC<3>
;ZERO AC<0>
;ZERO ALL ARRAY LOCATIONS
;INCREMENT POINT COUNTER
;INCREMENT POINT COUNTER
;NOT DONE--GET NEXT POINT
;# OF SWEEPS TO AC<0>
;# OF SWEEPS TO CNT1
;# OF POINTS/SWEEP TO AC<0>
;# OF POINTS/SWEEP TO IPT
;POINT SPACING TO AC<0>
;POINT SPACING TO CNT2
;DUMMY SAMPLE # TO AC<0>
;DUMMY SAMPLE # TO DCNT
;ARRAY SA TO AC<0>
;ARRAY SA TO CT1
;ADD 1 TO ARRAY SA
;ARRAY SA +1 TO CT2
;ZERO AC<0>
;ADDRESS D/A #0
;OUTPUT ZERO TO D/A #0
;START CONVERT, A/D #0
;INTERRUPT MASK TO AC<0>
;DISABLE ALL INTERRUPTS
;CONVERSION DONE?
;NO, KEEP WAITING
;DUMMY SAMPLES DONE?
;NO, TAKE ANOTHER
;ZERO AC<2>

```


B.2.4. Assembly Language Fast Fourier Transform Subroutine

```

$$$
SUBROUTINE FFT(ARRAY, NE, ISGN)
COMPLEX ARRAY(NE)
CONTINUE
A. DUSR FSP= 16
A. DUSR FPU= 76
A. DUSR FPU1= 74
A. DUSR FPU2= 75
A. DIAC PUSH= DOBS
A. DIAC PUSH= DOBS
A. DIAC POP= DOBP
A. DIAC POP= DOBP
A. DIAC XPUSH= DOBC
A. DIAC XPOP= DOB
A. DUSR FADD= DOC
A. DUSR FADD= DOC
A. DUSR FSUB= DOCS
A. DUSR FSUB= DOCS
A. DUSR FMUL= DOCP
A. DUSR FMUL= DOCP
A. DUSR FDIV= DOCC
A. DUSR FDIV= DOCC
A. DIAC XADD= DOA
A. DIAC XADD= DOA
A. DIAC XSUB= DOAS
A. DIAC XSUB= DOAS
A. DIAC XMUL= DOAP
A. DIAC XMUL= DOAP
A. DIAC XDIV= DOAC
A. DIAC XDIV= DOAC
A. DUSR FAB= NIOP
A. DUSR FNEG= NIOP
A. DUSR FLIP= NIOS
A. DUSR FNORM= NIOS
A. DIAC FLDEX= DOBC
0, FPU1
0, FPU2
0, FPU1
0, FPU2
0, FPU1
0, FPU1
0, FPU1
0, FPU2
0, FPU1
0, FPU2
0, FPU1
0, FPU2
0, FPU1
0, FPU2
0, FPU1
0, FPU2
FPU1
FPU1
FPU1
FPU2
0, FPU2

```

A. DIAC	DOB	0, FPU2
A. DIAC	DIA	0, FPU
A. DIAC	DIAC	0, FPU
A. DUSR	NIOC	FPU
A. DIAC	DOA	0, FPU
A	0, T, '3	
A	0, .BASE	
A	0, T, +2, 3	
A	0, SIGN	
A	1, T, +1, 3	
A	0, NMAX	
A	0, 1, SZC	
A	0, 1	
A	3, 3	
A	0, 0	
A	TEST	
A	0, 0	
A LOOP:	3, 3, SNC	
A ATEST:	1, 3, SNC	
A	LOOP	
A	0, 0	
A	0, KCTR	
A	3, 3	
A	3, I COUNT	
A	3, 3	
A ASORTL:	3, 3, SZC	
A	MAIN	
A	0, KCTR	
A	2, 2	
A	3, 1	
A	1, 1	
A	2, 2	
A	0, 0, SZR	
A	INUTL	
A	2, 3, SNC	
FSCAL=	LDA	
RCSR=	STA	
RCSR=	LDAG	
CSR=	STA	
LCSR=	LDAG	
	LDA	
	ADZ#	
	MOU	
	SUBZL	
	ADC	
	JMP	
	INC	
	MOUZL	
	ADZ#	
	JMP	
	NEG	
	STA	
	MOZR	
	STA	
	NEGZ	
	COM	
	JMP	
	LDA	
	SUB	
	MOU	
	MOZR	
	MOUL	
	INC	
	JMP	
	ADZ#	

```

SORTL
3,TST
3,3
2,2
1, BASE
1,3
1,2
0,0,2
1,0,3
0,0,3
1,0,2
0,1,2,3,3
1,1,3,3
0,1,2,3,3
1,2,3,3,2,2,3,3,2
0,2,2,3,3,2,2,3,3,2
1,2,3,3,2
0,3,3,2
1,3,2
3,TST
SORTL

```

```

JMP
STA
ADDZL
ADDZL
LDA
ADD
ADD
LDA
LDA
STA
STA
LDA
LDA
STA
STA
LDA
LDA
STA
STA
LDA
LDA
STA
STA
LDA
JMP 4096.

```

```

A A A A A A A A A A A A A A A A A A A A A A
ANMAX:
A.BASE:
ASIGN:
AICOUNT:
AJCOUNT:
AICTR:
AJCTR:
AKCTR:
AOFFSET:
AJSTART:

```

AISTEP:	0	0, CSR
AMPTR:	0	0
ATST:	0	
ACSRP:	3	3, WPTBL
ACSRN:	2	3, WPTBL
AWTBL:	WTBL	
ACM4:	-4	
ACM5:	-5	
AMAIN:	LDA	
A	LCSR	
A	LDA	
A	STA	
A	SUBZL	
A	STA	
A	LDA	
AKLOOP:	MOVZR	
A	STA	
A	STA	
A	LDA	
A	STA	
A	MOVZL	
A	STA	
A	ADDZL	
A	STA	
A	ADCZL	
A	ADDZL	
A	ADD	
A	STA	
A	LDA	
A	ADD	
AFIRST:	PUSHS	
A	PUSHS	
A	XPUSH	
A	XSUBS	
A	POPS	

```

AAAAAAA
FAODS
POPS
SUB 0,1
SUB 0,2
PUSHS
PUSHS 1
XPUSH 2
XSUBS 0
POPS 2
FAODS
POPS 1
ADD 3,1
ADD 3,2
DSZ ICTR
JMP FIRST
DSZ JCTR
JMP +2
JMP .KEND
SUB 2,2
STA 2,JSTART
LDA 3,MPTR
PUSHS 3
SUB 0,3
PUSHS 3
SUB 0,3
STA 3,MPTR
LDA 2,SIGN
MOVZL# 2,2,SNC
FNEG 0
XPUSH 0
XPUSH 2,I COUNT
LDA 2,ICTR
STA JSTART
ISZ 1,.BASE
LDA
AJLOOP:
AAAAAAA

```

```

A A A A A A A ILOOP:
LDA      3, JSTART
ADDZL   3, 3
ADD     3, 1
LDA     2, OFFSET
ADD     1, 2
PUSHS  2, 2
SUB     0, 2
PUSHS  2, CM4
LDA     0, 3
INC     0, 3
XPUSH  0 3
XMULS  0 3
XPUSH  0 3
XMULS  0 3
FSUBS  0 3
FLIP   0 3
LDA     0, CM5
XMULS  0 0
INC     0, 0
XPUSH  0 0
XMULS  0 0
FAODS  3 0
XPOP   0, 0
ADDZL  0, 2
ADD     0, 2
PUSHS  1 1
FLIP   0 0
XPUSH  0 2
XSUBS  0 2
POPS   1 1
FAODS  0, 1
POPS   0, 2
SUB     0, 1
SUB     0, 2
PUSHB  1 1

```



```

AAAAAA AAAAA AAAAA AAAAA AAAAA AAAAA AAAAA AAAAA AKEND: AAAAA AAAAA AAAAA AAAAA AAAAA AAAAA AAAAA AAAAA
FLIP  XPU  XSUB  POPS  FADD  POPS  LDA   ADD   ADD   DSZ  JMP   DSZ  JMP   SUB  XPOP  XPOP  XPOP  XPOP  ISZ  JMP   LDA  SKPBZ JMP   LCSR IORST JMP  LDA  INC   INC  XPU  XNUL  XNUL  FSUBS FLIP
002   1 3,1STEP 3,1 3,2 ICTR ILOOP JCTR UPDATE 0,0 0 0 0 0 0 KCTR KLOOP 0,CSRN FPU -1 0 RTN 1,CMS 1,2 2,3 2,3 2,3

```

```

A A A A A A A ANTBL:
XMLS 1
XPUSH 2
XMLS 2
FADDS 3
XPOP 3
FLIP JLOOP
JMP 0.0
1.0
0.707106781
0.707106781
0.923879533
0.382683432
0.980785280
0.195090322
0.995184727
9.80171403E-2
0.998795456
4.90676743E-2
0.999698819
2.45412285E-2
0.999924702
1.22715383E-2
0.999981175
6.13588464E-3
0.999995294
3.06795676E-3
0.999998824
1.53398017E-3
SUB 0.0
RETURN
END
ARTN:
*
```

B.2.5. General Time Domain/Frequency Domain Plot Program

```

$$$
Cxxxx
CX * * * * *
CX * * * * *
CX * * * * *
CX * * * * *
CX * * * * *
CX * * * * *
CX * * * * *
CX * * * * *
Cxxxx

PROGRAM GPLT
THIS IS A GENERAL PURPOSE PLOTTING ROUTINE
IT CAN GIVE LINEAR PLOTS, LNR-LOG, LOG-LNR OR LOG-LOG PLOTS
THE FILE TO BE PLOTTED SHOULD HAVE IN THE FIRST THREE VALUES :
NF : TOTAL NO. OF POINTS IN FILE
DIVX : HORIZONTAL SCALE IN UNITS/DIVISION ASSUMING TEN
      DIVISIONS AND UNITS IN EITHER NSEC OR MHZ
US : THE COEFF THAT THE FILE VALUES SHOULD BE MULTIPLIED BY TO
     BECOME IN PROPER UNITS, I.E. FILE VALUE * US = PLOT VALUE
IF FILE DOES NOT CONTAIN THESE VALUES THEY CAN BE ACCEPTED
WHILE RUNNING THE PROGRAM
DIMENSION Y1(1024),Y2(1024)
FORMAT (S8)
FORMAT (9H PLOT OF ,Z)
FORMAT (A2)
FORMAT (" VERT SC =",G12.4," MU/DIU",9X,
X
5 X
6 X
7 X
8 X
9 X
10 X
11 X
12 X
13 X

```

VERT SC =",G12.4," MU/DIU",9X,
 HORIZ SC =",G12.4," NS/DIU")
 VERT SC =",G12.4," UPS/DIU",9X,
 HORIZ SC =",G12.4," MHZ/DIU")
 VERT SC =",G12.4," DB/DIU",9X,
 HORIZ SC =",G12.4," MHZ/DIU")
 VERT SC =",G12.4," NEPERS/DIU",9X,
 HORIZ SC =",G12.4," MHZ/DIU")
 VERT SC =",G12.4," DEG/DIU",9X,
 HORIZ SC =",G12.4," MHZ/DIU")
 VERT SC =",G12.4," RADIANS/DIU",9X,
 HORIZ SC =",G12.4," MHZ/DIU")
 VERT SC =",G12.4," /DIU",9X,
 HORIZ SC =",G12.4," NS/DIU")
 VERT SC =",G12.4," /DIU",9X,
 HORIZ SC =",G12.4," MHZ/DIU")
 VERT SC =",G12.4," MU/DIU",9X,
 XMAX =",G12.4," NSEC")
 VERT SC =",G12.4," UPS/DIU",9X,

```

14 X   XMAX      =",G12.4," MHZ" )
    X   VERT SC  =",G12.4," DB/DIU",9X,
15 X   XMAX      =",G12.4," MHZ" )
    X   VERT SC  =",G12.4," NEPERS/DIU",9X,
16 X   XMAX      =",G12.4," MHZ" )
    X   VERT SC  =",G12.4," DEG/DIU",9X,
17 X   XMAX      =",G12.4," MHZ" )
    X   VERT SC  =",G12.4," RADIANS/DIU",9X,
18 X   XMAX      =",G12.4," MHZ" )
    X   VERT SC  =",G12.4," NSEC" )
19 X   XMAX      =",G12.4," MHZ" )
    X   VERT SC  =",G12.4," /DIU",9X,
20 X   XMAX      =",G12.4," MHZ" )
    X   VERT SC  =",G12.4," /DIU",9X,
21 X   XMAX      =",G12.4," MHZ" )
    X   VERT SC  =",G12.4," NSEC" )
22 X   XMAX      =",G12.4," MHZ" )
    X   VERT SC  =",G12.4," /DIU",9X,
100  IAU=0
105  TYPE " INPUT FILE NAME "
    READ (11,1) IFN
    CALL MSOPEN (6,IFN,"R")
    ACCEPT "NF,DIUX,US IN FILE? 1=YES, 0=NO
    IF (INF.EQ.1) GO TO 150
    IF (IAU.EQ.1) GO TO 110
    READ (6) (Y1(J),J=1,5)
    REWIND 6
    TYPE "XX THE FIRST FIVE VALUES IN FILE #1 ARE :      ",Y1(1)
    TYPE (Y1(J),J=2,5)
    GO TO 120
110  READ (6) (Y2(J),J=1,5)
    REWIND 6
    TYPE "XX THE FIRST FIVE VALUES IN FILE #2 ARE :      ",Y2(1)
    TYPE (Y2(J),J=2,5)
    ACCEPT "X OF POINTS TO BE PLOTTED IN THE FILE =?
    TYPE "VERTICAL SCALE MULTIPLYING FACTOR =?"
    TYPE "NOTE: IF FACTOR=1, DATA WILL BE PLOTTED AND"
120

```

```

TYPE "SCALED AS IT EXISTS IN THE FILE. THIS FACTOR"
ACCEPT "SHOULD BE ENTERED IN TERMS OF UNITS/DIVISION."
TYPE " "
TYPE "DO YOU WISH TO INPUT THE HORIZONTAL SCALE"
TYPE "IN TERMS OF SPACING BETWEEN POINTS (1) OR"
TYPE "UNITS PER DIVISION (2) BASED ON 10 DIVISIONS"
ACCEPT "OF TOTAL DATA WINDOW?"
IF (IDUM.EQ.2) GO TO 130
TYPE "NOTE: SPACING BETWEEN POINTS SHOULD BE INPUT"
TYPE "IN NSEC OR IN MHZ, AS APPROPRIATE."
ACCEPT "SPACING BETWEEN POINTS =?"
GO TO 140
TYPE "NOTE: UNITS PER DIVISION SHOULD BE INPUT"
TYPE "IN NSEC OR IN MHZ, AS APPROPRIATE."
ACCEPT "UNITS/DIVISION =?"
IF (IDUM.EQ.1) GO TO 140
DX=(DIUX*10.0)/FLOAT(NF)
ACCEPT "# OF VALUES TO BE IGNORED IN FILE BEGINNING=?
IF (INF.NE.0) READ (6) (A,J=1,INF)
GO TO 160
READ (6) NF,DIUX,VS
DX=(DIUX*10.0)/FLOAT(NF)
IF (IWJ.EQ.1) GO TO 170
READ (6) (Y1(J),J=1,NF)
GO TO 180
READ (6) (Y2(J),J=1,NF)
CALL FCLOS (6)
IF (IWJ.EQ.1) GO TO 190
TYPE "PLOT SECOND FILE ON THE SAME GRAPH? (1=YES, 0=NO)"
ACCEPT "NOTE: NF, DIUX AND DY MUST BE THE SAME IN BOTH FILES ",IWJ
IF (IWJ.EQ.1) GO TO 105
DO 200 J=1,NF
Y1(J)=Y1(J)*US
IF (IWJ.EQ.0) GO TO 200
Y2(J)=Y2(J)*US

```

","US

","IDUM

","DX

","DIUX

","INF

130

140

150

160

170

180

190

```

200 CONTINUE
TYPE "TYPE OF GRAPH ? (1=MV/T, 2= /T, 3=GAIN/F, 4=PH/F, 5=UPS/F, "
ACCEPT "6= /F, 9=U/F *XSPECIALXX)", IT
LG1=2
LG2=2
IF (IT.EQ.3) ACCEPT "NEPERS (1) OR DECIBELS (2)?" , LG1
IF (IT.EQ.4) ACCEPT "RADIANS (1) OR DEGREES (2)?" , LG2
IF (LG1.EQ.2) GO TO 210
IT=7
IF (LG2.EQ.2) GO TO 220
IT=8
IF (IT.NE.9) GO TO 225
IL2=0
ACCEPT "VDC =?"
GO TO 250
ACCEPT "LOG PLOT? (0=NO, 1=Y-LGX, 2=LGY-X, 3=LGY-LGX)
IL2=IL-IL/2X2
VSC=US
IF (IL.LT.2) GO TO 250
ACCEPT "FILE #1 VALUES? (0=POSITIVE, 1=NEGATIVE)
IF (IPN.NE.1) GO TO 250
DO 230 J=1,NF
Y1(J)=Y1(J)
IF (IMV.EQ.0) GO TO 250
ACCEPT "FILE #2 VALUES? (0=POSITIVE, 1=NEGATIVE)
IF (IPN.NE.1) GO TO 250
DO 240 J=1,NF
Y2(J)=Y2(J)
TYPE "XXXX",NF," POINTS IN FILE  XXXX"
ACCEPT " 0=PLOT ALL, 1=PLOT A PART
IF (IP.NE.0) GO TO 260
NB=1+IL2
NE=NF
N=NE-NB+1
GO TO 270
",VDC
",IL
",IPN
",IPN
",IP

```

" , NB
" , N

```
260 ACCEPT "START AT NB =? (>1 FOR LOG X )  
IF <IL2.NE.0.AND.NB.EQ.1> GO TO 260  
ACCEPT "# OF PLOTTED POINTS  
NE=NB+N-1  
IF <NE.GT.NF> NE=NF  
270 NB1=NB-1  
NE1=NE-1  
IF <IT.NE.9> GO TO 275  
XMIN=0.0  
XMAX=10.0  
YMIN=0.0  
YMAX=1.0  
HSC=1.0  
GO TO 370  
XMIN=NB1#DX  
XMAX=NEX#DX  
YMIN1=+1.E+40  
YMAX1=-1.E+40  
DO 280 J=NB,NE  
IF <Y1<J>.GT.YMAX1> YMAX1=Y1<J>  
IF <Y1<J>.LT.YMIN1> YMIN1=Y1<J>  
IF <IW.EQ.0> GO TO 295  
YMIN2=+1.E+40  
YMAX2=-1.E+40  
DO 290 J=NB,NE  
IF <Y2<J>.GT.YMAX2> YMAX2=Y2<J>  
IF <Y2<J>.LT.YMIN2> YMIN2=Y2<J>  
TYPE "###X XMIN & XMAX ARE : ", XMIN, XMAX, "  
ACCEPT "HORIZ SCALE : 0=FULL, 1=SPECIAL  
IF <IS.EQ.1> ACCEPT "NEW XMIN & XMAX ARE :  
HSC=(1-IL2)#X(XMAX-XMIN)/10.0+IL2#XMIN  
IF <IL2.NE.1> GO TO 300  
IF <XMIN.LT.1.0> GO TO 300  
MX=INT<ALOG10(XMIN)>+0.000001)  
MX1=INT<XMIN/10.0###MX>+0.000001)
```


" , IS
" , XMIN, XMAX

```

300 XMIN=MX1*10.0**MX
    GO TO 310
    MX=INT(ALOG10(XMIN))-0.999999)
    MX1=INT((XMIN/10.0**MX)+0.000001)
    XMIN=MX1*10.0**MX
310 IF (XMAX.LT.1.0) GO TO 320
    MX=INT(ALOG10(XMAX)+0.000001)
    MX1=INT((XMAX/10.0**MX)-0.000001)+1
    XMAX=MX1*10.0**MX
    GO TO 330
320 MX=INT(ALOG10(XMAX)-0.999999)
    MX1=INT((XMAX/10.0**MX)-0.000001)+1
    XMAX=MX1*10.0**MX
    CONTINUE
330 TYPE "xxxx YMIN1 & YMAX1 ARE :", YMIN1, YMAX1, "
    YMIN=YMIN1
    YMAX=YMAX1
    IF (IUV.EQ.0) GO TO 335
    TYPE "xxxx YMIN2 & YMAX2 ARE :", YMIN2, YMAX2, "
    IF (YMIN2.LT.YMIN1) YMIN=YMIN2
    IF (YMAX2.GT.YMAX1) YMAX=YMAX2
335 ACCEPT "VERT SCALE : 0=FULL, 1=SPECIAL
    IF (IS.EQ.0) GO TO 350
340 ACCEPT "NEW YMIN & YMAX ARE :
350 IF (IL.LT.2) GO TO 370
    YSIGN=YMIN*YMAX
    IF (YSIGN.GE.0.0) GO TO 370
    TYPE "FOR LOG Y PLOTS BOTH YMIN & YMAX MUST HAVE THE SAME SIGN."
    GO TO 340
370 USC=(1-IL/2)*(YMAX-YMIN)/10.0+IL/2*YMIN
    IF (IL.LT.2) GO TO 410
    IF (YMIN.LT.1.0) GO TO 380
    MY=INT(ALOG10(YMIN)+0.000001)
    MY1=INT((YMIN/10.0**MY)+0.000001)
    YMIN=MY1*10.0**MY

```



```

380 GO TO 390
MY=INT(ALOG10(YMIN))-0.999999)
MY1=INT((YMIN/10.0**MY)+0.000001)
YMIN=MY1*10.0**MY
IF (YMAX.LT.1.0) GO TO 400
MY=INT(ALOG10(YMAX)+0.000001)
MY1=INT((YMAX/10.0**MY)+0.000001)+1
YMAX=MY1*10.0**MY
GO TO 410
400 MY=INT(ALOG10(YMAX))-0.999999)
MY1=INT((YMAX/10.0**MY)+0.000001)+1
YMAX=MY1*10.0**MY
TYPE "XMIN=",XMIN," XMAX=",XMAX
TYPE "YMIN=",YMIN," YMAX=",YMAX
PAUSE
CALL INITT (0)
CALL DWINDO (XMIN,XMAX,YMIN,YMAX)
CALL TWINDO (0,1023,80,719)
IF (IL.NE.0) CALL LOGTRN (IL)
Q=YMIN
IF (IL.GE.2) GO TO 430
CALL MOVEA (XMIN,Q)
CALL DRAMA (XMAX,Q)
DO=USC
DO 420 J=1,10
Q=Q+DO
CALL MOVEA (XMIN,Q)
CALL DRAMA (XMAX,Q)
GO TO 470
DO 460 J=1,200
CALL MOVEA (XMIN,Q)
CALL DRAMA (XMAX,Q)
IF (Q.LT.1.0) GO TO 440
MY=INT(ALOG10(Q)+0.000001)
GO TO 450

```

```

440 MY=INT(ALOG10(Q))-0.9999999
450 Q=Q+10.0*XY
    IF (Q.GT.YMAX) GO TO 470
460 CONTINUE
470 Q=XMIN
    IF (IL2.EQ.1) GO TO 490
    CALL MOVEA (Q, YMIN)
    CALL DRAMA (Q, YMAX)
    DO=HSC
    DO 480 J=1,10
    Q=Q+DQ
    CALL MOVEA (Q, YMIN)
    CALL DRAMA (Q, YMAX)
480 IF (IT.EQ.9) GO TO 601
    GO TO 530
490 DO 520 J=1,200
    CALL MOVEA (Q, YMIN)
    CALL DRAMA (Q, YMAX)
    IF (Q.LT.1.0) GO TO 500
    MX=INT(ALOG10(Q))+0.000001
    GO TO 510
500 MX=INT(ALOG10(Q))-0.9999999
510 Q=Q+10.0*MX
    IF (Q.GT.XMAX) GO TO 530
520 CONTINUE
530 IF (IT.LE.2) GO TO 550
    NC=NB+1
    CALL MOVEA (NB*DX, Y1(NB))
    DO 540 J=NC,NE
    Z=FLOAT(J)
    CALL DRAMA (Z*DX, Y1(J))
    GO TO 570
540 CALL MOVEA (NB1*DX, Y1(NB))
550 DO 560 J=NB,NE1
    Z=FLOAT(J)

```

```

560 CALL DRAWA (Z*DX, Y1<J+1>)
570 IF (IW.EQ.0) GO TO 610
    IF (IT.LE.2) GO TO 590
    NC=NB+1
    CALL MOVEA (NB*DX, Y2<NB>)
    DO 580 J=NC, NE
    Z=FLOAT (J)
    CALL DRAWA (Z*DX, Y2<J>)
    GO TO 610
580 CALL MOVEA (NB1*DX, Y2<NB>)
    DO 600 J=NB, NE1
    Z=FLOAT (J)
    CALL DRAWA (Z*DX, Y2<J+1>)
    GO TO 610
600 XX=ALOG10(1.0/(DIUXX1.0E-8))
    CALL MOVEA (0.0, VDC)
    CALL DRAWA (XX, Y1<1>)
    DO 602 J=2, 1024
    Z=FLOAT (J)
    XX=ALOG10(1024.0/(1025.0-Z)*DIUXX1.0E-8))
    CALL DRAWA (XX, Y1<J>)
    XX=ALOG10(1.0/(DIUXX1.0E-8))
    CALL MOVEA (0.0, 0.0)
    CALL DRAWA (XX, Y2<1>)
    DO 603 J=2, 1024
    Z=FLOAT (J)
    XX=ALOG10(1024.0/(1025.0-Z)*DIUXX1.0E-8))
    CALL DRAWA (XX, Y2<J>)
    CALL HOME
    WRITE (10, 20) N, NB, XMIN
    WRITE (10, 21) YMAX
    CALL RESET
    CALL MOVABS (10, 00)
    CALL ANMODE
    WRITE (10, 22) YMIN

```

```

IF < IL2.NE.0 > GO TO 620
IF < IT.EQ.1 > WRITE < 10,4 > USC,HSC
IF < IT.EQ.2 > WRITE < 10,10 > USC,HSC
IF < IT.EQ.3 > WRITE < 10,6 > USC,HSC
IF < IT.EQ.4 > WRITE < 10,8 > USC,HSC
IF < IT.EQ.5 > WRITE < 10,5 > USC,HSC
IF < IT.EQ.6 > WRITE < 10,11 > USC,HSC
IF < IT.EQ.7 > WRITE < 10,7 > USC,HSC
IF < IT.EQ.8 > WRITE < 10,9 > USC,HSC
GO TO 630
IF < IT.EQ.1 > WRITE < 10,12 > USC,XMAX
IF < IT.EQ.2 > WRITE < 10,18 > USC,XMAX
IF < IT.EQ.3 > WRITE < 10,14 > USC,XMAX
IF < IT.EQ.4 > WRITE < 10,16 > USC,XMAX
IF < IT.EQ.5 > WRITE < 10,13 > USC,XMAX
IF < IT.EQ.6 > WRITE < 10,19 > USC,XMAX
IF < IT.EQ.7 > WRITE < 10,15 > USC,XMAX
IF < IT.EQ.8 > WRITE < 10,17 > USC,XMAX
WRITE < 10,2 >
READ < 11,3 > IC9DF
CALL HOME
ACCEPT " 0=STOP , 1=PLOT SAME FILE , 2=PLOT NEW FILE ",IC
IF < IC-1 > 999,220,100
999 END
*
```

B.3. Cable Modeling and Analysis Programs

B.3.1. Main Cable Model Program for Calculations of "m", "K", and Cable Impulse Response

```

$$$
C
CABLE MODEL PROGRAM USING PLANAR SKIN EFFECT MODEL
DIMENSION AK(300),BK(150),C(150),DK(1024),G(2),KK(2)
COMPLEX F(2048),SM,Z0,GM,RHO,AA,AB
PI=3.14159265
ACCEPT "CABLE LENGTH IN FEET CORRESPONDING TO M & K =?" " ,XLEN
ACCEPT "CABLE INDUCTANCE PER FOOT =?" " ,XL
ACCEPT "CABLE CAPACITANCE PER FOOT =?" " ,XC
ACCEPT "CABLE RESISTANCE PER FOOT =?" " ,R
ACCEPT "CABLE CONDUCTANCE PER FOOT =?" " ,XG
ACCEPT "INPUT OR COMPUTE M & K? (1=INPUT, 0=COMPUTE)" " ,N1
IF (N1.EQ.1) GO TO 130
TYPE " "
TYPE "CALCULATION OF M AND K:"
TYPE " "
NHARM=50
CALL MSOPEN (5,"MNEP","R")
READ (5) I
READ (5) DIVX
READ (5) X
DO 10 J=1,300
  READ (5) AK(J)
  AK(J)=AK(J)/XLEN
CALL FCLOS (5)
FO =DIVX*1.0E +6)/30.0
NH1=NHARM-1
XH1=FLOAT(NH1)
NH2=NH1+50
XH2=FLOAT(NH2)
DO 20 J=1,150
  XJ=FLOAT(J)
  F1=(XH1+XJ)*FOX2.0*PI
  F2=(XH2+XJ)*FOX2.0*PI
  BK(J)=(ALOG(AK J+NH2))-(ALOG(AK J+NH1))-(ALOG(F2)-ALOG(F1))
  EM=0.0
10
20

```

```

30      DO 30 J=1,150
        EM=EM+X*J)
        EM=EM/150.0
        PHI=(EM-1.0)*PI/2.0
        DO 70 J=1,150
            XK(1)=1.0E-15
            XK(2)=10.0
            XJ=FLOAT(J)
            M=0
            DO 50 K=1,2
                F1=(X*H1+X*J)*FO*2.0*PI
                X=XL+XK(K)*K*(F1*(EM-1.0))*COS(PHI)
                Y=-R/F1+XK(K)*K*(F1*(EM-1.0))*SIN(PHI)
                TTA=ATAN2(Y,X)
                A1=SQRT(X*X+Y*Y)
                A2=SIN(TTA/2.0)
                G(K)=A*(J+H1)+F1*SQRT(X*X+Y*Y)*A2
                M=M+1
                XKD=(XK(2)+XK(1))/2.0
                X=XL+XKD*(F1*(EM-1.0))*COS(PHI)
                Y=-R/F1+XKD*(F1*(EM-1.0))*SIN(PHI)
                TTA=ATAN2(Y,X)
                A1=SQRT(X*X+Y*Y)
                A2=SIN(TTA/2.0)
                GD=A*(J+H1)+F1*SQRT(X*X+Y*Y)*A2
                IF (ABS(GD).LE.1.0E-8) GO TO 70
                IF (M.GT.5000) GO TO 999
                IF (GD.GT.0.0) GO TO 60
                XK(2)=(XK(2)+XK(1))/2.0
                GO TO 40
            XK(1)=(XK(2)+XK(1))/2.0
            GO TO 40
        C(J)=(XK(2)+XK(1))/2.0
        EK=0.0
        DO 80 J=1,150

```

```

80  EK=EK+C<J>
    EK=EK/150.0
    SEM=0.0
    SK=0.0
    DO 90 J=1,50
    SEM=SEM+(EM-BX J)*X(EM-BX J)
    DO 100 J=1,50
    SK=SK+(EK-C<J>)*X(EK-C<J>)
    SEM=SQRT(SEM/49.0)
    SK=SQRT(SK/49.0)
    WRITE (10,110)EM,SEM
    WRITE (10,120)EK,SK
    FORMAT (1X,/' SLOPE M="F10.5" SIGMA M)="F10.5)
    FORMAT (1X,/' CONSTANT K="E13.5" OHMS/FTXHZOHM SIGMA K)="E13.5/
    TYPE "CALCULATION OF CABLE IMPULSE RESPONSE FROM MODEL."
    ACCEPT "DESIRED CABLE LENGTH IN FEET =?"
    ACCEPT "DESIRED FIRST HARMONIC IN HZ =?"
    IF (N1.EQ.0) GO TO 140
    ACCEPT "CABLE LOSS SLOPE M =?"
    ACCEPT "CABLE LOSS CONSTANT PER FOOT K =?"
    R0=SQRT(XL/XC)
    W=2.0*PI*XF1
    DC=2.0*XRO/(2.0*XRO+R*XLEN)
    F<1>=CMPLX(0.0,0.0)
    DO 150 J=1,511
    FJ=WXFLOAT<J>
    X=F J*XM
    X1=COS(EM*PI/2.0)
    X2=SIN(EM*PI/2.0)
    SM=X*CMPLX(X1,X2)
    X1=R+EK*REAL(SM)
    X2=XL*F J*EK*AIMAG(SM)
    AA=CMPLX(X1,X2)
    X1=XC*F J
    AB=AA/CMPLX(XG,X1)

```

```

X=CABS(AB)
X=SQRT(X)
X2=ATAN2(AIMAG(AB),REAL(AB))/2.0
Z0=XCMPLEX(COS(X2),SIN(X2))
AB=AA*CMPLX(XG,X1)
X=CABS(AB)
X=SQRT(X)
X2=ATAN2(AIMAG(AB),REAL(AB))/2.0
GM=XCMPLEX(COS(X2),SIN(X2))
X1=FJ*SQRT(XC*XL)
GM=GM*CMPLX(0.0,X1)
RHO=(R0-Z0)/(R0+Z0)
AA=(4.0*R0*Z0)/(R0+Z0)*(R0+Z0)*(R0+Z0)
AB=CEXP(-XLEN*GM)/(1.0-RHO*RHO)*EXP(-2.0*XLEN*GM)
F(J+1)=AA*AB
CALL MSOPEN(5,"MAG","W")
NPT=511
DIUX=F1*51.2E-6
DY=1.0
WRITE(5) NPT
WRITE(5) DIUX
WRITE(5) DY
DO 160 J=2,512
X=-20.0*XALOG10(CABS(F(J)))
WRITE(5) X
CALL FCLOS(5)
CALL MSOPEN(5,"PHAZ","W")
WRITE(5) NPT
WRITE(5) DIUX
WRITE(5) DY
SHIFT=0.0
DO 190 J=2,512
X=ATAN2(AIMAG(F(J)),REAL(F(J)))
X=XX*180.0/PI)
IF (J.EQ.2) GO TO 180

```

150

160


```

X1=X
PROD=X2**X
IF (PROD.GE.0.0) GO TO 180
IF (ABS(X).LE.90.0) GO TO 180
IF (X2.GT.0.0) GO TO 170
SHIFT=SHIFT-360.0
GO TO 180
SHIFT=SHIFT+360.0
X=X+SHIFT
X2=X1
WRITE (5) X
CALL FCLOS (5)
F(513)=(0.0,0.0)
DO 200 J=1,511
F(J+513)=CONJG(F(513-J))
N=1024
CALL FFT (F,M,-1)
DIUX=1.0E9/(10.0*F1)
TYPE "ESTABLISHMENT OF THE DC LEVEL FOR THE TIME DOMAIN IMPULSE"
TYPE "RESPONSE: DO YOU WISH TO INPUT THE 0.9T DC LEVEL (TYPE 1),"
TYPE "CALCULATE THE 0.9T DC LEVEL (TYPE 2) OR SET THE TAIL EQUAL" ",I
ACCEPT "TO ZERO (TYPE 3)"

DC
IF (IDC.EQ.2) GO TO 210
IF (IDC.EQ.3) GO TO 240
TYPE " "
ACCEPT "F(T) AT 0.9T =?"

T
GO TO 220
CALL DC(XL,XC,R,XG,EK,EM,XLEN,DIUX,FT)
Z=FT-REAL(F(922))/1024.0
DO 230 J=1,1024
DXJ=REAL(F(J))/1024.0
DXJ)=DXJ)+Z
GO TO 270

```

```

240 Z=0.0
250 DO 250 J=1010,1014
Z=Z+REAL(F(J))
Z=Z/5.0
260 DO 260 J=1,1024
DX(J)=REAL(F(J))-Z
DX(J)=DX(J)/1024.0
270 DX(1)=0.0
CALL MSOPEN (5,"TIR","W")
WRITE (5) M
DY=1.0
WRITE (5) DIUX
WRITE (5) DY
280 DO 280 J=1,1024
WRITE (5) DX(J)
CALL FCLOS (5)
ACCEPT "COMPARE MODEL WITH MEASUREMENT? (1=YES, 0=NO) " ,N2
IF (N2.EQ.0) GO TO 999
TYPE "RESPONSE WAVEFORM ACQUISITION--- SET S.O. TIME BASE"
TYPE "TO",DIUX," NS/CM"
ACCEPT "NUMBER OF POINTS PER X LOCATION =?"
ACCEPT "VERTICAL SCALE FACTOR IN MU/CM =?"
CALL 500 (10,1024,E)
CALL 500 (NPNT,1024,E)
290 DO 290 J=1,1024
E(J)=E(J)*DIUY/(NPNT*1638.4)
CALL MSOPEN (5,"T2M","W")
WRITE (5) M
WRITE (5) DIUX
WRITE (5) DY
300 DO 300 J=1,1024
WRITE (5) E(J)
CALL FCLOS (5)
TYPE "REFERENCE WAVEFORM ACQUISITION---SET S.O. TIME BASE"
TYPE "TO",DIUX," NS/CM"

```

NPNT
VERT

ACCEPT "NUMBER OF POINTS PER X LOCATION =?"
ACCEPT "VERTICAL SCALE FACTOR IN MU/CM =?"

CALL S00 (10,1024,E)
CALL S00 (NPNT,1024,E)

DO 310 J=1,1024
E(J)=E(J)*VERT)/(NPNT*1638.4)
Z=0.0

DO 320 J=10,29
Z=Z+E(J)
Z=Z/20.0

DO 330 J=1,1024
E(J)=E(J)-Z
DO 335 J=1,5
E(J)=0.0

DO 350 J=1,1024
Z=0.0

DO 340 K=1,J
Z=Z+DK)*E(J+1-K)
CONTINUE

F(J)=CMPLX(Z,0.0)
CALL MSOPEN (5,"T1M","W")

WRITE (5) M
WRITE (5) DIUX
WRITE (5) DY

DO 360 J=1,1024
WRITE (5) E(J)
CALL FCLOS (5)

CALL MSOPEN (5,"TIRXT1","W")
WRITE (5) M
WRITE (5) DIUX
WRITE (5) DY

DO 370 J=1,1024
X=REAL(F(J))
WRITE (5) X
CALL FCLOS (5)

310

320

330

335

340

350

360

370

999 END *

B.3.2. Main Cable Model Program for Calculation of Cable Step Response, Bit Error Waveform and Cable Square Wave Response

```

T$$
C
C
MAIN PROGRAM FOR CALCULATION OF CABLE IMPULSE RESPONSE, STEP
RESPONSE, BIT-ERROR WAVEFORM AND SQUARE WAVE RESPONSE.
DIMENSION DK(1024),E(1024)
COMPLEX F(1024),SM,Z0,G1,RHO,AA,AB,AC,AD
PI=3.14159265
ACCEPT "CABLE INDUCTANCE PER FOOT =?"
ACCEPT "CABLE CAPACITANCE PER FOOT =?"
ACCEPT "CABLE RESISTANCE PER FOOT =?"
ACCEPT "CABLE CONDUCTANCE PER FOOT =?"
ACCEPT "CABLE CONSTANT K =?"
ACCEPT "CABLE CONSTANT M =?"
ACCEPT "DESIRED CABLE LENGTH IN FEET =?"
ACCEPT "DESIRED FIRST HARMONIC IN HZ =?"
R0=SQRT(XL/XC)
N=2.0*PI*F1
UDC=2.0*RO/(2.0*RO+R*XLEN)
F(1)=CMPLX(0.0,0.0)
DO 10 J=1,511
FJ=AFLOAT(J)
X=FJ*AKEM
X1=DCOS(EM*PI/2.0)
X2=DSIN(EM*PI/2.0)
SM=X*CMPLX(X1,X2)
X1=R+EK*REAL(SM)
X2=XL*FJ*EK*XIMAG(SM)
AA=CMPLX(X1,X2)
X1=XCNFJ
AB=AA/CMPLX(XG,X1)
X=CABS(AB)
X=SQRT(X)
X2=ATAN2(XIMAG(AB),REAL(AB))/2.0
Z0=X*CMPLX(COS(X2),SIN(X2))
AB=AA*CMPLX(XG,X1)
X=CABS(AB)

```

```

",XL
",XC
",R
",XG
",EK
",EM
",XLEN
",F1

```

```

X=SQRT(X)
X2=ATAN2(AIMAG(AB),REAL(AB))/2.0
GM=XX*CMPLX(COS(X2),SIN(X2))
X1=F J*SQRT(XC*XL)
GM=GM-CMPLX(0.0,X1)
RHO=(R0-Z0)/(R0+Z0)
AA=(4.0*R0*Z0)/(R0+Z0)*(R0+Z0)
AB=(CEXP(-XLEN*GM))/(1.0-RHO*RHO*CEXP(-2.0*XLEN*GM))
F(J+1)=AA*AB
CALL MSOPEN(5,"MAG1","W")
NPT=511
DIUX=F1*51.2E-6
DY=1.0
WRITE(5) NPT
WRITE(5) DIUX
WRITE(5) DY
DO 20 J=2,512
X=-20.0*ALOG10(CABS(F(J)))
WRITE(5) X
CALL FCLOS(5)
CALL MSOPEN(5,"FAZ1","W")
WRITE(5) NPT
WRITE(5) DIUX
WRITE(5) DY
SHIFT=0.0
DO 50 J=2,512
X=ATAN2(AIMAG(F(J)),REAL(F(J)))
X=XX*180.0/PI)
IF (J.EQ.2) GO TO 40
X1=X
PROD=X2*XX
IF (PROD.GE.0.0) GO TO 40
IF (ABS(X).LE.90.0) GO TO 40
IF (X2.GT.0.0) GO TO 30
SHIFT=SHIFT-360.0

```

10

20

```

30 GO TO 40
SHIFT=SHIFT+360.0
40 X=X+SHIFT
X2=X1
50 WRITE (5) X
CALL FCLOS (5)
F(513)=(0.0,0.0)
DO 60 J=1,511
F(J+513)=CONJG(F(513-J))
M=1024
CALL FFT (F,M,-1)
DIUX=1.0E9/(10.0XF1)
TYPE "ESTABLISHMENT OF THE DC LEVEL FOR THE TIME DOMAIN IMPULSE"
TYPE "RESPONSE: DO YOU WISH TO INPUT THE 0.9T DC LEVEL (TYPE 1),"
TYPE "CALCULATE THE 0.9T DC LEVEL (TYPE 2) OR SET THE TAIL EQUAL"
ACCEPT "TO ZERO (TYPE 3)?"
IF (IDC.EQ.2) GO TO 70
IF (IDC.EQ.3) GO TO 100
TYPE " "
ACCEPT "F(T) AT 0.9T =?"
GO TO 80
70 CALL DC(XL,XC,R,XG,EK,EM,XLEN,DIUX,FT)
80 Z=FT-REAL(F(922))/1024.0
DO 90 J=1,1024
DX(J)=REAL(F(J))/1024.0
DX(J)=DX(J)+Z
GO TO 130
100 Z=0.0
DO 110 J=1010,1014
Z=Z+REAL(F(J))
Z=Z/5.0
DO 120 J=1,1024
DX(J)=REAL(F(J))-Z
DX(J)=DX(J)/1024.0
130 DX(1)=0.0
" ,FT

```

```

CALL MSOPEN (5, "TIR", "W")
WRITE (5) M
UY=1.0
WRITE (5) DIUX
WRITE (5) DY
DO 140 J=1,1024
X=DX*J)
WRITE (5) X
CALL FCLOS (5)
Z=0.0
DO 150 J=1,1024
Z=Z+DX(1025-J)
TYPE " "
TYPE "X DC) =",UDC
TYPE "U FINAL =",Z
TYPE " "
ACCEPT "SQUARE WAVE RESPONSE CALCULATION? (1=YES, 0=NO) " ,N1
IF (N1.EQ.0) GO TO 260
ACCEPT "REDUCE TMOOR TO N POINTS----N=? " ,NIMP
NJ=1024/NIMP
DO 160 J=1,NIMP
DX J)=FLOAT(NJ)*DX(1+NLX(J-1))
DO 170 J=NIMP,1024
DX J)=0.0
ACCEPT "# OF SQUARE WAVE CYCLES =? " ,NSQ
DO 180 J=1,1024
E(J)=1.0
NNEG=1024/(NSQ*2)
DO 190 J=1,NSQ
DO 190 K=1,NNEG
E(K+2*(J-1))*NNEG+NEG)=0.0
DIUX=DIUX+XNJ
CALL MSOPEN (5, "TIR1", "W")
WRITE (5) M
WRITE (5) DIUX

```



```

200 WRITE (5) DY
    DO 200 J=1,M
    WRITE (5) D(J)
    CALL FCLOS (5)
    CALL MSOPEN (5, "SQW", "W")
    WRITE (5) M
    WRITE (5) DIUX
    WRITE (5) DY
210 DO 210 J=1,M
    WRITE (5) E(J)
    CALL FCLOS (5)
    DO 230 J=1,1024
    Z=0.0
    DO 220 K=1,J
    Z=Z+D(K)*E(J+1-K)
    CONTINUE
220 F(J)=CMPLX(Z,0.0)
230 NSQ2=2*NSQ
    DO 240 J=1,NSQ2
    X=REAL(F(J*NEG))
    TYPE "U IN INTERVAL #",J," IS",X," VOLTS"
    CALL MSOPEN (5, "TIRXSQ", "W")
    WRITE (5) M
    WRITE (5) DIUX
    WRITE (5) DY
250 DO 250 J=1,1024
    X=REAL(F(J))
    WRITE (5) X
260 CALL FCLOS (5)
    ACCEPT "STEP RESPONSE CALCULATION? (1=YES, 0=NO) " ,N2
    IF (N2.EQ.0) GO TO 999
    Z=0.0
    DO 270 J=1,1024
    Z=Z+D(J)
    F(J)=CMPLX(Z,0.0)
270

```

```

CALL MSOPEN (5, "STEP", "W")
WRITE (5) M
WRITE (5) DIUX
WRITE (5) DY
DO 280 J=1,1024
X=REAL(F(J))
WRITE (5) X
CALL FCLOS (5)
CALL MSOPEN (5, "BR1", "W")
WRITE (5) M
WRITE (5) DIUX
WRITE (5) DY
DO 290 J=1,512
X=REAL(F(1025-J))
F(1025-J)=F(J)
F(J)=CMPLX(X,0.0)
DO 300 J=1,1024
X=REAL(F(J))
WRITE (5) X
CALL FCLOS (5)
CALL MSOPEN (5, "BR2", "W")
WRITE (5) M
WRITE (5) DIUX
WRITE (5) DY
DO 310 J=1,1024
X=VDC-REAL(F(J))
WRITE (5) X
CALL FCLOS (5)
END
999
*
```

280

290

300

310

999

*

B.3.3. Main Cable Model Program for Calculation of Unit Step TDR Waveform

```

$$$
C
MAIN PROGRAM FOR CALCULATION OF STEP TDR WAVEFORM
DIMENSION UK(2048)
ACCEPT "CABLE INDUCTANCE PER FOOT =?"
ACCEPT "CABLE RESISTANCE PER FOOT =?"
ACCEPT "CABLE LOSS SLOPE, M=?"
ACCEPT "CABLE LOSS CONSTANT PER FOOT, K =?"
ACCEPT "CABLE CHARACTERISTIC IMPEDANCE, Z0 =?"
ACCEPT "GENERATOR OUTPUT RESISTANCE, RG =?"
REFF=2.0*Z0/(Z0+RG)
PI=3.14159265
F=1.0E3
DF=1.0E3
F=F+DF
M=2.0*PI*X
Z=RXR/(M*M*X*X)
Z=Z+(2.0*RXR*X)/(EM-2.0)*COS(EM*PI/2.0)/(X*X)
Z=Z+EKX/(2.0*EM-2.0)/(X*X)
Z=SQRT(Z)
IF (Z.GE.1.0) GO TO 5
TL=1.0/F
TYPE "F<LONG>=",F," T<LONG>=",TL
ACCEPT "DESIRED DELTA T =?"
ACCEPT "DESIRED # OF POINTS =?"
ACCEPT "DESIRED # OF SERIES TERMS =?"
LL=0
12 IF (LL.EQ.1) NTERM=NTERM-1
DO 40 J=1,NPNT
IF (LL.EQ.1) J=NPNT
IF (LL.EQ.1) XX=0.5*REFF
IF (LL.EQ.0) UK(J)=0.5*REFF
FJ=FLOAT(J)-1.0
T=DT*XFJ
DO 30 N=1,NTERM
BN=SIGN(1.0/FLOAT(2*N+2),(-1.0)**(N+1))

```

",XL
 ",R
 ",EM
 ",EK
 ",Z0
 ",RG

",DT
 ",NPNT
 ",NTERM

```

BN=BN*REFF
DO 10 I=1,N
BN=BN*FLOAT(2*I-1)
BN=BN/FLOAT(2*I)
NN=NN+1
AN=0.0
DO 20 II=1,NN
I=II-1
ANI=GAMAX FLOAT(N+1)/GAMAX FLOAT(I+1)
ANI=ANI*(R**(N-I))/GAMAX FLOAT(N-I+1)
ANI=ANI*(E**(I))/(XL**(N))
ANI=ANI*(T**(N-I*EM))/GAMAX(N-I*EM+1)
AN=AN+ANI
IF (LL.EQ.1) XX=XX+ANXBEN
IF (LL.EQ.0) UK(J)=UK(J)+ANXBEN
CONTINUE
CONTINUE
IF (LL.EQ.1) GO TO 60
CALL MSOPEN (5,"TOR","W")
DY=1.0
DIUX=NPNT*DT*1.0E8
WRITE (5) NPNT
WRITE (5) DIUX
WRITE (5) DY
DO 50 J=1,NPNT
WRITE (5) UK(J)
CALL FCLOS (5)
LL=1
GO TO 12
XX=ABS(XX-UK(NPNT))
TYPE "MAXIMUM ERROR IN LAST POINT IS",XX," VOLTS"
TYPE "
END

```

*

B.3.4. Main Program for Calculation of Cable Matching Network Resistors

```

T$*
" T- OR H-MATCHING ANALYSIS FOR MATCHING GENERATORS TO"
" LOADS WITH EITHER A RESISTIVE T NETWORK (UNBALANCED LINES),"
" OR A RESISTIVE H NETWORK (BALANCED LINES): PROGRAM INPUTS"
" ARE TOTAL GENERATOR RESISTANCE, TOTAL LOAD RESISTANCE, AND"
" A START VALUE, STOP VALUE AND STEP SIZE FOR R3, THE NETWORK"
" SHUNT RESISTOR. THE PROGRAM THEN CALCULATES THE VALUES OF"
" R1, THE GENERATOR-SIDE RESISTOR(S), AND R2, THE LOAD-SIDE"
" RESISTOR(S), FOR EACH ASSUMED VALUE OF R3."
TYPE " "
TYPE " "
K1=1
ACCEPT "GENERATOR RESISTANCE = ?",RG
ACCEPT "LOAD RESISTANCE = ?",RL
ACCEPT "R3= ???",R3
IF (K1.EQ.1) GO TO 7
WRITE (10,6) RG,RL
GO TO 11
WRITE (10,8) RG,RL
TYPE " "
TYPE " "
B=2.0/R3
C=(RL-RG)*R3*(R3-RL*(RG/RG))/RL
IF (B*8.LT.4.0*8) GO TO 10
D=SQRT(B*8-4.0*8)
R1=(D-B)/2.0
R2=(RL*(R1+(RL-RG)*R3))/RG
IF (R2.LT.0.0) GO TO 10
IF (K1.EQ.1) R1=R1/2.0
IF (K1.EQ.1) R2=R2/2.0
WRITE (10,20) R3,R1,R2
GO TO 100
WRITE (10,30) R3
CONTINUE
FORMAT (1X,"FOR R3 =",F8.2," ,R1 =",F8.2," AND R2 =",F8.2)
10
100
20

```

```
30 FORMAT (1X, "FOR R3 =", F8.2, " SOLUTION IMPOSSIBLE" )  
6  FORMAT (1X, "UNBALANCED LINE WITH RG=", F8.2, " AND RL=", F8.2 )  
8  FORMAT (1X, "BALANCED LINE WITH RG=", F8.2, " AND RL=", F8.2 )  
    PAUSE  
    ACCEPT "ANOTHER RUN? (1=YES, 0=NO)", N  
    IF (N.EQ.1) GO TO 5  
    END
```

*

B.3.5. Main Program for Calculation of the Error Function

```

134
C
MAIN PROGRAM FOR COMPUTATION OF ERROR FUNCTION
DOUBLE PRECISION B1,B2,B3,B4,B5,P,X,Z,T,COF,COF1
B1=0.31938153000
B2=-0.35656378200
B3=1.78147793700
B4=-1.82125597800
B5=1.33027442900
P=0.231641900
ACCEPT "X(1)=?",X1
ACCEPT "X(2)=?",X2
ACCEPT "STEP SIZE =?",XS
DY=1.0
CALL MSOPEN (5,"COF","W")
NPNT=INT((X2-X1)/XS+0.0001)
DIUX=(X2-X1)/10.0
WRITE (5) NPNT
WRITE (5) DIUX
WRITE (5) DY
X=DBLE(X1)
DO 10 J=1, NPNT
Z=X
T=1.000/(1.000+P*XZ)
COF=1.000-(0.3989422804014300)*DEXP(-0.500*XZ*XZ)*X*(B1*XT+B2*XT*XT+B3*
1TX*XT+B4*XT*XT*XT+B5*XT*XT*XT*XT)
TYPE "X=",X
COF1=1.000-COF
TYPE "1-COF=",COF1
CO=SINGL(COF1)
WRITE (5) CO
X=X+DBLE(XS)
CONTINUE
CALL FCLOS (5)
END
10
*
```

B.3.6. Function Subroutine for Calculation of the Gamma Function

```

FUNCTION GAMA (X)
DOUBLE PRECISION XD,B1,B2,B3,B4,B5,B6,B7,B8,C1,GAM
B1=-0.57719165200
B2=-0.98820589100
B3=-0.89705693700
B4=-0.91820685700
B5=-0.75670407800
B6=-0.48219939400
B7=-0.19352781800
B8=-0.03586834300
XD=DBLE(X)-1.000
IF (XD.GE.0.000) GO TO 10
TYPE "ERROR---ARGUMENT OF GAMMA FUNCTION FOR THIS PROGRAM MUST BE"
TYPE "GREATER THAN OR EQUAL TO 1.0"
STOP
C1=1.000
IF (XD.LE.1.000) GO TO 30
C1=C1*XD
XD=XD-1.000
IF (XD.GT.1.000) GO TO 20
GAM=1.000+B1*XD+B2*XD*XD+B3*XD*XD*XD+B4*XD*XD*XD*XD
GAM=GAM+B5*XD*XD*XD*XD*XD+B6*XD*XD*XD*XD*XD*XD
GAM=GAM+B7*XD*XD*XD*XD*XD*XD*XD+B8*XD*XD*XD*XD*XD*XD*XD*XD
GAM=C1*GAM
GAMA=SNGL(GAM)
RETURN
END
10
20
30

```

*

B.3.7. Subroutine for Accurate Calculations of Cable Time Domain Impulse Response dc Level

```

SUBROUTINE DC(XLS,XCS,RS,XGS,EKS,EMS,XLENS,DIUXS,FTS)
DOUBLE PRECISION XL,XC,R,XG,EK,EM,XLEN,FK,R0,F1,W,DCO,X1,X2,X3,
1FFJ,FTT,X,PI,PN,FFJ,FT,DIUX
DOUBLE PRECISION COMPLEX SM,Z0,GM,RHO,AA,AB,AC
PI=3.14159265358979300
XL=DBLE(XLS)
XC=DBLE(XCS)
R=DBLE(RS)
XG=DBLE(XGS)
EK=DBLE(EKS)
EM=DBLE(EMS)
XLEN=DBLE(XLENS)
DIUX=DBLE(DIUXS)
ACCEPT "DESIRED FUNDAMENTAL FREQUENCY =?"
F1=DBLE(F1S)
FK=922.000
FN=1.024011/(F1*DIUX)
X1=XL/XC
R0=DSORT(X1)
W=2.000*PI*F1
DCO=2.000*R0/(2.000*R0+R*XLEN)
FT=DCO/FN
FTT=0.000
FFJ=0.000
ICT1=IDINT(FN/200.000)
TYPE "ICT1=",ICT1
ICT2=100
ICT3=ICT1-50
ICT4=ICT1-1
NCT1=0
NCT2=0
NCT1=NCT1+1
NCT2=NCT2+1
FFJ=FFJ+1.000

```

50

100

```

FJ=J*FFJ
X=F J*XM
X1=DCOS(EMPI/2.000)
X2=DSIN(EMPI/2.000)
SM=X*DCPLX(X1,X2)
X1=R+EK*DREAL(SM)
X2=XL*FJ*EK*DAIMAG(SM)
AA=DCPLX(X1,X2)
X1=X*FJ
AB=AA/DCPLX(XG,X1)
X=DCABS(AB)
X=DSORT(X)
X2=DATAN2(DAIMAG(AB),DREAL(AB))/2.000
Z0=X*DCPLX(DCOS(X2),DSIN(X2))
AG=X*DCPLX(XG,X1)
X=DCABS(AB)
X=DSORT(X)
X2=DATAN2(DAIMAG(AB),DREAL(AB))/2.000
GM=X*DCPLX(DCOS(X2),DSIN(X2))
X1=FJ*DSORT(XC*XL)
GM=GM-DCPLX(0.000,X1)
RHO=(R0-Z0)/(R0+Z0)
AA=(4.000*R0*Z0)/(R0+Z0)*(R0+Z0)*(R0+Z0)
AB=(DCEXP(-XLEN*GM))/(1.000-RHO*RHO*DCEXP(-2.000*XLEN*GM))
AC=DCONJG(AA*AB)
X1=2.000*PI*FFJ*FK/FN
X2=DREAL(AC)
X3=DAIMAG(AC)
FT=FT+(2.000*(X2*DCOS(X1)-X3*DSIN(X1)))/FN
IF (NCT1.LE.ICT4) GO TO 110
TYPE "F(T)=",FT
IF (NCT1.LE.ICT3) GO TO 120
FTT=FTT+FT
IF (NCT2.LT.ICT2) GO TO 100
IF (NCT1.LT.ICT1) GO TO 50

```

110

120

```
FTT=FTT/5000.000  
TYPE " "  
TYPE "F(T)=",FTT  
FTS=SNGL(FTT)  
RETURN  
END
```

*

APPENDIX C -- TIME DOMAIN DATA ACQUISITION SYSTEM DESCRIPTION

Figure C.1 is a simplified block diagram of the Automatic Pulse Measurement System (APMS) [6,7]. The sampling oscilloscope is a commercially available unit that has been modified to allow either stand-alone or computer-controlled operation. It should be noted that this type of oscilloscope is not a real time instrument. Rather, it acquires one voltage versus time point of the measured waveform per waveform occurrence. Thus only repetitive waveforms may be observed. The advantage of this sampling scheme over conventional real time oscilloscopes is the large amount of available bandwidth. Whereas conventional oscilloscopes are presently limited in bandwidth to below 1 GHz, the effective bandwidth of the sampling oscilloscope used in the APMS is about 18 GHz.

When the sampling oscilloscope is switched to computer-controlled operation, the oscilloscope is connected to the system minicomputer via an A/D-D/A unit and a digital control interface. Under program control, the computer sends the oscilloscope the desired time location at which a voltage sample is to be taken via the 14-bit D/A converter. After the waveform voltage sample has been taken it is recorded in the computer memory via the 14-bit A/D converter. The digital interface is designed to allow asynchronous (independent) clocking of the sampling oscilloscope with respect to the minicomputer.

The system minicomputer is a 16-bit machine with 32K words of core memory. With the peripherals shown in the block diagram, i.e., the flexible disk drive, the CRT graphics terminal, hard copy unit, paper tape punch (PTP) and paper tape reader (PTR), the system can generate either alpha-numeric or graphical data in either soft or hard copy. In addition, a hardware floating point number processor has been added to the computer to speed arithmetic calculations by an approximate factor of 10.

The APMS is capable of running at a maximum sampling rate of approximately 8 kHz. The useful signal voltage measurement range is ± 800 mV into the 50 Ω sampling head. The available real time equivalent sweep speeds range from 10 ps/cm to 500 μ s/cm in a 1-2-5 sequence.

The system software consists of a commercially available flexible disk operating system with such features as Basic and Fortran language support, disk files, text editor, and macro-command capability. The sampling oscilloscope waveform acquisition is done with assembly language programming while virtually all signal processing of the waveform is done in either Basic or Fortran. The software has been designed to achieve a happy medium between system versatility and ease of operation.

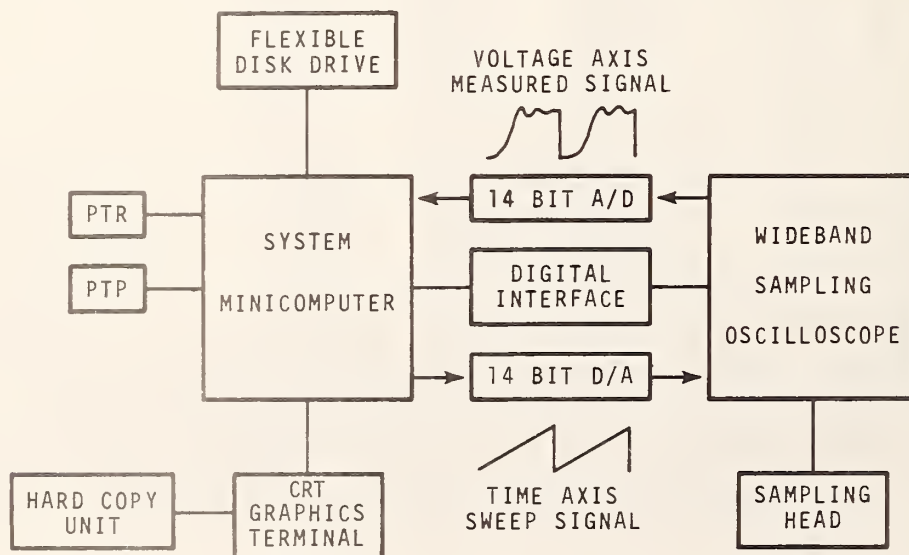


Figure C.1 Simplified block diagram of APMS

U.S. DEPT. OF COMM. BIBLIOGRAPHIC DATA SHEET	1. PUBLICATION OR REPORT NO. NBS TN-1042	2. Gov't. Accession No.	3. Recipient's Accession No.
4. TITLE AND SUBTITLE Shielded Balanced and Coaxial Transmission Lines - Parametric Measurements and Instrumentation Relevant to Signal Waveform Transmission in Digital Services		5. Publication Date June 1981	
7. AUTHOR(S) W. L. Gans and N. S. Nahman		6. Performing Organization Code	
9. PERFORMING ORGANIZATION NAME AND ADDRESS NATIONAL BUREAU OF STANDARDS DEPARTMENT OF COMMERCE WASHINGTON, DC 20234		8. Performing Organ. Report No.	
12. SPONSORING ORGANIZATION NAME AND COMPLETE ADDRESS (Street, City, State, ZIP) Dept. of the Army, US Army Communications Command Communications - Electronics Engineering & Installations Ag. Fort Huachuca, AZ 85613		10. Project/Task/Work Unit No.	
15. SUPPLEMENTARY NOTES <input type="checkbox"/> Document describes a computer program; SF-185, FIPS Software Summary, is attached.		11. Contract/Grant No.	
16. ABSTRACT (A 200-word or less factual summary of most significant information. If document includes a significant bibliography or literature survey, mention it here.) A method is presented for determining the impulse and step responses of a shielded cable using time domain terminal measurements and a physically based mathematical model for the transmission line properties of the cable. The method requires a computer controlled time domain measurement system and was implemented using the NBS Automatic Pulse Measurement System (APMS). Data are also developed for the frequency domain complex propagation function (attenuation and its related minimum-phase shift). The method is applied to 12 shielded paired-conductor (balanced) cables and 5 coaxial cables. Time domain responses are presented for three nominal cable lengths, 60 m (200 ft), 150 m (500 ft), and 300 m (1000 ft). The time domain responses are applied to the estimation of bit error rate increases due to the insertion of the cables into a digital signaling system employing a balanced polar NRZ waveform. Also discussed is the application of the time domain responses to time domain reflectometry techniques for cable acceptance tests and field-site testing of installed cables.		13. Type of Report & Period Covered	
17. KEY WORDS (six to twelve entries; alphabetical order; capitalize only the first letter of the first key word unless a proper name; separated by semicolons) Bit error rate; coaxial transmission lines; digital communication impulse response; instrumentation; measurements; shielded balanced transmission lines; time domain; transmission line model; waveform.		14. Sponsoring Agency Code	
18. AVAILABILITY <input checked="" type="checkbox"/> Unlimited <input type="checkbox"/> For Official Distribution. Do Not Release to NTIS <input type="checkbox"/> Order From Sup. of Doc., U.S. Government Printing Office, Washington, DC 20402. <input checked="" type="checkbox"/> Order From National Technical Information Service (NTIS), Springfield, VA, 22161	19. SECURITY CLASS (THIS REPORT) UNCLASSIFIED	21. NO. OF PRINTED PAGES 260	
	20. SECURITY CLASS (THIS PAGE) UNCLASSIFIED	22. Price \$ 20.00	

USCOMM-DC

NBS TECHNICAL PUBLICATIONS

PERIODICALS

JOURNAL OF RESEARCH—The Journal of Research of the National Bureau of Standards reports NBS research and development in those disciplines of the physical and engineering sciences in which the Bureau is active. These include physics, chemistry, engineering, mathematics, and computer sciences. Papers cover a broad range of subjects, with major emphasis on measurement methodology and the basic technology underlying standardization. Also included from time to time are survey articles on topics closely related to the Bureau's technical and scientific programs. As a special service to subscribers each issue contains complete citations to all recent Bureau publications in both NBS and non-NBS media. Issued six times a year. Annual subscription: domestic \$13; foreign \$16.25. Single copy, \$3 domestic; \$3.75 foreign.

NOTE: The Journal was formerly published in two sections: Section A "Physics and Chemistry" and Section B "Mathematical Sciences."

DIMENSIONS/NBS—This monthly magazine is published to inform scientists, engineers, business and industry leaders, teachers, students, and consumers of the latest advances in science and technology, with primary emphasis on work at NBS. The magazine highlights and reviews such issues as energy research, fire protection, building technology, metric conversion, pollution abatement, health and safety, and consumer product performance. In addition, it reports the results of Bureau programs in measurement standards and techniques, properties of matter and materials, engineering standards and services, instrumentation, and automatic data processing. Annual subscription: domestic \$11; foreign \$13.75.

NONPERIODICALS

Monographs—Major contributions to the technical literature on various subjects related to the Bureau's scientific and technical activities.

Handbooks—Recommended codes of engineering and industrial practice (including safety codes) developed in cooperation with interested industries, professional organizations, and regulatory bodies.

Special Publications—Include proceedings of conferences sponsored by NBS, NBS-annual reports, and other special publications appropriate to this grouping such as wall charts, pocket cards, and bibliographies.

Applied Mathematics Series—Mathematical tables, manuals, and studies of special interest to physicists, engineers, chemists, biologists, mathematicians, computer programmers, and others engaged in scientific and technical work.

National Standard Reference Data Series—Provides quantitative data on the physical and chemical properties of materials, compiled from the world's literature and critically evaluated. Developed under a worldwide program coordinated by NBS under the authority of the National Standard Data Act (Public Law 90-396).

NOTE: The principal publication outlet for the foregoing data is the Journal of Physical and Chemical Reference Data (JPCRD) published quarterly for NBS by the American Chemical Society (ACS) and the American Institute of Physics (AIP). Subscriptions, reprints, and supplements available from ACS, 1155 Sixteenth St., NW, Washington, DC 20056.

Building Science Series—Disseminates technical information developed at the Bureau on building materials, components, systems, and whole structures. The series presents research results, test methods, and performance criteria related to the structural and environmental functions and the durability and safety characteristics of building elements and systems.

Technical Notes—Studies or reports which are complete in themselves but restrictive in their treatment of a subject. Analogous to monographs but not so comprehensive in scope or definitive in treatment of the subject area. Often serve as a vehicle for final reports of work performed at NBS under the sponsorship of other government agencies.

Voluntary Product Standards—Developed under procedures published by the Department of Commerce in Part 10, Title 15, of the Code of Federal Regulations. The standards establish nationally recognized requirements for products, and provide all concerned interests with a basis for common understanding of the characteristics of the products. NBS administers this program as a supplement to the activities of the private sector standardizing organizations.

Consumer Information Series—Practical information, based on NBS research and experience, covering areas of interest to the consumer. Easily understandable language and illustrations provide useful background knowledge for shopping in today's technological marketplace.

Order the above NBS publications from: Superintendent of Documents, Government Printing Office, Washington, DC 20402.

Order the following NBS publications—FIPS and NBSIR's—from the National Technical Information Services, Springfield, VA 22161.

Federal Information Processing Standards Publications (FIPS PUB)—Publications in this series collectively constitute the Federal Information Processing Standards Register. The Register serves as the official source of information in the Federal Government regarding standards issued by NBS pursuant to the Federal Property and Administrative Services Act of 1949 as amended, Public Law 89-306 (79 Stat. 1127), and as implemented by Executive Order 11717 (38 FR 12315, dated May 11, 1973) and Part 6 of Title 15 CFR (Code of Federal Regulations).

NBS Interagency Reports (NBSIR)—A special series of interim or final reports on work performed by NBS for outside sponsors (both government and non-government). In general, initial distribution is handled by the sponsor; public distribution is by the National Technical Information Services, Springfield, VA 22161, in paper copy or microfiche form.

U.S. DEPARTMENT OF COMMERCE
National Bureau of Standards
Washington, D.C. 20234

OFFICIAL BUSINESS

Penalty for Private Use, \$300

POSTAGE AND FEES PAID
U.S. DEPARTMENT OF COMMERCE
COM-215



SPECIAL FOURTH-CLASS RATE
BOOK
